CSGI

Consorzio Interuniversitario per lo Sviluppo dei Sistemi a Grande Interfase

Report 2007

Outline

CSGI (Research Center for Colloids and Nanoscience) was established in December 1993. It has been officially recognized by the Italian Government in 1994, and is under the supervision and control of the Italian Ministry for University and Scientific Research (MIUR). Since 1995 CSGI began its scientific activity, devoted to basic research and to the development of high-tech new processes, and is supporting the activities of the small and medium size business industrial companies, that cannot afford the financial costs of an independent research activity.

In the last 12 years, CSGI has sponsored several different research programs, mainly supported by European Union grants, and partly also by other international and national Institutions, such as the Italian "Articolo 10, Law 46/1982", PNR, FISR, FIRB, CNR, and so forth.

CSGI has signed numerous contracts that involve about 70 national and international industrial companies, and some highly qualified research Centers, such as Procter & Gamble, Siemens, Tecnotessile SpA, Massachusetts Institute of Technology, Pharmacia-Upjon, Elf-Atochem, Ansaldo, Glaxo-Wellcome, Sintech, Inver, Cover, Tooling International Ltd, Industrial Materials Technology GmbH, MBN SpA, Inteti, Icmese, Comune di Firenze, VTT, etc. Such lively activity has brought to several International Patents and research agreements.

CSGI has reached a very qualified standard, and its level has been acknowledged abroad, in several fields. For example, CSGI is a leader in a number of applications of Nanotechnology, in the conservation of cultural heritage, and in the production of nanophasic powders (with MBN) for the production of special materials for aeronautics, high resistance coatings, etc. CSGI supports the local authorities for the safeguard and conservation of works or art ("Sovrintendenze Artistiche") in Tuscany and other Italian districts, with a set of technologies that have been developed for this aim. Similar actions have been promoted in agreement with the Mexican Federal Government for the conservation of monuments (Puebla Cathedral, Maya and Aztec heritage, the archaelogical site of Calakmul, Campeche).

CSGI is active also in the training of specialized researchers, has granted several fellowships, PhD supporting programs, post-doc grants, and other education projects, and has organized several national and international Meetings. In particular, during the year 2006, CSGI has issued 12 PhD scholarships, 35 fellowships, and 12 post-doc grants, and is actively participating in two European Master Programs: EMASCO-COSOM (European Master in Supramolecular and Colloidal Chemistry) and IMES (International Master on Bioenergy and Environment).

The CSGI financial plan is solid, with a strong growth of its financial assets, mainly due to EU funding.

The main topics of CSGI research activity are:

1) development of processes for the production of nanophasic systems, for the production of innovative textiles, for the synthesis of nanophasic alloys, ceramics and nanophasic or nanostructured composites (low temperature and low energy costs)
2) setup of new additives for cement products. These projects are mainly carried out in collaboration with Italcementi and MIT, and are aimed at investigating and optimizing the cement hydration process and the production of new, ceramics-like materials for the cement-related industry
3) formulation of dispersions in fluids, emulsions and inverted emulsions (paints, adhesives, sealing materials, detergents, etc.)

4) development of systems for the confinement of proteins and for the controlled release of pharmaceutics
5) development of food-related industrial processes (for example the treatment of milk and milk derivatives in supercritical phase)
6) development of innovative procedures for the conservation and restoration of works of art (paintings, frescoes and stone-based materials). CSGI is a world leader in this research activity, and is involved in a significant campaign for the recover of archaelogical treasures in Mexico (Calakmul), in the largest Maya site, and with the Maritime Museum in Stockholm for the conservation of the Vasa ship.

Fields of interest

Nanostructured and ultrafine materials.
Structure and dynamics of supramolecular assemblies (monolayers, micelles, liposomes, microemulsions, Langmuir-Blodgett films, host-guest systems).
Nanophasic ternary oxides.
Structural analysis of biomolecules in solution, interaction processes, recognition of ligands with macromolecular surfaces, theoretical and experimental analysis of cellular metabolism, interactions between metals and ligands, characterization of the interaction sites.
Formulation of nanophasic systems.
Innovative processes for the conservation and restoration of cultural heritage (stone materials, wood materials, paintings, frescoes, paper).

Structure and Organization of CSGI

Management Offices
President, Council, Director, Audit Council, Technical-Scientific Board.

Director of CSGI
Prof. Piero Baglioni, Department of Chemistry, University of Florence

President of CSGI
Prof. Giovanni Marletta, Department of Chemical Sciences, University of Catania

Website
http://www.csgi.unifi.it/

Foundation
December 21st, 1993

Official recognition by the Italian Government
November 15th, 1994 (G.U. Nr. 267)

Academic Locations and other associated Centers

University of Florence (headquarters)
University of Siena
University of Udine
University of Pavia
University of Cagliari
University of Napoli "Federico II"
University of Molise (Campobasso)
University of Catania
University of Bergamo
University of Milan, Bicocca
Polytechnic Institute of Milan
University of Perugia

Current Collaborations

Academic partners

ANU (Australian National University, Camberra), Argonne National Laboratory, Aston University (Birmingham, UK), Brookhaven National Laboratory, California Institute of Technology (CalTech), Centro di Istochimica del CNR di Pavia, Collège de France, Columbia University, CSIC (Siviglia), East China Normal University (Shangai), École Normale Supérieure (Lione), Escuela Superior Politecnica del Chimborazo (Ecuador), ETH (Zurigo), Hahn-Meitner Institut (Berlino), Hull University (Regno Unito), Institut de la Science et Génie des Matériaux et Procédés (Francia), Institut Laser Technology (Germania), Institut National Polytechnique de Lorraine (Nancy), Institute of Scientific Instruments (Repubblica Ceca), ITER (Germania), Laboratoire Leon Brillouin (Saclay), Lehstul Fertigungstechnologie (Germania), Massachusetts Institute of Technology (MIT), Max Planck Institut (Berlino), Museum of Fine Arts (Boston), Nuclear Research Institute (Praga), Oak Ridge National Laboratory, Risø National Laboratory (Danimarca), Technical University di Budapest, Tekniska Hogskolan I Lulea (Svezia), The Getty Conservation Institute (Los Angeles), Univeritat Gesamthoschule Kassel (Germania), Università "Louis Pasteur" di Strasburgo, Università degli Studi Bari, Università degli Studi Camerino, Università degli Studi Catania, Università degli Studi Chieti, Università degli Studi della Calabria, Università degli Studi di Parma, Università degli Studi Genova, Università degli Studi Milano, Università degli Studi Napoli, Università degli Studi Palermo, Università degli Studi Pisa, Università degli Studi Roma ("La Sapienza"), Università degli Studi Salerno, Università degli Studi Torino, Università degli Studi Trento, Università degli Studi Udine, Università degli Studi Urbino, Università di Grenoble, Università di Heidelberg, Università di Leida (Paesi Bassi), Università di Lund (Svezia), Universitad de Santiago de Compostela (Spagna), Universitad del Salvador Universitad Estadual de Campinas (Brasile), Université de Bourgogne, Université de Montpellier II, University College di Londra, CNIC (Cuba), University of Berkeley, University of Bristol, University of Detroit, University of York, University of Cambridge, University of East Anglia (Canada), University of Houston, University of South Florida, Weizmann Institute (Israele).

Industrial partners

Alcea, Alfa Test, Alfa Wasserman, Ansaldo, Aprilia, Ascor chimici, Ausimont, Bigagli, Biokimica S.p.A, Bioscreen Technology srl, BTG-Holland, Bitossi, Comune di Firenze, Consorzio delle Buone Idee, Chemia, Cover, D'Appolonia, Dynamotive, Elf-Atochem, ENEA (Energy Department – Casaccia), Eniricerche, Enitecnologie, EUBIA (European Biomass Industry Association, - Bruxelles, Belgium), Flory's, Getty Conservation Institute, Glaxo-Wellcome, Icmese, INASCO-Hellas (Integrated Aerospace Science Corporation - Greece), Industrial Materials Technology GmbH, Industrie Casearie Podda, Ineti, Institute for the Care of Hystorical Monuments (Prague), International Broker, Inver, IRBM, Italcementi S.p.A., Italfarmaco, Lamberti S.p.A., Lima, JRC (Joint Research Centre of the European Commission), Mapei, Mariplast, Martelli, MBN Nanomaterialia, Merk, Microtec (Germany), National Museum of Denmark, Nicox, Novuspharma Omrod Diesel (UK), Philips, Pharmacia-Upjon (USA and Sweden), Pharmaness, Procter & Gamble, Rifiniture BP, Sem, Siemens AG, S.I.F.I., Sintech, SIR Industriale, Sirio Panel, Solvay, Soprintendenze ai Beni Artistici e Storici di: Firenze-Prato-Pisatoia, Siena-Grosseto, Pisa-Lucca-Massa Carrara, Soprintendenze ai Beni Ambientali ed Architettonici di Arezzo, Firenze-Prato-Pisatoia, Roma, Veneto Orientale, Lombardia, Reggio Calabria, Tecnotessile SpA, TIL (Tooling International Ltd UK), TNO (Netherlands Organisation for Applied Scientific Research), 3M, Transfergomma (Padova), WIP (Germany), VTT (Finland).

Personnel

CSGI gathers about 300 researchers, including Full Professors, Associate Professors, University Researchers, that belong to the academic members.
Moreover, CSGI employs 71 researchers and 5 administration employees on its own. Several PhD and post-doc students are financially supported through CSGI fellowships. CSGI hosts researchers hired by industrial companies for training and specific research activities, in the framework of particular projects.

CSGI owes two research Laboratories, located in Vascon di Carbonera (Nanophases Laboratory) and in Prato (Laboratory for the refinement and surface modification of textiles). These plants collaborate closely with the local industrial activities.

CSGI owned Patents

1) Baglioni Piero, Dei Luigi, Ferroni Enzo, Giorgi Rodorico - Sospensioni stabili di idrossido di calcio. Brevetto Italiano FI/96/A000255 depositato il 31/10/1996.

2) Matteazzi Paolo, Baglioni Piero, Basset Diego - "Process for Recycling, by Milling, Solid Industrial Waste and Materials at the end of their Service Life" European Patent Application 97203735.2, Priority IT96 FI96A000280.

3) Grassi Giuliano, Chiaramonti David, Baglioni Piero – "Apparato a combustione di etanolo o miscele etanolo per cucine, stufe e illuminazione a uso domestico". Brevetto Italiano FI/98/A42 depositato il 24/ 02/ 98.

4) Ambrosone Luigi, Ceglie Andrea – "Software per l'analisi grafica e numerica di dati di Risonanza Magnetica Nucleare per la determinazione della polidispersità di emulsioni". Brevetto Italiano FI99A000044 depositato il 09/03/1999.

5) Baglioni Piero, Fratini Emiliano, Ricceri Riccardo, Sarti Giuseppe, Chiaramonti David - Engine fuels consisting of an emulsion comprising mineral and/or natural oils, their preparation and use in internal combustion engine. PCT Int. Appl. WO n. 99936473.0 del 02.07.99

6) Baglioni Piero, Carretti Emiliano, Dei Luigi - Microemulsioni ed emulsioni di olio in acqua, loro uso per la solubilizzazione di resine polimeriche e impacchi contenenti detti microemulsioni o emulsioni. Brevetto Italiano Fi99A000071 depositato il 02/ 04/ 99

7) Baglioni Piero, Bardi Ugo, Bonini Massimo -New method for the production of solid powder and films by compartimentalised solution thermal spraying (CSTS). Eur. Pat. Appl. EP 00-105673.8 delp. 17.03.2000

8) Baglioni Piero, Dei Luigi, Giorgi Rodorigo, Claudio Vinicius Schettino – Basic Suspensions their Preparation and Use in Processes for Paper Deacidification EP 02714088.8 del 15/01/02

9) Baglioni Piero, Dei Luigi, Fratoni Laura, Lo Nostro Pierandrea, Moroni Michelangelo - "Processo per la preparazione di nano e microparticelle di ossidi e idrossidi di metalli del secondo gruppo e di transizione, nano e microparticelle così ottenute e loro impiego in campo ceramico, tessile e cartario", DOMANDA BREVETTO N.FI2002A000052, depositata in data 28/03/2002 – EP 03745367.7

10) Baglioni Piero, Dei Luigi, Fratoni Laura, Lo Nostro Pierandrea, Moroni Michelangelo – "Preparation of nano- and micro-particles of group II and transition metals oxides and hydroxides and their use in the ceramic, textile and paper industries". PCT Int. Appl. (2003), 10 pp. CODEN: PIXXD2 WO 2003082742 A2 20031009 CAN 139:278604 AN 2003:796605

11) Baglioni Piero, Dei Luigi, Giorgi Rodorico, Ninham Barry W. – "Process for preparing nano- nad micro-sized particles of inorganic compounds" EP 04101822.7, 29/04/2004.

12) Angelico Ruggero, Ceglie Andrea, Hochoeppler Alejandro, Palazzo Gerardo, Stefan Alessandra – "Macroemulsioni acqua-in olio a lunga stabilità, loro preparazione ed uso" – DOMANDA BREVETTO N. FI2001A000016 depositata in data 29/01/01.

13) Ambrosone Luigi, Ceglie Andrea – "Materiale assorbente e suoi usi nei processi di bonifica di falde acquifere inquinate da prodotti chimici" – DOMANDA BREVETTO FI2003A000236 depositata iin data 11/09/03.

14) Ambrosone Luigi, Ceglie Andrea – "Gel stabili contenenti gelatina" – DOMANDA BREVETTO N. FI2003A000237 depositata in data 11/09/03.

15) Fratoni Laura, Lo Nostro Pierandrea – "Composizione detergente a base di un estere dell'acido L-ascorbico" – DOMANDA BREVETTO N. TO2003A001032 depositata in data 22/12/03.

16) Baglioni Piero, Ambrosi Moira, Dei Luigi, Faneschi Mauro, Mancioli Luciano, Santoni Sergio – "Ceramic products comprising nanoparticles of zirconium hydroxide and/or glass frits" – RIF. DOMANDA 7303 PTEP/2006 EP06112439.2 del 10.04.06

17) Ceglie Andrea, Venditti Francesco, Lopez Francesco, Palazzo Gerardo, Colafemmina Giuseppe, Angelico Ruggero, Ambrosone Luigi – "Materiale adsorbente contenente tensioattivo cationico, sua preparazione ed uso per la rimozione di metalli da soluzioni acquose" – DOMANDA BREVETTO N. FI 2006 A000113 – RIF. 7490 PTITdel 10.05.2006

18) Ambrosi Moira, Baglioni Piero, Bonini Massimo, Fratini Emiliano – "Nanoparticelle monodisperse di ossidi ed idrossidi metallici e loro applicazione nei settori tessile, cartario e ceramico" – DOMANDA BREVETTO FI 2006A000313 depositata in data 11/02/06.

List of publications 2005-2007

1. Insights into Hofmeister Mechanisms: Anion and Degassing Effects on the Cloud Point of Dioctanoylphosphatidylcholine/Water Systems. Lagi, M., Lo Nostro, P., Fratini, E., Ninham, B. W., Baglioni, P. *Journal of Physical Chemistry B* 111, 589-597 (2007)

2. Functionality of Photosynthetic Reaction Centers in Polyelectrolyte Multilayers: Toward an Herbicide Biosensor. Mallardi, A., Giustini, M., Lopez, F., Dezi, M., Venturoli, G., Palazzo, G. Journal of Physical Chemistry B 111, 3304-3314 (2007)

3. High-relaxivity supramolecular aggregates containing peptides and Gd complexes as contrast agents in MRI. Accardo, A., Tesauro, D., Morelli, G., Gianolio, E., Aime, S., Vaccaro, M., Paduano, L., Schillen, K. Journal of Biological Inorganic Chemistry 12 (2), 267-276 (2007)

4. Hofmeister Effects in Enzymatic Activity: Weak and Strong Electrolyte Influences on the Activity of Candida rugosa. Salis, A., Bilanicova, D., Ninham, B. W., Monduzzi, M. Journal of Physical Chemistry B 111, 1149-1156 (2007)

5. Light limitations to algal growth in tropical ecosystems. Loiselle, S., Cozar, A., Dattilo, A. M., Bracchini, L., Galvez, J. A. Freshwater Biology 52, 305-312 (2007)

6. Mesoscopic and Microscopic Investigation on Poly(vinyl alcohol) Hydrogels in the Presence of Sodium Decylsulfate. Mangiapia, G., Ricciardi, R., Auriemma, F., De Rosa, C., Lo Celso, F., Triolo, R., Hennan, R. K., Radulescu, A., Tedeschi, A. M., D'Errico, G., Paduano, L. Journal of Physical Chemistry B 111 (9), 2166-2173 (2007)

7. Nanostructures by Self-Assembling Peptide Amphiphile as Potential Selective Drug Carriers. Accardo, A., Tesauro, D., Mangiapia, G., Pedone, C., Morelli, G. Biopolymers 88 (2), 115-121 (2007)

8. A Study of the Microstructural and Diffusion Properties of Poly(vinyl alcohol) Cryogels Containing Surfactant Supramolecular Aggregates. Tedeschi, A. M., Auriemma, F., Ricciardi, R., Mangiapia, G., Trifuoggi, M., Franco, L., De Rosa, C., Hennan, R. K., Paduano, L., D'Errico, G. Journal of Physical Chemistry B 110 (46), 23031-23040 (2006)

9. Acid Titrations of poly(dG-dC)poly(dG-dC) in aqueous solution and in a w/o microemulsion. Airoldi, M., Boicelli, C. A., Gennaro, G., Giomini, M., Giuliani, A. M., Giustini, M. Journal of Biomolecular Structure & Dynamics 23, 465-477 (2006)

10. Anomalous surfactant diffusion living polymer system. Angelico, R., Ceglie, A., Olsson, U., Palazzo, G., Ambrosone, L. Physical Review E 74, 1403-1408 (2006)

11. Bacterial adhesion onto nanopatterned polymer surfaces. Satriano, C., Carnazza, S., Guglielmino, S., Marletta, G. Materials Science and Engineering C (2006)

12. Binary Mutual Diffusion Coefficients of Aqueous Solutions of Sucrose, Lactose, Glucose, and Fructose in the Temperature Range from (298.15 to 328.15) K. Ribeiro,

A.C.F., Ortona, O., Simões S.M.N., Santos, C.I.A.V., Prazeres P.M.R.A., Valente, A.J.M., Lobo, V.M.M., Burrows, H.D. Journal of Chemical and Engineering Data, 1836-1840 (2006)

13. Biocompatible Lipid-Based Liquid Crystals and Emulsions. Mosca, M., Murgia, S., Ceglie, A., Monduzzi, M., Ambrosone, L. Journal of Physical Chemistry B 110, 25994-26000 (2006)

14. Cathode materials (NiO-LiFeO2-LiCoO2) for molten carbonate fuel cell: a diffraction, NMR and conductivity study. Milanese, C., Berbenni, V., Bruni, G., Marini, A., Chiodelli, G., Villa, M. Solid State Ionics 177 (19-25), 1893-1896 (2006)

15. Cation Distribution in LiMgVO4 and LiZnVO4: Structural and Spectroscopic Study. Capsoni, D., Bini, M., Massarotti, V., Mustarelli, P., Belotti, F., Galinetto, P. Journal of Physical Chemistry B 110 (11), 5409-5415 (2006)

16. Colloidal aspects of photosynthetic membrane proteins. Palazzo, G. Current Opinion in Colloid & Interface Science 11, 65-73 (2006)

17. Comment on "Effective long-range attraction between protein molecules in solution studied by small angle neutron scattering" - Reply. Liu, Y.C., Fratini, E., L., Baglioni, P. Physical Review Letters 96, 21 (2006)

18. Comparative Analysis of the Effects of Locally Used Herbicides and Their Active Ingredients on a Wild-Type Wine Saccharomyces cerevisiae Strain. Braconi, D., Sotgiu,M, Millucci, L., Paffetti, A, Tasso, F, Alisi, C, Martini, S., Rappuoli, R, Lusini, P, Sprocati, AR, Rossi, C., Santucci, A. J. Agr. Food Chem (2006)

19. Comparison between Angular Dependent NEXAFS Analysis and Theoretical Calculations of Molecular Orientation of New Functional Mixed Aromatic Molecules Deposited onto Au/Si(111). Marletta, G., Gambino, G. L., Licciardello, A., Tuccitto, N. Nuclear Instruments & Methods in Physics Research Section B-Beam Interactions with Materials and Atoms 246, 145-150 (2006)

20. Conservation of acid waterlogged shipwrecks: nanotechnologies for de-acidification. Giorgi, R., Baglioni, P., Chelazzi, D. Applied Physics A: Materials Science & Processing 83, 669-673 (2006)

21. Densely-packed Self-assembled Monolayer on Gold Surfaces from a Conformationally-Constrained Helical Hexapeptide. Marletta, G. Surface Science 600, 409-416 (2006)

22. Drug-Protein Recognition Processes Investigated By NMR Relaxation Data. A Study on Corticosteroid-Albumin Interactions. Martini, S., Bonechi, C., Casolaro, M., Corbini, G., Rossi, C. Biochemical Pharmacology 71, 858-864 (2006)

23. Effect of mechanical activation on the formation of lead titanates from PbCO3 – TiO2. Berbenni, V., Milanese, C., Marini, A., Welham, N. J. Journal of Materials Science 41 (6), 1739-1744 (2006)

24. Electric-Field-Assisted Alignment of Supramolecular Fibers. Sardone, L., Marletta, G. Adv.Mat 18, 1276-1280 (2006)

25. Examining the dynamics of phytoplankton biomass in Lake Tanganyika using Empirical Orthogonal Functions. Bergamino, N., Loiselle, S., Cozar, A., Dattilo, A. M., Bracchini, L., Rossi, C. Ecological Modelling In press (2006)

26. Experimental evidence of fragile-to-strong dynamic crossover in DNA hydration water. Chen, S. H., Liu, L., Chu, X., Zhang, Y., Fratini, E., Baglioni, P., Faraone, A., Mamontov, E. Journal of Chemical Physics 125, 171103-171106 (2006)

27. Exploring interaction of beta-amyloid segment (25-35) with membrane models through paramagnetic probes. Esposito, C., Tedeschi, A. M., Scrima, M., D'Errico, G., Ottaviani, F., Rovero, P., D'Ursi, A.M. Journal of peptide science 12 (12), 766-774 (2006)

28. FbsA-Driven Fibrinogen Polymerization: A Bacterial ‘‘Deceiving Strategy’’. Pierno, M., Maravigna, L., Piazza, R., Visai, L, Speziale, P. Physical Review Letters 96, 028108 (2006)

29. Gi/o proteins: expression for direct activation enquiry. Di Cesare Mannelli, L., Pacini, A., Toscano, A., Fortini, M., Berti, D., Ghelardini, C., Galeotti, N., Baglioni, P. Protein Expression and Purification 47, 303-310 (2006)

30. Hofmeister effects in supramolecular and biological systems. Lo Nostro, P., Ninham, B. W., Milani, S., Lo Nostro, A., Pesavento G., Baglioni, P. Biophysical Chemistry 124, 208-213 (2006)

31. Hydration water and microstructure in calcium silicate and aluminate hydrates. Fratini, E., Ridi, F., Chen, S. H., Baglioni, P. Journal of Physics-Condensed Matter 18, S2467-S2483 (2006)

32. Incorporation of the sunscreen agent, octyl methoxycinnamate. Scalia, S., Tursilli, G., Bianchi, A., Lo Nostro, P., Bocci, E., Ridi, F., Baglioni, P. International Journal of Pharmaceutics 308, 155-159 (2006)

33. Influence of the Alkyl Tail Length on the Anionic Surfactant-PVP Interaction. Tedeschi, A. M., Busi, E., Basosi, R., Paduano, L., D'Errico, G. Journal of Solution Chemistry 35 (7), 951-968 (2006)

34. Interaction between cationic, anionic, and non-ionic surfactants with ABA block copolymer Pluronic PE6200 and with BAB reverse block copolymer Pluronic 25R4. Ortona, O., D'Errico, G., Paduano, L., Vitagliano, V. Journal of Colloid and Interface Science 301 (1), 63-77 (2006)

35. Interaction of Sodium Ions with Cationic Surfactant. Murgia, S., Portesani, F., Ninham, B. W., Monduzzi, M. Chemistry - A European Journal 12, 7689-7698 (2006)

36. Light scattering and cryo-transmission electron microscopy investigation of the self-assembling behavior of di-C12P-nucleosides in solution. Baldelli Bombelli, F., Berti,

D., Almgren, M., Karlsson, G.,. Journal of Physical Chemistry B 110, 17627-17637 (2006)

37. Limiting Partial Molar Volume of Sodium Chloride in 2-Methyl-2,4-pentandiol-Water Mixed Solvents at 25 °C. Capuano, F., Mangiapia, G., D'Errico, G., Sartorio, R. Journal of Solution Chemistry 35 (11), 1525-1535 (2006)

38. Lipase production by yeasts from extra virgin olive oil. Ciafardini, G., Zullo B.A., Iride A. Food Microbiology 23, 60-67 (2006)

39. Lipolytic activity of Williopsis californica and Saccharomyces cerevisiae in extra virgin olive oil. Ciafardini, G., Zullo B.A., Cioccia G., Iride A. International Journal of Food Microbiology 107, 27-32 (2006)

40. Lysozyme Mutual Diffusion in Solutions Crowded by Poly(ethylene glycol). Vergara, A., Capuano, F., Paduano, L., Sartorio, R. Macromolecules 39 (13), 4500-4506 (2006)

41. Metabolic response to exogenous ethanol in yeast: an in vivo NMR and mathematical modelling approach. Martini, S., Ricci, M., Bartolini, F., Bonechi, C., Braconi, D., Millucci, L., Santucci, A., Rossi, C. Biophysical Chemistry 120, 135-142 (2006)

42. Micro-laser sintering (microls) for rapid prototyping of metal-ceramics. Czerner, S., Stippler, P., Ostendorf, A., Matteazzi, P. Proceeding of the 2nd Pacific International Conference on Application of Lasers and Optics 2006 (2006)

43. Molecular Modeling of Interactions between L-lysine and functionalised quartz Surfaces. Gambino, G. L., Grassi, A., Marletta, G. Journal of Physical Chemistry B 110, 4836-4845 (2006)

44. Molecular Recognition and Controlled Release in Drug Delivery Systems Based on Nanostructured lipid Surfactants. Angius, R., Murgia, S., Berti, D., Baglioni, P., Monduzzi, M. Journal of Physics-Condensed Matter 18, S2203-S2220 (2006)

45. Nanosized LiMn2O4 from mechanically activated solid-state synthesis. Massarotti, V., Capsoni, D., Bini, M. Journal of Solid State Chemistry 179, 590-596 (2006)

46. Nanotechnology for Vasa wood de-acidification. Chelazzi, D., Baglioni, P., Giorgi, R. Macromolecular Synmposia 238, 30-36 (2006)

47. Nanotubes from a Vitamin C-based Bolaamphiphile. Ambrosi, M., Fratini, E., Alfredsson, V., Ninham, B. W., Giorgi, R., Lo Nostro, P., Baglioni, P. Journal of American Chemical Society 128, 7209-7214 (2006)

48. Near-Infrared Spectroscopy Investigation of the Water Confined in Tricalcium Silicate Pastes. Ridi, F., Fratini, E., Milani, S., Baglioni, P. Journal of Physical Chemistry B 110, 16326-16331 (2006)

49. NMR of Liquid Crystals and Micellar Solution - IV. Monduzzi, M., Murgia, S. in Nuclear Magnetic Resonance 35, 533-561 Ed. G. A. Webb, The Royal Society of Chemistry (2006)

50. Nuclear Magnetic Resonance for Studying Recognition Processes between Anandamide and Cannabinoid Receptors. Bonechi, C., Martini, S., Brizzi, V., Brizzi, A., Massarelli, P, Bruni; G., Rossi, C. Eur. J. Med, Chem. (2006)

51. Nuove prospettive di preparazione di array microbici come piattaforma per "lab-on-a-cell" chip e microsistemi diagnostici. Marletta, G., Satriano, C., Carnazza, S., Guglielmino, S. Atti del III Simposio sulle Tecnologie Avanzate. Utilizzo e Applicazioni. Ministero della Difesa. SEGREDIFESA. Roma. 22-23 Giugno 2006 (2006)

52. Observation of fragile-to-strong dynamic crossover in protein Chen, S. H., Liu, L., Fratini, E., Baglioni, P., Faraone, A. Proceedings of the National Academy of Sciences of the USA 103, 9012-9016 (2006)

53. Oxidation of water emulsified olive oils. Ambrosone, L., Mosca, M., Ceglie, A. Food Hydrocolloids 20, 1080-1086 (2006)

54. Physicochemical characterization of a peptide deriving from the glycoprotein gp36 of the feline immunodeficiency virus and its lipoylated analogue in micellar systems. Esposito, C., D'Errico, G., Armenante, M.R., Giannecchini, S., Bendinelli, M., Rovero, P., D'Ursi, A.M. Biochimica et Biophysica Acta-Biomembranes 1758 (10), 1653-1661 (2006)

55. Polymorphic Behavior in Protein-Surfactant Mixtures: The Water-Bovine Serum Albumin-Sodium Taurodeoxycholate System. Orioni, B., Roversi, M., La Mesa, C., Asaro, F., Pellizer, G., D'Errico, G. 110 (24), 12129-12140 (2006)

56. Relationships between wetland ecotones and inshore water quality in the Ugandan coast of Lake Victoria. Cozar, A., Loiselle, S., Mazzuoli, S., Bergamino, N., Bracchini, L., Dattilo, A. M. Wetlands Ecology and Management In press (2006)

57. RNA complementary to the 5 ' UTR of mRNA triggers effective silencing in Saccharomyces cerevisiae. Bonoli, M., Graziola, M., Poggi, V., Hochkoeppler, A. Biochemical and Biophysical Research Communications 339, 1224-1231 (2006)

58. SANS Analysis of the Microstructural Evolution during the Aging of Pyrolysis Oils from Biomass. Fratini, E., Bonini, M., Oasmaa, A., Solantausta, Y., Teixeira, J., Baglioni, P. Langmuir 22, 306-312 (2006)

59. Satellite based indices in the analysis of land cover for municipalities in the Province of Siena, Italy. Focardi, S., Loiselle, S., Mazzuoli, S., Bracchini, L., Dattilo, A. M., Rossi, C. Journal of Environmental Management In press (2006)

60. Self assembly of biologically inspired amphiphiles. Berti, D. Current Opinion in Colloid & Interface Science 110, 74-78 (2006)

61. Self-Assembly of ß-Cyclodextrin in Water. Part 1: Cryo-TEM and Dynamic and Static Light Scattering. Bonini, M., Rossi, S., Karlsson, G., Almgren, M., Lo Nostro, P., Baglioni, P. Langmuir 22, 1478-1484 (2006)

62. Self-organization of yeast cells on modified polymer surfaces after dewetting: new perspectives in cellular patterning. Carnazza, S., Satriano, C., Guglielmino, S. J. Physics: Condensed Matter, vol. 18, Special Issue 33: Nanoscience and Nanotechnology 18, S2221-S2230. (2006)

63. Smart Nanostructured Lipids for Drug Delivery. Murgia, S., Angius, R., Monduzzi, M. Rivista Italiana di Compositi e Nanotecnologie (Materiali, Aerospazio, Tecnologie Speciali) 2, 37-42 (2006)

64. Solid state synthesis of CaMnO3 from CaCO3- MnCO3 mixtures by mechanical energy. Berbenni, V., Milanese, C., Bruni, G., Cofrancesco, P., Marini, A. Zeitschrift Fur Naturforschung Section B. A Journal of Chemical Sciences 61b, 281-286 (2006)

65. Solid state synthesis of stoichiometric LiCoO2 from mechanically activated Co–Li2CO3 mixtures. Berbenni, V., Milanese, C., Bruni, G., Marini, A. Materials Chemistry and Physics 100 (2-3), 251-256 (2006)

66. Solution Behavior of a Sugar-based Carborane for Boron Neutron Capture Therapy: a Nuclear Magnetic Resonance. Bonechi, C., Ristori, S., Martini, S., Panza, L., Martini, G., Rossi, C., Donati, A. Biophysical Chemistry (2006)

67. Specific Anion Effects on Glass Electrode pH Measurements of Buffer Solutions: Bulk and Surface Phenomena. Salis, A., Pinna, M. C., Bilanicova, D., Monduzzi, M., Lo Nostro, P., Ninham, B. W. Journal of Physical Chemistry B 110, 2949-2956 (2006)

68. Specific anion effects on the optical rotation of glucose and serine. Lo Nostro, P., Ninham, B. W., Milani, S., Fratoni, L., Baglioni, P. Biopolymers 81, 136-148 (2006)

69. Spectroscopic and thermal investigation of hydrophobic and hydrophilic fractions of dissolved organic matter. Provenzano, M. R., Gigliotti, G., Clienti, A., Erriquens, F., Senesi,. Compost Science & Utilization 14, 191-200 (2006)

70. Static and Dynamic Features of a helical hexapeptide chemisorbed on a gold surface. Marletta, G. Materials Science & Engineering C-Biomimetic and Supramolecular Systems 26, 918-923 (2006)

71. Structural and Spectroscopic Properties of Pure and Doped Ba6Ti2Nb8O30 Tungsten Bronze. Massarotti, V., Capsoni, D., Bini, M., Azzoni, C. B., Mozzati, M. C., Galinetto, P., Chiodelli, G. Journal of Physical Chemistry B 110 (36), 17798-17805 (2006)

72. Structural Investigation of Bilayers Formed by 1-Palmitoyl-2-oleoylphosphatidylnucleosides. Milani, S., Baldelli Bombelli, F., Berti, D., Hauss, T., Dante, S., Baglioni, P. Biophysical Journal 90, 1260-1269

73. Supramolecular Aggregates of Amphiphilic Gadolinium Complexes as Blood Pool MRI/MRA Contrast Agents: Physicochemical Characterization. Vaccaro, M., Accardo, A., Tesauro, D., Mangiapia, G., Loef, D., Schillen, K., Söderman, O., Morelli, G., Paduano, L. Langmuir 22 (15), 6635-6643 (2006)

74. Susceptibility of water-emulsified extra virgin olive oils to oxidation. Ambrosone, L., Cinelli, G., Mosca, M., Ceglie, A. Journal of the American Oil Chemists Society 82, 165-170 (2006)

75. Synthesis and characterization of magnetic nanoparticles coated with a uniform silica shell. Bonini, M., Wiedenmann, A., Baglioni, P. Materials Science & Engineering C-Biomimetic and Supramolecular Systems 26, 745-750 (2006)

76. Synthesis and magnetic properties of ZnFe2O4 obtained by mechanochemically assisted low-temperature annealing of mixtures of Zn and Fe oxalates. Berbenni, V., Milanese, C., Bruni, G., Marini, A., Pallecchi, I. Thermochimica Acta 447 (2), 184-189 (2006)

77. Synthetic Polymers as Biomacromolecular Models for Studying Ligand-Protein Interactions: a Nuclear Spin Relaxation Approach. Corbini, G., Martini, S., Bonechi, C., Casolaro, M., Corti, P.,. Journal of Pharmaceutical and Biomedical Analysis 40, 113-121 (2006)

78. The "macromolecular tourist": Universal temperature dependence of thermal diffusion in aqueous colloidal Iacopini, S., Rusconi, Piazza, R. European Physical Journal E: Soft Matter 19, 59–67 (2006)

79. The bio-optical properties of CDOM as descriptor of lake stratification. Bracchini, L., Dattilo, A. M., Hull, V., Loiselle, S., Martini, S., Rossi, C. Journal of Photochemistry and Photobiology 85, 145-149 (2006)

80. The Effect of Salt on Protein Chemical Potential Determined by Ternary Diffusion in Aqueous Solutions. Annunziata, O., Paduano, L., Pearlstein, A. J., Miller, D. G., Albright, J. G. Journal of Physical Chemistry B 110 (3) (2006)

81. The Effect of Salt Stoichiometry on Protein-Salt Interactions Determined by Ternary Diffusion in Aqueous Solutions. Annunziata, O., Paduano, L., Albright, J. G. Journal of Physical Chemistry B 110 (32), 16139-16147 (2006)

82. The Maya site of Calakmul: "in situ" preservation of wall paintings and limestone by using nanotechnologies. Giorgi, R., Chelazzi, D., Carrasco, R., Colon, M., Desprat, A., Baglioni, P. in IIC Congress 2006, 162-169 Ed. D. Saunders et al., (2006)

83. The novel CTAB based organogel as reactor for ester synthesis by entrapped Candida rugosa lipase. Lopez, F., Venditti, F., Cinelli, G., Ceglie, A. Process Biochemistry 41, 114-119 (2006)

84. The role of wetlands in the chromophoric dissolved organic matter release and its relation to aquatic ecosystems optical properties. A case of study: Katonga and Bunjako Bays (Victoria Lake; Uganda). Bracchini, L., Cozar, A., Dattilo, A. M., Loiselle, S., Tognazzi, A., Azza, N., Rossi, C. Chemosphere, 1170-1178 (2006)

85. ToF-SIMS and PCA studies of Seggianese olives and olive oil. Focardi, S., Ristori, S., Mazzuoli, S., Tognazzi, A., Leach-Scampavia, D., Castner, D.G., Rossi, C. Colloids and Surfaces in press (2006)

86. Un nuovo processo biotecnologico per produrre biodiesel. Salis, A., Pinna, M., Solinas, V., Monduzzi, M. Rivista Italiana di Compositi e Nanotecnologie (Materiali, Aerospazio, Tecnologie Speciali) 2, 51-59 (2006)

87. Una prospettiva di studio per l'Isola di Montecristo e la sua zona costiera. Bracchini, L., Dattilo, A. M., Donati, A., Focardi, S., Loiselle, S., Mazzuoli, S., Tognazzi, A., Rossi, C. Etrurianatura 3, 96-99 (2006)

88. Use of lipases for the production of biodiesel. Salis, A., Monduzzi, M., Solinas, V. in Industrial enzymes, 315-337 Ed. J. Polaina, A. McCabe, Springer (2006)

89. Use of Rhodotorula minuta Live Cells Hosted in Water-in-Oil Macroemulsion for Biotrasformation Reaction. Cinelli, G., Cuomo, F., Hochkoeppler, A., Ceglie, A., Lopez, F. Biotechnology Progress 22, 689-695 (2006)

90. Viscoelastic Properties of Insoluble Surfactants Spread onto an Oscillating Aqueous Drop. Marletta, G. Journal of Colloid and Interface Science 296, 269-275 (2006)

91. Why pH Titration in Protein Solutions Follows a Hofmeister Series. Böstrom, M., Lonetti, B., Fratini, E., Baglioni, P., Ninham, B. W. Journal of Physical Chemistry B 110, 7563-7566 (2006)

92. Nanoparticles of Mg(OH)2: Synthesis and Application to Paper Conservation, Giorgi, R., Bozzi, C., Dei, L., Gabbiani, C., Ninham, B. W., Baglioni, P., Langmuir 21, 8495-8501 (2005)

93. Effects of counterion valency on the damping of phonons propagating along the axial direction of liquid-crystalline DNA, Liu, Y.C., Chen, S. H., Berti, D., Baglioni, P., Alatas, A., Said, A., Alp, E., Journal of Chemical Physics 123, 214909 (2005)

94. Self-assembly of magnetic nanoparticles into complex superstructures: Spokes and spirals, Neto, C., Bonini, M., Baglioni, P., Colloids and Surfaces a-Physicochemical and Engineering Aspects 269, 96-100 (2005)

95. Surfactant aggregates hosting a photoresponsive amphiphile: structure and photoinduced conformational changes, Bonini, M., Berti, D., Di Meglio, J.M., Almgren, M., Teixeira, J., Baglioni, P., Soft Matter 1, 444-454 (2005)

96. La Sfida delle Nanoscienze, Baglioni, P., Giorgi, R., Kos, 20-24 (2005)

97. Wax crystallization and aggregation in a model crude oil, Vignati, E., Piazza, R., Visintin, R, Lapasin, R., D'Antona, P, Lockhart, T., Journal of Physics-Condensed Matter 17, S3651-S3660 (2005)

98. Scattering, Rayleigh, Piazza, R., Degiorgio, V, in Encyclopedia of Condensed Matter Physics 5, 234-242 Ed. F. Bassani, G. L. Liedl, P., Elsevier (OXFORD) (2005)

99. Biocompatible lecithin organogels: microstructure and phase equilibria, Angelico, R., Ceglie, A., Colafemmina, G., Lopez, F., Murgia, S., Olsson,U., Palazzo, G., Langmuir 21, 140-148 (2005)

100. Specific ion effects on the growth rates of Staphylococcus aureus and Pseudomonas aeruginosa, Lo Nostro, P., Ninham, B. W., Lo Nostro, A., Pesavento G., Fratoni, L., Baglioni, P., Physical Biology 2, 1-7 (2005)

101. Anion Effects on Calixarene Monolayers: A Hofmeister Series Study, Lonetti, B., Lo Nostro, P., Ninham, B. W., Baglioni, P., Langmuir 21, 2252-2249 (2005)

102. Hofmeister effects in Biology: Effect of Choline addition on the salt-induced Superactivity of HRP and its implication for salt resistance of Plants, Pinna, M. C., Bauduin P., Touraud D., Monduzzi, M., Ninham, B. W., Kunz, W., Journal of Physical Chemistry B 109, 16511-16514 (2005)

103. Enzymes for biocatalysis in non aqueous media, Salis, A., Monduzzi, M., Solinas, V. in Biocatalysis: Chemistry and Biology, 29-53 Ed. A. Tricone, Research Signpost (2005)

104. Small-Angle Neutron Scattering of Ionic Perfluoropolyether Micellar Solutions: Role of Counterions and Temperature, Gambi, C. M. C., Giordano, R., Chittofrati, A., Pieri, R., Baglioni, P., Teixeira, J., Journal of Physical Chemistry B 109, 8592-8598 (2005)

105. Commercial lipase immobilization on Accurel MP1004 porous polypropylene, Salis, A., Sanjust, E., Solinas, V., Monduzzi, M., Bicatalysis and Biotransformations 23, 381-386 (2005)

106. Nanoparticles of Calcium Hydroxide for Wood Conservation. The Deacidification of the Vasa Warship, Giorgi, R., Chelazzi, D., Baglioni, P., Langmuir 21, 10743-10748 (2005)

107. Auto-organizzazione di cellule microbiche sottoposte a dewetting su superfici polimeriche modificate: nuove prospettive nel patterning cellulare, Satriano, C., Marletta, G., Carnazza, S., Guglielmino, S., Atti del II Simposio sulle Tecnologie Avanzate. Applicazioni delle Nanotecnologie per la Difesa nei Settori Strutturale, Elettronico, Biotecnologico. Ministero della Difesa. SEGREDIFESA. Roma. 23-24 Giugno 2005 (2005)

108. Biodiesel production from triolein and short chain alcohols through biocatalysis, Salis, A., Pinna, M., Monduzzi, M., Solinas, V., Journal of Biotechnology 119, 291-299 (2005)

109. Effective long-range attraction between protein molecules in solutions studied by small angle neutron scattering, Liu, Y.C., Fratini, E., Baglioni, P., Chen, W. R., Chen, S. H., Physical Review Letters 95, 118102 (2005)

110. Inelastic X-ray scattering studies of phonons propagating along the axial direction of a DNA molecule having different counter-ion atmosphere, Liu, Y.C., Berti, D., Baglioni, P., Chen, S. H., Alatas, A., Sinn, H., Said, A., Alp, E., Journal of Physics and Chemistry of Solids 66, 2235-2245 (2005)

111. A microscopic approach to thermophoresis in colloidal suspensions, Parola, A, Piazza, R., Journal of Physics-Condensed Matter 17, S 3639-S 3643 (2005)

112. Monitoring of Pictorial Surfaces by midFTIR Reflectance Spectroscopy: Efficiency of Innovative Colloidal Cleaning Agents, Carretti, E., Dei, L., Miliani, C., Rosi, F., Spectroscopy Letters 38, 459 (2005)

113. Genetic and phenotypic divergence and fitness convergence of Pseudomonas aeruginosa strains colonizing pulmonary environment, Carnazza, S., Gioffrè, A., Guglielmino, S., J. Clin. Microbiol (2005)

114. Radioattività delle unità litostratigrafiche vulcaniche, Villa, M., R. Tocci, in Progetto Città di Viterbo Cap. 12, 116-123 Ed. U. Chioccini, S. Madonna, (2005)

115. Enhanced secretion of heterologous proteins in Kluyveromyces lactis by over-expression of the GDP-mannose pyrophosphorylase, KlPsa1p, Uccelletti, D., Staneva, D., Rufini, F., Palleschi, C., FEMS Yeast Research 5, 735-746 (2005)

116. The Golgi Ca2+-ATPase KlPmr1p Function Is Required for Oxidative Stress Response by Controlling the Expression of the Heat Shock Element HSP60 in Kluyveromyces lactis, Uccelletti, D., Farina, F., Pinton, P., Goffrini, P., Mancini, L., Talora, C., Palleschi, C., Rizzuto, R., Molecular Biology of the Cell 16, 4636-4647 (2005)

117. Antimycobacterial compounds. Optimization of the BM 212 structure, the lead compound for a new pyrrole derivative class, Biava, M., Porretta, G. C., Deidda, D., Pompei, R., Tafi, A., Manetti, F., Bioorganic & Medicinal Chemistry 13, 1221-1230 (2005)

118. Phenolic constituents from Ephedra nebrodensis, Cottiglia, F., Bonsignore, L., Casu, L., Deidda, D., Pompei, R., Casu, M., Floris, C., Natural Product Research 19, 117-123 (2005)

119. Static and dynamic nonlineariy of A/D converters, J. Halamek, Viscor, I., Kasal, M., Villa, M., Radioengineering 1, 5 (2005)

120. Short time dynamics of solvent molecules and supramolecular organization of poly (vinyl alcohol) hydrogels obtained by freeze/thaw techniques, Ricciardi, R., D'Errico, G., Auriemma, F., Ducouret, G., Tedeschi, A. M.,De Rosa, C., Laupretre, F., Lafuma, F., Macromolecules 38 (15), 6629-6639 (2005)

121. Diffusion Coefficients for the Binary System Glycerol + Water at 25 °C. A Velocity Correlation Study, D'Errico, G., Ortona, O., Capuano, F., Vitagliano, V., Journal of Chemical and Engineering Data 49 (6), 1665-1670 (2005)

122. Galphas protein C-terminal alpha-helix at the interface: does the plasma membrane play a critical role in the Galphas protein functionality?, Albrizio, S., Caliendo, G., D'Errico, G., Novellino, E., Rovero, P., D'Ursi, A.M., Journal of peptide science 11 (10), 617-626 (2005)

123. Clock signal requirement for high frequency, high dynamic range acquisition systems, Viscor, I., J. Halamek, Villa, M., Review of Scientific Instruments 76 (2005)

124. Effect of the Addition of a Nonionic Surfactant on the Complex Poly(asparagine)-Cationic Surfactant, Roscigno, P., D'Auria, G., Falcigno, L., D'Errico, G., Paduano, L., Langmuir 21 (18), 8123-8130 (2005)

125. Mixed micellar aggregates of nonionic surfactants with short hydrophobic tails, Vitagliano, V., D'Errico, G., Ortona, O., Paduano, L., in Mixed Surfactant Systems (2nd Edition) 124, 165-204 CRC Press LLC (2005)

126. Le soluzioni micellari a base di propilene carbonato:una tecnica innovativa per la pulitura di superfici pittoriche, Macherelli, A., Carretti, E., Mauro, M., Salvadori, B., Dei, L., in Gli affreschi della scuola dei battuti di Conegliano, 424-425 Ed. G. Fossaluzza, Rotary Club, Conegliano Veneto, (2005)

127. Design and optimization of electrodes for fuel cells: new opportunities for materials science and engineering, Natali-Sora, I., Nelli, P., Villa, M., Chemical Engineering Transaction 8, 141-146 (2005)

128. Metabolic response to exogenous ethanol in yeast: an in vivo NMR and mathematical modelling approach, Martini, S., Ricci, M., Bartolini, F., Bonechi, C., Braconi, D., Millucci, L., Santucci, A., Rossi, C., Biophysical Chemistry 120, 135-142 (2005)

129. Chemically and Physically Induced (Reversible) Gelation of Organic Liquids by Monomeric and Polymeric Gelators, George, M., Luo, C., Wang, C., Carretti, E., Dei, L., Weiss, R.G., Macromolecular Synmposia 110, 173 (2005)

130. NMR of Liquid Crystals and Micellar Solution – III, Monduzzi, M., in Nuclear Magnetic Resonance 34, 523-552 Ed. G.A. Webb, The royal Society of Chemistry (2005)

131. Spatial and temporal variations of the inherent and apparent optical properties in a shallow coastal lake, Bracchini, L., Dattilo, A. M., Falcucci M., Loiselle, S., Hull, V., Arena, C., Rossi, C., Journal of Photochemistry and Photobiology 80, 161-177 (2005)

132. Role of hydrostatic paradoxes towards the formation of the scientific thought of students at academic level, Fontana, F., Di Capua, R., European Journal of Physics 26, 1017-1030 (2005)

133. Tribology of nanostructured plasma sprayed coatings, Celis, J.P., Basak, A.K,, Achanta, S., Vardavoulias, M., Matteazzi, P., NanoSMat Conference (2005)

134. Tribocorrosion Behaviour of Nano-structured Coatings for Automotive Application, Basak, A.K,, Matteazzi, P., Vardavoulias, M., Celis, J.P., EUROCORR 2005 (2005)

135. Corrosion-wear behaviour of thermal sprayed nanostructured FeCu/WC-Co coatings, Basak, A.K,, Matteazzi, P., Vardavoulias, M., Celis, J. P., Wear (2005)

136. New Possibilities by direct laser micro sintering for micro system technology components using nanophased powders, Becker, H., Ostendorf, A., Stippler, P., Matteazzi, P., AMST (2005)

137. Direct laser micro sintering using nanophased microscale powders, Becker, H., Ostendorf, A., Stippler, P., Matteazzi, P., Euro-u.Rapid 2005 (2005)

138. Technology improvements for microscale laser sintering, Becker, H., Ostendorf, A., Stippler, P., Matteazzi, P., OPTO-Ireland 2005 (2005)

139. Mechanochemically assisted solid-state synthesis of lithium gallates (LiGa5O8 and LiGaO2), Berbenni, V., Milanese, C., Bruni, G., Marini, A., Materials Chemistry and Physics 91-1, 180-184 (2005)

140. A new method to test the effectiveness of the teaching/learning process in basic courses at academic level, Fontana, F., European Journal of Physics 26, 331-339 (2005)

141. Structural Organization of Poly(vinyl alcohol) Hydrogels Obtained by Freezing and Thawing Techniques: A SANS Study, Ricciardi, R., Mangiapia, G., Lo Celso, F., Paduano, L., Triolo, R., Auriemma, F., De Rosa, C., Laupretre, F., Chemistry of Materials 17 (5), 1183-1189 (2005)

142. Surface Free Energy and Cell Adhesion onto Irradiated Polymer Surfaces, Satriano, C., Marletta, G., Carnazza, S., Guglielmino, S., (2005)

143. Transport and Structural Properties of Pure and Cr Doped Li3VO4, Massarotti, V., Capsoni, D., Bini, M., Mustarelli, P., Chiodelli, G., Azzoni, C. B., Galinetto, P., Mozzati, M. C., Journal of Physical Chemistry B 109, 14845-14851 (2005)

144. Characterization of a tethering system for biosensor applications, Blasi L., Pompa P.P., Pisignano D., Palazzo, G., Mallardi, A., Maruccio G., Maffei A., Ciccarella G., Vasapollo G., Calabi F., Cingolani R., Rinaldi R., in Nanotech 2005 1 Nano Science and Technology Institute (2005)

145. Lectins: tools for the molecular understanding of the glycocode, Ambrosi, M., Cameron, N.R., Davis. B. G., Organic & Biomolecular Chemistry 3, 1593-1608 (2005)

146. Investigation of the interaction between peanut agglutinin and synthetic glycopolymeric multivalent ligands, Ambrosi, M., Cameron, N.R., Davis. B. G., Stolnik-Trenkic, S., Organic & Biomolecular Chemistry 3, 1476-1480 (2005)

147. Tyrosinase activity and hemocyanin in the hemolymph of the slipper lobster Scyllarides latus, Olianas, A., Sanjust, E., Pellegrini, M., Rescigno, A., Journal of Comparative Physiology B 175, 405-411 (2005)

148. Nanostructured fluids based on propylene carbonate/water mixtures, Palazzo, G., Fiorentino, D., Colafemmina, G., Ceglie, A., Carretti, E., Dei, L., Baglioni, P., Langmuir 21 (2005)

149. Synthesis and characterization of Ce0.8Gd0.2O2-y polycrystalline and thin film materials, Chiodelli, G., Malavasi, L., Massarotti, V., Mustarelli, P., Quartarone, E., Solid State Ionics 176, 1505-1512 (2005)

150. Internal Dynamics and Protein-Matrix Coupling in Trehalose Coated Proteins, Cordone, L., Cottone, G., Giuffrida, S., Palazzo, G., Venturoli, G., Viappiani, C., Biochimica et Biophysica Acta-Proteins and Proteomics 1749, 252-281 (2005)

151. Supramolecular complexes of conjugated polyelectrolytes with poly(ethyleneoxide): multifunctional luminescent semiconductors exhibiting electronic and ionic transport, Sardone, L., Marletta, G., (2005)

152. Multiple scattering X-ray absorption studies of Zn 2+ binding sites in bacterial photosynthetic reaction centers, Giachini, L., Francia, F., Mallardi, A., Palazzo, G., Carpenè, E., Venturoli, G., Boscherini, F., Biophysical Journal 88, 2038-2046 (2005)

153. Dynamic scanning force microscopy of molecular surfaces, Pignataro, B., Marletta, G., Nanotechnology, 47-68 (2005)

154. Modelling the components of the vertical attenuation of ultraviolet radiation in a shallow lake ecosystem, Bracchini, L., Loiselle, S., Mazzuoli, S., Dattilo, A. M., Rossi, C., Ecological Modelling 186, 43-54 (2005)

155. Surface Design by Proteins on Polymer supports, Zhavnerko, H., Giamblanco, N., Seminara, G., Marletta, G., Physics, Chemistry and Application of Nanostructures, Eds. V.Borisenko, G.A.Gaponenko, V.S.Gurin; World Scientific Publisher, Singapore, 523-526 (2005)

156. The effect of irradiation modification and RGD sequence adsorption on the response of human osteoblasts to polycaprolactone, Marletta, G., Satriano, C., Pagani, G. A., Biomaterials 26, 4793–4804 (2005)

157. Analisi Ottica e Idrobiologia del Lago di Montepulciano, Mazzuoli, S., Focardi, S., Bracchini, L., Loiselle, S., Dattilo, A. M., Rossi, C., Etrurianatura 2 (2005)

158. ESR as a Valid Tool for the Investigation of the Dynamics of EPC and EPC/CHOL Liposomes Containing a Carboranylnucleoside, Rossi, S., Shimazi, R., Martini, G., Biochimica et Biophysica Acta-Bioenergetics in press (2005)

159. Bioengineering of a Cellulosic Fabric for Insecticide Delivery viaGrafted Cyclodextrin, Romi, R., Lo Nostro, P., Bocci, E., Ridi, F., Baglioni, P., Biotechnology Progress 21, 1724-1730 (2005)

160. La Scienza della Conservazione, Baglioni, P., Carretti, E., Dei, L., Ferroni, E., Giorgi, R., Darwin 5, 26 (2005)

161. Soft matter and art conservation: rheoreversible gels and beyond, Carretti, E., Dei, L., Weiss, R.G., Soft Matter 1, 17 (2005)

162. Hydration process of cement in the presence of a cellulosic additive. A calorimetric investigation, Ridi, F., Fratini, E., Mannelli, F., Baglioni, P., Journal of Physical Chemistry B 109, 14727-14734

163. Physical and Chemical Adsorption of Mucor javanicus Lipase on SBA-15

Mesoporous Silica. Synthesis, Structural Characterization, and Activity Performance, Salis, A., Meloni, D., Casula, M.F., Monduzzi, M., Solinas, V., Dumitriu, E., Langmuir 21, 5511-5516 (2005)

164. Report on oceanographic and geophysical investigation during cruise MFSTEP2 (April 2005) with R/V Urania, Northern Thyrrenian and Ligurian Sea, Bracchini, L., Tognazzi, A., ISMAR Bologna TECHNICAL REPORT 96, 1-40 (2005)

165. Adsorption of a cell-adhesive oligopeptide on polymer surfaces irradiated by ion beams, Satriano, C., Manso, M., Gambino, G. L., Rossi, F., Marletta, G., Bio-Medical Materials and Engineering 15, 87-89 (2005)

166. Fast exopolysaccharide secretion of Pseudomonas aeruginosa and polar polymers surfaces, Satriano, C., Guglielmino, S., Carnazza, S., Marletta, G., Journal of Colloid and Interface Science (2005)

167. Physicochemical Characterization of Lipoplexes and Their Transfection Efficiency as DNA Carriers, Salvati, A., Ciani, L., Masi, A., Arcangeli, A., Martini, G., Biochimica et Biophysica Acta-Biomembranes in press (2005)

168. Microemulsions and Micellar Solutions for Cleaning fresco Surfaces, Carretti, E., Salvadori, B., Baglioni, P., Dei, L., Studies in Conservation 50, 1 (2005)

169. Hofmeister Series: The Hydrolytic Activity of Aspergillus niger Lipase Depends on Specific Anion Effects, Pinna, M. C., Salis, A., Monduzzi, M., Ninham, B. W., Journal of Physical Chemistry B 109, 5406-5408. (2005)

170. Phase Separation in Binary Mixtures Containing LinearPerfluoroalkanes, Lo Nostro, P., Scalise, L., Baglioni, P., Journal of Chemical and Engineering Data 50, 1148-1152 (2005)

171. Reply to "Comments on 'Hofmeister Series: Hydrolytic Activity of Aspergillus niger Lipase Depends on Specific Anion Effects'", Pinna, M. C., Salis, A., Monduzzi, M., Ninham, B. W., Journal of Physical Chemistry B 109, 14752-14754 (2005)

172. Effect of 1-butanol on the microstructure of lecithin/water/tripalmitin system, Caboi, F., Lazzari, P., Pani, L., Monduzzi, M., Chemistry and Physics of Lipids 135, 147-156 (2005)

173. The influence of superplasticizers on the first steps of tricalcium silicate hydration studied by NMR techniques, Pirazzoli, I., Alesiani, M., Capuani, Silvia, Maraviglia, B., Giorgi, R., Ridi, F., Baglioni, P., Magnetic Resonance Imaging 23, 277-284 (2005)

174. Time dependent absorption evidence of Phenylurea derivatives herbicides on biomembrane models. A DSC study, Castelli, F., Envir. Chem 2, 63-70 (2005)

175. Examining the spatial distribution of the light environment in a neotropical shallow lake, Loiselle, S., Bracchini, L., Cozar, A., Dattilo, A. M., Rossi, C., Hydrobiologia, 181-191 (2005)

176. Spatial and temporal characterisations of the degradation of dissolved humic substances in freshwater lake, Mazzuoli, S., Focardi, S., Bracchini, L., Falcucci M., Loiselle, S., Rossi, C., Ecological Modelling 186, 55-62 (2005)

177. Nuove soluzioni per il recupero delle acque di vegetazione delle olive, Ciafardini, G., Zullo B.A., L'Informatore Agrario 28, 47-49 (2005)

178. Penetration of solar radiation into waters of Messina Strait (Italy), Dattilo, A. M., Decembrini, F., Bracchini, L., Focardi, S., Mazzuoli, S., Rossi, C., Annali di chimica 95, 177-184 (2005)

179. Spectroscopic and thermal investigations on compost improved by iron salt addition, Provenzano, M. R., Albuzio, A., D'Orazio, V., Journal of Agricultural and Food Chemistry 53, 374-382 (2005)

180. Effect of glycerol on micelle formation by ionic and nonionic surfactants at 25 °C, D'Errico, G., Ciccarelli, D., Ortona, O., Journal of Colloid and Interface Science 286 (2), 747-754 (2005)

181. The estimate of the effects of UV radiation on mortality of Artemia Franciscana in naupliar and adult stages, Dattilo, A. M., Bracchini, L., Loiselle, S., Carlini, L., Rossi, C., International Journal of Biometeorology 49, 388-395 (2005)

182. Characterization of indomethacin loaded lipid nanoparticles by differential scanning calorimetry, Castelli, F., Sarpietro, M.G., Int. J. Pharm 304, 231-238 (2005)

183. Evaluation of the interaction and drug release from alpha,beta-polyaspartamide derivatives to a biomembrane model, Castelli, F., Drug Delivery 12, 357-366 (2005)

184. Synthesis and biological activity of new iodoacetamide derivetives on mutants of squalene-hopene cylase, Castelli, F., Lipids 40, 729-735 (2005)

185. Influence of cardiolipin on the functionality of the QA-site of the photosynthetic bacterial reaction center, Giustini, M., Castelli, F., Husu I., Giomini, M., Mallardi, A., Palazzo, G., Journal of Physical Chemistry B 109, 21187-21196 (2005)

186. Study on the mechanisms of the antibacterial action of three monoterpenes, Castelli, F., Sarpietro, M.G., Antimicrobial Agents and Chemotherapy 49, 2474-2478 (2005)

187. I microrganismi dell'olio di oliva ne condizionano qualità e conservazione, Ciafardini, G., Zullo B.A., D'Amico A., L'Informatore Agrario 30, 41-46 (2005)

188. Remote sensing imagery analysis of the lacustrine system of Iberá wetland (Argentina) kmm, Cozar, A., Garcia, S.A., Loiselle, S., Galvez, J. A., Bracchini, L., Cognetta, A., Ecological Modelling 186, 29-42 (2005)

189. A mechanistic study of the permeation kinetics through biomembrane models: Gemcitabine-Phospholipid bilayers interaction, Castelli, F., J. Coll. Interf. Science 285, 110-117 (2005)

190. Sediment resuspension by wind in a shallow lake of Esteros del Iberá (Argentina): a model based on turbidimetry, Cozar, A., Galvez, J. A., Hull, V., Garcia, S.A., Loiselle, S., Ecological Modelling 186, 63-76 (2005)

191. Mitochondrial alterations and autofluorescent conversion of Candida albicans induced by histatins, Diaz, G., Polonelli, L., Conti, S., Messana, I., Cabras, T., Putzolu, M., Falchi, A. M., Fadda, M. E., Cosentino, S., Isola, R., Microscopy Research and Technique 66, 219-228 (2005)

192. Thermal decomposition of gallium nitrate hydrate
 Ga(NO3)3*xH2O, Berbenni, V., Milanese, C., Bruni, G., Marini, A., Journal of Thermal Analysis and Calorimetry 82, 401-407 (2005)

193. On the presence of Pseudo-Nitzschia calliantha Lundholm, Moestrup et Hasle and P. delicatissima (CLEVE) heiden in the southern adrietic sea (Mediterranean Sea, ITALY), Caroppo, C., Congestri, R., Bracchini, L., Albertano, P., Journal of Plankton Research 27, 763-774 (2005)

194. Adhesion Properties on nanometric scale of Silicon Oxide and Silicon Nitride Surfaces modified by 1-Octadecene, Pignataro, B., Renna, L., Marletta, G., Surface and Interface Analysis 33, 54-58 (2005)

195. Laccase overproduction in Pleurotus sajor-caju induced by ferulic acid, Sanjust, E., Rescigno, A., Sollai, F., The Italian Journal of Biochenmistry 54, 103 (2005)

196. Electronic structure of clusters (LiBC)n : n = 1, 2 and 4, Forte, G., Grassi, A., Physics Letters A 338, 303-308 (2005)

197. Bond-order correlation energies for small Si-containing molecules compared with ab initio results from low-order Moller-Plesset perturbation theory, Grassi, A., Forte, G., Mol. Phys. (2005)

198. Morphological anomalies in pollen tubes of Actinidia Deliciosa (kiwi) exposed to 50 Hz magnetic field, Dattilo, A. M., Bracchini, L., Loiselle, S., Ovidi, E., Tiezzi, A., Rossi, C., Bioelectromagnetics 26 (2), 153-156 (2005)

199. Neotropical Wetlands: New instruments in ecosystem management. Loiselle, S., Bastianoni, S., Bracchini, L., Rossi, C., Wetlands Ecology and Management 12, 587-596 (2004)

200. NMR of Liquid Crystals and Micellar Solutions-II. Monduzzi, M., in Nuclear Magnetic Resonance 33, 531-561 Ed. G.A. Webb, (2004)

201. Presence of microorganisms in flavoured extra virgin olive oil. Ciafardini, G., Zullo B.A., Pesca G., Annals of Microbiology 54, 33-40 (2004)

202. Wild-Type Strain of Saccharomyces cerevisiae. Martini, S., Ricci, M., Bonechi, C., Trabalzini, L., Santucci, A., Rossi, C., Febs Letters 564, 63-68 (2004)

203. Analysis of the p-tert-Butylcalix[4]arene derivative (Dc3)-Acetonitrile host-guest

complexing behaviour by Nuclear Magnetic Resonance (NMR) Spectroscopy and Computation Methods. Bonechi, C., Lonetti, B., Arduini, A, Baglioni, P., Donati, A., Martini, S., Pochini, A., Rossi, C., Journal of Physical Chemistry B 108, 7603-7610 (2004)

204. Self-Organization and Emergent Models in Bacterial Adhesion on Engineered Polymer Surfaces. Marletta, G., Carnazza, S., Guglielmino, S., Proceedings of the Int.Symp. on Circuits and Systems ISCAS 2004 4, 689-693 (2004)

205. Influence of functionalization on interaction and drug release from alpha,beta-Polyaspartylhydrazide derivatives to a biomembrane model. Evaluation by Differential Scanning Calorimetry technique. Castelli, F., Thermochimica Acta 423, 19-28 (2004)

206. Occurrence and characterization of yeasts isolated from artisanal Fiore Sardo cheese. Fadda, M. E., Massa, V., Pisano, B., Deplano, M., Cosentino, S. International Journal of Food Microbiology 95, 51-59 (2004)

207. Temperature and Pressure Dependence of Quercetin-3-O-Palmitate Interaction with a Model Phospholipid Membrane: Film Balance and Scanning Probe Microscopy Study. Sardone, L., Pignataro, B., Castelli, F., Sarpietro, M.G., Marletta, G., Journal of Colloid and Interface Science 271, 329-335 (2004)

208. Molecular Modeling of Interactions between Lysine and Quartz surface. Gambino, G. L., Grassi, A., Marletta, G., Journal of Physical Chemistry B 108, 2600-2607 (2004)

209. Irradiation-controlled Adsorption and Organization of Biomolecules on Surfaces: From the Nanometric to Mesoscopic Level. Marletta, G., Satriano, C., in Frontiers in Multifunctional Integrated Nanosystems, 71-94 Ed. E.Buzaneva and P.Scharff, Kluwer Academic Publisher (The Netherlands) (2004)

210. Langmuir-Schaefer films of new calix[4]pyrrole-based macrocycle exhibiting induced chirality upon differentiated binding with chiral alcohol vapours. Sortino, S., Petralia, S., Pignataro, B., Marletta, G., Conoci, S., Valli, L., in Proceedings of the 8th Italian Conference on Sensors and Microsystems, 103-108 (2004)

211. Pericyte adhesion and growth onto Polyhydroxymethylsiloxane Surfaces Nanostructured by Plasma Treatment and Ion Irradiation. Satriano, C., Marletta, G., Microvascular Research 68, 209-220 (2004)

212. Growth of ordered poly(ethylene-oxide) thin films from solutions: an SFM study. Sardone, L., Marletta, G., Synthesis and Reactivity in Inorganic and Metal-Organic Chemistry 147, 123-125 (2004)

213. Note. Xylose Production from Durum Wheat Bran: Enzymic versus Chemical Methods. Sanjust, E., Salis, A., Rescigno, A., Curreli, N., Rinaldi, A., Food Science and Technology International 10, 11-14 (2004)

214. Physicochemical Characterization of Acrylic Polymeric Resins coating Porous Materials of Artistic Interest. Carretti, E., Dei, L., Progress in Organic Coatings 49,

282 (2004)

215. Novel mannitol based non-ionic surfactants from biocatalysis - Part two: improved synthesis. Pinna, M. C., Salis, A., Monduzzi, M., Journal of Molecular Catalysis B: Enzymatic 27, 233-236 (2004)

216. FTIR spectroscopy to monitor selective cleaning on wall painting surfaces. Carretti, E., Macherelli, A., Mauro, M., Miliani, C., Rosi, F., Salvadori, B., Dei, L., in Proceedings of the VI IRUG congress, 239-243 (2004)

217. Rheo-reversible Polymeric Organogels: The Art of Science for Art Conservation. Carretti, E., Macherelli, A., Dei, L., Weiss, R.G., Langmuir 20, 8414 (2004)

218. Influence of cellulosic additives on tricalcium silicate hydration: nuclear magnetic resonance relaxation time analysis. Alesiani, M., Capuani, Silvia, Giorgi, R., Maraviglia, B., Ridi, F., Baglioni, P., Journal of Physical Chemistry B 108, 4869-4874 (2004)

219. Solution structure of folic acid. Molecular Mechanics and NMR investigation. Bonechi, C., Donati, A., Lampariello, R., Martini, S., Picchi, M. P., Ricci, M., Rossi, C., Spectrochimica Acta A 60, 1411-1419 (2004)

220. Solution Structure of Rifaximin and its Synthetic Derivative Rifaximin OR determined by Experimental NMR and Theoretical Simulation Methods. Martini, S., Bonechi, C., Corbini, G., Donati, A., Rossi, C., Bioorganic & Medicinal Chemistry 12, 2163-2172 (2004)

221. Interference of Some Tryptophan Metabolites in the Formation of Melanin In Vitro. Soddu, G., Sanjust, E., Murgia, S., Rescigno, A., Pigment Cell Research 17, 135-141 (2004)

222. Mixed micelles of homologous of Perfluopolyether Anionic Surfactant in Water. Mele, S., Murgia, S., Monduzzi, M., Journal of Fluorine Chemistry 125, 261-269 (2004)

223. Degradation of juglone by Pleurotus sajor-caju. Curreli, N., Rescigno, A., Rinaldi, A., Pisu, B., Sollai, F., Sanjust, E., Mycological Research 108 (2004)

224. Biocompatible Lipidic Formulations: Phase Behavior and Microstructure. Mele, S., Murgia, S., Caboi, F., Monduzzi, M., Langmuir 20, 5241-5246 (2004)

225. From Monolayers to Bilayers: Mesostructural Evolution in DDAB/Water/Tetradecane Microemulsions. Olla, M., Semmler, A., Monduzzi, M., Hyde, S., Journal of Physical Chemistry B 108, 12833-12841 (2004)

226. Hofmeister effects in cationic microemulsions. Murgia, S., Monduzzi, M., Ninham, B. W., Current Opinion in Colloid & Interface Science 9, 102-106 (2004)

227. Phase Behavior of Homologous Perfluoropolyether Surfactants: NMR, SAXS, and Optical Microscopy. Mele, S., Ninham, B. W., Monduzzi, M., Journal of Physical

Chemistry B 108, 17751-17759 (2004)

228. Fractionation of Sheep Milk Fat Via Supercritical Carbon Dioxide. Spano, V., Salis, A., Mele, S., Madau, P., Monduzzi, M., Food Science and Technology International 10, 421-425 (2004)

229. Enzymatic activity of lipase entrapped in CTAB/water/pentanol/hexane reverse micelles: a functional and microstructural inestigation. Lopez, F., Palazzo, G., Colafemmina, G., Cinelli, G., Ambrosone, L., Ceglie, A., Progress in Colloid & Polymer Science 123, 174-177 (2004)

230. Inhibition Effects of Ethanol on the Kinetics of Glucose Metabolism by S. Cerevisiae: NMR and Modelling Study. Ricci, M., Martini, S., Bonechi, C., Santucci, A., Trabalzini, L., Rossi, C., Chemical Physics Letters 387, 377-382 (2004)

231. Metastability and supersaturation limit for lysozyme crystallization. Carpineti, M, Piazza, R., Physical Chemistry Chemical Physics 6, 1506-1511 (2004)

232. Transfer of selected yeasts to oil through olive inoculation. Ciafardini, G., Cioccia G:, Pesca G., Zullo B.A., Italian Journal of Food Science 16, 105-111 (2004)

233. Allergy and tumour outcome after primary cancer therapy. Pompei, R., Lampis, G., Ingianni, A., Nonnis, D., Ionta, M. T., Massidda, B., International Archives of Allergy and Immunology 133, 174-178 (2004)

234. Alterations of O-glycosylation, cell wall and mitochondrial metabolism in Kluyveromyces lactis cells defective in KlPmr1p, the Golgi Ca2+-ATPase. Farina, F., Uccelletti, D., Goffrini, P., Butow, R.A., Abeijon, C., Palleschi, C., Biochemical and Biophysical Research Communications 318, 1031-1038 (2004)

235. Improved production of heterologous proteins by a glucose repression defective mutant of Kluyveromyces lactis. Donnini, C., Farina, F., Neglia, B., Compagno, M.C., Uccelletti, D., Goffrini, P., Palleschi, C., Applied and Environmental Microbiology 70, 2632-2638 (2004)

236. KlSEC53 is an essential Kluyveromyces lactis gene and is homologous with the SEC53 gene of Saccharomyces cerevisiae. Staneva, D., Uccelletti, D., Farina, F., Venkov. P., Palleschi, C., Yeast 21, 41-51 (2004)

237. Interaction between pentaethylene glycol n-octyl ether and low-molecular-weight poly(acrylic acid). D'Errico, G., Ciccarelli, D., Ortona, O., Paduano, L., Sartorio, R., Journal of Colloid and Interface Science 270 (2), 490-495 (2004)

238. Thermal lensing Measurement of particle thermophoresis in aqueous dispersions. Rusconi, Isa, L., Piazza, R., Journal of the Optical Society of America B 21, 605-616 (2004)

239. Mixed micelles composed of peptides and gadolinium complexes as tumor-specific contrast agents in MRI: a SANS study. Mangiapia, G., Accardo, A., Lo Celso, F., Tesauro, D., Morelli, G., Radulescu, A., Paduano, L., Journal of Physical Chemistry B

108 (45), 17611-17617 (2004)

240. Thermophoresis as a probe of particle-solvent interactions: the case of protein solutions. Piazza, R., Triulzi, B, Iacopini, S., Physical Chemistry Chemical Physics 6, 1616-1622 (2004)

241. Protein interactions and association: an open challenge for colloid science. Piazza, R., Current Opinion in Colloid & Interface Science 8, 515-522 (2004)

242. Particle thermophoresis in liquids. Parola, A, Piazza, R., European Physical Journal E: Soft Matter 15, 255-263 (2004)

243. Thermal forces in simple and complex fluids. Piazza, R., Giglio, M., European Physical Journal E: Soft Matter 15, 233-244 (2004)

244. New •-(N)-heterocyclichydrazones: evaluation of anticancer, anti-HIV and antimicrobial activity. Savini, L., Chiasserini, L., Travagli, V., Pellerano, C., Novellino, E., Cosentino, S., Pisano, B., Eur. J. Med, Chem. 39, 113-122 (2004)

245. Laccase induction by 4-hydroxybenzenesulfonic acid in Pleurotus sajor-caju. Sanjust, E., Corongiu, C., Rescigno, A., Sollai, F., The Italian Journal of Biochenmistry 53, 177 (2004)

246. KlPMR1 inactivation and calcium addition enhance secretion of non-hyperglycosylated heterologous proteins in Kluyveromyces lactis. Uccelletti, D., Mancini, P., Farina, F., Palleschi, C., Journal of Biotechnology 109, 93-101 (2004)

247. The spatial distribution of the optical properties in the UV and Visible in an aquatic ecosystem. Bracchini, L., Loiselle, S., Dattilo, A. M., Mazzuoli, S., Cozar, A., Rossi,C., Photochem. Photobiol. 80 (1), 139-149 (2004)

248. Genotypic and technological characterization of enterococci isolated from artisanal Fiore Sardo cheese. Cosentino, S., Pisano, B., Corda, A., Fadda, M. E., Piras, C., Journal of Dairy Research 71, 444-450 (2004)

249. PolyAT chemical denaturation in w/o microemulsion. Airoldi, M., Boicelli, C. A., Cadoni, F., Gennaro, G., Giomini, M., Giuliani, A. M., Giustini, M., Physical Chemistry Chemical Physics, 1453-1457 (2004)

250. Titration of poly(dA-dT) center dot poly(dA-dT) in solution at variable NaCl concentration. Airoldi, M., Boicelli, C. A., Cadoni, F., Gennaro, G., Giomini, M., Giuliani, A. M., Giustini, M., Biopolymers 75, 118-127 (2004)

251. Stretched chemical bonds in Si6H6: a transition from ring currents to localized π-electrons? Grassi, A., Journal of Chemical Physics 297, 13-19 (2004)

252. Dissociation energies in polyatomic molecules and metal clusters. Grassi, A., Forte, G., Recent Research Developments in Molecular Physics, Publisher: Transworld Research Network, 1-8 (2004)

253. Effect of glycerol on micelle formation by ionic and nonionic surfactants at 25 degrees C. D'Errico, G., Ciccarelli, D., Ortona, O., Journal of Colloid and Interface Science 286, 747-754 (2004)

254. Characterization of the Ugandan inshore waters of Lake Victoria based on temperature-conductivity diagrams. Cozar, A., Bracchini, L., Dattilo, A. M., Loiselle, S., Azza, N., Water Resources Research 40 (2004)

255. Using Satellite data for a territorial indicator in Tuscany. Focardi, S., Loiselle, S., Bracchini, L., Dattilo, A. M., Rossi, C., Sustainable City, 143 (2004)

256. Analysis of extinction in ultraviolet and visible spectra of water bodies of the Paraguay and Brazil wetlands. Bracchini, L., Cozar, A., Dattilo, A. M., Falcucci M., Gonzalez Vara y Rodriguez, A., Loiselle, S., Hull, V., Chemosphere 57, 1245-1255 (2004)

257. Microbial Synthesis of Poly(3-hydroxyalkanoates) by Pseudomonas aeruginosa from Fatty Acids: Identification of Higher Monomer Units and Structural Characterization. Barbuzzi, T., Giuffrida, M., Impallomeni, G., Carnazza, S.; Ferreri, A.; Guglielmino, S. P. P.; Ballistreri, A. Biomacromolecules 5, 2469-2478 (2004)

258. Strengthening in a Copper Based Nanocomposite. Marques, M. T., Correia, J. B., Matteazzi, P., Materials Science Forum 445-456, 244-248 (2004)

259. Temperature and concentration effects on supramolecular aggregation and phase behavior for poly(propylene oxide)-b-poly(ethylene oxide)- b-poly(propylene oxide) copolymers of different composition in aqueous mixtures, 1. D'Errico, G., Paduano, L., Khan, A., Journal of Colloid and Interface Science 279 (2), 379-390 (2004)

260. Physicochemical Properties of Mixed Micellar Aggregates Containing CCK Peptides and Gd Complexes Designed as Tumor-Specific Contrast Agents in MRI. Accardo, A., Tesauro, D., Roscigno, P., Gianolio, E., Paduano, L., D'Errico, G., Pedone, C., Morelli, G., Journal of American Chemical Society 126 (10), 3097-3107 (2004)

261. Multicomponent Diffusion in Crowded Solutions. 2. Mutual Diffusion in the Ternary System Tetra(ethylene glycol)-NaCl-Water. Vergara, A., Annunziata, O., Paduano, L., Miller, D. G., Albright, J. G., Sartorio, R., Journal of Physical Chemistry B 108 (8), 2764-2772 (2004)

262. Testing the Spectral Variation Hypothesis by using satellite multispectral images. Rocchini, D., Chiarucci, A., Loiselle, S., Acta Oecologica 26, 117-120 (2004)

263. Spontaneous emulsification of detergent solubilized Reaction Center: protein conformational changes precede droplets growth. Palazzo, G., Mallardi, A., Francia, F., Dezi, M., Venturoli, G., Pierno, M., Vignati, E., Piazza, R., Physical Chemistry Chemical Physics 6, 1439-1445 (2004)

264. Specific anion effects on the aggregation properties of anionic nucleolipids. Fortini, M., Berti, D., Baglioni, P., Ninham, B. W., Current Opinion in Colloid & Interface Science 9, 168-172 (2004)

265. Structural Investigation on the Poly(vinylpyrrolidone)-Water System in the Presence of Sodium Decyl Sulfate and Sodium Decanesulfonate: A Small Angle Neutron Scattering Study. Mangiapia, G., Berti, D., Baglioni, P., Teixeira, J., Paduano, L., Journal of Physical Chemistry B 108 (28), 9772-9779 (2004)

266. Association of sugar-based carboranes with cationic liposomes: an electron spin resonance and light scattering study. Morandi, S., Ristori, S., Berti, D., Panza, L., Becciolini, A., Martini, G., Biochimica et Biophysica Acta-Biomembranes 1664, 53-63 (2004)

267. Characterization of Carriers for Drug Delivery in Boron Neutron Capture Therapy (BNCT): ESR Study of Nitroxide-Containing Liposomes. Martini, G., Morandi, S., Rossi, S., Ristori, S., Progress in Colloid & Polymer Science 126, 146-150 (2004)

268. On the Carrier Properties of Perfluoropolyether-Betaine Mixed Vesicles: the Contribution of Electron Spin Resonance Spectroscopy. Martini, G., Balzi, M., Becciolini, A., Ristori, S., Rossi, S., Journal of Fluorine Chemistry 125, 253-260 (2004)

269. The role of the cosurfactant in the CTAB/water/n-pentanol/n-hexane system: Pentanol effect on the phase equilibria and mesophases structure. Palazzo, G., Cardone, L., Colafemmina, G., Angelico, R., Ceglie, A., Giustini, M., Physical Chemistry Chemical Physics 6, 1423-1429 (2004)

270. Borophenylalanine Insertion in Cationic Liposomes for Boron Neutron Capture Therapy. Martini, S., Ristori, S., Pucci, A., Bonechi, C., Donati, A., Becciolini, A.,Martini, G., Rossi, C., Biophysical Chemistry 111, 27-34 (2004)

271. Size Polydispersity Determination in Emulsion Systems by Free Diffusion Measurements via PFG-NMR. Ambrosone, L., Murgia, S., Cinelli, G., Monduzzi, M., Ceglie, A., Journal of Physical Chemistry B 108, 18472-18478 (2004)

272. Small Angle Polarized Neutrons (SANSPOL) Investigation of Surfactant Free Magnetic Fluid of Uncoated and Silica-Coated Cobalt-Ferrite Nanoparticles. Bonini, M., Wiedenmann, A., Baglioni, P., Journal of Physical Chemistry B 108, 14901-14906 (2004)

273. Synthesis and characterization of surfactant and silica-coated cobalt ferrite nanoparticles. Bonini, M., Wiedenmann, A., Baglioni, P., Physica A 339, 86-91 (2004)

274. Polyphenol oxidase expression in potato (Solanum tuberosum) tubers inhibited to sprouting by treatment with iodine atmosphere. Eolini, F., Hochkoeppler, A., Credi, A., Gonzalez Vara y Rodriguez, A., Poggi, V., Phytochemistry 65, 2181-2187 (2004)

275. Spectroscopic and Interfacial Properties of Myoglobin/Surfactant Complexes. Tofani, L., Feis, A., Snoke, R.E., Berti, D., Baglioni, P., Smulevich, G., Biophysical Journal, 1186-1195 (2004)

276. Fluorescence behaviour of Zn and NI complexes of humic acids from different origin. Provenzano, M. R., D'Orazio, V., Jerzykiewicz, M., Senesi, N., Chemosphere 55, 885-892 (2004)

277. DOTAP/DOPE and DcChol/DOPE Lipoplexes for Gene Delivery: Zeta Potential Measurements and Electron Spin Resonance Spectra. Ciani, L., Ristori, S., Salvati, A., Calamai, L., Martini, G., Biochimica et Biophysica Acta-Biomembranes 111, 70-79 (2004)

278. Electron transfer kinetics photosinthetic reaction centers enbedded in polyvinyl alcohol films. Francia, F., Giachini, L., Palazzo, G., Mallardi, A., Boscherini, F., Venturoli, G., Bioelectrochemistry 63, 73-77 (2004)

279. Probing light-induced conformational transitions in bacterial photosynthetic reaction center embedded in trehalose amorphous matrices. Francia, F., Palazzo, G., Mallardi, A., Cordone, L., Venturoli, G., Biochimica et Biophysica Acta-Bioenergetics 1658, 50-57 (2004)

280. Phase Behaviour of the lecithin/water/isooctane and lecithin/water/decane systems. Angelico, R., Ceglie, A., Colafemmina, G., Delfine, F., Olsson, U., Palazzo, G., Langmuir 20, 619. 631 (2004)

281. Does the Schulman's titration of microemulsions really provide meaningful parameters? Giustini, M., Murgia, S., Palazzo, G., Langmuir 20, 7381-7384 (2004)

282. Light-harvesting complex 1 stabilizes P+QB- charge separation in reaction centers of Rhodobacter sphaeroides. Francia, F., Dezi, M., Rebecchi, A., Mallardi, A., Palazzo, G., Melandri, B.A., Venturoli, G., Biochemistry 43, 14199-14210 (2004)

283. Viscoelastic and small angle neutron scattering studies of concentrated protein solutions. Lonetti, B., Fratini, E., Chen, S. H., Baglioni, P., Physical Chemistry Chemical Physics 6, 1388-1395 (2004)

284. Aqueous Polyacrylic Acid Based Gels: Physicochemical Properties and Applications in Cultural Heritage Conservation. Carretti, E., Dei, L., Baglioni, P., Progress in Colloid and Surface Science 123, 280 (2004)

285. Quasielastic and inelastic neutron scattering on hydrated calcium silicate pastes. Faraone, A., Fratini, E., Baglioni, P., Chen, S. H., Journal of Chemical Physics 121, 3212-3220 (2004)

286. Structural arrest in concentrated cytochrome C solutions: the effect of pH and salts. Baglioni, P., Fratini, E., Lonetti, B., Chen, S. H., Journal of Physics-Condensed Matter 16, S5003-S5022 (2004)

287. Role of the cosurfactant in water-in-oil microemulsion: Interfacial properties tune the enzymatic activity of lipase. Lopez, F., Cinelli, G., Ambrosone, L., Colafemmina, G., Ceglie, A., Palazzo, G., Colloids and Surfaces a-Physicochemical and Engineering Aspects 237, 49-59 (2004)

288. Gelatin microemulsion-based gels with the cationic surfactant etyltrimethylammonium bromide: a self-diffusion and conductivity study. Lopez, F., Venditti, F., Ambrosone, L., Colafemmina, G., Ceglie, A., Palazzo, G., Langmuir 20, 9449-9452 (2004)

289. Gelation in cytochrome C concentrated solutions near the isoelectric point: the anion role. Baglioni, P., Fratini, E., Lonetti, B., Chen, S. H., Current Opinion in Colloid & Interface Science 9, 38-42 (2004)

290. Langmuir monolayers of calix[8]arene derivatives: complexation of alkaline earth ions at the air/water interface. Lonetti, B., Fratini, E., Casnati, A., Baglioni, P., Colloids and Surfaces a-Physicochemical and Engineering Aspects 248, 135-143 (2004)

291. The present state of affairs with Hofmeister effects. Kunz, W., Lo Nostro, P., Ninham, B. W., Current Opinion in Colloid & Interface Science 9, 1-18 (2004)

292. New remarks on the high-polarizability perovskite-related materials CaCu3Ti4O12. Giulotto E., Mozzati, M. C., Azzoni, C. B., Massarotti, V., Capsoni, D., Bini, M., Ferroelectrics 298, 61-67 (2004)

293. Electric and dielectric properties of pure and doped CaCu3Ti4O12 perovskite materials. Chiodelli, G., Massarotti, V., Capsoni, D., Bini, M., Azzoni, C. B., Mozzati, M. C., Lupotto P., Solid State Communications 132, 241-246 (2004)

294. Role of doping and CuO segregation in improving the giant permittivity of CaCu3Ti4O12. Capsoni, D., Bini, M., Massarotti, V., Chiodelli, G., Mozzati, M. C., Azzoni, C. B., Journal of Solid State Chemistry 177, 4494-4500 (2004)

295. Mechanical activation of calcium titanate formation from CaCO3—TiO2 mixtures. Berbenni, V., Marini, A., Journal of Materials Science 39/16-17, 5279-5282 (2004)

296. Hofmeister Specific Ion Effects in Two Biological Systems. Lo Nostro, P., Lo Nostro, A., Ninham, B. W., Pesavento G., Fratoni, L., Baglioni, P., Current Opinion in Colloid & Interface Science 9, 97-101 (2004)

297. Water of Hydration in Coagels. Ambrosi, M., Lo Nostro, P., Fratoni, L., Dei, L., Ninham, B. W., Palma, S., Manzo, R. H., Allemandi, D., Baglioni, P., Physical Chemistry Chemical Physics 6, 1401-1407 (2004)

298. Novel mannitol based non-ionic surfactants from biocatalysis. Salis, A., Pinna, M. C., Murgia, S., Monduzzi, M., Journal of Molecular Catalysis B: Enzymatic 27, 139-146 (2004)

299. Inelastic X-ray Scattering Studies of Phonons in Liquid Crystalline DNA. Liu, L., Berti, D., Faraone, A., Chen, W. R., Alatas, A., Alp, E., Baglioni,P., Chen, S. H., Physical Chemistry Chemical Physics 6, 1499-1505 (2004)

300. Hydration, stability, and phase transformations of a new antitumor drug. Marini, A.,

Berbenni, V., Bruni, G., Cofrancesco, P., Margheritis, C., Orlandi, A., Villa, M., Journal of Pharmaceutical Sciences 93-9, 2222-2231 (2004)

301. A fast and low cost room temperature process fro TiB2 formation by mechanosynthesis. Matteazzi, P., Ricceri, R., Materials Science and Engineering C, 341-346 (2004)

302. Flexibility of Dilauroyl-Phosphatidyl-Nucleoside Wormlike Micelles in Aqueous Solutions. Baldelli Bombelli, F., Berti, D., Pini, F., Keiderling, U., Baglioni, P. Journal of Physical Chemistry B 108, 16427-16434 (2004)

Thesis (undergraduate, PhD, post-doc) 2005-2007

- Physico-chemical characterization of controlled-topology structures.
- Polyrotaxanes and host-guest systems: modellization of inclusion and aggregation phenomena.
- Role of water in biomolecular structure and dynamics: simulations and neutron scattering.
- Synthesis of metallic nanoparticles for innovative applications.
- Nanotechnology for artworks conservation.
- Nanostructured fluids with nucleic functionalizations.
- Development of new nanosystems for the cleaning and the consolidation of cultural heritage.
- Nanostructured systems as cleaning agents for painted surfaces: microemulsions, micelles, gels and foam of new generation.
- Multifunctional nanostructures.
- Self-assembled structures with lipophilic nucleosides for the construction of digitally addressable surfaces.
- Fluorinated emulsions.
- Paper degradation due to copper-rich iron-gall ink: evaluation of new strategies for conservation treatment.
- Addessable nanoarchitectures with optoelectronic and photovoltaic functionalities.
- Synthesis of functionalized magnetic powder and ferrogels.
- Interactions between Nucleolipids and Oligonucleotides.
- Structural and thermodynamic characterization of semi-ipn hydrogels from chitosan-polyvinylpyrrolidone.
- Lyotropic Effects and Non Covalent Interactions in Nanosystems.
- Ionic strength effect on the interactions between an anionic surfactant and a synthetic macromolecule.
- Nanoarchitectures for PLEDs (Polymer Light-Emitting Devices) based on Langmuir-Blodgett/Layer-by-Layer hybrid films.
- Physico-chemical properties of four component-fluorinated systems.
- Transport properties in systems based on macromolecules solutes: polyacrylic acid-polyvinyl alcohol-water.
- Synthesis of a new Vitamin C derivative and its characterization.
- Synthesis and functionalization of nanoparticles for treatments on textile samples.
- Optical properties of dissolved organic matter and physico-chemical properties of coastline waters in Lake Victoria (Kenya and Uganda).
- Characterization of structure and interactions in “arrested systems” of proteins and polymers.
- Nanosystems of amphiphiles functionalized with nuclei bases.
- Modifications of surfaces and textiles by using nanotechnoloy-based methods.
- Development of high-impact technology nanomaterials for industrial and art conservation application.
- Nanoarchitectures for PLEDs (Polymer Light-Emitting Devices) based on Langmuir-Blodgett/Layer-by-Layer hybrid films.
- Study of superplasticizers and modified cellulosic polymers effect on the microstructure and hydration of calcium silicate and aluminate.
- Characterization of vectors for gene delivery.
- Thermodynamic and microstructural characterization of hydrogels from poly(n-vinylpyrrolidone).

- Colloidal particles as diagnostic tools in MRI
- Determination of the spinoidal composition in a ternary system (acetic acid-chloroform-water).
- Transport phenomena in a solution containing a protein in a mixed solvent (2-methyl-2,4-pentanediol-water).
- Formulation and physico-chemical and microstructural characterization of hydrogels of chitosan with and without surfactants.
- Preparation and physico-chemical characterization of hydrogels of poly(n-vinylpyrrolidone) containing glycerol.
- NMR study of the recognition process between bioactive molecules and macromolecular receptors.
- NMR study of relaxation processes between bioactive molecules and models for receptors and cells.
- Study of bioaccumulation of As in Elodea densa for different radiative regimes.
- Study of the distribution of As, Cd, Cr, Pb, and Mn in the hydrograpgic basin of Cornia river.
- Analysis of the drug solid state during the phases of pharmaceutical dosage forms manufacturing.
- Physico-chemical characterization of liponucleosidic micellar solutions. Structural and Dynamic investigation in presence of molecular recognition between nucleic bases.
- Technologies on silicon surfaces for bio-electronic microsystems.
- Addressable Molecular Node Assembly – a Generic Platform of Nanoscale Functionalized Surfaces Based on a Digitally Adressable Molecular Grid.
- Physico-chemical study of the interface features of artistically and historically relevant porous materials.
- Study of surfaces modifications and Nanoparticles preparation.
- Nanophasic aggregated systems and the effect of lyotropic agents.
- Nucleation and Growth of Crystal Phases in Confined Micro- and Nano structured Regions in the presence of anti-scaling additives. Application for the conservation of Architectonic and Artistic Masterpieces.
- Characterization of alloys and natural or artificial patinae of historical or artistical metal artifacts by means of spectroscopic and diffraction techniques.
- Inorganic nanomaterials for the consolidation of artistic and architectonic artifacts.
- Consolidation of Globigerina stone from Malta by several organic and inorganic materials: a comparison study.
- In situ polymerization and innovative materials for the conservation of artifacts made of tufa.
- Physico-chemical characterization of painting materials.
- A physico-chemical study: liposomes for gene delivery and cell membranes.
- Kinetic glass transition in concentrated protein solutions.
- Functionalized nanodevices: from the molecular design to the physico-chemical characterization.
- Development of multifunctional microsystems for applications in clinical diagnostics and food analysis.
- Physico-chemical characterization of painting materials.

CSGI Activity in 2007-2009

CSGI is currently involved in 7 European programs, in several national projects, and in collaborations with small and medium size industrial companies.
CSGI has activated a triennial program with CNR on “Functionalities in surfaces and at interfaces (FUSINT)”.
CSGI is developing its own research activity in order to optimize the application of research projects inspired by the urging demands of small and medium size companies.
CSGI is actively working in order to offer a valid support to the Italian industrial system in the setting up and development of projects and pre-industrial processes.

Contact Details

Consorzio Sviluppo dei Sistemi a Grande Interfase
Department of Chemistry
University of Florence
via della Lastruccia, 3
50019 Sesto Fiorentino (Firenze)
Italy

voice: +39 055 457-3034
fax: +39 055 457-3036
E.mail: info@csgi.unifi.it
Internet: http://www.csgi.unifi.it/

Research themes

1A Hard Matter (Nanomaterials and Solid Interfaces) 1

- Biosensors based on nano-structured organic films
- Flame Spraying of Colloidal Suspensions
- Hydration kinetics and Microstructure of Portland Cement pastes
- Hydrogen Storage in Nanomaterials
- Multilayer Thin Films for molecular opto-electronics
- Multilayered Nanofilms for molecular opto-electronics
- NANOGRES: A novel nanostructured coating of ceramic materials
- Nanosensors based on ultrathin organic films
- Nanospraying - Thermal spraying of nanophased powders
- Nanostructured coatings for engineering tribological applications
- NIR investigation of the confined water into organic and inorganic systems
- Porous electrodes in alkaline fuel cells and electrolysers
- Thermal spraying of nanophased powders

1B Soft Matter (Nanomaterials and Liquid Interfaces) 42

- A microscopic model for colloid thermophoresis
- Addressable Molecular Node Assembly - a Generic platform of Nanoscale Functionalised Surfaces Based on a "Digitally Addressable" molecular Grid
- Bottom-Up strategies for the Self-Assembly of Biologically Inspired Surfactants
- Colloidal aspects of membrane proteins
- Cryo-TEM of Liposomes loaded with boron-coating compounds intended for Boron Neutron Capture Therapy (BNCT)
- Lipoplexes as non viral vectors for gene delivery
- Nanostructured Magnetic Fluids
- Nanostructured surfaces for controlled bacteria adhesion
- Perfluorocarbon O/W emulsions: physico-chemical characterization and Cell viability
- Phase behavior, microstructure and dynamics of surfactant systems: mecelles, liquid crystals, microemulsions, and emulsions
- Photoresponsive Surfactants
- Polymerization of human fibrinogen induced by pathogenic bacteria: a microbial "deceiving strategy"
- Self-assembly of β-Cyclodextrin in Water
- Self-Assembly of Biologically Inspired Surfactants
- Smart Nanostructured Materials: i) - Fluorinated Systems: NMR investigation; ii) - NMR studies in Micelles, Microemulsions, Emulsions and Liquid Crystalline systems based on biocompatible surfactnt systems for food, pharmaceutical and cosmetic applications; iii) - DDAB liquid Crystals, Microemulsions and Emulsions
- Specific ion effects
- Structure and Dynamics of membrane proteins
- Structure and Dynamics of Photosynthetic Reaction centers
- Study of the phase behavior of some fluorocarbon/hydrocarbon mixtures and of semifluorinated F_mH_n copolymers
- Surface imaging of Nanostructures: Brewster Angle Microscopy and Ellipsometric Mapping

- Structural properties of pure and doped Li_3VO_4 vanadate and Zn, Mg analogous compounds)
- Reactivity and Structure of Inorganic Compounds
- Stability and properties of spinel related phases
- Structural and spectroscopic investigation of pure and doped $Ba_6Zr_2Ta_8O_{30}$ tungsten bronze
- Structure, Reactivity and Characterization of Ternary Oxides for Energetic Uses
- Synthesis and Characterization of Advanced Materials for Energetic Studies
- Synthesis and characterization of pure and doped $Ba_6Ti_2Nb_8O_{30}$ ceramic materials
- Thermal stability and properties of pure $LiMn_2O_4$
- Y_2BaNiO_5 and related compounds

2C Biotechnology (Food, Pharmaceutics, Bioprocesses) 234

- Biocatalysis through immobilised lipases
- Bioconversion in emulsion systems
- Biotechnological Processes
- Characterization of anti-mycobacterial pyrrole derivates
- Characterization of autochtonous microflora from artisanal ewe's products
- Characterization of food products by ToF-SIMS and PCA
- Enzime activity in microemulsions
- Enzyme and coenzyme immobilisation
- Enzymes and their application to waste processing and bioremediation
- Formulations based on fully biocompatible surfactant systems for food, pharmaceutical and cosmetic applications
- In vivo expression of antisense RNAs leads to efficient silencing in Escherichia coli
- Lignocellulosics: degradation and recycling
- Nanostructured Media for Bacterial Production of Fine-Chemicals
- Organogel in Biotechnological processes
- Organogels in technological processes
- Ovine milk: composition, dairy processing and quality controls, fractionation as a source of raw materials, no food products, and dairy wastes
- Phase transitions and structure-properties in organic compounds
- Physico-Chemical Properties of Pharmaceutical Systems
- Polyphenol oxidases and enzymic browning
- Production of Recombinant Human Monoclonal Antibodies for Diagnostic and Therapeutic Use
- Selenium forms in solenium-enriched potato tubers
- Structure and oxidative stability of water-in-oil food emulsions
- Structure and stability in food emulsions
- Study of organic materials polymorphism

1A - Biosensors based on nano-structured organic films.

G. Caminati, B. Mecheri, F. Gambinossi, M. Puggelli, S. Morandi.

Aims

General aim of the present project is to gain a deeper knowledge on the mechanism of molecular recognition in interfacial biomimetic systems: spreading monolayers at water-air interface and ordered multilayer nanostructures. This type of investigation represents the basis for the development of biosensors using organized hybrid film technology: Self-Assembled Monolayers (SAM)/Langmuir-Blodgett (LB) devices and alternate LB structures of organic/inorganic materials.

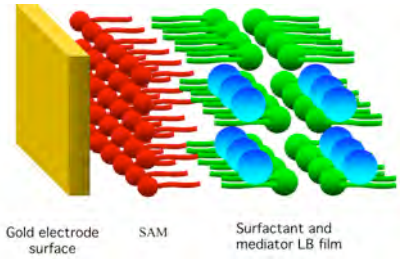

Fig. 1 Scheme of the multilayered architecture signed for the realization of the biosensors

We focused our studies on the recognition of food-contaminants whose widespread use is posing increasingly high risks to the health of the population.
The system described in figure 1 was used for the detection of food contaminants by means of electro-active molecules embedded in the hybrid nanostructure. In particular we investigated two main classes of contaminants: a) monosodium glutamate (MSG), heavily employed in food processing and responsible of disorders to central nervous system, and b) two of the most used families of veterinary antimicrobial substances, i.e. tetracyclines (TC), and rifamycins (RF). These compounds are well known to induce allergic syndromes and strain resistance to antibiotics. The long term goal of the present work is to develop new methods for the determination of toxic substances in waters and in edible materials.

Results

a) Biosensors for MSG.

Much effort has been devoted to the detection of glutamate in fluids not only for its biological relevance but also for the insurgence of allergic syndromes in the population due to its presence in food. Current detection methods are based on the reaction of oxidative deamination of glutamate, catalysed by glutamate dehydrogenase (GlDH) in the presence of nicotinamide adenine dinucleotide (NAD):

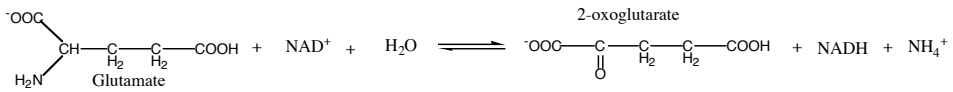

The NADH content, directly proportional to the glutamate concentration, can be determined either through direct spectroscopic observation or by electrochemical measurements. The electrochemical determination of MSG requires the use of a suitable redox mediator to

facilitate the long-range electron transport from the analyte molecule to the electrode surface according to the following scheme:

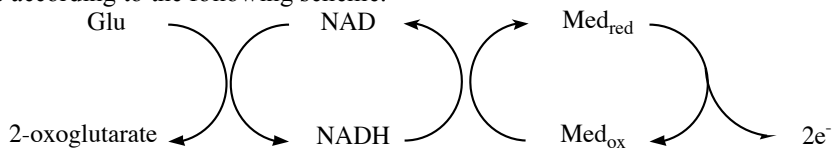

Electrode coating with organic ultra-thin films can be successfully used to immobilize such redox mediators. Organized thin films offer several advantages for the realization of novel modified electrodes: first of all the presence of hydrophobic compact layers may act as a selective barrier that can improve control of electrode processes. Secondly, the electrode coating with lipid layers allows immobilization of biomolecules such as enzymes. We focused on the use of different types of organized thin films in preparing sensitive layers containing electroactive molecules: Self-Assembled Monolayers (SAMs), Langmuir-Blodgett (LB) films and Hybrid Films (HFs). HF structures were realized by means of concurrent use of SAM and LB procedures in order to combine high molecular order and architectural control of the LB technology with chemical, mechanical and thermal stability of SAMs (see figure 1). Tipically, dipalmitoylphosphatidic acid (DPPA) was used as lipid matrix for LB fabrication whereas octadecylmercaptane (ODM) and octylmercaptane (OM) were used for the preparation of SAMs on gold surfaces.
Several redox mediators were screened on the basis of their redox features. In the case of non-amphiphilic redox mediators a preliminary study on the co-spreading process with the lipid matrix is performed at the water-air interface. Monolayers containing the desired redox mediator are transferred by LB deposition either directly on solid slides (LB), or on top of previously self-assembled monolayer (HF). Two different immobilization procedures were tested for the immobilization of the mediator in the LB film: a) co-transfer, i.e. direct deposition as LB film of the mixed monolayer; b) incubation, i.e. immersion of preformed thin films of the lipid in a solution containing the mediator. Such LB structures are characterized in terms of their electrochemical and spectroscopic behaviour. In the case of tetramethylbenzidine (TMB), the results indicate that the mediator is present in the film with unaltered electrochemical activity as reported in figure 2.

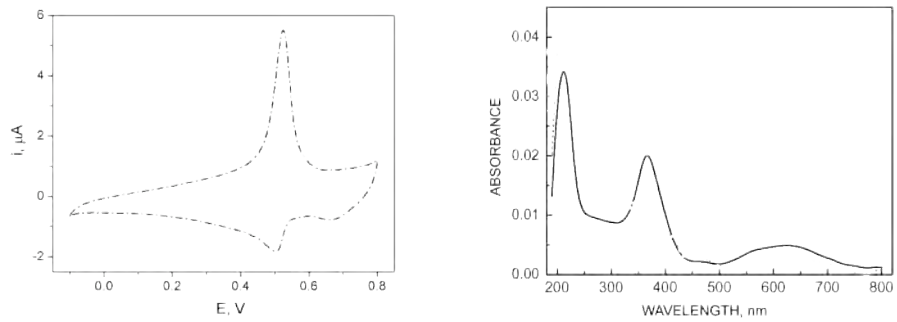

Fig. 2 (a) i-V profile and (b) absorbance of a typical phospholipid LB film containing TMB.

We tested the electrochemical response of such nanostructures for molecular recognition of NADH in solution.

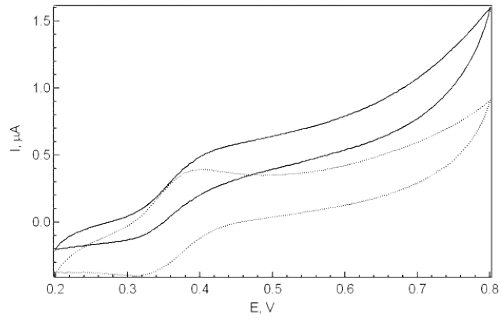

Fig. 3. Cyclic Voltammograms of a typical DPPA:TMB LB film in the absence (dotted line) and in the presence (solid line) of NADH in solution.

The figure shows that the electrochemical signal due to TMB in the film increases when NADH is added in solution; this finding demonstrates that the LB film is able to recognise the NADH molecules. NADH and MSG determination was also performed by means of spectroscopic techniques: the experimental results reveal that the designed architecture of the nanostructure strongly influences the interaction between the biomolecules and the film.

The body of the results indicates that LB nanostructures appear extremely interesting for molecular recognition of biological molecules by properly tuning the architecture and the composition of the film.

b) Biosensors for veterinary antibiotics.

Drug's residues deriving from the veterinary treatment of animals can survive the manufacturing cycle contaminating animal-derived food and the environment. Antibiotics are one of the most ubiquitous families of veterinary drugs which, on over-exposure of the consumer, rapidly induce the development of antibiotic resistance in the population. A rapid and effective control of the presence and level of antibiotic residues involves their fast identification both in animal-derived food and in polluted waters. The paradigm underlying the present research line is the study of the interaction of a suitable bio-reactant incorporated in a Langmuir-Blodgett system with the toxic compounds in the surrounding aqueous medium. The resulting multilayered nanosensor can be directly coupled to the detection devices: we explored both spectroscopic and electrochemical methods. Two typical antibiotic molecules studied are reported in figure 4.

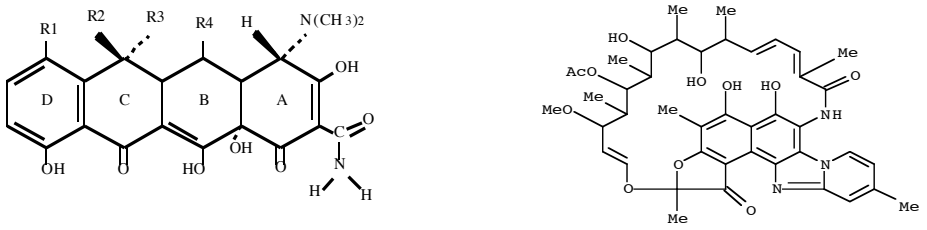

a **b**

Fig. 4 Chemical structures of tetracycline **(a)** and of rifampicin **(b)**.

We examined spreading monolayers of several amphiphiles in the presence of the antibiotic in the subphase by means of surface pressure-area and surface potential-area isotherms. We screened several phospholipids differing in the polar head group or in the length of the alkyl chain.

In the case of tetracycline, we found that interactions with the phospholipid molecules is highly dependent on the electric charge of the antibiotic and the ionisation state of the lipid. Significant interactions are established only between the negatively charged form of dipalmitoylphosphatidic acid (DPPA) and the protonated form of tetracycline although penetration through the hydrophobic layer can be excluded. In the case of rifamycins, a systematic study allowed to select dipalmitoylphosphatidyl glycerol sodium salt (DPPG-Na) as the most interactive lipid on the basis of the experimental characterization at water-air interface.

LB films of the selected matrix phospholipid were prepared and immersed in a solution containing the antibiotic under examination to allow incorporation of the drug. The resulting films were removed from the solution and characterized by means of contact angle and ellipsometric measurements. UV-Vis and FTIR/ATR spectroscopy as well as cyclic voltammetry were performed on the samples and provided direct evidence of the presence of the antibiotic in the film. For tetracycline, the results showed that TC diffuses from the solution towards the film crossing the alkyl chain layers to reach the interlayer hydrophilic zone. Analysis of the UV-Vis spectra and FTIR/ATR spectra (figure 5) in the Amide I and II region, showed that a specific interaction occurs between the A ring of the tetracycline molecule with the polar head group of DPPA.

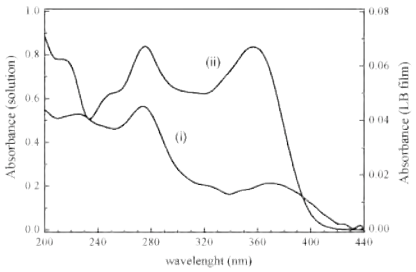

(a)

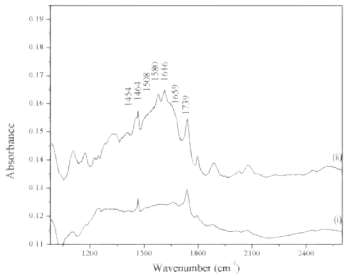

(b)

Fig. 5 (a) UV-Vis spectra of 5 DPPA LB layers immersed in TC solution (curve i) together with TC solution spectrum (curve ii); (b) FTIR-ATR spectra on germanium slides: (i) one LB layer of DPPA; (ii) one LB layer of DPPA/TC.

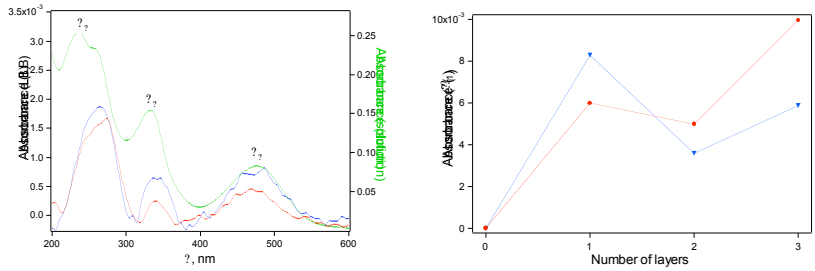

Fig. 6 **(a)** UV-Vis spectra of one DPPG-Na LB film transferred at 25 mN m^{-1} (red line) and 35 mN m^{-1} (blue line) immersed in 1 x 10^{-5} M Rfp solution together with Rfp solution spectra (green line); **(b)** absorbance maxima vs. number of LB layers transferred at 25 mN m^{-1} (red line) and 35 mN m^{-1} (blue line).

Preliminary results as a function of the antibiotic concentration in the examined solution revealed that the LB-based sensor can be used to determine the antibiotic concentration. In figure 7 we report the absorbance recorded for the LB film after removal from the TC solution. The results obtained with the incubation method open a new perspective for the realization of sensors for antibiotic residues in food by means of the LB technique coupled with a variety of detection systems such as UV-Vis and Fluorescence spectroscopy, Surface Plasmon Resonance and Quartz Crystal Microbalance.

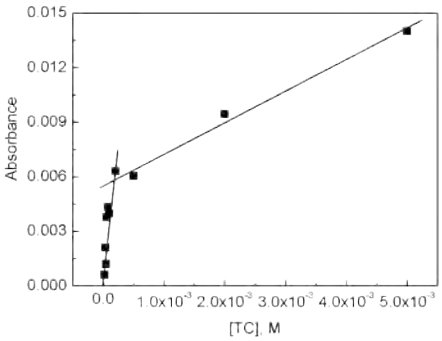

Fig. 7 Absorbance maxima for 3 DPPA/TC LB layers vs. TC concentration in solution.

References

F. Gambinossi, B. Mecheri, G. Caminati, M. Nocentini, M. Puggelli, G. Gabrielli, "*Antibiotic Interactions with Phospholipid Monolayers"*, Materials Science and Engineering C 22 (2002) 283-288.

G. Caminati, C. Focardi, G. Gabrielli, F. Gambinossi, B. Mecheri, M. Nocentini, M. Puggelli, *"Spectroscopic Investigation of Tetracycline Interaction with Phospholipid LB Films",* Materials Science and Engineering C 22 (2002) 301-305.

B. Mecheri, L. Piras, L. Ciotti and G. Caminati, "*Electrode coating with ultra-thin films containing electroactive molecules for biosensor applications",* IEEE Sensor Journal, accepted for publication.

B. Mecheri, L. Piras and G. Caminati, *"Langmuir-Blodgett Films incorporating redox mediators for molecular recognition of NADH"*, Bioelectrochemistry, accepted for publication.

S. Morandi, M. Nocentini, M. Puggelli and G. Caminati, *"Interaction of DPPG sodium salt with rifamycin antibiotic in Langmuir monolayers and Langmuir-Blodgett films"*, Physical Chemistry Chemical Physics, submitted for publication.

1A – Effect of Cellulose on Hydration and Microstructure of Cement pastes

Piero Baglioni, Emiliano Fratini, Francesca Ridi, Francesca Mannelli, Paola Luciani

Aims

Hydration Kinetics and Microstructure Characterization
Effect of Cellulose Ethers on Hydration Kinetics

Results

In cement industry the extrusion technique is used to produce flat shapes with improved resistance to compression. Extrusion is a plastic-forming process that consists of forcing a highly viscous plastic mixture through a shaped die. The material should be fluid enough to be mixed and to pass through the die and, on the other hand, the extruded specimen should be stiff enough in order to be handled without changing in shape or cracking. These characteristics are industrially obtained adding cellulosic polymers to the mixture. The aim of this work was to understand the action mechanism of this additive on the major pure phases constituting a typical Portland cement: tri-calcium silicate (C_3S), di-calcium silicate (C_2S), tri-calcium aluminate (C_3A) and tetra-calcium iron-aluminate (C_4AF). In particular, a methyl-hydroxyethyl cellulose, MHEC, was selected among the best-performing polymers. The effect of the additive on the hydration kinetics (rate constants, activation energies, diffusional constants) was evaluated by means of differential scanning calorimetry (DSC) while the hydration products were studied by using thermogravimetry-differential thermal analysis (TG-DTA), x-ray diffraction (XRD) and electronic microscopy (SEM). Furthermore we used ^{1}H-NMR relaxation times in order to investigate the pore structure evolution during the C_3S phase hydration process.
The calorimetric analysis (figures below) shows that a slight delay is produced in the setting of C_3S paste by means of MHEC, together with an improved hydration efficiency through an increased availability of the water in the hydration reaction. For example, in the case of the C_3S/water/MHEC paste cured at 20ºC, the acceleration period ends when only 20% of water remains unreacted (FWI=0.2); whereas for the C_3S/water paste cured at the same temperature the unreacted water is nearly 60%, meaning that in the presence of cellulose ether the C_3S can react with most of the available water to complete the hydration reaction.

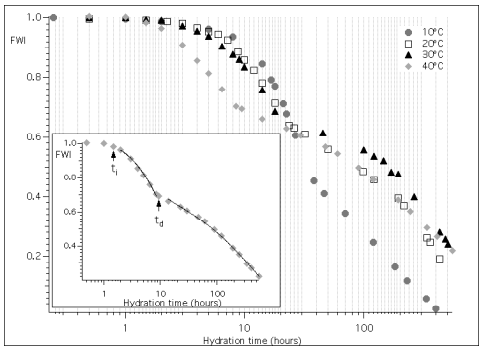

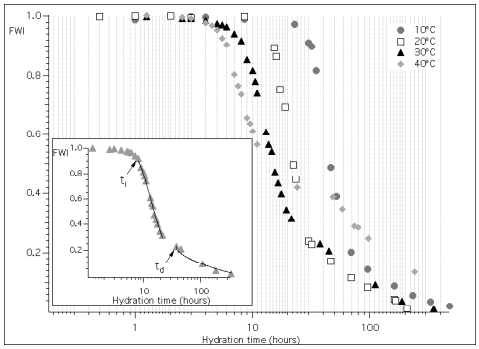

In the presence of cellulosic polymer the activation energy for the nucleation and growth process is essentially equal to that obtained with pure water. A value of 35 kJ/mol is estimated for the MHEC-added paste, not meaningfully different from 37 kJ/mol of the unmodified system. This result indicates that cellulose ether, differently from

superplasticizers (SPs), does not affect the hydration thermodynamics, i.e. the MHEC/C_3S interaction is negligible. However, the significant influence of this additive on the water availability suggests that, due to its highly hydrophilic chemical structure, it strongly interacts with the aqueous phase. The SEM micrographs performed on pastes of C_3S cured in pure water reveal a one-dimensional microstructure of the CSH, growing on the particle surfaces, in full accordance with the literature. The presence of MHEC in the paste produces some significant modification (after 12 hours of curing) in the appearance of the sample surfaces: the fibrils of the typical CSH growing phase are not present in the suggesting that the presence of the additive affects the shape of the hydrated CSH. NMR relaxation times (longitudinal and transversal) for C_3S/water and C_3S/MHEC/water systems were compared with the relaxation times of the MHEC/water mixture. T_1 and T_2 trends provided evidences of the strong interaction between the water and the cellulosic polymer. In particular, values of T_1=950 ms and T_2=4 ms have been found at the initial stage of the reaction in the C_3S/water paste and are reported in literature as indicative of water constrained in capillary pores. The induction period of C_3S/water/MHEC is characterized by T_1=1.18 s and T_2=6 ms, essentially the same as water entrapped in MHEC alone (T_1=1.23 s and T_2=5.75 ms). This result supports the hypothesis of a strong interaction between the water and the cellulosic molecules inside cementitious pastes. It is evident that also this interaction significantly modifies the CSH morphology. The presence of the cellulosic polymer also changes the appearance of fully hydrated C_3S pastes: the samples containing MHEC are much more compact in the respect to the standard pastes.

Di-calcium silicate, C_2S, is characterized by an extremely slow hydration process: it is necessary more than one year to complete the reaction. We acquired the whole hydration kinetics for the hydration of this phase with in pure water and in the presence of MHEC at 20°C. MHEC is found to have a slightly retardant effect. Due to the slowness of the reaction, the C_2S system shows two different nucleation-and-growth periods, as it is evident from the two different slopes in the plot of the Avrami-Erofeev plot

We utilized TG-DTA measurements to investigate the MHEC influence on the aluminate phases. We examined samples of C_3A and C_4AF powders mixed at 15ºC with water, with and without MHEC and we observed the time evolution during the hydration, of the thermal effects produced from the decomposition of the hydrated phases. Particular attention was paid on the early stages of the process when most of the water is consumed in the heterogeneous reaction with the rapid formation of hydrated phases.

As an evidence of the extremely high reaction rate of the aluminate phases, it has to be noted that immediately after the mixing of both C_3A and C_4AF with water some reaction products are formed: just after 5 minutes, the C_3A/pure water system presents two peaks at 128ºC and 280°C: with the progress of the hydration the intensity of this latter peak increases, with a corresponding progressive shift towards higher temperature, up to 316ºC after four days of curing. According to previous studies the decomposition occurring around 300°C has been assigned at stable cubic hydrogarnet phases. On the other hand, the XRD analysis performed on these samples effectively evidences the presence of C_3AH_6 (the cubic hydrogarnet product relative to the tricalcium aluminate hydration), together with some unreacted C_3A. No other XRD pattern is detectable, confirming the amorphous nature of the hydrated product responsible for the DTA peak at 128ºC. Another peak at 450ºC is present when the sample is cured four days, due to the loss of a remaining mol of crystal water from the hydrogarnet phase. When the MHEC is added to the paste a relevant inhibition in the formation of the cubic stable phase occurs in the first minutes of the reaction, as testified by the absence of the peak at 300°C, after 5 and 15 minutes from the mixing. These samples present endothermal features at 145, 230 and 260ºC. According to the XRD spectra, the hydrated products formed in these conditions are not crystalline since no additional pattern is present, apart from that of the anhydrous tricalcium aluminate. The

presence of the cellulose ether during the early stages of C_3A hydration stabilizes the amorphous gel, precursor of the stable C_3AH_6. At hydration times over 30 minutes the thermograms are identical to those obtained for C_3A/water. The micrographs obtained on the C_3A/water and C_3A/water/MHEC samples confirmed the results obtained with DTA technique. C_3A cured in pure water for 5 minutes shows a compact and featureless structure. When the cellulose ether is added to the mix the irregular foils, typical of the amorphous gel appear. When both the polymer-free and the polymer-added systems are cured for one hour or more, their morphologies are dominated by the cubic phase, C_3AH_6.
The C_4AF phase presents a similar behavior, with an even more accentuated inhibition effect of MHEC on the stable $C_3(AF)H_6$ during the first hour from the mixing.
The ^{1}H-NMR relaxation times analysis allowed inferring some interesting information about the mechanism of the progressive immobilization of water inside the paste, by comparing the results obtained with this technique with those produced by means of the DSC approach. In particular T_1 and T_2 vs hydration time trends account the different water population according to the Powers model. In this sense, NMR provides additional information about the early stages of hydration and probes the contribution of capillary water (free water) and gel water (physically bound water), which are not differentiate by DSC. Pore size distributions (PSD) of C_3S pastes in pure water and added with MHEC are reported in the figures below. The PSD of the C_3S/water paste (fig. A) in the first step of the hydration is centered in the interval 120-140 mm. After 9 hours the pore size dramatically shifts towards smaller values, in full accordance with previous results, and continue to decrease until 19 hours, when the distribution is almost entirely in the 0-20 mm interval. The system C_3S/water/MHEC (fig. B) presents a PSD centered in the interval 140-160 mm, in the first hours, and only a little shift can be observed in the first 19 hours until 100-120 mm.

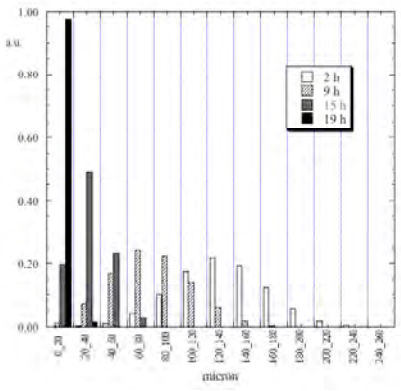

A)

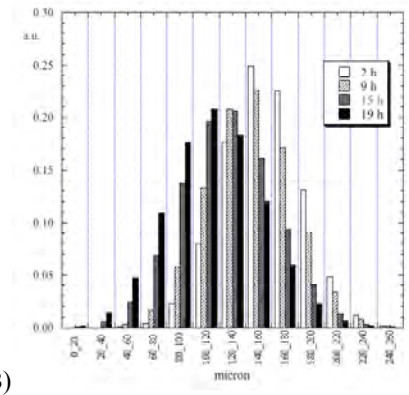

B)

References

M. Alesiani, S. Capuani, R. Giorgi, B. Maraviglia, I. Pirazzoli, F. Ridi and P. Baglioni: “Influence of cellulosic additives on tricalcium silicate hydration: nuclear magnetic resonance relaxatione time analysis". *Journal of Physical Chemistry B*, 108, 4869-4874, (2004).

F. Ridi, E. Fratini, F. Mannelli and P. Baglioni: “Hydration process of cement in the presence of a cellulosic additive. A calorimetric investigation". *Journal of Physical Chemistry B*, 109, 14727-14734, (2005).

1A – Flame Spraying of Colloidal Suspensions

Massimo Bonini and Piero Baglioni, in collaboration with: Niccolo' Baldanzini, Alessandro Giorgetti, Federico Casucci, Paolo Citti (DMTI, Faculty of Engineering, Univ. of Florence)

Aims

Aim of this project is to demonstrate on a lab-scale the feasibility of the flame spraying of colloidal suspensions. This new methodology has been recently patented by CSGI [1] and it allows the preparation of nanostructured coatings or powders, constituted by discrete sub-units as small as a few nanometers.

Results

On a lab-scale, flame spraying has already proved to be an effective synthetic route to obtain really nanostructured coatings, i.e. films constituted by discrete nanodimensioned sub-units. Stable suspensions of nanoparticles are synthesized and then used to feed the flame spraying system. The chemical composition and the dimensions of the nanoparticles can be easily tuned, making so possible to design a surface both form a chemical and a physical point of view.

A prototype capable to produce coatings by means of flame spraying of colloidal suspensions was recently designed and assembled at the CSGI unit of Florence (see figure 1). This machine can produce uniform nanostructured coatings on objects, as large as 500 mm in diameter and 800 mm in length.

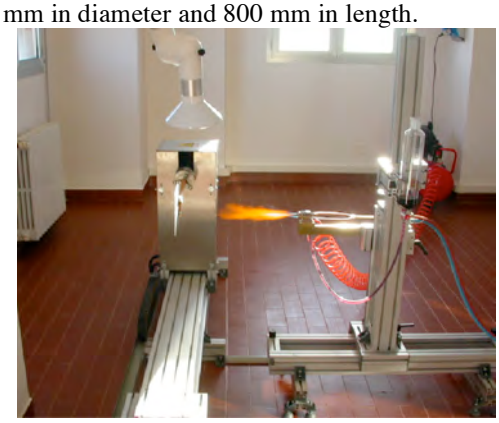

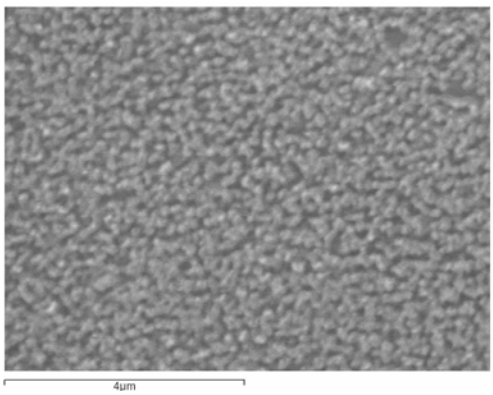

Fig. 1. The flame spraying prototype installed at the CSGI unit of Florence.
Fig. 2. Glass coated through Flame Spraying of a TiO_2 nanoparticle suspension.

References

[1] Baglioni, P., U. Bardi, and M. Bonini, *New process for the production of nanostructured solid powders and nano-particles films by compartimentalised solution thermal spraying (CSTS),* 2001, EP1134302.

1A - Hydration kinetics and Microstructure of Portland Cement pastes

Piero Baglioni, Emiliano Fratini, Francesca Ridi, Paola Luciani

Aims

Hydration Kinetics and Microstructure Characterization
Effect of Cellulose Ethers on Hydration Kinetics

Results

In cement industry the extrusion technique is used to produce flat shapes with improved resistance to compression. Extrusion is a plastic-forming process that consists of forcing a highly viscous plastic mixture through a shaped die. The material should be fluid enough to be mixed and to pass through the die and, on the other hand, the extruded specimen should be stiff enough in order to be handled without changing in shape or cracking. These characteristics are industrially obtained adding cellulosic polymers to the mixture. The aim of this work was to understand the action mechanism of this additive on the major pure phases constituting a typical Portland cement: tri-calcium silicate (C_3S), di-calcium silicate (C_2S), tri-calcium aluminate (C_3A) and tetra-calcium iron-aluminate (C_4AF). In particular, a methyl-hydroxyethyl cellulose, MHEC, was selected among the best-performing polymers. The effect of the additive on the hydration kinetics (rate constants, activation energies, diffusional constants) was evaluated by means of differential scanning calorimetry (DSC) while the hydration products were studied by using thermogravimetry-differential thermal analysis (TG-DTA), x-ray diffraction (XRD) and electronic microscopy (SEM). Furthermore we used ^{1}H-NMR relaxation times in order to investigate the pore structure evolution during the C_3S phase hydration process.
The calorimetric analysis (figures below) shows that a slight delay is produced in the setting of C_3S paste by means of MHEC, together with an improved hydration efficiency through an increased availability of the water in the hydration reaction. For example, in the case of the C_3S/water/MHEC paste cured at 20ºC, the acceleration period ends when only 20% of water remains unreacted (FWI=0.2); whereas for the C_3S/water paste cured at the same temperature the unreacted water is nearly 60%, meaning that in the presence of cellulose ether the C_3S can react with most of the available water to complete the hydration reaction.

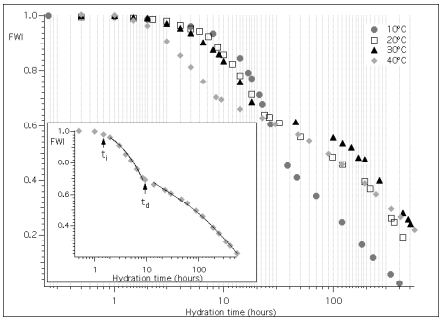

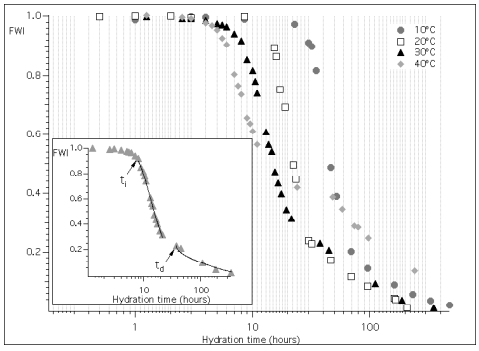

In the presence of cellulosic polymer the activation energy for the nucleation and growth process is essentially equal to that obtained with pure water. A value of 35 kJ/mol is

estimated for the MHEC-added paste, not meaningfully different from 37 kJ/mol of the unmodified system. This result indicates that cellulose ether, differently from superplasticizers (SPs), does not affect the hydration thermodynamics, i.e. the MHEC/C_3S interaction is negligible. However, the significant influence of this additive on the water availability suggests that, due to its highly hydrophilic chemical structure, it strongly interacts with the aqueous phase. The SEM micrographs performed on pastes of C_3S cured in pure water reveal a one-dimensional microstructure of the CSH, growing on the particle surfaces, in full accordance with the literature. The presence of MHEC in the paste produces some significant modification (after 12 hours of curing) in the appearance of the sample surfaces: the fibrils of the typical CSH growing phase are not present in the suggesting that the presence of the additive affects the shape of the hydrated CSH. NMR relaxation times (longitudinal and transversal) for C_3S/water and C_3S/MHEC/water systems were compared with the relaxation times of the MHEC/water mixture. T_1 and T_2 trends provided evidences of the strong interaction between the water and the cellulosic polymer. In particular, values of T_1=950 ms and T_2=4 ms have been found at the initial stage of the reaction in the C_3S/water paste and are reported in literature as indicative of water constrained in capillary pores. The induction period of C_3S/water/MHEC is characterized by T_1=1.18 s and T_2=6 ms, essentially the same as water entrapped in MHEC alone (T_1=1.23 s and T_2=5.75 ms). This result supports the hypothesis of a strong interaction between the water and the cellulosic molecules inside cementitious pastes. It is evident that also this interaction significantly modifies the CSH morphology. The presence of the cellulosic polymer also changes the appearance of fully hydrated C_3S pastes: the samples containing MHEC are much more compact in the respect to the standard pastes.

Di-calcium silicate, C_2S, is characterized by an extremely slow hydration process: it is necessary more than one year to complete the reaction. We acquired the whole hydration kinetics for the hydration of this phase with in pure water and in the presence of MHEC at 20°C. MHEC is found to have a slightly retardant effect. Due to the slowness of the reaction, the C_2S system shows two different nucleation-and-growth periods, as it is evident from the two different slopes in the plot of the Avrami-Erofeev plot.

We utilized TG-DTA measurements to investigate the MHEC influence on the aluminate phases. We examined samples of C_3A and C_4AF powders mixed at 15ºC with water, with and without MHEC and we observed the time evolution during the hydration, of the thermal effects produced from the decomposition of the hydrated phases. Particular attention was paid on the early stages of the process when most of the water is consumed in the heterogeneous reaction with the rapid formation of hydrated phases.

As an evidence of the extremely high reaction rate of the aluminate phases, it has to be noted that immediately after the mixing of both C_3A and C_4AF with water some reaction products are formed: just after 5 minutes, the C_3A/pure water system presents two peaks at 128ºC and 280°C: with the progress of the hydration the intensity of this latter peak increases, with a corresponding progressive shift towards higher temperature, up to 316ºC after four days of curing. According to previous studies the decomposition occurring around 300°C has been assigned at stable cubic hydrogarnet phases. On the other hand, the XRD analysis performed on these samples effectively evidences the presence of C_3AH_6 (the cubic hydrogarnet product relative to the tricalcium aluminate hydration), together with some unreacted C_3A. No other XRD pattern is detectable, confirming the amorphous nature of the hydrated product responsible for the DTA peak at 128ºC. Another peak at 450ºC is present when the sample is cured four days, due to the loss of a remaining mol of crystal water from the hydrogarnet phase. When the MHEC is added to the paste a relevant inhibition in the formation of the cubic stable phase occurs in the first minutes of the reaction, as testified by the absence of the peak at 300°C, after 5 and 15 minutes from the mixing. These samples present endothermal features at 145, 230 and 260ºC. According to

the XRD spectra, the hydrated products formed in these conditions are not crystalline since no additional pattern is present, apart from that of the anhydrous tricalcium aluminate. The presence of the cellulose ether during the early stages of C_3A hydration stabilizes the amorphous gel, precursor of the stable C_3AH_6. At hydration times over 30 minutes the thermograms are identical to those obtained for C_3A/water. The micrographs obtained on the C_3A/water and C_3A/water/MHEC samples confirmed the results obtained with DTA technique. C_3A cured in pure water for 5 minutes shows a compact and featureless structure. When the cellulose ether is added to the mix the irregular foils, typical of the amorphous gel appear. When both the polymer-free and the polymer-added systems are cured for one hour or more, their morphologies are dominated by the cubic phase, C_3AH_6.
The C_4AF phase presents a similar behavior, with an even more accentuated inhibition effect of MHEC on the stable $C_3(AF)H_6$ during the first hour from the mixing.
The ^{1}H-NMR relaxation times analysis allowed inferring some interesting information about the mechanism of the progressive immobilization of water inside the paste, by comparing the results obtained with this technique with those produced by means of the DSC approach. In particular T_1 and T_2 vs hydration time trends account the different water population according to the Powers model. In this sense, NMR provides additional information about the early stages of hydration and probes the contribution of capillary water (free water) and gel water (physically bound water), which are not differentiate by DSC. Pore size distributions (PSD) of C_3S pastes in pure water and added with MHEC are reported in the figures below. The PSD of the C_3S/water paste (fig. A) in the first step of the hydration is centered in the interval 120-140 mm. After 9 hours the pore size dramatically shifts towards smaller values, in full accordance with previous results, and continue to decrease until 19 hours, when the distribution is almost entirely in the 0-20 mm interval. The system C_3S/water/MHEC (fig. B) presents a PSD centered in the interval 140-160 mm, in the first hours, and only a little shift can be observed in the first 19 hours until 100-120 mm.

References

M. Alesiani, S. Capuani, R. Giorgi, B. Maraviglia, I. Pirazzoli, F. Ridi and P. Baglioni: “Influence of cellulosic additives on tricalcium silicate hydration: nuclear magnetic resonance relaxatione time analysis". *Journal of Physical Chemistry B*, 108, 4869-4874, (2004).

F. Ridi, E. Fratini, F. Mannelli and P. Baglioni: “Hydration process of cement in the presence of a cellulosic additive. A calorimetric investigation". *Journal of Physical Chemistry B*, 109, 14727-14734, (2005).

1A - Hydrogen Storage in Nanomaterials

C. Milanese, V. Berbenni, G. Bruni, P. Cofrancesco, A. Marini

Aims

Study of hydrogen sorption properties (maximum reversible intake, absorption and desorption minimum temperatures, sorption kinetics, and cycling effects) of mechanically activated nanopowders of Mg-rich metallic alloys, bcc and Ti alloys, and complex hydrides.
Search for innovative materials that allow obtaining both the gravimetric and the volumetric hydrogen storage densities and the sorption kinetics required for automotive applications.

Results

These first results concern the hydrogen sorption properties of Mg-rich activated metallic alloys. The interest in magnesium as a hydrogen – storage material originates from the lighter weight, the higher hydrogen weight % of the metal hydride MgH_2 (7.6 %), and the lower price compared with other types of metal – hydrogen systems. However, the slow hydriding / dehydriding kinetics of Mg and the high dissociation temperature of MgH_2 currently limit the practical applications of this system for hydrogen storage. Alloying magnesium with transition metals and rare – earth elements is one of the approaches employed to enhance the reaction thermodynamics and hydrogen – sorption kinetics. Reducing the particles and grain size of the alloys by mechanical milling and adding catalysts have also been used successfully to improve the hydriding kinetics.
In this study, the samples were prepared by high-energy milling of Mg with 10 different metals M (= Al, Cu, Fe, Mo, Ni, Si, Sn, Ti, Zn, Zr) in various weight ratios. The studies were performed on 100 mg samples in a thermogravimetric instrument (Intelligent Gravimetric Analyzer IGA, Hiden Isochema, UK) having a mass resolution of 0.2 μg. The pressure and temperature operative ranges are from 10^{-6} bar to 20 bar and from -15 °C to 400 °C respectively.
Before the analyses, all the samples were "activated" at 400 °C by cycling hydrogen pressure from 1 bar to 20 bar for 4 times, as can be seen in Figure 1. This standard procedure is needed to improve the sorption properties of the milled materials and to obtain homogenous and comparable data for all the mixtures.

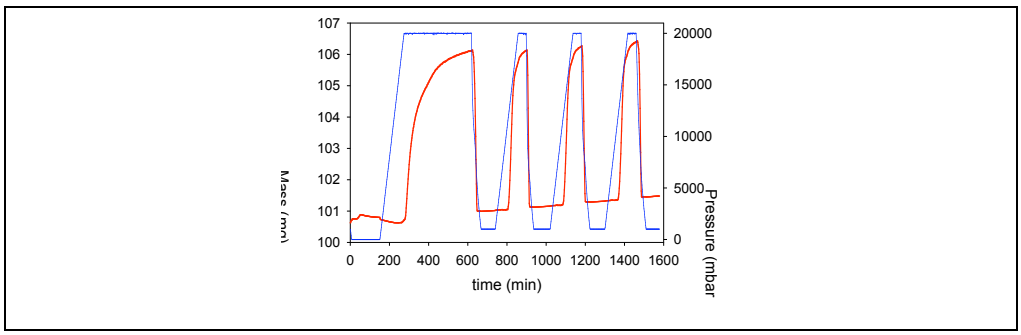

Fig. 1: Pressure (blue line) and weight (red line) profiles recorded during the activation procedure of a Mg-Ni binary mixture.

After the activation, the maximum intake of hydrogen of the samples was measured during 6 hours isobar/isotherm at 20 bar and 370°C ("charge step"). Subsequently, in order to asses if the process was reversible and to gain information about the desorption (minimum desorption temperature and kinetics), the "H_2 charged samples" were subjected to 4 isobars/isotherms steps of 3 hours at 1 bar and increasing temperatures of 250 °C, 300 °C, 350 °C, 400 °C ("discharge step"). Finally, the charge and discharge steps were repeated to test if there was an ageing effect on the sorption properties of the powders. In Figure 2 the mass profile recorded for a Mg – Ni mixture during all the steps of the analysis is reported together with the pressure and temperature signals.

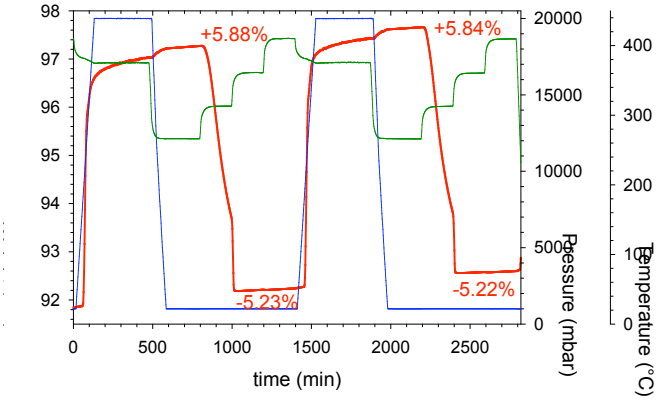

Fig. 2: Weight (red line), pressure (blue line) and temperature (dark green line) profiles recorded during the analysis of a Mg-Ni binary mixture. The values in red correspond to the hydrogen weight % absorbed or desorbed.

Table 1 summarizes the sorption properties for the Mg 70% (in weight) - M 30% binary mixtures. The samples with M = Ni and Cu seem the most promising ones, because of the higher hydrogen maximum intake combined with a good reversibility. Unfortunately, also for these samples the desorption temperatures are higher than 300°C, still too high for automotive applications.

Table 1: Sorption properties for Mg 70% (in weight) - M 30% binary mixtures.

M	**Max wt % absorbed H_2 (1° charge)**	**wt % desorbed H_2 (1° discharge)**	**Min T_{des} (°C)**	**Reversibility = f (n° cycles)**
Ni	+6.0	-6.0	320	No
Cu	+5.1	-5.1	345	No
Mn	+4.4	-2.9	340	Yes
Zn	+4.4	-4.2	365	No
Al	+4.2	-4.2	320	No
Fe	+3.5	-2.5	320	Yes
Ti	+3.3	-2.7	320	Yes
Sn	+3.2	-1.1	400	Yes
Mo	+3.4	-3.1	360	Yes
Zr	+1.6	-0.5	320	Yes

For all the families, reducing the Mg% in the mixtures leads to a decrease of the desorption temperature (to a minimum of 260 °C), but also to a reduction of the maximum H_2 intake (see Table 2).

Table 2: Comparison of the sorption properties of binary mixtures Mg – M with decreasing Mg content.

Composition (weight %)	Max wt % absorbed H_2	Min T_{des} (°C)	wt % desorbed H_2
Mg 77% + Ni 20% + catalyst	+ 6.1	320	- 6.0
Mg 75% + Ni 20% + catalyst	+5.9	320	- 5.8
Mg 54% + Ni 44% + catalyst	+ 4.3	280	- 4.2
Mg 34% + Ni 64% + catalyst	+ 2.5	260	- 2.4
Mg 70% + Cu 30%	+ 5.1	345	- 5.1
Mg 43% + Cu 57%	**+ 3.2**	**280**	**- 3.2**
Mg 70% + Al 30%	+ 4.2	320	- 4.2
Mg 55% + Al 45%	+ 3.8	340	- 2.8
Mg 37% + Al 63%	+ 1.3	350	- 0.7
Mg 70% + Zn 30%	+ 4.4	350	- 4.2
Mg 50% + Zn 50%	+ 2.9	330	- 2.6

In order to gain information about the mechanism of hydrogenation/dehydrogenation, X-ray powders diffraction analysis was performed on the mixtures after both the charge and the discharge steps. After absorption, the peaks of the Mg hydride phase (MgH_2) are present in all the analyzed mixtures. For M = Ti also the binary metal hydrides $TiH_{1.971}$ and $TiH_{1.924}$ and for M = Ni the two ternary hydrides Mg_2NiH and Mg_2NiH_4 form, too. When the sorption process is not fully reversible, MgH_2 is still present after the discharge step.

References

Zaluski L., Zaluska A., Ström-Olsen J.O. – Hydrogen absorption in nanocrystalline Mg_2Ni formed by mechanical alloying. *Journal of Alloys and Compounds* **1995**, 217, 245-249.

Liang G., Boily S., Huot J., Van Neste A., Schulz R. – Mechanical alloying and hydrogen absorption properties of the Mg-Ni system. *Journal of Alloys and Compounds* **1998**, 267, 302-306.

Janot R., Cuevas R., Latroche M., Percheron-Guégan A. – Influence of cristallinity on the structural and hydrogenation properties of Mg_2X phases. *Intermetallics* **2006**, 14, 163-169.

Shao H., Wang Y., Xu H., Li X. – Preparation and hydrogen storage properties of nanostructured Mg_2Cu alloy. *Journal of Solid state chemistry* **2005**, 178, 2211-2217.

1A - Multilayer Thin Films for molecular opto-electronics

G. Caminati, F. Gambinossi, B. Mecheri, P. Baglioni

Aims

Organized molecular assemblies containing surface-active chromophores show specific and useful responses which cannot be achieved in randomly dispersed systems. Molecular design of functional compounds and molecular control of their arrangements will be essential for the construction of highly efficient and functional materials. Langmuir-Blodgett deposition is one of the best methods to prepare highly organized molecular thin films, in which various molecular parameters such as distance, orientation, extent of chromophore interaction or redox potential can be controlled independently in each monolayer. We have been studying photochemical and electrochemical properties of LB films containing electrochromic or photochromic moieties in order to construct molecular electronic and photonic nanodevices.

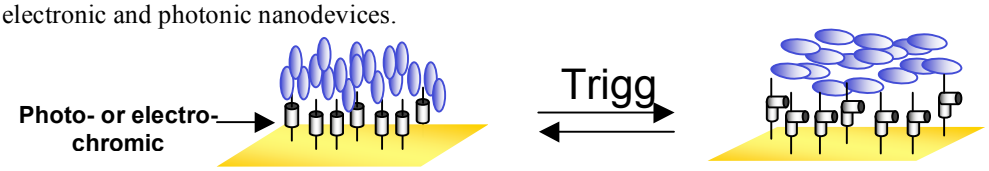

Fig. 1 Schematic representation of an example of the working principle of a "smart" molecular devices.

Results

a) Electrochromic nanodevices

The potential sensitive fluorescent molecules, Di-n-ANEPPS are known to respond to changes in the surrounding medium by modifying their electronic properties.

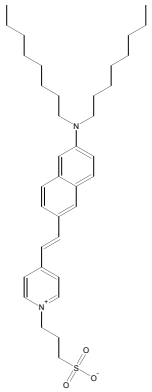

Fig. 2 Chemical structures of Di-8-ANEPPS.

We studied the interfacial behaviour of Di-4-ANEPPS and Di-8-ANEPPS (figure 2) and we found that, like other styryl dyes, these molecules exhibit a strong tendency to aggregate in monolayer and in multilayer systems. In the attempt to avoid undesired aggregation phenomena in the monomolecular layer, we studied mixtures of the dyes with an amphiphilic matrix.

We used different double and single chain amphiphilic compounds both with charged and uncharged head groups.
The film forming properties of the dye in the mixtures were investigated at the water-air interface by means of surface pressure (p) and surface potential (DV) versus molecular area isotherms.
The results show that the stability of monolayers containing Di-8-ANEPPS can be controlled by the appropriate choice of the amphiphile and of the mixing ratio used: stable monolayers were obtained using either DHP (dihexadecylphosphate) and OTMA (Octadecyltrimethylammonium bromide), although p-A isotherms reveal lower stability and higher fluidity in the case of OTMA.
The spectroscopic behaviour of pure and mixed films at the liquid-air interface as well as in LB films was investigated and compared with the electronic spectra of Di-8-ANEPPS in solution.
The absorption spectra of the pure dye and of the mixtures at liquid-air interface show the formation of domains of H-aggregates within the amphiphilic matrices. In particular, in the case of Di-8-ANEPPS/OTMA mixtures with low content of the chromophore no monomer species are detected in Langmuir and in LB films neither by absorbance spectroscopy nor by fluorescence emission. Interestingly, no aggregates were detected in the absorption and emission electronic spectra of the 4:1 Di-8-ANEPPS/OTMA monolayer, either at water-air interface and in LB film; in both cases we determined that the chromophoric part of the dye molecule resides in a polar environment.

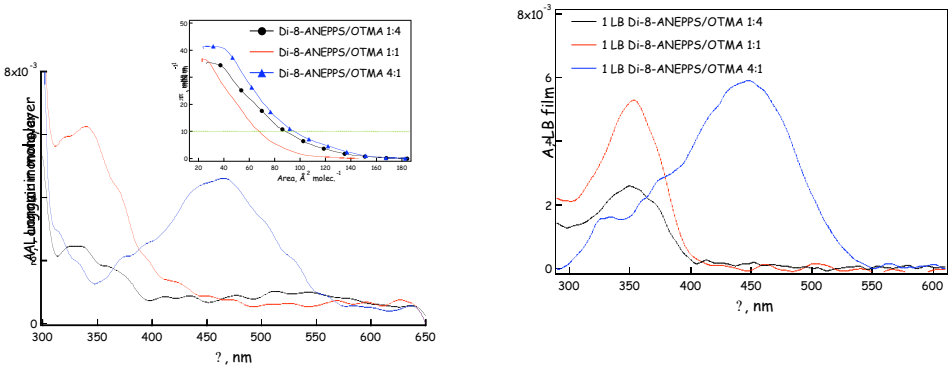

Fig.3 UV-Vis absorption spectra of some Di-8-ANEPPS/OTMA monolayers at water-air interface **(a)** and as LB films **(b)**.

These results on the aggregation behaviour in an organic matrix appear particularly relevant since the understanding of energy migration and transfer in monolayers and LB systems is essential for the rational design and fabrication of microelectronic devices based on vectorial energy and electron transport.

b) Photochromic nanodevices

Photochromic materials in organized molecular assemblies have been the subject of extensive investigations in recent years because of their potential applications in optical switches, memories and displays. When photochromic moieties are introduced in a polypeptide matrix their photoisomerisation reactions can induce conformational changes of the whole macromolecule, amplifying the perturbation due to the single chromophore. Therefore, photochromic polypeptide assemblies can be highly promising materials for photomodulated devices.

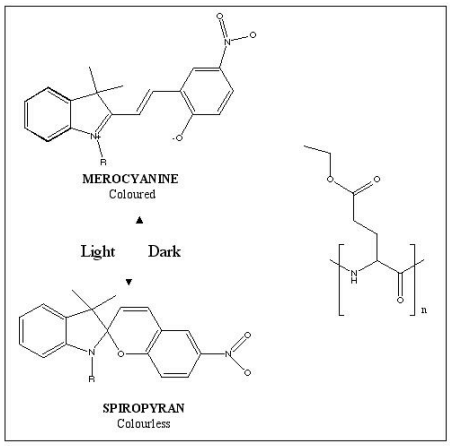

Fig. 4 Chemical structure of PSG. The reversible isomerization between the open merocyanine form (trans) and the close spiropyran one (cis) is driven by the molecule irradiation.

We focused our studies on the investigation of the structural and optical properties of bi-dimensional systems of a merocyanine-substituted poly (L-glutamic acid), PSG (see figure 4). In hexafluor-2-propanol solution, the irradiation with visible light promotes the reversible isomerization of the merocyanine units to spiropyran form. We found that the photochromic biopolymer, PSG, forms stable floating monolayers at the water air-interface that were characterised by means of Surface Pressure-Molecular Area (p-A) and Surface Potential-Molecular Area (DV-A) isotherms, typical results are reported in figure 5.
The shape and the features of the isotherms are different in the case of dark-adapted and irradiated monolayers, indicating that the photoisomerization between merocyanine and spiropyran occurs also at the water-air interface.

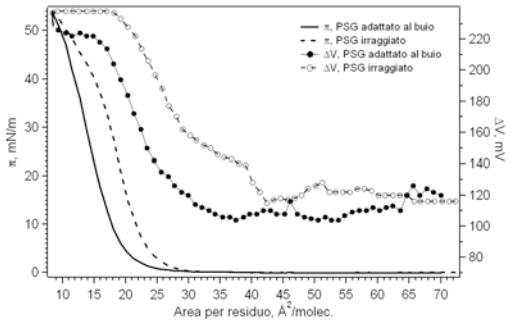

(a)

(b)

Fig. 5 **(a)** Spreading isotherms p-A e DV-A of dark-adapted and irradiated PSG monolayers. **(b)** Scheme of the different packing of the PSG molecules in monolayer induced by irradiation.

Moreover we transferred polypeptide monolayers onto solid supports, by means of the Langmuir-Blodgett technique.
UV-Vis Absorption and Circular Dichroism Spectra, acquired on dark-adapted and irradiated LB films, showed how the biopolymer films respond to the sunlight irradiation.

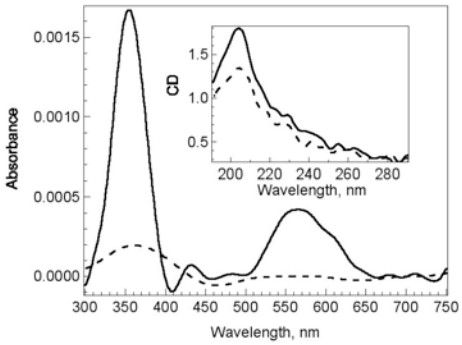

Fig. 6 UV-Vis Absorption Spectra (inset Circular Dichroism Spectra) of typical LB film of PSG transferred onto quarz. Solid line: dark-adapted film. Dashed line: irradiated film.

References

H. Huesmann, G. Gabrielli, G. Caminati, *"Monolayers and Langmuir-Blodgett films of the electrochromic Dye Di-8-ANEPPS"*, Thin Solid Films 327-329 (1998) 804-807.

F. Gambinossi, M. Mannini, P. Baglioni, G. Caminati, *"Spectroscopic properties of Langmuir-Blodgett films of a potential-sensitive dye"*, Materials Science and Engineering C 23 (2003) 897-902.

B. Mecheri, P. Baglioni, O. Pieroni, G. Caminati, "*Molecular Switching in Nano-Structured Photochromic Films of Biopolymers"*, Material Science and Engeneering C 23 (2003) 893-896.

F. Gambinossi, P. Baglioni and G. Caminati, *"Spectroscopic characterization of a styryl dye in monolayer at liquid-air interface"*, Physical Chemistry Chemical Physics, submitted for publication.

B. Mecheri, G. Caminati, P. Baglioni, C. Satriano, A. Auditore, A. Licciardello, G. Marletta, "*Optical Properties and Morphology of Langmuir-Blodgett Fims of Photochromic Biopolymers"*, Physical Chemistry Chemical Physics, submitted for publication.

1A – Multilayered Nanofilms for molecular opto-electronics

G. Caminati, F. Gambinossi, B. Mecheri, S. Ciappelli, P. Baglioni

Aims

The project is focused on the study of nano-films containing electrochromic, photochromic or electroluminescent moieties in order to construct nanodevices for molecular electronics and photonics.

Results

The field of nanotechnology for molecular electronics ties two areas together: the search for compounds with the desirable function and the assembly of the individual molecules into new devices with superior properties.

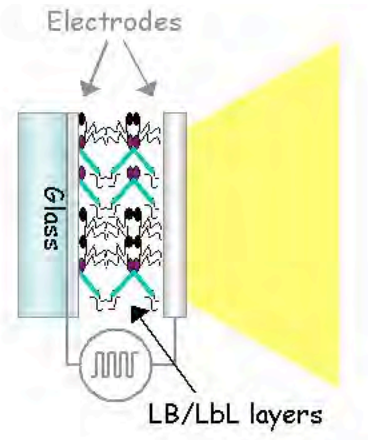

Fig. 1 Schematic representation of an example of the working principle of a molecular device.

Most of these applications require preparation of stable and well-organized films with fast fabrication processes. Langmuir-Blodgett multilayer deposition is one of the best methods to prepare highly organized molecular thin films, but large scale production is prevented by the lack of information on the parameters ruling the efficiency of the process in LB super-lattices and by the relative poor stability of these assemblies. The research activity has shown that stable assemblies of controlled thickness and known in-plane structure can be successfully fabricated by means of a combination of different nano-techniques: Langmuir-Blodgett (LB) method, chemical Self-Assembly and Layer-by-Layer (LbL) polyelectrolytes deposition. Moreover, proper tailoring of the layer sequence will provide the desired spacing and coating of the nanosystem.

a) Electrochromic materials

The potential-sensitive fluorescent molecules, DI-n-ANEPPS respond to changes in the surrounding medium by modifying their electronic properties. We studied the interfacial behaviour of DI-8-ANEPPS (figure 2) and we found that this molecule exhibits a strong tendency to aggregate in monolayer and in multilayer systems. In the attempt to avoid undesired aggregation phenomena in the monomolecular layer, we studied mixtures of the dyes with an amphiphilic matrix.

The film forming properties of the dye in the mixtures were investigated at the water-air interface by means of surface pressure - area (π-A) and surface potential – area (ΔV-A) isotherms. The results show that the stability of monolayers containing DI-8-ANEPPS can be controlled by the appropriate choice of the amphiphile and of the mixing ratio used.
In particular we found the highest compactness and stability for DI-8-ANEPPS monolayers mixed with a large amount of an anionic surfactant, DHP (figure 2).

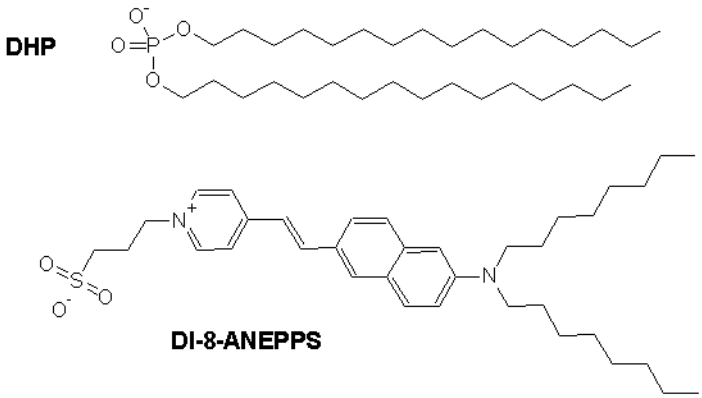

Fig. 2 Chemical structures of DHP and DI-8-ANEPPS.

Information on the mechanism of dye aggregation in LB film as a function of the stabilization time of the floating monolayer was obtained by means of UV-Visible absorption spectroscopy (figure 3).

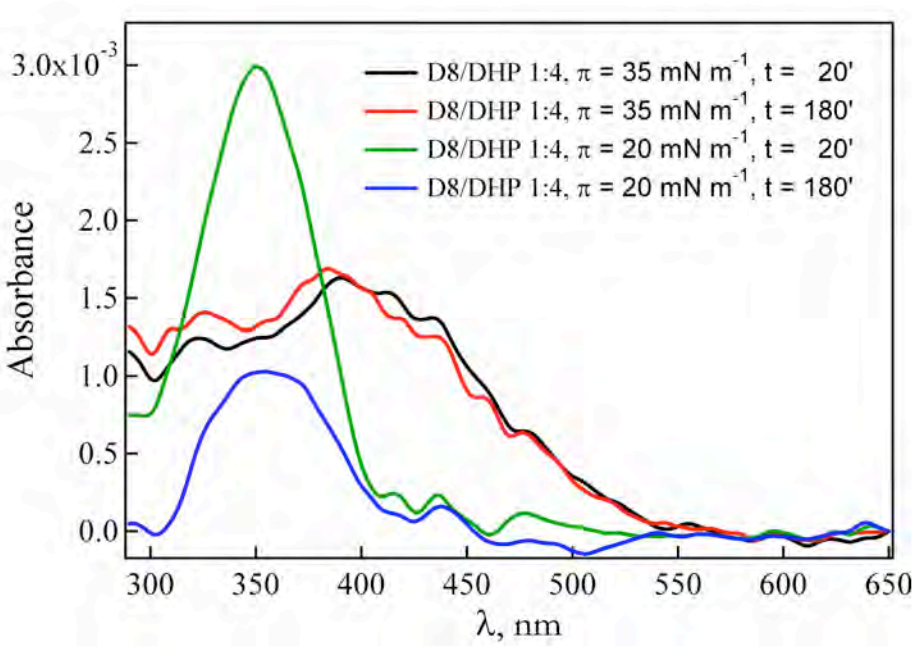

Fig. 3 UV-VIS absorption spectra of DI-8-ANEPPS/DHP LB film.

The absorption spectra of 1 LB of the DI-8-ANEPPS/DHP mixture transferred at π = 35 mN m^{-1} do not show any variation in wavelength and absorbance with the stabilization time. The broader band is centred at 400 nm and it is responsible of the π - π^* transition of the monomeric dye. On the contrary the UV-Visible absorption of one monolayer of DI-8-ANEPPS/DHP transferred at 20 mN m^{-1} shows a marked decrease with time of absorbance at 350 nm due to the contribution of H-aggregate molecules. Moreover, preliminary studies on the inspection of the multilayers structure through confocal laser scanning microscopy (CLSM) reveals the presence of strongly fluorescent circular domains (figure 4). Exciting the nanostructures with an Ar laser at 458 nm, we observe two bands at 600 and 630 nm, the latter band is ascribed to the emission of the monomer species.

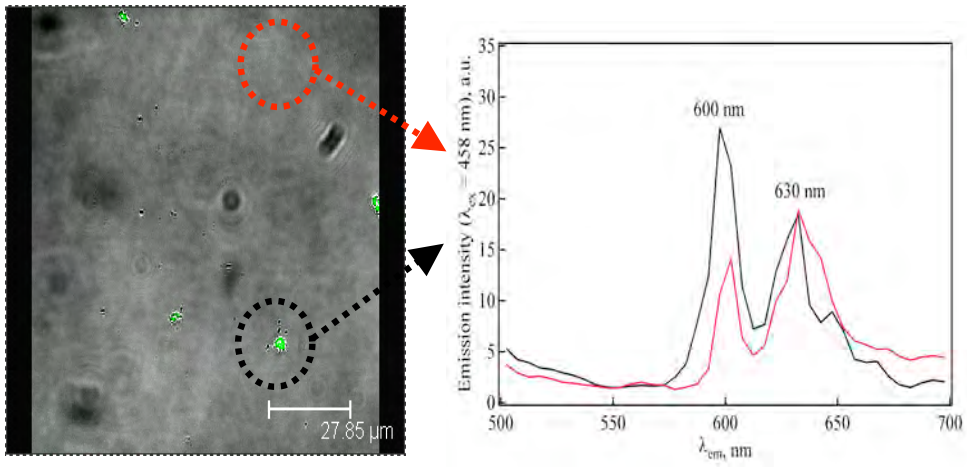

Fig. 4 Confocal Laser Scanning Microscopy images of 1 LB layer of the DI-8-ANEPPS/DHP mixture.

Aggregation behaviour results may help in understanding the processes of energy transfer in restricted geometries since energy migration is an essential step for the design and fabrication of devices based on vectorial energy and electron transport.

b) Photochromic nano-devices

Photochromic materials in organized molecular assemblies have been the subject of extensive investigations because of their applications in optical switches, memories and displays. We investigated the photochromic behaviour of a spyropyran-containing Poly (L-glutamic acid) in 2-dimensional structures, i.e. Langmuir Monolayers and Langmuir-Blodgett films. The photochromism of spiropyrans is due to the photoisomerization between the closed spiropyran form and the open merocyanine one. When photochromic moieties are introduced in polypeptide matrices their photoisomerisation reactions can induce conformational changes of the whole macromolecule, amplifying the perturbation due to the single chromophore. Therefore, photochromic polypeptide assemblies can be highly promising materials for photomodulated devices. We investigated the structural and optical properties of a merocyanine-substituted poly (L-glutamic acid), PSG, in solution as well as in bi-dimensional systems. In hexafluor-2-propanol solution, the irradiation with visible light promotes the reversible isomerization of the merocyanine units to spiropyran form. We found that the photochromic biopolymer, PSG, forms stable floating monolayers at the water air-interface that were characterised by means of Surface Pressure-Molecular

Area isotherms. Moreover we transferred polypeptide monolayers onto solid supports, by means of the Langmuir-Blodgett technique. UV-Vis Absorption and Circular Dichroism Spectra, acquired on dark-adapted and irradiated LB films, showed how the biopolymer films respond to the sunlight irradiation. The morphology, compactness and chemical structure of the deposited PSG films were investigated by means of Atomic Force Microscopy, Time-of-Flight Secondary Ion Mass Spectrometry as well as Ellipsometry. Typical AFM results are reported in figure 5.

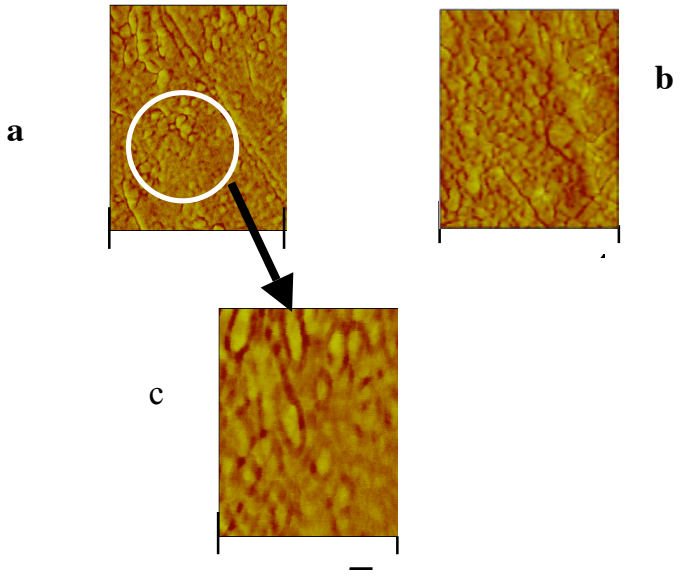

Fig. 5 AFM images of 1 (a) and 3 LB (b) layers (1x1 μm). (c) 500x500 nm enlargment of (a).

The results indicated a dishomogeneous coverage and significant morphological differences between mono- and multilayers of PSG, which could be related to the different packing of PSG molecules.

c) Electroluminescent polymers

We investigated the performances of a molecularly organized Organic Light Emitting Diode (OLED), constructed using a combination of polyelectrolyte Layer-by-Layer (LbL) assembly and Langmuir-Blodgett (LB) deposition. The hetero-structure was based on a poly(p-phenylenevinylene) (PPV) derivative and on poly(methacrylic acid) (PMA). Furthermore, we inserted clay layers in different positions of the multilayered structure in the attempt to overcome the problem of reduced OLED efficiency due to the presence of oxygen and humidity. Figure 6 shows a schematic representation of the sequence of layers chosen for the hybrid nanostructure.

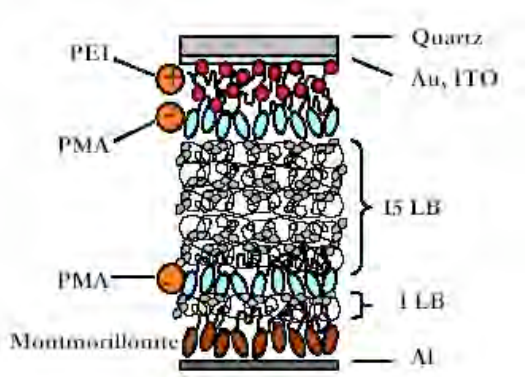

Fig. 6 Hybrid multilayered structure.

The polyelectrolytes used in this study were the cationic polyethylenimine (PEI) and the anionic polymethacrylate (PMA): the monomer units of the polymer and of the polyelectrolytes are shown in figure 7.

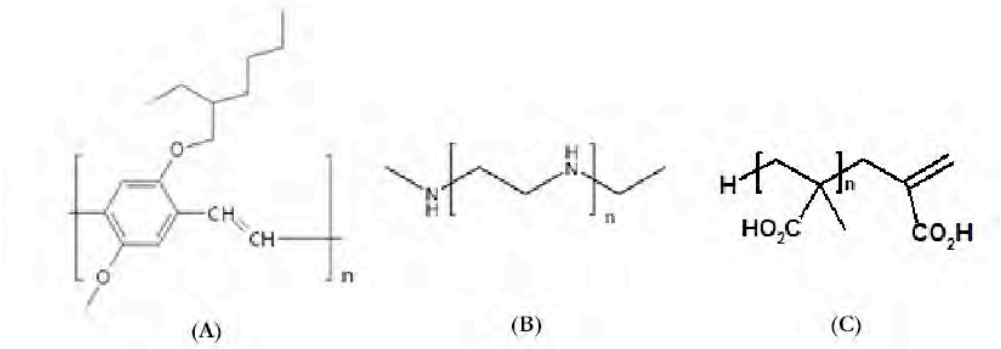

Fig. 7 Monomeric units of MEH-PPV (**A**), PEI (**B**) and PMA (**C**).

The film-forming properties of the PPV derivative were investigated at the water-air interface by recording surface pressure and surface potential isotherms. The results were correlated to the morphological structure of the polymer monolayer investigated by means of Brewster Angle Microscopy (BAM). LB transfer was achieved for different molecular packing of the PPV monolayer.
The assembling process of the LbL multilayers on the LB film was analyzed in situ by Quartz Crystal Microbalance (QCM) measurements. The growth of such multilayered hybrid structures was successfully followed by means of acoustic shear waves investigation. Information on the damping of the acoustic waves provided direct access to the viscoelastic properties of each single layer of the nanodevice.
Figure 8 shows the layer-by-layer adsorption of PEI and PMA at the third, the fifth, the seventh and the ninth overtones.
PEI and PMA were adsorbed from solution of 0.1 M NaCl, adjusted to pH 10 and 3.5, respectively. A rinsing step consisting of an aqueous solution of 0.1 M NaCl was included between the adsorption of the polyelectrolytes.

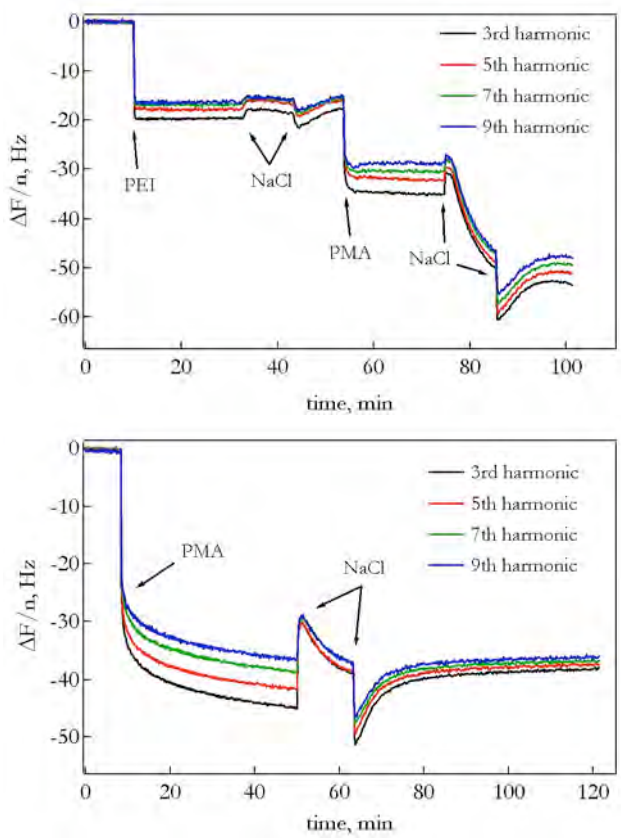

Fig. 8 QCM data showing the change in normalized frequency as a function of the adsorption of polyelectrolyte layers of PEI and PMA onto gold coated quartz **(A)** and onto MEH-PPV LB films **(B)**.

A rapid decrease in frequency is observed due to the adsorption of the cationic PEI to the substrate. After proper rinsing, addition of PMA solution in the measuring chamber resulted in a further decrease of the resonant frequency due to the formation of a PMA overlayer.
The sensor crystal was then dismounted from the chamber and connected to the dipper of a film balance. We deposited 15 Y-type layers of MEH-PPV on top of the LbL film. Figure 8 B shows the adsorption of a second PMA layer over the LbL/LB sequence.
To obtain further information on the thickness and on the viscoelastic properties of the layers we analyze the QCM data by using two models: a rigid film (RF) and a viscoelastic film (VF) model. Both the model gave good agreement between calculated and experimental curves of Δf and ΔD. The optical response of the hybrid multilayer was tested measuring the electronic absorption and the emission spectra as a function of LB packing and for different LB/LbL/Clay combinations.

References

Gambinossi, F., Baglioni, P., Caminati, G., *Structural and optical properties of a supramolecular assembly of poly[2-methoxy-5-(2'-ethylhexyloxy)-1,4-phenylenevinylene)]*, VII Congresso Nazionale di Chimica Supramolecolare, Firenze (Italy), September 2005.

Caminati, G., Baglioni, P., Gambinossi, F., *In situ investigation of the morphology and of the interaction of charged surfactants with a styryl dye by absorbance spectroscopy and Brewster angle microscopy at the water-air interface,* IXth European Conference on Organised Films (ECOF 2004), Valladolid (Spain), July 2004.

Caminati, G., Baglioni, P., Gambinossi, F., *Multilayer structures of electroluminescent polymers based on a combination of Layer-by-Layer assembly and Langmuir-Blodgett deposition,* IXth European Conference on Organised Films (ECOF 2004), Valladolid (Spain), July 2004.

Mannini, M., Gambinossi, F., Baglioni, P., Caminati, G., *Immobilization of a fluorescent dye in Langmuir-Blodgett films*, Bioelectrochemistry 2003, 63(1-2), 9-12.

Gambinossi, F., Baglioni, P., Caminati, G., *Self-aggregation and phase separation of a styryl dye in monolayer at the liquid-air interface and in Langmuir-Blodgett films,* Physical Chemistry Chemical Physics 2004, 6(7), 1587-1591.

Gambinossi, F., Mannini, M., Baglioni, P., Caminati, G., *Spectroscopic properties of Langmuir-Blodgett films containing a potential-sensitive dye*, Materials Science and Engineering C 2003, 23(6-8), 897-902.

Mecheri, B., Caminati, G., Baglioni, P., Satriano, C., Auditore, A., Licciardello, A., Marletta, G., *Optical Properties and Morphology of Langmuir-Blodgett Fims of Photochromic Biopolymers,* in preparation

Gambinossi, F., Mannini, M., Baglioni, P., Caminati, G., *Morphological and spectroscopic studies on Langmuir-Blodgett films of an electro-active molecule*, to be submitted to Advanced Materials.

1A –NANOGRES®: A novel nanostructured coating of ceramic materials

Moira Ambrosi, Luigi Dei, Piero Baglioni

Aims

The improvement of both mechanical and stain resistance properties of ceramic products are central issues for the manufacturing of high quality flooring and coating materials. As it is known, by coating either a finished or crude ceramic support with a powder of glassy material (commonly called "frit" and consisting of a mixture of oxides melted, rapidly cooled down and finally ground) and by subsequent baking it at temperatures ranging between 600 and 1450 °C, a more or less transparent layer can be obtained, depending on the frit used. Although the glassy layer protects the possible underglaze decoration and reduces stain penetration, the need of relatively high thickness results in a remarkable decrease of mechanical properties, such as hardness and resistance to abrasion, so accelerating the product usury. Evolution in technical porcelain grés manufacturing allowed production of tiles with more homogeneous composition, harder and more resistant to usury, slip and low temperatures than the traditional glazed ceramics. Nevertheless, due to their natural surface microporosity, unglazed porcelain stoneware are susceptible to dirt penetration and therefore scarcely stain resistant.
The aim of our work was to develop a versatile procedure that allowed to solve the above mentioned technical grés stain resistance problem with simultaneous enhancement of hardness and resistance to usury.

Results

It was found that by applying to tiles a particular mixture of ceramic oxides, called NANOGRES®, both mechanical and stain resistance properties could be improved.
The ceramic oxides nano- and micro-particles were dispersed in water and the so obtained suspension applied onto the ceramic supports by spraying during the usual productive cycle before baking. The desired amount of oxides mixture was deposited filling the microporoes of the crude material. During baking, glass melted within the surface cavities filling them and making the final product smooth and stain resistant. Moreover, the particular composition of the mixture used increased the tile hardness and resistance to abrasion.
Thus, NANOGRES® becomes the ideal coating several ceramic products, definitively solving any problem of stain-resistance, mechanical resistance and permeability of materials featured by a surface microporosity. Without altering the optical appearance, NANOGRES® can be used with light colors, usually avoided due to the possible stains formation.
The modest cost and versatility makes the application procedure easily extendible on an industrial scale to a wide range of ceramic products, such as floorings, coatings, dishes and crockery, table and kitchen products, sanitary and high tech objects like insulators.

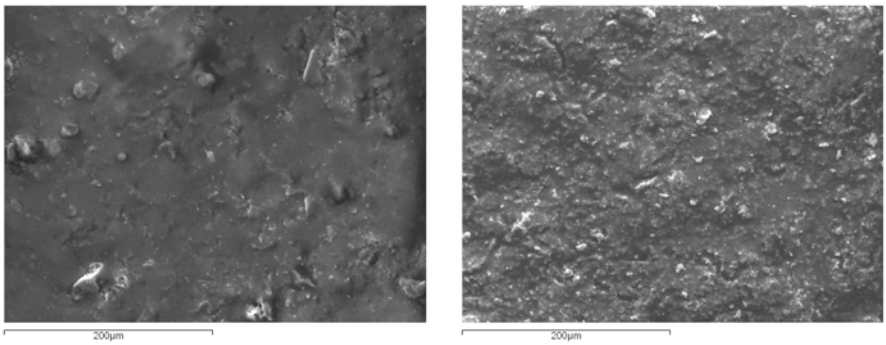

(a) (b)

Fig. 1. Unglazed porcelain grés. a), Untreated; b), Treated by NANOGRES®: significant closure of surface microporosity.

(a) (b)

Fig. 2. Unglazed porcelain grés. a), Untreated; b), Treated by NANOGRES®: The tile becomes totally stain-resistant.

Sample	**Treatment**	**Vickers hardness, HV (± 10%)**	Critical surface tension, γ_c / **$mN \cdot m^{-1}$ (± 5%)**	Stain resistance
Technical porcelain grés	Untreated	800	7.8	NO
	NANOGRES®	Up to 2100	12.3	YES

Table 1. Vickers hardness, HV, critical surface tension, γ_c, and stain resistance of technical porcelain grés before and after treatment by NANOGRES®.

1A – Nanosensors based on ultrathin organic films

G. Caminati, F. Gambinossi, M. Puggelli, S. Morandi.

Aims

The research is focused on the preparation of new molecular devices for sensor applications by means of a combination of different nanotechniques tailored to meet specific requirements: Langmuir-Blodgett (LB), Self-Assembly (SA) and Layer-by-Layer (LbL) technologies.

Results

Our previous research activity has shown that monomolecular layer transfer (LB) alone or combined with covalent self-assembly and/or Layer-by-layer deposition allow to produce stable structures with controlled geometry and desired functionalities. This approach is applied to the construction of novel miniaturized devices for diagnostic purposes (either in biomedical, environmental or food-safety fields). Such nanodevices can be directly coupled to diverse detection systems to achieve maximum response in the quantitative determination of a variety of water-soluble substances.

We focused our studies on the recognition of food-contaminants whose widespread use is posing increasingly high risks to the health of the population. The proposed nanodevice can be used either in screening test at the end of the manufacturing cycle or for clinical biodagnostics.

In particular we investigated three main classes of contaminants: a) heavy metal ions such as Nickel, Cobalt and Copper, b) pesticides, heavily employed in agricultural processing and responsible of disorders of the central nervous system, and c) one of the most used families of antibiotic substances, i.e. rifamycins.

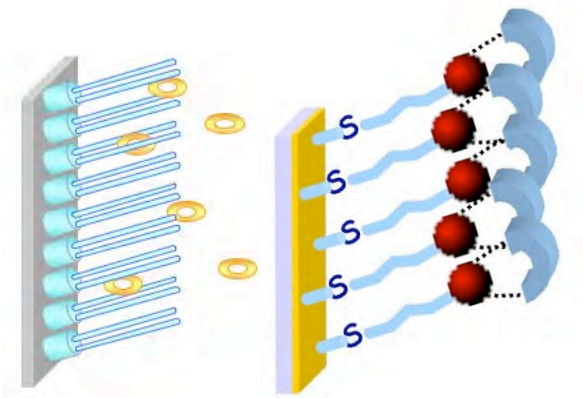

(a) (b)

Fig. 1 Scheme of the architectures designed for the realization of the sensors.

We adopted two different approaches depending on the substance to be detected. In the case of drug molecules we exploited their affinity with phospholipid membrane to promote their incorporation into the LB system as reported in figure 1 a. For the other two examples we chose the self-assembly method either on gold or quartz surfaces (figure 1b).

a) Nanosensors for the detection of heavy metals in water

The nanoassemblies were constructed on gold surfaces as well as on quartz substrates to allow the flexible choice of different experimental methodologies for their characterization.

Moreover, diverse utilization strategies may be envisaged for the final device depending on the substrate adopted. We studied the reactivity of a functionalized surface of self-assembled nanostructures towards metal ions complexation. The formation of the complex at the surface was successfully monitored by means of two different but complementary detection methods, i.e. Quartz Crystal Microbalance with dissipation monitoring (QCM) and UV-Vis-Nir absorption spectroscopy.
A scheme of the working principle of a typical QCM instrument is reported in figure 2.

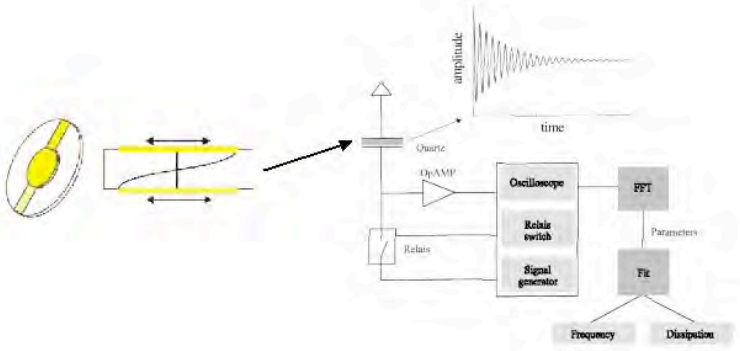

Fig. 2 Scheme of a QCM instrument.

Nanosensors for the determination of heavy metal ions in water were constructed both on gold and quartz substrates. In the former case we used a class of thiols that directly chemisorbed on the surface, whereas silanizing agents were chosen for the quartz based systems. The complexation of the metal ions was followed monitoring the increase of the characteristic absorption bands for SAM functionalized quartz slides.

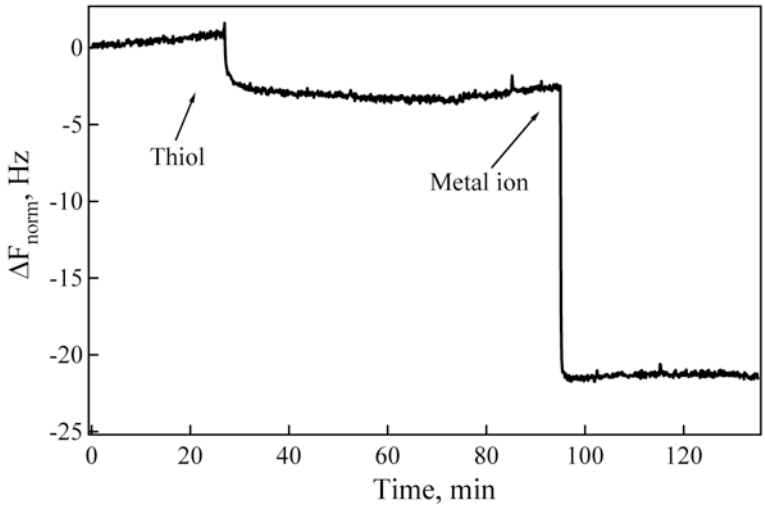

Fig. 3 QCM data showing the change in normalized frequency (third harmonic) upon addition of a solution of functionalized thiols and of metal ions.

QCM measurements were employed to study the complexation process for self-assembled monolayers of organic chelants on gold (see figure 3).

The results indicated that the functionalized molecules form a rigid self-assembled film on gold that strongly associate with the metal ions when they are added in the measurement chamber. Moreover, we analyzed the electrochemical properties of the self assembly during the adsorption process, adding a potentiostat to the QCM instrument. This technique allowed to use the redox fingerprint of the metal complex to determine the complexation kinetics and the association constant at the SAM surface. The data were correlated to the complexation constant extracted from the spectroscopic data obtained for quartz and ITO substrates.

b) Pesticides in fluid matrices

The above self-assembled system was further exploited for the detection of pesticide in fluid matrices monitoring the variation in the QCM signal upon addition of the analyte in the measuring chamber. Figure 4 shows the frequency decrease due to the adsorption of the pesticide molecule on the QCM crystal.

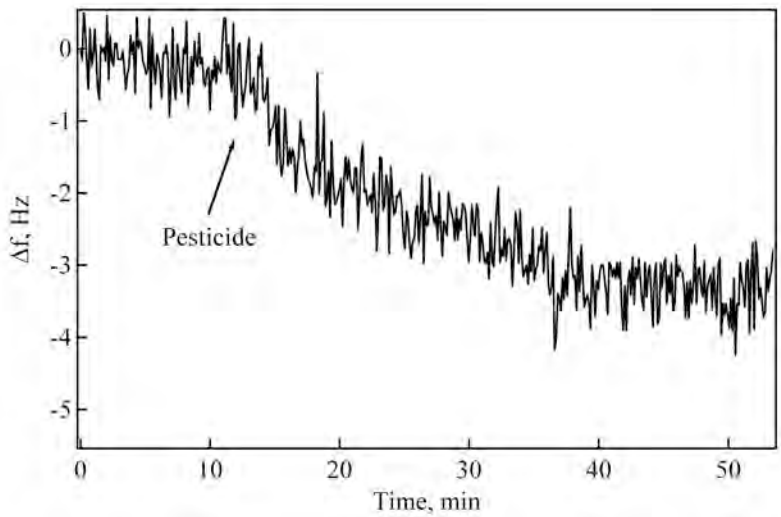

Fig. 4 QCM data showing the change in frequency at the third harmonic upon addition of pesticide on the functionalized gold coated quartz.

c) Biosensors for veterinary antibiotics.

The present research line is focused on the study of the interaction between a suitable bio-reactant used for the construction of a Langmuir-Blodgett system and a toxic compounds localized in the surrounding aqueous medium.

The resulting nanofilm can be directly coupled to the detection devices: we explored both spectroscopic and electrochemical detection methods in order to build a screening sensor for the determination of residues of Ryfamicin in aqueous matrices. These compounds belong to a class of antibiotics well known to induce strain resistance. The chemical structure of typical drug molecule studied is reported in figure 5.

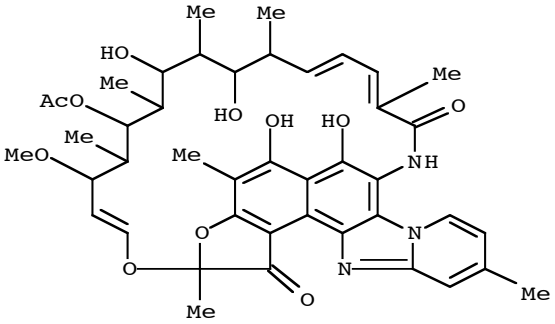

Fig. 5 Chemical structure of rifaximin

In previous studies, we examined spreading monolayers of several amphiphiles in the presence of Ryfamicins (Rfs) in the subphase by means of surface pressure-area and surface potential-area isotherms combined with Brewster Angle Microscopy. We screened several phospholipids differing in the polar head group or in the length of the alkyl chain. A systematic study allowed to select Dipalmitoyl Phosphatidylglycerol (DPPG) as the most interactive phospholipid on the basis of the experimental characterization at water-air interface.

LB films of DPPG matrix were prepared and immersed in a solution containing the antibiotic under examination to allow the incorporation of the drug in the nanofilm. UV-Vis spectroscopy as well as cyclic voltammetry were performed on the samples, both methods evidenced the presence of the drug molecule in the LB film. In figure 6 we report the increase in oxidation current upon increasing content of rifaximin in solution for bare glassy carbon (GC) electrode as well as for LB covered glassy carbon. The effect of signal amplification due to presence of the LB nanofilm on the surface is evident.

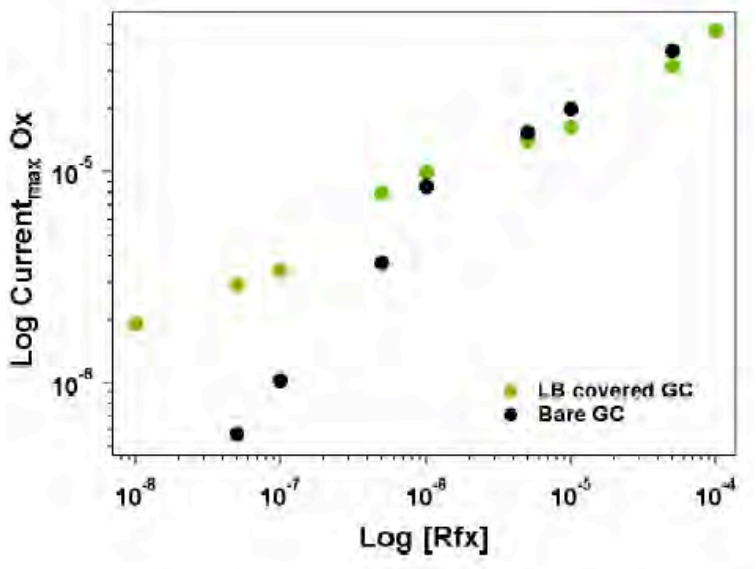

Fig. 6 Peak oxidation current as a function of Rfx concentration.

The data in figure 6 clearly highlight that it is possible to detect Rfx concentrations lower than $1x10^{-8}$ M only when the GC electrode is functionalized with an LB film of DPPG.

This result is particularly relevant for sensor applications since the MRL (Maximum Residue Limit) set by the EU for Rifaximin in milk is $1x10^{-7}$ M.

References

Mecheri, B., Gambinossi, F., Nocentini, M., Puggelli, M., Caminati, G., *Modulation of tetracycline-phospholipid interactions by tuning of pH at the water-air interface,* Biophysical Chemistry 2004, 111(1), 15-26.

Gambinossi, F., Mecheri B., Nocentini, M., Puggelli, M., Caminati, G., *Effect of the phospholipid head-group in antibiotic-phospholipid association at water-air interface,* Biophysical Chemistry 2004, 110(1-2), 101-117.

Morandi, S., Nocentini, M., Puggelli, M., Caminati, G., *Spectroscopic investigations of antibiotic interaction with phospholipid monolayers and Langmuir-Blodgett films*, XVII Conference of the European Colloid and Interface Society, Florence (Italy), September 2003.

Morandi, S., Nocentini, M., Puggelli, M., Caminati, G., *Langmuir-Blodgett technology as an useful tool for biosensor building to antibiotic recognition*, XXI Congresso Nazionale della Società Chimica Italiana, Torino (Italy), June 2003.

Gambinossi, F., Baglioni, P., Caminati, G., *Nanosensors for the detection of pesticides in fluid matrices*, Patent to be submitted.

Morandi, S., Puggelli, M., Caminati, G., *Phospholipid nanofilms for the detection of Rifaximin in solution*, International Journal of Environmental and Analytical Chemistry 2005, 85, 665-673.

1A - Nanostructured coatings for engineering tribological applications

P. Matteazzi in collaboration with MBN (I), HEF R&D (FR), Liebeherr Aerospace Tolouse S.A. (FR), IfU GmbH Privates Institut für Umweltanalysen (D), Poeton Industries Ltd (UK), Ecole Nationale d'ingenieurs de Saint Etienne (F).

Aims

Novel nanophased powders materials to be applied for fabrication of nanostructured solid lubricants coatings with enhanced wear-resistance at high temperatures and loads;
Energy beam synthesis of nanostructured wear resistant coatings for machine-building industry with the following parameters: thickness100-500 μm; operating temperature up to 900°C, allowable Hertz pressure up to 1100 Mpa, friction coefficient 0.06-0.20;
Thermodiffusion synthesis of solid lubricant compositions based on refractory metals disulphides for aerospace and automotive industries with the following parameters: htickness1-100 μm; operating temperature up to 800°C, allowable Hertz pressure up to 1200 Mpa, friction coefficient 0.01-0.12.

Results

The activity foreseen the development of advanced high-performance Solid Lubricant Coatings (SLC) through materials engineering approach in which required properties will be finely tuned by: designing an appropriate matrix for the solid lubricant as a high performance material (nanostructured, functionally graded), and synthesising by Mechanomaking (the industrial evolution of mechanical alloying and mechanosynthesis) of nanophased powder materials to be applied for coating fabrication. In order to obtain powders best suited for Tribo applications an air-classifier has been developed and assembled. Subsequently it has been equipped with a Jet-mill systems (low energy milling) in order to improve the shape of the particles: it permits to obtain particles more rounded (see *Fig.1*) with better flowability.

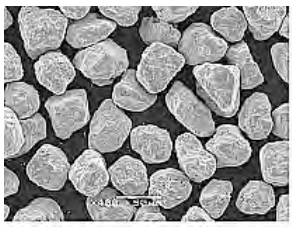

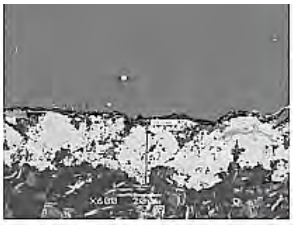

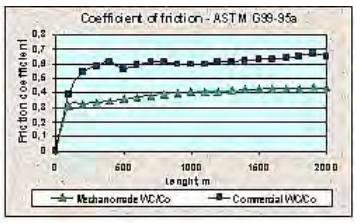

Different processes of spraying have been used and different results have been obtained. The wear tests are performed for Plasma Spraying, HVOF (High Velocity Oxy fuel) spraying, laser cladding, D-gun spraying and thermo-diffusion synthesis.
The coatings, obtained with nanophased powders, demonstrate advantages in terms of structure, porosity rate (about 1%), pore distribution and result of tribological tests are promising (see *Fig.3*). In order to improve the lubrication performance, a new powder with addition of solid lubricant ($WC/Co/CaF_2$) has been produced by energy milling and processed by HVOF spraying. The results of erosion and tribological tests on these coatings are expected. Full-scale industrial test (under conditions imitating real exploitation environment), will be performed if the tribolological tests will be positive.

1A – NIR investigation of the confined water into organic and inorganic systems

E. Fratini, P. Luciani, S. Milani, F. Ridi, C. Vannucci, P. Baglioni

Aims

Investigation of the properties of confined water by means of NIR spectroscopy in hydrating inorganic samples (silicate and aluminate pastes) and proteins.

Results

The study of water confined in restricted geometries has a particular relevance in many chemical and biological processes. The structure and the biological activity of the proteins, for example, are essentially determined by the presence of a few layers of water molecules, strongly interacting at the protein surface. The influence of the surface hydrophilicity-hydrophobicity on the structural and dynamical properties of the water molecules (at the nanoscale level) has been extensively investigated in inorganic model systems such as carbon nanotubes or silica gels. In this regard, cementitious pastes are 'sui generis' systems worth of investigation, since they evolve continuously from both a chemical and a mechanical point of view. Cement develops its characteristics as a result of heterogeneous reactions between solid phases (calcium silicates and/or aluminates) and water.

Near infrared spectroscopy (NIR) provides information on the vibrational low harmonics modes of stretching and bending of hydrogen bonds. The absorption bands in the near infrared region are known to be excellent markers of the state of water O-H bonds, since both the strength and the geometry of these bonds affect the frequency of the absorption peaks. The "state" of water molecules has been previously studied for different matrices as pure water, electrolytic solutions, and hydrogels. In particular, the first overtone band of the O-H stretching mode of water (~7000 cm^{-1}) has been deeply investigated and several structural models have been proposed to account for the peculiar vibrational spectrum of the water.

We acquired the NIR spectra of hydrating tricalcium silicate and tetracalcium ferro-aluminate (two of the major components of a common cement powder) pastes as a function of the hardening time. After three hours from the mixing the spectrum is dominated by the spectroscopic features of the liquid water, with two broad bands approximately at 7000 cm^{-1} and 5000 cm^{-1}, attributed respectively to the first overtone of OH stretching and to the combination band (stretching + bending). During the hydration process the total intensity of the characteristic bands decreases, because of the conversion of the water into hydrated phases. Contextually the intensity of the sharp peak at 7083 cm^{-1} increases, due to the formation of portlandite, $Ca(OH)_2$.

We performed a Gaussian de-convolution in terms of five components on the 7000 cm^{-1} band in order to have a deeper insight on both the state of water inside the pastes and its evolution during the hydration reaction. The Gaussian de-convolution results are shown in the figure 1.

We used five Gaussian functions to fit the experimental data, denoted with Greek characters (α, β, γ, δ and ε). The Gaussian ε has been used to account for the very sharp peak at 7083 cm^{-1} coming from the first overtone of the O-H stretching in $Ca(OH)_2$. According to the existing literature the Gaussian β and γ, respectively at 6600 and 6900 cm^{-1}, are referred as coming from a continuum of strongly hydrogen bonded water molecules rather than attributed to a specific molecular classes. The δ component is used as a background contribution to account for the absorption wing coming from the 5000 cm^{-1}

band. Finally, the α Gaussian (around 7070 cm^{-1}), is attributed to a particular class of water molecules: this contribution to the first overtone absorption band has been assigned to the oscillation of weak O-H bonds. It has been experimentally demonstrated that in bulk the "weakly hydrogen bonded" water population increases in intensity with increasing temperature and also by means of the geometric constrains imposed to the water phase by a solid matrix. Our data provide a strong evidence of the existence of these two types of water molecules in the silicate and aluminate hydrating systems: a fraction of the water being in close contact with the pores surfaces (accounted by the α Gaussian) and a second fraction practically unaffected by the solid matrix (Gaussian β and γ).

According to the literature we used the combination band at ~5000 cm^{-1} in a quantitative way for the determination of total amount of water still present in the sample. We compared the trend of the Free Water Index vs time, as obtained with the differential scanning calorimetry, with the overall area of the ~5000 cm^{-1} band, normalized to the area registered at the beginning of the hydration process. Despite the conceptual difference between the two experimental techniques, an excellent agreement exists between this method and the differential scanning calorimetry approach.

The contribution of α, β and γ components to the 7000 cm^{-1} band has been estimated by measuring the area of each peak at each hydration time and normalizing it to the area of the 5000 cm^{-1} band at the same time. The evolution of the three bands during the hydration evidences that, while the β and γ components decrease in time, the α band increases. This support that the water inside the pores becomes progressively less mobile, i.e. the "bulk-like" water, responsible for the β and γ spectral contributions, gradually disappears, while the percentage of the "surface-interacting" water (that origins the α peak, because of the weakened hydrogen bonds) becomes preponderant.

Moreover, the analysis of the α peak position shows that the wavenumber progressively increases, from 7065 to 7082 cm^{-1}. It is worth noting that in the literature a value of 7066±3 cm^{-1} is reported for the a component of bulk water, while 7088±2 cm^{-1} is typical of the same component in a dry silica hydrogel.

Figure 2 shows the comparison between the increase of the surface-interacting water in the sample and the ratio of the surface area to weight of dry C_3S. This quantity has been determined from the surface to volume ratio, obtained from NMR spin-spin relaxation data. It is evident that the two quantities have the same trend.

We can conclude that the proposed Gaussian de-convolution allows the straightforward quantification of the evolution of the surface interacting water, being this quantity directly connected to the surface development of the hydrated products. The extension of this method to other systems as hydrated protein and DNA is currently under investigation.

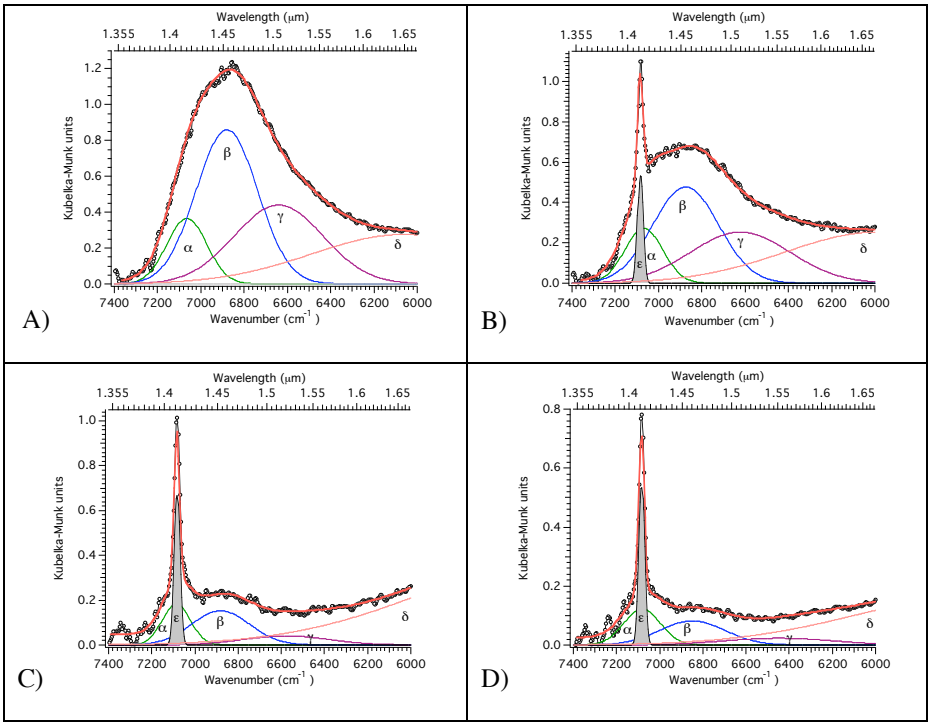

Fig. 1: NIR spectra (7400-6000cm^{-1}) registered at increasing hydration times for the C_3S/water paste (w/c=0.4): A) 3h, B) 1 day (25h), C) 19 days (456h), D) 27 days (648h) after mixing.

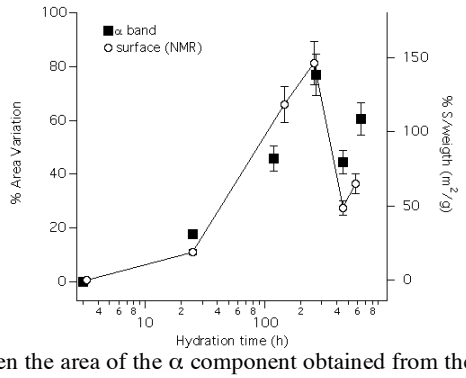

Fig. 2: Comparison between the area of the α component obtained from the deconvolution of the NIR absorption (7400-6000cm^{-1}) and the surface to volume ratio, as obtained from NMR spin-spin relaxation data.

References

Ridi F., Fratini E., Milani S. and Baglioni P., *NIR investigation of the water confined in tricalcium silicate pastes*, Journal of Physical Chemistry B 2006, accepted for publication.

1A - Porous electrodes in alkaline fuel cells and electrolysers

Marco Villa, Carla Antoci, Chiara Milanese, Paolo Nelli, , Giovanni Zangari (*)
Dipartimento di Progettazione e Tecnologie – Facoltà di Ingegneria, Dalmine
(*) Department of Materials Science, Un. Of Virginia, Charlottesville, VA (USA)

Aims

Fundamental studies of interfacial phenomena in alkaline cells.
Development of new electrode materials
Characterizing and improving air electrodes through voltage and pressure modulation techniques

Results

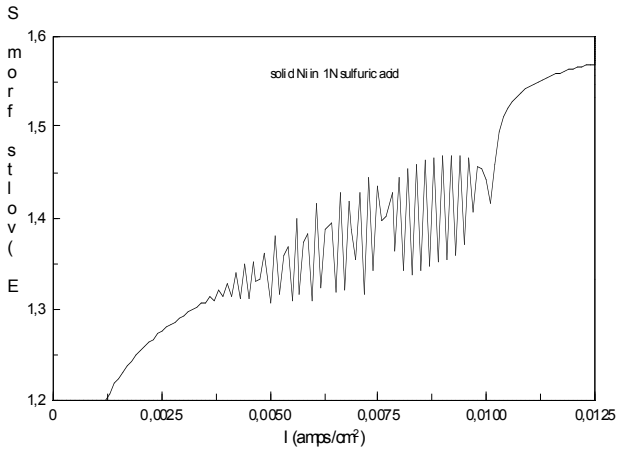

We are conducting a systematic study of the electrochemical behaviour of Ni-based electrodes in the hydrogen (HER) and oxygen (OER) evolution reaction; this field is very popular and technologically promising, being Ni one of the most cost-effective catalysers, but many basic questions still answers. Our data demonstrate the relevance of items mostly ignored in the recent literature: 1) role of the hydriding and oxidation reactions in the catalytic and conduction properties of Ni; 2) partial irreversibility of these reactions and associated surface modification effects; 3) influence on the Fermi level of alloying with precursors elements (such as Al, Zn in Raney Nickel) or with cations from solution. In addition, a host of other effects contributes to a rather complex phenomenology. . As an example, we illustrate an interesting oscillatory phenomenon just discovered in Nickel electrodes, both in acidic and alkaline solutions [1]. We have collected the characteristic V-I curve of many electrodes by slowly sweeping the current from the HER to the OER region and back. A portion of this galvanodynamic scan presenting an unexpected oscillatory behaviour is shown in the figure on the side . This instability phenomenon has the following characteristics: i) it is observed in galvanodynamic scans when decreasing current below the OER voltage, sometimes down into the HER region; ii) it apparently does not depend upon the scan rate or the pH of the solution, iii) the amplitude and position of the oscillation are influenced by morphology and "age" of the electrode, and are only

weakly related with the size of the current step. This oscillatory phenomenon is characterized by the onset of a mechanism which counters the forces driving the system towards equilibrium [2,3]. The phenomenon is likely to be related with cyclic oxidation-reduction reactions taking place in the small pores, or cracks, of a solid catalyst. It is peculiar in the fact that a very small perturbation (the current step) may drive a large response in a direction away from equilibrium. An understanding of these phenomena may provide guidelines for the improved design of such catalysts.

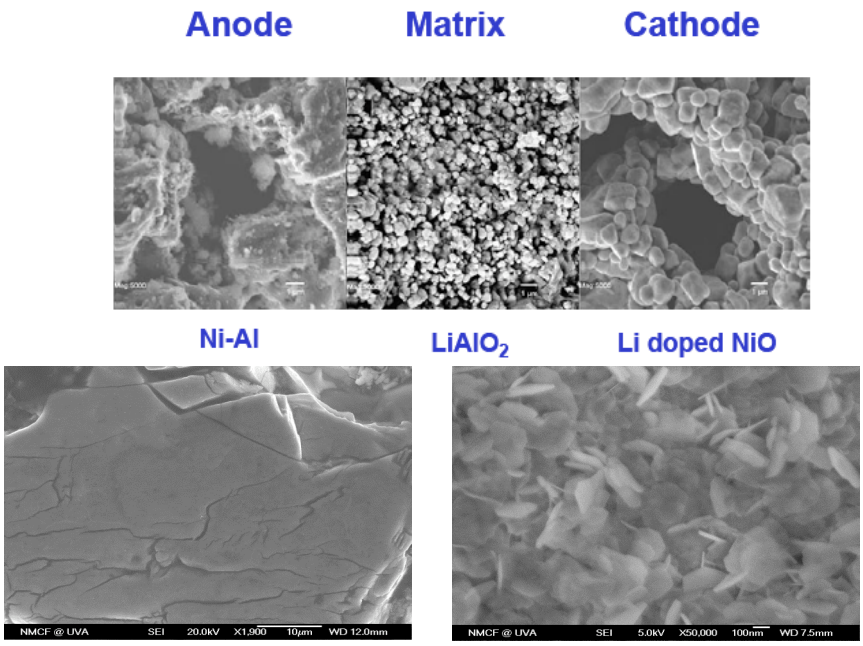

The main gains in efficiency and lifetime of electrolysers are expected to come from new materials and processes for electrode production. We have sintered a semi-conducting Li-doped Nickel oxide, originally to be used as a cathode in a molten carbonate fuel cell (see figure at left), and found it to be most suitable as oxygen electrode in an alkaline electrolyser. We have found that improved wetting characteristic of PTFE-bonded Raney-Ni electrodes may be achieved by coating and oxidizing treatments. With the same type of electrode, treatment in boiling 7mol KOH drastically changes the creaked surface of the Raney-Ni grains (first figure at the right) leaving a roughened surface with sub-micron features (second figure) and a reduce HER activity.

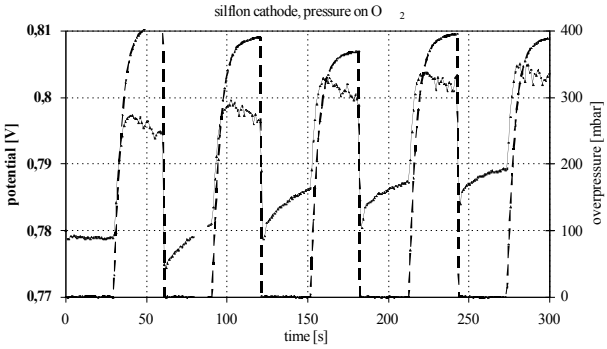

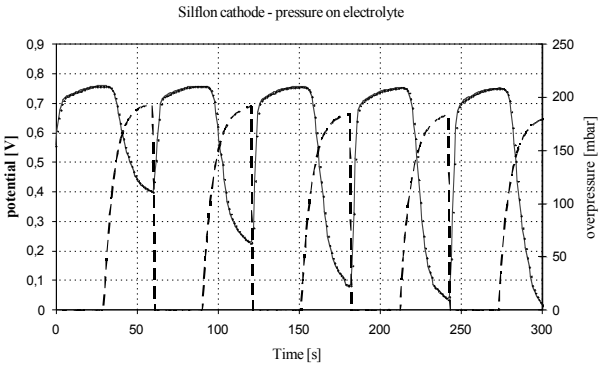

Many electrochemical devices, and alkaline fuel cell in particular, consist of two porous gas electrodes enclosing a liquid electrolyte. In this type of device, a high area active layer is sandwiched between a "gas diffusion layer", with large hydrophobic pores impervious to the electrolyte, and a "gas barrier", where the electrolyte is wetting a microporous hydrophilic material. In most of the alkaline cells we have tested, we have been able to improve the triple-phase boundary, without causing a flow of fluid(s) across the electrode, by applying an overpressure on the electrolyte or a gas compartment side. We have show [4] that the electrochemical response of a cell to a change of overpressure is a very sensitive indicator of the status of the interface, and a flexible tool of characterization for either alkaline fuel cells or electrolysers. As an example, in the figure at the right, we have applied pressure pulses (dashed curve) on the oxygen compartment of an alkaline fuel cell and found that the voltage of silfon electrode (solid curve) improves but, above 400mbar, ii signal the noise due to oxygen bubbles enetering the electrolyte. In the figure at the right, the pressure is applied on the electrolyte; above 180mbar the voltage of the fuel cell drops to zero. With these types of experiments we find the optimal working conditions and estimates the average size of the hydrophobic and hydrophilic pores located, respectively, on the gas and electrolyte sides.

References

Villa M., Nelli P., Zangari G., Galvanodynamic studies and oscillatory reactions at Ni electrodes, submitted to ECS Transactions (Chicago, May 2007)

Zaikin A.N, Zhabotinsky A.M., Nature (1970) 225, 535.

Prigogine I., The End of Certainty, The Free Press, New York (1997).

Villa M, Nelli P., Kohnke H-J, Zangari G., Effects of pressure modulation on porous gas electrodes submitted to ECS Transactions (Chicago, May 2007)

1B - A microscopic model for colloid thermophoresis

Roberto Piazza
and Alberto Parola (Università dell'Insubria)

Topic

In the recent past, thermophoresis (i. e. particle transport driven by thermal gradients, which is akin to the Soret effect in simple fluid mixtures) has been the subject of an increasing number of experimental investigations. In dilute suspensions the mass flow J can be written as $J = -D\nabla n - nD_T\nabla T$, where n is the particle number density, D is the usual Brownian diffusion coefficient, and D_T is called the coefficient of thermal diffusion. In the absence of convection, and assuming that the thermal gradient is directed along z, Soret-coupling of heat and mass transfer leads therefore to a steady-state concentration gradient given by:

$$\frac{dn}{dz} = -nS_T \frac{dT}{dz}$$

where $S_T = D_T / D$ is called the Soret coefficient.
With respect to electrophoretic or rheological studies, thermophoretic measurements present several practical advantages for what concerns the design of the measuring setup. The main reason why they have not so far been comparatively exploited in colloidal science is probably the lack of any general model of particle thermophoresis in liquids. Theoretical approaches have been mostly built for specific colloidal systems but, so far, no general physical picture of why, and in what direction, should a particle move when placed in a temperature gradient has been presented.

Aims

i) Providing a statistical mechanics description of particle thermophoresis phenomena
ii) Relating the Soret coefficient to microscopic particle/solvent interactions

Results

At variance with what happens in colloid sedimentation or electrophoresis, no real external field is present in thermophoretic transport: yet, similarly to gravitational settling and at variance with electrophoresis, experiments often probe the system in steady conditions that, although not corresponding to an equilibrium thermodynamic state, are typified by the absence of a net particle flow. The strategy we followed consists in trying to see whether, as in the case of "real" external volume forces, a treatment at the colloidal level of the steady-state is still feasible. In other words, the main question we have addressed is the following: Can we envisage a "fictitious" external force" f_z leading to an equilibrium colloid concentration profile that coincides with the steady-state distribution induced by the thermal gradient? Once f_z is found the Sorret coefficient follows from the Smoluchowski equation as : $S_T = -(k_B T\, dT/dz)^{-1} f_z$. To construct f_z, we followed a macroscopic hydrodynamic approach assuming that the particle acts on the fluid as an external field **F** stemming from the interfacial molecular forces between the colloid and the solvent. It turns out that, while in isothermal conditions and for spherical colloids **F** is a conservative field with spherical symmetry, in the presence of a thermal gradient breaking the symmetry **F** contains an additional non-conservative contribution that is the sole responsible for particle drift.

This treatment leads to a general expression for the Soret coefficient for spherical colloids dispersed in a solvent of density r in terms of the particle-solvent interaction potential u(r, T) that, when u is short-ranged compared to the particle radius a (quasi-planar approximation) reads:

$$S_T = \frac{4\pi a\rho}{k_B T}\int_0^\infty ru(r,T)dr$$

We have used the former general expression to evaluate the Soret coefficient for charged colloids interacting via a DH screened potential, obtaining results that are in full agreement with those formerly found in specific approaches.

At variance with thermophoresis in liquids, a convincing theoretical explanation of the thermophoretic phenomena in gases was achieved a long time ago. In a following paper [2], we have therefore attempted to develop a general formalism which, in the case of gases, is able to reproduce the known results obtained via the kinetic theory but can, at the same time, be applied to denser systems. We have first shown that, as for dilute gases, in thermally inhomogeneous liquids no off-diagonal momentum flux is present and the full pressure tensor is unaffected by the presence of the thermal gradient. The case, however, is different when the presence of a surface breaks space homogeneity. This circumstance does indeed occur when colloidal particles are present in the solvent. In such a case the structure of the pressure tensor predicted by linear response theory is richer, and a net momentum transfer between the fluid and the colloid sets in. By applying this approach to a dilute suspension of hard spheres, we found that the Soret coefficient may also be written as:

$$S_T = \frac{4\pi a}{k_B T}\frac{\partial}{\partial T}\int_0^\infty dx\, x[p - p_T(x)]$$

where $p_T(x)$ is the tangential component of the fluid pressure tensor, which depends on the distance from the (quasi-planar) interface, and p is the bulk pressure. The quantity appearing on the right hand side of the former equation is just the temperature derivative of the product of the surface tension γ times a characteristic length that measures the size of the liquid layer where the pressure tensor is anisotropic. Therefore, the Soret coefficient is basically related to the particle/solvent interfacial tension, and thermophoretic measurements can be used to probe particle-solvent interaction at the microscopic level.

References

Parola A. and Piazza R. , Particle thermophoresis in liquids*, European Physical Journal E* 15, 255-263 (2004

Parola A. and Piazza R., A microscopic approach to thermophoresis in colloidal suspensions *Journal of Physics.: Condensed Matter 17, S 3639-S **3643** (2005)*

1B - Addressable Molecular Node Assembly - a Generic Platform of Nanoscale Functionalised Surfaces Based on a "Digitally Addressable" Molecular Grid

Piero Baglioni, Gabriella Caminati, Debora Berti, Francesca Baldelli Bombelli, Martina Banchelli, in collaboration with Bengt Nordén, Department of Chemistry and Bioscience, Chalmers University of Technolgy, Gothenburg, Sweden; Tom Brown Bio-Organic Chemistry in the School of Chemistry, University of Southampton, Southampton, UK; Jean-Marie Lehn, I.S.I.S., Université Louis Pasteur, Strasbourg, France

Aims

AMNA is a STREP (Specific Targeted Research Project) funded by the 6th Framework Program (EU). The project receives its funding from the area "Nano-technologies and nanosciences - Self-organisation and self-assembling".The goal of the project is a nano-technology platform based on a 100 nm size grid of addressable molecular building blocks (using three-armed nodes), a novel bottom-up modular approach to place functional groups at defined positions in space with sub-nm precision. An almost complete freedom of choice, for grid assembly as well as for positioning of functional groups, is afforded by a “digital” (in contrast to analogue) code for molecular recognition. High structural fidelity and convenient assembly rates are achieved using DNA base-pair recognition and stacking into rigid double-helical structures. Each node has typically three oligonucleotide strands and a moiety for attaching either a functional group or a lipid anchoring group, so that a group of six nodes are connected to form a hexagon providing a planar network of hexagons.

Results

The project is still at its early stages; specific task of the Florence unit is to engineer a 2-D matrix that can suitably host the nodes, without losing their structural fidelity and their assembly rates; our first results concern the incorporation of a single-stranded 18-er oligonucleotide with a cholesteryl anchoring unit, specifically synthesized in Southampton, onto phospholipid vescicles. The inclusion has been followed through Quasi Elastic Light Scattering and characterized through UV Absorption and CD. Quantitative information has been achieved thanks to QCM (Quartz Crystal Microbalance). Hybridization with the complementary water-soluble strand, labelled with a fluorescent tag, has been monitored by UV, CD and Fluorescence techniques. Variation of membrane fluidity and surface charge can be considered to achieve higher inclusion and better coupling efficiency. Our current efforts are devoted to design a suitable three-arm node, as far as packing properties and liphophilicity are concerned, whose synthetic feasibility will be evaluated by the Southampton group. This molecule will be incorporated in membranes of varying composition and fluidity and coupling with complementary strands will be studied.

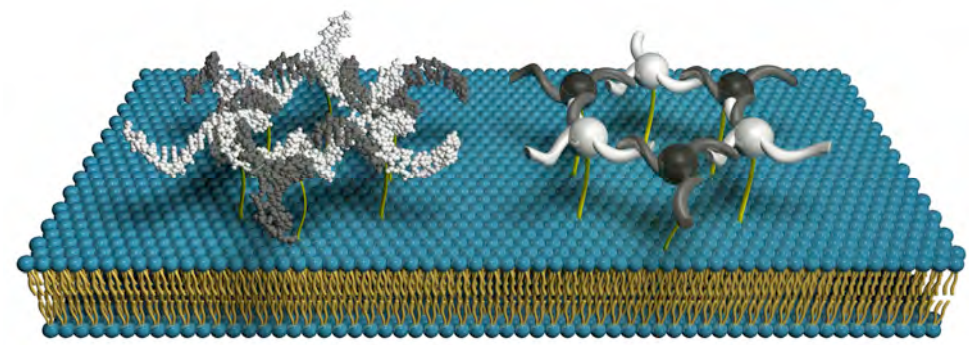

Left - molecular model, and to the right - schematic picture of start hexagon consisting of six nodes, each bearing three deoxyribonucleotide (DNA) arms with mutually complementary sequences of ten bases. Lipid chains, covalently tethered to the DNA strands, serve the role of anchoring the hexagon to a lipid matrix. The grid will be built up, radially from the start hexagon, by a net of hexagons and nodes, each being uniquely addressable by its base-sequence code. © AMNA project

References

http://www.phc.chalmers.se/english/res_AMNA.html;

http://europa.eu.int/comm/research/headlines/news/article_04_10_04_en.html;

http://www.voyle.net/Nano%20Funding/Funding2004-00014.htm;

http://www.nanotechnology.com/?name=News&file=article&sid=5002

1B - Bottom-Up strategies for the Self-Assembly of Biologically Inspired Surfactants

Debora Berti, Francesca Baldelli-Bombelli, Martina Fortini and Piero Baglioni

Aims

We have undertaken a structural study of supramolecular structures formed by the self-assembly of recently sinthesized nucleolipids that is double-chain phospholipids undergone to an enzymatic modification that transfers a nucleoside on the polar head. This work is motivated by the interest in the expression of molecular functions in self-organized systems, where the driving force of aggregation has a hydrophobic nature, which is the exclusion of hydrocarbon chains from the contact with aqueous medium. The molecular information (i.e. packing parameter and molecular recognition capacity) is amplified in the supramolecular arrangement and rules phase behavior. Their self-assembly can be fine-tuned by a proper choice of the alkyl chains of the lecithin in the synthetic step. But most important is the molecular information contained in the polar head, standing its biological relevance: like in nucleic acids its functionality is triggered by the macromolecular organization, in our case is the self-aggregation that makes possible base-base interactions

Results

In 1994 we started to implement a remarkably elegant to perform an enzymatic functionalization of phospholipids with nucleic acids in a one-pot combination of natural building blocks.

The reaction proved to be quite flexible and allows the exchange of a choline headgroup in a lecithin with a nucleoside: the resulting derivative has a nucleotide in the polar head reproducing the charge of each DNA monomer and is called phosphatidylnucleoside. The initial interest in such derivatives was boosted by their possible use as liphophilic nucleoside analogues derivatives in mieloyd leukemia treatment. More recently the use AZT (3'-azido, 3'-deoxythymidine, a modified nucleoside) in HIV therapy and the realization that the "bare" nucleoside is inefficient in entering the blood-brain barrier (the most important reservoir of HIV is the central nervous system), sparkled the use of "smart prodrugs". Phosphatidylnucleosides are transformed in nucleoside-triphosphates, that exert antiviral action by inhibiting the reverse transcriptase, in a metabolic pathway carried on by Phospholipases.

A morphoplogical characterization of bilayer-forming phosphatidylnucleoside by TEM techniques, showed a correlation between stacking and H-bonding efficiency of the base on the polar head and the morphology of the aggregate: we would like to stress the attention on the fact that these lipids have a net negative charge per monomeric unit, just like nucleic acids, while the studies until then concerned interactions between ***neutral or oppositely charged groups***. How the stacking H-bonding network propagates along the mesosocopic interface is still unclear and subject of debate.

We have studied phosphatidylnucleosides' aggregation and molecular recognition properties in some details at the water-air interface. A dependence of the limiting areas per molecule on stacking attitudes of the base was found and deviations from the ideal behavior when two complementary-base derivatives were mixed in monolayer reported, suggesting specific interactions between complementary bases.

The extension of the study of molecular recognition to mesoscopically extended interfaces was the obvious development of these studies and stable liposomes formed from unsaturated phosphatidylnucleosides have been investigated. Monodisperse vesicles have

been prepared from DOP-Adenosine, DOP-Uridine, DOP-Cytidine and DOP-ethenoAdenosine (ε- Adenosine). Uracil and Adenine are RNA complementary bases. Cytidine is a pyrimidinic base like Uridine, and it has a similar sterical hindrance, while ε-Adenosine is a $1,N^6$ etheno bridged modification of Adenosine where the amino group of the purine is no longer available for H bonding. The UV spectra of vesicular solutions of DOP-Adenosine, DOP-Cytidine and to a lesser extent DOP-ε-Adenosine, show consistent hypochromicity if compared to those obtained dissolving the vesicles by action of a detergent to obtain mixed micelles. Upon mixing two equimolar vesicle populations formed from complementary bases, changes in Circular Dichroism and UV spectra were detectable on the same time scale, indicating "excess" in the stacking interactions. The whole process occurred without fusion or alteration of the size distribution of the liposomes. The time-scale indicated a mixing process mediated by monomeric exchange. At equilibrium spectroscopic features were identical to those shown by vesicles prepared by hydration and extrusion of a mixed DOP-Adenosine/DOP-Uridine films. The evidence of H-bonding was however indirect, since NMR spectra are not sufficiently resolved in lipid vesicles due to large spectral broadening. The ideal behavior of DOP-Cytidine/DOP-Uridine systems indicated a Watson-Crick selectivity pattern. DPP-nucleoside derivatives exhibited a time-dependent annealing morphology and eventually evolved to elongated non-liposomal structures.

The search for molecular recognition at mesoscopically extended interface evolved toward micellar aggregates where aggregation, shape, and size are ruled by thermal equilibrium and can be altered through the variation of a control parameter. Vesicular aggregates can be considered static metastable structures while micelles are equilibrium assemblies deriving from spontaneous association of monomers as a result of delicate balance of hydrophobic and hydrophilic interactions. This means that either the onset of aggregation and the structural properties of the aggregates can give insights into base-base interactions. Another important aspect concerns the feasibility of ^{1}H-solution NMR investigations, since the fast tumbling of micellar aggregates allows a narrowing of the broad lines observed for bilayered structures and a direct detection of recognition patterns typical of nucleic acids.

The structure of micelles formed by dioctanoylphosphatidylnucleosides (diC8P-Adenosine, diC8P-Uridine and their 1/1 mole ratio mixture) has been studied by Small Angle Neutron Scattering as a function of pH and amphiphile concentration. Several indications of deviation from ideal behavior can be found in the cmc, in the area per polar head and in spectroscopic properties of bases. Selective and preferential interactions have been identified between adenine and uracil moieties, according to a pattern resembling molecular recognition in nucleic acids. In particular NMR, UV-Vis and CD spectroscopies indicate that in mixed micelles, formed from diC_8P-Adenosine and diC_8P-Uridine phosphatidylnucleosides, both stacking and hydrogen bonding interactions are present between the bases at the micellar surface. NMR indicates that a H-bonded Watson-Crick adduct is formed despite the exposure of the bases to the highly competitive aqueous environment.

A similar characterization of micelles from monoalkyl-phosphoryl nucleosides (C_{16}-AMP, C_{16}-CMP and C_{16}-UMP) has highlighted excess stacking interactions in the ternary system formed by Watson-Crick complementary nucleolipids. The same aggregates have also been investigated by means of NMR techniques. Some selective interactions between bases have been found in the mixed micellar system and an average orientation of the aromatic system parallel to the micellar surface has been deduced.

A recent interesting progress concerns the fromation of flexible polymerlike micellar structures by dilauroylphosphatidylnucleosides. The interfacial curvature is intermediate between globular micelles and bilayers, and like in natural nucleic acids, very different

length scales are interplaying. The size and shape of aggregates show strong dependence on the nucleolipid volume fraction and on the nature of the polar head. In fact strong stacking interactions between neighboring bases have been found for DLP-Adenosine, while DLP-Uridine has in the aggregate electronic properties similar to the momomer. Some twisted ribbon-like helical structures have been found for DLP-Adenosine at low volume fractions (see Figure below), while for higher concentrations flexible entangled objects are formed.

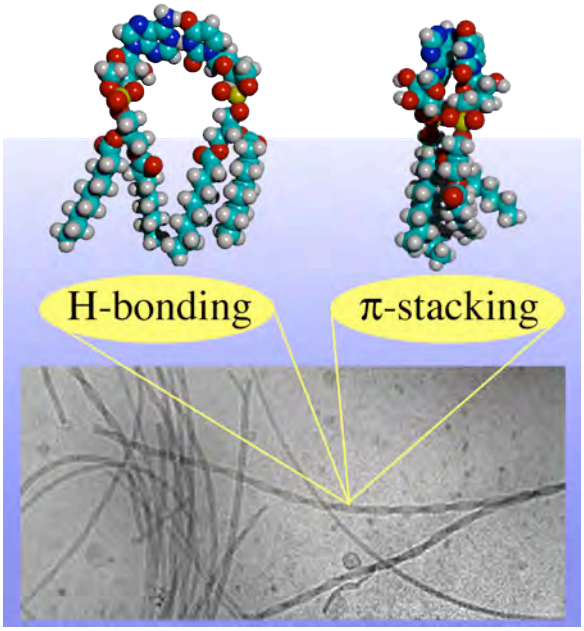

References

Berti D, Barbaro P, Bucci I, Baglioni P: *Molecular recognition through H-bonding in micelles formed by dioctylphosphatidyl nucleosides*. Journal of Physical Chemistry B 1999, 103:4916-4922.

Berti D, Pini F, Baglioni P, Teixeira J: *Micellar aggregates from short-chain phospholiponucleosides*: *A SANS study*. Journal of Physical Chemistry B 1999, 103:1738-1745.

Berti D, Pini F, Baglioni P, Teixeira J: *A SANS investigation on micelles from short-chain phospholiponucleosides*. Physica B 2000, 276:334-336.

Berti D, Luisi PL, Baglioni P: *Molecular recognition in supramolecular structures formed by phosphatidylnucleosides-based amphiphiles*. Colloids and Surfaces a-Physicochemical and Engineering Aspects 2000, 167:95-103.

Baldelli Bombelli F, D.; Keiderling, U.; Baglioni, P.: *Giant Polymerlike Micelles Formed by Nucleoside-Functionalized Lipids*. J. Phys. Chem. B. 2002, 106:11613-11621.

D. Berti, U. Keiderling, P.Baglioni, *Supramolecular structures formed by Phospholiponucleosides*, Prog. Colloid Polym. Sci, 2002, 120, 64-73.

Baglioni, P. *Rhodia Prize Lecture*, ECIS conference, Paris 2002.

D. Berti, E. Fratini, S. Dante, T. Hauss, P. Baglioni, *A structural study of Lamellar Phases formed by Nucleoside lipids*, Applied Physics A, 74, S(2002), 522-524.

F. Baldelli Bombelli, D. Berti, U. Keiderling, P. Baglioni, *Living polynucleotides formed by the spontaneous aggregation of dilauroylphospholiponucleosides*, Applied Physics A, 74, S (2002), 1270-1273.

P. Baglioni and D. Berti, *Self Assembly in micelles combining stacking and H-bonding*, Current Opinion in Colloid and Interface Science, 2003,8, 55-61.

D. Berti, F. Baldelli Bombelli, M. Almgren and Piero Baglioni, *Micellar Aggregates Formed by Dilauroylphosphatidylnucleosides* in Self-Assembly, Ed. Brian H. Robinson, IOS Press: Amsterdam, the Netherlands, 2003, 348-357.

1B – Colloidal aspects of membrane proteins

G. Palazzo, A. Mallardi, M. Giustini, F. Lopez, G. Venturoli, R. Piazza

Aims

Study of the solution properties of membrane protein and of interactions between surfactants (lipids included) and membrane properties.

Results

Although the first membrane protein to be crystallised *in surfo* was the photosynthetic bacterial RC, studies of the solution properties of photosynthetic membrane proteins are still rare. Our recent works, performed on reaction center complex (RC) from *Rhodobacter sphaeroides*, have unexpectedly revealed quite rich phase behaviour of systems made of RC, lauryldimethylaminoxide (LDAO) and water. Ionisation of LDAO bound to RC induces reversible emulsification of the protein over a narrow acidic pH range, resulting in stable micrometric RC-surfactant droplets. The droplet size undergoes a fast initial growth, followed by a relatively steady stage. The earliest growth is roughly consistent with a $t^{1/3}$ time dependence of the droplet size suggesting that the droplets increase in size through Ostwald ripening. After this initial growth, droplets persist in a quasi-stationary state for very long time. It was proposed that Ostwald ripening could be hindered by the presence within the droplets of the water-insoluble RC, due to competition between Laplace pressure and osmotic pressure of the trapped component, preventing collapse of the small ones. Electrostatic interactions play a key role in the phase separation process, as shown by a systematic analysis of ionic strength effects and by the use of a cationic detergent (dodecyltrimethylammonium bromide) that mimics, also at basic pH, the ionised form of LDAO. Phase segregation was coupled to changes of the RC absorption suggesting that surfactant-protein interactions leading to phase separation also induce a conformational transition of the RC. Time-resolved absorption spectra recorded during the emulsification process reveal that such a conformational change is always faster than droplets formation.

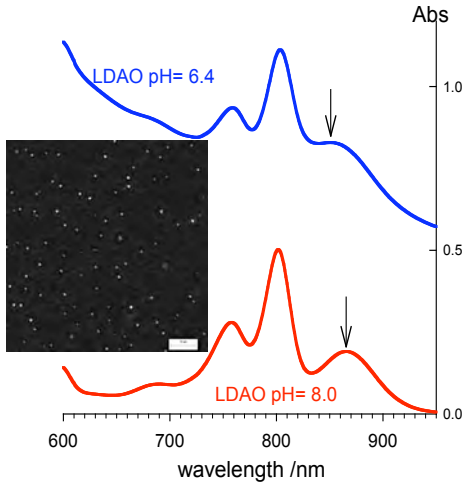

Fig.1 *Visible-NIR absorbance spectra of RCs solubilized by LDAO at pH= 8.0 and 6.4.*

Inset: micrograph of phase-separated droplets at pH= 6.4.

In recent years, the presence of a binding site for a cardiolipin molecule was assessed by several crystallographic studies performed on both wild-type and mutant RCs crystallised *in surfo* and *in cubo* . We have found that cardiolipin does not affect the affinity of the protein for ubiquinone, but has a marked influence on the rate of charge recombination. It appears that the main effect of cardiolipin on the electron transfer can be ascribed to a destabilisation of the charge-separated state. Results obtained in micelles and vesicles

follows the same titration curve when cardiolipin concentration evaluated with respect to the apolar phase is used as relevant variable. The dependence of the $P^+Q_A^-$ recombination rate on cardiolipin loading suggests two classes of binding sites. In addition to a high-affinity site (compatible with previous crystallographic studies) a cooperative binding, involving about four cardiolipin molecules takes place at high cardiolipin loading.
Membrane proteins, must be secluded in suitable lipophilic domains in order to study them *in vitro*. A drawback of the use of membrane mimetic systems formed by disconnected hydrophobic domains (such as micelles and vesicles) is the scarce control on their occupancy by lipophilic guests. To account for the non-exponential kinetics of charge recombination of RCs embedded in vesicles a new approach was developed few years ago. It was based on the assumption that the size polydispersity of proteoliposomes and the distribution of quinone molecules among them result in a quinone concentration distribution function, P(Q). The first and second moments of P(Q) have been evaluated from the size distribution of proteoliposomes probed by dynamic light scattering. Following these premises, the kinetics of $P^+Q_B^-$ recombination can be described by a truncated cumulant expansion. This analysis accounts satisfactorily for the non-exponential kinetics of $P^+Q_B^-$ recombination observed over a range of temperatures. The model (subsequently extended to the case of low quinone/RC ratios) provides a means of determining the equilibrium constant of quinone binding and of electron transfer processes involving RCs in liposomes. Lately, several evidences indicate that reaction centers experience disconnected quinone domains not only in artificial liposomes but also *in vivo*.

References

Giustini, M., Castelli, F., Husu, I., Giomini, M., Mallardi, A., Palazzo G., *Influence of cardiolipin on the functionality of the Q_A-site of the photosynthetic bacterial reaction center*, J. Phys. Chem. B 2005, *109*, 21187-21196.

Francia F., Dezi, M., Rebecchi, A., Mallardi, A., Palazzo, G., Melandri, B.A., Venturoli,G., *Light-harvesting complex 1 stabilizes $P^+Q_B^-$ charge separation in reaction centers of Rhodobacter sphaeroides*, Biochemistry 2004, *43*, 14199-14210.

Francia F., Dezi, M., Rebecchi, A., Mallardi, A., Palazzo, G., Melandri, B.A., Venturoli,G., *Light-harvesting complex 1 stabilizes $P^+Q_B^-$ charge separation in reaction centers of Rhodobacter sphaeroides*, Biochemistry 2004, *43*, 14199-14210.

Palazzo G., Mallardi, A., Francia F., Dezi, M., Venturoli, G., Pierno, M., Vignati, E., Piazza, R., *Spontaneous emulsification of detergent solubilized Reaction Center: protein conformational changes precede droplets growth*, Phys.Chem. Chem. Phys. 2004, *6*, 1439–1445.

Piazza, R., Pierno, M., Vignati, E., Francia F., Venturoli, G., Mallardi, A..,Palazzo G., :*Liquid-liquid phase separation of a surfactant-solubilized membrane protein*, Phys. Rev. Letters 2003, 90, article n. 208101.

Ambrosone, L., Mallardi, A., Palazzo, G., Venturoli, G.,:*Effect of heterogeneity in the distribution of ligands and proteins among disconnected particles: the binding of ubiquinone to bacterial reaction center*, Physical Chemistry Chemical Physics 2002, 4, 3071-3077.

Palazzo, G., Mallardi, A., Giustini, M., Berti, D., Venturoli, G., *Cumulant analysis of charge recombination kinetics in bacterial reaction centers reconstituted into lipid vesicles*, Biophys. J. 2000,79, 1171-1179.

1B - Cryo-TEM of Liposomes loaded with boron-containing compounds intended for Boron Neutron Capture Therapy (BNCT)

Simona Rossi and Giacomo Martini (in collaboration with *K. Edwards, Dept. of Physical Chemistry, Uppsala University, Sweden*).

Aims

Cryo-TEM investigation of structure and stability of liposomes intended for drug delivery in BNCT.
ESR analysis of phospholipids bilayer of liposomes loaded with amphiphilic drugs.

Results

Electron microscopy constitutes an powerful method for the determination of aggregate morphology in dilute lipid solutions. Lipid aggregates, such as liposomes and micelles, are, however, very labile and extremely sensitive to small changes in concentration and composition. Cryo-transmission electron microscopy (Cryo-TEM) is a relatively new technique that offers unique possibilities for direct visualization of labile microstructures in dilute aqueous solutions[1,2]. This technique makes it possible to obtain images that are two-dimensional projections of all of the aggregates in water suspension without the need of treating the sample with fixation reagents or other chemicals. The cryo-TEM involves ultra-fast cooling of thin liquid films (by rapidly plunging the samples into liquid ethane held at ~ 100K) to vitrify the samples, that are examined in the electron microscope at cryogenic temperatures.
We used Cryo-TEM to obtain structural information on the effect of boronated drugs on aggregate structure in samples containing small unilamellar liposomes (diameter =100nm) with varying bilayer composition. In addition, the Electron Spin Resonance (ESR) spectroscopy of lipophilic spin labels (*5*-, 7- *and 16-* doxyl stearic acid, n-DSA, cholestane-doxyl derivatives) give us interesting information on the dynamic perturbation of the liposome bilayer after boronated drug insertion within membrane. ESR spin labelling has, in fact, proved to be a powerful technique for studying liposome bilayers and drug-lipid interactions [3-5].
The compounds used are based on a boron rich carborane cage: the lactosyl carborane [1,2-dicarba-closo-dodecarboran(12)-1-ylmethyl] (D-galactopyranosyl)-(1→4)-gluco-pyranoside (LCOB) (kindly provided by Prof. L. Panza, Università del Piemonte Orientale) and b–5–*o*-carboranyl-2'-deoxyuridine (CDU) (kindly provided by Prof. Schinazi, Emory University Atlanta, USA).
In LCOB the carborane moiety has been coupled to an hydrophilic lactosyl moiety[6] which increases the solubility in water of the compound and escorts and binds the boronated compound to the tumor cell surface.

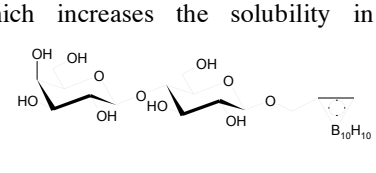

LCOB

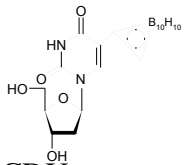

CDU

The second compound, CDU, is a non-toxic pyrimidine nucleoside analogue designed for BNCT of brain tumors, which has been extensively studied for its cytotoxicity, anticancer, antiviral activity and cellular uptake[7]. Since both compounds have high hydrophobicity because of their ortho-carborane domain they are expected to locate inside the hydrophobic region of the membrane.

We investigated and characterised unilamellar liposomes with different membrane composition[8]: *i)* egg phosphatidylcholine (EPC), *ii)* distearoyl phosphatidylcholine (DSPC) *iii)* EPC/Cholesterol and DSPC/Cholesterol at molecular ratio 55/45. In many pharmaceutical formulations, cholesterol is included in the lipid mixture to further increase the *in vivo* stability. In addition, saturated phospholipids are preferred when considering the long-term stability of the liposomes.
ESR results proved that CDU insertion into the liposome membrane gave rise to a strong variation of the fluidity and order degree of the bilayer. The EPC bilayers became more packed in the presence of the carboranyl-nucleoside and this effect tookplace both in the hydrophilic glycerol moiety and in the deepest interior of the hydrocarbon regions. This effect was stronger in EPC liposomes than in EPC/Chol liposomes, where it occurred at lower CDU concentration.
In LCOB-loaded liposomes LCOB insertion into the phospholipid bilayer increased the packing order in the vicinity of the water/hydrocarbon interface whereas the inner hydrophobic region of the bilayer was unaffected.
Cryo-TEM micrographs revealed a significant change in the size distribution when the LCOB molar fraction increased in the liposomes dispersion. The lactosyl-carborane induced the formation of extremely small liposomes with diameters ranging from 10 to 30 nm in coexistence with liposomes in the size range of 80-100 nm. A second interesting effect caused by the incorporation of LCOB was that both populations of the liposomes developed a tendency to aggregate and form clusters, a phenomenon which was proved by turbidity measurement. When the LCOB concentration was further increased, the number of small liposomes increased. At x_{LCOB} =0.82 the sample contained only a limited number of intact liposomes and most of them showed bilayer openings from which originated short threadlike micelles, a few tens of nanometers in length (figure 1).

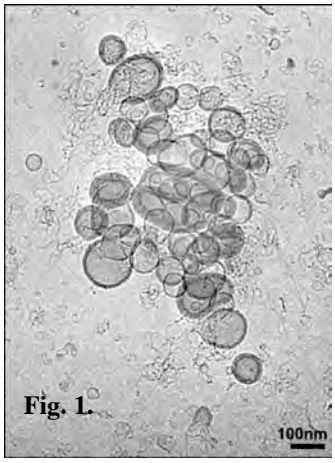

Fig. 1.

References

Dubochet J., Adrian M., Chang J.-J., Homo J.-C., Lepault J., McDowall A.W. and Schultz P., *Cryo-electron microscopy of vitrified specimens,* Quart. Rev. Biophys. 21, 1988, 129-228.

Almgren, M. Edwards, K. and Gustaffson J., *Cryotransmission electron microscopy of thin vitrified samples,* Curr. Opin. Colloid Interface Sci. 1996, 1 (2), 270-278.

Marsh, D., Kurad D. and Livshits V.A., *High-field electron spin resonance of spin labels in membranes*, Chemistry and Physics of Lipids, 116 (1-2), 2002, 93-114.

Štrancar J., Šentjurc M. and Schara M., *Fast and Accurate Characterization of Biological Membranes by EPR Spectral Simulations of Nitroxides*, Journal of Magnetic Resonance, 142 (2), 2000, 254-265.

Benatti C.R., Feitosa E., Fernandez R.M. and Lamy-Freund M.T., *Structural and thermal characterization of dioctadecyldimethylammonium bromide dispersions by spin labels*, Chemistry and Physics of Lipids, 111 (2), 2001, 93-104.

Tietze, L.F.; Bothe, U. *Ortho-carboranyl glycosides of glucose, mannose, maltose and lactose for cancer treatment by boron neutron-capture therapy* Chem. Eur. J. 4 (7), 1998, 4, 1179-1183.

Schinazi R.F., Goudgaon N.M., Fulcrand G., Kattan Y.E., Lesnikowsky Z., Ullas G., Moravek J., Liotta D.C., *Cellular pharmacology and biological activity of 5-carboranyl-2'-deoxiuridine*, Int. J. Radiat. Oncol. Biol. Phys. 28 (5), 1994, 1113-1120.

Rossi, S.; Karlsson, G.; Martini, G.; Edwards, K.; *Combined cryo-TEM and ESR studies of EPC liposomes loaded with a carboranyl compound intended for BNCT,* Langmuir 19 (14), 2003; 5608-5617.

1B - Lipoplexes as non viral vectors for gene delivery

Laura Ciani, Giacomo Martini, Sandra Ristori, Anna Salvati, in collaboration with the Department of Pathology (Prof. Annarosa Arcangeli , Univ. Of Florence.

Aims

Physico-chemical characterization of several lipoplexes to establish valuable systems for non toxic and highly efficient gene transfection.

Results

Human genome characterization and recombinant DNA technology have created tremendous opportunities for gene therapy. However, delivery of the large anionic bioactive DNA into the cell is not simple, because it must arrive intact to the nucleus, after crossing the cell and nuclear membranes. In recent years, cationic lipid/liposomes have emerged as useful carriers,[1,2] because they exhibit ease of manipulation, reproducibility, and versatile preparation. We made use of positively charged unilamellar vesicles, formed by a cationic surfactant, DOTAP or DC-Chol, and a zwitterionic phospholipid, DOPE, as helper lipid.

Model lipoplexes were first prepared by using small oligonucleotides, either in the form of a single strand (PolyA and PolyT) or of the corresponding double strand. Their characterization was performed by Zeta Potential, Microcalorimetry and Electron Spin Resonance.[3] Both zeta potential and microcalorimetric titration showed that a stable complex could be formed between oligonucleotides and cationc liposomes. In particular, zeta potential measurements showed that: for DOTAP/DOPE liposomes, the two single-strand oligos had the inversion point of the zeta potential (corresponding to the formation of a neutral complex) at 0.50 charge ratio. This meant that neutralization took place when the negative phosphate groups of the added oligo reached half the concentration of the cationic lipids. We thus deduced that, in this case, only the lipids located on the liposome external surface interacted with DNA fragments. A similar behaviour was observed in the titration of DC-Chol/DOPE, but in this case the inversion point was different for different oligos: This was due to specific interactions between the DNA bases and the external surface of the DC-Chol/DOPE liposomes.

The thermodynamic data of the complex formation, obtained by microcalorimetry, where in agreement with zeta potential data.

The status of the lipid bilayer as a function of oligonucleotide addition was monitored at molecular level by introducing appropriately tailored ESR spin probes. In particular, 5-doxyl stearic acid showed that interactions between oligos and liposomes did not change either the dynamics or the structural properties of the bilayer. (fig. 1). ESR probes also showed enhanced rigidity in the DC-Chol/DOPE bilayer with respect to the DOTAP/DOPE bilayer, which is in line with the well known condensing effect that cholesterol and its derivatives exert on fluid lipid assemblies.

From the above analysis the following scheme of lipoplex could be deduced for single strand oligos interacting with both type of cationic liposomes, and for the double strand oligo interacting with DC-Chol/DOPE liposomes: DNA fragments simply “wrapped up” the external surface of liposomes, which remained substantially intact. On the contrary, DOTAP/DOPE liposomes showed a more complicate behavior when interacting with the double strand oligo. This difference could be traced back to the higher fluidity of their bilayer, that allowed more marked deformations.

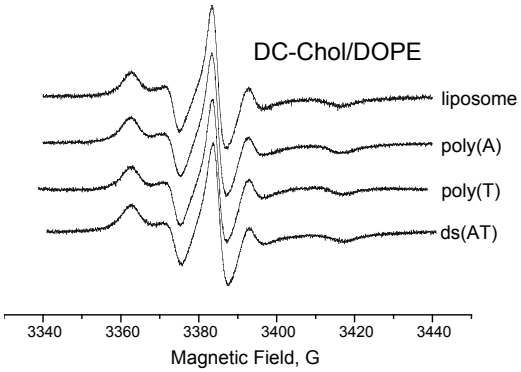

Fig 2. 310 K ESR spectra of 5-DSA inserted in plain DC-Chol/DOPE liposomes and in lipoplexes containing single and double strand oligonucleotides.

Transfection experiments toward CHO cells were then performed with lipoplexes made up by liposomes and the pEGFP plasmid, that carries the information to produce a fluorescent protein. Preliminary results showed that: i) marked transfection was achieved by the lipoplexes; ii) DOTAP/DOPE liposomes were less toxic, but also less efficient, than DC-Chol/DOPE liposomes and (iii) Lipoplex charge and lipoplex/cell ratio were critical parameters for transfection efficiency. Figure 2 shows a comparison between experiments performed at two different lipoplex charge values, with constant cell/lipoplex ratio.

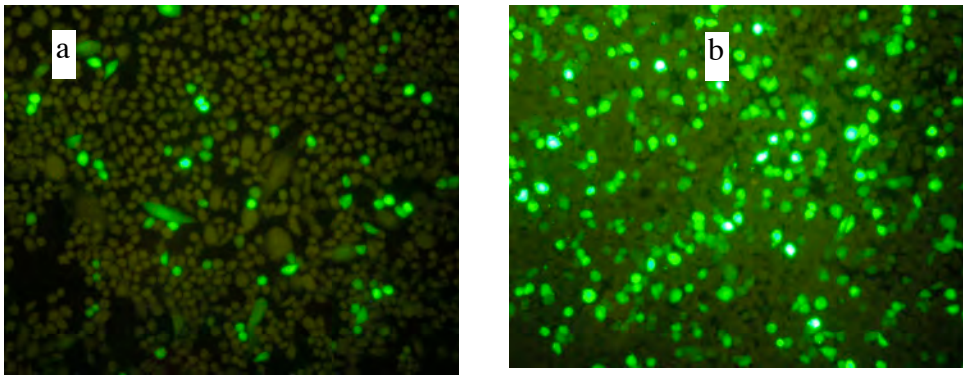

Fig. 2. Fluorescence microscopy images of cell transfected with the pEGFP plasmid/DC-Chol/DOPE lipoplex. (a): $DNA^-/lipide^+ = 0.07$ and (b): $DNA^-/lipide^+ = 0.7$ 48 h from the injection.

References

Kataoka, K.; Harashima, H., Gene delivery systems: viral vs. non-viral vectors**,** *Adv. Drug Delivery Rev.,* 52, 151, **2001**.

Zhdanov, R I; Podobed, O V; Vlassov, V. V., Cationic lipid-DNA complexes-lipoplexes-for gene transfer and therapy, *Bioelectrochemistry,* 58, 53, **2002.**

Ciani, L.; Ristori, S.; Salvati, A.; Calamai, L.; Martini, G., DOTAP/DOPE and DC-Chol/DOPE Lipoplexes for Gene Delivery: Zeta Potential Measurements and Electron Spin Resonance Spectra. *Bichim. Biophys. Acta,* submitted for publication.

1B - Nanostructured Magnetic Fluids

Massimo Bonini and Piero Baglioni, in collaboration with Albrecht Wiedenmann (HMI, Berlin)

Aims

Aim of this project was the synthesis of magnetic fluids constituted by magnetic nanoparticles dispersed in both water and organic solvents. We focused in preparing magnetic nanoparticles stabilized either by a surfactant shell, by the charges present on their surfaces or by an outer shell of an inert material.

Results

Ferrofluids are stable dispersions of magnetic nanoparticles in a liquid carrier. During this project, three different synthetic strategies were explored: synthesis in reverse micelles, preparation from super-saturated solutions and thermal decomposition. These techniques lead to different results in terms of dimensions, polydispersity and maximum amount of dispersed solid material [1]. In order to characterize the ferrofluids, microscopy (TEM and AFM) and scattering (DLS, SAXS and SANS) techniques were used.

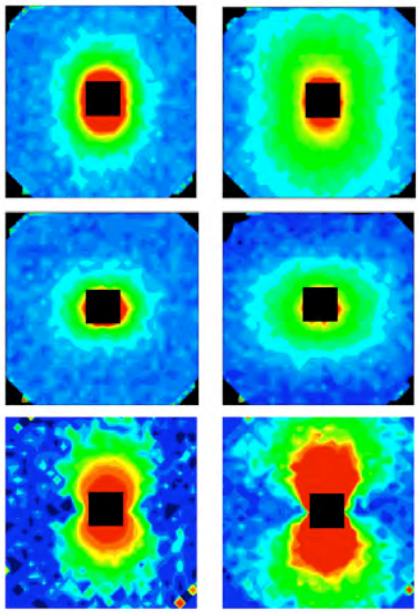

Figure 1. SANSPOL iso-intensity plots of silica-coated cobalt ferrite nanoparticles.

A particular attention was devoted to the preparation of core-shell nanoparticles from supersaturated solutions, the core being constituted of cobalt-ferrite, $CoFe_2O_4$, while the outer shell was silica. These particles are of particular interest because of their bio-compatibility, due to the inert silica shell. A detailed characterization was obtained by means of Small Angle Scattering of Polarized Neutrons (SANSPOL), a recently developed technique available at the Berlin Neutron Scattering Center, Hahn-Meitner Institute, Berlin (Germany). Results showed that core-shell cobalt-ferrite nanoparticles present a uniform silica shell that can be obtained by a very simple synthetic procedure. The thickness of this coating does not depend on the size of the cobalt-ferrite particles and it doesn't change the shape of the coated particle. Moreover the thickness of the outer shell can be easily tuned during the synthesis.

References

Bonini, M.; Wiedenmann, A.; Baglioni, P. J. Phys. Chem. B 2004, 108, 14901-14906.

Bonini, M.; Wiedenmann, A.; Baglioni, P. Physica A 2004, 339, 86–91.

Bonini, M.; Wiedenmann, A.; Baglioni, P. Materials Science and Engineering C In Press.

1B - Nanostructured surfaces for controlled bacteria adhesion

C.Satriano, G.M.L.Messina and G.Marletta
LAMSUN-CSGI at Dept.of Chemistry, Univ. of Catania
S.Carnazza and S.Guglielmino,
Dept. of Microbiology, Univ. of Messina

Aims

Fabrication of topographically and chemically nanostructured surfaces. Adhesion tests of bacteria on the nanostructured surfaces.

Results

Spherical polystyrene (PS) colloidal particles of 200 nm of diameter and functionalized by carboxylate groups have been immobilized onto a hydrophilic and flat polysiloxane surface by dewetting-driven self-assembling from aqueous dispersion. At the end of the process the colloids were hexagonally close packed into tree-dimensional crystal lattices (Figure1).

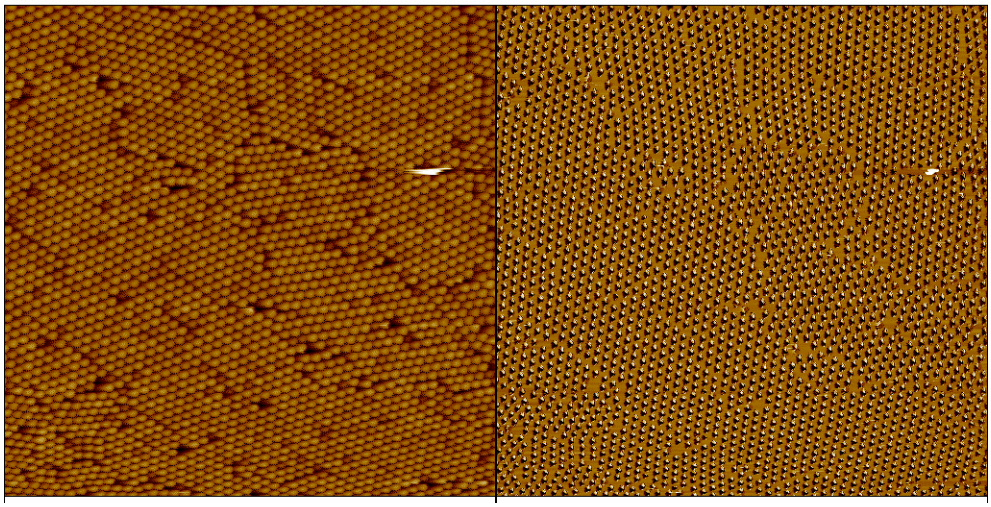

Fig. 1- Tappping mode AFM height (left hand side, z range= 200 nm) and phase (right hand side, z range= 90°) images of hexagonally packed PS colloids.

A polymer solution has been allowed to fill the interstitial spaces and after mechanical removal of colloidal masks the resulting 2D pattern consisted of hydrophilic pores surrounded by a hydrophobic matrix (Figure 2). The maximum extent of the nanopatterned arrays was only of few ten of microns, for each array the pore pitch being of 200 nm, diameter and rim of 110.9±7.4 nm, and 4.3±2.1 nm, respectively.

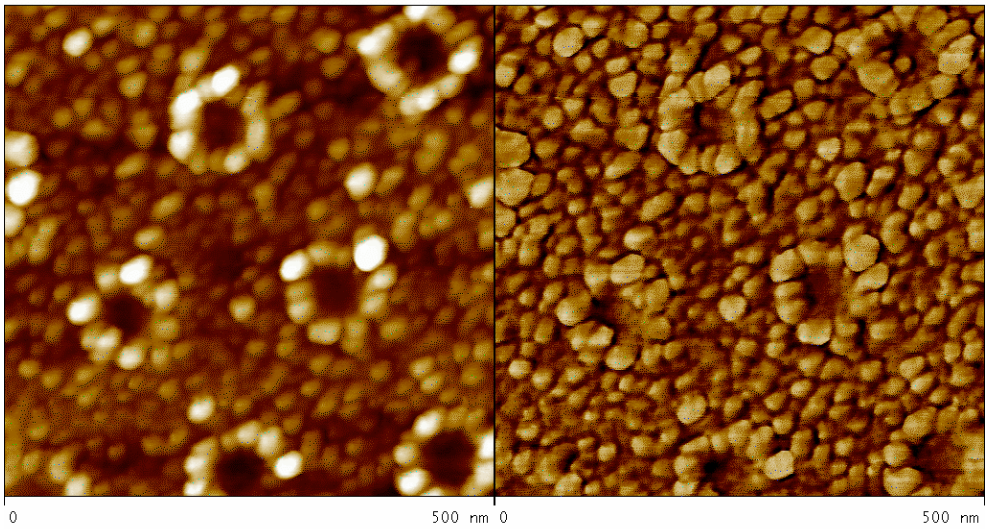

Fig. 2 - AFM height (left hand side, z range= 10 nm) and phase (right hand side, z range= 15°) images of nanostructured surfaces.

Adhesion experiments for 2 hours-incubation of *Pseudomonas Aeruginosa* evidenced a sparse grown of biofilm-like structures with respect to homogeneous hydrophilic and hydrophobic surfaces, respectively. The observed effects have been interpreted in terms of the very "active" role of the internal area of nanopores, which may affect the bacterial response, prompting the formation of biofilm-like aggregates only above a given extent of the nanopore-containing areas.

References

Satriano, C, Messina, G.M.L., Carnazza, S., Guglielmino S., Marletta, G., *Bacterial adhesion onto nanopatterned polymer surfaces*, Material Sci. Eng. C, (2006), in press.

Satriano, C, Messina, G.M.L., Marletta, G., *A colloidal-based nanofabrication method for topographically and chemically patterned polymer surfaces*, manuscript in preparation.

1B - Perfluorocarbon O/W emulsions: physico- chemical characterization and Cells viability

*Pierandrea Lo Nostro, Simona Rossi, Lorenzo Tattini, Piero Baglioni (*in collaboration with *Monica Monici, CEO - Centre of Excellence in Optronics, c/o Sect. Medical Physics, Dept. of Clinical Physiopathology University of Florence and Gloriano Moneti, Centre of Gas Chromatography and Mass Spectrometry, CISM).*

Aims

The purpose of the present study – in the framework of a research project sponsored by the Italian Ministry for Health - is the investigation of the aging mechanisms of perfluorocarbon emulsions using image analysis and light scattering method.
Interaction of perfluorocarbon O/W emulsions with human blood cells has been evaluated with cell viability, morphological and metabolism changes.

Results

Perfluorocarbons (PFCs) are highly fluorinated, inert organic compounds that dissolve large volumes of respiratory gases such as oxygen and carbon dioxide. Liquid PFCs are colorless, odorless, and noncorrosive. As they are immiscible in aqueous systems, including biological fluids such as plasma and cell culture medium, they have to be emulsified for intravascular administration and for use in biological reactors. It has been shown that the toxicity of the emulsion is directly related to the emulsion droplet diameter [1]; above 300 nm, the toxicity of the emulsion increases markedly. It is therefore vital to ensure that destabilization of the emulsion is prevented or controlled as far as possible if the emulsion is destined for intravenous use.
There has been a considerable effort to formulate stable PFC emulsions and to understand the driving forces and mechanisms responsible for their aging. Emulsion stability can be studied through the evolution of the droplet size and size distribution. The increase in droplet diameter is an indicator of the loss of stability of the emulsion and the growth rate of the droplets reveals the mechanism responsible for the aging. Two main mechanisms have been proposed for the loss of stability of these emulsions: coalescence and molecular diffusion.
Oil-in-water emulsions of four perfluorocarbons (perfluorooctane, perfluorodecalin, perfluorooctyl bromide, perfluorotributylamine) were prepared with Pluronic F-68 (PL-68) as emulsifiers. Moreover a semifluorinated alkane (diblock $F(CF_2)_m(CH_2)_nH$ short-chain copolymers such as F_8H_{16}) with a phospholipid (namely DPPC) has been used for the formulation of quaternary oil-in-water emulsions composed of the same PFCs. The emulsions were prepared by a preliminary high energy dispersion methodology (Ika Ultra-Turrax disperser) and a subsequent sonication. All emulsions were autoclaved after preparation and their stability was followed through optical microscopy in phase contrast mode and dynamic light scattering. All formulations slowly sedimented their fluorocarbon droplets over a period of several days, and formed a gel which was, however, easily redispersible without any change in droplet diameters. The stability of emulsions was checked at three different temperatures: 4°C, 25°C and 37°C.
Light scattering and optical microscope (Figure 1, left) experiments revealed that perfluorotributylamine /PL-68 retained its initial diameter of 200 nm throughout the duration of the experiment at all storage temperatures. All other formulations based on PL-68 showed an increased diameter especially at higher temperature. The perfluorodecalin-

based emulsion had a significantly larger and heterogeneous droplet diameter (Figure 1, right).
The aging mechanism seems to be dependent on both the composition of the emulsion and the conditions of storage. For example, perfluorodecalin/PL-68 suffer degradation by coalescence, except for the emulsions stored at lower temperature, where the molecular diffusion plays a dominant role. A different behaviour was found for PFC/F_8H_{16}/DPPC emulsions where the smaller size distribution and higher stability with aging was attributed to the perfluorodecalin base emulsion.

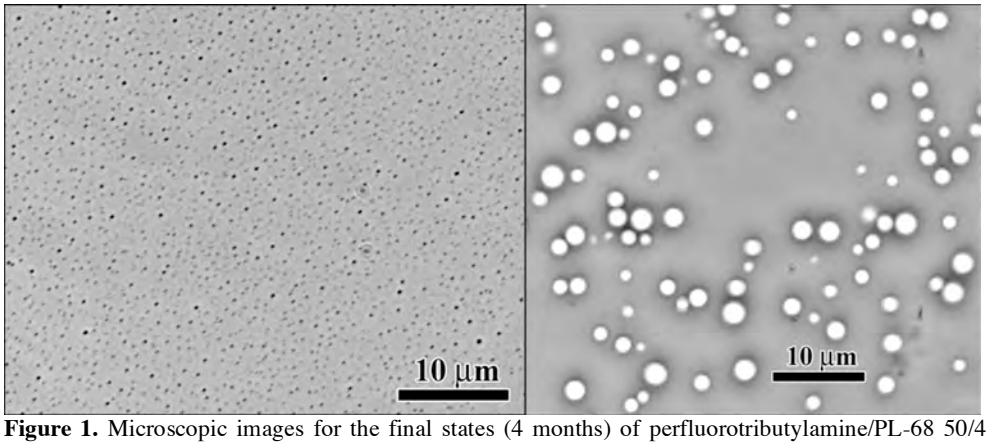

Figure 1. Microscopic images for the final states (4 months) of perfluorotributylamine/PL-68 50/4 %w/v(left) and perfluodecalin/PL-68 50/4 %w/v (right) aged at 25°C.

Cell viability experiments confirmed the key-role played by emulsion droplet size distribution: in fact, perfluorotributylamine/PL-68 and perfluorodecaline/ F_8H_{16}/DPPC emulsions showed higher cell viability. Cell size increased of 30-40% after 24 hours incubation at 37°C.

1B - Phase behavior, microstructure and dynamics of surfactant systems: micelles, liquid crystals, microemulsions, and emulsions

M.Monduzzi, F. Caboi, S. Mele, S. Murgia, P. Baglioni, L. Ambrosone, R. Angelico, M. Olla, in collaboration with P. Lazzari (Atlantis, Cagliari),A. Chittofrati (Ausimont CRS, Milano -Italy), O. Soderman (Lund, Sweden), A. Khan (Lund, Sweden), B.W. Ninham (Canberra, Australia)

Aims

Phase diagrams characterization
Relationship between surfactant shape and microstructure
Microstructural transitions in microemulsions:percolative behavior

Results

Some perfluopolyether carboxylates having Na^+, K^+ or NH_4^+ counterions and hydrophobic chains constituted by perfluoropropilene oxide units and mostly $Cl\text{-}C_3F_6O$- terminated, were investigated for phase behavior through surface tension, conduxctivity, optical microscopy and NMR. Different hydration and binding degree of the different counterions cause variations in the extension of the micellar region and in the type of liquid crystalline phases. This, in turn, implies variation of the effective packing parameter v/al.

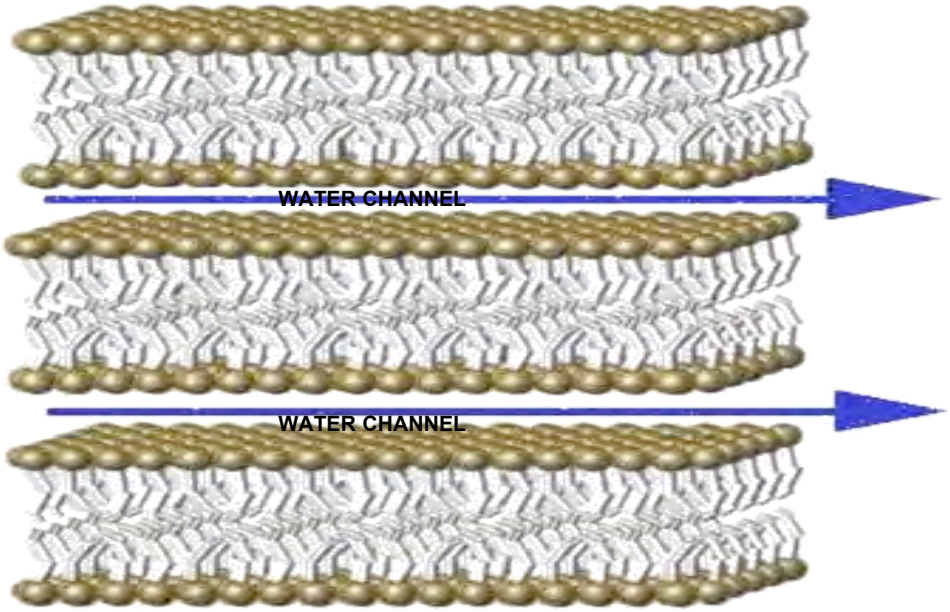

Lamellar Liquid Crystals

a 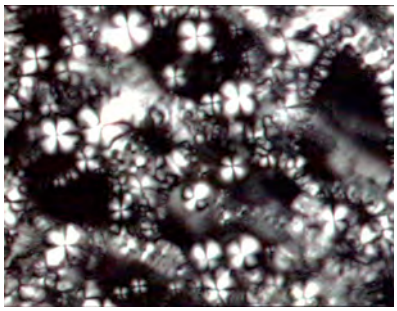 b 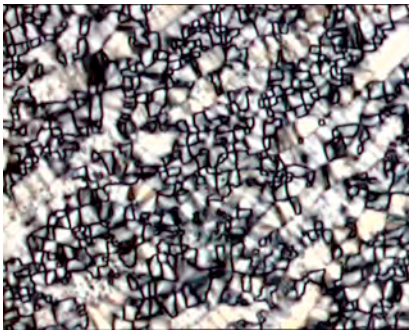

Optical micrographs in polarized light of different lamellar phases

Investigations on the microstructural transitions occurring in the w/o microemulsions phase formed by Na-AOT and Ca-AOT with decane and isooctane oils were carried out through NMR self-diffusion measurements. Diffusion data along with conductivity measurements allowed to establish that w/o spherical droplets form only in a very limited range of compositions and close to the oil corner.
Several studies were carried out on ternary systems, based on DDAB surfactant.

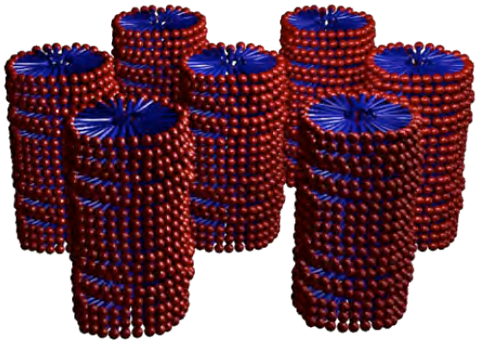 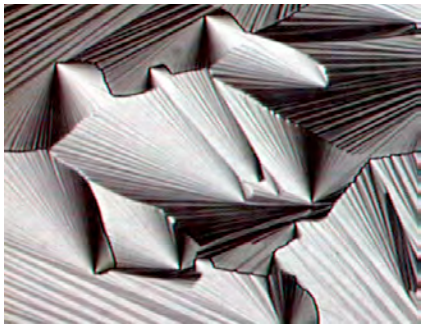

Hexagonal Liquid Crystals and typical pattern at the Optical microscope in polarized light

Phase diagrams were characterized in the presence of some aromatic oils such as toluene and trifluoro-methylbenzene, and semifluorineted linear alkane oils such as C_4F_9 C_4H_9 and C_8F_{17} $C_{16}H_{33}$, and also a fully perfluoropolyether oil, or perfluorooctane oil. Aromatic oils allow the formation of microemulsion regions characterised, at high oil content, by the presence of DDAB molecules almost molecularly dispersed. This arises from the strong aromatic oil stacking. The presence of semifluorinated or fully fluorinated oils induces the formation of higly stable emulsions which were characterised through NMR self-diffusion, and optical microscopy . The most significant result in the case of a semfluorinated oil (C_4F_9 C_4H_9) is that w/o droplets having bimodal size distribution form [3]. Conversely, in the case of fully fluorinated oils oil-in-lamellar liquid crystals (DDAB/W lamellar phases) emulsions occur.

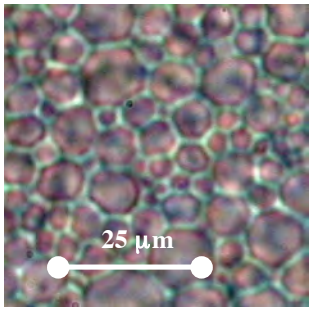

a

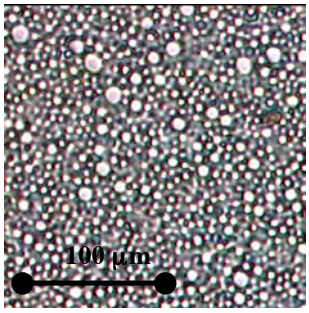

b

Optical micrographs of droplets in concentrated emulsion samples

Some DDAB/water/oil (decane, dodecane, toluene) microemulsions were investigated along oil dilution lines through ^{14}N NMR relaxation. The analysis of relaxation data in terms of the two step model along with percolation theory allowed to quantify the range of the correlation times which characterise the interactions (staic and dynamic percolation regimes) among the DDAB aggregates as a function of the oil content.
A review paper on the microstructural transitions occurring in concentrated w/o microemulsions allowed to emphasize furthermore that w/o spherical droplets seldom occur. In many cases, particularly for surfactants having packing parameters close to unity, non spherical closed water domains are often present at low volume fractions of the dispersed phase also.

References

Caboi F., Chittofrati A., Lazzari P., Monduzzi M. (1999) *Counterion effect on the phase behavior of Perfluoropolyether carboxylates: 1. Micelles and Liquid Crystals in Water.* Colloids and Surfaces A, **160,** 47-56

Olla M., Monduzzi M., Ambrosone L. (1999) *Microemulsions and emulsions in DDAB/W/Oils Systems* Colloids and Surface A, **160,** 23-36

Pitzalis P., Angelico R., Soderman O., Monduzzi M. (2000) *A structural investigation of Ca-AOT/water/oil microemulsions* Langmuir, **16**, 442-450

Olla M., Monduzzi M. (2000) *On DDAB microemulsions: Influence of an Aromatic Oil on the microstructure* Langmuir, **16**, 6141-6147

Monduzzi M., Mele S. (2001) *A novel NMR approach to model percolation in w/o microemulsions* J. Phys. Chem. B, **105**, 12579-12582

Mele S., Khan A., Monduzzi M. (2002) DDAB Ternary System: characterization of three-phase Emulsions J. Surf. Deterg., **5**, 381-389

M. Monduzzi (2003) *NMR of Liquid Crystals and Micellar Solutions* in Nuclear Magnetic Resonance, Specialistic Periodical Report, ISBN 0-85404-342-X , Ed. G.A. Webb, The Royal Society of Chemistry, Thomas Graham House, Cambridge (UK), Vol 32, Chap. 15, 520-558

Monduzzi M., Caboi F., Mele S., Murgia S., Baglioni P., Ninham B.W. (2003), *Microstructure and Percolation of Concentrated w/o Microemulsions* In Self-assembly, ISBN 1-586033824 Ed. B.H. Robinson, IOS Press, Amsterdam pp. 251-259

Mele S., Murgia S.,Monduzzi M. (2004) *Mixed micelles of homologous of PerfluopolyetherAnionic Surfactant in Water* J. Fluorine Chem. **125**, 261-269

Mele S., Chittofrati A., Ninham B. W., Monduzzi M. *^{19}F NMR investigation of mixed surfactant partitioning and kinetic stability of fluorinated nanodroplets in water*. J. Phys. Chem. B, submitted (2004)

M. Olla, A. Semmler, M. Monduzzi, S. Hyde From mono to bilayer: mesostructural evolution in the ternary cationic microemulsion *DDAB/water/tetradecane*. J. Phys. Chem. B, submitted (2004)

Mele S., Ninham B.W., Monduzzi M. Phase behavior and microstructure of perfluoropolyether surfactants. NMR, SAXS, and Optical Microscopy Studies. J. Phys. Chem. B, submitted (2004)

1B – Photoresponsive Surfactants

M. Bonini, D. Berti and P. Baglioni

Aims

Aim of the project is the investigation of the photoresponsive properties of cationic bolaphorm surfactants, where an azobenzene moiety connects two identical hydrophobic chains terminated by quaternary ammonium groups. Such molecules forms supramolecular assemblies in water in a way similar to ordinary surfactants, but both interfacial and associative properties can be modulated or even fine-tuned by shining the sample with appropriate wavelength light. Since the isomerization is accompanied by a change in conformation, whose extent is determined by the derivatization of the chromophore, they represent excellent candidates for optical storage devices, where the information is contained in the light induced alteration of conformational properties.

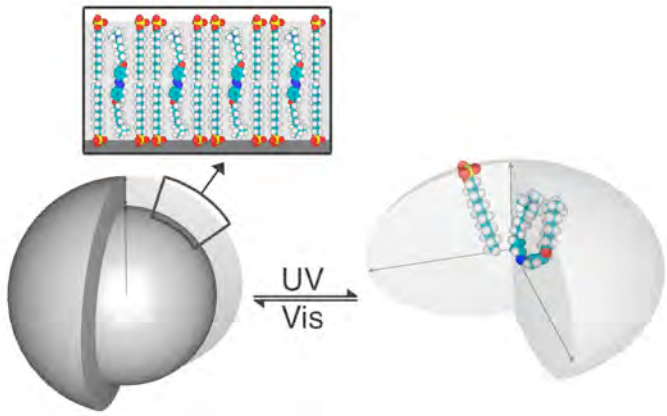

Results

Azobenzene derivatives present unique electronic properties, since their cis-trans isomerization, driven by light absorption in the UV-Vis range, presents an elevate reversibility, thus allowing the cycling of photoconversion.

Isomerization kinetics have been explored both in binary and in ternary systems (mixed with SDS at different mole ratios) in water. To map the photostationary states in different supramolecular assemblies, we have monitored structural properties at precise stages of a photoisomerization cycle, whose kinetics is dependent on surfactant concentration for binary systems and on SDS/BTHA mole ratio for ternary systems. This is due to the fact that concentration drives self-aggregation and isomerization itself is strictly connected to the packing constraints of the active molecule, dependent on size and shape of the aggregates.

Therefore, in order to gain a deeper insight on this mechanism and also to design supramolecular architectures with the desired structure/performance properties it was necessary to perform a structural investigation, employing the classical techniques of soft matter physical chemistry.

Mesoscopic length scales, that is the dimensional realm of nanosciences, are traditionally investigated by means of scattering techniques, in our case Photon Correlation Spectroscopy and Small Angle Neutron Scattering. For some selected samples spectra have been recorded as a function of the photoisomerization.

Very different results have been obtained for the binary and the ternary systems. This characteristic shed light on the isomerization behavior and also opens the way for possible product formulation.
For bynary systems Dynamic Light Scattering yields results that are consistent with the presence of aggregates with characteristic dimensions typical of the mesoscopic scale. However each intensity autocorrelation functions is not a simple single-exponential function, indicating the presence of different populations. This prevents a straightforward and precise analysis of the data by means of DLS.
Further evidence can be inferred from direct imaging techniques. Cryo-TEM investigation show that closed hollow structures, spherical and rod like micelles are present in the 1 mM BTHA sample in lab-adapted conditions. Simple packing considerations regarding the structure and sterical hindrance of the surfactant in its two isomeric forms (see Figure) are consistent with the fact that micellar structures can be formed preferentially by the cis isomers, while trans molecules can favorably pack in locally planar structures that eventually close in spherical vesicles.
The presence of two well-defined environments, one for each isomer, deduced by the isosbestic presence, further reinforces this hypothesis. For ternary systems, we have found that a particular composition (that is SDS:BTHA 4.8:1) yields the preferential formation of bilayered structures when trans conformation is prevailing, i.e. catanionic photoresponsive vesicles that provide distinctive features to photoisomerization properties. Since cis conformation has packing preferences toward micellar aggregates, this is the composition that, upon irradiation, brings about the highest changes in bulk solutions.

References

D. Berti, M. Bonini, G. Debrégeas, J.M. Di Meglio, P. Baglioni, “Surfactant aggregates hosting a photoresponsive amphiphile: structure and photoinduced conformational changes”, XVI Conference of the European Colloid and Interface Society, Paris (France), September, 2002.

D. Berti, M. Bonini, P. Baglioni, “Surfactant aggregates hosting a photoresponsive amphiphile: structure and photoinduced conformational changes”, XXI Congresso Nazionale della Societa’ Chimica Italiana, Torino (Italia), Giugno 2003.

M. Bonini, D. Berti, J.M. Di Meglio, M. Almgren, J. Teixeira and P. Baglioni *Surfactant aggregates hosting a photoresponsive amphiphile: structure and photoinduced conformational change*, Soft Matter, 2005, 1(6), 444.

1B - Polymerization of human fibrinogen induced by pathogenic bacteria: a microbial ‘‘deceiving strategy’’

Matteo Pierno, Laura Maravigna, and Roberto Piazza
Livia Visai and Pietro Speziale (Università di Pavia)

Topic

Protein aggregation processes, either due to structural mutations or to metabolic dysfunctions, are increasingly seen as the main source of serious pathologies that include for instance Alzheimer, Parkinson, and prionic diseases. Yet, extensive protein association effects can also be brought in by external microbial agents. Pathogenic bacteria have indeed developed a number of strategies to overcome the protective barriers of their hosts, which range from hampering recognition by the immune system, to hedging against antibacterial effectors and escaping from phagocyte attack. Phagocytosis can also be hindered by subtle strategies, aimed at deceiving phagocyte recognition. We have unraveled a peculiar “deceiving strategy” developed by *Streptococcus agalactiae* (also named GBS), the main microbial cause of bacterial sepsis and meningitis in neonates, which exploits FbsA, a cell wall protein to induce aggregation of fibrinogen (Fbg), an important plasma glycoprotein playing a key role in hemostasis. This aggregation process drives the buildup of a Fbg layer on bacterial cells, protecting GBS against phagocytosis.

Aims

i) Detecting by Dynamic Light Scattering fibrinogen aggregation induced by FbSA and providing a structural analysis aggregates.
ii) Analyzing the effects of fibrinogen aggregation on GBS bacterial cells in vivo.
iii) Investigating the consequences of FbsA-induced fibrinogen aggregation on the immuno response to Streptococcus Agalactiae.

Results

FbsA was added to dilute Fbg solutions at physiological pH in variable molar ratio, and the kinetics of aggregation followed by Dynamic Light Scattering (DLS) as a function of the time t_{agg} after mixing. The addition of FbsA yields a rapid and substantial increase of the decay time of the DLS correlation functions $g(t)$, which grows by 2 orders of magnitude in less than two hours. All DLS correlation functions are all correlation functions are well fitted, except at very short times, by a stretched exponential $g(t) = \exp[-(t / t)^{a}]$, where the stretch exponent $a \approx 0.70 \pm 0.05$ does not appreciably depend on t_{agg}, while at very short time the shape of g(t) is a simple exponential. This behaviour of $g(t)$ is commonly found for solution of semiflexible polymer, like for instance actin. The analogy with the behaviour of semirigid polymers is further confirmed by the dependence on the scattering wave-vector q of the short-time decay rate, which is found to scale as q^3.
FbsA-induced fibrinogen aggregation takes place not only in solution, but also directly on the bacterial cell wall. GBS cultures, exposed to fibrinogen tagged by Fluorescein isothiocyanate (FITC) are shown in in Fig.1 (left), which shows that fluorescent fibrinogen is fully concentrated around the GBS cells. Vice versa, no similar effect is found for *Dfbs*A GBS, a bacterial strain missing FbsA. The same effect takes place on polystyrene colloids laden with FbsA (see Fig.1, right) shows, while no Fbg binding is detected when other serum proteins like albumin are formerly adsorbed on the particle surface.

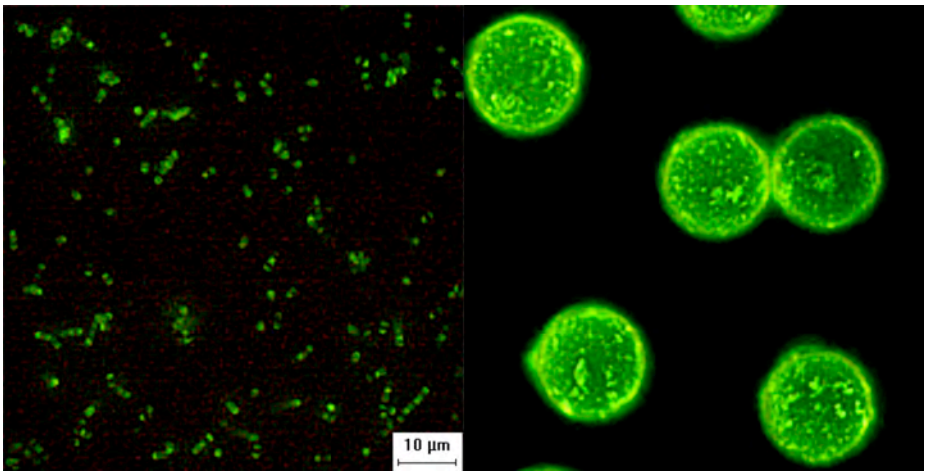

Fig. 1. Fbg polymerization on GBS cells (left) and on FbsA-laden PS particles (right)

Finally, we have compared macrophage phagocytosis for (a) GBS cells formerly exposed or not to Fbg, and (b) GBS cells expressing or not FbsA. Standard invasion essays show that exposure to Fbg reduces phagocytosis of almost a factor of 10, while no similar effects are detected for the DfbsA mutant. This evidence suggests that Fbg surface aggregation could be a relevant GBS adaptive strategy.
Protection against phagocytosis is probably not the only adaptive advantage of FbsA action on Fbg. Colonization and penetration of epithelial and endothelial tissues, which is an essential prerequisite for bacterial invasion, is certainly favored by the presence on the cell wall of a thick polymerized Fbg layer. FbsA-induced polymerization of Fbg is also very likely involved in favoring thrombus formation and endocarditis.

References

Pierno, M,, Maravigna, L., Piazza, R. Visai, L., and Speziale, P., *FbsA-Driven Fibrinogen Polymerization: A Bacterial ''Deceiving Strategy''* Physical Review Letters, **96,** 028108 (2006)

1B - Self-Assembly of β-Cyclodextrin in Water

*Massimo Bonini, Simona Rossi, Pierandrea Lo Nostro and Piero Baglioni (*in collaboration with *Goran Karlsson and Mats Almgren, Dept. of Physical Chemistry, Uppsala University)*

Aims

Although cyclodextrins (CDs) have been extensively studied for more than four decades, the self-aggregation of cyclodextrins in water has been postulated only recently. Therefore, the aim of this investigation is to confirm the existence of supramolecular assemblies in b-CD/water dispersions, and to evaluate the main structural and geometrical features of such mesoscopic structures. In order to determine both the size and the structure of the self-assembled structures, we used dynamic (DLS) and static (SLS) light scattering, in combination with cryogenic Transmission Electron Microscopy (cryo-TEM). Electron Spin Resonance (ESR) experiments were performed to study the effect of β-CD self-aggregation in water on the formation of inclusion compounds with doxyl-stearic acid-based spin probes (n-DSA).

Results

The results of this investigation definitely confirm that β-CD monomers do aggregate in water at room temperature in differently shaped particles, depending on the concentration. A critical aggregation concentration (c.a.c.) between 2 and 3 mM was determined by using Dynamic (DLS) and Static (SLS) Light Scattering. Above 3 mM aggregates are formed in water, with a minimum hydrodynamic radius of about 90 nm. These particles are in equilibrium with larger objects at higher solute concentrations. Transmission Electron Microscopy at cryogenic temperature (Cryo-TEM) was used to detect the structural features of cyclodextrin self-aggregates. The results show the occurrence of polymorphism depending on the β-CD concentration: polydisperse objects with diameters of about 100 nm are present at lower concentrations, while micrometer planar aggregates are predominant at higher concentrations. Upon sonication the large bidimensional sheets turn into entangled long fibers and folded lamellae. Static light scattering experiments were performed to evaluate the fractal nature of the particles.

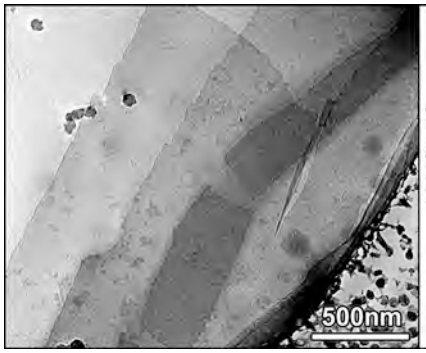

Figure 1. Cryo-TEM micrograph showing the planar aggregates formed by β-CD in water at high concentration.

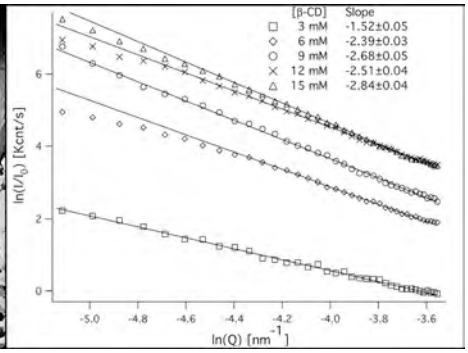

Figure 2. Static Light Scattering results of β-CD solutions in water at various concentrations.

In order to explore the aggregation of β-cyclodextrin in water and its influence on the inclusive properties, the interaction of amphipilic spin labels with b-cyclodextrin has been investigated using conventional electron spin resonance (ESR) spectroscopy. Stearic acid spin probes (n-DSA) which contain a doxyl group, a cyclic nitroxide with unpaired electrons, covalently linked to the aliphatic chain carbon in position 5, 7, 12 and 16 were used. The most relevant finding from the ESR experiments is the detection of two spectral components differing in line-width, and thus in dynamics. The faster ESR component (Component 1), which was detected in all the investigated n-DSA/b-CD systems, has been simulated in order to extract the dynamic and polarity properties experienced by the spin probes (t, <A>). The comparison of the simulation results with the spectrum obtained from the n-DSA in aqueous solutions definitely show that the Component 1 ESR signal is due to the inclusion of the stearic chain in the b-cyclodextrin inner cavity. However, the decrease in <A> does not account for the insertion of the doxyl group into the hydrophobic cavity of b-cyclodextrin, but it's consistent with its location in proximity of the hydrophilic rim.
The broader lines and lower <A> values observed for the slower ESR spectral component (Component 2) indicate that the rotational diffusion of the probes is slower, and that they experience a less polar microenvironment. This result suggests that the probes interact with large aggregates that offer different domains with different polarities. The appearance of two separated signals shows that the frequency of exchange between the two sites is low if compared to the experimental time-scale accessible through ESR, confirming the existence of stable aggregates of b-CD in water.

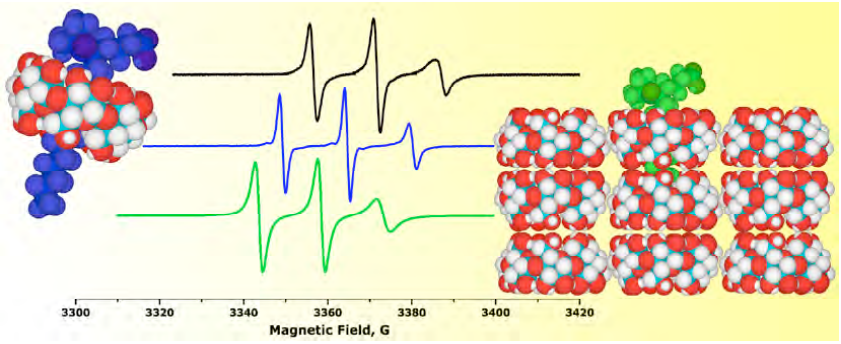

References

Bonini, M.; Rossi, S.; Karlsson, G.; Almgren, M.; Lo Nostro, P.; Baglioni, P. Langmuir ***2006***, 22, *1478-1484*.

1B - Self-Assembly of Biologically Inspired Surfactants

Debora Berti, Francesca Baldelli Bombelli, Martina Banchelli, Francesca Betti, Silvia Milani and Piero Baglioni

Aims

Aim of this project is the design of complex supramolecular structures, achieved by embedding biologically inspired "chemical information units" into surfactant molecules. The synthetic amphiphiles under investigation reproduce on their polar head the chemistry and the charge of DNA monomers and, beside their biological relevance, have considerable potential for application in Nanbiotechnologies. Over the last years we have undertaken a structural study of supramolecular structures formed by their self-assembly. The leading energetic term in determining the aggregate morphology is the choice of the hydrophobic assembler, but a fine tuning can be introduced by proper selection of the polar head. This latter contribution does not only originate from electrostatic or excluded volume interactions, as in conventional surfactants, but rather in specific recognition properties of bases. Self-assembly triggers specific base-base interaction, while the chemistry of biologically relevant polar heads implies mutual interactions in the aggregate, and modulate properties on the mesoscale. Curvature elasticity is the key energetic parameter for understanding static and dynamic properties of surfactant systems. Our ultimate aim is to higlight how self-assembly and molecular recognition interplay in determining the phase behavior (in terms of size shape and curvature elasticity) and show how this predictive knowledge can be exploited to engineer smart nanodevices.

Results

In 1994 we started to systematically implement an enzymatic route to functionalize phospholipids with nucleic acid bases in a one-pot combination of natural building blocks. The initial interest in such derivatives was boosted by their possible use as liphophilic nucleoside analogues derivatives in mieloyd leukemia treatment and HIV.

Our interest was instead directed towards a microstructural characterization of the aggregates formed by self-assembly of these amphiphiles and to highlight how molecular recognition is expressed according to interfacial curvature of these aggregates and in turn how selective interactions affect particle size and shape.

The first evidence of an interplay between molecular recognition (in terms of stacking and H-bonding efficiency of the base) and self-assembly has been obtained through a TEM morphological characterization of spontaneous self assemblies from phosphatidylnucleoside bilayers (zero curvature). Liposomes formed from unsaturated phosphatidylnucleosides (DOP-Adenosine, DOP-Uridine, DOP-Cytidine and DOP-ethenoAdenosine, ε-Adenosine) have also been investigated. Uracil and Adenine are RNA complementary bases. Cytidine is a pyrimidinic base like Uridine, and it has a similar sterical hindrance, while ε-Adenosine is a $1,N^6$ etheno bridged modification of Adenosine where the amino group of the purine is no longer available for H bonding. The UV spectra of vesicular suspensions of DOP-Adenosine, DOP-Cytidine and to a lesser extent DOP-ε-Adenosine, show consistent hypochromicity if compared to those obtained dissolving the vesicles by action of a detergent to obtain mixed micelles. Upon mixing two equimolar vesicle populations formed from complementary bases, changes in Circular Dichroism and UV spectra were detectable on the same time scale, indicating “excess” in the stacking interactions. The whole process occurred without fusion or alteration of the size distribution of the liposomes. The time-scale indicated a mixing process mediated by monomeric

exchange. At equilibrium spectroscopic features were identical to those shown by vesicles prepared by hydration and extrusion of a mixed DOP-Adenosine/DOP-Uridine films. The ideal behavior of DOP-Cytidine/DOP-Uridine systems indicated a Watson-Crick selectivity pattern. DPP-nucleoside derivatives exhibited a time-dependent annealing morphology and eventually evolved to elongated non-liposomal structures.
A recent progress in this field, which is currently investigated, concerns concetrated dispersions (up to 90% w/w). Bilayers of palmitoyl-oleoyl phosphatidylnucleoside derivatives (POP-Adenosine and POP-Uridine) have been for instance investigated in the low-water content regime by a combination of neutron diffraction and linear FTIR dichroism. Attention has been focused on the modulation of structural properties operated by the presence and the kind of nucleic acid base; base substitution causes major differences in phase behavior of the phospholipids, i.e. water sorption from a controlled humidity atmosphere and smectic periodicity. Besides a confirmation of the diffraction data, FTIR has also provided evidence that the same chemical groups at the bilayer interface (namely the sugar-phosphate) have a different orientation depending if the base is a purine or a pyrimidine.

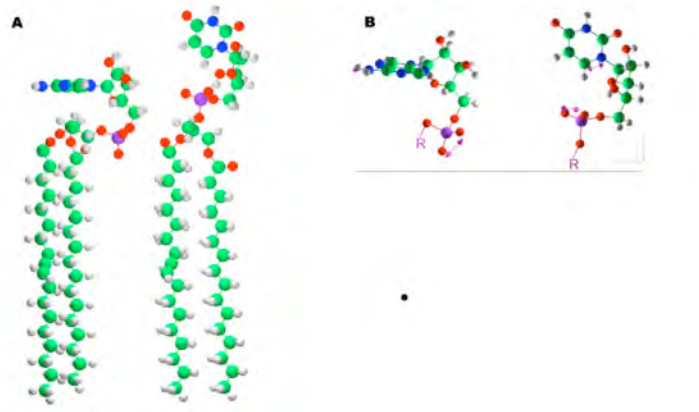

A very simple geometrical optimization agrees with this observation. This indicates that a different pattern of base interaction is operating in the two cases and that base substitution acts as a modulator of the phase properties.

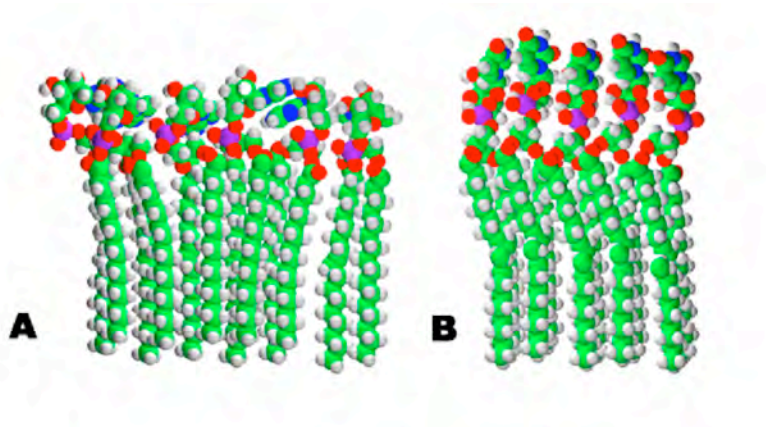

The search for molecular recognition at mesoscopically extended interface evolved toward micellar aggregates where aggregation, shape, and size are ruled by thermal equilibrium and can be altered through the variation of a control parameter. Vesicular aggregates can be considered static metastable structures while micelles are equilibrium assemblies deriving from spontaneous association of monomers as a result of delicate balance of hydrophobic and hydrophilic interactions.

The structure of micelles formed by dioctanoylphosphatidylnucleosides (diC8P-Adenosine, diC8P-Uridine and their 1/1 mole ratio mixture) has been studied by Small Angle Neutron Scattering as a function of pH and amphiphile concentration. Several indications of deviation from ideal behavior can be found in the cmc, in the area per polar head and in spectroscopic properties of bases. Selective and preferential interactions have been identified between adenine and uracil moieties, according to a pattern resembling molecular recognition in nucleic acids. In particular NMR, UV-Vis and CD spectroscopies indicate that in mixed micelles, formed from diC_8P-Adenosine and diC_8P-Uridine phosphatidylnucleosides, both stacking and hydrogen bonding interactions are present between the bases at the micellar surface. NMR indicates that a H-bonded Watson-Crick adduct is formed despite the exposure of the bases to the highly competitive aqueous environment.

Interactions of such micelles with nucleic acids ic currently being investigated, highlighting again Watson-Crick selectivity of interaction.

A recent interesting progress concerns the fromation of flexible polymerlike micellar structures by dilauroylphosphatidylnucleosides. The interfacial curvature is intermediate between globular micelles and bilayers, and like in natural nucleic acids, very different length scales (cross section and contour length) are interplaying. The size and shape of aggregates show strong dependence on the nucleolipid volume fraction and on the nature of the polar head. In fact strong stacking interactions between neighboring bases have been found for DLP-Adenosine, while DLP-Uridine has in the aggregate electronic properties similar to the momomer. Some twisted ribbon-like helical structures have been found for DLP-Adenosine at low volume fractions, while for higher concentrations flexible entangled objects are formed.

As already mentioned, micellar size and shape are extremely responsive to medium conditions. Current investigation concerns structural transitions in wormlike phases induced by the introduction of a third component (oil or “inert” surfactant, like SDS). The presence of oil (solubilized in the micellar apolar interior) or of another surfactant, controls the orientation and the distance between nucleoside groups at the interface, modulating therefore the recognition pattern between complementary bases onto the same aggregate. Hexane, cyclohexane, octane and decane can be solubilized in the interior of wormlike micelles to form oil-in-water microemulsions. We will undertake a structural investigation as a function of the chemical nature of the polar head and of the oil volume fraction.

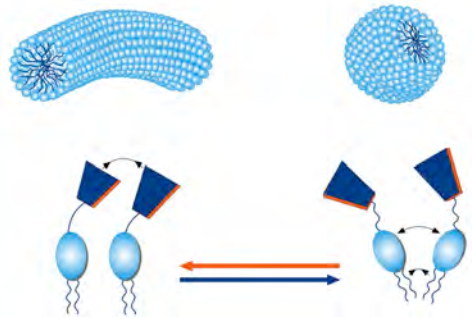

We expect to observe a stepwise transition from locally cylindrical to globular structures as oil content is increased. The persistence of a cylindrical local structure as oil content is increased has specific connections with interfacial elastic properties, connected to monomer chemical structures and is therefore the expression of molecular specificity on the mesoscale.

References

Berti, D. *Reattivita´e Riconoscimento Molecolare in Sistemi Organizzati*, Tesi di Dottorato di Ricerca in Scienze Chmiche (IX Ciclo), Universita´degli Studi di Firenze (**1997**), Biblioteche Nazionali di Roma e Firenze.

Berti D, Franchi L, Baglioni P, Luisi PL: *Molecular recognition in monolayers. Complementary base pairing in dioleoylphosphatidyl derivatives of adenosine, uridine, and cytidine*. Langmuir 1997, 13:3438-3444.

Bonaccio, S., Wessicken, M., Berti, D., Walde, P., Luisi, P. L. L. *Relation Between the Molecular Structure of Phosphatidyl Nucleosides and the Morphology of their Supramolecular and Mesoscopic Aggregates*, Langmuir, 1996, 12, 4976.

Berti D, Baglioni P, Bonaccio S, Barsacchi-Bo G, Luisi PL: *Base complementarity and nucleoside recognition in phosphatidylnucleoside vesicles*. Journal of Physical Chemistry B 1998, 102:303-308.

Berti D, Barbaro P, Bucci I, Baglioni P: *Molecular recognition through H-bonding in micelles formed by dioctylphosphatidyl nucleosides*. Journal of Physical Chemistry B 1999, 103:4916-4922.

Berti D, Pini F, Baglioni P, Teixeira J: *Micellar aggregates from short-chain phospholiponucleosides*: *A SANS study*. Journal of Physical Chemistry B 1999, 103:1738-1745.

Berti D, Pini F, Baglioni P, Teixeira J: *A SANS investigation on micelles from short-chain phospholiponucleosides*. Physica B 2000, 276:334-336.

Berti D, Luisi PL, Baglioni P: *Molecular recognition in supramolecular structures formed by phosphatidylnucleosides-based amphiphiles*. Colloids and Surfaces a-Physicochemical and Engineering Aspects 2000, 167:95-103.

Baldelli Bombelli F, D.; Keiderling, U.; Baglioni, P.: *Giant Polymerlike Micelles Formed by Nucleoside-Functionalized Lipids*. J. Phys. Chem. B. 2002, 106:11613-11621.

D. Berti, U. Keiderling, P.Baglioni, *Supramolecular structures formed by Phospholiponucleosides*, Prog. Colloid Polym. Sci, 2002, 120, 64-73.

Baglioni, P. *Rhodia Prize Lecture*, ECIS conference, Paris 2002.

D. Berti, E. Fratini, S. Dante, T. Hauss, P. Baglioni, *A structural study of Lamellar Phases formed by Nucleoside lipids*, Applied Physics A, 74, S(2002), 522-524.

F. Baldelli Bombelli, D. Berti, U. Keiderling, P. Baglioni, *Living polynucleotides formed by the spontaneous aggregation of dilauroylphospholiponucleosides*, Applied Physics A, 74, S (2002), 1270-1273.

P. Baglioni and D. Berti, *Self Assembly in micelles combining stacking and H-bonding*, Current Opinion in Colloid and Interface Science, 2003,8, 55-61.

D. Berti, F. Baldelli Bombelli, M. Almgren and Piero Baglioni, *Micellar Aggregates Formed by Dilauroylphosphatidylnucleosides* in Self-Assembly, Ed. Brian H. Robinson, IOS Press: Amsterdam, the Netherlands, 2003, 348-357.

Baldelli Bombelli, F., Berti, D., Pini, F., Keiderling, U., Baglioni, P., Flexibility of Dilauroyl-Phosphatidyl-Nucleoside Wormlike Micelles in Aqueous Solutions, Journal of Physical Chemistry B 108, 16427-16434 (2004) 1.

Francesca Baldelli Bombelli, Debora Berti, Mats Almgren, Göran Karlsson and Piero Baglioni, Light Scattering and Cryo-TEM Investigation of the Self-Assembling Behavior of di-C_{12}P-Nucleosides in Solution, J. Phys. Chem. B , 2006 in press

Silvia Milani, Francesca Baldelli Bombelli, Debora Berti, Thomas Hauß, Silvia Dante, Piero Baglioni, Structural Investigation of Bilayers Formed by 1-Palmitoyl-2-oleoylphosphatidylnucleosides, Biophysical Journal, 2006, 90 (4)

D. Berti, Self assembly of biologically inspired amphiphiles, Current Opinion In Colloid & Interface Science 11 (1), 2006

Fortini, M., Berti, D., Baglioni, P., Ninham, B. W.Specific anion effects on the aggregation properties of anionic nucleolipids, Current Opinion in Colloid & Interface Science 9, 168-172 (2004)

1B – SMART NANOSTRUCTURED MATERIALS
i - Fluorinated Systems: NMR investigations

M. Monduzzi, S. Murgia, S. Mele (Euroallumina, Portoscuso-Cagliari), A. Chittofrati (Solvay Solexis, Milan, Italy), B.W. Ninham (A.N.U., Canberra, Australia)

Aims

PFPE surfactants and oils
Micelles, mixed micelles, liquid crystal and microemulsions
Kinetic stability of fluorinated nanodroplets

Results

The mixtures of sodium and ammonium salts of three homologous perfluoropolyether carboxylic acids having Cl- terminated perfluoroalkyl group (Cl-PFPE) and differing in the average molecular weight were examined. The surfactants, namely n2, n3 and n4, have respectively two, three and four PFPE units.
The sodium and ammonium salts of perfluoropolyether acids utilized in the present work have the following general structure:

$$Cl-\left(C_3F_6O\right)-\left(C_3F_6O\right)_{n-1}-CF_2COO^-X^+$$

where $X^+ = Na^+$ or NH_4^+ and n= 2, 3, 4. In these compounds, chlorine is present only in the terminal unit, while the chain is fully fluorinated; a $-CF_3$ group is always present in the terminal unit and this group was chosen to follow the chemical shifts by the NMR technique. Each surfactant was studied alone and in mixture with the other surfactants with the same counterion. ^{19}F NMR chemical shifts were measured for each surfactant and for the mixtures in different concentrations. For a given mixture the micelle composition, X_i, can be determined from the observation of the chemical shifts of the micellar components. It was found that Cl-PFPE surfactant mixtures form in water mixed micelles which contain the surfactants in equilibrium with monomeric species. The analysis of ^{19}F NMR chemical shift variations allowed evaluating the partition of the various surfactants in the mixed aggregates as a function of the total concentration.
The observed chemical shift can be related to the aggregate and monomer chemical shifts and to the molar fraction of the surfactant in the bound and free state (X_{bound} and X_{free}) according to the relation:

$$d_{obs} = X_{bound}\,(d_{bound} - d_{free}) + d_{free} \qquad (1)$$

If the monomer and aggregate shifts are known, the bound surfactant molar fraction X_{bound} can be calculated at any given surfactant concentration.
For a mixed micellar system it is assumed that each fluorine chemical shift depends on micellar composition, which generates for each atom an average shielding effect. Extending the typical two-site model to mixed surfactant systems allows evaluating the micelles composition, using the equations:

$$\delta_{obs}n2 = \left[1+\left(\frac{\alpha n2-1}{\alpha n2}\right)\left(\frac{Xn2}{1-Xn2}\right)\left(1-\frac{\delta_{obs}n3-\delta_{bound}n3}{\delta_{free}n3-\delta_{bound}n3}\right)\right]\left(\delta_{free}n2-\delta_{bound}n2\right)+\delta_{bound}n2$$

$$\delta_{obs}n3 = \left[1+\left(\frac{\alpha n3-1}{\alpha n3}\right)\left(\frac{Xn3}{1-Xn3}\right)\left(1-\frac{\delta_{obs}n2-\delta_{bound}n2}{\delta_{free}n2-\delta_{bound}n2}\right)\right]\left(\delta_{free}n3-\delta_{bound}n3\right)+\delta_{bound}n3 \qquad (2)$$

where n2 and n3 are two different surfactants, e.g. two homologous surfactants differing in the average molecular weight. In this equation, Xn2 and Xn3 represent the fractions of n2

and n3 surfactant molecules in the bound micellar state and an2 and an3 are the corresponding molar fractions.

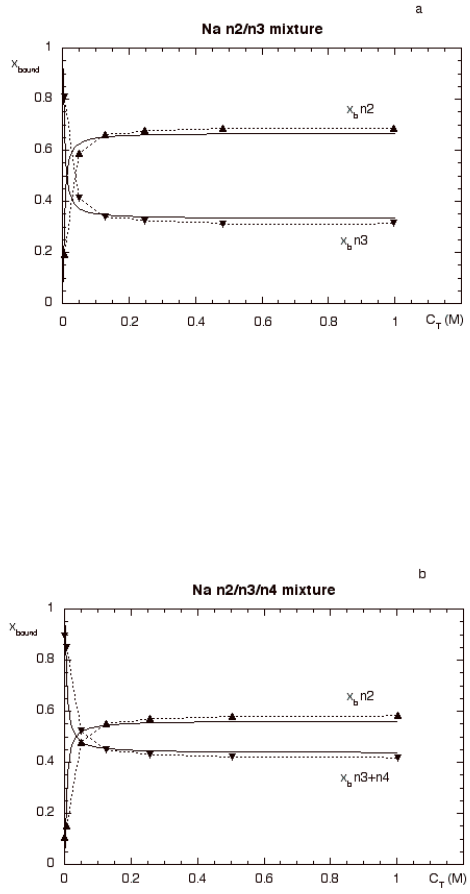

Fig. 1. Composition of the Cl-PFPE-Na micelles as a function of the total surfactant concentration C_T (M). **a**) Na n2/n3 = 60/40 binary mixture; **b**) Na n2/n3/n4=47/33/20 ternary mixture.

Composition of mixed micelles resembles ideal mixing predictions particularly at high surfactant concentrations. Self-assembled structures formed by perfluoropolyether carboxylates with hydrophobic chain terminated by $Cl\text{-}C_3F_6O$, and either sodium or ammonium counterions, have been explored in aqueous binary systems. The focus is on the different counterion specific micelles and liquid crystals formed. These have been detected and characterized via optical microscopy, SAXS and NMR. Fig. 2 shows the main features of the phase diagrams determined for the two homologous series having sodium and ammonium counterion.

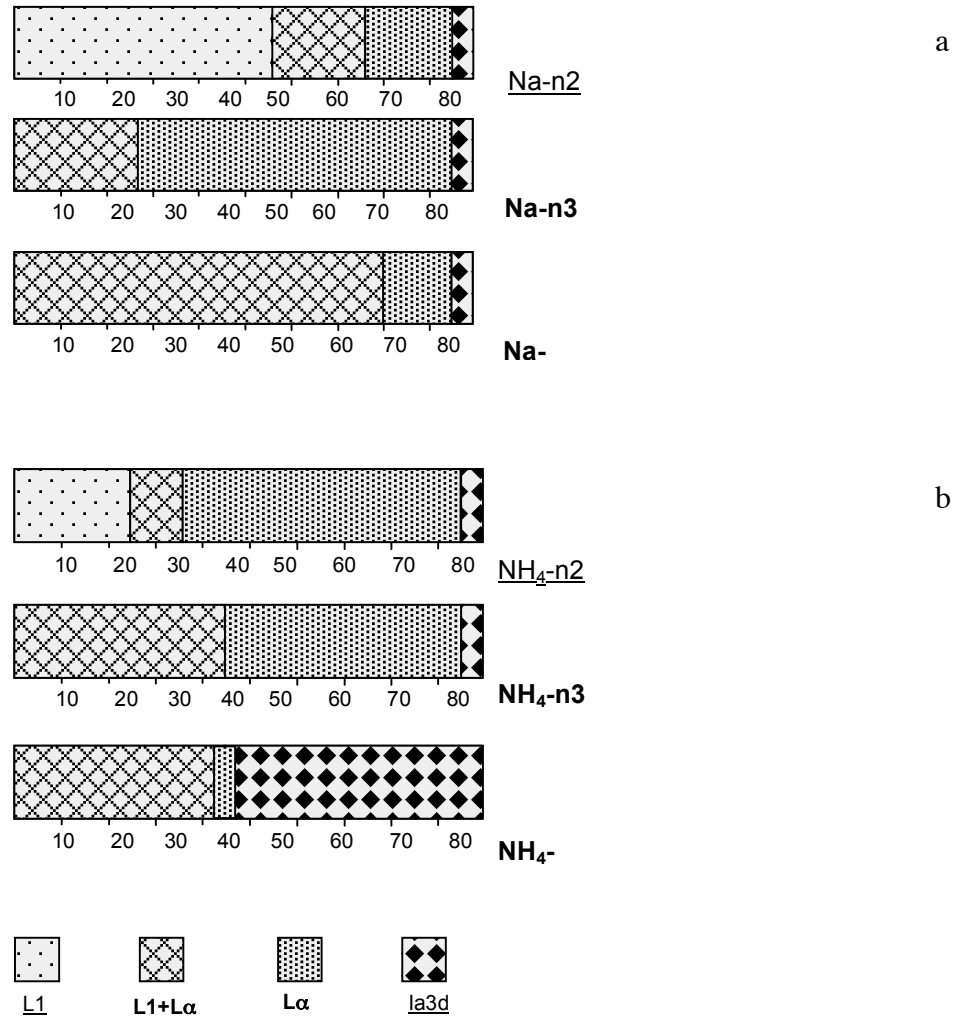

Fig. 2. Binary phase diagrams of PFPE surfactants with different chain lengths (n2, n3 and n4) and respectively Na^+ counterion (Figure 2a) and NH_4^+ counterion (Figure 2b). L_1: micellar solution; L_α: lamellar liquid crystal ; Ia3d: cubic bicontinuous liquid crystal.

All Cl-PFPE surfactants form lamellar and cubic liquid crystals independently of chain length and counterion. Non spherical micelles for the shortest PFPE chain surfactants, and anomalous swelling of the lamellar phases for almost all surfactants were ascertained. On the contrary regular Ia3d space group was ascertained for all cubic phases.

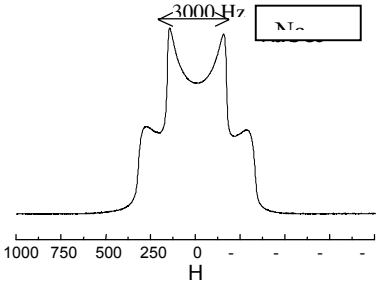

Fig. 3 ^{2}H NMR spectra showing the quadrupolar splittings for Na-n3 80% in ^2H_2O and relative optical micrograph in polarized light

It should be reminded that nuclei with a spin quantum number I≥1, such as ^{2}H, have an electric quadrupolar moment that can interact with non zero net electric field gradients giving multiple resonance of 2I peaks, separated by the splitting:

$$Dn_q=(3/m)P_b\, c\, S_b \quad (3)$$

Where m = 4 and m = 8 for the lamellar and hexagonal phase respectively, P_b is the fraction of the observed nucleus in the bound state, c is the quadrupolar coupling constant and $S_b=1/2(3\cos^2 J_D-1)$ is the order parameter related to the average time orientation (J_D) of the nucleus with respect to the surfactant chain axis. For water molecules, P_b is linearly dependent on the surfactant/water (s/w) molar ratio and thus eq. (3) can be rewritten as:

$$Dn_q=(3/m)\, n_b\, (s/w)\; c\, S_b \quad (4)$$

where n_b is the number of bound water molecules per polar head. The straight line of eq. (4) would pass through the origin at low surfactant concentration.

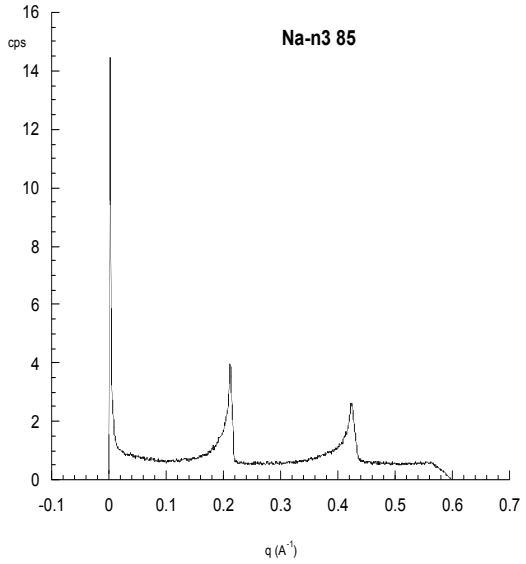

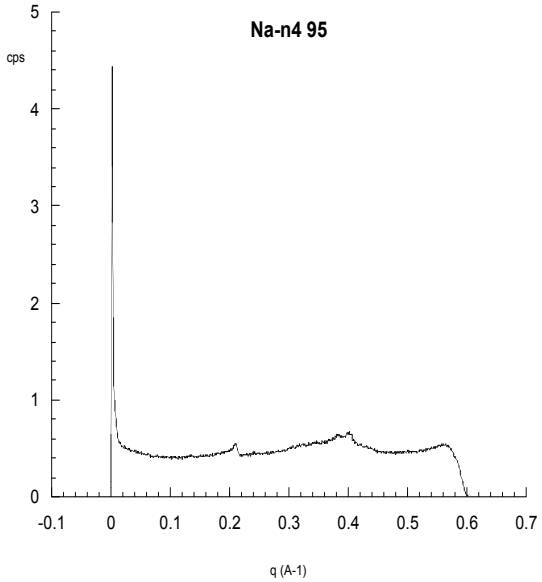

Fig. 4. Typical SAXS patterns, cps (counts per second) vs. q ($Å^{-1}$), relative to a) lamellar phase for sample Na-n3 85 wt% in H_2O b) cubic Ia3d phase for sample Na-n4 95 wt% in H_2O.

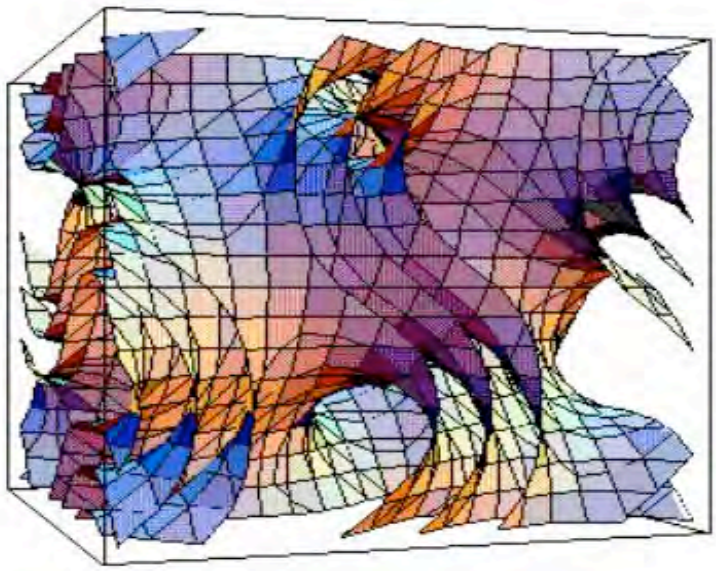

Fig. 5. IPMS surface of the Ia3d bicontinuous cubic phase.

Oil-in-water fluorinated microemulsion aggregates were diluted at high water content, so taking the system outside the regime of thermodynamic stability. The kinetic stability of aggregates was studied by an analysis of ^{19}F NMR chemical shifts. The microemulsions were formed from mixtures of three homologous perfluoropolyether (PFPE) sodium carboxylates of high purity. They had a Cl- terminated perfluoroalkyl group and differed in the number of perfluoro-iso-propoxy units in the chain. Two PFPE oils having different chain lengths and n-perfluorooctane were used to obtain the o/w fluoro-nanodroplets. The

partitioning of the individual surfactants between aqueous phase and mixed fluoro-nanodroplets as a function of total surfactant concentration was determined.
From the analysis of the ^{19}F NMR chemical shifts given in eq. 1 (for microemulsions based on n2 surfactant only), and eqs. 2 (for microemulsions based on surfactant mixtures), the degree of surfactant binding was evaluated for the nine microemulsions.
For each microemulsion the surfactant binding is reported for the different dilutions at 2, 10, and 20 g/L. As mentioned above the most dramatic effect on binding of surfactants occurs immediately after the dilution procedure.

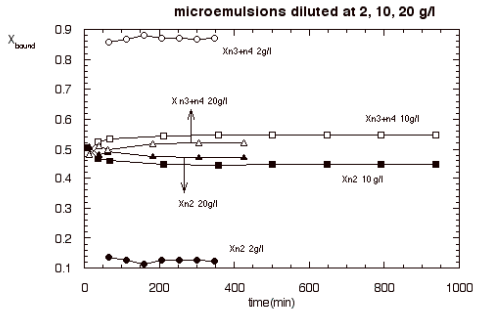

Fig. 6. Effect of dilution on the kinetic stability of the microemulsions formed by n2/n3/n4 surfactant mixture, water and a PFPE oil (MW 580)

The xn2 and (xn3+n4) molar fractions of the bound n2 and (n3+n4) surfactants are reported vs. time (minutes) for the dilutions at 2{n2(**l**),n3+n4(m)}, 10 {n2(**n**),n3+n4(c)}and 20 {n2(s), n3+n4(ê)}g/l.

References

Mele S., Murgia S., Monduzzi M., *Mixed micelles of homologousof PerfluopolyetherAnionic Surfactant in Water,* J. Fluorine Chem. 2004, 125, 261-269

Mele S., Chittofrati A., Ninham B. W., Monduzzi M. *^{19}F NMR investigation of mixed surfactant partitioning and kinetic stability of fluorinated nanodroplets in water* - J. Phys. Chem. B, 2004, 108, 8201-8207

Mele S., Ninham B.W., Monduzzi M. *Phase behavior and microstructure of perfluoropolyether surfactants. NMR, SAXS, and Optical Microscopy Studies* - J. Phys. Chem. B, 2004, 108, 17751-17759

Monduzzi M., *NMR of Liquid Crystals and Micellar Solutions in Nuclear Magnetic Resonance*, in Specialistic Periodical Report, ISBN 0-85404-342-X, Ed. G.A. Webb, The Royal Society of Chemistry, Thomas Graham House, Cambridge (UK), Vol 34, Chap. 14, 523-552 (2005)

1B - ii - NMR studies on Micelles, Microemulsions, Emulsions and Liquid Crystalline systems based on biocompatible surfactant systems for food, pharmaceutical and cosmetic applications

M. Monduzzi, S. Murgia, P. Lazzari and L. Pani (Pharmaness, Cagliari), T. Nylander and H. Larsson (Lund Unversity, Sweden), K. Larsson and H. Ljusberg-Wahren (Camurus Lipid Research, Lund, Sweden), N. Krog (Danisco Ingredients, Bradmont, Denmark)

Aims

Biocompatible and stable formulations. Cubosomes and Hexosomes
Structural characterizations by Optical Microscopy, NMR and SAXS
Dynamic aspects by NMR techniques

Results

Drug delivery systems based on liquid crystalline matrices have been developed in the recent years. The liquid crystals, generally of cubic or hexagonal space group, are formed by naturally occurring lipids such as monoglycerides or polyglycerides and phospholipids.

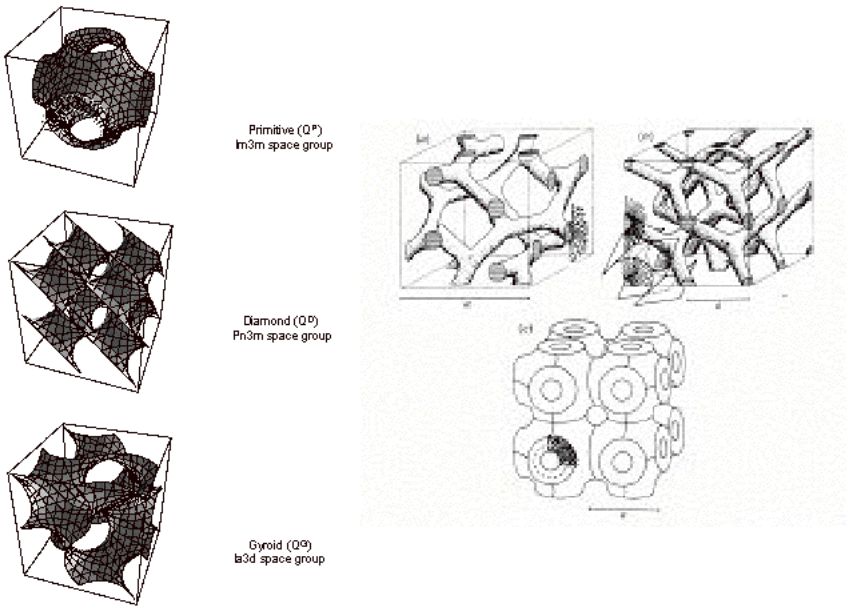

Fig, 1. IPMS and representations of bicontinuous cubic LC phases.

Particularly Glycerol monooleate-based aqueous systems were considered. The aim was the preparation of high-performance biocompatible formulations which might solubilize a large variety of additives
The characterisation of the phase behavior and of the microstructural transitions occurring in multicomponent systems was performed through optical microscopy, NMR and SAXS techniques. Thermal stability of the monophasic regions and microstructural transitions vs.

time were investigated, particularly when the volume fraction of the dispersed phase increases. Acyl migration and hydrolysis of the monoglyceride are the most significant phenomena, whose rate increases with increasing temperature and water content. Acyl migration in few months reaches the thermodynamic equilibrium that is G1MO:G2MO = 9:1 approximately.

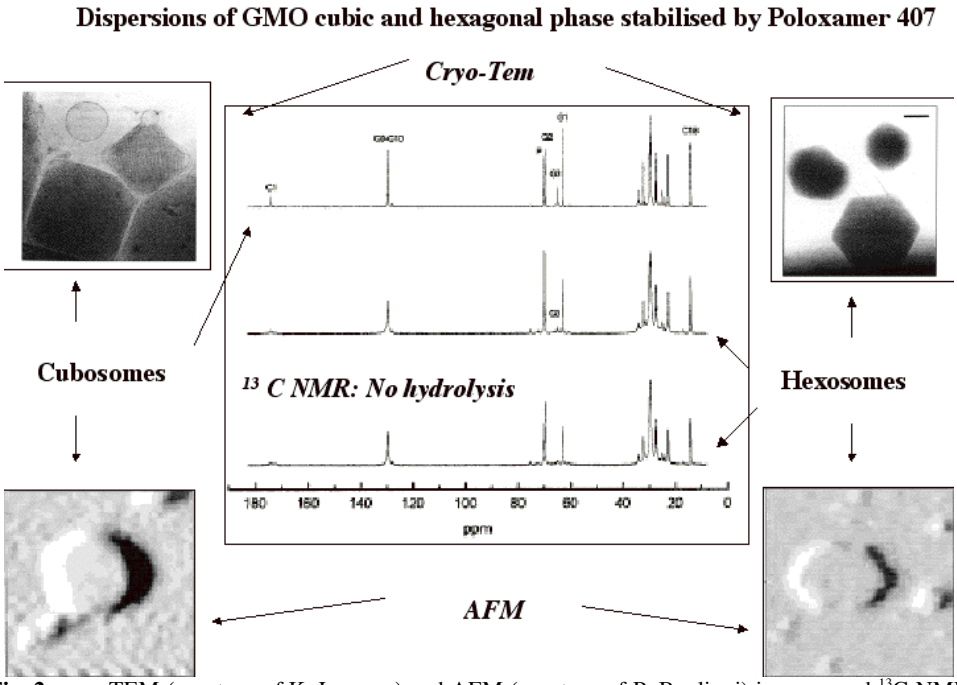

Fig. 2. cryo-TEM (courtesy of K. Larsson) and AFM (courtesy of P. Baglioni) images, and ^{13}C NMR spectra of cubosomes and hexosomes

Hydrolysis tends to progress with storage time and often the various GMO liquid crystalline phases (lamellar and cubic) undergo a transition to a reverse hexagonal phase within 6-8 months of storage due to the formation of at least 10-12 wt% of oleic acid. Some additives (for instance sodium decanoate) act sinergically with oleic acid thus the reverse hexagonal phase forms within 1-2 month from preparation of the sample. Other additives such as diglycerol monooleate - a lamellar phase forming surfactant - counteract the effect due to hydrolysis products and cubic or lamellar microstructures can be retained for years. Interestingly, GMO based systems can protect for years easily oxidazing substances such as retinol.

Cubic and hexagonal liquid crystalline phases of GMO can be dispersed in nanoparticles which display mostly cubic (cubosomes) and hexagonal (hexosomes) shape respectively as demonstrated by SAXS and also AFM techniques. The nanoparticles can be stabilised in aqueous solution for several months through addition of a triblock non ionic copolymer (poloxamer 407) which, besides the stabilizing action, prevents hydrolysis phenomena of the monoglycerides as shown by NMR spectra.

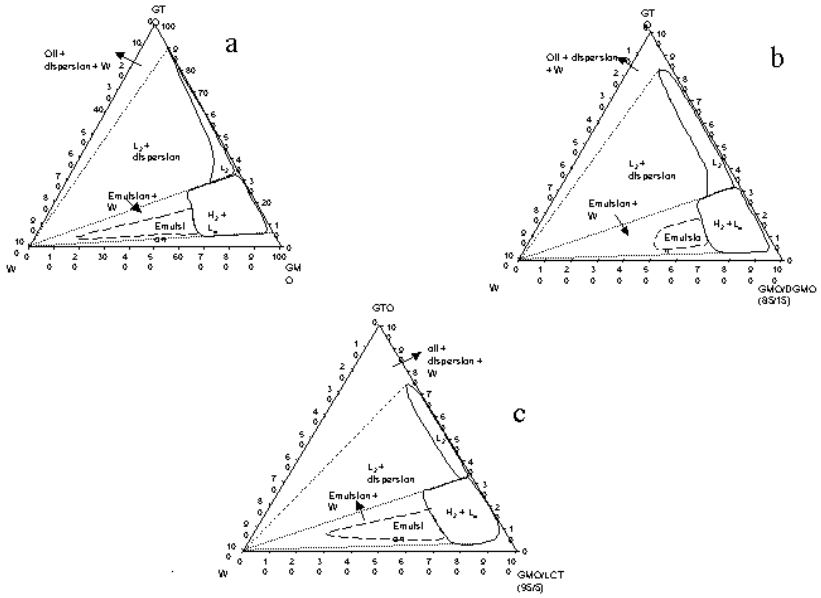

Fig. 3. Schematic diagram of: **a)** GMO/GTO/W at 25°C. **b)** GMO-DGMO (85/15)/GTO/W at 25°C. **c)** GMO-LCT (95/5)/GTO/W at 25°C. L_2: microemulsion region; H_2+L_a: two-phase region, where a reverse hexagonal (H_2) and a lamellar (L_a) LC phase coexist. The boundaries of the emulsion area are determined within ±2.5%.

^{13}C NMR relaxation experiments performed on reverse micellar solutions and various liquid crystalline phases of GMO/water, GMO/water/additive and also on cubosomes and hexosomes showed that the monoolein hydrophobic skeleton is scarsely affected by the nature of the system. The local arrangement and the dynamics are retained in all systems.
The significant variations of the relaxation times observed for the polar head were easily related to the interfacial curvature which is zero for lamellar and bicontinuous cubic phases and becomes negative for reverse micellar and hexagonal phases.
Ternary phase diagrams of mixtures of natural lipids (glycerol trioleate, glycerol monooleate, diglycerol monooleate and lecithin) and water were investigated by means of optical microscopy in polarized light and by multinuclear NMR spectroscopy. All systems showed a microemulsion region at high oil content and a large area of coexistence of two liquid crystalline (hexagonal and lamellar) phases. ^{1}H and ^{13}C NMR self-diffusion measurements were used to characterize microstructural features of the microemulsions. On water dilution the two-phase liquid crystalline region transforms into a creamy emulsion area where the droplets of water are stabilized by both the lamellar and the hexagonal phases, as indicated by ^{2}H NMR measurements. Due to the very effective dispersing action of the two liquid crystalline phases these emulsions show a high stability towards phase separation.
Warm microemulsions based on lipids characterized by a melting point over 50 •C have been successfully used as starting matrix in a quenching process to obtain solid lipid nanoparticles (SLN). In this work, we have investigated the effect of 1-butanol (B) on the phase behavior of the lecithin (LCT)/water (W)/tripalmitin (TP) system at 70 •C. The study has been carried out at LCT/B = 1 (weight ratio). Emulsion and liquid crystalline phase regions have been observed in the ternary phase diagram, while the presence of 1-butanol in

the LCT/W/B/TP system allows the formation of a wide area of liquid isotropic phase from the whole (LCT + B)/TP binary axis up to 37 wt% of water.

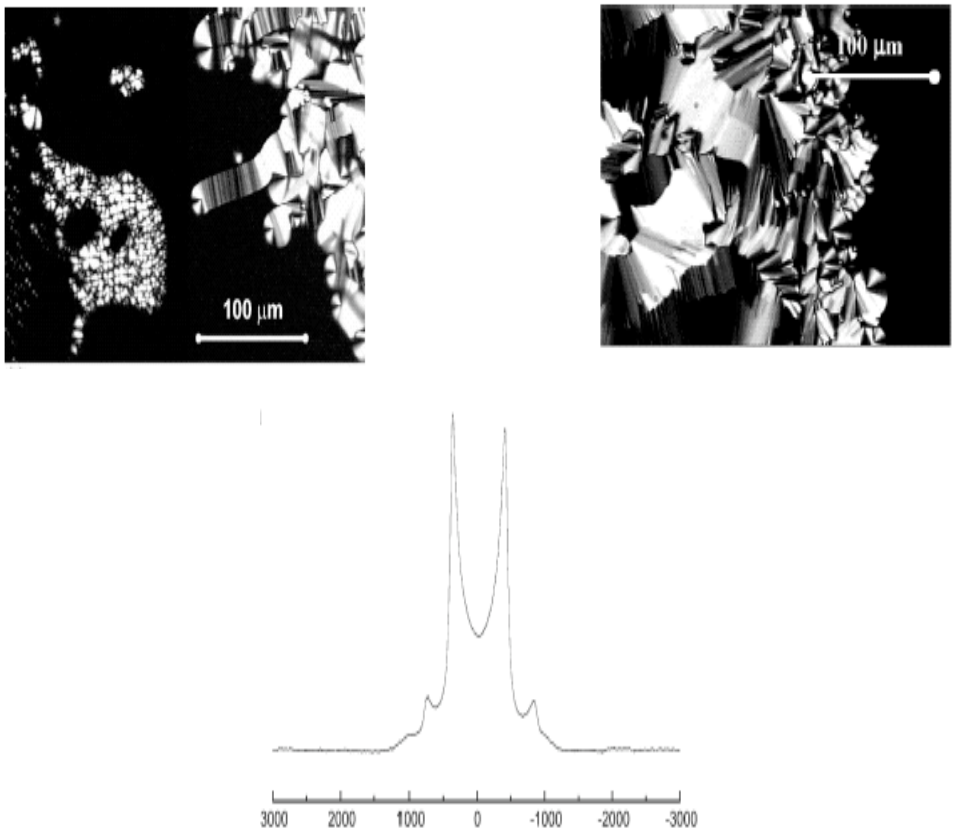

Fig. 4. Optical micrographs and ^{2}H NMR spectrum showing the coexistence of H_2 and L_a LC in the emulsion region of GMO/$^{2}H_2O$/GTO system.

The microstructure of this isotropic phase has been investigated by means of ^{1}H NMR PGSE technique. The self-diffusion coefficients of the different components along oil and water dilution lines indicate a microstructural organization characterized by a highly connected water in oil domains.
Two reviews on the use of NMR techniques to investigate liquid crystals and micellar solutions are here mentioned because of the wide interest on biocompatible systems.

References

Monduzzi M., Caboi F., Nylander T., Larsson K., *Phase behavior, microstructure, and stability of three-component Systems stabilized by a fully biocompatible surfactant.* J. Surfactant & Deterg. 1999, 2, 441

Pitzalis P., Krog N., Larsson H., Ljusberg-Wahren H., Monduzzi M., Nylander T., *Characterization of the liquid crystalline phases in the Glycerol-onooleate/Diglycerol-Monooleate/Water System,* Langmuir 2000, 16, 6358-6365

Monduzzi M., Ljusberg-Wahren H., Larsson K., *A ^{13}C NMR Study of Aqueous Dispersions of Reversed Lipid Phases,* Langmuir 2000, 16, 7355-7358

Caboi F., Amico G.S., Pitzalis P., Monduzzi M., Nylander T., Larsson K., *Addition of Hydrophilic and Lipophilic Compounds of Biological Relevance to the onoolein/Water System. I - Phase Behavior by NMR and SAXS,* Chem. Phys. Lipids 2001, 109, 47-62

Murgia S., Caboi F., Monduzzi M., *Addition of Hydrophilic and Lipophilic Compounds of Biological Relevance to the Monoolein/Water System. II - Dynamics by ^{13}C NMR,* Chem. Phys. Lipids 2001, 110, 11-17

Murgia S., Caboi F., Monduzzi M., Ljusberg-Wahren H., Nylander T., *Acyl migration and hydrolysis in monoolein based systems,* Progr. Colloid Polym. Sci. 2002, 120, 41-46

Caboi F., Murgia S., Monduzzi M., Lazzari P., NMR investigation on Malaleuca alternifolia essential oil dispersed in the Monoolein aqueous system: phase behavior and dynamics, Langmuir 2002, 18,7916-7922

Mele S., Murgia S., Caboi F., Monduzzi M., *Biocompatible lipid formulations: Phase diagrams and microstructures from Optical Microscopy and multinuclear NMR Spectroscopy,* Langmuir 2004, 20, 5241-5246

Caboi F., Lazzari P., Pani L., Monduzzi M., *Effect of 1-butanol on the microstructure of lecithin/water/tripalmitin system* Chem. Phys. Lipids 2005 135, 147-156

Angius R., Murgia S., Berti D., Baglioni P., Monduzzi M., *Molecular recognition and controlled release in drug delivery systems based on nanostructured lipid surfactants*
J. Phys: Condensed Matter 2006, 18, S2203-S2220

Murgia, S., Angius, R., Monduzzi, M., *Smart Nanostructured Lipids for Drug Delivery*
Rivista Italiana di Compositi e Nanotecnologie (Materiali, Aerospazio, Tecnologie Speciali*)* 2006, 2, 37-42

Monduzzi M., *NMR of Liquid Crystals and Micellar Solutions* in Nuclear Magnetic Resonance, Specialistic Periodical Report, ISBN 0-85404-342-X, Ed. G.A. Webb, The Royal Society of Chemistry, Thomas Graham House, Cambridge (UK), 2004 Vol 33, Chap. 15, 531-561

Monduzzi M., *NMR of Liquid Crystals and Micellar Solutions* in Nuclear Magnetic Resonance, Specialistic Periodical Report, ISBN 0-85404-342-X, Ed. G.A. Webb, The Royal Society of Chemistry, Thomas Graham House, Cambridge (UK), 2005 Vol 34, Chap. 14, 523-552

Monduzzi M., Murgia S., *NMR of Liquid Crystals and Micellar Solutions* in Nuclear Magnetic Resonance, Specialistic Periodical Report, ISBN 0-85404-357-8 Ed. G.A. Webb, The Royal Society of Chemistry, Thomas Graham House, Cambridge (UK), Vol 35, 533-561 (2006)

1B - iii - DDAB Liquid Crystals, Microemulsions and Emulsions

M. Monduzzi, S. Murgia, S. Hyde and B.W. Ninham (Canberra, Australia)

Aims

Microstructural transitions in microemulsions:percolative behavior
Specific ion effects

Results

Several studies were carried out on ternary systems, based on DDAB surfactant.

Phase diagrams were characterized in the presence of some aromatic oils such as toluene and trifluoro-methylbenzene, and semifluorineted linear alkane oils such as C_4F_9 C_4H_9 and C_8F_{17} $C_{16}H_{33}$, and also a fully perfluoropolyether oil, or perfluorooctane oil. Aromatic oils allow the formation of microemulsion regions characterised, at high oil content, by the presence of DDAB molecules almost molecularly dispersed. This arises from the strong aromatic oil stacking. The presence of semifluorinated or fully fluorinated oils induces the formation of higly stable emulsions which were characterised through NMR self-diffusion, and optical microscopy . The most significant result in the case of a semfluorinated oil (C_4F_9 C_4H_9) is that w/o droplets having bimodal size distribution form. Conversely, in the case of fully fluorinated oils oil-in-lamellar liquid crystals (DDAB/W lamellar phases) emulsions occur.

Some DDAB/water/oil (decane, dodecane, toluene) microemulsions were investigated along oil dilution lines through ^{14}N NMR relaxation. The analysis of relaxation data in terms of the two step model along with percolation theory allowed to quantify the range of the correlation times which characterise the interactions (staic and dynamic percolation regimes) among the DDAB aggregates as a function of the oil content.

Small-angle X-ray (SAXS) scattering and ^{14}N NMR relaxation were determined for microemulsion samples formed from didodecyl dimethylammonium bromide (DDAB), water, and tetradecane to deduce the associated microstructures. The swelling features within the tetradecane microemulsion are unusual compared with those of DDAB/water/alkane analogues formed with shorter *n*-alkanes: tetradecane-containing microemulsions do not show the characteristic anti-percolation transition seen for the latter microemulsions.

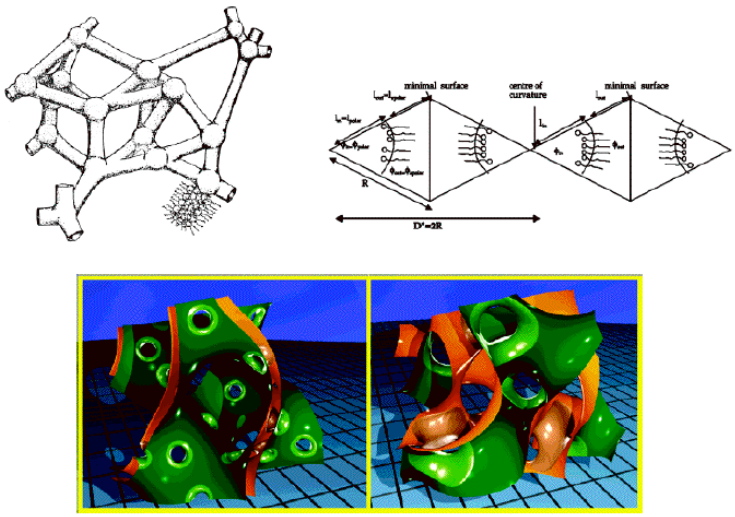

Fig. 1. Modeling of the nanostructure of DDAB/W/Tetradecane microemulsion

Experimental data along tetradecane dilution lines are consistent with a continuous transition from a bilayer to monolayer structure of the surfactant interface. The evolution is topologically complex. It involves the annealing of bilayer punctures that occur on oil dilution. A quantitative model that allows continuous transformation from multihandled bilayers (typical of L3 sponge mesophases) to multihandled monolayers (typical of microemulsions modeled with shorter chained alkanes) is proposed that well fits the observed behavior.

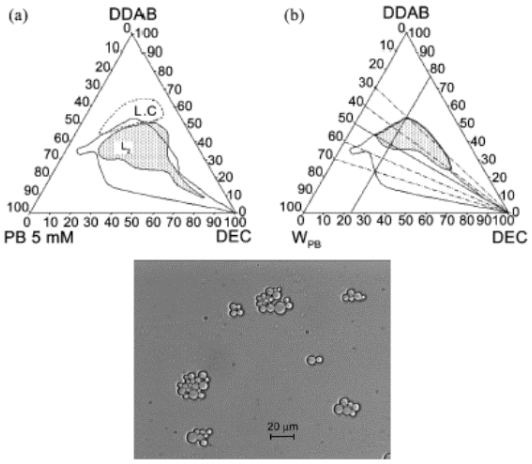

Fig. 2. Phase diagrams of DDAB/W/Decane microemulsion: (a) Phosphate Buffer 5 mM solution instead of pure water (b) fixed molar ratio [DDAB]/[PB] = 200

Ternary oil-water double chained cationic microemulsions provide a sensitive system to explore specific ion effects. Very slight changes in ionic concentrations of perturbing Hofmeister ions show up dramatic changes in bulk phase behavior that seem to throw some new light on the problem of water structure.

References

Olla M., Monduzzi M., *On DDAB microemulsions: Influence of an Aromatic Oil on the microstructure,* Langmuir 2000, 16, 6141-6147

Monduzzi M., Mele S., *A novel NMR approach to model percolation in w/o microemulsions,* J. Phys. Chem. B 2001, 105, 12579-12582

Mele S., Khan A., Monduzzi M., *DDAB Ternary System: characterization of three-phase Emulsions,* J. Surf. Deterg. 2002, 5, 381-389

Monduzzi M., Caboi F., Mele S., Murgia S., Baglioni P., Ninham B.W., *Microstructure and Percolation of Concentrated w/o Microemulsions,* In Self-assembly, ISBN 1-586033824 Ed. B.H. Robinson, IOS Press, Amsterdam 2003, pp. 251-259

Olla M., Semmler A., Monduzzi M., Hyde S., *From mono to bilayer: mesostructural evolution in the ternary cationic microemulsion DDAB/water/tetradecane,* J. Phys. Chem. B, 2004, 108, 12833-12841

Murgia S., Monduzzi M., Ninham B.W., Hofmeister effects in cationic microemulsions Current Opinion Colloid Interface Science 2004, 9, 102-106

Murgia S., Portesani F., Ninham B.W., Monduzzi M., Sodium ion interactions with cationic surfactant interfaces, Chemistry – A European Journal, 2006, 12, 7689-7698

1B - Specific ion effects

Pierandrea Lo Nostro, Barry W. Ninham, Marco Lagi, Simona Rossi, Piero Baglioni

Aims

Effect of cations and anions at different interfaces ("Hofmeister series").

Results

We examined the characteristic experimental parameters of some different systems in the presence of concentrated salt solutions (i.e. between 0.1 and 1 M).
In particular, we studied:

- the formation and precipitation of polypseudorotaxanes obtained from a- or b-cyclodextrins and PEG or PPG derivatives with different molecular weights in the presence of different electrolyte solutions (measured parameter: threading time; figure 1)
- the coagel-to-micelle or the coagel-to-gel phase transitions induced in aqueous mixtures of ascorbyl-alkanoates at different concentrations in the presence of different salts, sugars and urea (measured parameters: transition temperature and enthalpic change; figure 2)
- the water absorbency of natural wool fibers in controlled conditions (temperature and relative humidity) in the presence of different salt solutions (measured parameter: weight gain after immersion in water or solution; figure 3)
- the growth of Staphylococcus aureus (a halophilic bacterium) in standard conditions, and in the presence of some water solutions of electrolytes (measured parameter: growth rate of bacteria; figure 4)
- optical rotation of some D- and L-aminoacids

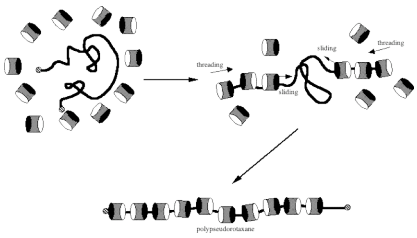

Fig. 1

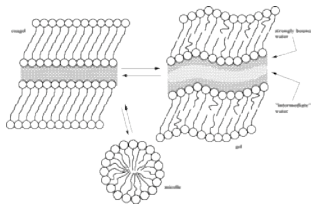

Fig. 2

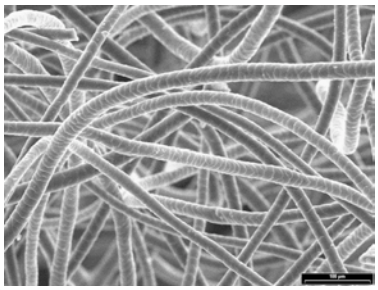

Fig. 3

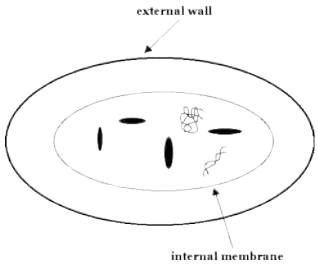

Fig. 4

In each case we checked the variation of the examined characteristic parameter as a function of some physico-chemical properties that are directly related to the dispersion interactions (i.e. lyotropic number, free energy of hydration, radius of hydrated ion, partial molar volume, molal surface tension increment, polarizability and molar refractivity).
The results indicate that in all these cases the phenomenon is ruled by dispersion forces, that originate from the different microscopic atomic properties of the single ions (namely polarizability and ionization potential).

References

Lagi, M., Lo Nostro, P., Fratini, E., Ninham, B.W., Baglioni, P. *Insights into Hofmeister Mechanisms: Anion and Degassing Effects on the Cloud Point of Dioctanoylphosphatidylcholine/Water Systems*. J. Phys. Chem. B 2007, 111, 589-597.

Lo Nostro, P., Ninham, B.W., Milani, S., Lo Nostro, A., Pesavento, G., Baglioni, P., *Hofmeister effects in supramolecular and biological systems*. Biophys. Chem. 2006, 124, 208-213

Lo Nostro, P., Ninham, B.W., Milani, S., Fratoni, L., Baglioni, P. *Specific anion effects on the optical rotation of glucose and serine*. Biopolymers 2006, 81, 136-148

Becheri A., Lo Nostro P., Ninham B.W., Baglioni P. *The Curious World of Polypseudorotaxanes: Cyclodextrins as Probes of Water Structure* Journal of Physical Chemistry B 2003, 107, 3979-3987

Lo Nostro P., Ninham B.W., Ambrosi M., Fratoni L., Palma S., Allemandi D., Baglioni P. Hofmeister *Effect in Coagels of Ascorbic Acid-based Surfactants* Langmuir 2003, 19, 9583-9591

Lo Nostro P., Ninham B.W., Fratoni L., Palma S., Manzo R.H., Allemandi D., Baglioni P. *Effect of Water Structure on the Formation of Coagels from Ascorbyl-Alkanoates* Langmuir 2003, 19, 3222-3228

Lo Nostro P., Fratoni L., Ninham B.W., Baglioni P. *Water Absorbency by Wool Fibers: Hofmeister Effect* Biomacromolecules 2002, 3, 1217-24

Lo Nostro P., Lopes J.R., Ninham B.W., Baglioni P. *Effect of Cations and Anions on the Formation of Polypseudorotaxanes* J. Phys. Chem. B 2002, 106(9), 2166-2174

Lo Nostro P., Ceccato M., Baglioni P. *a-Cyclodextrin/Polyethylene Glycol Polyrotaxane: A Study of the Threading Process* Langmuir 1997, 13(9), 2436-39

1B - Structure and dynamics of membrane proteins

G.Palazzo, A. Mallardi, G. Venturoli, R. Piazza

Aims

Study of the coupling of intra-protein electron transfer to protein dynamics in bacterial reaction centers embedded in glassy or polymer matrix

Insight on protein-protein and protein-detrgent interactions in the case of membrane proteins

Results

We have investigated the coupling of protein motions to intra-protein long-range electron transfer and to inter-protein interactions. All the investigations were carried out on a given protein: the *bacterial photosynthetic reaction center* of purple bacterium *Rhodobacter sphaeroides*. This protein provides an excellent model system for the detailed study of reaction substates and the free-energy barriers between them. The reactions can be probed by means of spectroscopical techniques, and it is possible to initiate electron-transfer in reaction centers (RC) with a pulse of light. This allows synchronized, single turnover measurements over a wide range of time scales. Reactions are reversible, allowing signal averaging.

The reduction of protein dynamics by incorporation into trehalose glasses and in polyvinylalcohol films has been used to investigate the coupling of long-range electron transfer to internal protein dynamics. Therefore the measurements here reported have the advantage of studying electron transfer in the reaction centers, when the protein dynamics approaches the one of a harmonic solid *at room temperature*.

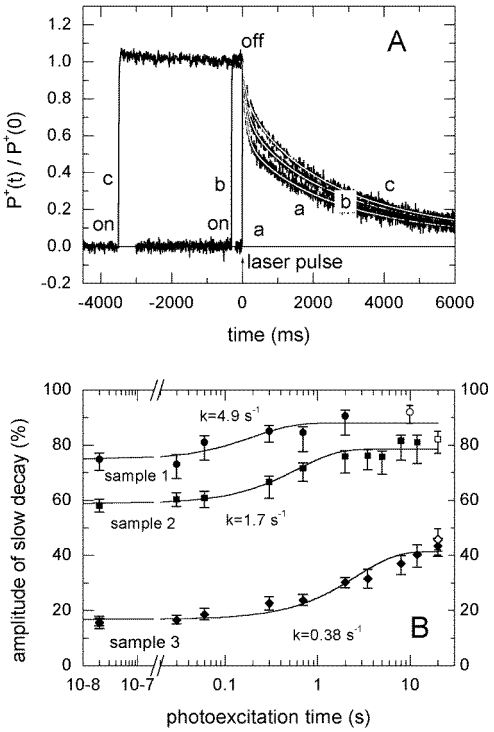

Kinetics of charge recombination following continuous illumination of RCs embedded in trehalose glasses. Panel A. P^+ decay following a laser pulse (trace a) and continuous illumination of 300 ms (trace b) and 3.5 s (trace c). Continuous curves are best fit to the sum of two power laws. Panel B. Amplitude of the slow component of charge recombination as a function of the duration of photoexcitation at increasing degree of dehydration of the trehalose matrix.

When the above internal motions are slowed down on the time scale of the studied reaction a continuous spectrum of reaction rates is observed (inhomogeneous reaction kinetics). This spectrum reflects the heterogeneity of the ensemble of the protein molecules frozen in different conformational substates, each characterized by a different reaction rate. This means that non-orthodox analyses are required to extract from the observed reaction kinetics pieces of information.

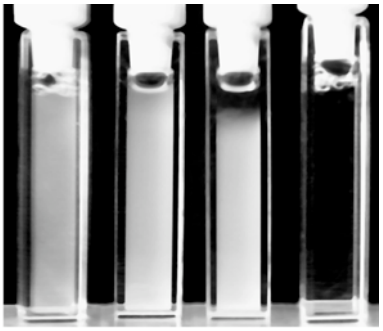

From left to right: pictures of RC/DDAO samples at pH=6.5 taken 200 s, 12 h, and 4 days after mixing, compared to a sample at pH= 8.0 (last image), remaining fully transparent for indefinite time.

We have also found that, in solution, the presence of a strong electrostatic interaction between the protein and cationic detergents, leads to the phase segregation of reaction centers into mesoscopic ‘‘droplets,’’ with a typical size of the order of a few μm and a relatively narrow size distribution. Such a phase-segregation is coupled with a conformational transition of the reaction center. To the best of our knowledge this is the first report on liquid-liquid phase separation tacking place in membrane protein solutions.

References

F. Francia, G. Palazzo, A. Mallardi, L. Cordone, G. Venturoli “Residual water modulates Q_A^- to Q_B electron transfer in bacterial reaction centers embedded in trehalose glasses”, Biophys. J., 85, 2760-2775 (2003)

R. Piazza, M. Pierno, E. Vignati, F. Francia, G. Venturoli, A. Mallardi, G. Palazzo “Liquid-liquid phase separation of a surfactant-solubilized membrane protein”, Phys. Rev. Letters, 90, article n. 208101, (2003)

Palazzo, G., Mallardi, A., Hochkoeppler, A., Cordone, L., Venturoli, G., "Electron transfer kinetics in photosynthetic reaction centers embedded in trehalose glasses: trapping of conformational substates at room temperature", Biophysical Journal, 82, 558-568, (2002)

Ambrosone, L., Mallardi, A., Palazzo, G., Venturoli, G., "Effect of heterogeneity in the distribution of ligands and proteins among disconnected particles: the binding of ubiquinone to bacterial reaction center", Physical Chemistry Chemical Physics, 4, 3071-3077, (2002)

Palazzo, G., Mallardi, A., Giustini, M., Berti, D., Venturoli, G., "Cumulant analysis of charge recombination kinetics in bacterial reaction centers reconstituted into lipid vesicles", Biophys. J.,79, 1171-1179, (2000)

1B - Structure and Dynamics of Photosynthetic Reaction Centers

G. Palazzo, A. Mallardi, G. Venturoli

Aims

Study of the coupling of intra-protein electron transfer to protein dynamics in bacterial reaction centers embedded in glassy or polymer matrix.

Results

Proteins are soft materials. Indeed, a protein is not rigid, rather it can undergo a variety of (fast) vibrations and (slower) structural rearrangements, these latter being called *protein-specific motions*. A protein share with supercooled liquids and glasses the existence of a very large number of non-identical conformation (substates)and separated by free-energy barriers. All possible substates together form the energy landscape, where a substate is pictured as a valley in the landscape. We have investigated the coupling of protein motions to intra-protein long-range electron transfer and to inter-protein interactions. All the investigations were carried out on a given protein: the *bacterial photosynthetic reaction center* of purple bacterium *Rhodobacter sphaeroide*s.

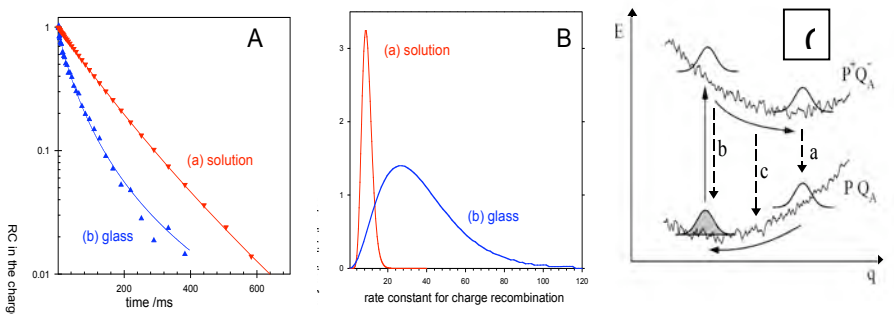

Fig. 1 *Kinetic analysis of charge recombination following laser flash excitation of RC in a trehalose solution and glass.* ***(A)*** *Normalized decay of the charge separated state measured in a 0.4 M trehalose solution (trace a), and in a dry glass (water/trehalose mole ratio of 0.47; trace b).* ***(B)*** *The corresponding distribution functions.* ***(C)*** *The corresponding evolution of the protein ensembles in a simplified diagram showing relaxation on the energy surfaces associated with the neutral (PQ_A) and the charge separated state ($P^+Q_A^-$); the abscissa q represents a generic conformational coordinate*

This protein provides an excellent model system for the detailed study of reaction substates and the free-energy barriers between them. The reactions can be probed by means of spectroscopical techniques, and it is possible to initiate electron-transfer in reaction centers (RC) with a pulse of light. This allows synchronized, single turnover measurements over a wide range of time scales. Reactions are reversible, allowing signal averaging.

Hindering of protein specific motions coupled to long-range electron transfer has been detected in RC embedded in trehalose glasses at room temperature. According to our investigations, conformational relaxations occurring in response to primary charge separation decrease both the free energy gap and the electronic coupling between acceptor and donor states, resulting in the observed stabilisation of the charge-separated state. Fig 1 shows the decay kinetics of laser induced charge separated state (panel A) and the corresponding rate distribution functions (panel B) obtained in solution (a) and in trehalose glass (b). Incorporation of the protein into a rigid the trehalose-water matrix leads to a

substantial increase of mean rate of charge recombination and of the distribution width. Both the acceleration and the spreading of the recombination kinetics observable at room temperature in extremely dried trehalose-water matrices are quite comparable with those detected upon cooling the RC in the dark below 60 K. The coupling between relaxation and electron transfer is shown schematically in Panel C, which depicts simplified free energy surfaces of the electronic states of neutral and charge-separated RC as a function of a generic conformational coordinate q. Within the Franck-Condon approximation, transitions between the $P^+Q_A^-$ and PQ_A electronic states are vertical in this diagram. The electron transfer rate is controlled by the energy gap ε, i.e. by the vertical separation between the two surfaces. Since ε varies with q, the charge recombination kinetics reflects the evolution of the protein ensemble on the lower or upper energy surfaces. In trehalose glass, the RC relaxation from the *dark-adapted* to the *light-adapted* conformation, which stabilises primary charge separation in solution at room temperature (see transition *a* in Fig2C), is prevented over the time scale of $P^+Q_A^-$ recombination. This results in an accelerated charge recombination, occurring in a structurally inhomogeneous population of essentially non-relaxed *dark-adapted* proteins (see transition *b* in Fig.2C). In moderately 'soft' matrices, a partial relaxation takes place over the time scale of charge recombination, leading to intermediate recombination kinetics (see transition *c* in Fig. 2C).

References

Cordone L., Cottone G., Giuffrida S., Palazzo G., Venturoli G., Viappiani C., *Internal Dynamics and Protein-Matrix Coupling in Trehalose Coated Proteins*, Biochim. Biophys. Acta 2005, *1749*, 252-281.

Francia F., Palazzo G., Mallardi A., Cordone L., Venturoli G., *Probing light-induced conformational transitions in bacterial photosynthetic reaction centers embedded in trehalose amorphous matrices*, Biochim. Biophys. Acta 2004, 1658, 50-57.

Francia F., Giachini L., Palazzo G., Mallardi A., Boscherini F., Venturoli G., *Electron transfer kinetics in photosynthetic reaction centers embedded in polyvinyl alcohol films*, Bioelectrochemistry 2004, 63, 73-77.

Francia F., Palazzo G., Mallardi A., Cordone L., Venturoli G.,*Residual water modulates Q_A^- to Q_B electron transfer in bacterial reaction centers embedded in trehalose glasses*, Biophys. J. 2003, 85, 2760-2775.

Palazzo G., Mallardi A., Hochkoeppler A., Cordone L., Venturoli G., *Electron transfer kinetics in photosynthetic reaction centers embedded in trehalose glasses: trapping of conformational substrates at room temperature*, Biophysical J. 2002, 82, 558-568.

1B - Study of the phase behavior of some fluorocarbon/hydrocarbon mixtures and of semifluorinated FmHn copolymers

P. Lo Nostro

Aims

Phase diagram of fluorocarbon/hydrocarbon mixtures
Self-assembly of semifluorinated alkanes in selective solvents

Results

The mutual conformational incompatibility between fluorocarbons (FC) and hydrocarbons (HC) generates a set of interesting phenomena in all states of matter. These are expression in micro-phase separation (Figure 5), segregation and self-assembly. For example, semifluorinated alkanes (F_mH_n) form ordered smectogenic liquid crystals, adsorb at the air/hydrocarbon interface, and produce gels (Figure 6: gels from F_8H_{16}/C_8F_{18} mixtures) in different organic liquids (fluorocarbons, hydrocarbons, dimethylsulfoxide, dimethylformamide, tetrahydrofurane and so on). F_mH_n can also behave as surface active agents in selected solvents. The nature of common surfactants is based on the 'chemical' antipathy of surfactant head and the tail (reminiscent of the archaic and vague concept of 'affinity'), and on their opposite 'sympathy' for water molecules. Here the mutual repulsion is simply due to the different conformations allowed—the concept and consequences of structural incompatibility are essential. SFA molecules act as "emulsifying" agents in FC/HC mixtures, increasing the miscibiliy of the two liquids, and producing a shift in the upper consolute temperature to lower *T*.

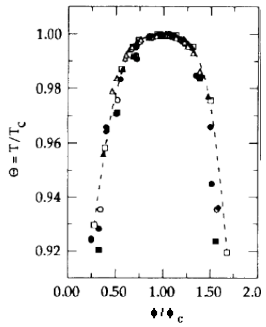

Fig. 5

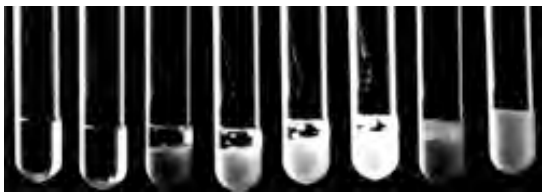

Fig. 6

References

Lo Nostro, P., *Aggregates from semifluorinated n-alkanes: how incompatibility determines self-assembly,* Curr. Opinion Coll Interface Sci. 2003, 8(3), 223-226.

Sloutskin, E., Kraak, H., Ocko, B., Ellmann, J., Möller, M., Lo Nostro, P., Deutsch, M., *The Thermal Expansion of Surface-frozen Monolayers of Semi-fluorinated Alkanes*, Langmuir 2002, 18(6), 1963-1967.

Geppi, M., Pizzanelli, S., Veracini, C.A., Cardelli, C., Tombari, E., Lo Nostro, P., *Investigation of the solid state behaviour of a semi-fluorinated n-alkane by means of NMR, calorimetric and dielectric techniques,* J. Phys. Chem. B 2002, 106(7), 1598-1605.

Lo Nostro, P., Cardelli, C., Chen, S.H., *Phase separation of fluorocarbon/hydrocarbon mixtures in the presence of semifluorinated copolymers,* Polymer Preprints 1999, 40(2), 1101-1102.

Lo Nostro, P., Choi, S.M., Ku, C.Y., Chen, S.H., *Fluorinated Microemulsions: A Study of the Phase Behavior and Structure,* Journal of Physical Chemistry B 1999, 103, 5347-5352.

Ku, C.Y., Lo Nostro, P., Chen, S.H., Structural Study of the Gel Phase of a Semifluorinated Alkane in a Mixed Solvent, *Journal of Physical Chemistry B 1997, 101, 908-14*.

1B – Surface Imaging of Nanostructures: Brewster Angle Microscopy and Ellipsometric Mapping.

G. Caminati, S. Morandi, F. Gambinossi, S. Ciappelli, P. Baglioni.

Aims

Brewster Angle Microscopy (BAM) and Ellipsometric mapping were used to control the structural organization of the bidimensional morphology of thin films at liquid and solid interfaces.

Results

Brewster Angle Microscopy (BAM) offer unique possibilities to explore the bidimensional morphology of ordered nanofilms. A recent improvement of BAM technology allows to add the simultaneous ellipsometric imaging of the entire surface with a lateral resolution of 2 mm, a scheme of the EP3-BAM instrumentation (Nanofilm technologie GmbH, Germany) is reported in figure 1.

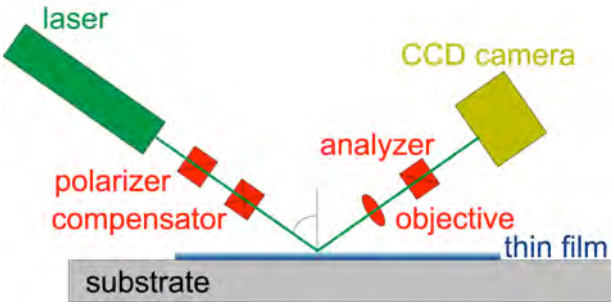

Fig. 1 Schematic representation of a Brewster Angle Microscope combined with an imaging ellipsometer.

BAM analysis is usually applied to amphiphilic molecules spread at the water-air interface in order to follow the formation of different phase domains upon compression.
We have employed these methods for the surface characterization of amphiphilic films at liquid interfaces as well as multilayers transferred on different substrates.
In the case of spreading monolayers, the present study emphasizes the importance of a careful morphological study of the bidimensional structure both before and after the transfer of the film onto the solid substrate. Such information has proved to be essential for the construction of efficiently performing nanostructures.
Furthermore, we have implemented this method for the study of adsorption films at water-air interface and for the interfacial characterization of film-forming compounds used for the construction of functional nanodevices.

a) Adsorption film at water-air interface

Adsorption films of drug molecules have been investigated adding BAM imaging to conventional surface techniques, i.e. surface tension- and surface potential – area isotherms. We focused on an important family of antibiotic, Rifamycins (Rfs), used for the treatment of several diseases, in human and veterinary medicine. Rfs structure consists in a naphtohydroquinone group spanned by an aliphatic chain, Rfs family members differ only in the substituent group of the aromatic moiety. The study evidenced that all the Rifamycins investigated are surface active and aggregate in solution above a critical

concentration (C.A.C., Critical Aggregation Concentration). Rifaximin (Rfx) and Rifampicin (Rfp) behave similarly at the water-air interface, whereas Rifamycin SV (Rsv) is more surface-active and shows different aggregation behavior. The results obtained for the modeling of surface tension data with different equations of state suggested that molecular aggregation occurs also at the interface. This hypothesis was further supported by surface potential measurements. Direct visualization of the adsorption film obtained with Brewster Angle Microscopy allowed to identify the shape and size of the aggregated domains. In figure 2 we report surface tension as a function of Rfx concentration; typical BAM images of the adsorption film are reported for the concentrations indicated by the arrows in the graph.

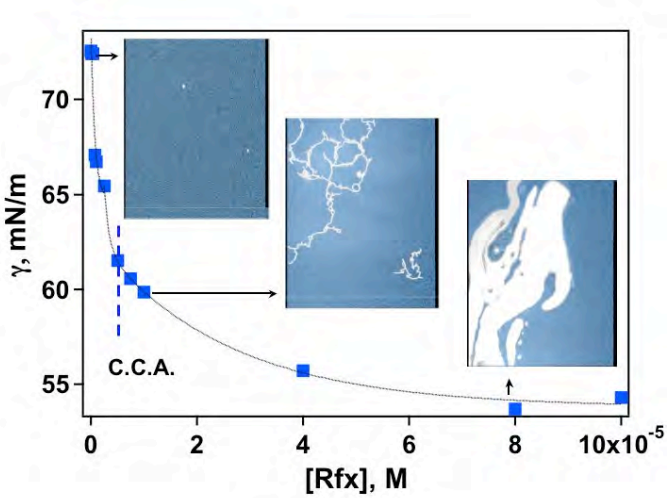

Fig. 2 Surface tension as a function of Rfx concentration coupled with BAM images (400x500 mm).

At low concentrations dark images were recorded: this indicates the presence of an extremely expanded film. Interestingly, after the C.A.C. necklace domains of condensed phase appear. A further increase of concentration leads to the formation of extremely bright regions of highly packed or collapsed material.

b) Langmuir monolayer at water-air interface

We investigated the surface morphology of a fluorescent molecule, DI-8-ANEPPS, mixed with an amphiphilic matrix. Such systems are the precursors of electrochromic nanodevices.

The film forming properties of the floating monolayers were analysed at the water-air interface by means of Brewster Angle Microscopy during surface pressure-area isotherms acquisition (figure 3).

All the mixtures are characterized by a *plateau* occurring at $p_{tr,1}$ = 28 mN m^{-1}. Below $p_{tr,1}$, the curves move towards higher molecular areas, according to the hypothesis that DI-8-ANEPPS lies flat at the interface between the matrix molecules. On the other hand, above $p_{tr,1}$, the mean molecular areas shift towards lower values with increasing concentration of the dye, suggesting a phase segregation effect of DI-8-ANEPPS. At low concentration of DI-8-ANEPPS, the mixed monolayer are more stable than the pure components as shown by the higher collapse surface pressure values; the corresponding isotherms are characterized by a second plateau, $p_{tr,2}$, around 40 mN m^{-1}.

These findings were confirmed by the visualization of the mixture morphology at the water-air interface by means of Brewster Angle Microscopy (BAM) as shown in figure 3.

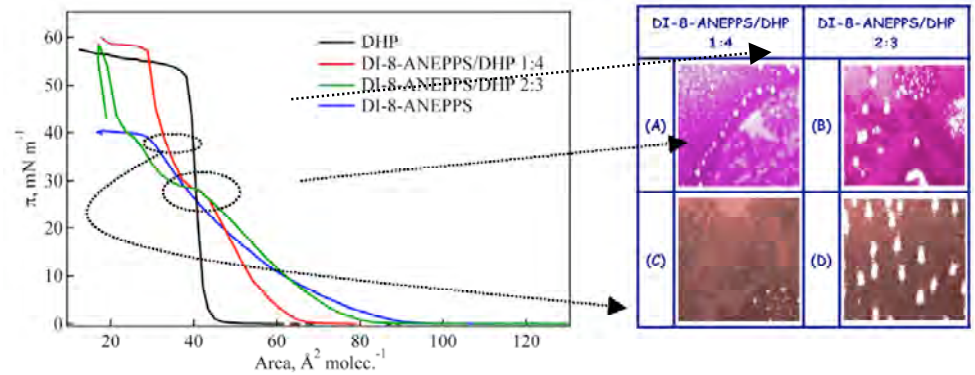

Fig. 3 Spreading isotherms and Brewster Angle Microscopy images (160 mm x 160 mm).

In fact, close to $p_{tr,1}$ the images show phase domains that grow to form circular structures containing bright spots of aggregated or partially collapsed material (A and B). Between $p_{tr,1}$ and $p_{tr,2}$, the behaviour is completely different: in the case of the 1:4 mixture (C), the film is formed by a homogeneous pattern of bright areas, while for the 2:3 mixed monolayer (D) the bright spots are regularly organized on a dark background.
These results are particularly important if such monolayers are used for the construction of nanofilms on solid support. In fact, to fabricate efficient nanodevices it is mandatory to obtain stable and homogeneous monolayers before film transfer onto the desired substrate.

c) Langmuir-Blodgett Films

Multilayer assemblies of a fluorescent polymer, MEH-PPV are promising systems to be used for OLED (Organic Light Emitting Diode) technology. We are currently studying a new molecular architecture for such systems using a combination of polyelectrolyte Layer-by-Layer (LbL) assembly and Langmuir-Blodgett (LB) deposition. To this end, a step-by-step characterization is necessary to ensure the desired hybrid layer sequence. For this purpose, we used contact angle measurement combined with film thickness determination.
A mapping of the thickness and optical constants of the film surface was accomplished using combined BAM and ellipsometric imaging of the surface. A typical thickness profile is reported in figure 4 for the hybrid LbL/LB system.

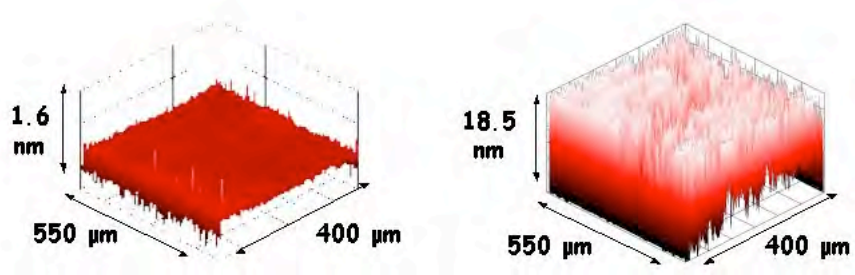

Fig. 4 Ellipsometric mapping of MEH-PPV LB films on LbL layers.

In figure 4 a, we report the ellipsometric mapping of the LbL film composed by PMA and PEI on ITO supports, the results provided a thickness value of 1.6 nm. After transferring 15

MEH-PPV layers on top of the LbL film by means of the Langmuir Blodgett technique, we obtained multilayer structures with a homogeneous pattern and an average total thickness of 18.5 nm, i.e. 1.2 nm for each layer, a value in agreement with a single MEH-PPV monolayer (see figure 4 b).
The optical response of the hybrid multilayered structure was tested measuring the electronic absorption and emission spectra. UV-Vis spectroscopy characterization of the resulting structures demonstrated that a linear growth was maintained over several deposition cycles.

References

Gambinossi, F., Baglioni, P., Caminati, G., *Structural and optical properties of a supramolecular assembly of poly[2-methoxy-5-(2'-ethylhexyloxy)-1,4-phenylenevinylene)],* VII Congresso Nazionale di Chimica Supramolecolare, Firenze (Italy), September 2005.

Caminati, G., Baglioni, P., Gambinossi, F., *In situ investigation of the morphology and of the interaction of charged surfactants with a styryl dye by absorbance spectroscopy and Brewster angle microscopy at the water-air interface,* IXth European Conference on Organised Films (ECOF 2004), Valladolid (Spain), July 2004.

Caminati, G., Baglioni, P., Gambinossi, F., *Multilayer structures of electroluminescent polymers based on a combination of Layer-by-Layer assembly and Langmuir-Blodgett deposition,* IXth European Conference on Organised Films (ECOF 2004), Valladolid (Spain), July 2004.

Gambinossi, F., Mannini, M., Baglioni, P., Caminati, G., *Morphological and spectroscopic studies on Langmuir-Blodgett films of an electro-active molecule*, to be submitted to Advanced Materials.

Mannini, M., Gambinossi, F., Baglioni, P., Caminati, G., *Immobilization of a fluorescent dye in Langmuir-Blodgett films*, Bioelectrochemistry 2003, 63(1-2), 9-12.

Gambinossi, F., Baglioni, P., Caminati, G., *Self-aggregation and phase separation of a styryl dye in monolayer at the liquid-air interface and in Langmuir-Blodgett films*, Physical Chemistry Chemical Physics 2004, 6(7), 1587-1591.

Gambinossi, F., Mannini, M., Baglioni, P., Caminati, G., *Spectroscopic properties of Langmuir-Blodgett films containing a potential-sensitive dye*, Materials Science and Engineering C 2003, 23(6-8), 897-902.

Morandi, S., Puggelli, M., Caminati, G., *Study of Langmuir monolayers and LB film containing drug molecules for biosensor applications*, VI Workshop on Biosensor and bioanalytical m-techniques in environmental and clinical analysis, Rome (Italy), October 2004.

Morandi, S., Caminati, G., *Adsoption films of Rifamycins at water-air interface*, submitted to Langmuir.

1B – Surface modification of polymers for controlled cell adhesion

C.Satriano and G.Marletta
LAMSUN-CSGI at Dept.of Chemistry, Univ. of Catania
G.Ciapetti, S.Pagani and N.Baldini
Laboratory for Pathophysiology of Orthopaedic Implants, Istituto Ortopedico Rizzoli, Bologna
G.Lupo, C.Anfuso, G.Assero and M.Alberghina
Dept. of Biochemistry, Univ. of Catania

Aims

Surface modification of polymers by ion beams and plasmas to trigger the cell response onto the irradiated surfaces. Elucidation of cell adhesion mechanism with respect to surface chemical structure and properties.

Results

The surface modification of carbon-based (e..g, polyethylenetherephtalate, PET, and poly-ε-caprolactone, PCL) and silicon-based (polyhydroxysiloxane, PHMS) polymers has been obtained either by inert ion beams (Ar^+ or He^+) at low energy (5-50 keV) in the fluence range of 10^{14}-10^{16} ion/cm^2 or radiofrequency cold plasmas of Ar and O_2. In the case of ion irradiation the thickness of the modified layers has been evaluated in the range of 100-200 nm, depending on the ion type and energy as well as the target material, while in the case of plasma treatments narrower modified depths of tens of nanometers have estimated.
The main changes of the chemical structure and composition of surfaces consisted in the formation respectively of amorphous phases a-C:H_xO_y for the carbon-based polymers and SiO_xC_y for the silicon-based material, as evidenced by X-Ray Photoelectron Spectroscopy (XPS) and Time-of-Flight Secondary Ion Mass Spectrometry (ToF-SIMS).
The characterization of the surface morphology and roughness on the micro- and nanoscale by Atomic Force Microscopy (AFM) evidenced a general smoothening of surfaces (very significant, for example in the case of PCL, where the root mean squared roughness decreases even of 2-3 times, less marked for the almost atomically flat PHMS). The wettability and surface free energy (SFE) parameters, evaluated by static and dynamic contact angle measurements, evidenced that the various modification treatments could allow to span from a very hydrophobic character (as in the case of unmodified PHMS, ~90° of water contact angle, WCA) to moderately hydrophilic (WCA~45°-50° for the ion irradiated PHMS) and very hydrophilic one (WCA~0-10° for oxygen-plasma treated PHMS), corresponding to the change of relevance of the polar acid-base components of SFE with respect to the dispersive Lifshitz van der Waals.
The surface-modified polymers have been tested with several cell lines, including fibroblasts, pericytes and osteoblasts.
In general, an improvement of cell adhesion has been observed for both ion and plasma-treated surfaces. Fig.1 shows an example of the enhanced adhesion and spreading behaviour of osteoblasts onto PCL ion-irradiated surfaces.

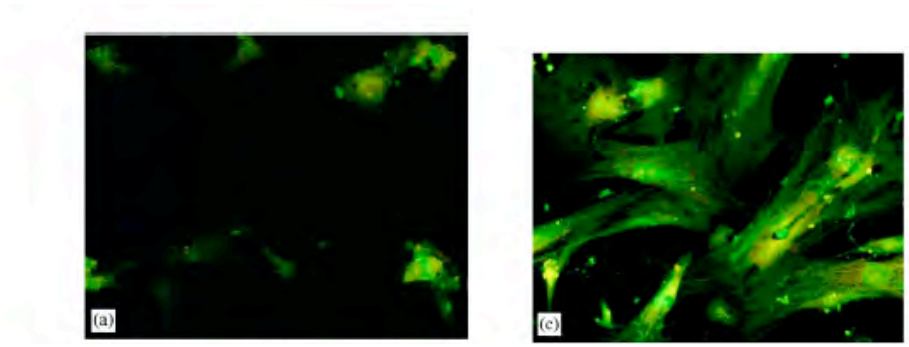

Fig. 1- Spreading of osteoblasts on PCL untreated (a) and 50 keV Ar^+ irradiated (c) surfaces. Ref. 1

A comparative study of the adhesion of pericytes cells onto oxygen-plasma treated or ion irradiated PHMS surfaces, evidenced as to the long-term cell-surface interaction, the ion-irradiated surfaces as the most promising substrates for the optimal cell spreading and proliferation process. As an example, Figure 2 shows the different adhesive response of pericytes onto unmodified, O_2-plasma treated and Ar^+ irradiated PHMS surfaces (Ref 2).

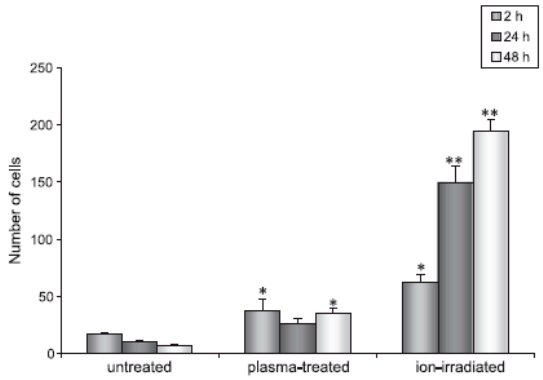

Fig. 2- Adhered pericytes on various PHMS surfaces. Cells viability was determined by trypan blue vital staining. Pericytes were plated at a density of $2x10^4$ cells/cm^2. Data shown are representative of three separate experiments (*P<0.05; ** P<0.01 compared to untreated control by Student's t test)

The observed cell behaviour has been related to the physico-chemical properties of the investigated surfaces, and some critical parameters have been found such as the polar term of surface free energy and the surface charge.

References

G. Assero, C. Satriano, G. Lupo, C.D. Anfuso, G. Marletta, and M. Alberghina, Pericyte Adhesion and Growth onto Polyhydroxymethylsiloxane Surfaces Nanostructured by Plasma Treatment and Ion Irradiation, Microvascular Research Journal, 68 (2004) 209-220.

G. Marletta, G. Ciapetti, C. Satriano, S. Pagani, N. Baldini, The effect of irradiation modification and RGD sequence adsorption on the response of human osteoblasts to polycaprolactone, Biomaterials 26 (2005) 4793–4804.

1B - Thermophoresis in macromolecular solutions and colloidal suspensions

Sara Iacopini, Andrea Guarino, Benedetta Triulzi, and Roberto Piazza.

Topic

Thermal diffusion, or Ludwig-Soret effect, is the relative matter flow induced in fluid mixtures by a temperature gradient, driving the components in opposite *-thermal gradient, is a closely akin effect taking place both for airborne particles and in complex liquids like colloidal suspensions, polymer solutions, or biological fluids. Transport of fluids or particles driven by thermal gradients takes place in many situations of basic and practical interest. Thermal diffusion in simple mixtures is generally a weak effect, but still it dramatically lowers thermal convection thresholds, playing therefore a crucial role in many naturally-occurring convective processes like thermohaline convection in oceans, and component segregation in oil wells, volcanic lava, and the Earth mantle. Particle thermophoresis in macromolecular solutions or colloidal dispersion is a much stronger effect: in DNA solutions, for instance, synergy of thermal convection and thermophoresis may lead to amplification of the local macromolecular concentration up to a thousand fold, suggesting the feasibility of Soret-driven bio-reactors. Thermophoresis is known since a long time, yet it still lacks a clear microscopic picture: for instance, in most cases particles diffuse towards the colder region, but examples of reverse behaviour are common, and no model can so far predict the direction of thermodiffusive motion. In dilute suspensions (particle weight fraction $w << 1$), the mass flow J can be written as $J = -D\nabla c - cD_T\nabla T$, where c is particle concentration in mass per unit volume, D is the usual Brownian diffusion coefficient, and D_T is called the coefficient of thermal diffusion. In the absence of convection, and assuming that ∇T is directed along z, Soret-coupling of heat and mass transfer leads therefore to a steady-state concentration gradient given by

$$dc/dz = -cS_T dT/dz,$$

where $S_T = D_T / D$ is called the Soret coefficient. S_T is therefore positive when particle are "thermophobic" (they move to the cold) and negative when they are "thermophilic" (drifting to the hot side).

Aims

- Unraveling the microscopical roots of thermophoresis
- Pointing out the role of particle-solvent interfacial properties in driving thermophoretic motion.

Experimental method.

In order to investigate thermophoresis in disperse systems, we have used a beam-deflection method, exploiting the deflection of a laser beam due to the concentration, and therefore refractive index gradient induced by the imposed temperature field. Our experimental apparatus consists first of all of a thermal--diffusion cell, made of two horizontal closely spaced plates separated by an optical--glass frame, with an optical path length of 40 mm and a sample volume of about 300 ml. Tuning of plate temperatures is achieved using two independently-controlled Peltier modules, placed in closed thermal contact with the plates. Typically, a temperature difference $\nabla T \approx 0.5 - 1^\circ$ C is applied in a time scale of few tens of seconds between the initially isothermal plates, and kept fixed within ±5 mK up to several hours. A laser beam is mildly focused through the plate gap, and the position of the

transmitted beam is monitored by a position-sensitive detector with a resolution of few mm, placed far from the cell. The beam suffers first a very rapid downward deflection $(\Delta z)_{th}$ due to the temperature dependence of the refractive index of the solution, followed by a much slower change $\Delta z_S(t)$ due to the progressive build-up of the Soret-induced concentration gradient, reaching exponentially an asymptotic limit $(\Delta z)_S$ with a time constant t set by the particle Brownian diffusion time over the plate separation distance. Due to the wide separation of the time scales between thermal expansion and Soret effect, S_T can be simply determined from the ratio of these two displacement.

Results

a) Charged colloids. By measuring the Soret coefficient of SDS micelles, we have shown that thermophoresis in charged micellar solutions has a very distinctive behaviour. In the limit of very low concentration, S_T sensibly drops by adding salt. In other words, the single particle Soret effect strongly increases with the Debye-Hückel screening length l_{DH}. However, intermicellar interactions play a strongly conflicting role, to such an extent that even at moderately low SDS concentration the situation gets totally reversed, and S_T *increases* with increasing salt concentration. Quantitatively, the single-particle Soret coefficient S_{T0} is found to scale as the square of l_{DH}. Collective effects show the same ionic-strength dependence as the solution osmotic compressibility: they increase, or conversely reduce the Soret coefficient compared to S_{T0} depending on the fact that intermicellar interactions are, respectively, attractive or repulsive. Both single particle behaviour and collective contributions can be understood in terms of model originally proposed by Eli Ruckenstein, relating thermophoresis to gradients of the particle-solvent interfacial tension *g*. According to this view, thermophoresis can be envisaged as a microscopic "thermocapillarity effect": attractive (repulsive) solvation interactions U_S `pull' particles along (`push' particles down) ∇U_S, because of unbalanced tangential stresses in a thin sublayer close to the particle surface, which can be envisaged as an effectively unbalanced *g*.

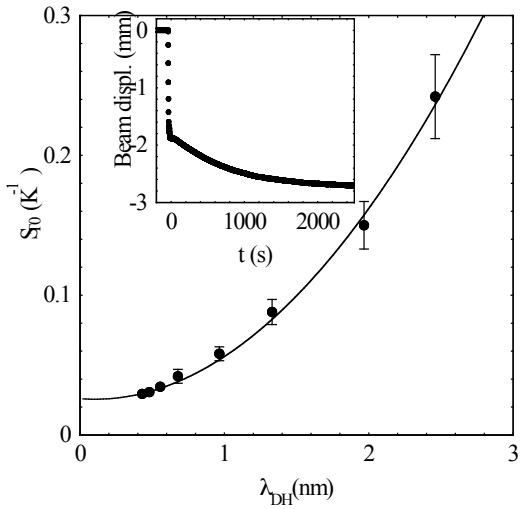

Fig.1: Soret coefficient for SDS micellar solution, in the dilute limit, as a function of l_{DH}. The insert shows a typical beam-deflection signal

b) Thermophoresis in protein solutions. Proteins in `salting-out' conditions, that is in the presence of a sufficient amount of added salt, display strongly temperature-dependent solution properties. We have found out a very puzzling behaviour of thermophoresis in lysozyme solutions [3]: particle motion can indeed be *tuned* from thermophobic to thermophilic by decreasing temperature. Moreover, by lowering T the absolute value of S_T increases exponentially, with a growth parameter that weakly depends on the ionic strength. Finally, a strong correlation of S_T with lysozyme equilibrium solubility was observed. Later [4], we have further expanded the analysis to include effects of particle charge and of the addition of different salts, and analysed transient effect to derive the temperature dependence of the thermal diffusion coefficient D_T, which was found to grow linearly with temperature, showing as S_T sign-reversal at a temperature that weakly depends on pH or ionic strength. Presently we are performing measurements suggesting that a very similar behaviour is shared by a wide class of aqueous disperse systems, ranging from synthetic polyelectrolytes to amphiphilic aggregates and rigid latex particles. In particular, the observed functional form of the temperature dependence for the Soret coefficient seems to be an universal feature of aqueous colloidal suspensions. Although we are still on the way of extending Ruckenstein's suggestion to a wider class of colloidal systems, all preliminary theoretical results seem to point out that thermophoresis takes place because of interfacial stress developing in a thin layer close to the particle surface where the solvent properties differ from the bulk. The net hydrodynamic effect of such stresses can be envisaged as a violation of the equilibrium stick boundary conditions, resulting in an effective particle slip (this is quite similar to what happens for other "phoretic" effects like electro- and diffusio-phoresis) [5]. Were this interpretation correct, thermophoresis could be used as an useful probe of particle-solvent interfacial properties

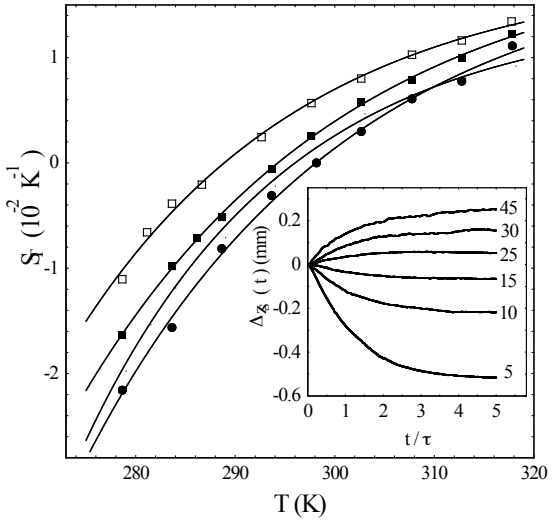

Fig.2: Soret coefficient versus temperature for c= 7 g/l lysozyme solutions at pH= 4.65, in the presence of 7.5 (open squares), 20 (full squares), 100 (full dots), and 400 mM open dots) NaCl. Full lines are fits to the exponential law proposed in ref. [3]. Inset: Soret contribution to the beam-deflection signal for lysozyme solutions at various temperatures, indicated to the right in °C: Dz_S is conventionally drawn as positive if it goes along with Dz_{th}, and each transient is plotted versus t/t for graphical convenience.

References.

R. Piazza and A. Guarino, *"Soret effect in interacting micellar solutions"*, Phys. Rev. Lett. **88**, 208302 (2002)

R. Piazza "Thermal diffusion in ionic micellar solutions", Phil. Mag. **83**, 2067 (2003)

S. Iacopini and R. Piazza, "Thermophoresis in Protein solutions", Europhys. Lett., **63**, 247 (2003)

R. Piazza, B. Triulzi, and S. Iacopini "*Thermophoresis as a probe of particle-solvent interactions: the case of protein solutions"*, Phys. Chem. Chem.Phys., **6**, 1616 (2004)

R. Piazza, *"Thermal forces: colloids in temperature gradients"*, J. Phys.: Cond. Matt. (submitted)

1B – Wax crystallization and aggregation in a model crude oil

Emanuele Vignati and Roberto Piazza
Ruben Visintin and Romano Lapasin (Università di Trento)
Paolo D'Antona and Thomas Lockhart (EniTecnologie S.p.A.)

Topic

The paraffinic (wax) component of crude oils is prone to phase separation (crystallization) at low temperature. The temperature at which wax crystals first appear as an oil is cooled is defined as the cloud point (CP), or the wax appearance temperature. Wax deposits can form on the walls of pipelines where the temperature of the external environment is below the CP, a situation commonly encountered in offshore and arctic production. Because wax deposition leads to progressive restriction of the pipeline, oil companies invest considerable effort into evaluating the risk of deposit formation and defining effective countermeasures. Below the CP, many crude oils undergo a rheological transition over a narrow temperature range to a gel-like phase characterized by a significant yield stress. This is referred to as the pour point (PP),which, as the name suggests, corresponds to the temperature below which the crude oil no longer flows. Crude oil gelation represents a threat wherever the temperature external to the pipeline lies below the PP of the oil: prolonged interruption of flow will lead to cooling of the oil and, inevitably, gelation. Because the gelled oil displays yield behaviour, significant pressure must be applied to re-start flow; in many operational scenarios, the pipeline may not be able to withstand this pressure. Thus, predicting the conditions for oil gelation and the pressure required to re-start flow are also important in the design of offshore/artic field developments.

Aims

i) Developing a "model" system, reproducing the aggregation, gelation and rheological properties of common crude oils.
ii) Describing oil gelation as a colloidal aggregation process driven by dispersion forces between the nucleated wax crystallites.
iii) Analyzing the interplay between wax crystals nucleation and growth and diffusion-limited crystallite aggregation.

Results

The model oil employed in these studies consisted of a mixture of high-mw linear (C_{20}–C_{55}) and branched paraffins (C_{18}–C_{38}) dissolved in a saturated hydrocarbon solvent (C_{11}–C_{14}). The concentration of the n- and iso-paraffins was adjusted to achieve wax crystallization and gelation over a temperature range convenient for the experimental studies (CP, 58°C; PP, 39°C). Addition of the branched paraffins proved essential to obtaining a system that closely mimics the gelation behaviour of real crude oils. The model closely resembles the crude oil in terms of its rheological behaviour. In particular, the storage and loss moduli and the shear viscosity increase several orders of magnitude over a relatively narrow temperature range around the PP (see Fig. 1). Using a custom build low-to-medium angle light scattering setup, which exploits an inverted telescope to extend the detected q-range, and a very short (200 mm) optical path cell, we have determined the structural properties of the model system as a function of T [1]. Due to the strong scattering cross section, measurements were limited to a relatively narrow temperature range below the CP. Nonetheless the systems, although macroscopically fluid, show a distinct microscopic dynamic arrest just below the CP ("physical gelation"). The light scattering data provide

strong support for several essential elements of the physical mechanism formerly proposed [2] to account for the gelation of waxy crude oils: i.e., that attractive interactions (very probably due to dispersion forces) drive aggregation of the wax solids into an extended, fractal network. Wax precipitation progressively takes place between the CP and the PP. In this region, rapid wax aggregation leads to formation of a dynamically arrested structure, whose fractal dimension is consistent with Diffusion Limited Cluster Aggregation (see Fig.2).The strength of the network increases as the amount of crystallized wax grows, to the point that the gel becomes capable of sustaining gravitational stresses. By performing settling experiments, we also obtained an estimate for the yield stress in the weak "physical" gel region just below the CP.

One of the issues raised by our results concerns the relation between dynamic arrest and mechanical rigidity. While the former requires only the build-up of a percolating network encompassing and framing all particles, the latter is related to the overall isostaticity of the structure. That is, assessment of mechanical rigidity (for a given applied stress) requires careful consideration both of the forces and of the torques acting on the structural bonds of the gel.

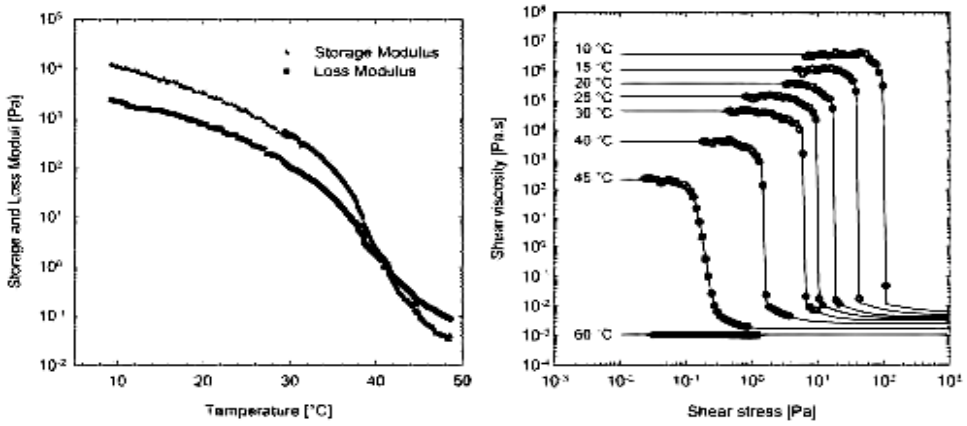

Fig. 1: Storage and loss moduli versus temperature (left, fix cooling rate, 1°C/min) and flow curves at different temperatures for the model system.

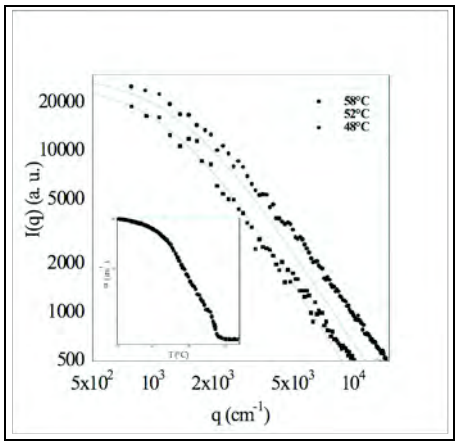

Fig. 2: Scattered intensity from the model system, fitted by a Fisher-Burford law for a fractal gel. The temperature dependence of the sample turbidity is shown in the inset.

References

Vignati, E., Piazza, R., Visintin R., Lapasin, R., D'Antona, P., Lockhart, T.P., Journal of Physics: Condensed Matter **17,** S3651-S3660 (2005),

Visintin R., Lapasin R., Vignati E., D'Antona P., Lockhart T.P., "*Rheological behavior and structural interpretation of waxy crude oil gels"* Langmuir **21**, 6240-6249 (2005)

1B - 'Weak' physical gel in organic media

A. Ceglie, R. Angelico, L. Ambrosone, G. Palazzo, G. Colafemmina, U. Olsson

Aims

Microstructure of micellar networks
Phase behavior of lecithine-water-oil ternary systems
Dynamic investigations on shear-induced phase transitions

Results

Microstructure of Lecithin organogels in Isooctane as deduced by surfactant self-diffusion NMR experiments. (**A**) Network of long worm-like micelles with few junction points (branches), whose mean density increases with increasing both micellar volume fraction and water content (**B** and **C**).

The shear-induced Isotropic → Nematic transition in Lecithin organogels in Cyclohexane presents the unusual property – for a micellar system – to have a very long relaxation time for the process of re-entanglement back to the disordered phase. This phenomenon, which is reminiscent of a mechanism where nematic state slowly re-melts to isotropic, has been recorded by performing time-resolved SANS experiments as shown below:

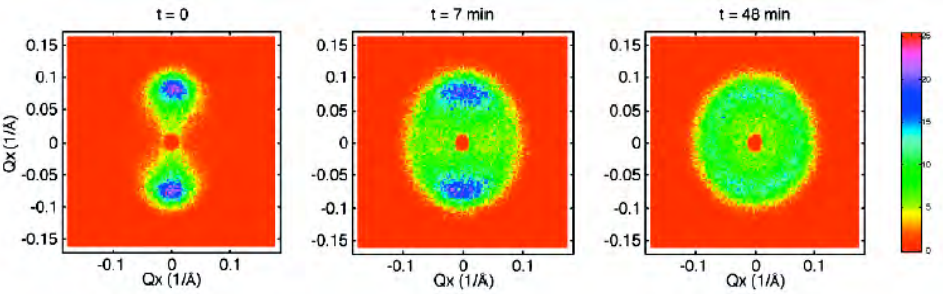

The detailed phase diagram investigation of the system Lecithin-Water-Cyclohexane at 25°C:

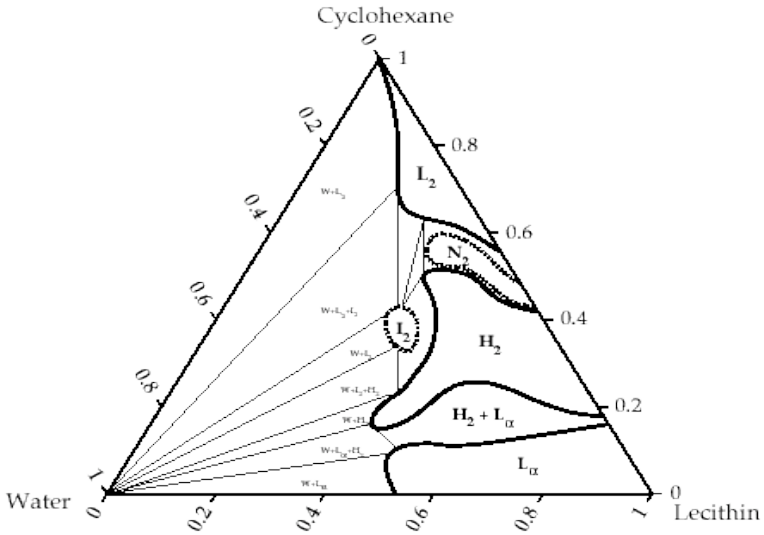

References

Angelico, R., Balinov, B., Ceglie, A., Olsson, U., Palazzo, G. and Soderman, O. "Water diffusion in polymer-like reverse micelles 2: composition dependence", Langmuir 15, 1679-1684 (1999).

Angelico, R., Ceglie, A., Olsson, U. and Palazzo, G. "Phase diagram and phase properties of the system lecithin-water-cyclohexane", Langmuir 16, 2124-2132 (2000).

Ambrosone, L.,Angelico, R., Ceglie, A., Olsson, U. and Palazzo, G. "Molecular diffusion in living networks", Langmuir 17, 6822-6830, (2001)

Angelico R., Olsson, U., Mortensen, K., Palazzo, G. and Ceglie, A. "Relaxation of shear-aligned wormlike micelles", Journal of Physical Chemistry B 106, 2426-2428 (2002)

Angelico, R., Burgemeister, D., Ceglie, A., Olsson, U., Palazzo, G. and Schmidt, C. "Deuterium NMR Study of Slow Relaxation Dynamics in a Polymer-like Micelles System after Flow-Induced Orientation", Journal of Physical Chemistry B 107, 10325-10328 (2003)

1C - Conformational Analysis of Biomolecules in Solution Using Theoretical and Experimental NMR and Molecular Simulation Methods

Claudia Bonechi, Silvia Martini, Maso Ricci, Alessandro Donati, Claudio Rossi

Aims

Determination of geometrical constraints for the structures in solution using experimental 2D-NMR techniques.
Identification of one stable conformation or families of conformations for molecules with important biological properties such as protein, nucleic acid, peptides, drugs, self-assembling polymers, etc.
The study of the relationship between structure determination and biological functions.

Results

The conformational and dynamical studies in solution, carried out with nuclear magnetic resonance techniques, are of great importance to obtain information on molecular mechanisms for biologically active molecules.
The structural determination of biological macromolecules is a fundamental step for further studies at the molecular level for their interactions with other structures. This differentiation in terms of molecular structure can be connected to the difference of biological functionality of these compounds.
Combined use of NMR experimental results, theoretical simulations of two-dimensional NMR spectra by Complete Relaxation Matrix Analysis (CORMA) and molecular dynamics calculations, represents a powerful approach in the determination of the structure of organic compounds in solution.
NOESY (Nuclear Overhauser Effect Spectroscopy) experiments are usually used to identify spatial connectivities between nuclei which are dipolarly coupled, since the size of the NOE depends inversely on the distance between two interacting spins. Geometrical constraints were obtained from 2D-NOESY and/or 2D-ROESY cross-peak intensities using the MARDIGRAS program. The derived proton-proton and proton-carbon distances were used in the molecular dynamics simulations and the accuracy of the final structures was obtained generating the theoretical 2D-ROESY spectra by CORMA program. From the protons cartesian coordinates of a molecular structure with CORMA program it is possible to determine quantitatively the entity of the dipolar interactions, including the phenomenon of spin-diffusion. In the refinement procedure the accuracy of the models obtained after molecular dynamics calculations was evaluated on the basis of the crystallographic-type R-factor, comparing experimental and theoretical NOESY spectra.
In order to obtain one single conformation or a family of conformations it is important to apply the molecular and dynamic calculations using the experimental geometrical distances as constraints. In order to take in account the conformational complexity of macromolecules with biological interest during the structural determination in solution we optimized various approaches.
For the structure calculations different methodologies have been applied. We used the restrained molecular dynamics (rMD) with the aim to explore the entire conformational space a Montecarlo method. In particular the approach based on molecular dynamics, known with the name of MDtar (Time Averaging Molecular Dynamic), has provoked remarkable interest. In this procedure the geometric constraints are not satisfied at every step of the simulation but only for a specific definable time.

This approach was applied to the study of different macromolecules and bio-molecules in solution.
We investigated the conformational properties of rifaximin and its derivative, rifaximin OR, which belongs to a more recent class of ansamycin derivatives. The conformational analysis allowed the identification of one stable conformation for rifaximin and highlighted that the brake of the aliphatic bridge of rifaximin didn't give raise to strong conformational modifications, nevertheless some important structural rearrangements involving the aliphatic chain of rifaximin OR have been found.

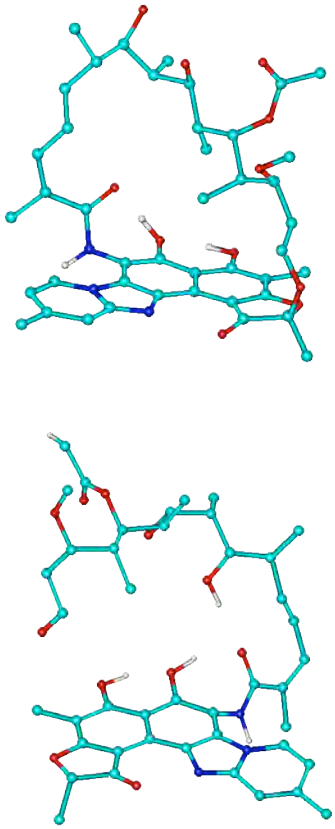

Fig. 1 *Structure of rifaximin and rifaximin Or obtained by experimental NMR and theoretical caluclations methods.*

We analized the conformation of natural products as anandamide. This compound mimics the pharmacological effects of Δ^9-tetrahydrocannabinol. In this case the results show that a single conformation is not present in solution. By cluster analysis procedure we found twenty-two conformational families able to describe the behavior of anandamide in solution.

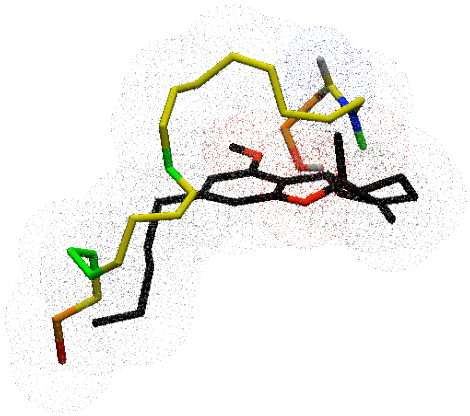

Fig. 2 *Comparisons of one structure of anandamide (obtained by cluster analysis) and* D^9*-THC structures (RMS=1.64).*

This approach has been used to analyze the conformational properties of different bioactive compounds, such as peptides (bradikinin), oligosaccharides (hyaluronic acid), drugs (carborane, antibiotics, calyx[n]areni), natural products, etc.

References

A. Donati, A. Magnani, C. Bonechi, R. Barbucci and C. Rossi: "Solution structure of hyaluronic acid oligomers by experimental and theoretical NMR, and molecular dynamics simulation". *Biopolymers*, 2001, 59 (6), 434-44.

C. Bonechi, A. Brizzi, V. Brizzi, A. Donati and C. Rossi: "Conformational Analysis of the N-Arachinylethanolamide (Anandamide) using Nuclear Magnetic Resonance and Theoretical Calculations". *Magnetic Resonance in Chemistry*, 2001, 39 (8), 432-437.

S. Martini, A. Magnani, P. Corti, G. Corbini, R. Lampariello, M.P.Picchi, M. Ricci and C. Bonechi: "Spectroscopic Investigation of the Conformational Properties and Self-Association Behaviour of Natural Compounds in Solution". *Spectroscopy Letters*, 2002, 35 (4), 581-602.

C. Rossi, A. Donati, C. Bonechi, M. Ricci, S. Martini: "Solution structure of folic acid. Molecular Mechanics and NMR investigation". *Spectrochimica Acta part A: Molecular and Biomolecular Spectroscopy*, 60/7, 1411-1419 (2004).

S. Martini, C. Bonechi, A. Donati, A. Magnani and C. Rossi: "Solution Structure of Rifaximin and its Synthetic Derivative Rifaximin OR determined by Experimental NMR and Theoretical Simulation Methods". *Biorganic and Medicinal Chemistry*. 2004 (in press).

1C – Intermolecular forces and specific ion effects

M. Monduzzi, A. Salis, M.C. Pinna, P. Lo Nostro, B.W. Ninham (A.N.U. Canberra, Australia), [P. Bauduin, D. Touraud and W. Kunz (Regensbourg University, Germany)]

Aims

Ion specific effects
Enzymatic activity
Hofmeister Series

Results

Specific ion effects are universal in biology, biochemistry, chemistry and chemical engineering. Franz Hofmeister, Professor of Pharmacology at the University of Prague, was the first to study these effects systematically.

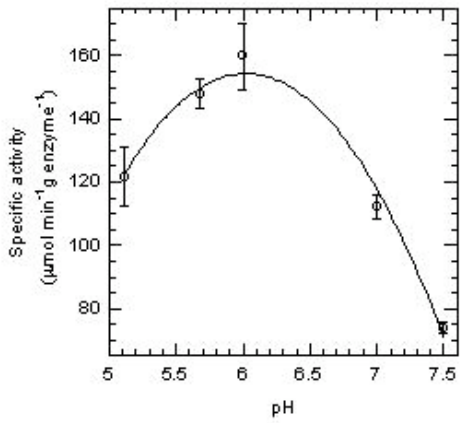

Fig. 1. Enzymatic activity of lipase A (*Aspergillus niger*) in phosphate buffer 5 mM solution at different pH values.

For over a hundred years Hofmeister effects have not been encompassed by theories of solution or colloid chemistry. In his pioneering work starting in 1888, Hofmeister studied specific ion effects of various salts, at a fixed ionic strength, for precipitation (salting-out) of ovalbumin. The precipitation efficiency of the anions of sodium salts was in the order:
$H_2PO_4^- > SO_4^{2-} > F^- > Cl^- > Br^- > NO_3^- > I^- > ClO_4^- > SCN^-$
This usual Hofmeister series ordering is qualitative.
Initially, the colligative properties of colloids were related to what Hofmeister called "the water withdrawing power of salts", and what we now call bulk hydration or activity coefficients of salts. Hofmeister considered this by far the most important. However, the effects he observed also seemed to be associated with what we would call specific ion adsorption, hydration-dehydration, ion exchange effects that occur at colloidal surfaces.
Hofmeister effects or sequences refer to the relative effectiveness of anions or cations, on a wide range of phenomena. They remain unexplained by present theories of physical chemistry. They play a role in many phenomena from solubility of salts, electrolyte activities, surface tensions to ion exchange resin, pH measurements, zeta potentials, buffers,

micellar cmcs, microemulsion microstructure, cloud points of non-ionic surfactants, ion binding to micelles, proteins and membranes, transport across membranes, gel-coagel transitions, molecular forces and colloid stability.
In some preliminary papers attempts have been made to accommodate Hofmeister effects in terms of NES forces acting on ions in adsorption, namely the high frequency, or dispersion part. For aqueous solutions it turned out that this high-frequency contribution is only a small part of the full dispersion interactions. The lower frequency contributions in the microwave and infrared, dipolar and induced dipole-dipole that give rise to hydration, or "dressed" ions are evidently here more important.
In the framework of the conventional language for the description of water structure and electrolytes, ions are designated as kosmotropic or chaotropic. The former are supposed to act as structure makers, and form the left-hand side of the Hofmeister series. The sequence then merges into the chaotropic species, the supposed structure breakers. Ions with small size and high charge (fluoride, sulfate, calcium, aluminum) belong to the kosmotropic class, while large and monovalent ions (thiocyanate, iodide, cesium) are considered to be chaotropes. This classification relates the observed Hofmeister effects to the ability of ions to strengthen or to break hydrogen bonds in aqueous solutions. In essence ion specificity is attributed to a non-local bulk effect that is determined by solvation processes and energies.

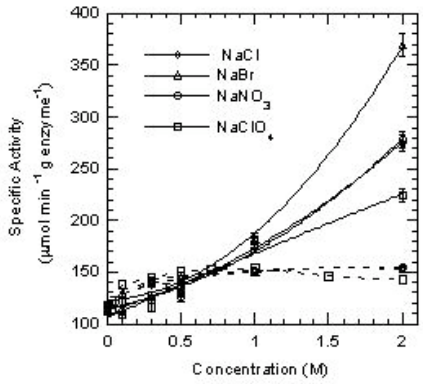

Fig. 2. Anions effect on the hydrolytic activity of lipase A in phosphate buffer (5 mM, pH = 7) solution with increasing concentration of salts. Experimental activities (solid lines), calculated activities (dashed lines).

The specific activity of lipase A (*Aspergillus niger*) toward the hydrolysis of p-nitrophenyl acetate (p-NPA) is shown to increase as a result of sodium salts addition according to specific ion effects of the Hofmeister series. This shows explicitly that the Hofmeister effect is due to the different specific interactions between anions and the enzymatic surface.
From this work some important conclusions on the comprehension of the real nature of the Hofmeister effect arise. If salts addition was responsible of water structure modification (bulk phenomena), the corresponding pH change should have produced the increase of enzymatic activity predicted by theoretical curves. But this is not. The present results can be justified only in terms of a specific interaction of Br^- anions at the enzyme surface.

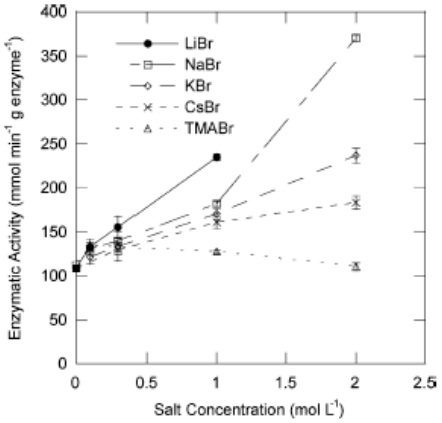

Fig. 3: Cation effect on enzymatic activity of lipase A (*Aspergillus niger*) in phosphate buffer (5 mM, pH 7) solution with increasing the concentration of bromide salts.

Table 1: Observed Molar Extinction Coefficients ($e_{obs.}$) of p-nitrophenol (p-NP-OH) / p-nitrophenloate (p-NP-O^-) Determined from Calibration Lines Performed at Different Sodium Salt Concentrations.

Salt Concentration (M)	$e_{obs.}$ (NaCl)	e_{obs} ($NaNO_3$)	e_{obs} (NaBr)	e_{obs} ($NaClO_4$)
0	8990	8990	8990	8990
0.1	6220	6260	6070	6160
0.3	4770	4740	4690	4620
0.5	4200	3980	4000	3590
1	2910	2830	2750	2380
2	2050	1760	1400	1210

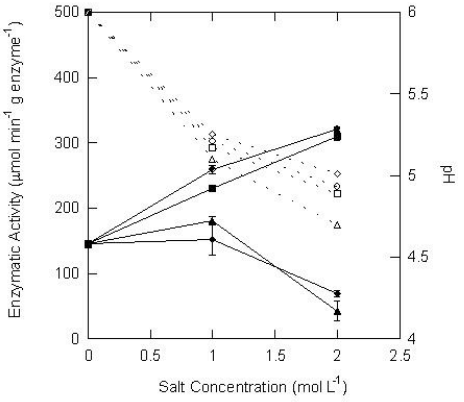

Fig. 4 - Enzymatic activity (filled symbols, left *y* axis) and pH (empty symbols, right *y* axis) of lipase A (*Aspergillus niger*) in phosphate buffer (5 mM, pH 6) solution with increasing concentration of sodium salts NaCl (n), NaBr (g), NaSCN (u), and $NaClO_4$ (5).

Clearly, the final outcome is that the enzyme comes to a very active conformation for the catalytic process. Hence, the main conclusion is that, in the studied case, enzymatic activity

is deeply related to surface phenomena. However, as mentioned above, it should be recalled that surface phenomena may occur at the glass electrode surface also. Consequently the measured pH may not be the real bulk pH of the solution. Even so, Hofmeister series effects on the hydrolytic activity of lipase A do not change. One may not even be sure of the pH reading, but the superactivity induced by adding specifically NaBr 2M in phosphate buffer at pH)=7 (that is not the optimal pH without added salts) seems to be a quite remarkable result. Substantially it turns out that it is more convenient to obtain the apparent optimal pH conditions by adding salts rather than by using an 'ad hoc' buffer solution only.

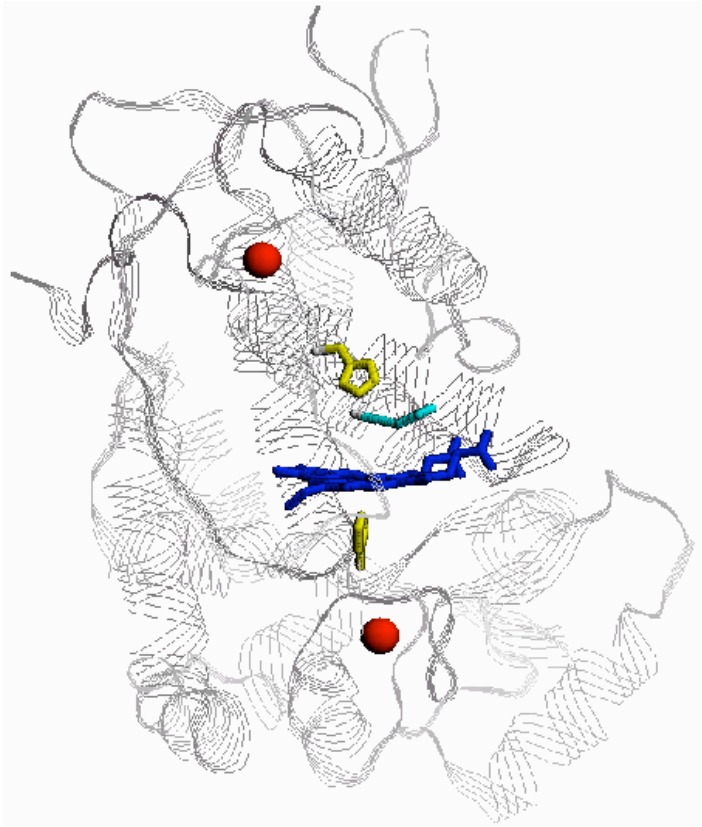

Horse Radish Peroxidase Picture

The effect of choline addition on the salt-induced super activity of horseradish peroxidase (HRP) is investigated. HRP is presented in the literature as an efficient H2O2 scavenger, and choline is the precursor of glycine betaine, a strong osmoprotectant molecule. Both the regulations of H2O2 and of osmoprotectant concentrations are implicated in plants in order to counteract salt-induced cell damage. For the oxidation of 2,2-¢-azino-bis-(3-ethylbenzothiazoline-6-sulfonic acid) diammonium salt (ABTS), sulfate anions were found to play a crucial role in the increase of HRP activity. This induced super activity can be strongly reduced by adding choline chloride. The phenomena provide an example of physicochemical Hofmeister effects playing a central regulatory role in an important biological system.

Finally a systematic work on the effect of salt addition on the pH measuremnts via glass electrodes has been carried out

The effect of electrolytes on pH measurements via glass electrodes is explored with solutions buffered at pH 7 (phosphate and cacodylate). Salt and buffer concentrations are

varied. Direct and reverse Hofmeister effects are observed. The phenomena are significant for salt concentrations above 0.1 M and for buffer concentrations below 20 mM. Changes in measured pH show up most strongly with anions. They can be related to the usual physicochemical parameters (anion molar volumes, molar refractivity, and surface tensions) that are characteristic of Hofmeister series. They correlate strongly with anionic excess polarizabilities; this suggests the involvement of non-electrostatic, or dispersion, forces acting on ions. These forces contribute to ionic adsorption at the glass electrode surface, and to the liquid junction potential.

References

Pinna M.C., Salis A., Monduzzi M., Ninham B.W., *Hofmeister Series: The hydrolytic activity of Aspergillus niger lipase depends on specific anion effects,* J. Phys. Chem. B, 2005, 109, 5406-5408

Pinna M.C., Bauduin P., Tourand D., Monduzzi M., Ninaham B.W., Kunz W., *Hofmeister Effects in Biology: Effect of Choline addition on the salt-induced Superactivity of HRP and its implicatiopn for salt resistance of Plants;* J. Phys. Chem. B, 2005, 109, 16511-16514

Pinna M.C., Salis A., Monduzzi M., Ninham B.W., *Reply to Comments on Hofmeister Series: The hydrolytic activity of Aspergillus niger lipase depends on speciofic anion effects,* J. Phys. Chem. B 2005, 109, 14752-14754

Salis A., Pinna M.C., Bilanicova D., Monduzzi M., Lo Nostro P., Ninham B.W., Specific Anion Effects on Glass Electrode pH Measurements of Buffer Solutions: Bulk and Surface Phenomena, J. Phys. Chem. B 2006, 110, 2949-2956

1C - Ligand-Macromolecules Interaction as observed by Nuclear Relaxation Analysis

Silvia Martini, Claudia Bonechi, Alessandro Donati, Maso Ricci, Claudio Rossi

Aims

Definition of experimental parameters from selective nuclear relaxation analysis in order to evaluate the strength of the overall complexation behaviour of small ligands (drugs, xenobiotics, etc.) toward biomacromolecules (Nucleic acids, Proteins, etc.).
Identification of the functional groups of the ligands involved in the binding sites and the effects of the bound ligand on macromolecule conformation by the combined use of different spectroscopic techniques (NMR, IR).
Extension of the methodology to solvent-macromolecule interaction studies, in particular water-protein interactions.

Results

Biological reactions are mostly concerned with selective interactions between small ligands and macromolecular receptors. In particular interactions with bioactive molecules are of primary interest for defining the biological role of large biopolymers and for the activation of specific chemical processes.
In order to be able to compare the extent of recognition processes occurring between ligands and macromolecules, an "Affinity Index", representing the global affinity between the ligand and the receptor, was calculated from selective relaxation rate measurements. We applied this methodology to different systems in order to compare the strength of the interaction processes between the same ligand and different receptors, as well as between a macromolecules and different ligands. The investigation is based on the comparison of selective (R_1^{SE}) and non-selective (R_1^{NS}) proton spin-lattice relaxation rate analysis of the ligand in the presence and absence of the macromolecular receptor. The formation of intermolecular adducts affects R_1^{NS} and R_1^{SE} to different extents, depending on the dynamical parameters (i.e. the correlation time τ_c), assuming fast chemical exchange between the bound and the free environments with respect to both chemical shift difference and proton relaxation rate (Figure 1). In particular, the slower ligand dynamics in the ligand-macromolecule complex mostly affects R_1^{SE}. In the presence of well resolved proton resonances R_1^{SE} can be easily determined in different systems.

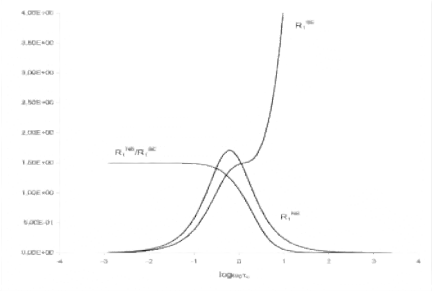

Fig. 1 R_1^{NS} and R_1^{SE} of a proton pair in relation to $\omega_H\tau_c$ assuming a constant r_{i-j} distance for the i-j dipolar interaction.

We investigated the interaction between lamotrigine , an antiepileptic drug, and some plasma proteins such as albumin, a-globulin, b -globulin and g -globulin. The selective (R_1^{SE}) and non-selective (R_1^{NS}) spin-lattice relaxation rates analysis, allowed the identification of interaction processes between lamotrigine and these plasma proteins. In particular the calculation of the *Affinity Index*, suggested that the interaction was selective and the drug had specificity for certain proteins (Figure 2).
We also investigated the effects of a second ligand (lamotrigine in this case) on the interaction process between carbamazepine (another antiepileptic drug) and albumin. The results suggested that lamotrigine is able to play a different role at low concentrations, reinforcing the carbamazepine-albumin interaction, in respect to higher concentrations producing competitive effects. The cooperative role of lamotrigine at low concentration was also revealed by the higher value of the "*affinity index*" in the ternary system with respect to carbamazepine-albumin. The synergic effect was probably more evident at low lamotrigine concentrations, since at higher concentrations the carbamazepine and lamotrigine ligands could compete for similar receptor sites.

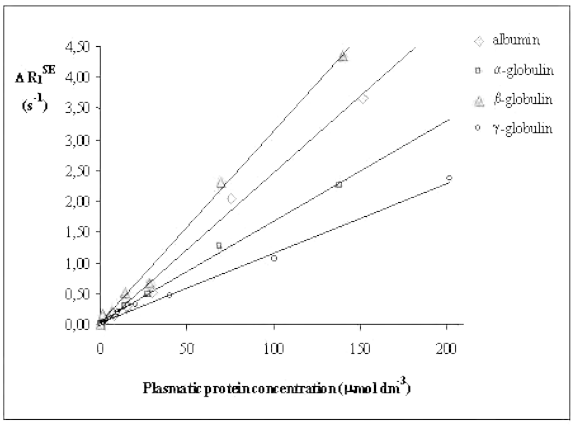

Fig. 2 *Linear relationship between H4' selective relaxation enhancements and ovine plasma protein concentrations.*

Another study concerned the interaction between ovine serum albumin and two amphenicolic antibiotics [cloramphenicol (CAP) and tiamphenicol (TAP)], using a combined approach based on NMR and IR methodologies, furnishing complementary information about the recognition process occurring within the two systems. The two ligands, despite their similar structures, showed a different affinity toward albumin. The results obtained by both NMR and IR spectroscopy suggest that the driving force for the albumin-ligand interactions is in general a recognition process with low specificity. In particular we found that both the CAP and TAP ligands interact with the albumin mainly via aspecific interactions, the interaction with TAP has a more denaturing effect on the protein than that occurring with CAP and the ligand portions responsible for the binding with the protein are mainly the aromatic and amidic regions.
Water relaxation behaviour can be used to monitor the ligand-macromolecule interaction as well as the protein hydration. The results obtained from a study involving water-albumin

system showed the existence of a significant contribution to the bulk water molecules in the presence of the protein. This contribution contains two terms: the first arises from the long-lived buried water molecules surrounded by the macromolecular constituents, the second is due to water molecules present in the hydration shell around the macromolecular surface which are affected by some extent in their dynamical properties by the presence of the protein.
The same approach was used to evaluate the strength of the interaction between anandamide (AEA) and cannabinoid receptors. In particular, different interactions are analysed using three brain sections, the whole brain, the cerebral cortex and the cerebellum. Knowing the distribution of the CB1 receptors in the brain is useful in the analysis of the molecular recognition phenomena between a specific ligand and different sample obtained from three zone of brain.
Selective and non-selective proton spin-lattice relaxation rate analysis of anandamide in the presence of different cerebral receptors allowed the identification of interaction processes occurring at different strengths. In particular AEA was found to interact preferentially with cannabinoid receptors present in the cerebellum in respect of these found in the whole brain and cerebral cortex. This study confirms the biological role played by AEA in simulating trans-delta-9-tetrahydrocannabinol effects on cerebral receptors.

References

C. Bonechi, A. Donati, S. Loiselle**,** S. Martini, M. Ricci and C. Rossi:" Ligand-Macromolecules Interaction as observed by Nuclear Relaxation Analysis", *Trends in Chemical Physics, Research Trends*, 2000, vol. 8, 35-47.

C Rossi, S. Bastianoni, C. Bonechi, G. Corbini, P. Corti, A. Donati. "Ligand-Protein recognition studies as determined by nuclear relaxation analysis", *Chem Phys. Lett.*, 310, 495-500, 1999.

C. Rossi, C. Bonechi, S. Martini, M. Ricci, G. Corbini, P. Corti, and A. Donati: "Ligand-Macromolecule Complexes: the Affinity Index Determination by Selective Nuclear Relaxation Analysis", *Magn. Reson. Chem.*, 39, 8, 457-462, 2001.

S. Martini, C. Bonechi, A. Magnani, N. Marchettini, P. Corti, G. Corbini and C. Rossi: "Nuclear Magnetic Resonance And Infrared Spectroscopy Combined Use as a Tool for Studying Recognition Processes between Amphenicolic Antibiotics and Albumin.", *Magn. Reson. Chem.*, 2003, 41(7), 489-502.

C. Rossi, S. Martini, M. Ricci, M.P. Picchi and C. Bonechi: "Water-protein and ligand-protein interactions as determined by selective NMR relaxation studies", *Macromolecular Synmposia,* 2003, 203, 89-101.

C. Bonechi, S. Martini, M. Ricci, A. Donati, P. Massarelli, G. Bruni, A. Brizzi, V. Brizzi, C. Rossi "Nuclear Magnetic Resonance for Studying Recognition Processes between Anandamide and Cannabinoid Receptors". *Biophys. Chem.* (2004) submitted.

1C - NMR data analysis in complex and simple liquid mixtures

A. Ceglie, L. Ambrosone, G. Palazzo, G. Colafemmina,

Aims

Determination of size distribution in emulsions by NMR
Deconvolution of echo decays coming from overlapping peaks
Analysis of anomalous diffusion

Results

We presented a new method to analyse pulsed gradient spin-echo (PGSE) NMR data from a mixture of compounds sharing the same NMR resonance (e.g. polymer solutions or mixtures of aliphatic compounds). If all the spin-bearing species undergo Brownian motion, their contribution to the experimental echo decay is exponential.
For the case of more than one diffusing species at a given chemical shift, the echo attenuation is the Laplace transform of the distribution function of the self-diffusion coefficients. Applying the algorithm previously developed by us, we solve the integral equation, obtaining the distribution function of the diffusion coeffcients. The method is tailored for small data sets (10 – 30 points) typical of PGSE-NMR measurements.

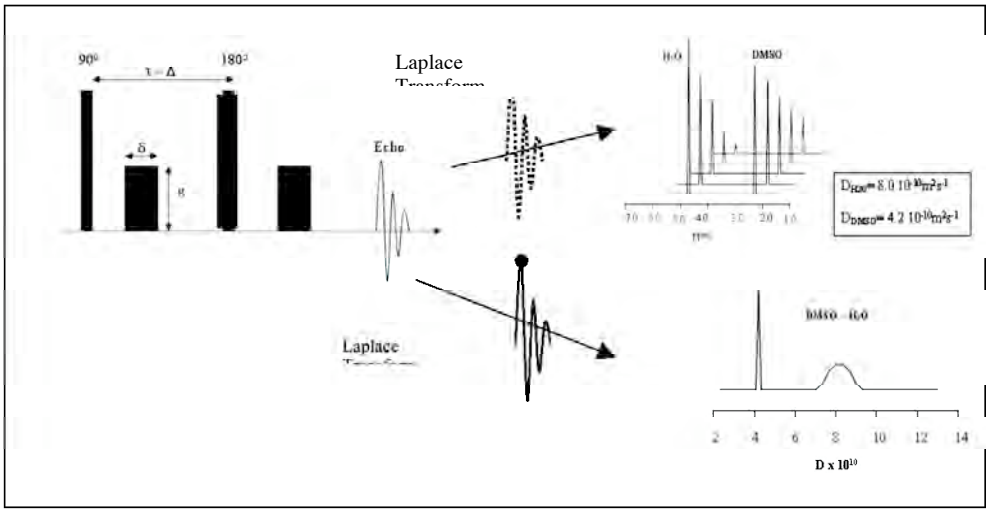

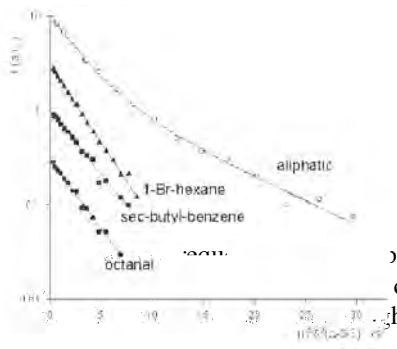

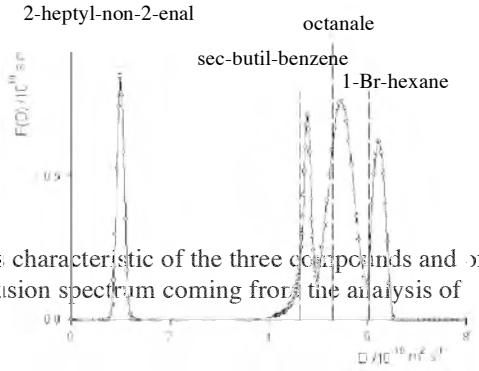

Ech peaks characteristic of the three compounds and of the diffusion spectrum coming from the analysis of onl ht).

References

L.Ambrosone, A.Ceglie, G.Colafemmina, G.Palazzo, "General methods for determining the droplet size distribution in emulsion systems", J.Chem.Phys., 102 , 797-804, (1999)

L.Ambrosone, A.Ceglie, G.Colafemmina, G.Palazzo, "Emulsions: a time-saving evaluation of the droplets polydpersity and of the dispersed phase self diffusion coefficient", Langmuir,15, 6775-6780, (1999)

L.Ambrosone, A.Ceglie, G.Colafemmina, G.Palazzo, "A new strategy for evaluating the self-diffusion coefficient in restricted diffusion. Case of polydisperse emulsions with small mean radii", J.Phys.Chem.B, 104, 786-790, (2000)

L.Ambrosone, A.Ceglie, G.Colafemmina, G.Palazzo, "Resolving complex mixtures by means of Pulsed Gradient Spin Echo NMR experiments", Phys.Chem.Chem.Phys., 4, 3040-3047, (2002)

1C - Solution Behavior of a Sugar-based Carborane: a Nuclear Magnetic Resonance Investigation

Alessandro Donati, Claudia Bonechi, Silvia Martini, Maso Ricci, Claudio Rossi

Aims

Analysis of physico-chemical properties of carborane molecules in solution.
Determination of intra-molecular CH…X(N, O) bonds in crystals, and their persistence in solution were observed in molecules containing, carba-borane cage and amidic groups, by X-ray and NMR techniques.
Validation of experimental data by theoretical ab initio calculation.

Results

Polyhedral boranes and heteroboranes have been the subject of widespread interest for at least fifty years and this was mainly due to the ability of boron atoms to catenate and form molecular networks with rather peculiar geometries. Nuclear Magnetic Resonance has proven to be a suitable technique for the physico-chemical characterization at a molecular or micellar level, and it has been used since long to obtain valuable information on surfactant-based systems
The existence, the persistence in solution and the chemical properties of unusual hydrogen bonds are recently emerged as an argument of extensive debate, reflecting the extreme interest of this topic, both for theory of chemical bonding and its applications in several fields. Multiple withdrawing groups attached to a sp^3-hybridized carbon, should be the necessary condition to make the carbon a proton donor. New techniques and refinement of theoretical calculation allowed a more accurate description of this subtle interaction.
We analize the behaviour of C-H donor included in the cage of a carbaborane compounds, designed to develop an alternative mechanisms of action in Boron Neutron Capture Therapy (BNCT). In these molecules the CH enclosed in the cage, which presents H-donor behaviour, can form intra-molecular C-H···O bond and C-H···N bond, which surprisingly appears to be both persistent in solution. Nuclear Magnetic Resonance data showed that the conformation in which C-H···O interaction occur is favored, even if other reasons, than intrinsic C-H···X strength only (i.e. steric hindrance), are co-responsible for this behaviour.
X-ray crystallography, 2D-NMR and *ab initio* calculations confirmed this finding. Structure

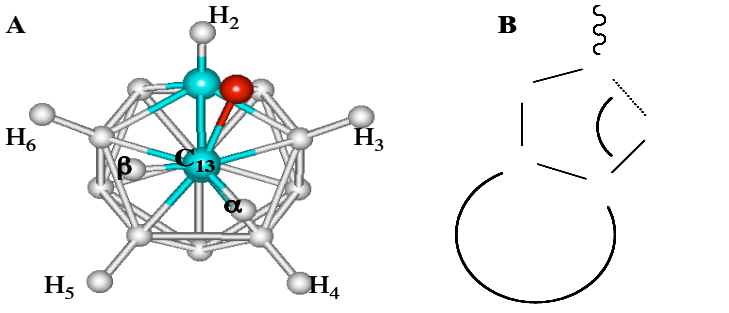

Figure 2.A: View of the carboranyl cage along the C_{13}-C_1 bond of the GCOB model optimized by *ab initio* calculation. Protons H_{13} and $H_{13'}$ are indicated as a and b respectively. The glucosyl portion is omitted for clarity. **B**: Sketch of the five member ring in which the proposed H-bond is involved.

of both species has been proposed together with detailed geometries of the respective CH···X bonds.
Regarding the persistence of CH···X(O,N) bonds in solution, at the best of our knowledge this is the first case in which an intra-molecular CH···N interaction has been recognised with a very high degree of confidence and the geometrical parameters determined. On the other hand the persistence of the CH···O bond interaction is a clear confirmation of other recent findings in the field.
The occurrence and the persistence in solution of CH···X(O,N) bonds has been demonstrated for carba-boranyl derivatives of pharmaceutical interest. The activated CH group of the carborane cage results as an important probe for the evaluation of chemical behaviour of this non-classic interaction, with group of biological interest. In this case crystallographic studies demonstrated that the amidic oxygen was involved as hydrogen acceptor in the bond, allowing the determination of accurate geometric parameters.
All the experimental data presented in this research were in agreement for describing the carborane molecules as remarkably rigid objects, whose two main portions (the sugar rings and the carborane cage) were held fixed with respect to each other by means of a H-C···O bond. Temperature variations and aggregate formation were not able to disrupt this intramolecular bond, and thus did not introduce any substantial change at a molecular level. In this respect carborane molecule,has a different behaviour from classical surfactant systems, where structural changes have been shown to take place as a consequence of micelle formation. Quantum mechanical calculation strongly supported this model.
On the other hand, the analysis of nuclear relaxation parameters indicated that in aggregating condition an equilibrium existed between monomers and micelles, which is in line with the picture of typical surfactant behaviour.
The occurrence and persistence in solution of CH···X(N,O) bonds was demonstrated for the two rotamers of a carba-boranyl derivative of potential pharmaceutical interest. The activated CH group of the carborane cage can thus be considered an important probe for the evaluation of the chemical behaviour in this non-classic interaction, especially when groups of biological interest such as the amide are involved. Crystallographic studies demonstrated that the amide oxygen was involved in the bond as hydrogen acceptor. This allowed the accurate determination of geometric parameters, from which it was possible to extract information on the forces involved in the hydrogen bond. Moreover, this intra-molecular CH···O interaction was demonstrated to persist in solution, showing its importance in driving conformational properties of bio-macromolecules and supra-molecular complexes.
The occurrence of a CH···N bond in solution was also demonstrated by NMR studies and was confirmed by *ab initio* calculations. The strength of both these interactions and their geometrical parameters were found to be in the same range of classical hydrogen bonds. In particular, in the case of the CH···N for the cis rotamer, the H atom directly pointed toward

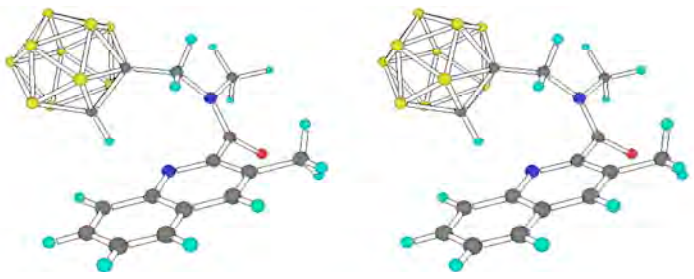

Figure: Stereo view of DDQC*cis* model optimized by *ab initio* calculation at RHF/6-31G** level. Boron bonded hydrogens were omitted for clarity.

the nitrogen sp^2 lone-pair, whereas in the case of the CH···O bond for the trans rotamer a higher deviation from planarity was observed (q=10.2° and q=41.2° respectively). However, for the CH···O bond we should consider that a seven member ring was formed, in which geometrical constraints are more effective.

References

Donati, S. Ristori, C. Bonechi, L. Panza, G. Martini and C. Rossi: "Evidences of strong C-H···O bond in a ortho-carboranyl b-lactoside in solution". *J. Am. Chem. Soc.* 2002, 124 (30), 8778-8779.

Cappelli, A., Pericot Mohr,G., Gallelli, A., Giuliani, Anziani, G., M., Vomero, S., Fresta, M., Porcu, P., Ma ciocco, E., Concas, A., Biggio, G., Donati, A. (2003). Structure-Activity Relationship Studies on Carboxamide Derivatives Focused to the Targeted Delivery of Radionuclides and Boron Atoms by Means of Peripheral Benzodiazepine Receptor Ligands. *Journal of Medicinal Chemistry* **46(17)**, 3568-3571.

Cappelli, A., Pericot Mohr,G., Anzini, M., Vomero, S., Donati, A., Casolaro, M., Mendichi, R., Giorni, G. (2003). Synthesis and Characterization of a New Benzofulvene Polymer Showing Self-Assembling and Thermal-Induced Disassembling Properties. *Journal of Organic Chemistry* **68(24)**, 9473-9476.

Cappelli, A., Giorgi, G., Anzini, M., Vomero, S., Ristori, S., Rossi, C., Donati, A. (2004). Caracterization of C-H···X(N,O) bonds in carboranyl compounds in solid state and solution. *Chemistry: A European journal* (in press)

Donati, A., Ristori, S., Bonechi, C., Martini, S., Panza, L., Martini, G., Rossi C. (2004): Solution Behavior of a Sugar-based Carborane: a Nuclear Magnetic Resonance Investigation. *J. Phys. Chem.* (submitted)

1C – Structure and dynamics of four component microemulsions

G. Palazzo, G. Colafemmina, F. Lopez, M. Giustini, A. Ceglie

Aims

Structural determination in multicomponent microemulsions.
Full comprehension of the cosurfactant and/or cosolvent role in surfactant systems.

Results

Under suitable conditions (T, P, composition) water, apolar compounds, and surfactants give rise to thermodynamically stable mixtures called microemulsions. The structure of microemulsions can be idealized as a set of interfaces dividing polar and apolar domains. Characteristic lengths are in the range 1÷100 nm, so that they appear optically transparent (some times bluish) and the thermodynamical stability is achieved by a very low the oil/water interfacial tension. However, in order to attain the appropriate packing of amphiphiles at interface, the addition of others surface-active substances is often required. These cosurfactants partition themselves among the oil, water, and interface domains. Therefore, without a quantitative description of the dependence of the partition equilibria on the system composition, a full understanding of quaternary microemulsions cannot be attained.

We have studie in detail the microstructure of the quaternary CTAB/water/n-pentanol/n-hexane system. By increasing the pentanol/CTAB mole ratio, the system evolves from oil-in-water to water-in-oil structures. For very large 1-pentanol loading some water is expelled from the reverse micelles resulting in a L_2 *plus* water equilibrium (emulsification failure). The adsorption of cosurfactant at the interface of direct micelles, planar lamellae, bicontinuous microemulsions, and spherical reverse micelles follows the same adsorption isotherm (independently from the curvature of the interface). Moreover, the results obtained unambiguously show that the interface composition dictates the spontaneous curvature of interfacial film. Actually positive, null, and negative curvatures correspond to different compositions of the interfacial film. Once the influence of cosurfactant on the spontaneous curvature of the interface is understood, the appearance of the emulsification failure upon pentanol loading can be rationalised within the framework of the flexible surface model. The interface composition at the phase boundaries was determined by means of Schulman's titrations. To evaluate interfacial composition in single-phase w/o microemulsion, PGSE-NMR data have been collected along two composition paths: (i) water dilution lines, where the interface composition remains constant; (ii) paths where the interface composition is changed at fixed water/surfactant ratio (due to the partition equilibrium, such paths

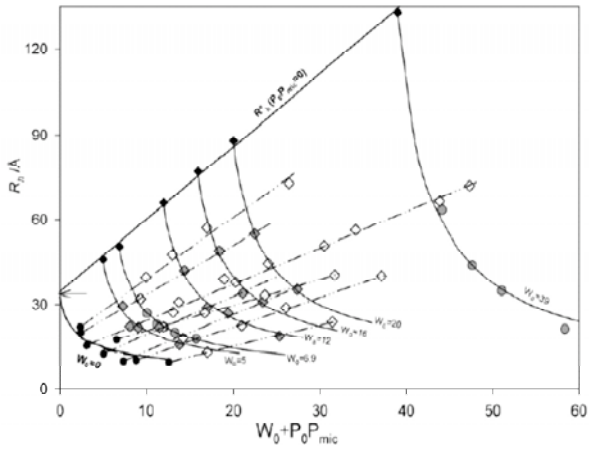

correspond either to cosurfactant dilution either to oil dilution). As shown in the figure, all the data recorded along different paths can be analysed by the same "master plot".
We are investigating oil-in-water microemulsion as well. In particular, the microstructure of aggregates formed by sodium dodecyl sulfate (SDS) and 1-pentanol in mixtures of water and a polar aprotic solvent (propylene carbonate) was investigated by means of PGSE-NMR, dynamic light scattering, viscosity and conductivity measurements. Propylene carbonate partitions itself between micelles and aqueous bulk. The fraction of micellized propylene carbonate remains constant along PC-dilution, and the phase separation takes place when the composition of continuous phase attains the PC/water miscibility gap. The micellized propylene carbonate is present mainly in the micelle's palisade and strongly increases the total interfacial area, thus acting as a cosurfactant.

References

Venditti F., Angelico R., Palazzo G., Colafemmina G., Ceglie A., Lopez F., *Hydrolysis of Tetraethoxysilane in CTAB reverse micelles: effects of the formed ethanol on the microstructure,*. Langmuir, 2006, submitted.

Palazzo G., Fiorentino D., Colafemmina G., Ceglie A., Carretti E., Dei L., Baglioni P. *Nanostructured fluids based on propylene carbonate/water mixtures*, Langmuir,2005, 21, 6717-6725.

Lopez F. Venditti F., Ambrosone L., Colafemmina G., Ceglie A., Palazzo P., *Gelatin Microemulsion-Based Gels with the Cationic Surfactant Cetyltrimethylammonium Bromide: A Self-Diffusion and Conductivity Study,* Langmuir 2004, 20, 9449-9452.

Giustini, M., Murgia S., Palazzo G., *Does the Schulman's titration of microemulsions really provide meaningful parameters?*, Langmuir, 2004, 20, 7381-7384.

Palazzo G., Carbone L., Colafemmina G., Angelico R., Ceglie A., Giustini, M., *The role of the cosurfactant in the CTAB/water/n-pentanol/n-hexane system: Pentanol effect on the phase equilibria and mesophases structure*, Phys.Chem.Chem.Phys., 2004, *6*, 1423 – 1429.

Palazzo G., Lopez F., Giustini, M., Colafemmina G., Ceglie A., *Role of cosurfactant in the CTAB/water/n-pentanol/n-hexane water-in-oil microemulsion: 1. Pentanol effect on the microstructure*, J.Phys.Chem.B, 2003, 107, 1924-1931.

1C - The cosurfactant role in four component microemulsions: microstructure determination and model prediction

A. Ceglie, G. Palazzo, G. Colafemmina, F. Lopez, M.Giustini

Aims

Structural determination in multicomponent microemulsions
Full comprehension of the cosurfactant role in surfactant systems

Results

The microstructure of the quaternary water-in-oil microemulsion CTAB/water/n-pentanol/n-hexane has been investigated over a wide range of composition. The dependence of the interface composition on the overall composition is described satisfactorily by a simple partition equilibrium. This permits a quantitative analysis of the experimental data. To achieve this result, a new strategy has been developed for two composition paths: (i) water dilution lines, where the interface composition remains constant; (ii) paths where the interface composition is changed at fixed W_0 (due to the partition equilibrium, such paths correspond either to cosurfactant dilution either to oil dilution). All the data recorded along different paths can be analysed by the same "master plot". Moreover, the effect the behaviour of nucleic acids solubilized in such microemulsion was studied in detail.

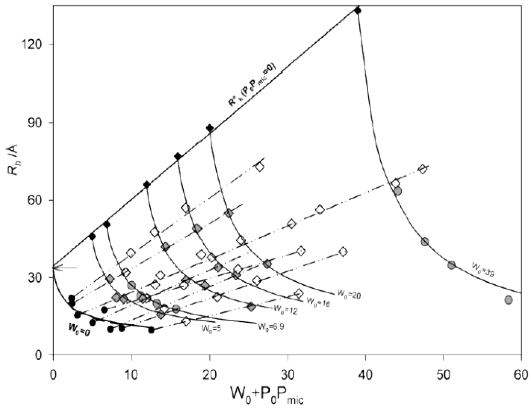

References

G. Colafemmina, G. Palazzo, E. Balestrieri, M. Giomini, M. Giustini, A. Ceglie, "Towards the comprehension of the cosurfactant role: a NMR self-diffusion and conductivity study of a four-components water-in-oil microemulsion", Progress Colloid & Polymer Sci., 105 , 281-289, (1997)

Airoldi, M., Boicelli, C.A., Gennaro, G., Giomini, M., Giuliani, A.M., Giustini, M., "A spectroscopic study of polt(dAdT)poly(dAdT) in microemulsions", Phys. Chem. Chem. Phys., 2, 4624-4641, (2000)

Airoldi, M., Boicelli, C.A., Gennaro, G., Giomini, M., Giuliani, A.M., Giustini, M., Scibetta, L. "Different factors affecting polyAT conformation in microemulsions: effect of variable Po and KCl concentration", Phys. Chem. Chem. Phys., 4, 3859-3864, (2002)

G.Palazzo, F.Lopez, M.Giustini, G.Colafemmina, A.Ceglie "Role of cosurfactant in the CTAB/water/n-pentanol/n-hexane water-in-oil microemulsion: 1. Pentanol effect on the microstructure" J.Phys.Chem.B, 107, 1924-1931, (2003)

1C – Theoretical modeling of amino acids and peptides on surfaces

A.Grassi, G. Forte and G.Marletta

Aims

A growing interest is devoted to the understanding of the interaction processes of biomolecules onto inorganic surfaces, due to their applications in biotechnology, biomaterials, biosensors, etc., etc.. areas. Scope of our work is to study these interaction processes in biosurfaces obtained from the adsorption of L-lysine onto a functionalised quartz surfaces (SiOH, $SiCH_3$ and mixed $SiOH/SiCH_3$) with particular attention to the variation of the strength and of the nature of the molecule-surface interaction on varying the functional group.

Moreover, it is known from literature that the solvent play a fundamental role in adsorption phenomena of biomolecules and therefore a theoretical study finalised to modelling these processes must include the solvation effects. At this end in our works, the modelling has been performed at static and dynamic levelsincluding the solvent effect. In our works both Molecular Mechanics and semiempirical quantum mechanics techniques as been used. In order to analysed "macroscopic" properties of a biosurface (self-assembling, friction force, mechanical properties, etc.. etc..), Molecular Mechanics method, based on the Force Field Theory, is a very suitable technique. Moreover, due to the computational effort, MM methods are the best approach to study dynamical and static processes involving a very large number of molecules, as for example a large cluster of molecules to simulate the surface, the adsorbed biomolecule (peptide, protein, etc.. etc..) and a large number of water molecules to simulate the solvent environment. On the other hand, the strength and the nature of the molecule-surface interaction are localized effects involving a few number of atoms and therefore the study these effects can be performed using quantum-mechanics techniques (such as semi-empirical quantum mechanics methods).

Results

The in aqueous solution the L-lysine molecule show three different forms. Depending of the pH value these forms are showed in fig.1.

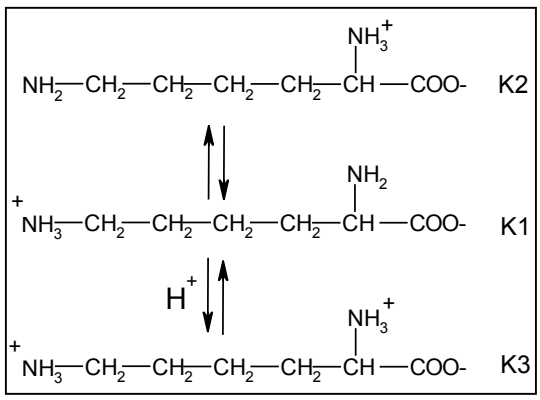

Fig.1 - Equilibrium representation of three principal form of lysine, K1, K2 and K3, at isoelectric pH.

In water, the aminoacids tend to assume a linear conformation due to the dipole-dipole interaction of the carboxylic and the amino groups with the solvent molecules. In our works we have focused the attention on the species present at isoelectric pH.
The static and dynamical calculations performed on the adsorbed L-lysine onto a hydroxilated (fully hydrophilic) silanol quartz surface, indicate that a strong interaction occurs between the ε-protonated amino group of the L-lysine with the surface. Furthermore, the aminoacid

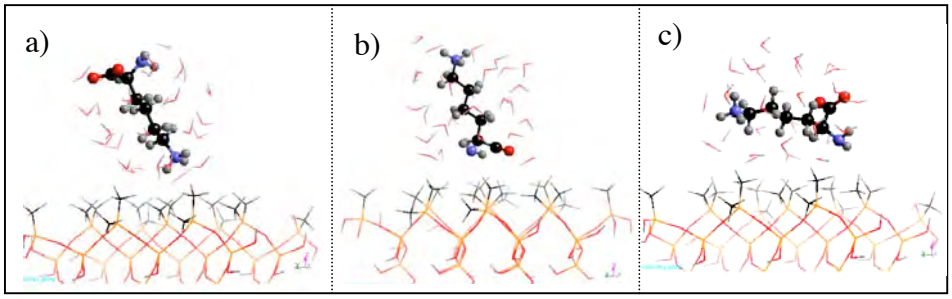

Fig.2 - L-lysine in K1 form in the three orientation: *end-on*, with ε–amino group pointing towards the surface (a), *end-on* with the α-amino group pointing towards the surface (b), and *side-on* (c) with respect to the surface.

molecule has a preferred *end-on* orientation (fig.2) with respect to the surface, with the ε-protonated
amino group pointing toward the surface. The statistical analysis of the system trajectories reveals that the relatively ordered water-shell structure of the aminoacid molecule in the *bulk* solution is broken when the molecule approaches the surface because of the reciprocal perturbation of the molecule and surface solvation shells.
To analyze the substrate effect on the adsorption process, the same calculations were performed for partially hydrophilic surfaces formed by silanol and methyl groups with a ratio 1:5, and hydrophobic fully methylated surfaces.
Molecular dynamics and static calculations indicate that L-Lysine does not show any significant interaction with fully methylated surfaces, while its interaction with hydroxylated/methylated surfaces is dominated by electrostatic and H-bond terms.
In the first case there is no preferential orientation of L-Lysine with respect to the surface, while in the second case, the L-Lysine-surface interaction mainly depends on the molecular orientation, with a preferred geometry involving the ammonium group pointing towards the silanol site.
The structure of water shells around L-Lysine molecules was shown to be strongly affected by the relative hydrophilic/hydrophobic character of the surfaces. In particular, the order is almost completely lost for partially hydrophilic surfaces, while well defined hydration shells around L-Lysine are obtained for hydrophobic surfaces.

2A - A prospective for Global Change analysis: the inter annual dynamics of the dissolved organic carbon in aquatic ecosystems

Luca Bracchini, Steven Loiselle , Arduino Massimo Dattilo, Stefania Mazzuoli, Nadia Bergamino, Antonio Tognazzi, Silvia Focardi, Claudio Rossi

Aims

Study the impact of environmental local and global changes from dissolved organic carbon prospective. Risks analyses and remediation.

Results

The impact of the global and local changes on aquatic ecosystems is related to significant variations in climatic series measurements of temperature, rain, solar radiation and other. In the stratosphere the Ozone and other allotropic species of oxygen absorb UV irradiance at low wavelength. In the past, the pollutants (e.g. CFC) released by human activities reduced the ozone concentration in the stratosphere. This reduction was related with an enhanced of UV irradiance in the biosphere. The role of ozone in the absorption of the UV irradiance in atmosphere is played, in aquatic environments, by the chromophoric portion of dissolved organic carbon (CDOM). The sources, sinks and dynamics of this heterogeneous compound of molecules is sensitive to the temperature and pH of the water, to the rain (terrigenous inputs), to the biological cycles (from bacterial activity to fishes degradation, autochthonous inputs) and irradiance exposure. The inter annual variation of the solar UV irradiance absorption of CDOM is driven by its concentration and by photodegradation and photobleaching. The construction of a temporal series of the optical properties of CDOM can be use to evidencing anomalous variations of this important parameter controlling the propagation of the irradiance in the water. The measured absorption during the year in the Fogliano Lake was presented in figure 1. In this shallow coastal lake, the protection against the UV irradiance appear to be high in the summer season and the photobleaching, if active, is completely obscured by summer production of CDOM. On the contrary in the winter and autumn season the absorption of CDOM is low

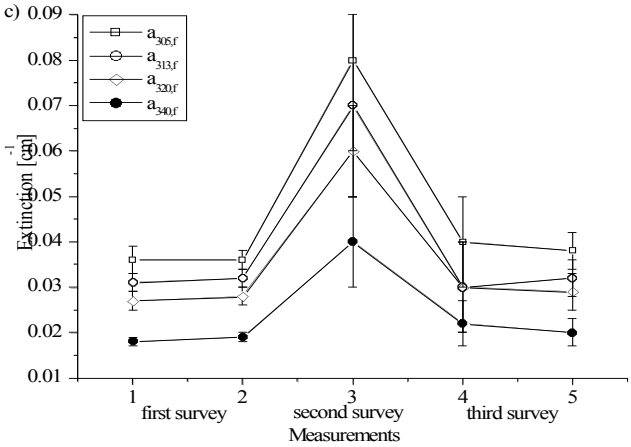

Figure 1: The absorption in the Fogliano Lake during the spring (first survey), summer (second survey) and autumn seasons (third survey).

The spectral slope temporal variation was presented in figure 2

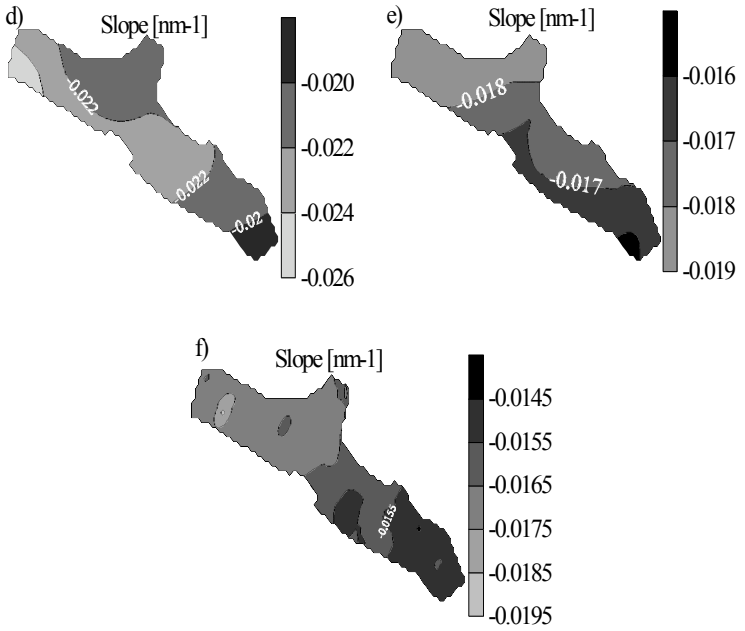

Figure 2: Spectral slope in spring (d), summer (e) and autumn (f) seasons.

From this data the lower molecular weight was founded during the spring season and propagation of UV irradiance is favourite.
The complete inverse pattern was observed in Salto Lake where the summer photobleaching was clearly evidenced (figure 3). In this ecosystem the epilimnion appear to be exposed by high flux of UV photons during the summer season.

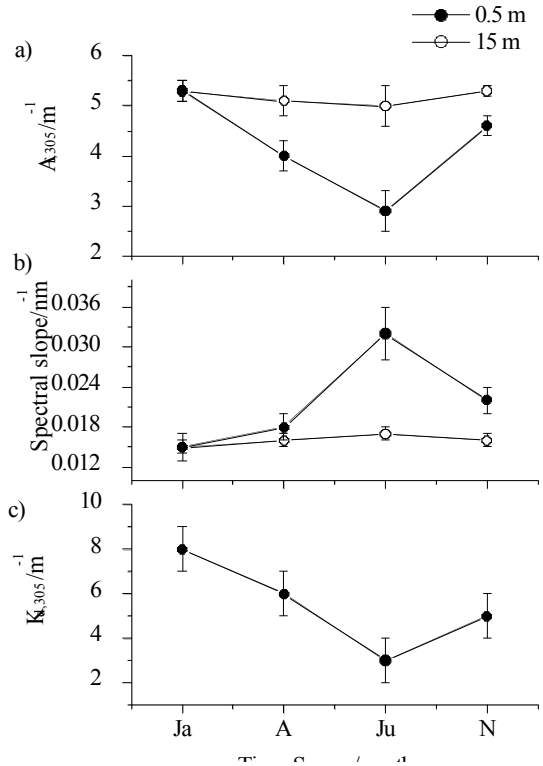

Figure 3: Inter annual optical and bio-optical variation in the Salto Lake

References

Bracchini L., S.A. Loiselle, A. M. Dattilo, S. Mazzuoli, A. Cózar, C. Rossi. 2004.The spatial distribution of the optical properties in the UV and Visible in an aquatic ecosystem., Photochem. Photobiol., 80(1) 139-149.

Bracchini L., A. Cozar, A. M. Dattilo, M. Falcucci, R. Gonzales, S. Loiselle and V. Hull, Analysis of extinction in ultraviolet and visible spectra of water bodies of the Paraguay and Brazil wetlands, Chemosphere 57 (2004) 1245-1255

Bracchini L., Dattilo A.M., Falcucci M., Loiselle S.A., Hull V., Arena C., Rossi C. Spatial and temporal variations of the inherent and apparent optical properties in a shallow coastal lake,. Journal of Photochemistry and Photobiology B: Biology, 2005, 80, 161-177

Bracchini L., Dattilo A.M., Loiselle S.A., Cozar A., Tognazzi A., Azza N., Rossi C., The role of wetlands in the chromophoric dissolved organic matter release and its relation to aquatic ecosystems optical properties. A case of study: Katonga and Bunjako Bays (Victoria Lake; Uganda), Chemosphere, In press.
Bracchini, L., Dattilo, A.M., Loiselle, S., Spatial and temporal characterization of the inherent and apparent optical properties in an aquatic ecosystem. (submitted to Photochemical and Photobiological Sciences, 2006)

2A - Analysis of the water masses in the marine and freshwater systems using bio-optical properties of chromophoric dissolved organic carbon (CDOM)

Arduino Massimo Dattilo, Luca Bracchini, Steven Loiselle, Stefania Mazzuoli, Nadia Bergamino, Antonio Tognazzi, Silvia Focardi, Claudio Rossi

Aims

Evaluation and differentiation of the water masses from DOC/CDOM prospective. The UV photoactive layer of the water column.

Results

The key study of oceanographic physic is the evaluation of the different water masses in the water column and dynamics. Our group use DOC/CDOM properties to distinguish surface (until 300 m) and deeper (below 300 m) water masses. In the surface layer particular attention is related to the UV photoactive layer of the water column in which photodegradation of CDOM and impact on biotic systems is active. In the deeper layer the CDOM and DOC properties modification are related to the consummation and production of bacterial substrate.

These studies are executed in both marine (Mediterranean Sea) and freshwater (Lakes) systems. CDOM description of the water masses are related not only with chemical physical properties but also with optical and biological properties.

The method was execute in the eastern basin of the Mediterranean Sea using data from a oceanographic survey (R/V Urania, Samca MedBio, figure 1).

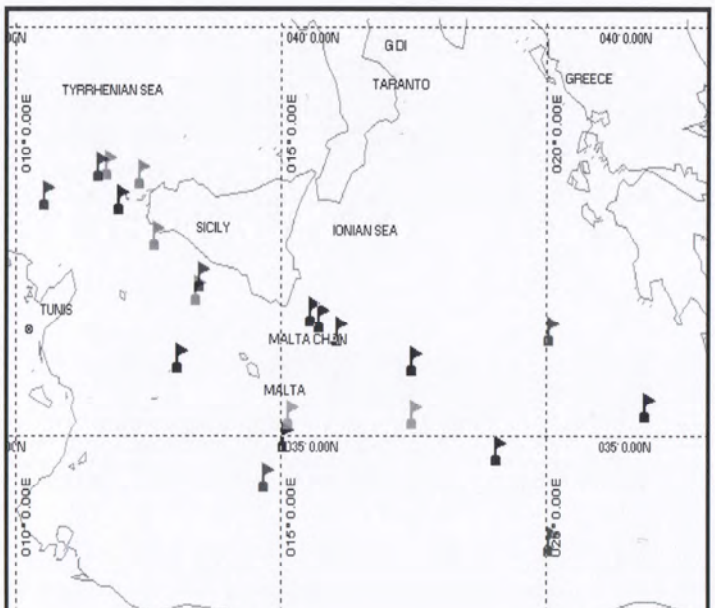

Figure 1: The sampling stations in the SAMCA 5 MEDBIO survey.

The solar spectral irradiance investigation in the upper layer of the water column is used to determine the UV photoactive and photic layers (figure 2)

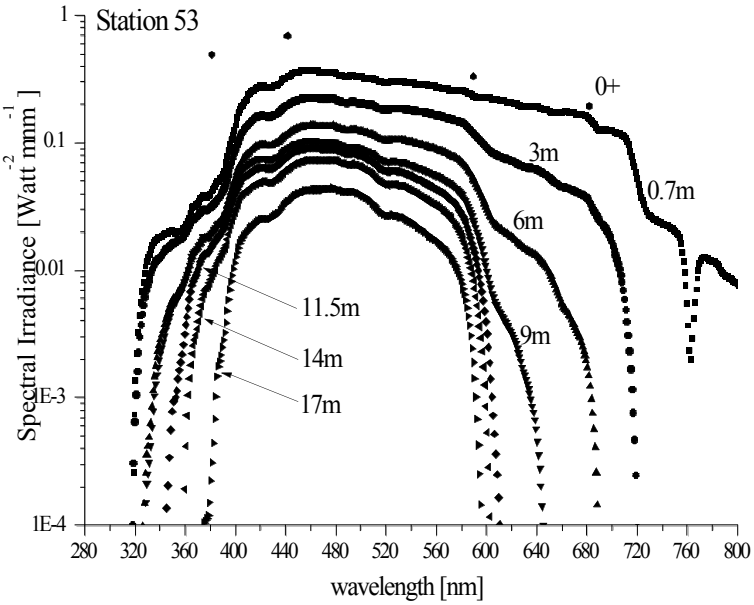

Figure 2: The spectral irradiance in the sub surface layer of the water column.

The optical properties of Chromophoric Dissolved Organic Matter (CDOM) were analized from absorption (m^{-1}) and spectral slope value (s) according to the equation:

$$a(\lambda)_f = Ae^{-s(\lambda-\lambda_0)} + \gamma$$

where, 240 nm ≤ λ ≤ 400 nm, λ_0 = 240 nm, A+γ is the absorption at 240 nm and s is the spectral slope of the spectra (nm^{-1}, evaluated with a non linear algorithm).
The spectral slope and absorption profiles are determined by interaction of CDOM with solar irradiance in the sub surface layer (where solar ultraviolet irradiance is present) by degradation of biotic systems and by bacterial activity. The s and absorption at 290 nm data collected in a station were presented in figure 3. The absolute minimum value of the spectral slope was observed at 75 m of depth where UV irradiance in not present and the presence of phytoplankton communities is maximal. In this case it is possible conclude that the CDOM is originated from degradation of phytoplankton. At the same time, the absorption of CDOM is maximal at this depth. This is related with high concentration of CDOM but also by a minimal photodegradation (at this depth the CDOM is produced and it can be call "new CDOM"). In the sub surface depth (10 m) the CDOM is photodegraded (high s respect to the s at 75 m) and photobleached (low absorption respect to the absorption at 75 m). At 300 m of depth absolute maximum of s was measured. This layer of the water column, in this basin, is called Levantine Intermedie Water (LIV), and it is the old water (it is sink from a long time). The CDOM optical properties changes in this layer are determined by bacterial activity.

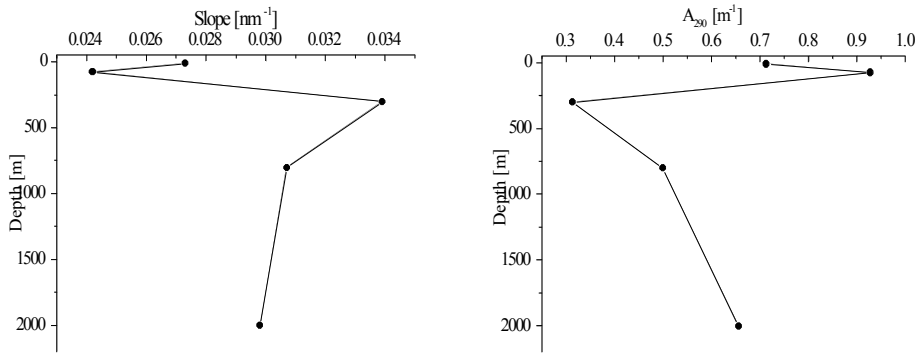

Figure 3: The spectral slope and absorption profiles in a station of eastern Mediterranean Sea

Representing all data collected during the cruise, an average spectral slope profile can be evaluated for this basin and a negative non linear relation with dissolved oxygen was observed (figure 4 and 5).

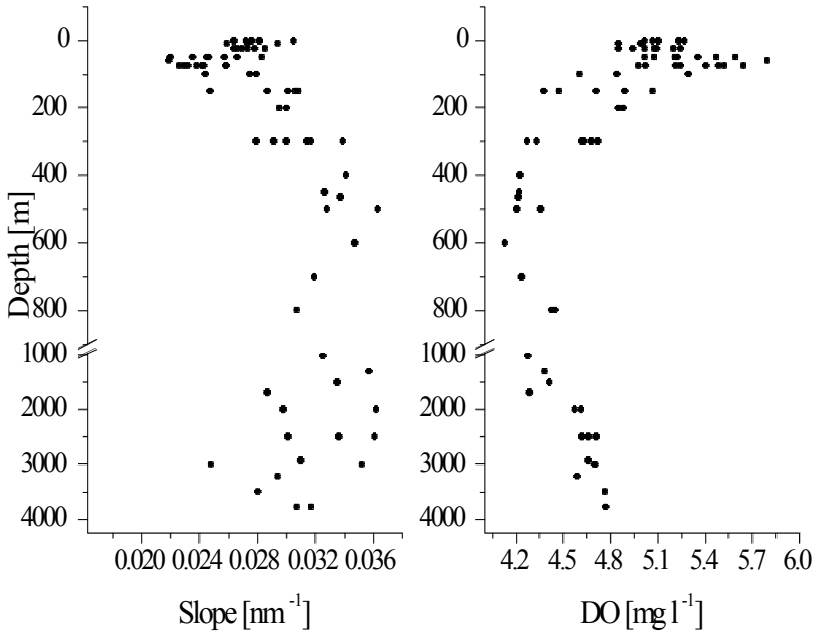

Figure 4: The average spectral slope (Slope) and dissolved oxygen (DO) profiles.

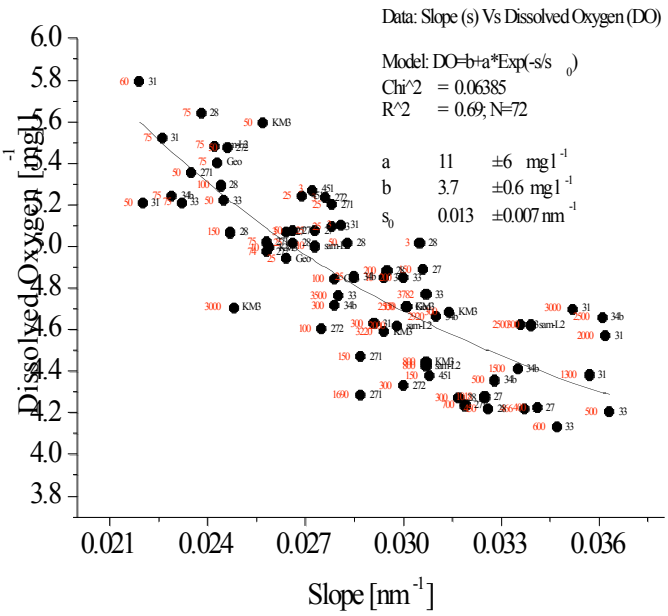

Figure 5: Relationship between spectral slope and DO

In deep lakes (e.g. Salto Lake) the water column is commonly subdivided in to three layers. The epilimnion (Upper Layer Water, ULW), the metalimnion (Frontal Water, FW) and the hypolimnion (Deep Layer Water, DLW) clearly evidenced by temperature/conductivity (T/C) diagram (Figure 6).

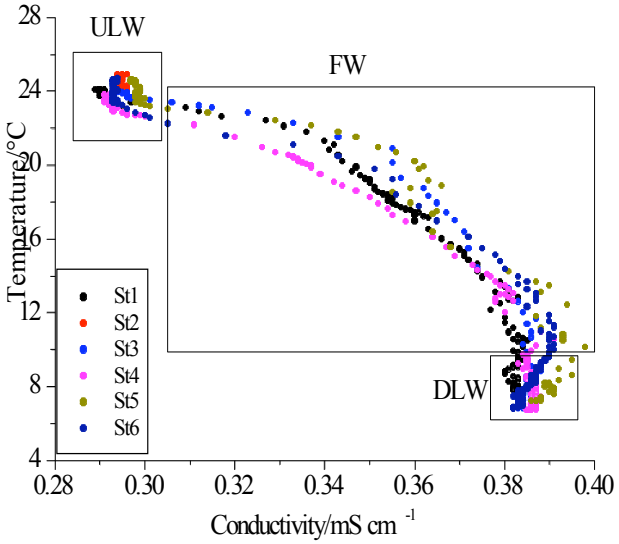

Figure 6: T/C diagram in Salto Lake

In the ULW the solar ultraviolet irradiance is present and it interact with biotic and abiotic systems. From CDOM optical properties prospective a chemical physical, optical and biological subdivision of the water masses can be adopted considering CDOM spectral slope and absorption diagram (s/A diagram figure 7)

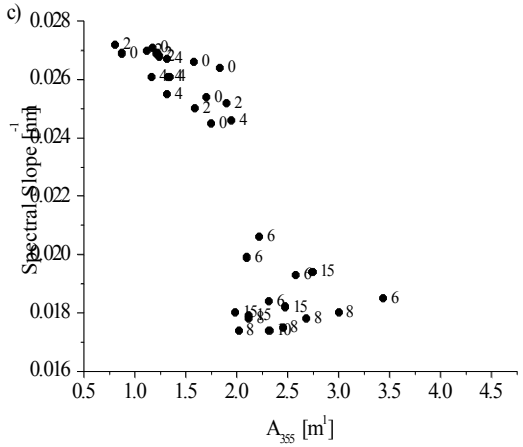

Figure 7: Subdivision of the water masses from s/A diagram. The labels are the sampling depths.

The ULW (0, 2 and 4 m sample depths) is characterized by high s and low A_{355}. This is related with the photodegradation and photobleaching of CDOM exposed to UV solar irradiance. At the same time in the FW and DLW (6, 8, 10, 15 m sample depths) the CDOM is characterized by low s and high A_{355}. The spectral slope profiles (figure 8) were characterized by high value of s in the ULW and low s in the DLW. An absolute minimum of s was observed in the FW where the production of new not photodegraded CDOM is present. This production was originated by degradation/exudation of phytoplankton..

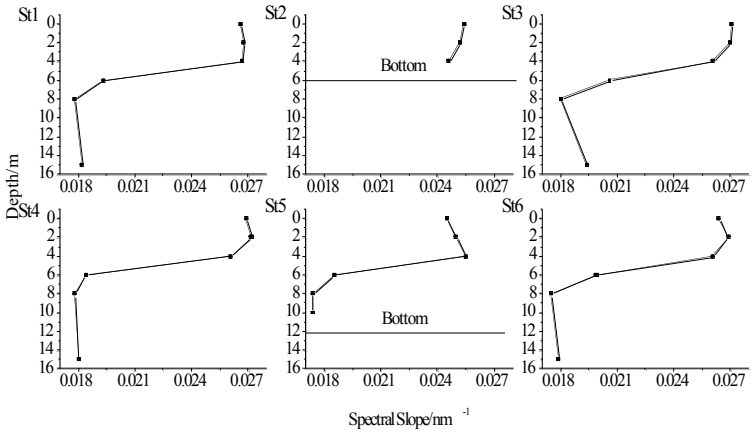

Figure 8: Spectral slope profile during a summer survey in Salto Lake.

Both chemical physical and CDOM descriptions of the water masses con be use to improve the comprehension of the aquatic ecosystems in relation of the biological functions.

References

Cózar, A., L. Bracchini, A. Dattilo S. Loiselle and N. Azza, Characterization of the Ugandan inshore waters of Lake Victoria based on temperature-conductivity diagrams, Water Resources Research Vol. 40, W12303, doi:10.1029/2004WR003128

Borghini, M., Bozzano, R.,, Schiano, E. Bracchini, L., et al., Report on oceanographic and geophysical investigation during cruise MFSTEP2 (April 2005) with R/V Urania, Northern Thyrrenian and Ligurian Sea, CNR, ISMAR-CNR Cataloging-In-Publication data: ISMAR Bologna TECHNICAL REPORT N. 96, pp 40.

Dattilo A. M., Decembrini F., Bracchini L., Focardi S., Mazzuoli S., Rossi C., Penetration of solar radiation into waters of Messina Strait (Italy)., Annali di Chimica, 2005, 95, 3-4, 177-184

Caroppo C., Congestri R., Bracchini L., Albertano P.. On the presence of *Pseudo-Nitzschia calliantha Lundholm, Moestrup et Hasle* and *P. delicatissima (CLEVE) heiden* in the southern adrietic sea (Mediterranean Sea, ITALY), Journal of Plankton Research, 2005, 27, 763-774.

Dattilo, A.M., Bracchini, L, Loiselle, S., Decembrini, F., Rossi, C., Spectral attenuation of solar radiation and optical characterizationof surface coastal waters related to the Straits of Messina, Estuarine, Coastal and Shelf Science (In review 2006).

2A - Characterization of food products by ToF-SIMS and PCA

Antonio Tognazzi[a], Sandra Ristori[b], Stefania Mazzuoli[a], Silvia Focardi[a] and Claudio Rossi[a]
[a]Dipartimento di Scienze e Tecnologie Chimiche e dei Biosistemi,Università degli Studi di Siena
[b]Dipartimento di Chimica, Università degli Studi di Firenze

Aims

In recent years the analysis of agricultural products has focused on nutritional properties, which are both related to farming techniques (e.g. use of chemicals) and geographic origin. In this project we study the influence of different factors on olives and olive oil, with the aim of using extensive physico-chemical characterization to promote the final quality of this food.

Results

Extra-virgin olive oil represents one of the major high-quality agricultural product in Italy, and Tuscany ranks among the top producers. Besides the generally acknowledged good flavour and organolectic excellence of extra virgin olive oil, it has now been established that its regular use in the human diet is able to diminish the occurrence of circulatory diseases and cancer. This is mainly due to the high content of antioxidants in olives and olive oil, especially mono-unsaturated fats. However, it has been demonstrated [1] that a more subtle balance between major components and micronutrients may also play a role in determining olives and olive oil healthy properties.

Effects of chemical treatments

Chemical treatment may not only introduce traces of exogenous compounds, but it may also induce permanent alterations on plants and fruits, which compromise their overall quality. In this framework, the complexity of agricultural systems has to be taken into account during the course of investigation. In this context, fingerprint analysis is a valuable tool for complementing more conventional analytical methods.

In this study [2] we compared the chemical composition of three different groups of olives belonging to the Seggianese cultivar, that is one of the most abundant in the south of Tuscany. Samples were either taken from organic or conventional farming, and were labelled as “untreated”(UT), “treated-unwashed” (TU) and “treated-washed” (TW), according to the type of process they had undergone. Chemical treatment was carried out with an insecticide (dimethoate) and a fungicide (copper oxychloride), while washing was simply performed with cold water, according to a well established procedure. Intact olive slices and olive oil (spread as thin films on silicon wafers) were analyzed by ToF-SIMS and Principal Component Analysis (PCA) of the mass spectra was used to investigate similarities among samples. The entire ToF-SIMS spectrum is particularly suited to be used in pattern recognition and statistical analysis, since it bears high information, and it has been widely used in the characterization of complex systems.

Results showed that treated-washed olives were more similar to untreated samples. However, the washing process was not totally effective, since the treatment was able induce

alterations in the olive composition (figure 1). Similar results were obtained on oils, studied with the same procedure.

Figure 2 shows the loadings for PC1(a) and PC2 (b) vs the corresponding m/z value. The loading plot indicates that lower mass peaks (i.e. m/z = 1-60) were more intense in the treated-unwashed samples (positive loadings correspond to positive scores in Figure 1), whereas higher mass peaks were more intense in the spectra of unwashed and treated-washed samples. For the second principal component the difference between groups of samples were less clearly defined.

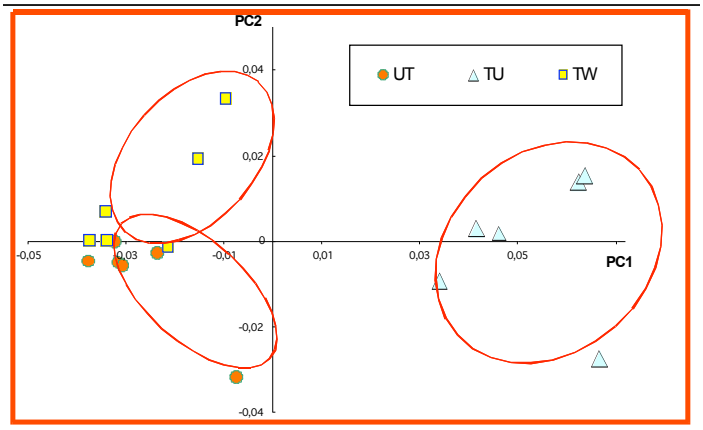

Figure 1. PC1 (90.27% of variance) and PC2 (6.16% of variance) score plot for the positive ToF-SIMS spectra of olives.

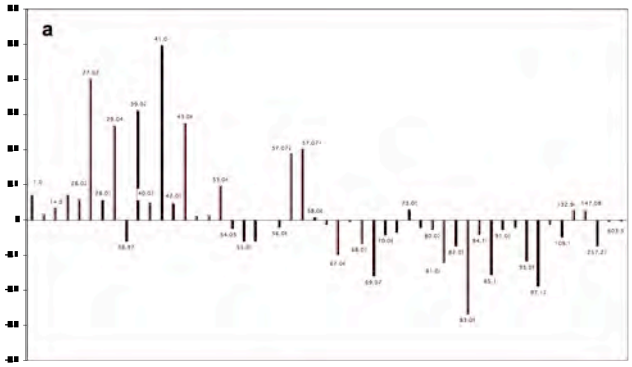

Figure 2. (a) PC1 loadings on PC1 for the score plot shown in Figure 1.

The SIMS data reported in figs 1 and 2 suggested that the chemicals used in the treatment were able to change the olive surface composition. Indeed, there were signals having higher intensity in TU than in UT or TW olive spectra, which were also found either in the dimethoate or in the copper oxychloride spectrum. For general discussion, it should be recalled that SIMS spectra of complex systems, such as the surface of intact fruits, can

hardly be described by pointing out single features and a more correct description is usually obtained by statistical tools. In this respect, the results reported in figures 1 and 2 provide an overview of the analyzed samples. However, special focus has to be placed on the intermediate region of the mass spectrum, where the quasimolecular ion of dimethoate and/or copper oxychloride are expected, together with characteristic peaks of palmitic acid (MW = 256.240), oleic acid (MW = 282.256), double chain derivatives of tripalmitin, triolein and mixed triglicerides (e.g. CH_3-$CH(OCOC_{15}H_{31})$-$CH_2(OCOC_{15}H_{31}^+)$, MW = 552.512; (CH_3-$CH(OCOC_{15}H_{31})$-$CH_2(OCOC_{17}H_{33}^+)$, MW = 578.527; CH_3-$CH(OCOC_{17}H_{33})$-$CH_2(OCOC_{17}H_{33}^+)$; MW = 604.543;), etc..

Fig 3 reports the positive SIMS spectra of representative olive samples and of the two chemicals used for treatment, in the 200-650 u.m.a. region.

It was observed that none of the most characteristic peaks of dimethoate and copper oxychloride had significant intensity in the spectra of treated olives and, in general, only low molecular weight species were detected. For instance, the Cu^+ peaks (at m/z ≈ 63 and m/z ≈ 65) from the fungicide and the parent ion of dimethoate ($C5H12NO3PS2^+$ at m/z ≈ 230), were not recorded in the spectra of TW or TU samples. The lack of significant amounts of the chemicals employed for the treatment was in line with data reported in the literature, since the two products used for Seggianese olives are considered among the most easily eliminable ones and, if properly administered, no trace of their presence should be retained by the edible products.

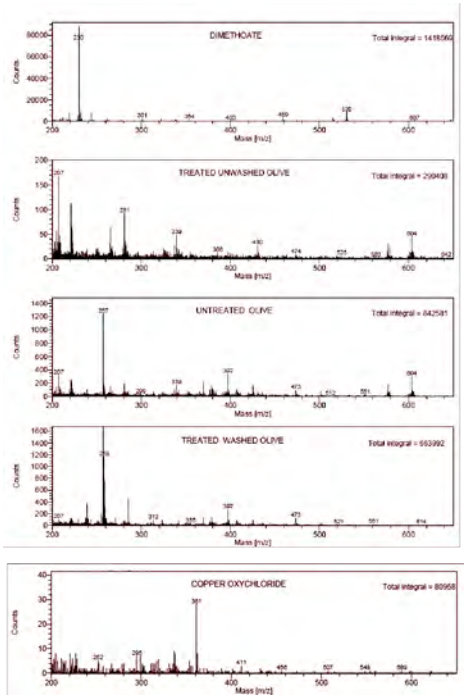

Figure 4. Intermediate (200-650 a.m.u.) region of the positive ToF-SIMS spectrum for different sample types.

Results obtained with the negative ion SIMS were in agreement with the above findings and, essentially, the same sample grouping was obtained from the principal component analysis of negative spectra. As in the case of positive ions, no peaks typical of the

chemicals used in the treatment (e.g the phosphate or sulphur negative ions) showed high intensity. This implies that the difference among olive groups were due to changes induced by the chemicals (degradation of molecules present in the olives, deposition of contaminants, etc.), rather than to the presence of the chemicals themselves.

In conclusion, we observed that TU olives were appreciably different from UT and TW samples. Oils from UT and TW olives were also found to be different. Smaller differences between UT and TW specimens were detected. Distinction among sample groups was not due to the presence of the chemicals used, since most of the peaks which are specific of dimethoate and copper oxychloride SIMS spectra were not significantly more intense for TW samples. However, a general change in the ToF SIMS spectra of olives with different history was evidenced, and it was attributed to chemical modifications in the surface of treated samples.
It has been reported that pesticides, and dimethoate in particular, are able to alter the lipid biosynthesis in olives. For example, Rutter et al. showed that lipid and fatty acid patterns are affected by treatment with this pesticide, even though it rapidly disappears from the food product [3]. Our results are consistent with this finding.

Cultivar and Geographical Characterization

The quality of olives depends on many factors. Some of them are intrinsic to the fruit, such as cultivar type and geo-climatic growing conditions; other factors depends on the farming and collection modalities. All these variables are reflected on the organolectic (aroma, odour, flavour) and chemical (composition, acidity, etc.) characteristics of olives. It is therefore important to create a reliable method for the classification of olives and oils on the base of cultivar and geographic origin. For this purpose, we used ToF-SIMS and PCA and we analyzed three olive varieties (Correggiolo, Moraiolo and Leccino), obtained by organic farming. This cultivars are simultaneously grown in different geographic areas of southern Tuscany and were collected in the areas of Follonica, Murlo and Trequanda. The sample labelling is listed in Table 1.

	Leccino	**Moraiolo**	**Correggiolo**
Follonica	LF	MF	CF
Murlo	LM	MM	CM
Trequanda	LT	MT	CT

Table 1. Samples used in cultivar and geographical characterization

Preliminary results showed that a simple two dimensional analysis is not able to differentiate geographical origin and cultivar type within the same dataset. Three dimensional PCA provides a more detailed description, and in our case it was able to operate such distinction.
However, a single characteristic at a time could be appropriately handled by bi-dimensional treatment. For instance, Fig 5 shows the PC2-PC3 score plot for the three cultivars. In each graph, samples with different geographical origin were well separated. For this analysis

PC1 was not chosen, since it gave positive scores for all samples and, therefore, mainly reported on the same olive characteristics.

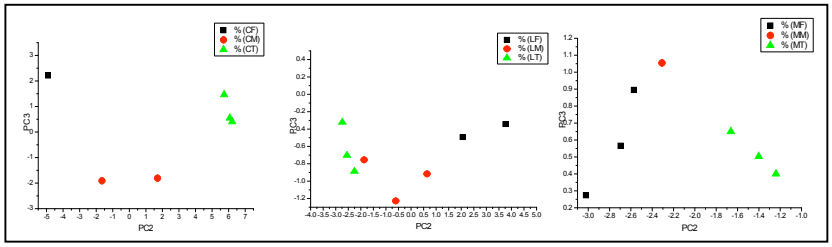

Figure 5. PC2-PC3 score plot for the three different cultivars.

Fig 6 shows the PC1-PC2-PC3 score plot, where samples are grouped according to both cultivar and geographical origin.

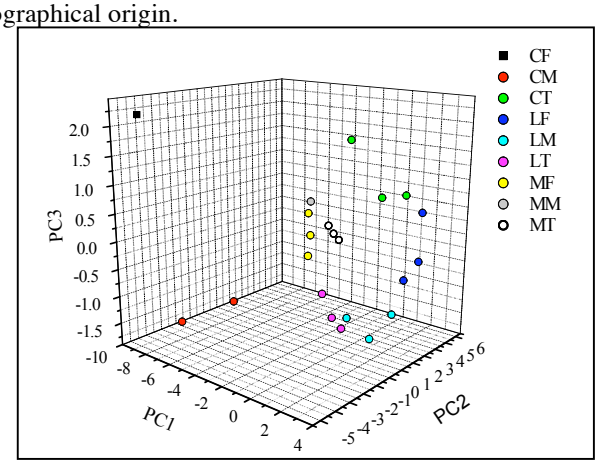

Figure 6. Three dimensional score plot for different cultivars and geographical origin.

Further studies are in progress to strengthen our method and build up a procedure for the identification of different olive types.

References

F.Visioli, C.Galli, *The effects of minor constituents of olive oil on cardiovascular disease: new findings*, Nutrition Review 56 (1998) 142-147.

S. Focardi, S. Ristori, S. Mazzuoli, A. Tognazzi, D. Leach-Scampavia, D. G. Castner, C. Rossi, *ToF-SIMS and PCA studies of olives and olive oil,* Colloids and Surfaces A, 2006, in the press (DOI: 10.1016/j.colsurfa.2006.01.003)

A. J. Rutter, J. Sanchez, J.L. Harwood, *The effect of dimethoate on lipid biosynthesis in olive (Olea europaea) callus cultures, Phytochemistry* 47 (1998) 735-741.

2A - Colloidal Science and Nanotechnology for Cultural Heritage Conservation

P. Baglioni, E. Carretti, D. Chelazzi, L. Dei, R. Giorgi, S. Grassi, A. Macherelli

Aims

- Nanomaterials for wall paintings and stones conservation.
- Autogeneously air-setting mortar
- Nanotechnology for paper deacidification.
- Wood deacidification of ancient shipwrecks: the Vasa case studies
- Nanocontainer solutions for wall painting and stone surfaces.
- Innovative gels for easel paintings conservation.

Results

The scientists' contribution to conservation of cultural heritage has grown to a great extent in the last decade. Chemists and physicists can greatly contribute to the preservation of artefacts because they can provide useful and reliable predictions of the degradation of Cultural Heritage materials and delay, as far as possible, the complete degradation of the artefacts themselves.

Criteria for treatments, such as compatibility, minimal intervention or reversibility, have found only in the last years some practical applications with the emerging of new techniques based on nanotechnologies. Nanotechnology is based on the recognition that particles of size below 100 nm impart to nanostructures formed from them new behaviour and properties.

Some innovative inorganic methods based on nanotechnologies, for example, have provided new ways for the consolidation of paintings. In particular, by using these compatible methods, it is possible to perform interventions without modification of the physico-chemical and mechanical behaviour of the materials, ensuring long-lasting effects.

CSGI is involved in several projects aiming to improve materials and techniques for the conservation of cultural heritage. The city of Florence is one of the most appropriate "environments" for these studies. After the 1966 Florence flood, the research group directed by the CSGI co-founder Prof. Enzo Ferroni was one of the first Academic Institutions that applied a rigorous scientific approach to the investigation of Cultural Heritage conservation. The peculiarity of the research in the Science for Cultural Heritage resides in its multidiscipinarity, where basic studies are usually associated to technological researches.

Several restorations have been carried out with CSGI scientific consultancy, and using innovative methodologies developed in the CSGI Laboratories (Masaccio's wall paintings in Cappella Brancacci, and Beato Angelico's wall paintings in San Marco Abbey, in Florence, Piero della Francesca's wall paintings in Arezzo, Maya paintings in Calakmul - Mexico, etc.).

CSGI contribution mainly consists of a co-operation with conservators and private and public institutions for experimentation of the innovative methodologies; this approach provides a continuous improvement of the conservation procedures. Moreover, CSGI offers also physico-chemical diagnostics of materials: in particular, CSGI expertise is related to the characterization of pigments, dyes, fibers, and binders used in wall or easel paintings, and also of the degradation products, as salts, varnishes and aged adhesives, in stones, wall paintings, paper, and wood.

Nanomaterials for wall paintings and stones conservation

European wall paintings have been made with slaked lime according to the fresco technique. Although very stable over a long period of time, wall paintings often suffer of several decay processes. Natural ageing originates the flaking of the paint layer and the powdering of the painted surface. This is due to the "chemical corrosion" of the binder, calcium carbonate, with loss of cohesion between pigments and substrate. Consolidation of mural painted surfaces (or stones) by inorganic treatments should provide the right content of carbonate binders to confer long-term preservation to the works of art. Historically, the Ferroni-Dini method, also called the "barium" method, was the first method that provided reliable results and its success was mainly related to the possibility of removing salts that threaten the paintings, reinforcing at the same time the porous structure.

The evolution of Ferroni-Dini is based on calcium hydroxide that is the best binder for limestone and wall paintings. In fact, the whole physico-chemical compatibility between the original and the restoration materials can be completely achieved by using calcium hydroxide. This is the best remedial for wall paintings reinforcement, since $Ca(OH)_2$ is the 'original' binder used by artists.

However, a direct use of aqueous solutions of calcium hydroxide is limited by the low solubility of the salt (1.6 g/L). A way to increase the lime concentration would be the use of lime dispersions in water. Unfortunately, water dispersions of commercially available $Ca(OH)_2$ cannot be used since the particle sizes are too large and the sedimentation rate is too fast, producing white glazing over painted surfaces. Particles have a broad size distribution and the mean size is larger than several micrometers. Dispersions of nanosized particles in non-aqueous solvents produce kinetically stable systems and can solve most of the drawbacks above mentioned.

We were among the first able to synthesize nanoparticles in nonaqueous solvents with the optimal properties for application to cultural heritage conservation. Kinetically stable dispersions can be obtained in short-chain aliphatic alcohols. Alcohols are environmentally friendly, volatile, and, compared to other solvents, have a low toxicity. Surface tension is small enough to ensure optimal wetting that is responsible for high penetration of the dispersions within the porous structure of the wall paintings.

The dispersions of nanoparticles are similar to an extremely concentrated solution of lime water (up to 30% volume fraction), well above the physico-chemical limit imposed by the solubility of calcium hydroxide in water.

Nanomaterials are characterized by high surface area that mainly influences the chemical reactivity of nanoparticles, producing just few days after the application a consistent consolidation of the treated surfaces.

We used successfully innovative methods based on nanotechnologies for the *in situ* consolidation of paintings and limestone in "*La Antigua Ciudad Maya de Calakmul*", a UNESCO World Heritage Site since year 2002 (Campeche, Mexico).

Traditional conservation methods used for the European Cultural Heritage have been extensively used in the past for the conservation of pre-Columbian artefacts. Unfortunately, synthetic polymers, such as Paraloid B72, Mowilith 30, and Primal AC 33, largely used for the conservation of several archaeological sites, have produced devastating and completely unexpected degradation processes on Mexican cultural heritage. The use of synthetic polymers to fix powdered and flaked paints in Palenque and Cacaxtla, and to re-adhere detached polychrome-modelled stucco fragments in Kohunlich, produced just after a few years dramatic effects on the artefacts, as detachment and flaking of surfaces and a strong acceleration of the chemical reactions involved in the paintings degradation.

$Ca(OH)_2$ nanoparticle application have provided in Calakmul excellent results. At the moment nanotechnology application in the field of wall painting conservation can be considered as a revolutionary alternative to the use of polymers.

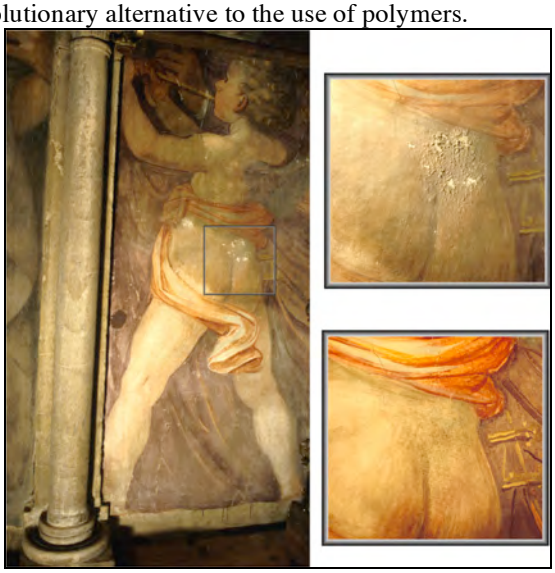

Cathedral of Florence, Santi di Tito's wall paintings: conservation carried out by means of $Ca(OH)_2$ nanoparticle dispersions

Santa Maria Novella Basilica in Florence, wall paintings by Andrea da Firenze: conservation carried out by means of lime/alcohol dispersions

La Antigua Ciudad Maya de Calakmul, Mexico: pyramid and wall paintings recently discovered therein and preserved by using $Ca(OH)_2$ nanoparticle dispersions

Autogeneously air-setting mortar

Mural paintings and decorative stucco are layered structures. A common consequence of degradation processes is the weakening of interfaces, leading to the complete or partial flaking or detachment of these layers. Several materials have been used to re-adhere delaminating layers and/or fill voids in degraded limestone. A grouting with the same composition of the original material is preferable for the conservation treatment, since the new introduced materials should be, in principle, compatible with the wall paintings and/or limestone.

Lime based adhesives have the same physico-chemical properties of wall painting, but they require CO_2 to set. Unfortunately, the CO_2 uptake by diffusion deeply into a porous structure is too slow and inefficient for setting. Therefore, a possible solution is the use of lime-based grouts with an additive that slowly produces carbon dioxide.

Additives producing CO_2 by reaction with water in an alkaline environment have been identified in the group of carbonic acid esters, and tested for wall paintings consolidation. These compounds are carbamates, with general formula R-O-CO-NR'_2, where R=C_2H_5 and R'=H in ethyl carbamate. Ethyl carbamate, was successfully used for the consolidation through injection of frescoes by Masaccio, Lippi, and Masolino in the Brancacci chapel in Florence (Italy).

Mortars containing carbamates were called “autogeneous mortars”, since the setting process occurs without involving CO_2 from the air. Carbon dioxide is produced *in situ* and all the other decomposition products are released without damage to the work of art.

Mortars with ammonium carbamate have been used for repairing of detached stucco fragments and also for the filling of voids and re-adhesion of flaked layers of wall paintings in the Maya site of Calakmul (Mexico).

Re-adhesion of polychrome-modeled stucco fragments by using autogeneously air-setting mortar. Calakmul - Mexico.

Nanotechnology for paper deacidification

Alkaline nanosized particles, used as nonaqueous dispersions, have been found particularly efficient for the preservation of cellulose-based materials that degrade through an acid-catalyzed process, which leads to chemical disruption of the cellulose polymer. It has been shown that acid-catalyzed hydrolysis is the main chemical route for cellulose de-polymerization. The overall effect is the shortening of the average chain length of cellulose that leads to a catastrophic loss of paper strength.

These processes can be stopped or consistently slowed down by a deacidification treatment. $Mg(OH)_2$ and $Ca(OH)_2$ are excellent de-acidifying agents, since they ensure a fair physico-chemical compatibility with the support, and after their transformation into the corresponding carbonate work very well as alkaline reservoir without originating any undesirable side-products.

$Mg(OH)_2$ and $Ca(OH)_2$ nanoparticles dispersions in alcohols, but the method is not restricted to these solvents and other less polar solvents can be employed as well, may be applied on paper by spraying or by impregnation in a chamber similarly to Bookkeeper, Battelle and Wei t'o methods (worldwide used methods for deacidification). All these methods produce hydroxide *in situ,* but originate some side-products, and require

dispersants to stabilize the systems. Our methodology use directly hydroxide as nanoparticles and this overcome the main limitations above reported. The used solvents are volatile, environmentally friendly and with low surface tension so that they properly work as carrier for solid particles, ensuring a homogeneous and penetration depth within the paper fibres.

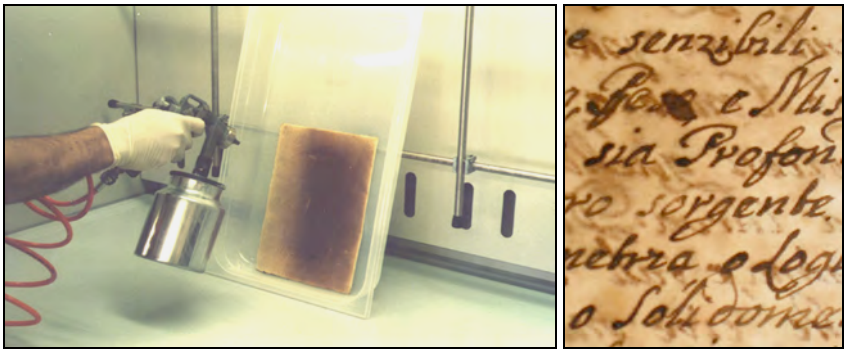

Deacidification of paper by sprayed lime nanodispersions

Innovative methodologies for inhibition of salt crystallization in porous media

The growth of crystal phases within a porous matrix is one of the main sources of the degradation affecting the historical building materials. The formation of salts is connected to the environmental conditions and, therefore, in many cases they are not completely removable. Less disrupting effect, inside the porous matrix, would be obtained if we were able to minimize the growth of crystals (and the volume). Inhibitor molecules or *habitus* modifiers, adsorbing on crystalline growing faces or over the crystallization nuclei, provide the right way to do it.

The research project is devoted to the study of inhibition or modification effects by some classes of molecules. The research project is planned as follows:

1 - preparation of laboratory samples impregnated by saturated salt solution;

2 - physicochemical characterization of the crystalline phases, and the porous materials;

3 - monitoring of the crystallization process and analysis of the inhibition activity of additives after crystallization-dissolution cycles carried out in climatic chamber.

This approach aims to control the growth of crystalline phases, by reducing the mechanical stresses of the pore walls. The project contribution to the conservation field is remarkable because it offers new tools for prevention of the degradation processes, instead of mechanical cleaning of surfaces affected by salt crystallization.

Wood deacidification of ancient shipwrecks: the Vasa case studies

The deacidification treatment of acidic wood samples from the famous Swedish warship Vasa was an interesting application of hydroxides nanoparticles for the conservation of Cultural Heritage.

The preservation of archaeological and waterlogged wood is a complex challenge in the conservation of ancient shipwreck. In fact, wood presents may show several concomitant degradation processes. For example, Vasa wood is very rich of iron salts, coming from bolts and cannon balls, which catalyze the oxidation of sulfur and sulfides, largely present inside the wood, to sulfuric acid. The large quantity of elemental sulfur in the timbers was shown to be the result of bacterial activity in near-anoxic conditions of the harbor seabed, and might produce up to 5000 kg of sulfuric acid when fully oxidized. At the moment, the

acid-catalyzed hydrolysis of the cellulose, which would reduce the stability of the wood, is seriously worrying the Vasa curators.
Vasa wood acidity can be neutralized by the application of nanoparticles of earth-alkaline carbonates and/or hydroxides, which provides also an alkaline reservoir inside the wood. Nanoparticles soaked in the wood from an alcoholic dispersion adhere to the wood wall and release hydroxyl ions leading to wood neutralization. Oak and pine samples from the Vasa wreck were characterized and treated with alkaline magnesium or calcium nanoparticle dispersions in non-aqueous solvents. Deacidification was monitored by pH changes and thermal analysis and all the treated samples were submitted to thermal artificial ageing in order to demonstrate the efficacy of the method. The excellent results obtained are now opening a new perspective in waterlogged wood conservation.

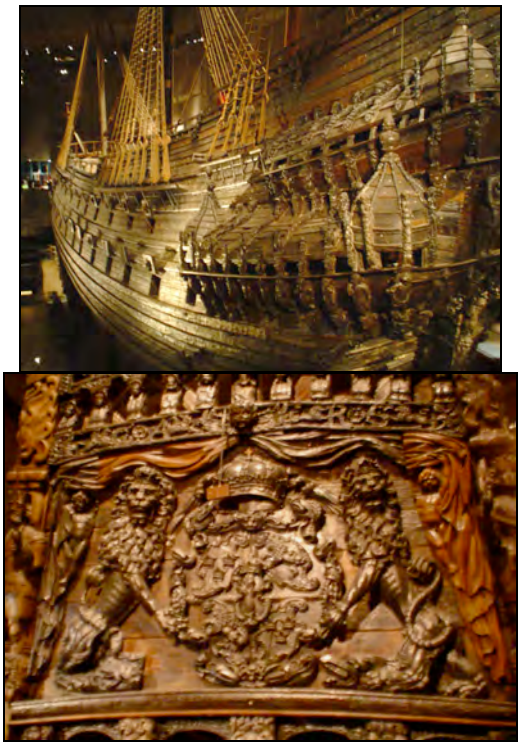

Vasa shipwreck at Swedish Maritime Museum in Stockholm

Nanocontainer solutions for wall painting and stone surfaces
Oil-in-water microemulsions and aqueous micellar solutions have been formulated for the application to wall paintings, easel paintings and stones, in order to remove hydrophobic materials (wax, fats, acrylic and vinyl resins, etc.) from the works of art surfaces. The first example of microemulsion application for cleaning organic contaminants (bee wax spots) on fresco paints was performed on Masaccio, Lippi, and Masolino masterpieces in Florence (Brancacci chapel).
Past restoration treatments, based on the use of synthetic materials, failed since of their degradation. In fact, they are unstable in most of the environmental conditions: drastic temperature and relative humidity changes, mechanical abrasion by dust and wind, rain and water condensation, light, and pollution promote degradation. The final effect is the

oxidation of polymer end-groups or side-groups, the chemical breakdown of polymer chain (chain-scission), and cross-linking reactions. All these processes lead to the loss of pigments adhesion, yellowing of polymers, decrease of polymer solubility and loss of treatment reversibility. The only way for removing them is, at the moment, limited to the usage of toxic mixtures of solvents.

Three (water, oil, surfactant), four (water, oil, surfactant, and co-surfactant), and five components (water, oil A, oil B, surfactant, and co-surfactant) systems were set up and checked in laboratory as 'cleaning agents'. New formulations were tested in some case studies in the framework of the restoration of the wall paintings by Filippo Lippi in Prato Cathedral and Spinello Aretino in the Guasconi chapel in San Francesco Church, Arezzo. The removal from wall paintings surfaces of hydrophobic polymeric resins, was complete and, even eight years after their application, no side effects came out.

Recently, these systems have been adopted in several restorations for the removal of vynil and acrylic polymers from very extended areas of painted surfaces. Microemulsions and micellar solution developed at the CSGI Center were used in the Sacristy of San Salvador Church in Venice (60 m^2), for cleaning of the mural paintings of the Conegliano (near Venice) Cathedral Façade (250 m^2) and also in the mural paintings of the Old Sacristy of Santa Maria della Scala in Siena (90 m^2).

Brancacci chapel in Florence: painting by Masaccio before and after the removal of wax spots. The left image shows a wax spot under UV light.

Detail of the fresco attributed to Camillo Capelli called “Il Mantovano” (16th century) in the San Salvador Church in Venice before (A) and after (B) cleaning with an oil-in-water microemulsion developed *ad hoc* for the removal of acrylic resins.

Innovative gels for easel paintings conservation
In the last two years the Florence unit of CSGI has developed new gel systems with potential application for easel paintings conservation. The basic idea is to overcome the problems associated to the residues of gelators with high molecular weight (very high viscosity creates difficulties during the removal from the painted surfaces) by developing system with a gelator precursor (polyallylamine) that becomes a true gelator after CO_2 bubbling with consequent formation of the polyallylammoniunm carbamate which behaves as a very good gelator for many solvents commonly used in easel paintings cleaning. Then the gelator can be easily removed disrupting the gel network by simple weak acid hydrolysis that gives back the polyallylamine precursor. This approach seems to have very stimulating outputs for potential application in cultural heritage conservation: important tests are in progress in cooperation with Museums and Galleries in Florence and Siena.

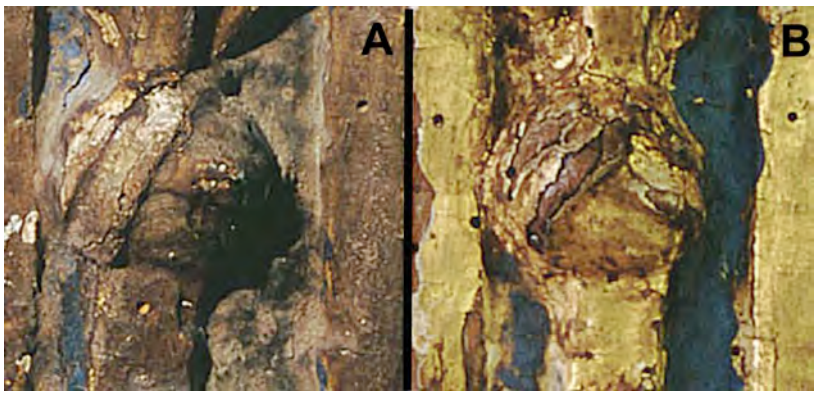

A 19th century gilded frame overlaid with a surface layer of a degraded natural varnish before (A) and after (B) application and removal of CSGI innovative gels.

References

Baglioni, P., Giorgi, R., *Soft and Hard nanomaterials for restoration and conservation of cultural heritage*, Soft Matter, 2, 2006, 293-303.

Giorgi, R., Chelazzi, D., Carrasco, R., Colon, M., Desprat, A., Baglioni, P., *The Maya site of Calakmul: "in situ" preservation of wall paintings and limestone by using nanotechnologies*, The Object in Context: Crossing Conservation Boundaries, Munich IIC Congress 2006: proceedings, Edited by David Saunders, Joyce H. Townsend and Sally Woodcock, 2006, 162-169.

Chelazzi, D., Giorgi, R., Baglioni, P., *Nanotechnology for Vasa Wood De-Acidification*, Macromolecular Symposia (Special Issue: Macromolecules in Cultural Heritage, Issue Edited by F. Cappitelli, Y. Shashoua, E. Vassallo.) 238 (1), 2006, 30-36.

Chelazzi, D., Giorgi, R., Baglioni, P., *Nanotechnologies for the conservation of waterlogged wood: the Vasa case studies,* Heritage, Weathering and Conservation conference (HWC-2006): proceedings, edited by R.Fort, M.Alvarez de Buergo, M.Gomez-Heras & C.Vazquez-Calvo, Taylor & Francis/A.A.Balkema Publishers, London, 2006, 797-

802.

Giorgi, R., Chelazzi, D., Baglioni, P., *Conservation of acid waterlogged shipwrecks: nanotechnologies for de-acidification*, Applied Physics A: Materials Science & Processing (Special issue: Materials Science and Cultural Heritage, Guest Editor(s): M.-C. Corbeil, M. Stuke, M. Menu, G. Padeletti), 83 (4), 2006, 567-571.

Baglioni, P., Giorgi, R., Chelazzi, D., Chen, C.C. *Nanoscience for the Conservation of Cultural Heritage and the Emergence of A Powerful Digital Image Collection*, Proceedings of The 8th National Russian Research Conference RCDL2006 - Digital libraries: advanced methods and technologies, digital collections. Suzdal (Russia), October 17-19, 2006

Vervat, M., Baglioni, P., Chelazzi, D., Favaro, M., Giorgi, R., Mosto, V., Vigato, P.A., Vigna, A., *Test preliminari per la valutazione di metodologie innovative per la pulitura di tinte labili: i verdi e i neri nella pittura italiana del XIX secolo*, in Lo Stato dell'Arte 4, Atti del IV Congresso Nazionale IGIIC, Siena, 28-30 Settembre 2006, Nardini Editore, p. 87-93.

Vervat, M., Baglioni, P., Chelazzi, D., Giorgi, R., Mosto, V., *Studio dello stato di degrado delle tele di lino di Giovanni Fattori*, in Lo Stato dell'Arte 4, Atti del IV Congresso Nazionale IGIIC, Siena, 28-30 Settembre 2006, Nardini Editore, p. 101-108.

Carretti, E., Dei, L., Weiss, R. G., *Soft matter and art conservation: rheoreversible gels and beyond*, Soft Matter, 1, 2005, 1-6.

Giorgi, R., Bozzi, C., Dei, L., Gabbiani, C., Ninham, B.W., Baglioni, P., *Nanoparticles of $Mg(OH)_2$: synthesis and application to paper conservation*, Langmuir, 2005, 21, 8495-8501.

Giorgi, R., Chelazzi, D., Baglioni, P., *Nanoparticles of calcium hydroxide for wood conservation. The deacidification of the Vasa warship*, Langmuir, 2005, 21, 10743-10748.

Carretti, E., Salvadori, B., Baglioni, P., Dei, L., *Microemulsions and Micellar Solutions for Cleaning fresco Surfaces*, Studies in Conservation, 50, 2005, 1-8.

Carretti, E., Dei, L., Miliani, C., Rosi, F., *Monitoring of Pictorial Surfaces by mid-FTIR Reflectance Spectroscopy: Efficiency of Innovative Colloidal Cleaning Agents*, Spectroscopy Letters, 2005, 38, 459-475.

Bitossi, G., Giorgi, R., Mauro, M., Salvadori, B., Dei, L., *Spectroscopic techniques in cultural heritage conservation: a survey*, Applied Spectroscopy Reviews, 2005, 40, 187-228.

Carretti, E., Dei, L., *Applications of Gels*, in Molecular Gels: materials with self-assembled fibrillar networks, P. Terech and R. G. Weiss Eds., Springer 2005, New York.

Chelazzi, D., Giorgi, R., Dei, L., Baglioni, P., *Nanotecnologie per la conservazione del patrimonio culturale*, La Chimica e l'Industria, 2005, 87 (10), 78-82.

Baglioni, P., Carretti, E., Dei, L., Ferroni, E., Giorgi, R., *La Scienza della Conservazione*, Darwin, 5, 2005, 26-33.

Palazzo, G., Fiorentino, D., Colafemmina, G., Ceglie, A., Carretti, E., Dei, L., Baglioni, P., *Nanostructured fluids based on propylene carbonate/water mixtures*, Langmuir, 2005, 21, 6717-6725.

Croveri, P., Dei, L., Giorgi, R., Salvadori, B., *Consolidation of globigerina limestone (Malta) by means of inorganic treatments: preliminary results*, in Proceedings of the 10th International Congress on Deterioration and Conservation of Stone, vol.1, D. Kwiatkowski & R. Lofvendahl Ed., Stockholm, 2004.

Vervat, M., Vigna, A., Baglioni, P., Giorgi, R., Chelazzi, C., *Il ritratto di Diego Martelli di Federico Zandomeneghi della Galleria d'Arte Moderna di Firenze: un restauro secondo il principio del minimo intervento*, in Atti del II Congresso Nazionale IGIIC - Lo stato dell'arte. Conservazione e restauro. Confronto di esperienze, Genova, 27/29 Settembre 2004, 392-401.

Carretti, E., Dei, L., *Physicochemical Characterization of Acrylic Polymeric Resins coating Porous Materials of Artistic Interest*, Progress in Organic Coatings, 2004, 49, 282-289.

Carretti, E., Macherelli, A., Dei, L., Weiss, R.G., *Rheo-reversible Polymeric Organogels: The Art of Science for Art Conservation*, Langmuir, 2004, 20, 8414-8418.

Baglioni, P., Carretti, E., Dei, L., Giorgi, R., *Nanotechnology for Wall Paintings Conservation*, in Self-Assembly, B. H. Robinson Ed., IOS Press Ohmsha, Amsterdam, 2003, 32-41.

Baglioni, P., Giorgi, R., Chen, C.C., *Nanoparticle technology saves cultural relics: potential for a multimedia digital library*, in Proceedings of the Workshop on Multimedia Contents in Digital Libraries, Chania (Grecia), 2003.

Carretti, E., Dei, L., Baglioni, P., *Solubilization of Acrylic and Vinyl Polymers in Nanocontainer Solutions. Application of Microemulsions and Micelles to Cultural Heritage*, Langmuir, 2003, 19, 7867-7872.

Nanni, A., Dei, L., *$Ca(OH)_2$ Nanoparticles from W/O Microemulsions*, Langmuir, 2003, 19, 933-938.

Salvadori, B., V. Errico, M. Mauro, E. Melnik and L. Dei, *Evaluation of Gypsum and Calcium Oxalates in Deteriorated Mural Paintings by FTIR Spectroscopy*, Spectroscopy Letters, 36, 2003, 501-513.

Baglioni, P., E. Carretti, L. Dei and R. G. Weiss, *Physicochemical Properties of Polyallylamine Based Gels with CO_2 as Gellant*, Journal of American Chemical Society, 2003, 125, 5121-5129.

Giorgi, R., Dei, L., Ceccato, M., Schettino, C.V., Baglioni, P., *Nanotechnologies for conservation of Cultural Heritage: paper and canvas deacidification*, Langmuir, 2002, 18, 8198-8203.

Carretti, E., Dei, L., Baglioni, P., *Aqueous Polyacrylic Acid Based Gels: Physicochemical Properties and Applications in Cultural Heritage Conservation*, Progress in Colloid and Polymer Science, 119, 2002, 280-283.

Baglioni, P., Ceccato, M., Dei, L., Giorgi, R., Schettino, C. V., *Nanotechnologies for Conservation of Cultural Heritage: Paper and Canvas Deacidification*, Langmuir, 2002, 18, 8198-8203.

Giorgi, R., Dei, L., Schettino, C., Baglioni, P., *A new method for paper deacidification based on calcium hydroxide dispersed in non-aqueous media*, Preprint of the IIC Baltimore Congress 2002, Works of Art on Paper, Books, Documents and Photographs: Techniques and Conservation, P. Smith Ed., 2002, 69.

Salvadori, B. Dei, L., *Synthesis of $Ca(OH)_2$ nanoparticles from diols*, Langmuir, 17, 2001, 2371-2374.

Ambrosi, M., Baglioni, P., Dei, L., Giorgi, R., Neto, C., *Nanosized crystals of $Ca(OH)_2$: properties and application*, Langmuir, 2001, 17 4251-4255.

2A - Enzymes, Synzymes and their application to waste processing and bioremediation.

E. Sanjust, A. Rescigno, S. Murgia, A. Salis (CSGI), in cooperation with F. Sollai, G. Vivona, J.V. Bannister (University of Malta, Msida, Malta)

Aims

Synthetic techniques: selection of macromolecular supports and redox mediators for synzyme synthesis
Characterization procedures for enzymes and synzymes
Applied techniques: treatment of polluted water from agrofood industries, biotransformations and biomass production and analysis

Results

Many wastes from agrofood industrial processes contain high concentrations of organic products, requiring at least one oxidation step to be safely disposed. Chemical oxidations are often depending on aggressive chemicals such as hypochlorites, ozone and so on; high costs and/or formation of toxic byproducts could be a serios limitation. On the other hand, biological treatments take place under relatively mild conditions but their application is usually prevented by long times and/or poor availability and high costs of the used enzymes. Therefore an integrated project is now in progress, devoted to optimise the production of selected highly active oxidases from edible white-rot fungi such as *Pleurotus*. The fungus could be directly employed in bioconversion processes, leading to formation of edible biomass and substantial reduction of the recalcitrant substrates. Alternatively, the involved oxidases could be extracted form suitable culture media, purified, and possibly immobilized on suitable supports. Among fungal oxidases, laccases and tyrosinases have drawn our attention and are under study as regards their induction, substrate specificity, action mechanism(s) and operational stability.
Synzymes are artificial enzymes, made by assembling naturally occurring moieties such as proteins and coenzymes, or also assembling suitable non-proteinaceous polymers and redox mediators, both natural or synthetic. Our attention is now focused on quinonoid synzymes, acting as amine oxidases to deaminate primary aliphatic amines to aldehydes, and especially to artificial peroxidases, capable of oxidatively degrading a wide range of aromatic molecules by means of hydrogen peroxide or also molecular oxygen. A number of such artificial peroxidase have been synthesised starting from water soluble or water insoluble polymers, coupled with both natural and synthetic metalloporphins and metalloporphyrins. Preliminary work has shown the promising features of these proparations as it regards ease of preparation, low cost, stability and catalytic activity. Also good substrate specificity towards non-phenolic substrates has been reached with ceratin preparations. The synzyme technology is obviously not limited to bioremediation and could find deep application in other technological processes such as drug biosynthesis: to this purpose, a flavosynzyme acting as a $NAD(P)^+$ regenerating tool has been recently synthesized and characterized.
A review on bioremediation through microbial agents was published.

References

Lepori M., MSc Thesis (Supervisor: Sanjust E.), 2001 *Enzyme induction in* Pleurotus *spp*

Pompei R. (2001) *"Bioremediation" microbica per il risanamento dell'ambiente terrestre e marino*." In RECUPERO AMBIENTALE: Tecnologie, Bioremediation e Biotecnologie. pp 443-455, UTET, Torino,.

Serra A. MSc Thesis (Supervisor: Sanjust E.) *Peroxidase activity of some immobilized metalloporphyrins*, 2002

Sanjust E., Cocco D., Curreli N., Rescigno A., Sollai F., Bannister J.V. (2002) Flavin-grafted poly(vinyl alcohol): preparation and properties Journal of Applied Polymer Science, , 85, 2471-2477

Sanjust E., Cecchini G., Sollai F., Curreli N., Rescigno A. (2003) *3-Hydroxykynurenine as a Substrate/Activator for Mushroom Tyrosinase* Arch. Biochem. Biophys. 412, 272-278

Sanjust E., Salis A., Rescigno A., Curreli N., Rinaldi A., (2004) Note.Xylose production from durum wheat bran: enzymic versus chemical methods Food Science and Technology International, in the press

Curreli N., Rescigno A., Rinaldi A., Pisu B., Sollai F., Sanjust E., (2004) Degradation of juglone by Pleurotus sajor-caju Mycological Research, in the press

Soddu G., Sanjust E., Murgia S., Rescigno A., (2004) Effect of 3-hydroxyanthranilic acid and 3-hydroxykynurenine on formation of melanin in vitro Pigment Cell Research, in the press

2A - Physical, Chemical and Limnological characterization of aquatic ecosystems. Study of impacts of solar radiation (UV and Visible): in situ and laboratory measurement and model descriptions.

Luca Bracchini, Steven Loiselle , Arduino Massimo Dattilo, Stefania Mazzuoli, Andres Cozar, Antonio Tognazzi, Silvia Focardi, Claudio Rossi
(Department of Chemical and Biosystem Sciences, University of Siena, Via Aldo Moro 2, 53100 Siena, Italy)

Aims

Determination of the temporal and spatial distribution of the optical characteristics of natural aquatic ecosystems
Determination of the impact of UV and Visible radiation on aquatic ecosystems
Models elaboration to examine the impact of the radiation on living systems

Results

The flux of solar UV (290 nm-400 nm) and visible (400 nm – 700 nm) radiation is one of the most important flux that determines ecosystem behaviour. UV radiation is the most energetic, for each incident photon, and damaging for the ecosystem. This radiation can have a significant impact on the metabolic activity of the primary producers, on the chemical characteristics of the biotic and abiotic compartments and on the biological functions of the fauna. Visible radiation is the fundamental energy source for all photosynthetic activities and therefore is the building block for the trophic web.
The measurement of the flux of radiation is particularly important in aquatic ecosystems. The manner in which the available radiation is attenuated depends upon the optical path that the electromagnetic wave follows within the study medium. In an aquatic ecosystem, besides the optical path of the water, there are a number of other important elements that need to be considered as having an important impact on the optical properties of the water medium. Dissolved organic matter, phytoplankton and suspended solids can cause a significant modification of the optical characteristics of the ecosystem. It is therefore important to measure the concentrations of the main components of the aquatic medium. These physical chemical characteristics will vary seasonally and spatially, as well as be influenced by the activities of man in and around the ecosystem. Man's activities can directly impact the material and energy flows that determine the ecological and chemical-physical status of natural systems. In fact, increases of allocthonous matter and changes in the distribution of solar radiation are the main threats to aquatic ecosystems both nationally and internationally. Both of these flows have a direct effect on the quality and productivity of these systems through modifications in the radiation field available within the water body.
More recently, to study the effect of different level in qualities (photon wavelength) and quantities (number of photons) on abiotic and biotic community of the aquatic ecosystems, The group is initiating a study with a large enclosure (10 m^3) constructed in the lake. With help of selective filters that cut-off a part of solar spectrum and a part of lamps spectrum (with well know spectral emission) it will be possible to study the effects of the modified radiation on the biotic and the abiotic systems, and the interaction between them.
Different aquatic ecosystems are interested by the research of the group: Iberà Lake in North East of Argentina, Victoria Lake in Uganda/Kenya, Salto Lake in Rieti province, Pontine lagoons in Latina Province, Montepulciano Lake in Siena Province and many other

sites (eg in Manfredonia Gulf, Puglia). The laboratory studies consist in the analysis of optical characteristic of the filtered (absorption and scattering of dissolved matter) and unfiltered (scattering and absorption of the total suspended solid) water sample and the analysis of the mortality and development of organism in controlled and repetitive condition. In aquatic ecosystems, in particular in wetland lake, the spatial, with a non Gaussian distribution, and temporal variation of the physical and chemical condition suggest a non total deterministic georeferenced maps representation (Kriging with help of variogramm model) of measurement and algorithm developed. The attenuation coefficients of the environmental solar radiation give many information on the difference of habitat in the same lake (local scale) and give much information on functionality of the boundary (eg wetland, agricultural and urban activities).
Some example of the results of the researches group are represented in the followed figure:

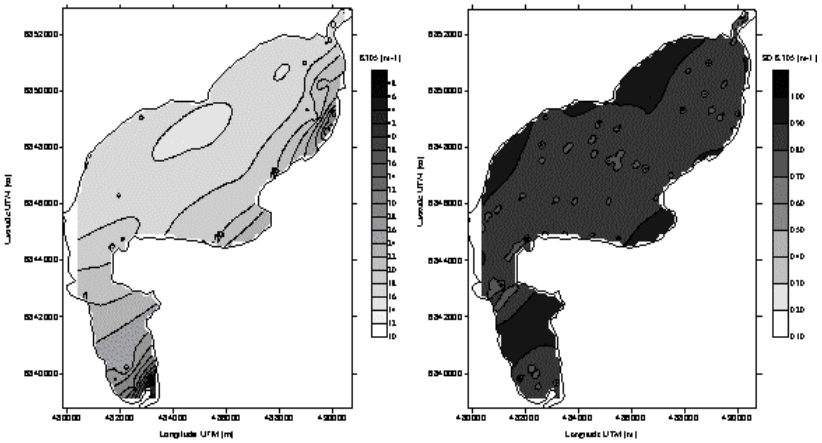

Fig. 1 *Map representation of 305 nm attenuation (K305, m^{-1}) and standard deviation (SD, m^{-1}) of interpolating grid of 77 stations in the Iberà Lake*

The extremely variation of the 305 nm attenuation coefficient have suggest us to divide the lake in three distinct basins: south, centre and north. The resulting map is well correlated with the Dissolved Organic Matter (DOC, mg l^{-1}, figure 2) measured from a sample at 0.25 m from surface of the lake:

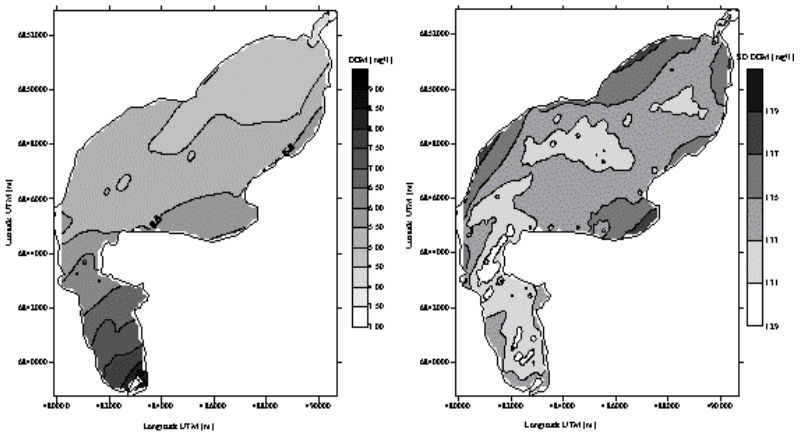

Fig. 2 *DOM [mg l^{-1}] distribution in Iberà Lake and Standard Deviation [mg l^{-1}] of interpolating grid*

The attenuation distribution of the Visible radiation (with a PAR sensor) in the Katonga bay and Bumjako bay in North West of Victoria Lake (Uganda) is presented in figure 3:

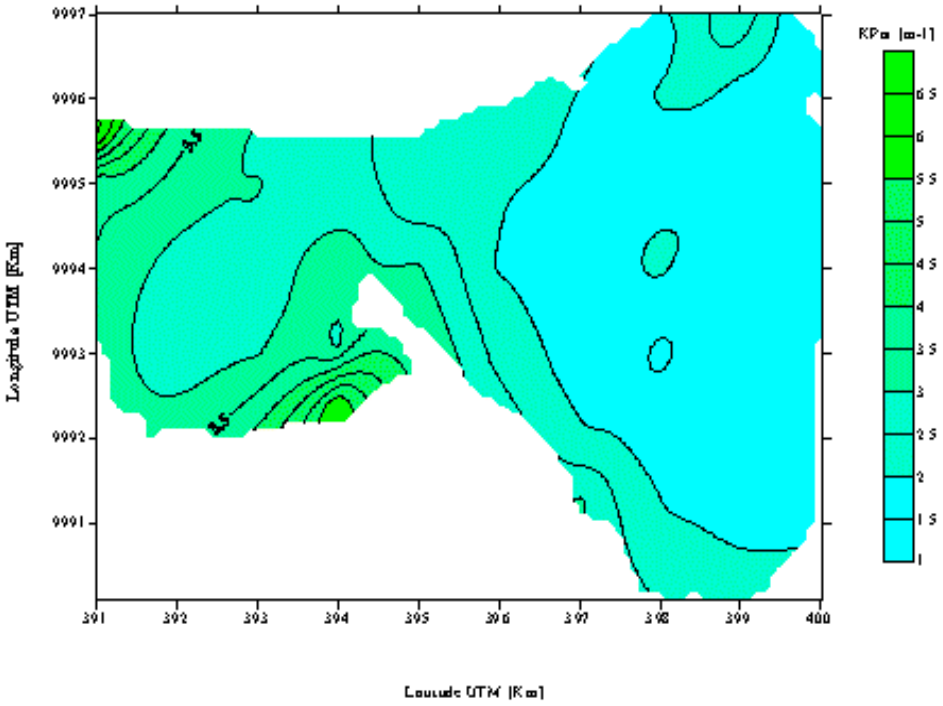

Fig. 3 *Attenuation of Visible radiation in Victoria Lake*

With the same statistical technique it is possible represent the Turbidity and Fluorescence measurements (figure 4) obtained from sample of water collected at 0.25 m of depth

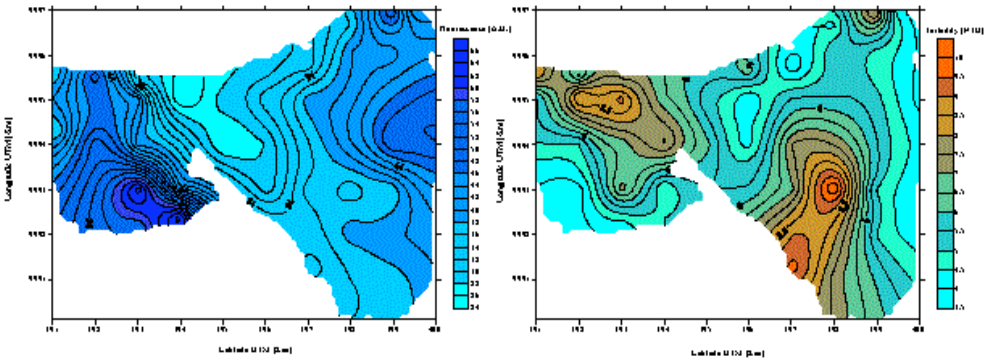

Fig. 4 *Fluorescence [Arbitrary Units] and Turbidity [Nephelometric Turbidity Units] in two bays of Victoria Lake*

The correlation between the in situ measurements of Chlorophyll α and the florescence and turbidity permit the determination of the distribution of fitoplankton in all studied section of the lake (figure 5):

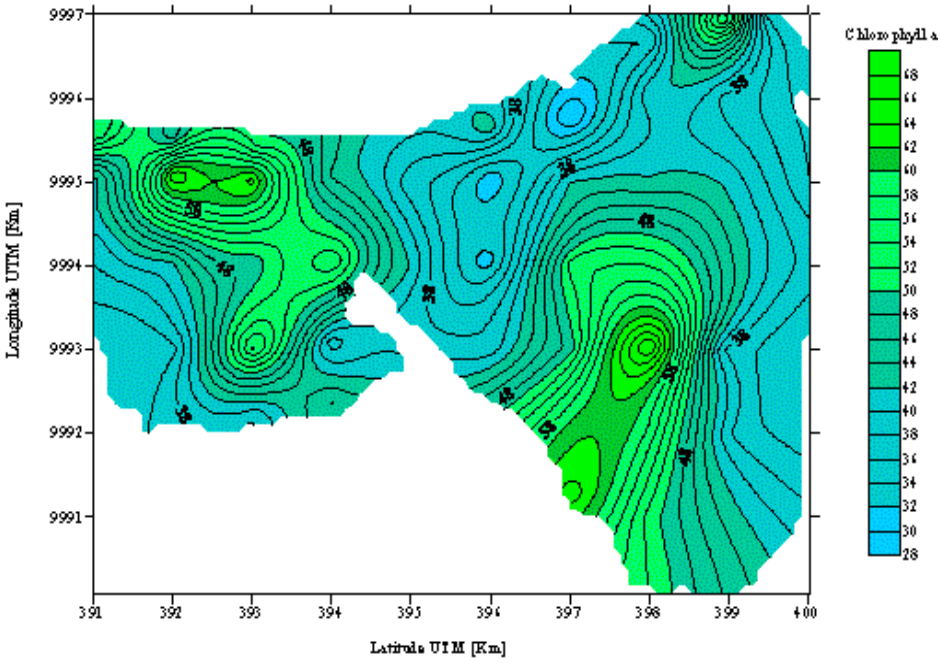

Fig. 5 *Chlorophyll a distribution obtained from multiple linear regression of the Turbidity, Fluorescence and in situ measurement of fitoplankton*

In the same way it is possible represent the effect of rivers and wetlands on aquatic environment. In particular it is possible to study from the molecular weight and the photobleaching of dissolved organic matter, the chemical quality of the water (figure 6 and 7)

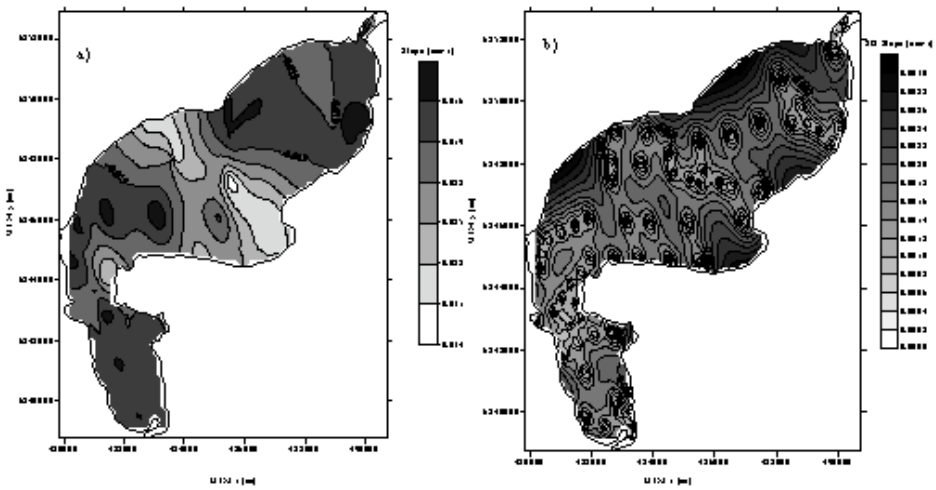

Fig. 6 *DOM chemical quality transported by two river in the Iberà Lake. The maximum values of photobleaching was found in central part of Lake*

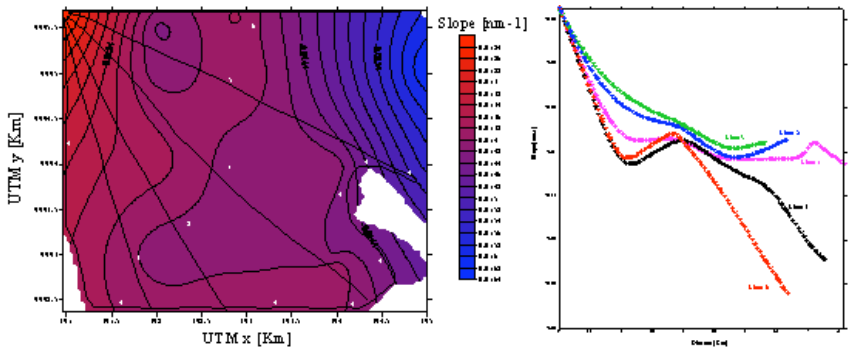

Fig. 7 *Effect of the wetland on DOM release (Victoria Lake, Uganda)*

The group is interested to modelling the light environment. In particular was develop a model to estimate the upwelling radiation (equation 1) with help of Secchi disk depth measurements (figure 8)

$$A = -\frac{1}{2} Ln\left(\frac{I_{uw}}{I_o}\frac{1}{r(\lambda)}\right) = 1.78 \pm 0.03 \quad (1)$$

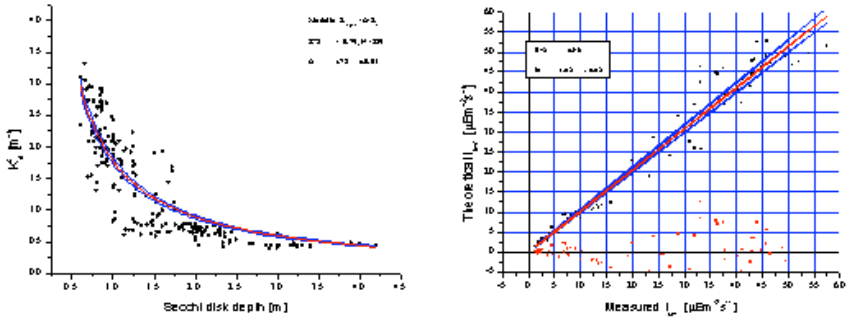

Fig. 8 *Secchi disk model results*

With the synergism between in situ and laboratory optical measurements it is possible to distinguish the role of the dissolved and suspended matters in the attenuation of solar radiation as function of wavelength (figure 9a and 9b):

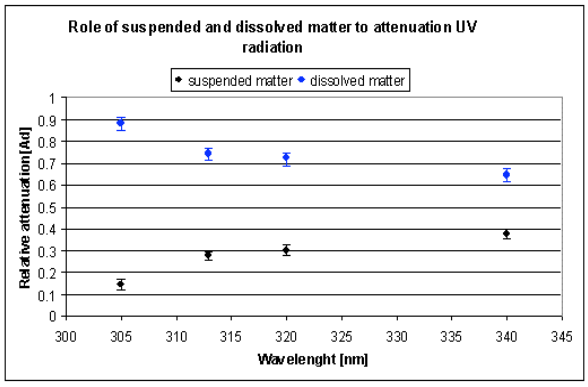

Fig. 9a *Importance of the dissolved and suspended matter to the attenuation of UV radiation in eutrophic Lake (Montepulciano Lake)*

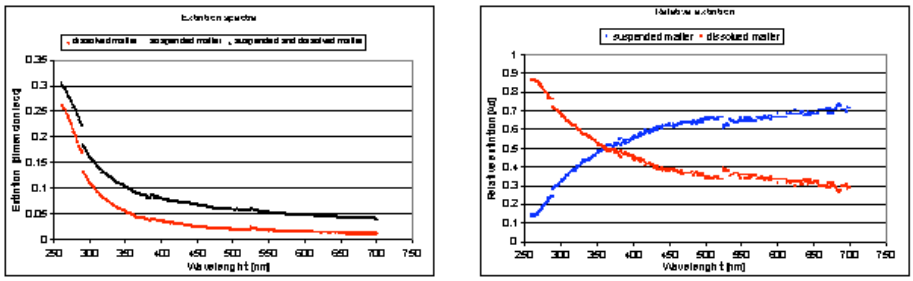

Fig. 9b *Extinction spectra and relative extinction of UV and Visibile radiation in Montepulciano Lake*

With the extinction properties it is possible obtain some information about in solution and suspended matter (figure 10)

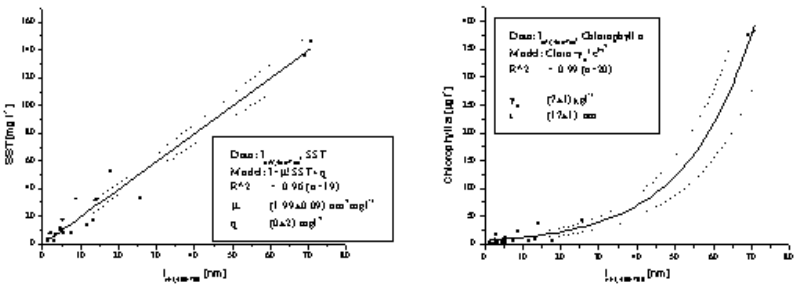

The impact of UV radiation (wave centered on 310 nm) on living systems was performed in laboratory; the resulting mortality model (eg. on *Artemia Franciscana*) is showed in figure 11a (Mortality in the adult stage) and 11b (Mortality in the Naupliar stage):

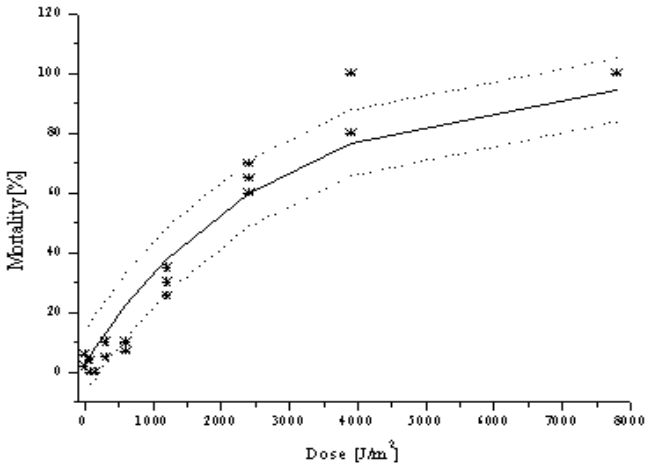

Fig. 11a *Mortality of Artemia franciscana in adult stage exposed to a different doses of artificial UV radiation*

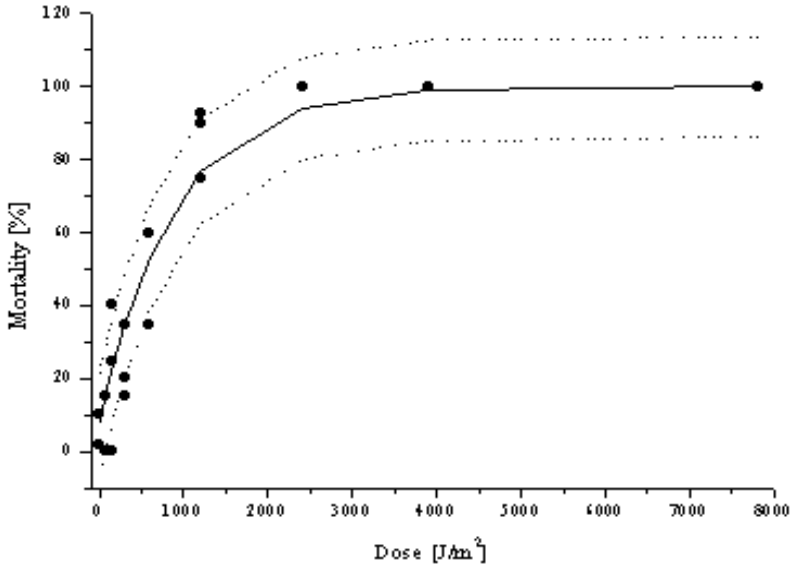

Fig. 11b *Mortality of Artemia franciscana in naupliar stage exposed to a different doses of artificial UV radiation*

References

Bracchini, L., S. Loiselle, A Cózar, A.M. Dattilo, M.P.Picchi and C. Rossi (accepted for publication 2003) Modelling The Components Of The Vertical Attenuation Of Ultraviolet Radiation In A Wetland Lake Ecosystem. Ecological modelling

Cózar, A., C. M. García, J. A. Gálvez, S. A. Loiselle, L. Bracchini and A. Cognetta (accepted for publication 2003). Spatial and temporal analysis of the lacustrine system of Iberá wetland (Argentina) based on remote sensing imagery. Ecological modelling

Cózar, A., J. A. Gálvez, V. Hull, C. M. García and S. A. Loiselle (accepted for publication 2003). Sediment resuspension by wind in a shallow lake of Esteros del Iberá (Argentina): a model based on turbidimetry. Ecological modelling

Mazzuoli, S., L. Bracchini, S. Loiselle, and C. Rossi (accepted for publication 2003). An analysis of the evolution of humic substances in a shallow lake ecosystem. Ecological modelling

Loiselle, S., L. Bracchini, A. Cózar, A. M. Dattilo and C. Rossi (accepted for publication 2003) Examining the spatial distribution of the light environment in a neotropical shallow lake. Hydrobiologia

Mazzuoli, S., S. Loiselle, V. Hull, L. Bracchini and C. Rossi (accepted for publication 2003), The analysis of the seasonal, spatial and compositional distribution of humic substances in a subtropical shallow lake.

Acta Hydrochimica

Loiselle S, S. Bastiononi, L. Bracchini and C. Rossi (accepted for publication 2003) Neotropical Wetlands: New Instruments In Ecosystem Management. Wetlands Ecology and Management

Rocchini, D., A. Chiarucci, S. Loiselle (accepted for publication 2003) Testing the Spectral Variation Hypothesis by using satellite multispectral images. Acta Oecologica

2A - SANS Investigation of Biomass Pyrolysis Oils

*Emiliano Fratini, Massimo Bonini, and Piero Baglioni (*in collaboration with *Anja Oasmaa and Yrjo Solantausta VTT Processes, P.O. Box 1601, 02044 VTT, Finland, and Jose' Teixeira, Laboratoire Léon Brillouin, CEA-CNRS, Saclay, 91191 Gif-sur-Yvette, France)*

Aims

Oils obtained by flash pyrolysis of biomass are good candidates as potential substitutes for fossil fuels. Unfortunately, these oils are poorly stable since numerous reactions take place after the production making them very reactive and leading to several problems in their handling and utilization. In particular, compared to mineral fuels, pyrolysis oils (POs) show a lower long-term instability and a relevant dependency on the storage temperature. Therefore the characterization of the composition of POs and the way it is affected by aging represents a crucial step in order to employ these oils in practical applications and, in particular, as substitutes of mineral oils. In this study, Small Angle Neutron Scattering (SANS) was used to study the evolution of the microstructure of oils obtained from pyrolysis of pine sawdust.

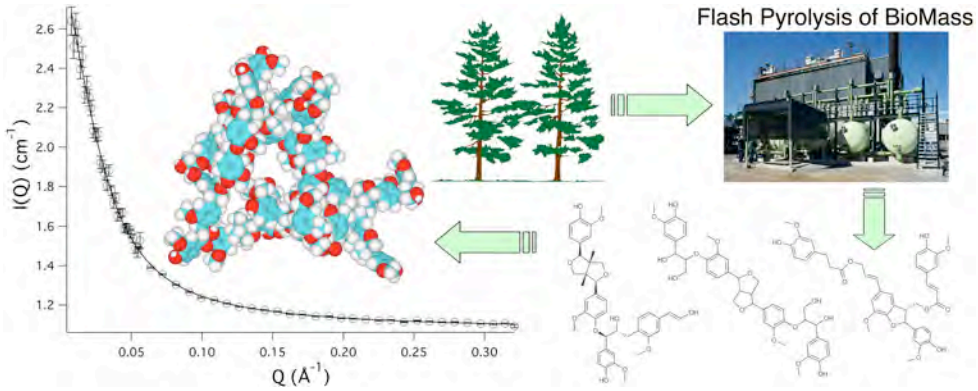

Results

Several models have been explored in order to fit the SANS experimental data. The fractal model introduced by Chen and co-workers [1] accurately describes the system and its evolution. Nanostructures formed by the association of lignin tetramers are present in PO. These clusters have a branched structure characterized by a fractal dimension, D_f, between 1.4 and 1.5, and an aggregation number, *S*, between 50 and 80. The microstructural characterization fully supports the thermal ejection theory, recently formulated by Piskorz [2], where lignin oligomers are considered to be directly expelled from wood particles as a result of a partial cracking of lignin molecules during the pyrolysis. These oligomers polymerize during storage, and this process continues until the heaviest lignin-rich fraction separates out of the matrix as a viscous sludge. In agreement with the chemical analysis results, this process mainly occurs during the first 6-7 months of aging, followed by a decrease in the aggregation rate.

References

Liu, Y. C.; Sheu, E. Y.; Chen, S. H.; Storm, D. A. *Fuel* **1995**, *74*, 1352-1356.

Piskorz, J.; Majerski, P.; Radlein, D. In: *Biomass. A Growth Opportunity in Green Energy and Value-Added Products*; Overend, R. P., Chronet, E., Eds.; Elsevier: Amsterdam, 1999.

Fratini, E.; Bonini, M.; Oasmaa, A.; Solantausta, Y.; Teixeira, J.; Baglioni, P. *Langmuir*; **2006**; *22*; 306-312.

2A - Surface modification of textile materials

Pierandrea Lo Nostro, Eugenio Bocci, Ester Falletta, Alessio Becheri, Massimo Bonini, Piero Baglioni

Aims

Modification of the surface of textile materials

Results

Modification of the surface of textile materials, mainly wool and cellulosic fabrics (cotton and Tencel®), was obtained through:

- grafting of a cyclodextrin derivative in order to endow the surface with empty hosting cavities that can be used for uptake/release of fragrances, insect repellents, antimicrobials, etc. (Figure 7)
- deposition of metal, or metal oxide nanoparticles (mainly Ag, ZnO and TiO_2) for antimicrobial activity or anti-UV shield and comfort upgrade (Figure 8)
- flame retardancy through surface reaction of cellulosic fibers with ammonium sulfammate and urea water solutions

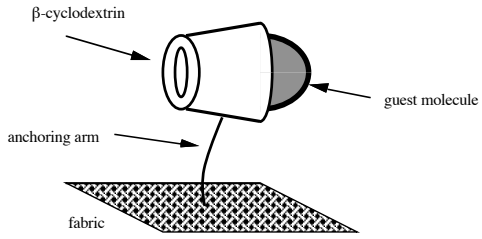

Fig. 7

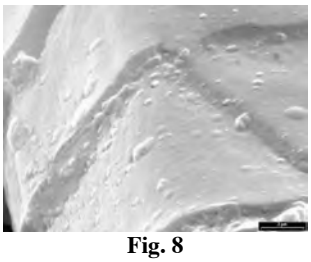

Fig. 8

The formation of stable inclusion compounds at the fabrics' surface was tested with several techniques: UV-VIS spectrophotometry (with integrating sphere), back-extraction with organic solvents, calorimetry, aroma testing and insect repellency tests (in collaboration with the Italian National Institute of Health, Rome). Figures 9 and 10 show a specimen of Tencel® treated with monochlorotriazinyl-β-cyclodextrin and then with DEET, a common insect repellent.

Fig. 9

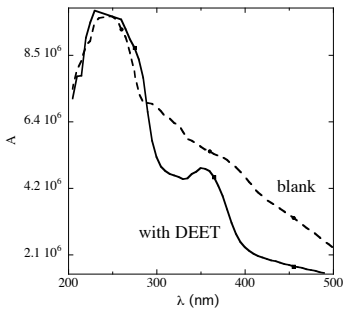

Fig. 10

References

Lo Nostro, P., Fratoni, L., Ridi, F., Baglioni, P., *Surface Treatments on Tencel® fabric: grafting with β-cyclodextrin,* J. Appl. Polym. Sci. 2003, 88, 706-715.

Lo Nostro, P., Fratoni, L., Baglioni, P., *Modification of a Cellulosic Fabric with β-Cyclodextrin for Textile Finishing applications,* Journal of Inclusion Phenomena and Macrocyclic Chemistry 2003, 44, 423-427.

Romi, R., Lo Nostro, P., Bocci, E., Ridi, F., Baglioni, P., *Bioengineering of a Cellulosic Fabric for Insecticide Delivery via Grafted Cyclodextrin*. Biotechnol. Prog. 2005, 21, 1724-1730.

Scalia, S., Tursilli, R., Bianchi, A., Lo Nostro, P., Bocci, E., Ridi, F., Baglioni, P. *Incorporation of the sunscreen agent, octyl methoxycinnamate in a cellulosic fabric grafted with β-cyclodextrin*. Int. J. Pharm. 2006, 308, 155-159.

2A - The analysis of the controlling factors of productivity in aquatic ecosystems

Steven Loiselle, Andres Cozar, Nadia Bergamino, Arduino Massimo Dattilo, Luca Bracchini, Stefania Mazzuoli, Silvia Focardi, Antonio Tognazzi, Claudio Rossi

Aims

The spatial and seasonal variations in primary production and the concentrations of phytoplankton can be pronounced in large lakes. These intra and interannual modifications can have a strong spatial heterogeneity due to complex links between hydrodynamics and local ecological factors. To understand the effects of local and global environmental forcing factors on the ecosystem cycles and biodiversity, it is fundamental to develop and analyse spatial databases that address their interannual and seasonal variability. Seasonal cycles of light availability and nutrients can vary geographically, controlling the phytoplankton blooms. In the past, phytoplankton studies in these extensive ecosystems focused mostly on point stations over a limited number of years. The activities of the Environmental spectroscopy group at UNISI is focusing on the combination of in situ measurements, ecological modelling and spatio-temporal data to determine the variations of phytoplankton biomass concentrations in several of the worlds largest lakes. These include Lake Tanganyika, Lake Victoria, Lake Malawi, Laguna Ibera. Ecological models have been develop that relate the available solar energy in the mixed water column and the carrying capacity of ecosystem to support algal biomass. Using this approach, as well as regional meteorological data analysis, it is possible to analyse spatial variations in primary productivity. The resulting hypothesis is then confronted with satellite measurements of surface biomass concentrations to link forcing functions with biomass and estimate how changing climate patterns may effect ecosystem functioning.

Results

Model development.

The patterns of abundance of algal biomass in aquatic ecosystems depend upon on the supply of resources (both nutrients and solar irradiance) as well as upon dominant loss processes (such as grazing and sedimentation). The balance between production and losses determines where and when phytoplankton community will grow and to what extent. We develop an ecosystem specific approach for determining the algal biomass carrying capacity under light limiting conditions. The model is based on the relationship between the total solar energy available and the energy stored (algal biomass) within the ecosystem at steady state. We applied this model to describe real conditions in two disparate algal communities; the phytoplankton community in Lake Victoria, East Africa and the microphytobenthos community in lacustrine system of Esteros del Iberá (South America).

Aquatic autotrophs have nutritional and energetic requirements that are necessary for their photosynthetic carbon fixation and growth. However, the upper limits of growth in light limiting conditions remain poorly understood with respect to nutrient-controlled capacities. This bias has partly arisen due to the complexity in modelling light availability in aquatic environments. The main challenges are the spatio-temporal variability of light within the water column, the competition for light with abiotic components and the negative feedback of algal auto-shading.

Attempts to describe light control of algal carrying capacities have followed two general

The algal concentrations at different solar irradiances for the pelagic environment of Lake Victoria and the benthic ecosystem of the lakes of Ibera wetland was used to derive the carrying capacity for each system from the upper concentration limits.

Lake Victoria, Africa

Lake Victoria, the second largest lake in the world, represents a unique reservoir of tropical biodiversity as well as a fundamental resource for the 30 million persons living within its catchment. Beginning in the past century, increasing human activity has led to changes in the distribution and bio-availability of the nutrient pools in the watershed, airshed and lakes. Because of the extensive nature of Lake Victoria, the impact of the climate factors may be highly differentiated in space (Plisnier et al. 2000).

A series of calibrated SeaWiFS images acquired from NASA archive was used to identify the lake regions sharing a similar temporal co-variation in chlorophyll-*a* concentration. A single value decomposition analysis (SVD) was applied to a matrix of 680 lake sections (9×9 km^2) for 150 scenes, covering biweekly the period from August 1997 to March 2004. Gaps in the biweekly-averaged scenes were previously filled through a kriging spatial interpolation. It was found that Lake Victoria can be mainly divided into three large regions; north, south, and an intermediate section. Other four small inshore regions (Murchinson Gulf, Winam Gulf, Sese Islands and Bumburi Channel) were also found to co-vary independently. The study period covered different El-Niño (1997-98 and 2002-03) and La-Niña (1998-99) events. To examine the possible influence of these global climate events on the interannual variability of lake production cycles, the temporal series of each lake region were subsequently decomposed into seasonal and trend components following an ARIMA-model based method.

Lake Victoria showed a regular seasonal variability in phytoplankton biomass (Fig. 1). An appropriate average seasonal series of surface meteorology was used to determine the climate influence on the spatial heterogeneity of the seasonal chlorophyll-*a* cycles. Regional differences in the stratification-mixing cycle of the lake were analyzed from lake surface energy budgets. Results show that the mixing phase determined in the north lake initiates with the maximal heat loses during July-August throughout the lake. However wind forcing is significantly stronger in south, where southeasterly monsoons enter the lake. A lengthy mixing reduces the exposition of the phytoplankton cells to the solar irradiance. The manifestation of this disturbed condition on the productivity of Lake Victoria is regulated by climate anomalies teleconnected to El-Niño phenomenon. Results show that El-Niño explained 71% of the variability in phytoplankton biomass over the last seven years (1997-2004). The close linkage between lake production and El-Niño has important implications on the lake's response to future global climate fluctuations.

The lakes of the Esteros del Ibera wetland, Argentina

The "Esteros del Iberá" is one of the largest pristine inland wetland ecosystems in South America. The seasonal dynamics of the lacustrine systems within the wetland were analysed using the EOF methodology. To compare the temporal variations in the lake optical characteristics in different lakes, the temporal trend in each lake section was compared. The deviation in the temporal trend of each site when compared to the EOF mode was used to examine the differences in the temporal trends of each lake section. The lakes present in the border agricultural and population centres (L. Mercedita y Cambí Retá) show a larger deviation ($R < 0.80$). These areas are subject to nutrient flows that may lead to changes in the seasonal cycle of phytoplankton. The analysis of the seasonal trend within the artificial reservoir of the hydroelectric dam (Lago Yacyretá) on the Paraná River demonstrated a completely different behaviour in relation to the EOF mode ($R < 0.50$) and wetland lakes. The rain periods coincided with a increase in water transparency, apparently due to the "washing" of the basin when the Paraná river passes through the floodplain. Similar observations have been made in Venezuela in the Orinoco floodplain (Castillo 2000).

The analysis of the spatial and temporal trends of the lacustrine ecosystems of the Iberá wetland system showed a clear north-south difference. In the north, differences in water quality along the east-west gradient were also determined. In the spatial analysis, this was clearly determined in the cluster analysis of the water optical properties using the monthly averages of the four years of satellite data. Those wetland lakes that strayed from this behaviour were those that were located in border areas in which agricultural activities were present. These three regions (NE, NW and S) within the wetland were differentiated by both water quality measurements as well as geomorphology.

In summary, the Ibera wetland can be defined as a system of lakes and marshes, whose characteristics have regional and temporal gradients. These gradients are effected by the flowrate and retention time of each lake, the presence of agricultural activities near the lake and the geomorphological characteristics of the bio-geographic region.

Lake Tanganyika

The spatial and seasonal variations in phytoplankton concentrations can be pronounced in large lakes and this is particularly true in Lake Tanganyika. In the present work, spatial and temporal variations of surface chlorophyll-a concentrations for the whole of Lake Tanganyika have been determined using a seven-year time-series (1997-2004) of satellite observed measurements. Statistical analysis was used to define regions with similar temporal co-variation of phytoplankton biomass and to extrapolate their bloom seasonality.

The different phytoplankton cycle of each Lake region provides information on the relationship between climate and productivity.

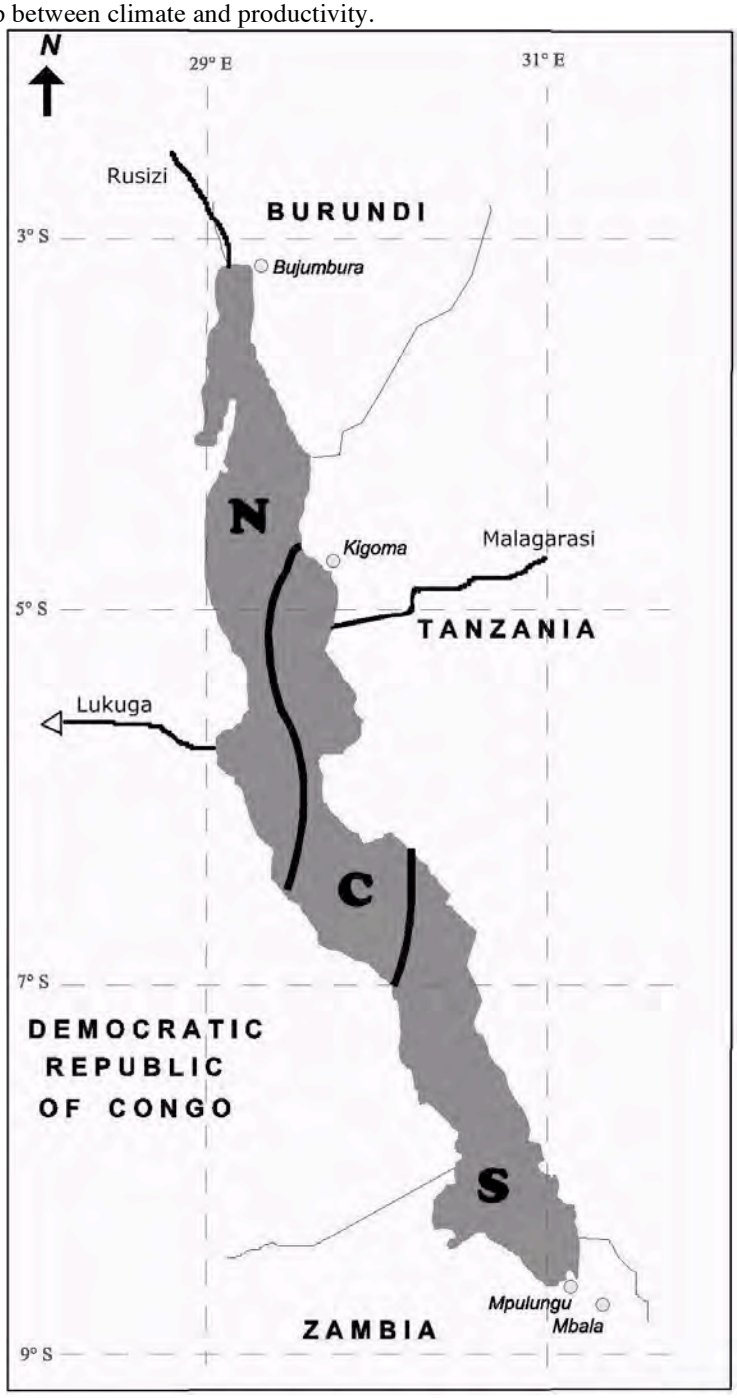

A shift in the phytoplankton seasonality was observed at the end of 2000, showing the high sensitivity of the Lake to regional climate patterns. This assessment of phytoplankton variability in large lakes is a prerequisite for the understanding of long-term changes

References

Loiselle, S. A., Bracchini, L., Rossi, C., Modelling energy fluxes in remote wetland ecosystems with the help of remote sensing, Ecological Modelling 145, (2001) 245-261

Cózar, A. C. M. García, S. A. Loiselle, J. A. Gálvez, L. Bracchini and A. Cognetta, Remote sensing imagery analysis of the lacustrine system of Iberá wetland (Argentina) Ecological Modelling 186, (2005) 29-42

Rocchini, D., A. Chiarucci, S. Loiselle, Testing the Spectral Variation Hypothesis by using satellite multispectral images. Acta Oecologica 26 (2004) 117-120

Loiselle, S. A., A. Cózar, A. van Dam, F. Kansiime, P. Kelderman, M. Saunders, S. Simonit, Development of tools for wetland ecosystem resource management in Eastern Africa, in Springer Ecological Studies; *Wetlands as a Natural Resource* (ed. J. T. A. Verhoeven) (in press)

Loiselle S:A., V. Hull, J. A. Galvez, C Rossi, “Qualitative modelling tools for rural ecosystem management", International Journal of Sustainable Development and World Ecology, 8, (2001) 1-14.

Cózar, A., A. Dattilo, N. Bergamino, L. Bracchini and S. A. Loiselle, Nutrient enrichment of Ugandan inshore waters: possible changes in the historical trend of Lake Victoria (accepted for publication Wetlands Ecology and Management, 2006)

Loiselle S.A., A Cózar, A. Dattilo, L. Bracchini A.A. Galvez, Light limitations to algal growth in tropical ecosystems Freshwater Biology (2006) DOI 10.1111

Bergamino, N. S. A. Loiselle, A. Cozar, A.M Dattilo, L. Bracchini, C. Rossi 2006 Examining the dynamics of phytoplankton biomass in Lake Tanganyika using Empirical Orthogonal Functions. Ecological Modelling (accepted for publication)

2A - The use of satellite based optical sensors to examine the chemical, physical and biological properties of aquatic ecosystems

Steven Loiselle, Nadia Bergamino, Silvia Focardi, Andres Cozar, Arduino Massimo Dattilo, Luca Bracchini, Stefania Mazzuoli, Claudio Rossi.
Department of Chemical and Biosystem Sciences, University of Siena, Via Aldo Moro 2, 53100 Siena, Italy

Aims

The combination of biological, chemical and optical measurements with the satellite based emission and reflectance measurements is an important tool in the study of the spatial and temporal characteristics of aquatic ecosystems. The CSGI Siena environment group has used these instruments in collaboration with researchers in a number of important research projects studying Lake Victoria in East Africa, the Ibera wetland in Argentina, the Nembuucu wetland in Paraguay and the Lake Montepulciano in Italy. The objective is usually to examine season and spatial changes in water and habitat quality and model these changes to understand the impact of changes in local and global climate, resource uses and hydrological conditions. Doing so, satellite derived information about lake shape, distribution, optical characteristics (Secchi depth, turbidity, concentration of dissolved organic matter) can be used to examine the role of resource utilisation on ecosystem quality. The satellite systems most often used are the SAC-C satellite MMRS sensors, the EO1 ASTER sensors and the Landsat ETM sensors. The wavebands that are usually used are visible and infrared. The availability of a time series of images from satellites with similar characteristics allows for a macro-scale comparisons related to the temporal co-variation of the ecosystem characteristics. Present efforts are being dedicated to the development of new analysis and modelling techniques for the study of the organic carbon cycle in the Mediterranean sea, combining oceanographic data with new satellite technologies, in collaboration with other national and European partners.

Results

Lake Victoria, Africa

SAC-C images were used to perform the classification of the wetland areas of the Ugandan coast and the Kenyan coast acquired on 23/06/2002 and 04/09/2002 . Images were georeferenced using the geocorrection file for each acquisition date. At sensor radiances were obtained using the published values. Path irradiance was removed by using 1% dark object subtraction. The surface reflectance was calculated by determining the sun elevation at the centre of each scene at the time and the MMRS spectral responses supplied by CONAE. Clouds present in the resultant images were then removed and those areas impacted were not considered in the analysis.

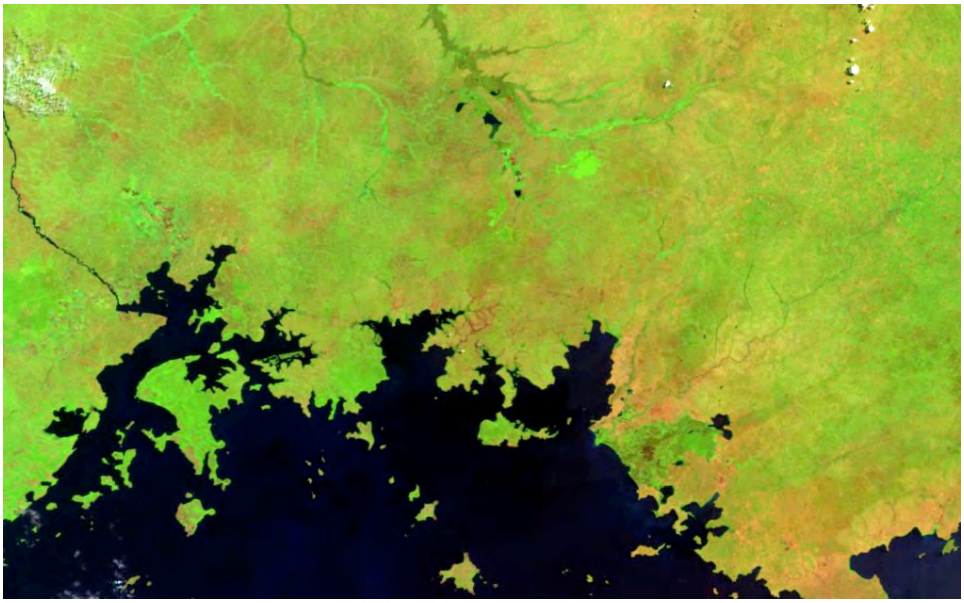

Plots of known vegetation composition in the Kirinya and Nabugabo wetlands were then used as training areas. A classification was performed using four main classes; wetland dominated by *Cyperus papyrus* with *Tyhpa latifolia* and *Phragmites domenginensis*, wetlands dominated by *Miscanthidium violecium* with areas of *Typha latifoli* and *Phragmites domenginensis*, non wetland areas (forests and agricultural areas obtained using land use maps from 1992) and open water areas. Plots (17) in the Yala and Katonga wetlands were used to control the accuracy of the abelled pixels of the two classified images created. The overall accuracy of the two wetland classes were 64 % (papyrus dominated) and 66 % (miscanthidium dominated).
The results of the analysis indicate that the wetlands along the western shore have a higher density than the northeastern shore. This is most likely the result of water and air circulation in this equatorial setting as well as the increased population density along the northern shore. The resulting impact on water quality in the Lake is presently being investigated, but the combination of lower wetland presence and increase population density will undoubtedly lead to poorer water quality in the northern bay areas where much of the lake population lives.

Ibera wetland, Argentina
The "Esteros del Iberá" is one of the largest pristine inland wetland ecosystems in South America. The analysis of the wetland was made to determine the seasonal changes in water quality in the large number of wetland lakes. Landsat TM and SAC-C MMRS satellite images were processed using radiometeric correction models created for each satellite system utilised. Digital numbers were transformed to radiances on the sensor according to the calibration data for each scene. The path irradiance of the measured exo-atmospheric radiance was removed by using the dark object subtraction. The reflectance was calculated by determining the sun elevation at the centre of each scene at the time and date of each image. Lake morphology and lakes distribution (geomorphologic analysis) was performed thought the spectral analysis of the near-infrared band of the MMRS sensor of the SAC-C satellite. A single image of spring 2001 was used to determine the size and location of all major open water bodies (> 0.5 km^2) in the wetland area. The reflectance data of each

image was then sampled for each lake and each lake subsection.. Samples of permanent water bodies just beyond the wetland borders were also sampled for comparison purposes. A database of 63 lake sections of a total of 25 water bodies was obtained. Using the corrected at-surface reflectance of each lake section, the average reflectance for all sections in the visible and infrared wavelengths was then recorded for 39 image dates from March 1997 until November 2001. When clouds covered a particular lake section, a weighted average of the preceding and following images was used to complete the matrix.

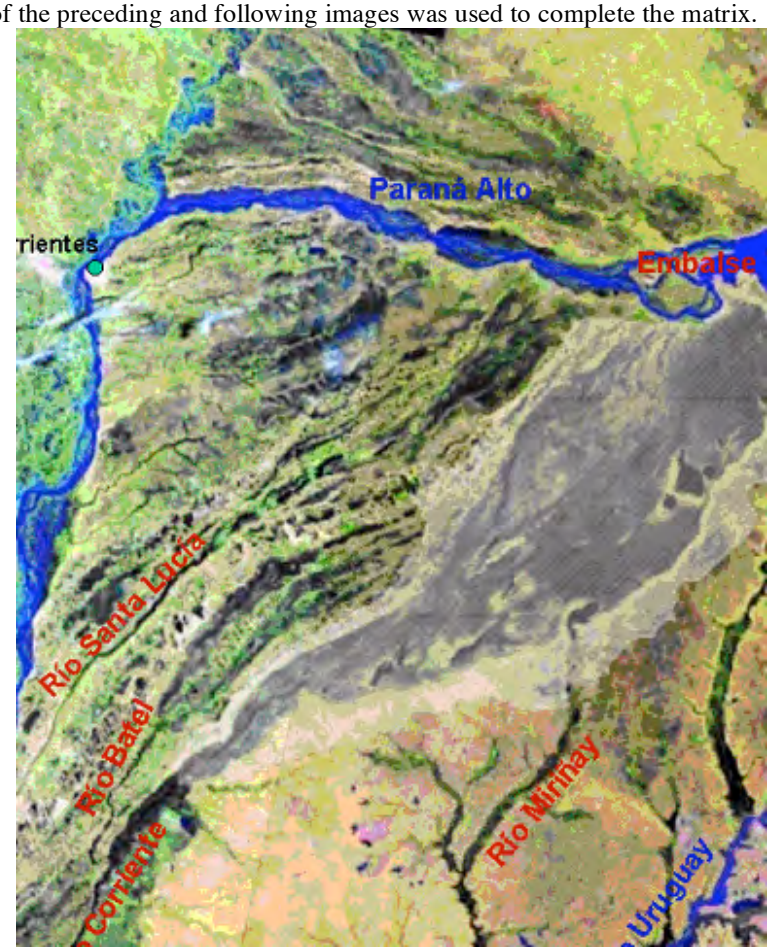

The determination of optical properties of the lake waters by satellite measured reflectances was made by comparing on site measurements with coincident satellite images. The on site measurements were made over a two year period in two of the permanent wetland lakes, Laguna Ibera (54 km2) and Laguna Galarza (14 km2). Georeferenced satellite images obtained in the same period (± 3 days) were used to create a series of algorithms that related the reflectances in the visible wavebands (bands 1,2,3 on all sensors) and infrared wavebands (band 4 and 5) to measured water optical properties. These included the Secchi depth, the nephelometric turbidity and the concentration of dissolved organic matter, which consisted mostly of dissolved humic and fulvic acids.

On the basis of the changes in lake and wetland morphology, the wetland was divided into three regions and the qptical characteristics of each region were determined. The spatial distribution of the optical properties show strong similarities with the geomorphogical regions. The water quality of the lakes of Southern Region generally showed higher transparency, that is, higher S_d values (media e SD). The most transparent waters were

located in the central zone of this Region, in particular in Laguna Medina and the northern sections of Laguna Trin. The lakes of Northeast and Northwest basin showed lower transparency. Laguna Luna and Laguna Iberá in the Northeast basin shows a different behaviour with respect to the "north-south" pattern of transparency in the macrosystem. The lakes selected outside the wetland in the active floodplain of the Mid Parana river showed the lowest transparency of all the sampled areas.

Temporal analysis

The seasonal dynamics of the lacustrine systems within the wetland were analysed using the EOF methodology of the series of Secchi depth estimations. The first EOF mode (first principal component) extracted from the covariance matrix of S_d explained the 56.4% of the variance of the collection of temporal series. The remainder of the modes always explained less 44% of the variability. The first mode corresponded with the seasonal nature of the wetland, showing transparency maxima during June and minima during January (fig. 4.9). This pattern approximately coincides with the maxima and minima of solar irradiance in the region as well as measured lake water temperature. The monthly maxima and minima of water temprature respectively coincided with the maxima and minima of S_d. Phytoplankton dynamics of two of the wetland lakes also displayed similar dynamics (L. Galarza and L. Ibera south basin).

To compare the temporal variations in the lake optical characteristics in different lakes, the temporal trend in each lake section was compared to the first EOF mode. The deviation in the temporal trend of each site when compared to the EOF mode was used to examine the differences in the temporal trends of each lake section. The lakes present in the border agricultural and population centres (L. Mercedita y Cambí Retá) show an even larger deviation ($R < 0.80$). These areas are subject to nutrient flows that may lead to changes in the seasonal cycle of phytoplankton. The analysis of the seasonal trend within the artificial reservoir of the hydroelectric dam (Lago Yacyretá) on the Paraná River demonstrated a completely different behaviour in relation to the EOF mode ($R < 0.50$) and wetland lakes. The rain periods coincided with a increase in water transparency, apparently due to the "washing" of the basin when the Paraná river passes through the floodplain. Similar observations have been made in Venezuela in the Orinoco floodplain (Castillo 2000).

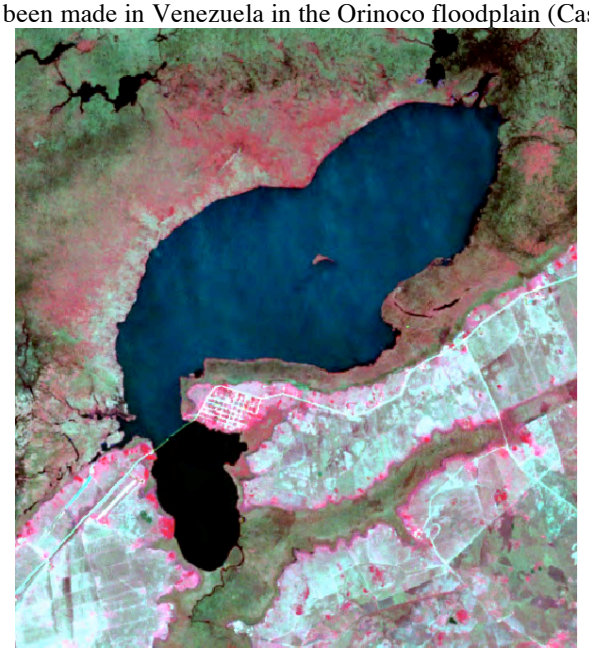

The analysis of the spatial and temporal trends of the lacustrine ecosystems of the Iberá wetland system showed a clear north-south difference. In the north, differences in water quality along the east-west gradient were also determined. In the spatial analysis, this was clearly determined in the cluster analysis of the water optical properties using the monthly averages of the four years of satellite data. Those wetland lakes that strayed from this behaviour were those that were located in border areas in which agricultural activities were present. These three regions (NE, NW and S) within the wetland were differentiated by both water quality measurements as well as geomorphology.
In summary, the Ibera wetland can be defined as a system of lakes and marshes, whose characteristics have regional and temporal gradients. These gradients are effected by the flowrate and retention time of each lake, the presence of agricultural activities near the lake and the geomorphological characteristics of the bio-geographic region.
Other areas under study are the Lake Montepulciano (Italy) and the Nembuucu wetland in Paraguay.

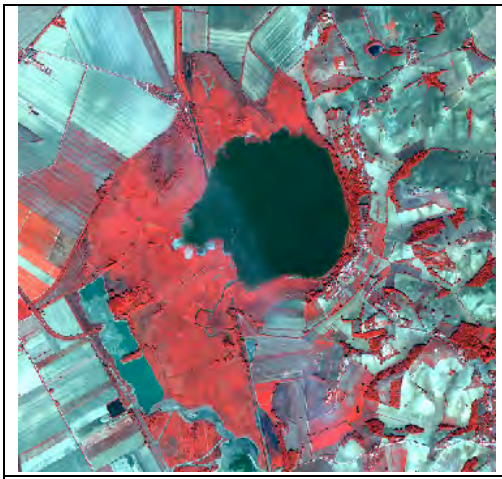

Lake Montepulciano, Italy (IKONOS satellite)

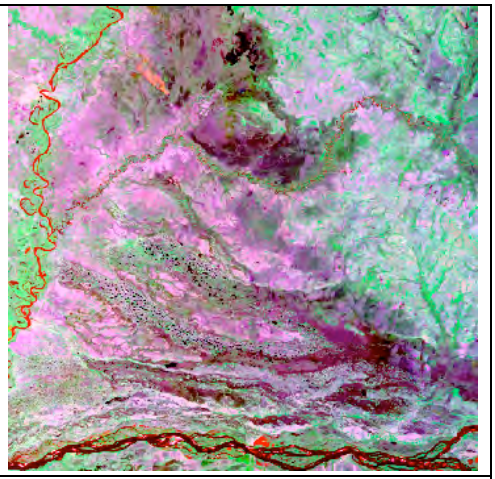

Nembuucu wetland and Paraguay river (SAC-C MMRS)

References

S. A. Loiselle, L. Bracchini, C. Rossi, Modelling energy fluxes in remote wetland ecosystems with the help of remote sensing, Ecological Modelling 145, (2001) 245-261

S. A. Loiselle, L. Bracchini, A. Cozar, A. Cognetta, C. Rossi, Determination of water optical parameters in a large wetland using TM bands, In: Proceedings from the 29th International Symposium on Remote Sensing of Environment, Buenos Aires, AR

S. A. Loiselle, G. Canziani, G. Sabio, C. Rossi, "The use of systems analysis methods in the sustainable management of wetlands" Hydrobiologia, 458. 191-200, 2001

S. A. Loiselle, S. Bastianoni, L. Bracchini C. Rossi "Neotropical wetlands: new instruments in ecosystem management". Wetlands Ecology and Management, 12 (2004) 587 - 596

D. Rocchini, A. Chiarucci, S. Loiselle, Testing the Spectral Variation Hypothesis by using satellite multispectral images. Acta Oecologica 26 (2004) 117-120

A. Cózar, C. M. García, S. A. Loiselle, J. A. Gálvez, L. Bracchini and A. Cognetta "Remote sensing imagery analysis of the lacustrine system of Iberá wetland (Argentina) Ecological Modelling 186, (2005) 29-42

N. Bergamino, S. A. Loiselle, A. Cozar, A.M Dattilo, L. Bracchini, C. Rossi 2006 Examining the dynamics of phytoplankton biomass in Lake Tanganyika using Empirical Orthogonal Functions. Ecological Modelling (accepted for publication)

S. Focardi, S.A. Loiselle, S. Mazzuoli, L., Bracchini, A. M. Dattilo, C. Rossi Satellite based indices in the analysis of land cover for municipalities in the Province of Siena, Italy. Journal of Environmental Management (2006) DOI 10:1016

S. Focardi, I. Corsi, Mazzuoli, S., Vignoli, L., Loiselle, S.A., Focardi, S. Integrating Remote Sensing Approach with Pollution Monitoring Tools for Aquatic Ecosystem Risk Assessment and Managment: A Case Study of Lake Victoria(UGANDA), Environmental Monitoring and Assessment, 2006, 122: 275-287

2A - Vectors as Carrier of Drugs

G. Martini, L. Ciani, A. Salvati, S. Ristori, A. Arcangeli (Dip. Patologia e Oncologia, Università di Firenze), L. Calamai (Dip. Scienze del Suolo, Università di Firenze) and G. Ricciardi (Dip. Chimica, Università della Basilicata)

Aims

Physico-chemical characterization and biological effects evaluation of supramolecular complexes between surfactant aggregates and boro-compounds or DNA for treating a wide variety of human diseases.

Results

Lipoplexes for Gene Therapy

Human genome characterization and recombinant DNA technology have created tremendous opportunities for gene therapy. However, delivery of large anionic bioactive DNA into the cell is not simple. As a first step, DNA must arrive intact to the nucleus, after crossing the cell and nuclear membranes. For this purpose viral vectors are commonly used as efficient delivery agents, although they present non negligible safety concerns. Cationic liposomes-DNA complexes (lipoplex) are a powerful alternative to viral systems in gene therapy.

Cationic unilamellar vesicles with 100 nm mean diameter were prepared from the cationic DC-Chol and the zwitterionic phospholipid DOPE as helper lipid. Zeta potential was measured on the above liposomes complexed with a plasmid encoding for the Enhanced Green Fluorescent Protein (pEGFP) and Electron Spin Resonance (ESR) spectra were recorded using appropriately tailored paramagnetic probes. Both kinds of measurements were carried out in the same conditions (medium composition, pH, temperature) employed for transfection experiments.

Results showed that liposomes loaded with the plasmid (lipoplexes) remained intact while DNA wrapped the external surface of liposomes, as it has been proposed by the so called external model (figure 1).

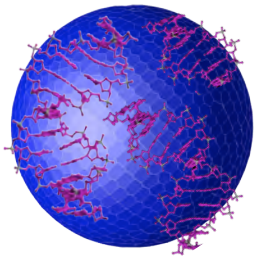

Fig.1 Model of lipoplex.

Transfection experiments of the pEGFP plasmid were checked on CHO cells. The critical parameters for transfection efficiency were found to be: composition and pH of the medium, surface charge of the liposome membrane, lipoplex charge and lipoplex/cell ratio, cell proliferation (cell culture conditions) and amount of lipoplexes added to the cell culture.

Our target is now to transfect human glioblastome cells in vitro. This tumor cells are well known to be hardly transfected. Preliminary results, obtained with the U138 cell line, are very promising, since the transfection efficacy of DOTAP/DOPE and DC-Chol/DOPE lipoplexes is well above the performance of a typical commercially available kit (figure 2).

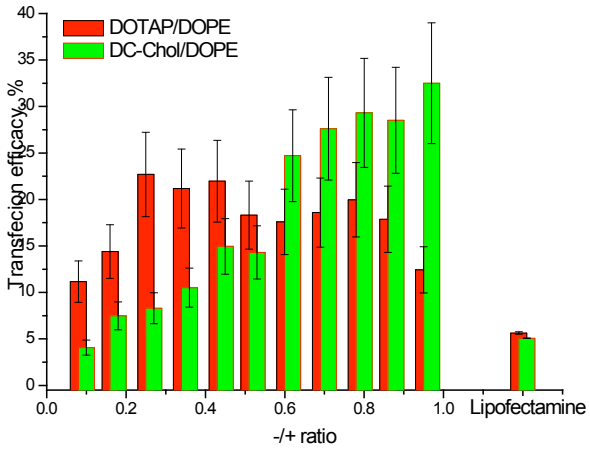

Fig.2 Transfection efficacy of DOTAP/DOPE and DC-Chol/DOPE lipoplexes on U138 cell line at 48 hours, evaluated as the number of cells that produce GFP over the total number of live cells.

siRNA: a new frontier for gene regulation

RNA interference (RNAi) is an evolutionary conserved mechanism, based on the action of short antisense (interfering) RNAs (siRNAs). It is capable to operate the silencing of several genes in eukaryotic organisms, and nowadays it represents a powerful research tool for knocking down undesired gene transcripts in Gene Therapy protocols. Different strategies to induce RNAi in mammalian cells have been developed. Furthermore, many efforts are being made to improve transfection efficiency as well to eliminate potential off-target and non-specific effects. However, the molecular mechanisms underlying the interaction between vectors used to transfect siRNAs and the plasma membrane is still unclear, and a detailed knowledge of the complex (vector + siRNAs) characteristics is required to design appropriate carriers for siRNAs delivery.

Current investigation with cationic liposomes gave a biological response comparable to commercial kits.

Carrier of different nature, such as micelles of cationic gemini surfactants, are also under study in collaboration with Dr. Martin In (Montpellier University). In this project the complex between cationic surfactants and siRNA analogues (siDNA) was formed above the c.m.c., to ensure that the supramolecular interaction was between siDNA and micelles. The obtained complexes were analyzed either with Zeta potential and ESR of amphiphilic paramagnetic probes. The former allowed to follow complex formation through surface charge variation, the latter gave insights on the molecular environment before and after oligo binding to the cationic micelles (figure 3).

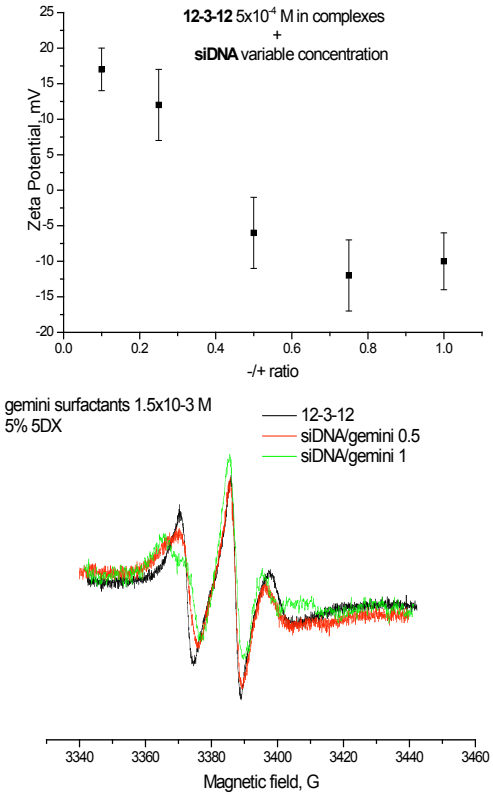

Fig.3 Zeta potential value (left) and ESR spectra (right) of complexes as a function of siDNA concentration.

Liposomes as Vectors for poly-carboranylalkylthio-porphyrazines in Anticancer Therapy

In tumor treatment liposomes act as suitable carriers for a large variety of drugs. Maximal loading occurs for monolamellar structures with 100-200 nm diameter.

This project concerns the physico-chemical characterisation of newly synthesized poly-carboranylalkylthio-porphyrazines (OCASPzs), to be loaded into liposomes of varying lipid composition. An example is reported in Figure 4 (Mg-OCASPz).

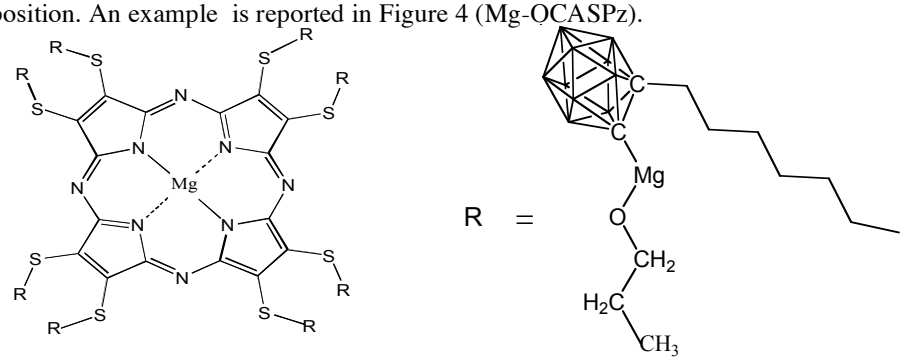

Fig.4 Chemical structure of Mg-OCASPz. On theright side the formula of the pendent chains, bearing a o-carboranyl unit (B10C2), is reported.

In the context of carboranyl-tetrapyrroles, OCASPzs represent an important improvement, in that they conjugate a high degree of peripheral carboranyl substitution and the peculiar electronic properties of the octathiolato-porphyrazine core. Therefore, besides carrying a huge amount of boron (i.e. 80 atoms per molecule), OCASPzs are of great interest for the multiple approach they offer in anticancer therapy, viz., in Photothermal Therapy, Photodynamic Therapy and Boron Neutron Capture Therapy (BNCT).
The liposomes chosen in this study were formed by lipids with oleoyl chains, that gave a fluid and thick limiting bilayer (total length of the plain lipid layer is ≈ 4 nm). Interestingly, the lenght of Mg-OCASPzs with extended lateral chains (i.e. its maximal size) is just 4nm. In this study different surface charges were chosen, since this feature is usually important in determining the interaction with living cells. The surface charge variation was followed as a function of Mg-OCASPz content by Zeta potential measurements. Contemporarily, the mean size of plain and drug loaded liposomes was measured. Table 1 illustrates the characteristics of three liposome types (made by positive, zwitterionic and negative lipids) loaded with Mg-OCASPz at two different lipid to porphyrin ratios.

SAMPLE	Zeta Potential, mV	Mean diameter, nm
DOTAP/DOPE	+45 ± 5	112 ± 4
DOTAP/DOPE with lipid : Mg-OCASPz = 200 : 1	+37 ± 5	120 ± 6
DOTAP/DOPE with lipid : Mg-OCASPz = 100 : 1	+33 ± 8	126 ± 8
DOPC/DOPE	-18 ± 2	120 ± 5
DOPC/DOPE with lipid : Mg-OCASPz = 200 : 1	+5 ± 3	218 ± 30
DOPC/DOPE with lipid : Mg-OCASPz = 100 : 1	+15 ± 5	190 ± 50
DOPA/DOPE	-65 ± 8	117 ± 5
DOPA/DOPE with lipid : Mg-OCASPz = 200 : 1	-50 ± 10	150 ± 20
DOPA/DOPE with lipid : Mg-OCASPz = 100 : 1	- 47 ± 10	150 ± 30

Table 1. Surface charge and mean diameter of different liposomes loaded with OCASPz porpyrin, bearing eight carboranyl cages. In these experiments total lipid content was kept constant at 4.10-2 mol/dm3

Results showed that the liposome insertion of Mg-OCASPz was obtained, notwithstanding its bulky structure. The general trend shows an increase in the mean size of liposomes, following Mg-OCASPz uptake. Preliminary SANS and SAXS measurements are in agreement with this observation.
Porphyins with different chemical structure (e.g. the free base) and different lateral chains are currently under study to obtain the highest loading ratio with minimal deformation of the host liposomes.

References

Ciani L., Ristori S., Salvati A., Calamai L., Martini G., *DOTAP/DOPE and DC-Chol/DOPE lipoplexes for gene delivery: zeta potential measurements and electron spin resonance spectra*, Biochim. Biophys. Acta 2004, 1664, 70-79.

Salvati A., Ciani L.,Ristori S., Martini G., Masi A., Arcangeli A., *Physical Chemical Characterization of Lipoplexes and their transfection efficiency as DNA carrier*, Biophys. Chem. 2005, 121, 21-29.
Luguya R.J., Fronczec F.R., Smith K.M. and Vicente M.G.H., *Carboranylcorroles*, Tetrahedron Letters 2005, 46, 5365-5368.

Gottumukkala V., Luguya R.J., Fronczec F.R. and Vicente M.G.H., *Synthesis and cellular studies of an octa-anionic 5,10,15,20-tetra[3,5-(nido-carboranylmethyl)phenyl]porphyrin (H2OCP) for application in BNCT*, Bioorganic and Medicinal Chemistry 2005, 13, 1633-1640.

2B – Direct ultraprecision manufacturing (MANUDIRECT)

P. Matteazzi, R. Trevisan

Aims

This project is funded by the European Commission' Sixth Framework Programme, under priority 3: Nanotechnology and nanosciences, knowledge-based multifunctional materials and new production processes and devices (NMP).
The manufacturing technologies to date available are limited in space resolution to some 200 μm in particular for bulk metallic components.
Direct, bottom up, fabrication, with much improved space resolution and increased productivity, could be made available.
The first level objective of the project is to provide the manufacturing industry with an entirely new platform for manufacturing, by the way of high productivity-high resolution direct, one step, laser sintering using metals and ceramic materials.
This leading objective represents a key factor for future competitivity of EU based manufacturing industry.
The project will develop the new Direct Manufacturing Platform by providing:

1) several powders grades developed for the technology, integrated in the micro/nanoscale;
2) highly localized powder and laser fluxes;
3) high productivity combined with spatial resolutions in the scale of 50 μm;
4) new methodologies for integrated materials and components design;
5) the developed platform to be available for exploitation within the EU manufacturing industry.

The impact of the project and its success will be horizontal to many sectors and vertical in engineering methodologies. Virtual engineering concepts and design will be translated into products without the need of prototyping steps.
Economic impact can be evaluated for some sectors, for example microengineering, biomedical and others. But the impact is much wider, because it open the way to direct macroscale fabrication.

Results

Work in progress (project started in September the 1st , 2006)

References

1. H. Becker; A. Ostendorf; P. Stippler; P. Matteazzi, Technology improvements for microscale laser sintering, OPTO-Ireland 2005 ,4–6 April 2005 Royal Dublin Society Dublin, Ireland.

2. H. Becker, A. Ostendorf, P. Stippler, P. Matteazzi, Direct laser micro sintering using nanophased microscale powders, Euro-u.Rapid 2005; 10-12 May 2005.; Leipzig, Germany

2B - Doped $LiMn_2O_4$ spinel and Jahn-Teller distortion

V. Massarotti, D. Capsoni, M. Bini

Aims

Study of the inhibition of the Jahn-Teller cooperative distortion in $LiMn_2O_4$ by doping with transition metal and Ga ions.
Characterization of the homogeneous dilution of doping ions and the valence state of Mn ion in the spinel lattice.
Determination of the charge distribution model related to the cationic substitution.

Results

The study of the occurrence near room temperature of Jahn-Teller (J-T) transition in $Li_{1.02}M_xMn_{1.98-x}O_4$ with $0.0<x<0.06$ and M=Ni, Co, Cr and Ti [22] and with Ga ions [32] is performed. The EPR spectra and magnetic susceptibility data are related to the valence state of M and Mn, and to the homogeneous distribution of the dopant. The J-T distortion, which is associated with a drop in conductivity with decreasing temperature is suppressed by substituting Mn with 3% Co^{3+} or Cr^{3+}, with 2% Ga^{3+} or by substituting an even smaller amount of Ni^{2+} (1%). It is found that the J-T distortion inhibition is possible when $r=|Mn^{4+}|/|Mn^{3+}| \geq 1.18$. Doping with the tetravalent cation Ti^{4+}, which always decreases the r value, does not suppress the J-T transition [22].
NMR measurements indicate that Ga^{3+} ion substitute chiefly in the octahedral sites, Mn^{4+} ions occupy regular and distorted octahedral sites. At the same time, the value of the lattice parameters remain unchanged. Mn^{2+} ions are present in the tetrahedral site and Li^+ increases in the octahedral sites as a consequence of Li-Mn/Ga inversion. Such mechanism increases the efficiency of J-T inhibition by Ga doping in comparison with transition cation having the same valence [32].
Al-doped lithium manganese spinel showed homogeneous distribution of Al^{3+} ions in both cationic sites by XRD, NMR and EPR analysis [41]. The J-T distortion is shifted towards lower temperature by very low Al-substitution.
The charge distribution in Mg-doped lithium manganese spinel is discussed and compared to those of the other M-doped samples: the sensitivity of the cationic sublattice in displaying electronic and magnetic changes is remarked [40].

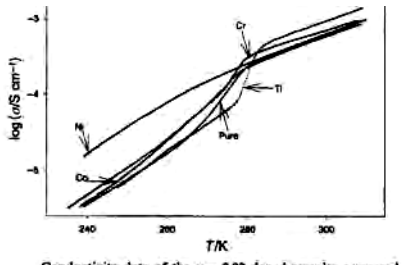

Conductivity data of the x = 0.02 doped samples compared with the pure spinel.

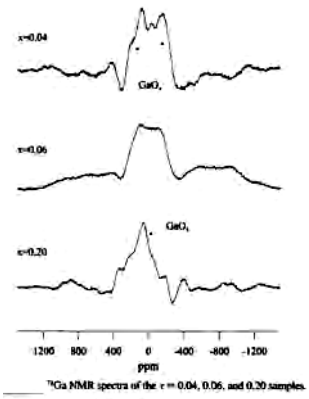

⁷¹Ga NMR spectra of the x = 0.04, 0.06, and 0.20 samples.

References

Capsoni, D., Bini, M., Chiodelli, G., Massarotti, V., Azzoni, C.B., Mozzati, M.C., Comin, A. *Inhibition of Jahn-Teller cooperative distortion in $LiMn_2O_4$ spinel by transition ions doping*. Physical Chemistry Chemical Physics 2001, 3, 2162.

Capsoni, D., Bini, M., Chiodelli, G., Mustarelli, P., Massarotti, V., Azzoni, C.B., Mozzati, M.C., Linati, L., *Inhibition of Jahn-Teller cooperative distortion in $LiMn_2O_4$ spinel by Ga^{3+} doping*. J. Phys. Chem. B 2002, **106**, 7432.

Capsoni, D., Bini, M., Chiodelli, G., Massarotti, V., Mustarelli, P., Linati, L., Mozzati, M.C., Azzoni, C.B. *Jahn-Teller transition in Al^{3+} doped $LiMn_2O_4$ spinel*. Solid State Communications 2003, **126**, 169.

Capsoni, D., Bini, M., Chiodelli, G., Massarotti, V., Mozzati, M.C., Azzoni, C.B. *Structural transition in Mg-doped $LiMn_2O_4$: a comparison with other M-doped Li-Mn spinels*. Solid State Communications 2003, **125**, 179.

2B - Formation of elemental metal powders by room-temperature mechanosynthesis

Riccardo Ricceri , Paolo Matteazzi

Aims

Mechanosynthesis has been shown to be very effective for the preparation of many metals with high melting points and ceramic materials (1,2). The aim of this work was to produce elemental metals like tungsten and boron using magnesium and metal oxides as starting materials by a mechanochemical process. Both these metals are presently produced by processes based on long and expensives routes: the reported process takes place ion both cases at room temperature, and is relatively unexpensive, requiring also a simple equipment in comparison with the industrial processes in use. The studied reactions are:

$B_2O_3 + 3\ Mg \rightarrow 2\ B + 3\ MgO$ and
$WO_3 + 3\ Mg \rightarrow W + 3\ MgO$

Mechanosynthesis reactions were performed in a vibratory ball mill (Spex 8000 Mixer Mill) using carbon steel balls as grinding media under argon atmosphere.

Results

Elemental boron powder of submicron size has been obtained with 82% yield after very short milling times (as short as 9 minutes): the powder was crystalline and of very high purity (>99%), after leaching with diluted HCl of the milled powders in order to remove the unwanted MgO product. In fig.1 the XRD spectrum of the purified elemental crystalline boron powder is reported. Elemental tungsten was obtained thanks to a similar procedure: submicron crystalline metallic tungsten powder was obtained after 8 minutes milling with 84% yield: a high purity metal powder (>99% also in this case) was obtained after leaching of the milled powders with diluted HCl in a similar way to that reported for boron powders. In fig.2 the XRD spectrum of the purified elemental crystalline tungsten powder is reported.

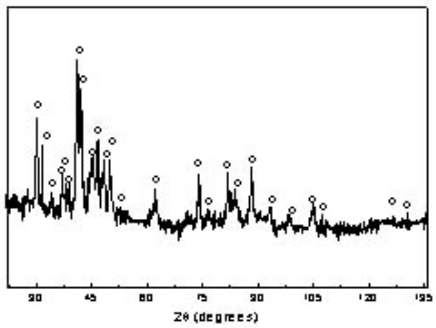

Fig.1 *XRD trace of purified boron. (o) metallic B.*

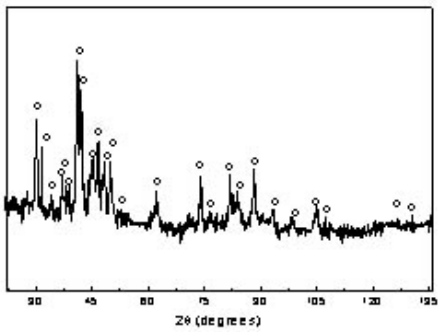

Fig.2 *XRD trace of purified tungsten. (*) metallic W.*

References

Matteazzi, G. Le Caër, *Mater. Sci. Eng.,* 1992, vol. A156, p.229.

P. Matteazzi, G. Le Caër, " *J. Am. Ceram. Soc.,* 1992, vol. 75, no.10, p.2749.

R.Ricceri, P.Matteazzi, "Formation of elemental boron by mechanosynthesis", *Int. J. Powder. Met.* (2003), in press.

R.Ricceri, P.Matteazzi, "A study of formation of nanometric W by Room temperature mechanosynthesis", *J. Alloys Comp.* (2003), in press.

2B - Interactions of Carboranyl-Nucleosides with *Stealth* Liposomes

*Simona Rossi (*in collaboration with *K. Edwards, Dept. of Physical Chemistry, Uppsala University, Sweden and R. F. Schinazi, Veterans Affairs Medical Center, Decatur, and Laboratory of Biochemical Pharmacology, Department of Pediatrics, Emory University School of Medicine, Atlanta, USA).*

Aims

The purpose of the present study is the characterization of pegilated liposomes containing hydrophobic carboranyl–derivatives. Cryo-transmission electron microscpopy (cryo-TEM) was used to visualize changes in aggregate structure caused by inclusion of the boronated compounds within bilayer. In addition, electron paramagnetic resonance (EPR) spectroscopy confirmed the effects of the boronated coumponds on lipid packing order and motional features of liposomal membrane.

Results

Liposomes are able to encapsulate many different classes of therapeutic agents within a biocompatible bilayer shell. Furthermore, liposomes mediate changes in drug pharmacokinetics and biodistribution that can decrease toxicity and drug metabolism and/or enhance cellular or tumor drug delivery. Liposomes used, or intended, for drug delivery are often sterically stabilized to extend their circulation time in the blood stream. Normally, the stabilization is achieved via incorporation of an appropriate amount of lipid with a covalently anchored homo-polymer, usually a poly(ethylene glycol) (PEG) chain.

Liposomes constituted by DSPC and cholesterol display long circulation times and also low leakage of many drugs, such as doxorubicin, encapsulated in their inner aqueous compartment. Interestingly, the presence of cholesterol appears to have a negative influence on the retention of certain more hydrophobic compounds [1] and formulations based on PEG-stabilized cholesterol-free DSPC liposomes may in these cases be preferable.

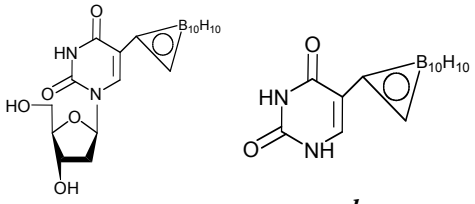

a ***b***

The compounds used in this study are b–5–*o*-carboranyl-2'-deoxyuridine (CDU, scheme *a*) and carboranyl-2'-uracyl (CU, scheme *b)*: non-toxic molecules designed for BNCT of brain tumors, which have been extensively studied for their cytotoxicity, anticancer, antiviral activity and cellular uptake[2].

The results show that the presence of CDU affects the integrity of the phospholipid membrane and may have a dramatic effect on the overall aggregate structure in the dispersions. The cryo-TEM investigations reveal that EPC:DSPE-PEG_{2000} (96:4 mol/mol) liposomes containing CDU are not stable over time but go through a slow transformation into thread-like micelles. In particular, time dependent structural rearrangements occur in the CDU-loaded pegilated EPC aggregates. After a few days of incubation at 25 °C large openings and membrane pores were evident in samples

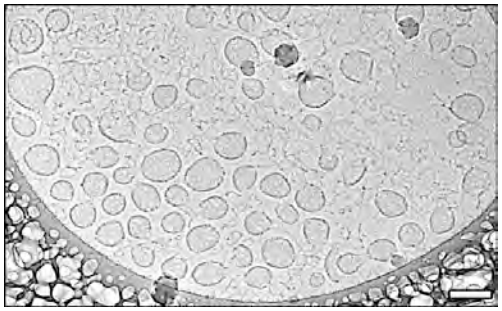

containing 10 to 43 mol% CDU. Eventually all liposomes developed perforated membranes and a significant proportion of the lipid material changed into networks of branched and entangled cylindrical micelles (Figure 1). The carborane-nucleoside is able to act as an edge-actant and stabilize the hydrophobic rim of membrane pores and open bilayer structures. Incorporation of CDU leads to severe packing disturbances and creation of highly unfavourable voids in the inner hydrophobic part of the membrane as indicated by ESR results. The lowered order parameter of the n-DSA suggests that the aggregates are less structured. It is interesting that 5-DSA is more sensitive to the variation of bilayer packing whereas the inner hydrophobic domain monitored by 16-DSA is the most affected in both ordering and segmental mobility. The deeper penetration of CDU into the membrane core has been also suggested by the occurrence of an additional spectral component at low temperature. The slow motion component could be connected with spin probes embedded in CDU rich domains, resembling restricted molecular motion, while the narrow component corresponds to the spin probes in the fluid phospholipid environment.

A fundamentally different structural behaviour was observed when CDU was included in PEG-stabilized membranes composed of the saturated phospholipid DSPC. In this case CDU promoted the formation of open bilayer discs, as well as small extremely angular bilayer structures (Figure 2a). Flat circular membrane discs are known to form in mixtures of DSPE-PEG_{2000} and DSPC. These discs are well described by an ideal disc model assuming partial component segregation, i.e. the PEG-lipids preferentially accumulate at the edge whereas the DSPC molecules make up the flat bulk of the disc. In pure DSPC/PEG-lipid mixtures bilayer discs do not become apparent, however, until PEG-lipid concentrations reach about 10 mol%. The PEG-lipid concentration was in the present study merely 4 mol%, and thus the presence of CDU helps shift the balance from closed liposomes to open circular discs. It is clear that bilayer structures with sharp angles and edges cannot form if all lipids exist in a true, well ordered gel-state. Instead, the accumulation of CDU helps create and stabilize such less well packed, more fluid-like, domains in the highly ordered gel-phase bilayer. The average size of membrane discs increased with aging: in contrast to fresh dispersions, were the disc-size rarely exceeded 150 nm, the 10 day old samples contained a population of flat discs with diameters of up to 400 nm. Cryo-TEM micrographs obtained 20 days later indicated that the discs continued to grow with time and eventually collapsed into large bilayer sheets (Figure 2b).

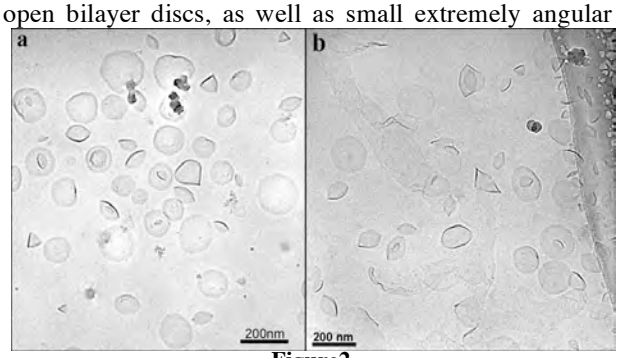

Figure2

References

Rossi, S.; Schinazi, R. F.; Martini, G. Biochim. Biophys. Acta 1712, 2005, 81-91.

Schinazi R.F., Goudgaon N.M., Fulcrand G., Kattan Y.E., Lesnikowsky Z., Ullas G., Moravek J., Liotta D.C., Cellular pharmacology and biological activity of 5-carboranyl-2'-deoxiuridine, Int. J. Radiat. Oncol. Biol. Phys. 28 (5), 1994, 1113-1120.

2B - Magnetic investigations in Mn substituted titanates

V. Massarotti, D. Capsoni, M. Bini

Aims

EPR determination of Mn oxidation state
XRD characterization of perovskitic solid solutions
Microstructure and grain boundary study of substituted $SrTiO_3$

Results

Electron paramagnetic resonance (EPR) and static magnetization data on Mn substituted (up to 3 mol%) strontium titanate samples are used to determine the Mn oxidation states: Mn^{4+} and Mn^{2+} states are observed. The behavior of their intensity vs temperature is also determined and suggests the presence of antiferromagnetic interactions in heavily Mn doped grain boundaries. X-ray diffraction analysis shows two coexisting perovskite-type phases, whose abundance depends on the Mn content [14].

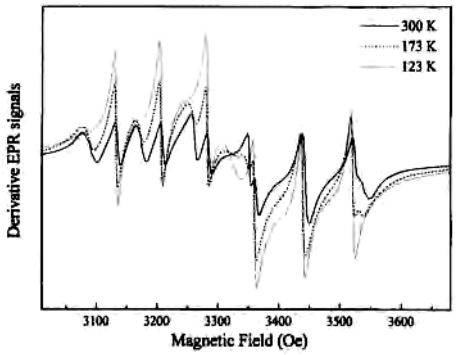

Temperature dependence of derivative EPR signal of the 2.5 mol% Mn sample.

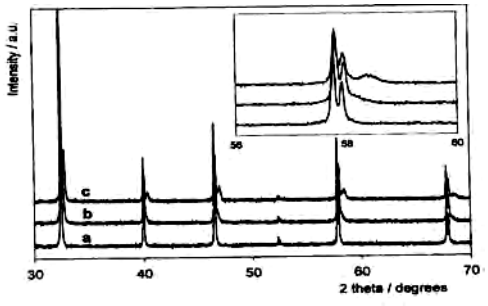

XRD patterns of samples (a) 1 mol%Mn, (b) 2.5 mol%Mn and (c) 3 mol% Mn

When La and Mn are simultaneously substituted (up to 10 mol%) in $SrTiO_3$ the EPR signals indicate the nearly complete stabilization of the Mn^{3+} oxidation state. X-ray diffraction analysis shows in each sample a single cubic perovskite phase with lattice parameter depending on the degree of substitution.[15]

Electron paramagnetic resonance (EPR) on polycrystalline $CaCu_3Ti_4O_{12}$ have been performed and are discussed within a crystal-field approach. A symmetric signal centred at g=2.15 is observed for T>25 K, with no evidence of hyperfine structure. At this temperature an antiferromagnetic transition is observed by static magnetization measurements.

V, Cr, Mn and La substituted samples are also investigated to understand the nature of the observed paramagnetic centre. A strong copper-hole delocalization may justify the EPR response [42].

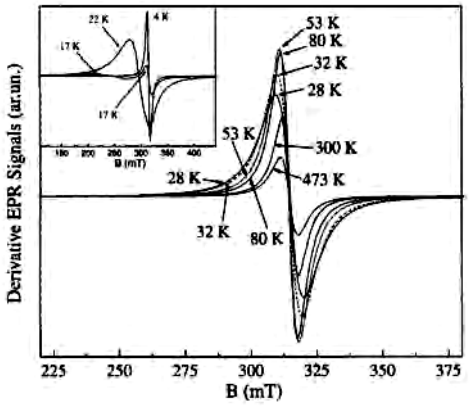

EPR spectra of the pure-a sample for $T > T_N$. The inset shows EPR spectra at 22 and 17 K (amplified by a factor 10) and at 4 K (amplified by a factor 2).

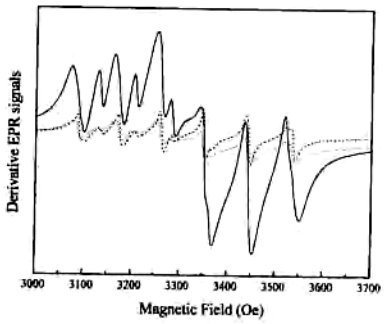

Structured part of the EPR signals at 300 K of 5 mol% (dashed line) and 10 mol% La,Mn samples (dotted line) compared with 3 mol% Mn:$SrTiO_3$ (solid line).

References

Azzoni C.B., Mozzati M.C., Paleari A., Massarotti V., Bini M., Capsoni D., *Magnetic evidence of different environments of manganese ions in Mn-substituted strontium titanate,* Solid State Commun. 2000, **114**, 617.

Azzoni C.B., Mozzati M. C., Galinetto P., Paleari A., Massarotti V., Bini M., Capsoni D., *Magnetic investigation of Mn ions in La,Mn:$SrTiO_3$.,* Solid State Commun. 2000, **116**, 303.

Mozzati M. C., Azzoni C. B., Capsoni D., Bini M., Massarotti V., *Electron paramagneticresonance investigation of polycrystalline $CaCu_3Ti_4O_{12}$.,* J. Phys.: Condens. Matter 2003, **15**, 7365.

2B - Microscale fabrication of graded materials components

P. Matteazzi, R. Rolli, in collaboration with MBN (I), INASCO (EL), Ltm (F), LZH (D), SIEMENS (D), TIL (UK), IMNR (RO)

Aims

Scientific research objectives: 1) realize nanophased powders materials (3-10μm); 2) conceive a laser/powder head being capable of spatial resolution of better than 50 μm; 3) microscale fabrication of materials with gradients resolution in the 10-50 μm range. Technological research objectives: 1) micromaking machine for graded materials, with a productivity in the order of 0.1 g/s; 2) fully dense micromade components with graded materials (tolerances within 10 μm). Technical achievements: 1) micromade recess tools for the aeronautics fasteners industry, with improved wear resistance and service life; 2) micromade tools inserts for plastics injection molding, with graded wear resistance, thermal conductivity and cooling channels; 3) process conditions of Micromaking for laser sintering of nanophased powders.

Results

The activity is divided into different parts to develop the small scale sintering technology employing a fusion produced by the laser beam with the coaxial powder injection into the action zone. Another large part of the activity is the design of materials for some demonstrative applications and the development of the suitable powder.

The Micromaking machine (see *Fig.1*) has been assembled and some nanophased powders have been tested. One of the main objectives has been reached: starting from laser tracks (2 Dimensional) now it is possible to make objects 3D with a spatial resolution of 50 μm (see *Fig. 2-3-4*) using the Micromaking machine.

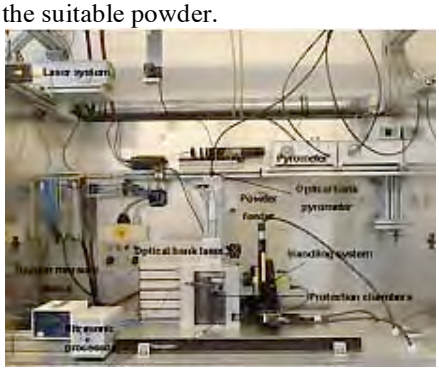

Fig.1 Micromaking machine prototype

In order to obtain a powder best suited for Micromaking application the air-classifier (already designed and assembled) has been equipped with Jet-mill system (low energy milling): it permits the control of sizes distribution of particles (range 3-10 μm) and their shape (more rounded to obtain improvement of flowability).

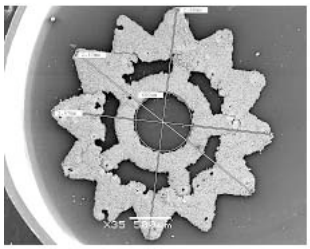

Fig.2 Gear: SEM image

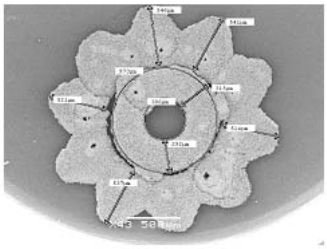

Fig.3 Gear: SEM image

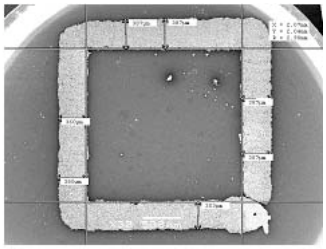

Fig.4 Frame: SEM image

2B – Nanosinter

P. Matteazzi, R. Rolli, C. Zambon

Aims

"Nanosinter" is an industrial research project, financed by Veneto Region. It concerns the manufacturing of mechanical components (made by innovative "nano-structured Titanium based alloys"), through the development of the Sintering process under controlled atmosphere and conditions.
The aim of the research activity regards the development of the Sintering technology in order to achieve the possibility to produce (on industrial scale) the sintered nanostructured Titanium components that satisfy the specific market requirements.

The main target of the plan is to carry out some demonstrative examples of mechanical components. This will allow to demonstrate also in Veneto the existence and the availability of vanguard synthesis technologies and high innovative and competitive nano-materials, like the "nanostructured Titanium alloys",
Therefore, the project is focused on the introduction in Veneto of this new forming technology (hot sintering) putting in evidence the market potentialities of these new nano-materials in order to increase the products quality and the industrial competitive level of Veneto manufacture system.
The solutions proposed may have many final applications in many sectors of the Veneto industry. Among them we have considered: glasses industry, sport equipment sector, the knives field, the automotive and the biomedical ones, etc.
The Project aims are:

Development of a synthesis technology: hot sintering under controlled atmosphere.
Development of nanostructured Titanium alloys with enhanced performances.
Diffusion on Regional (Veneto), National, and European level, of the technology and of the innovative nano-materials employed and developed.

Results

The NANOSINTER project allowed, through the research activity performed, to achieve various results that can be summarised as it follows:

- Development of a new process of synthesis (titanium sintering) for the realization of mechanical components –for the Veneto industry –
- Use of innovative materials for their manufacture –nanostructured titanium alloys – and demonstration of their possible employment inside to the traditional Veneto industry fields;
- Attainment of components with mechanical property suitable to be employed in their reference fields;
- Reduction of materials and reduction of energy demand for their manufacture;
- Reduction of the unit costs of the components respect to the traditional manufacturing process;
- Wide diffusion of knowledge and technologies – at National (Veneto in particular) and International level.

These results are emerged thanks to a careful evaluation of all the aspects belonging the developed processes - performance of materials achieved, economical and energetic evaluations – and the activities and experiences performed within the project.

References

Mechanical alloying of the Ti-Al system in atmosphere of hydrogen and argon, , Akito Takasaki and yoshio Furuya, Nanostructured Materials, vol. 11, No. 8 pp.1205-1207, 1999

Thermal stability of Hydroxylapatite -Titanium and hydroxylapatite-Titania Composites, Celaletdin Ergun, Robert H. Doremus, Turkish J. Eng. Sci. 27 (2003) 423-429

Production and characterization of fully dense hydrogenated γ-TiAl by blended elemental approach, J.I.Qazi, J. Rahim, O.N. Senkov, F.H. Froes, M.L. Ovecoglu and A. Genc.,

2B - New insights into the magnetic properties of the $Ca_2Fe_2O_5$ ferrite

V. Massarotti, D. Capsoni, M. Bini

Aims

Study the changes of $Ca_2Fe_2O_5$ (C2F) magnetic properties when Ca^{2+} or Fe^{3+} ions are substituted with small amount of isovalent and aliovalent ions (Mg^{2+}, Al^{3+}, Ti^{4+}, Ge^{4+}).
Clarify the origin of the weak ferromagnetic component reported in literature from single crystal measurements.
Ascertain the influence of low amount of Fe_3O_4, detected by XRD in all the samples, on the C2F magnetic behavior.

Results

The presence of spurious ferrimagnetic Fe_3O_4 phase strongly influences the magnetization data and the related hysteresis curves show a great resemblance to those obtained from the undoped single crystals described in literature. Taking also into account that an accurate sample characterization of the above mentioned samples is really absent, a combined use of spectroscopic (EPR), structural (XRPD), magnetic (SQUID magnetometry) and microscopic (Scanning Electron Microscopy, SEM) techniques has been carried out to get new insights into the origin of the discussed ferromagnetic component.

2B – Produzione e Stoccaggio di Idrogeno in Nanomateriali (NANOSTORE)

P.Matteazzi, A.Colella, R.Rolli, F.De Ros,
in collaboration with
MBN (I), Università di Pavia (I), Università di Bergamo (I)

Aims

The goal of this project is to work out the bottlenecks hampering hydrogen production (supply) and solid storage as fuel for a widespread mobile use. An innovative approach to this field has been developed through the following steps:

- improvement of the efficiency of common industrial electrolyzers/fuel cells in order to reduce energy waste and commercial costs and development of a small cell/ demonstrative prototype electrolyzer

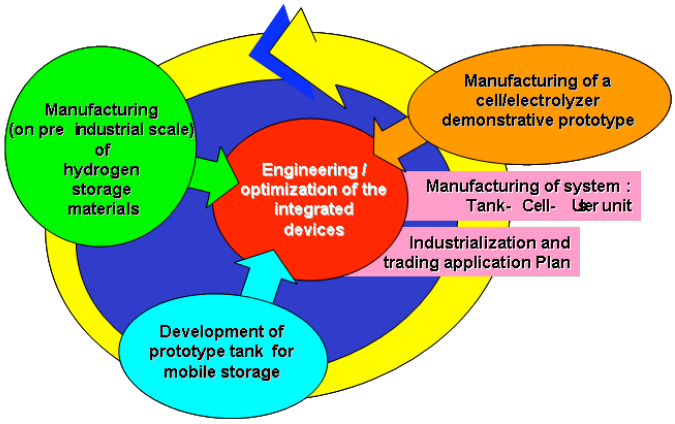

- design and development, through combinatory methods, of innovative nanomaterials for solid hydrogen storage synthesized by mechano-chemical processing (high energy milling) and manufacture of a prototype tank

- manufacture and engineering of a demonstrative device for mobile use which integrates both the tank and the cell prototypes. The ultimate purpose will be to optimize the device for an industrialization and trading application plan

Results and project activities

During the 1st year of NANOSTORE the activities are being carried out in the first two work packages regarding both the Hydrogen production and Nanomaterials for Hydrogen storage.

Hydrogen production

The research group of the "Università di Bergamo" has been developing original methods of modulation techniques of pressure and voltage which permit:

- to improve electrolysis in alkaline ambient
- to better understand the mechanisms which contribute to the electric losses in the cell

The manufacturing and the optimization of new electrodes, in collaboration with Gaskatel, is the key to enhance the electrolytic process in the WP continuation.

Nanomaterial for Hydrogen storage

The purpose of this WP is to design, produce and test 1000 different materials; therefore, an experimental design plan is needed. The innovative work methodology is based on the optimization of materials enhancing their performance through a consecutive step experimental plan.

During the first screening step, a wide range of materials were planned among the following classes:

- Metal hydrides (Mg alloys, bcc alloys, Ti alloys)
- Complex hydrides (Alanates, Borohydrides)
- Ammides
- PDMH (Polymer dispersed metal hydrides)

Nanomaterials compounds have been designed and produced by modifying the composition and process parameters in order to change their thermodynamic and kinetic behavior in the hydrogenation reaction and to develop innovative synthesis paths.

In order to tailor materials suitable for a hydrogen mobile storage, possessing properties well matched with European SRA targets, the following selection criteria were determinated:

- good reversibility;
- low release temperature with suitable kinetic at atmospheric pressure;
- fast absorption kinetic at suitable temperature;
- material cost and H_2 storage capacity

In order to check rapidly (1000 specimen are scheduled) if the materials possess the required properties to meet these criteria, a new instrumental device has been developed to get a multiple activation system. Moreover, suitable methodologies of characterization have been developed such as temperature scan dehydrogenation and hydrogenation (fig 1).

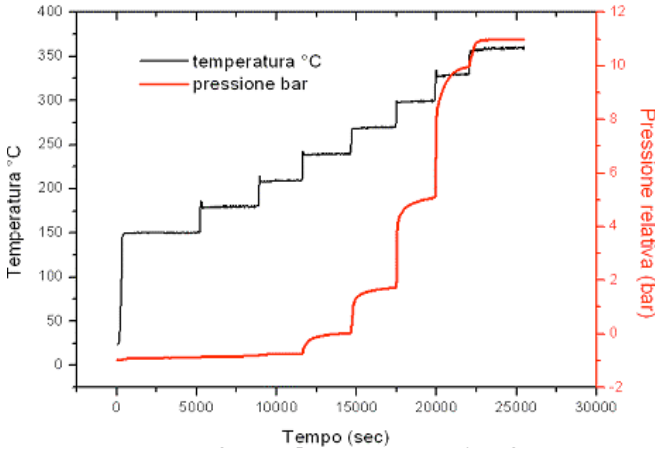

In the following steps, experiments are planned through a statistical method (Taguchi approach) which allows to significantly reduce the number of trials in order to individuate how parameter change affects material behavior. In this way, data collected from the tests are being analyzed with combinatory methods and only materials which meet the targets will be subsequently investigated.

Although the project is at the beginning stage, a range of good results seem to stand out which represents an encouraging starting point for further developments. A wide series of results data obtained will be presented during the CSGI congress.

References

L. Zaluski, A Zaluska, J.O Strom-Olsen , *Hydrogenation properties of complex alkali metal hydrides fabricated by mechano-chemical synthesis,* J. of All. and Comp. 290 (1999) 71-78

J.L Bobet, E Grigorova, *Hydrogen sorption properties of graphite-modified magnesium nanocomposites prepared by ball-milling,* J. All. and Comp. 366 (2004)298-302

Borislav Bogdanovic, Gary Sandroc, *Catalyzed Complex Metal Hydrides,* MRS Bullettin September 2002, 712-716

Douglas C. Montgomery *Design and Analysis of Experiments*. John Wiley2001

2B - Proprietà strutturali e di trasporto del vanadato Li_3VO_4 puro e drogato e analoghi con Zn e Mg (Transport and structural properties of pure and doped Li_3VO_4 vanadate and Zn, Mg analogous compounds)

V. Massarotti, D. Capsoni, M. Bini

Aims

- Investigation of the dopant influence on the transport and structural properties of lithium ortovanadate
- Determination of cation distribution on tetrahedral and octahedral sites by the combined use of different structural and spectroscopic techniques.

Results

The Lithium Vanadates are materials suitable for applications in the fields of optics, electrochemistry and electronics. For what concerns the transport properties, these compounds behave as solid ionic conductors due to the high mobility of lithium ions in the structure.

The effects of 5 and 10% chromium additions on the transport and structural properties of Li_3VO_4 compounds. The Cr-substitution is easily obtained without impurity phases and does not affect the room- and high-temperature host crystal structure, as evidenced by X-ray powder diffraction and Micro Raman analysis.

The EPR signals are interpreted in terms of quantified amounts of Cr ions in 5+ and 3+ valence states. Suitable ^{7}Li and ^{51}V MAS-NMR spectra simulations agree with the EPR results about the relative amount of Cr^{5+} and Cr^{3+} ions substituted in V^{5+}- and Li^{+}-sites respectively. The Cr^{3+} presence on Li-site, also suggested by Raman results and Rietveld refinements, requires Li-vacancies to maintain the charge neutrality. The p-type conductivity suggested by the positive thermoelectric power coefficients, significantly increases by the cation doping up to an order of magnitude.

The Mg and Zn substitution leads to two different crystallographic structures with respect to Li_3VO_4. The room temperature cation occupancy in $LiMgVO_4$ and $LiZnVO_4$ crystallographic sites is obtained by means of the combined use of X-ray powder diffraction (XRPD), ^{7}Li and ^{51}V MAS-NMR and micro-Raman measurements.
In $LiMgVO_4$ Cmcm orthorhombic structure the 4*c* (C_{2v} symmetry) tetrahedral vanadium site is fully ordered; on the contrary, the Li 4*c* tetrahedral site and the 4*b* (C_{2h} symmetry) Mg octahedral site display about 22% of reciprocal cationic exchange.
Higher cationic disorder is observed in $LiZnVO_4$: the three cations can distribute on the three tetrahedral and distinct sites of the R-3 structure. XRPD and MAS-NMR analysis results highly agree for what concerns vanadium ion distribution on the three cationic sites (about 25%, 26% and 47%). From the full profile fitting of XRPD patterns with the Rietveld method it is also obtained that Li^{+} displays a slight preferred occupation of T1 position (~ 55%) and Zn^{2+} of T2 position (~46%). The vibrational spectra of the two compounds are characterized by different peak position and broadening of the Raman modes reflecting the cation distribution and the local vibrational units distortion. A comparison is also made with recent Raman results on Li_3VO_4.

High temperature XRPD measurements rule out possible structural transitions up to 673 K for both compounds.

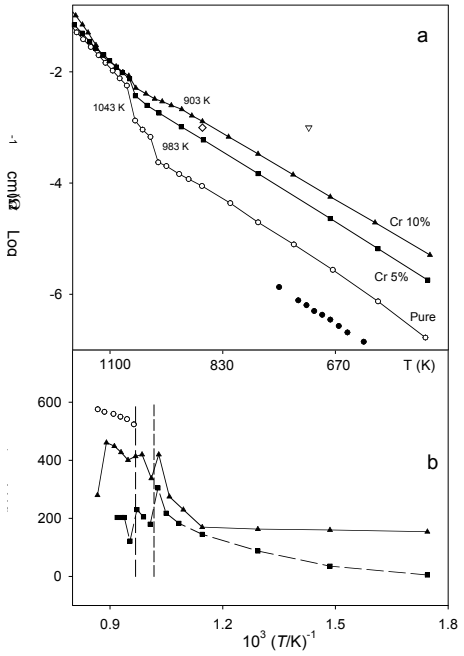

a) Arrhenius plots and b) thermoelectric power (a) of pure and doped samples. In a) down triangle, open diamond and full circle (single crystal) are literature data.

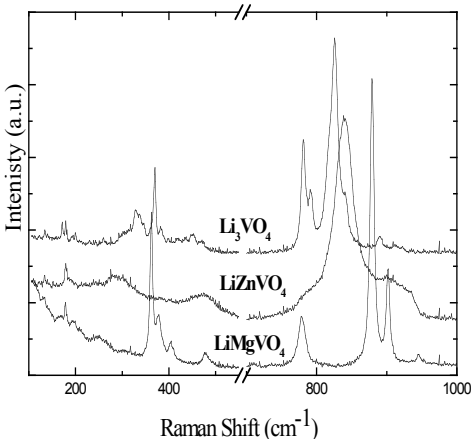

Comparison between the Raman spectra of $LiMgVO_4$ and $LiZnVO_4$ with the spectrum of Li_3VO_4 compound[17]. All the spectra have been collected in the same experimental conditions.

References

Massarotti, V., Capsoni, D., Bini, M., Mustarelli, P., Chiodelli, G., Azzoni, C.B., Galinetto, P., Mozzati M.C. *Transport and structural properties of pure and Cr doped Li_3VO_4.* J. Phys. Chem. B 2005, 109, 14845.

Capsoni, D., Bini, M., Massarotti, V., Mustarelli, P., Belotti, F., Galinetto, P. *Cation distribution in $LiMgVO_4$ and $LiZnVO_4$: structural and spectroscopic study.* J. Phys. Chem. B 2006, 110**.**

2B – Reactivity and Structure of Inorganic Compounds

V. Berbenni, G. Bruni, P. Cofrancesco, A. Marini, C. Milanese

Aims

Solid state synthesis of ternary oxides for energetic uses.
Study of the effect of mechanical activation by high energy milling on solid state reactions.

Results

The solid state reactions occurring in the mechanically activated systems:

a. $PbCO_3$-TiO_2;
b. Li_2CO_3-Ga_2O_3;
c. Co-Li_2CO_3;
d. $CaCO_3$-$MnCO_3$;
e. $ZnC_2O_4 \cdot 1.8H_2O$-$2FeC_2O_4 \cdot 2H_2O$ and $ZnC_2O_4 \cdot 1.8H_2O$-$Fe_2(C_2O_4)_3 \cdot 6H_2O$.

have been studied using thermal analysis (TGA, DSC), X-ray powder diffraction (XRPD), scanning electron microscopy (SEM) and surface area determination (BET) .

a. $PbCO_3$-TiO_2 system

Lead Titanate, $PbTiO_3$ is a perovskite-type ferroelectric material with noticeable dielectric, pyroelectric and piezoelectric properties. It is stable at room temperature as tetragonal phase, that transforms to a cubic phase at T ≈ 490°C (temperature of ferroelectric anomaly). Synthesis of $PbTiO_3$ both in form of powder and as thin film has been accomplished by different routes such as sol-gel and hydrothermal process. Nanosized lead titanate powders have also been obtained by calcinating a polymeric precursor prepared by the Pechini process and via mechanochemical route starting from PbO and TiO_2.
We prepared $PbTiO_3$ powders by mild annealing (2 h at 600°C) of $PbCO_3$:TiO_2 1:1 mixtures previously subjected to mechanical activation, (a thermal treatment of about 12 h at T > 850°C was needed to obtain $PbTiO_3$ in the absence of mechanical activation).
TG/DSC measurements (Figure 1) showed that the temperature range of lead carbonate decomposition didn't depend from mechanical activation that, on the contrary, sensibly affected the energetics of $PbTiO_3$ formation: indeed the milled mixtures showed an exothermic peak that was related to the formation of the product from the two nascent oxides PbO and TiO_2.

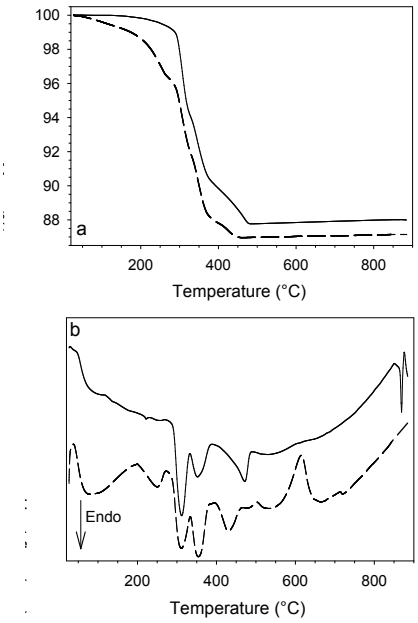

Figure 1 - TG (a) and DSC (b) curves obtained under nitrogen at 5K/min on $PbCO_3$ -TiO_2 mixtures: physical mixtures (full line); milled mixtures (dashed line).

Furthermore, SEM micrographs and the XRPD line broadening allowed to conclude that $PbTiO_3$ powders obtained from activated mixtures are of nanometric size.

$PbTi_3O_7$ has been prepared starting from mechanically activated $PbCO_3$ - $3TiO_2$ mixtures by 1 h annealing at 850°C (a thermal treatment as long as 100 h at 800°C was required to yield this compound from unmilled mixtures). The DSC analysis of the milled mixture suggested that the reaction proceeded in two steps: formation of $PbTiO_3$ and reaction of this compound with excess TiO_2 to yield $PbTi_3O_7$.

b. Li_2CO_3 - Ga_2O_3 system

In recent years lithium gallate ($LiGaO_2$) has attracted interest as substrate material for the growth of GaN thin films and as potential alternative matrix material for electrolyte support in molten carbonate fuel cells. On the other hand, the compound $LiGa_5O_8$ has been widely studied to test its viability as tunable laser system, both in pure form and doped with Ni^{2+}, Mn^{2+}, Co^{2+} and Fe^{3+} ions. The principal use of these gallates is in gas-discharge lamps for document reproduction. $LiGa_5O_8$ can be prepared by firing at 1000°C a stoichiometric mixture of lithium carbonate and gallium oxide, whereas $LiGaO_2$ has been synthesized by heating an equimolar mixture of the same reactants between 600 and 1500°C.

We synthesized $LiGaO_2$ and $LiGa_5O_8$ by solid-state reaction between Li_2CO_3 and Ga_2O_3 starting either from physical mixtures and from mixtures mechanically activated by high energy milling. By combined XRPD and TG evidences, it has been demonstrated that the milling of a 1:5 (molar ratio) mixture of Li_2CO_3–Ga_2O_3 results in the partial formation of lithium gallate $LiGa_5O_8$ at room temperature (Figure 2). The synthesis of this phase was completed after an annealing of 24h at 630°C.

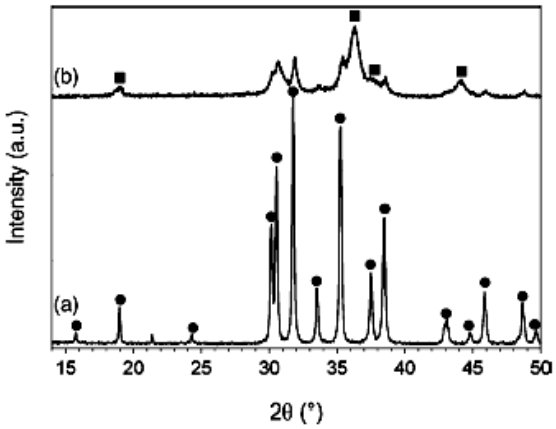

Figure 2: XRPD patterns of 1:5 (molar ratio) Li_2CO_3–Ga_2O_3 mixtures: (a) physical mixture; (b) mechanically activated mixture. Filled circles: Ga_2O_3; filled squares: $LiGa_5O_8$.

On the other hand, when synthesis was performed starting from physical mixtures, $LiGaO_2$ formed as an intermediate compound and pure $LiGa_5O_8$ was obtained only after a thermal treatment of 24h at 850°C. Another effect of the milling was the significantly lower crystal size (6–9 nm) of the product with respect to that of the powders synthesized from the physical mixture (~54 nm).

In the case of the 1:1 (molar ratio) mixture, the influence of the mechanical treatment was less evident either on the temperature of solid-state synthesis and on the crystal size of the product. Pure $LiGaO_2$ was obtained in both case after annealing at 830°C. Furthermore, no evidence was obtained of formation of $LiGaO_2$ and/or $LiGa_5O_8$ at room temperature during milling.

c. Co - Li_2CO_3 system

Lithium cobalt oxide (Lithium cobaltite, $LiCoO_2$) is attracting interest for possible applications as cathode material for lithium batteries due to its high specific capacity, low self discharge and long operating life. Furthermore, $LiCoO_2$ has been recently introduced into Molten Carbonate Fuel Cells (MCFC) to act as a protective layer of the cathode constituted by $Li_xNi_{1-x}O$ against dissolution in the molten carbonate electrolyte. At first, lithium cobaltite has been prepared by solid state reaction at temperatures of ~ 850 - 900°C. Then, in order to obtain ultrafine $LiCoO_2$ powders, a wide range of synthetic routes have been applied such as sol-gel, freeze–drying, molten salts synthesis and hydrothermal synthesis. Furthermore, mechanical activation (MA) combined with thermal treatment at moderate temperatures has been used to prepare highly dispersed $LiCoO_2$ starting from LiOH + CoOOH and LiOH + $Co(OH)_2$ mixtures.

We synthesized stoichiometric $LiCoO_2$ starting from both physical and mechanically activated mixtures in the solid state system Co-0.5Li_2CO_3.

From TG and XRPD measurements, it has been demonstrated that the steps taking place during heating from room temperature to 850°C are the oxidation of Co to Co_3O_4, and the decomposition of Li_2CO_3. This last one is "driven" by the presence of nascent Co_3O_4 and leads to the formation of $LiCoO_2$.

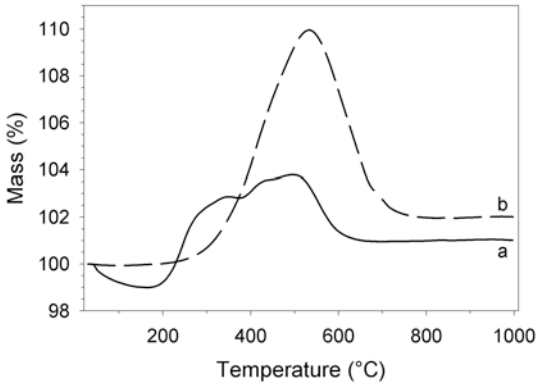

Figure 3: TG curves recorded in air at 1 K/min on a Co-0.5 Li_2CO_3 milled mixture (a, full line) and on a physical mixture (b, dashed line).

When starting from milled mixtures, all the processes began and ended at temperatures about 120°C lower than those recorded for physical mixtures and the solid state reaction was already completed at 680°C. Nanometric powders of pure $LiCoO_2$ were obtained from milled mixtures after a thermal treatment of 48h at a temperature as low as 400°C, while starting from physical mixtures an annealing of 12h at 680°C was needed to give micrometric particles.

a

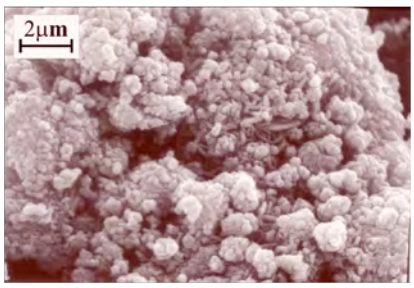

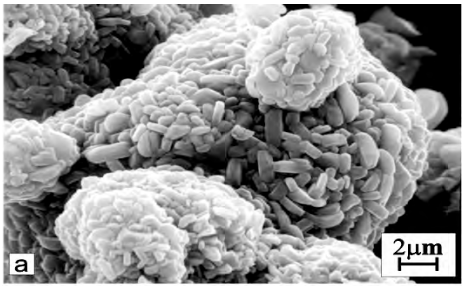

Figure 4: SEM micrographs of Co-0.5 Li_2CO_3 mixtures. (a) milled mixtures annealed 48h at 400°C. (b) physical mixtures annealed 12h at 680°C.

d. $CaCO_3$ - $MnCO_3$ system

$CaMnO_3$ is the end member of the perovskite related mixed oxides $Ca_{1-x}F^{III}_xMnO_3$ where F^{III} is a trivalent cation that substitutes for Ca in the perovskite lattice so that Mn is stabilized into the mixed valence status (Mn^{III} / Mn^{IV}). Such a status is also exhibited by the non stoichiometric calcium manganite ($CaMnO_{3-x}$) with oxygen vacancies that significantly affect the magnetic and electronic properties of the compound. Indeed the stoichiometric oxide $CaMnO_3$ has an orthorhombic perovskite structure and it is a G-type antiferromagnetic insulator with a Neel temperature of 120K. With decreasing oxygen content, the $CaMnO_{3-x}$ phase shows stronger ferromagnetic interactions with a slight increase in Neel temperature and an increase in conductivity in that it becomes a n-type semiconductor. The synthesis of $CaMnO_{3-x}$ oxide was usually performed by solid state reaction involving high temperature and long reaction time (1400°C, 15h), so leading to samples with large particle size.

To try and solve this problem different synthetic routes have been devised such as, for example, the thermal decomposition of metallo-organic precursors (Ca, Mn malonates). Other Authors have simply modified the solid state route by using as precursor the solid solution $CaCO_3$-$MnCO_3$ prepared by wet methods or by using the Pechini process.

We describe a solid state synthesis of $CaMnO_3$ starting from equimolecular mixtures $CaCO_3$:$MnCO_3$ subjected to mechanical activation. During milling, a $CaCO_3$ - $MnCO_3$ solid solution of nanometric particle size formed and this phase seems a well suited precursor to yield pure nanosized $CaMnO_3$ at around 900°C.

By milling up to 25h, a mixture $CaCO_3$-0.5 Mn_2O_3 was the intermediate phase obtained at ≈560°C. With longer milling times, the reaction course was different: both decomposition of $MnCO_3$ to MnO_2 and ~60% $CaCO_3$ to CaO occurred within 660°C. Non stoichiometric $CaMnO_{3-x}$ formed up to 950°C. By increasing milling time an increasing share of $MnCO_3$ decomposes to give Mn_3O_4 during milling.

It is to point out that no complete formation of $CaMnO_3$ occurred by annealing samples of physical mixture for times up to 48h at 1200°C.

e. $ZnC_2O_4 \cdot 1.8H_2O$-$2FeC_2O_4 \cdot 2H_2O$ and $ZnC_2O_4 \cdot 1.8H_2O$-$Fe_2(C_2O_4)_3 \cdot 6H_2O$ systems

$ZnFe_2O_4$ crystallizes with a spinel lattice with Zn^{2+} in tetrahedral interstices and Fe^{3+} in the octahedral ones (direct spinel structure). In fact it is known that the distribution of the cations between the two types of site changes as the crystallite size decreases and that this fact leads to the phenomenon of superparamagnetism on heating. Several synthetic routes have been proposed to prepare $ZnFe_2O_4$ and this work reports a synthesis of nanometric $ZnFe_2O_4$ from a combination of mechanical activation of solid mixtures of metal oxalates [Zinc Oxalate and Fe(II) or Fe(III) oxalates] followed by annealing under air flow. By combination of TG/DSC measurements and XRPD it has been shown that, independently on the iron precursor selection, the mechanical activation of the starting systems results in the formation of nanocrystalline product within 500°C, while only a mixture of the constituents oxides (ZnO and Fe_2O_3) is obtained when starting from the physical mixtures. Furthermore, in the case of the activated mixtures, the formation enthalpy of $ZnFe_2O_4$ has been estimated.

The analysis of the XRPD patterns of the different mixtures after they have been thermally treated in oven showed that a mild annealing in air (1h at 500°C) of the mechanically activated mixtures succeeded in obtaining nanocrystalline $ZnFe_2O_4$. On the contrary prolonged annealing at 1000°C is needed to obtain microcrystalline $ZnFe_2O_4$ when starting from non activated mixtures.

Moreover the SEM observations and the specific surface area measurements showed that the mechanical activation results in a microstructure that significantly differs from that of the physical mixtures particularly in the case of the Fe(III)-based mixture. Finally the determination of the magnetic properties demonstrated that the subsequent annealing of the milled mixtures leads to a sensible enhancement of the "pinning" of the magnetic domains.

References

Berbenni V., Milanese C., Marini A., Welham N.J. – Effect of mechanical activation on the formation of lead titanates from $PbCO_3$ – TiO_2 mixtures. *Journal of Materials Science* **2006**, 41 (6), 1739-1744.

Berbenni V., Milanese C., Bruni G., Marini A. – Mechanochemically assisted solid-state synthesis of lithium gallates ($LiGa_5O_8$ and $LiGaO_2$). Materials Chemistry and Physics **2005**, 91(1), 180-184.

Berbenni V., Milanese C., Bruni G., Marini A. – Solid state synthesis of stoichiometric $LiCoO_2$ from mechanically activated Co-Li_2CO_3 mixtures. *Materials Chemistry and Physics* **2005**, 91 (1), 180-184.

Berbenni V., Milanese C., Bruni G., Cofrancesco P., Marini A. – Solid state synthesis of $CaMnO_3$ from $CaCO_3$-$MnCO_3$ mixtures by mechanical energy. *Z. Naturforsch. B* **2006**, 61 (3), 281-286.

Berbenni V., Milanese C., Bruni G., Marini A., Pallecchi I. – Synthesis and Magnetic Properties of $ZnFe_2O_4$ obtained by mechanochemically assisted low-temperature annealing of mixtures of Zn and Fe Oxalates. *Thermochimica Acta* **2006**, 447, 184.

2B - Stability and properties of spinel related phases

V. Massarotti, D. Capsoni, M. Bini et al.

Aims

Identification of the Mn_5O_8 Raman spectrum
Investigation on structural transformation thermally induced in Mn_5O_8 lattice by laser beam

Results

The Raman spectrum of the metastable Mn_5O_8 phase, obtained from slow oxidation of Mn_3O_4 at low temperature, is analyzed for the first time and the thermal stability is monitored by the changes in Raman spectra due to laser induced thermal treatments. A structural transformation toward the spinel phase Mn_3O_4 is observed at T>1000 K. Other Mn oxides, characterized by intermediate Mn oxidation states, are not detected below o during the transformation. A compositional model of the sample grains is also proposed by comparing Raman data with X-ray diffraction and scanning electron microscopy measurements [10].

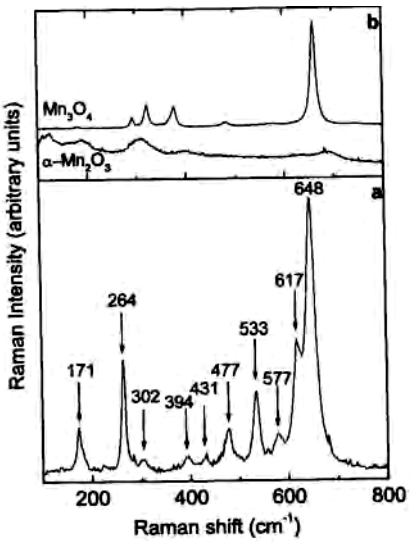

(a) Raman spectrum of a representative sample attributed to Mn_5O_8 phase. (b) Raman spectra of the pure Mn_3O_4 and α-Mn_2O_3 reference samples. Spectra have been collected at about 800 K.

References

Azzoni C.B., Mozzati M.C., Galinetto P., Paleari A., Massarotti V., Capsoni D., Bini M. , *Thermal stability and structural transition of metastable Mn_5O_8: in situ micro-Raman study*. Solid State Commun. 1999, 112, 375.

2B - Structural and spectroscopic investigation of pure and doped $Ba_6Zr_2Ta_8O_{30}$ tungsten bronze

V. Massarotti, D. Capsoni, M. Bini

Aims

Study of the cation doping influence on ferroelectric and structural properties of $Ba_6Zr_2Ta_8O_{30}$ (BZT)

Results

Members of this family display interesting ferroelectric features at room temperature. These materials can find applications in microelectronic and electro-optical devices. A doping of 3% on Zr site by transition cations (Fe, Mn, Cr, Co and Ni) can influence the physical and chemical properties of BZT. Structural and spectroscopic investigations were carried out with XRPD, EPR and micro-Raman measurements and results were compared with those obtained on the analogous $Ba_6Ti_2Nb_8O_{30}$ tungsten bronze.

2B - Structure, Reactivity and Characterization of Ternary Oxides for Energetic Uses

V. Berbenni, A. Marini, G. Bruni

Aims

Synthesis, structural and microstructural characterisation of $Li_xNi_{1-x}O$ solid solution for use as cathodic material in MCFC

Solid state synthesis of ternary oxides from mechanically activated mixtures

Results

The thermal decomposition processes taking place in solid state mixtures Li_2CO_3–$MnCO_3$ (x_{Li}=0.10–0.50, x_{Li}=lithium cathionic fraction) have been studied (both in air and nitrogen flow) by thermogravimetric analysis (TGA), in order to get a better understanding of the different possible by-products, and by X-ray powder diffractometry (XRD) to assess the equilibrium compounds [23]. As concerns the measurements performed in air, $LiMn_2O_4$ and excess Mn_2O_3 are the equilibrium products obtained for x_{Li} up to 0.33. By $0.33 < x_{Li} < 0.50$ a mixture of $LiMn_2O_4$ and Li_2MnO_3 is obtained. In this case the TGA data show that an excess lithiated spinel ($Li_{1+x}Mn_2O_4$) is obtained as an intermediate phase. The measurements performed in nitrogen (x_{Li} up to 0.33) show, when examined by TGA, the formation reaction of $LiMn_2O_4$ and Mn_3O_4 which is completed within about 720 °C. At higher temperatures a rather complex reaction takes place between $LiMn_2O_4$ and the excess Li_2O present at 720 °C, leading to the formation of the compounds $Li_2Mn_2O_4$ and $LiMnO_2$ again with excess of Mn_3O_4. At higher mixture lithium content ($0.33 < x_{Li} < 0.50$) $LiMn_2O_4$, Li_2MnO_3 and Mn_3O_4 form up to about 720 °C. At higher temperatures $LiMnO_2$ is by far the majority phase present which is formed by solid state reactions occurring between $LiMn_2O_4$ and Li_2MnO_3 and between Li_2MnO_3 and Mn_3O_4 (Fig. 1).

In another paper [24], the thermal decomposition processes taking place in solid state mixtures Li_2CO_3–MnO (x_{Li}=0.10–0.50, x_{Li}=lithium cathionic fraction) have been studied (in air) by High Resolution Thermogravimetric Analysis (HRes-TGA), Heat Flux Differential Scanning Calorimetry (Heat Flux-DSC) and temperature variable X-ray Powder Diffractometry (HT-XRPD), in order to get a better understanding of the intermediate reaction stages and to assess the equilibrium compounds as well. As concerns the measurements performed on mixtures with $x_{Li} < 0.33$, $LiMn_2O_4$ and excess Mn_2O_3 are the obtained equilibrium products. By $0.33 < x_{Li} < 0.50$ a mixture of $LiMn_2O_4$ and Li_2MnO_3 is obtained whose proportions depend on the reaction path followed. A stoichiometric model, where both lithium manganese oxides form simultaneously, holds for x_{Li}=0.45 and 0.50 mixtures. A two stage model, where Li_2MnO_3 forms first, followed by reaction with excess Mn_2O_3 to yield $LiMn_2O_4$, is the reaction path for the x_{Li}=0.35 mixture.

Solid State Reaction study has been performed on the systems Li_2CO_3-$FeC_2O_4{\cdot}2H_2O$ and Li_2CO_3-$Fe_2(C_2O_4)3{\cdot}6H_2O$ in the composition range x_{Li} (lithium cationic fraction) = 0.10-0.50 [11]. By means of high resolution TGA, XRPD and DSC, it has been shown that, starting from iron(II) oxalate, Fe_2O_3 forms which starts to react with Li_2CO_3 well below its temperature of spontaneous decomposition (ca. 650 °C). The reaction product is a mixture of lithium ferrites ($LiFe_5O_8$ and $LiFeO_2$) whose relative amounts depend on the starting composition. The microstructure of the ferrites obtained by this system appears to be sensibly different from that of the same compounds prepared from the Li_2CO_3-Fe_2O_3 reacting system. High resolution TGA, combined with TG/FT-IR and Diffuse Refectance FT-IR Spectroscopy, reveals that, in the case of the second system the reaction takes place between iron(III) oxide and lithium carbonate even at lower temperature than it was the

case of iron(II) oxalate. The reaction mechanism is rather a complex one but the reaction product is still a mixture of the same lithium ferrites. SEM micrographs showed that, in this case, the ferrite microstructures are quite similar to those formed starting from the reacting system Li_2CO_3-Fe_2O_3.

a) b)

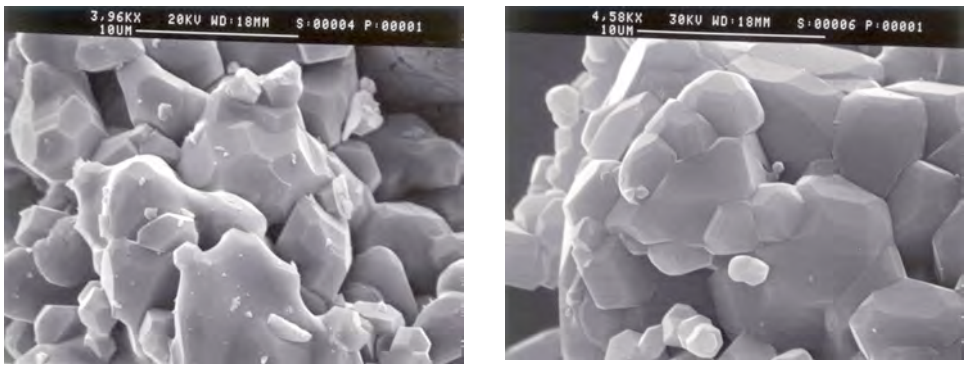

Fig. 1 *–SEM micrographs of the x_{Li}=0.33 activated mixture. (a) cycled in air between 25 and 1200 °C, (b) annealed in air for 12 h at 800 °C*

The formation of lithium ferrites ($LiFe_5O_8$ and $LiFeO_2$) from mechanically activated mixtures of Li_2CO_3–Fe_2O_3 has been studied using thermal analysis (TGA,DSC), evolved gas analysis (TG/FT-IR), X-ray powder diffraction (XRPD), scanning electron microscopy (SEM) and particle size analysis [25]. It is shown that mechanical activation of the precursors considerably enhances the reactivity of the solid system analysed and makes it possible to obtain reaction products with a much lower expense of thermal energy. In particular, lithium ferrites can be obtained at temperatures at least 160 °C lower than those necessary in the absence of mechanical activation. Moreover, both the microstructure and the allotropic ratio of the products, as well as the reaction path, are affected by mechanical activation.

The solid state reactions occurring in the mechanically activated system $SrCO_3$-Fe_2O_3 [composition: x_{Fe} (iron cationic fraction) = 0.50-0.92] have been studied [29]. At x_{Fe} = 0.50, $SrFeO_{2.5+x}$ (brownmillerite) forms by annealing of the activated mixture at 850 °C under nitrogen, while the non-stoichiometric perovskite ($SrFeO_{3-x}$) is the equilibrium product when annealing is performed under air. At x_{Fe} = 0.66 a mixture of $SrFe_2O_4$ and $SrFe_2O_5$ is the final product, no matter what is the annealing atmosphere. The enthalpies of reaction at these compositions have been determined. By increasing iron content (x_{Fe} = 0.80), the annealing at 850 °C of the activated mixture leads to $SrFe_2O_4$, $SrFe_2O_5$ and $SrFe_{12}O_{19}$ (hexaferrite). Finally, at x_{Fe} = 0.92, $SrFe_{12}O_{19}$ is produced from the mechanically activated mixture at temperatures lower (~800 °C) than in the case of conventional solid state route. In the case of last two compositions, no reaction enthalpy can be determined as the process is too slow.

The formation of barium hexaferrite, $BaFe_{12}O_{19}$, from a 1:6 molar ratio mixture of barium oxalate and iron oxide has been investigated (Fig. 2) [35]. Thermogravimetry (TGA), high temperature X-ray powder diffraction (HT-XRPD), differential scanning calorimetry (DSC) and micro-Raman spectroscopy have been used to determine the effect of mechanical activation on the solid state reactions occurring during heating. The resulting magnetic properties were investigated measuring hysteresis loops. For the activated mixtures, the mass loss is over at ~600 °C i.e. well below the temperature where $BaCO_3$ spontaneous

decomposition is complete (T>850 °C). Such a noticeable temperature lowering is a consequence of the high energy milling enhancing the formation of $BaFe_2O_4$. After heating the milled mixture to 850 °C, $BaFe_{12}O_{19}$ was rapidly formed from the $BaFe_2O_4$ and residual Fe_2O_3. Starting from an unmilled mixture, only minor amounts of $BaFe_{12}O_{19}$ were formed by heating to 850 °C. The favourable formation of barium hexaferrite, when starting from milled powders, has been confirmed by micro-Raman spectroscopy. The powder from the activated sample was shown to have far better magnetic properties than the unactivated sample.

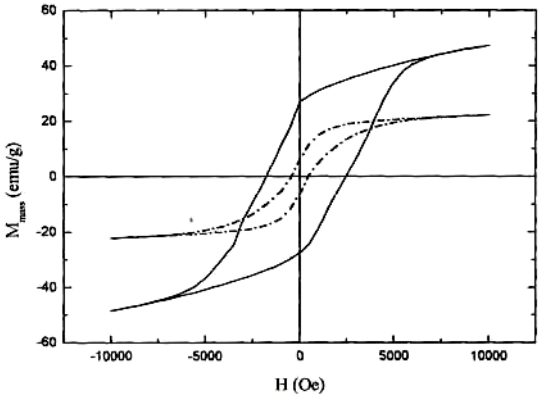

Fig. 2 *Hysteresis loop at r.t. obtained from unmilled (dashed line) and milled (solid line) BaC_2O_4+6Fe_2O_3 mixtures annealed at 850 °C*

Barium metatitanate ($BaTiO_3$) is widely used because of its high dielectric constant, ferroelectric properties and positive temperature coefficient of electrical resistivity. The compound has been synthesized by milling and annealing mixtures of $BaCO_3$ and TiO_2 (rutile) [19]. High energy milling of $BaCO_3$-TiO_2 equimolecular mixture resulted in a noticeable drop of the temperature where the reaction can occur. The formation of single phase $BaTiO_3$ was confirmed by thermogravimetric analysis (TGA) (both alone and coupled with Fourier transform infrared spectroscopy (FT-IR) evolved gas analysis), by differential scanning calorimetry (DSC) and x-ray powder diffractometry (XRPD). The formation of phases like Ba_2TiO_4 (orthotitanate), which are known to be detrimental for $BaTiO_3$ end performances, has only been revealed as an intermediate minor phase that disappears by annealing at temperatures as low as 750 °C. At such temperatures the crystal size of the product is ~400 Å. $BaTiO_3$ formation occurs either by a slow heating (2 K/min) of the milled mixture, or by a rapid heating followed by an isothermal annealing.

By thermoanalysis (TGA and DSC) and X-ray powder diffraction it has been shown that the compounds $SrTiO_3$ and Sr_2TiO_4 can be prepared by mechanical activation of, respectively, 1:1 and 2:1 $SrCO_3$ –TiO_2 (rutile) mixtures followed by annealing for 12 h at 3 2 800–850 °C [20]. These compounds could not be obtained by heating the physical mixtures to temperatures as high as 1000 °C. Moreover, the enthalpies of the reactions leading from Sr carbonate and rutile to the formation of these compounds have been determined. By combining these data with the enthalpy of $SrCO_3$ decomposition, also obtained in this work, the enthalpies of formation of $SrTiO_3$ and Sr_2TiO_4 have been calculated. On the contrary, no $Sr_3Ti_2O_7$ was shown to form, by the same annealing

procedure, when starting from a mechanically activated mixture. DSC and XRD results agree in indicating that a mixture of Sr_2TiO_4 and $SrTiO_3$ forms instead.

References

Berbenni, V., Marini, A., Bruni, G., Riccardi R., *Solid State Reaction Study in the Systems Li_2CO_3-$FeC_2O_4{\cdot}2H_2O$ and Li_2CO_3-$Fe_2(C_2O_4)_3{\cdot}6H_2O$* Thermochim. Acta 2000, **346**, 115.

Berbenni, V., Marini, A., Bruni, G., *Effect of Mechanical Milling on Solid State Formation of $BaTiO_3$ from $BaCO_3$ – TiO_2 (Rutile) Mixtures* Thermochim. Acta 2001, **374** (2), 151.

Berbenni, V., Marini, A., Bruni, G., *The Effect of Mechanical Activation on the Preparation of $SrTiO_3$ and Sr_2TiO_4 Ceramics fron the Solid State System $SrCO_3$ – TiO_2*, Journal of Alloys and Compounds 2001, 329/1-2, 230.

Berbenni, V., Marini, A., *Thermogravimetry and X-Ray Diffraction Study of the Thermal Decomposition Processes in Li_2CO_3-$MnCO_3$ Mixtures,* J. Anal. Appl. Pyrol. 2002, 62/1, 45.

Berbenni, V., Marini, A., *Thermoanalytical (TGA-DSC) and High Temperature X-Ray Diffraction (HT-XRD) Study of the Thermal Decomposition Processes in Li_2CO_3 – MnO Mixtures,* J. Anal. Appl. Pyrol. 2002, 64, 43-58.

Marini, A., Berbenni, V., Matteazzi, P., Ricceri, R., Welham, N.J., *Solid State Formation of Lithium Ferrites from the Mechanically Activated System Li_2CO_3 – Fe_2O_3* J. Eur. Ceramic Soc. 2002, 23/3, 527.

Berbenni, V., Marini, A., *Solid State Synthesis of Strontium Oxoferrates from the Mechanically Activated System $SrCO_3$ – Fe_2O_3* Materials Research Bullettin 2002, **37**/2, 221.

Berbenni, V., Marini, A., Welham, N.J., Galinetto, P., Mozzati, M.C., *The Effect of Mechanical Milling on the Solid State Reactions in the Barium Oxalate – Iron (III) Oxide System* J. Eur. Ceramic Soc. 2003, **23**/1, 179.

Berbenni, V., Marini, A., Solid State Synthesis of Lithiated Manganese Oxides From Mechanically Activated Li2CO3 – Mn3O4 Mixture. J. Anal. Appl. Pyrol. 2003, 70, 437.

Berbenni, V., Marini, A., Profumo, A., Cucca, L., *The Effect of High Energy Milling on the Solid State Synthesis of $MnFe_2O_4$ from Mixtures of MnO-Fe_2O_3 and Mn_3O_4-Fe_2O_3* Z. Naturforsch. 2003, **58b**, 415 - 422.

Berbenni, V., Marini, A., *Oxidation Behaviour of Mechanically Activated Mn_3O_4 by TGA/DSC/XRPD*
Materials Research Bulletin. 2003, **38**, 1859 - 1866.

2B – Synthesis and Characterization of Advanced Materials for Energetic Studies

V. Berbenni, G. Bruni, P. Cofrancesco, A. Marini, C. Milanese

Aims

Synthesis and characterization of NiO-based solid solutions employing as cathode materials in molten carbonate fuel cells (MCFC).
Analysis of the role of mechanical activation of the reactants on the solid state synthesis.

Results

In the development of molten carbonate fuel cells (MCFC), the "state of the art" cathodic material (lithiated nickel oxide, $Li_xNi_{1-x}O$) presents a good electronic conductivity and catalytic activity as well [1] but it does not provide enough chemical stability in the molten carbonate electrolyte [2,3]. This fact shortens the operating life of the cell with respect to the target of 40000 hours.
In this sense addition of $LiFeO_2$ (lithium ferrite, second component) to NiO is known to improve the chemical stability of the electrodic system [4] though at expense of conductivity, that can be improved by addition of $LiCoO_2$ (lithium cobaltite, third component) [5]. NiO and $LiFeO_2$ have the same fcc structure with very similar lattice parameters while $LiCoO_2$ is trigonal. As expected, NiO and $LiFeO_2$ are fully soluble one in the other, while ternary solid solutions are believed to form only for small (<18%) and high (>90%) $LiCoO_2$ molar content [6].

a) Preparation of binary NiO-$LiFeO_2$ solid solutions
As a first step in the study of the ternary NiO-$LiFeO_2$-$LiCoO_2$ system, we explore [7] the preparation procedures, solid state reactions, and thermal treatments which lead to the binary solid solution NiO-$LiFeO_2$ starting from the reacting system Ni-Li_2CO3- Fe_2O_3. The mixtures were prepared over the entire composition interval ($LiFeO_2$ molar fraction X_{LiFeO2} = 0.1 to 0.9) in two ways: a) by stirring the reactants in acetone suspension for 2 hours and subsequently drying in oven for 2 hours (physical mixture); b) by grinding for extended time intervals in a planetary ball mill (high energy mechanical activation). Reactions temperatures and annealing procedures where chosen based upon thermogravimetry (TG), differential scanning calorimetry (DSC), and high temperature X-rays powder diffraction (HT-XRPD) experiments.
The mechanism of the solid state reactions leading to formation of the solid solutions clearly emerges from thermal analyses (Figure 1).

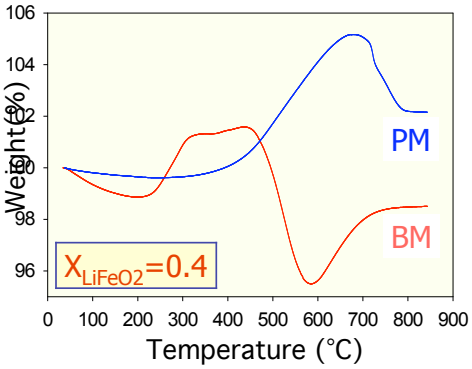

Fig. 1 - TG traces of X_{LiFeO2} = 0.4 samples heated at 5K/min up to 850°C. Red: ball milled mixture; PM: physical mixture.

The steps are the following: a) oxidation of Ni to NiO, b) thermal decomposition of Li_2CO_3, c) reaction between Li_2O and Fe_2O_3 to yield $LiFeO_2$, d) formation of a solid solution between NiO and $LiFeO_2$. An unexpected effect of mechanical activation is that it causes Ni oxidation even at room temperature; as a consequence, the mass variation during heat treatment is noticeably less than expected; however, this phenomenon is significant only for $X_{LiFeO2} \leq 0.4$.
The temperature ranges in which these four reactions take place are strongly dependent upon the mechanical treatment, as confirmed also by HT-XRPD (Figure 2).

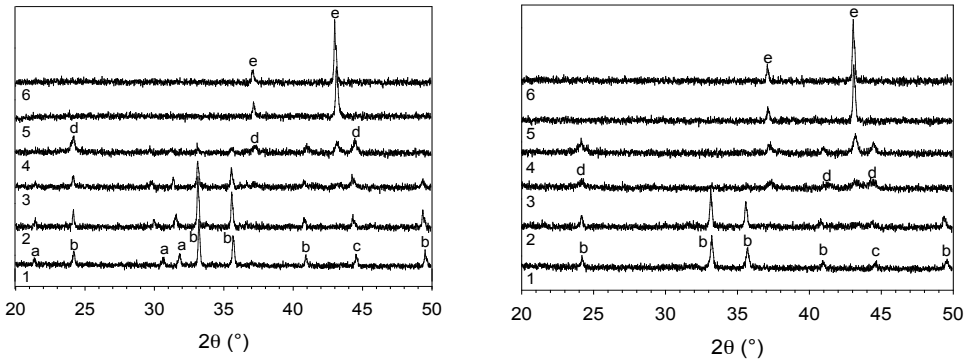

Fig. 2 - X-Ray Powder Pattern of a X_{LiFeO2} =0.9 sample treated at different temperatures. (a) Physical Mixture (b) Milled Mixture. 1. 25°C 2. 400°C 3. 500°C 4. 580°C 5.730°C 6. 800°C. Patterns a. Li_2CO_3 b. Fe_2O_3 c. Ni d. γ-$LiFeO_2$ e. solid solution.

As regards the physical mixtures (Figure 2a), steps a) and b) begin approximately around 350°C and 500°C, respectively. The diffraction peaks of the reactants are present up to 580°C. At this temperature the peaks of the products γ-$LiFeO_2$ (the low temperature tetragonal form of lithium ferrite)and NiO are showing up. At 730°C the α→γ transition has occurred and the solid solution NiO-$LiFeO_2$ has formed.
In the milling mixtures (Figure 2b), steps a) and b) begin approximately around 200°C and 350°C and the peaks of the reactants are present only up to 400°C. At 580°C the formation of the solid solution is completed.
As regards the solid state synthesis, a 12h annealing at 580°C followed by a further 6h annealing at 730°C are needed to obtain an homogeneous product starting from the physical

mixtures, while a thermal treatment of 6h at 580°C is enough to prepare the binary solid solution when starting from the activated mixtures.

b) Preparation of ternary NiO-$LiFeO_2$-$LiCoO_2$ solid solutions

We investigate [8,9,10] the line of the ternary diagram with a constant $NiO/LiFeO_2$ molar ratio of 3:1 and increasing content of $LiCoO_2$ (from 5 to 30% mol). These compositions were chosen because, according to literature [6], they seems to have the best performance as cathodic materials in MCFC.

The samples have been prepared from weighted mixtures of NiO-$LiCoO_2$-$LiFeO_2$ which were made from precursors through oxidation/decomposition performed in air at 850°C for 12h. The physical ternary mixtures were obtained by weighting appropriate amounts of the three components, stirring them in acetone suspension for 2 hours, drying in oven for 2 hours. About 500 mg of mixture was placed in an alumina boat and into a tubular furnace (Carbolite, UK Model MTF 1200). Our "standard thermal treatment" consists of 24h at 800°C followed by 2h sintering at 1000°C. Annealing times at 1000°C were subsequently extended up to 300h, or until changes in X-rays patterns were no longer appreciable. Lattice parameters and their standard errors have been computed from X-ray powder diffraction through an iterative minimum-square-deviation procedure which included most peaks. Electrical conductivity has been measured in DC with a four-electrodes probe from room temperature up to 800°C.

Figure 3 shows the XRPD patterns recorded on samples containing between 5% and 30% mol $LiCoO_2$ after the standard thermal treatment. According to the literature [6], a homogeneous solution is obtained for $LiCoO_2$ molar fractions below 15%. Above this composition, the diffraction peaks of cobaltite have been observed. With the standard thermal treatment, all samples show the presence of more than one phase in XRPD. The presence of a cobaltite phase is confirmed also by SEM analysis: in the micrograph of the mixtures subjected to the standard thermal treatment the microstructures of either NiO and $LiCoO_2$ can be recognized.

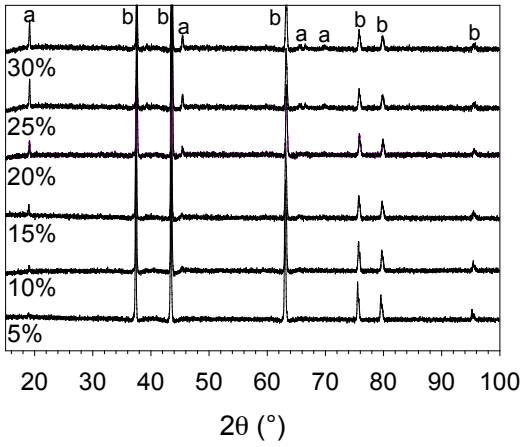

Fig. 3 - X-Ray Powder Patterns of mixtures containing a constant $LiFeO_2/NiO$ molar ratio of 1:3 and increasing content of $LiCoO_2$ (from 5 to 30% mol) after a thermal treatment of 24h at 800°C + 2h at 1000°C. Patterns: a. $LiCoO_2$; b. NiO-$LiFeO_2$-$LiCoO_2$ solid solution.

By annealing the mixtures at 1000°C for longer times, the peaks assigned to $LiCoO_2$ progressively disappear (Figure 4). This is verified for molar contents of cobaltite up to

25%, which is well above the solution limit reported in the literature. With increasing $LiCoO_2$ content, the annealing time required to obtain a single-phase product increases from 24h with 5% mol cobaltite to 96h for 25% mol. For the sample containing 30% mol $LiCoO_2$, the most intense peak of this component is still present after 300h annealing. We remark that no Li-release occurs even with a week-long annealing at 1000°C; in other words, these ternary solid solutions have very good thermal stability.

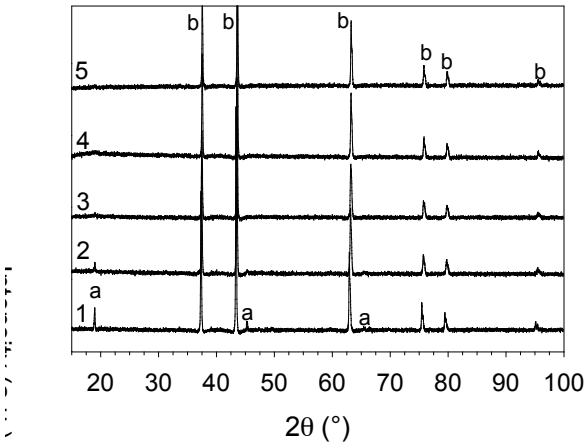

Fig. 4 - X-Ray Powder Patterns of the mixture containing a constant $LiFeO_2$/NiO molar ratio of 1:3 and 15% mol $LiCoO_2$ after thermal treatments of: (1) 24h at 800°C; (2) 24h at 800°C + 2h at 1000°C; (3) 24h at 800°C + 36h at 1000°C; (4) 24h at 800°C + 48h at 1000°C; (5) 24h at 800°C + 60h at 1000°C. Patterns a. $LiCoO_2$; b. NiO-$LiFeO_2$-$LiCoO_2$ solid solution.

Figure 5 shows the trend of conductivity obtained at 650°C (the work temperature of MCFC) for the mixtures with a nominal fraction of cobaltite from 0 to 30% mol, after the standard thermal treatment (two-phases products). For samples containing 5% and 20% mol $LiCoO_2$ the values recorded after prolonged annealing at 1000°C (single phase product) are also reported (triangles).

According to the literature, the conductivity increases with addition of cobaltite up to 25% molar, and it is distinctly higher in the two-phase samples. However, our best conductivity values (at 650°C) are, in the average, about 7 times smaller than those reported [6], and our conductivity is about the same below and above the demixing boundary. If we consider our samples as Co-doped NiO-$LiFeO_2$ solutions, we may say that doping substantially enhances conductivity. For a $LiCoO_2$ molar content between 10% and 30%, σ (650°C) increases four times or more by addition of Co.

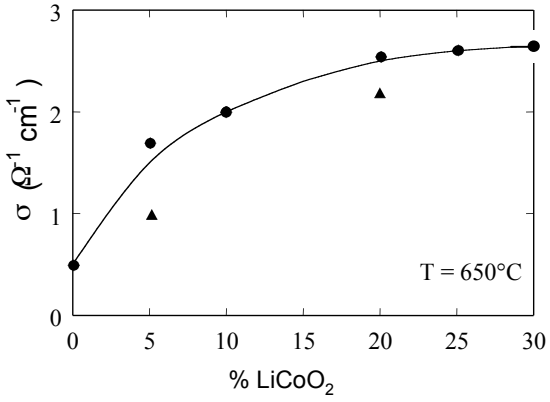

Fig. 5 - Conductivity (measured at 650°C) of mixtures with increasing nominal $LiCoO_2$ content. Circles: mixtures annealed 24h at 800°C + 2h at 1000°C (two-phases products); triangles: mixture annealed for a longer time (that is 24h for 5% mol $LiCoO_2$ and 72h for 20% mol $LiCoO_2$) at 1000°C (one-phase product).

References

[1] Gorin, E., Recht, H.L., in "Chemical Technlogy VI", W. Mitchell Jr. Ed., Academic Press, New York 1963, p.193.

[2] Selman, R., in "Fuel Cell Systems", L.J.M.J. Blomen and M.N. Mugarwn Editors, Plenum Press, New York 1993, Chap 9.

[3] Veldhuis, J.B.J., Eckes, F.C., Plomp, L., J. Electrochem. Soc. 1992, 139, 16.

[4] Singh, P., Bernard, R.M., Paetsch, L.M., Chamberlin, R.D., US Patent 4 1991, 992, 342.

[5] Bloom, I., Lanagan, M.T., Krumpelt, M., Smith, J.L., J. Electrochem. Soc. 1999, 146(4), 1336.

[6] Wijayasinghe, A., Bergman, B., Lagergren, C., Electrochim. Acta 2004, 49, 4709.

[7] Milanese, C., Berbenni, V., Bruni, G., Marini, A., Chiodelli, G., *Preparation of NiO-$LiFeO_2$ solid solutions: role of mechanical and thermal treatments*, 2005, Baden Baden (Germany), International Conference on Solid State Ionics (SSI-15)- Poster Session.

[8] Milanese, C., Berbenni, V., Bruni, G., Marini, A., Chiodelli, G., Villa, M., *Cathode materials (NiO-$LiFeO_2$-$LiCoO_2$) for molten carbonate fuel cell, a diffraction and conductivity study*, 2005, Baden Baden (Germany), International Conference on Solid State Ionics (SSI-15)- Poster Session.

[9] Villa, M., Berbenni, V., Chiodelli, G., Milanese, C., Marini, A., *An NMR study of NiO-$LiFeO_2$-$LiCoO_2$ solid solution: relationship with conductivity and homogeneity*, 2005, Baden Baden (Germany), International Conference on Solid State Ionics (SSI-15)- Talk.

[10] Milanese C., Berbenni V., Bruni G., **Marini A.**, Chiodelli G., Villa M. – Cathode materials (NiO-$LiFeO_2$-$LiCoO_2$) for molten carbonate fuel cell: a diffraction, NMR and conductivity study. *Solid State Ionics* **2006**, 177 (19-25), 1893-1896.

2B - Synthesis and characterization of pure and doped $Ba_6Ti_2Nb_8O_{30}$ ceramic materials

V. Massarotti, D. Capsoni, M. Bini

Aims

Study the influence of cation doping on local structure, cation oxidation state and defect formation.
Propose charge compensating defect equilibria on the basis of thermoelectric power measurements and EPR valence state results.
Study the influence of cation doping on the conductivity of the samples.

Results

The $Ba_6Ti_2Nb_8O_{30}$ (BTN) compound is a member of the tetragonal (space group *P4bm*) tungsten bronze family. Its structure consists of corner-sharing BO_6 octahedra (B = Ti and Nb) with peculiar Raman bands observed at about 260, 590 and 630 cm^{-1}. It displays peculiar ferroelectric, electro-optical and non linear optical properties both in polycrystalline and single crystal form. Many papers are reported in literature concerning the substitution on the different cationic sites with several types of atoms.
We synthesized pure and Fe, Mn, Cr and Y/Fe substituted BTN to obtain $Ba_6Ti_{2-x}M_xNb_8O_{30}$ (x=0.06 and 0.18) and $Ba_{6-x}Y_xTi_{2-x}Fe_xNb_8O_{30}$ (x=0.18) respectively. The crystal structure of substituted materials is the same of pure BTN and the cell volume is approximately constant independent of the type and amount of substitution. By Rietveld refinement of occupancy factors a random distribution of Ti and Nb on the two octahedral sites is found, in agreement with data previously reported.
For what concerns the valence state of the doping ions and their distribution on the BTN cations sites, interesting information have been obtained by EPR signals. In the case of Fe doped samples, two main EPR signals attributed to Fe^{3+} ions are obtained with $g_{eff} = 4.3$ and $g_{eff} = 2$; this suggests that Fe^{3+} cations occupy at least two different environments, such as the two octahedral sites present in the BTN structure. The EPR signals of the Mn doped samples can be attributed to Mn^{2+} cations distributed on both octahedral sites and from the signal areas it can be deduced that 2+ is the only oxidation state of the Mn ions in the samples. For Cr ions, on the basis of signal simulation, three main components can be observed, due to Cr^{3+} ions in three octahedral environments, one of them significantly occupied (~94 and ~90% for x_{Cr}=0.06 and x_{Cr}=0.18 respectively). A Cr distribution in good agreement with the EPR results has been obtained by additional Rietveld refinement of XRPD data on the basis of a compositional model starting from equal distribution of Cr^{3+} on the two octahedral sites.
The conductivity results can be explained on the ground of suitable defect model prevailing under the different doping conditions: oxygen vacancies and substitutional atomic defects.

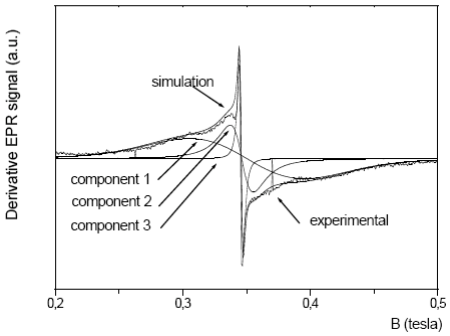

EPR signal deconvolution by numerical methods for x_{Cr}=0.06 sample.

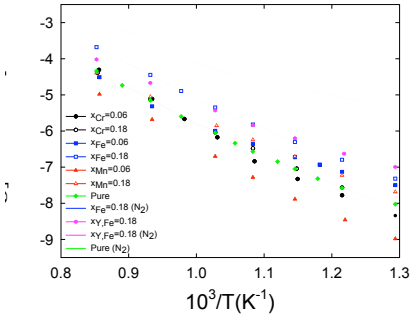

Arrhenius plots of BTN samples in the temperature range 773-1073 K. The x_{Fe}=0.18, $x_{Y,Fe}$=0.18 and pure samples data collected in N_2 flow are also reported.

References

Massarotti V., Capsoni D., Bini M., Azzoni C.B., Mozzati M.C., Galinetto P., Chiodelli G. - Structural and spectroscopic properties of pure and doped $Ba_6Ti_2Nb_8O_{30}$ tungsten bronze. *Journal of Physical Chemistry B* **2006**, 110 (36), 17798-17805.

2B - Thermal stability and properties of pure $LiMn_2O_4$

V. Massarotti, D. Capsoni, M. Bini, V. Berbenni, A. Marini

Aims

Properties-composition relationships in $LiMn_2O_4$ spinel obtained from sol-gel and solid state syntheses

Understanding of the mechanisms of thermal decomposition of the spinel phase as a function of oxygen partial pressure in the T range 25-1050°C

Results

Lithium manganese spinel $Li_{1+y}Mn_{2-y}O_4$ ($0.00<y<0.07$) synthesized by the sol-gel process is studied with a focus on the effects on the changes of formation conditions which can sensibly

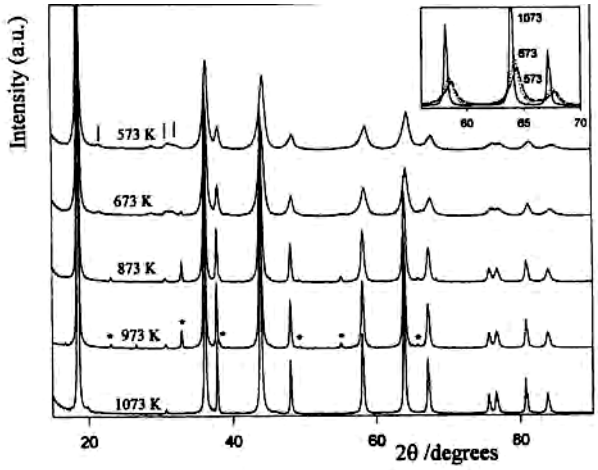

XRD patterns of the samples synthesized via the sol–gel method annealed at different temperatures. Positions of the main peaks of Mn_3O_4 and Mn_2O_3 are marked with bars and stars, respectively. In the inset some profile details are shown.

determine the mean crystallite size from a few nanometers to several hundreds nanometers. Changes of stoichiometry and abundance of the spinel phase can be observed in the $573<T_A/K<1073$ range of annealing temperature (T_A). Comparing spinel phase obtained by sol-gel and solid state synthesis evidences the correlation among composition, structure and electric and magnetic properties [8].

The structural evolution of $LiMn_2O_4$ spinel was followed from 320 K down to 10 K. The structural transformation takes place near room temperature with a significant hysteresis: the high-T cubic phase transforms into a superstructure orthorhombic cell.

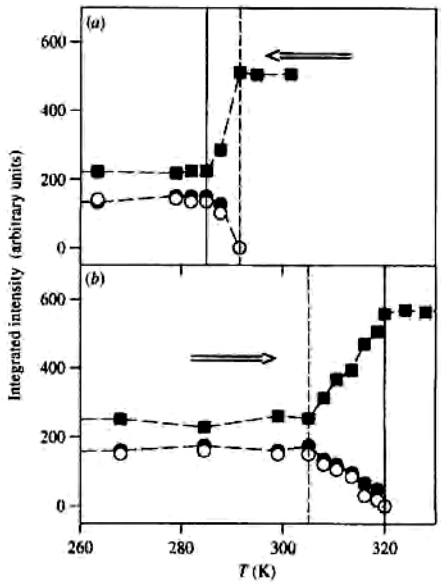

Trend of integrated intensity *versus* temperature for the triplet observed in the 27.5–28.5° 2θ range using $\lambda = 1.200$ Å (central peak, filled squares; left lateral peak, filled circles; right lateral peak, open circles) for the cooling (*a*) and heating (*b*) processes. Dashed lines are given as an aid to the eye. Vertical lines indicate the beginning (dash) and the end (line) of the transformation.

The study indicates that the nuclear structure is stable down to 10 K, while neutron diffraction patterns below 80 K show the rise of a magnetic ordering. From Mn-O bond length analysis of the MnO_6 octahedra, a temperature-independent charge ordering can be deduced [9].

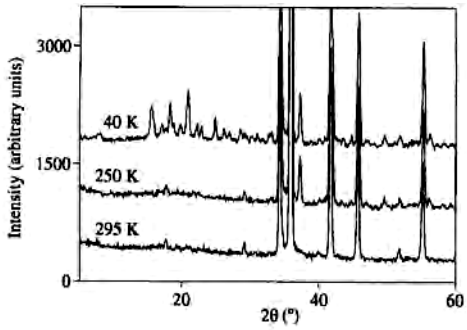

Comparison of neutron patterns collected at 295, 250 and 40 K.

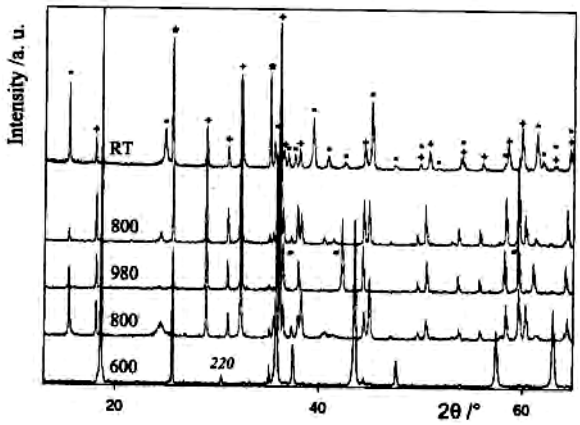

Most significant XRD patterns obtained in a heating/cooling cycle under N_2. The symbols are pertinent to the phases: Al_2O_3 (*), Mn_3O_4 (+), o-$LiMnO_2$ ($''$) and $Li_xMn_{1-x}O$ (→).

Reversible and irreversible transformations in $LiMn_2O_4$ are studied under different atmospheres (air, O_2 and N_2) in the temperature range 25-1050°C. In air and O_2, a reversible cation exchange occurs. For T>800°C Mn^{2+} ions substitute Li^+ at the tetrahedral (8a) position and Li^+ shifts to interstitial octahedral (16c) sites. Under N_2 flow, a first decomposition occurs between 600 and 800°C and yields Mn_3O_4, orthorhombic $LiMnO_2$ and O_2. Minor O_2 release occurs when heating above 900°C, which is accompanied by the transformation of o-$LiMnO_2$ into a cubic $Li_xMn_{1-x}O$ solid solution (x<0.5), consistent with a decrease in the average oxidation state of Mn ions. This cubic phase decomposes upon cooling (T<800°C) giving Mn_3O_4 and o-$LiMnO_2$ [33].
The electrical conductivity of $Li_{1+y}Mn_{2-y}O_4$ (-0.36<y<0.16) spinels is analyzed. Li-rich spinels show conductivity values higher than that observed in stoichiometric $LiMn_2O_4$. A conductivity drop, associated with a structural phase transition at about 280 K in $LiMn_2O_4$, progressively disappears by decreasing Li content, while it is absent in Li-rich samples. Stoichiometry effects on the concentration of charge carriers and on the available sites for the hopping transport process are evaluated. The role of the Jahn-Teller effect on the conductivity behavior is also considered [7].

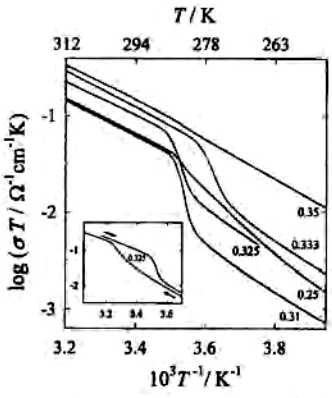

Temperature dependence of the conductivity of representative samples with $0.25 \leq x \leq 0.35$ near the temperature of the structural transition observed at about 290 K in stoichiometric spinel. A hysteresis loop for $x = 0.325$ is shown in the inset.

References

Massarotti, V., Capsoni, D., Bini, M., Chiodelli, G., Azzoni, C.B., Mozzati, M.C., Paleari, A., *Characterization of sol-gel $LiMn_2O_4$ spinel phase,* J. Solid State Chem. 1999, 147, 509.

Massarotti, V., Capsoni, D., Bini, M., Scardi, P., Leoni, M., Baron, V., Berg, H., *$LiMn_2O_4$ low temperature phase: synchrotron and neutron diffraction study,* J. Appl. Cryst. 1999, 32, 1186.

Massarotti, V., Capsoni, D., Bini, M., Stability of $LiMn_2O_4$ and new high temperature phases in air, O_2 and N_2, *Solid State Commun. 2002, 122, 317.*

Azzoni, C.B., Mozzati, M.C., Paleari, A., Bini, M., Capsoni, D., Chiodelli, G., Massarotti, V., *Stoichiometry effects on the electrical conductivity of lithium-manganese spinels,* Z. Naturforsch, 1999, 54a, 579.

2B - Y_2BaNiO_5 and related compounds

V. Massarotti, D. Capsoni, M. Bini, P. Galinetto (INFM, Pavia), M. Merli (University of Pavia), A. Rigamonti (INFM, Pavia), F. Tedoldi (INFM, Pavia), R. Santachiara (INFM, Pavia), M. Orvatic (Grenoble, France), L. Linati (CGS, Pavia), A. Altomare (IRSMC-CNR, Bari), A.G.G. Moliterni (IRSMC-CNR, Bari)

Aims

Structural determination by ab initio procedures from X-ray powder data
Cationic substitution and lattice stability by X-ray diffraction and NMR
Vibrational characteristics and phase stability range of doped samples by micro-Raman technique
Chemical bonding study in Ca substituted compounds by analysis of charge density distribution

Results

The procedure of *ab-initio* structure solution is successfully applied to Y_2BaO_4 [5] and a series of $Y_{2-x}Ca_xBaNiO_5$ compounds ($0<x<0.33$) [6]. The cation substitution does not influence the success of structure determination by using the EXPO code for direct method procedure. The structural parameters obtained for samples with different x values are compared with those reported in the literature. It is pointed out that the knowledge of the dependence of lattice parameters and cell volume on the cation site occupancy factors allows the direct determination of the degree of substitution of calcium on the yttrium site of the sample [5, 6].

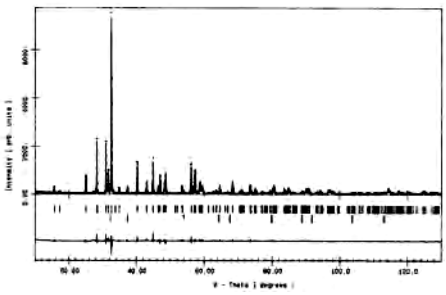

A comparison between observed (dots) and calculated (solid line) pattern after Rietveld refinement for x_{Ca} =0.5 shows very low residuals as difference curve (lower line).

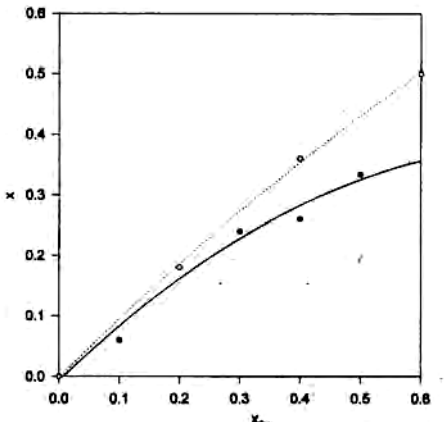

The trend of the experimental Ca content (x, closed circles) as a function of the nominal x_{Ca}, content is well compared with literature data (open circles) in a wide range of values.

Cation substitution by Mg and Zn on the Ni site of Y_2BaNiO_5 compound has been investigated by NMR and micro-Raman techniques. The presence of Mg makes possible to resolve the signals associated to different Ni ions in the Haldane chains of this compound, the finite length being created by substituting Ni^{2+} (S=1) by Mg^{2+} (S=0) [13].
Zn substitution on Ni site induces a structural change for x>0.13, while for x<0.13 two structural types coexist. The lack of the inversion symmetry on the Zn-substituted structure

causes the appearance of peculiar Raman modes in the frequency region between 260 and 340 cm^{-1}, shown in figure below.

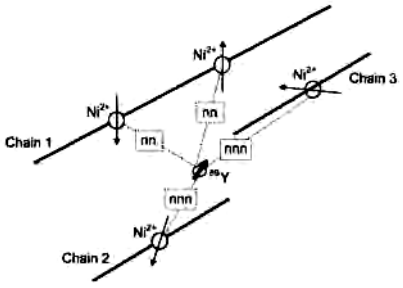

Schematic representation of the magnetic structure around a given ^{89}Y nucleus in Y_2BaNiO_5.

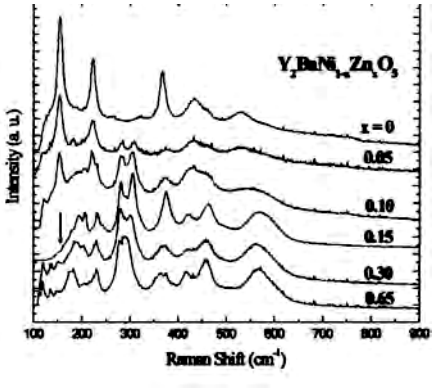

Energy and intensity of these modes are discussed taking into account the role of the doping level and of the phase abundance of the samples. A possible assignment of the modes is proposed [34].

We investigate how the presence of Ca^{2+} substituted in Y^{3+} site can influence the electronic charge distribution and the bond character in the Y_2BaNiO_5 compound. The electronic density map (r(r)) is derived from powder X-ray diffraction patterns with a novel procedure based upon a correlative use of two methods: Maximum Entropy Method (MEM) and Whole Powder Profile Fitting (WPPF). The substantial contraction of NiO_6 octahedra with increasing Ca content is related to an Ni-O bond which becomes more ionic as x increases up to x=0.24. The covalency becomes stronger above x=0.24 particularly along some Ba-O bonds [31].

References

Massarotti V., Capsoni D., Bini M., Altomare A., Moliterni A. G. G. (1999). X-ray diffraction study of polycrystalline Y_2BaO_4: a test of the new EXPO program. *Z. Kristallogr*. **214**, 200.

Massarotti V., Capsoni D., Bini M., Altomare A., Moliterni A. G. G. (1999). Ab initio structural approach on polycristalline $Y_{2-x}Ca_xBaNiO_5$ ($0 \leq x \leq 0.33$) compound*s*. *Z. Kristallogr*. **214**, 205.

Tedoldi F., Rigamonti A., Santachiara R., Horvatic M., Linati L., Bini M., Capsoni D., Massarotti V. (2000). Boundary effects in finite Heisenberg AF S=1 chains: ^{89}Y NMR in $Y_2BaNi_{1-x}Mg_xO_5$. *Appl. Magn. Res*. **19**, 381.

Capsoni D., Bini M., Massarotti V., Galinetto P. (2002). Micro-Raman and X-ray diffraction study of $Y_2BaNi_{1-x}M_xO_5$ (M=Mg, Zn) polymorphs. *Solid State Commun*. **122**, 367.

Merli M., Capsoni D., Bini M., Massarotti V. (2002). Chemical bonding study in Ca substituted Y_2BaNiO_5 by analysis of charge density distribution. *Solid State Commun*., **121**, 193.

2C - Biocatalysis through immobilised lipases

M. Monduzzi, V. Solinas, E. Sanjust, R. Pompei, S. Murgia, A. Salis, S. Mele, C. Pinna, in cooperation with P. Adlercreutz (Chemical Centre, Lund, Sweden)

Aims

Immobilisition procedures
Characterization of enzymes activity
Biocompatible processes to obtain no food products
Biosurfactants and Biodiesel

Results

Sucroesters represent a relatively new class of surfactants showing high performances and biocompatibility. The problem is related to traditional synthesis involving organic solvents. New types of synthesis, based on lipase enzymatic catalysis were tested. On the basis of promising results previously obtained to produce wax esters the commercial immobilized lipases (Candida Anthartica, Candida rugosa and Mucor miehei) will be investigated . The effect of loading and enzymatic activity will be investigated in the range of temperature 40-60°C. Optimum conditions of temperature and water activity to produce sucroesters should be ascertained.
Such system has been successfully used to produce selected glycerides.
In collaboration with a Swedish research group of the Chemical Centre of Lund, a small SCF plant will be arranged to test immobilized lipases (Candida Anthartica, Candida rugosa and Mucor miehei) for the sysnthesis of sucroesters based on glucose and galactopyranose together with linear hydrocarbon C12-C18 chains.
The new molecules were characterized for the physico-chemical properties and for the molecular structures by NMR technique.

References

Salis A., Solinas V., Monduzzi M. (2003) Wax esters synthesis from heavy fraction of sheep milk fat and cetyl alcohol by immobilised lipases J. Molec. Catalysis B, **21**, 167-174

Salis A., Svensson I., Solinas V., Monduzzi M., Adlercreutz P., (2003) *The atypical lipase B from candida antarctica is better adapted for organic media than the typical lipase from thermomyces lanuginosa* BBA - Proteins and Proteomics, **1646**/1-2,145-151

Salis A., Sanjust E., Solinas V., Monduzzi M., (2003) Characterization of Accurel MP1004 Polypropylene powder and its use as a support for lipase immobilization. J. Molec. Catalysis B **24-25**, 75-82

Salis A., Pinna M.C., Murgia S., Monduzzi M., (2004) Novel mannitol based non-ionic surfactants from biocatalysis J. Molec. Catalysis B, **27**, 139-146

Pinna M.C., Salis A., Monduzzi M., (2004) Novel mannitol based non-ionic surfactants from biocatalysis-part two- *Improved sythesis,* J. Molec. Catalysis B, in press

2C - Bioconversion in emulsion systems

A.Ceglie, A. Hochkoeppler, G. Palazzo, F. Cuomo, A. Stefan

Aims

Studies on the correlation between the supramolecolar structure and the reactivity induced by biological guest

Results

A large body of data has been collected in the last 20 years in the growing field of biotransformations in organic environments studies dealing with reactions catalyzed by enzymes solubilized in microemulsion systems or with reactions performed in non aqueous media have been extensively described in the literature.
One of the most attractive goals in this field is represented by the utilization of appropriate systems to host living cells which are particularly challenging as low-cost sources of enzymes. Until now attempts involving whole cells in biocatalysis reactions have been performed in biphasic systems and in w/o microemulsions. Although biphasic systems have the advantage of preserving the viability of microbial cells, their use for large scale reactors is hampered by the small interface area available for mass transfer between the two phases. On the contrary, w/o microemulsions feature a considerable interface but the viability of the cells hosted in these systems is rather poor.

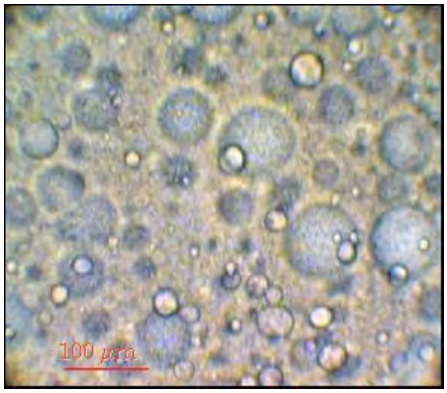

Water-in-oil emulsion systems sustain viability of a eukaryotic cell. The droplets are stabilized by a Lα phase. When water-insoluble compounds are involved they are solubilized in organic bulk but the diffusion between the interphase allows microorganism growth in the dispersed phase. Microphotograph was obtained by VEM technique.

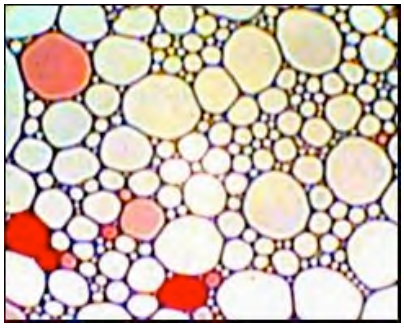

A SDS/Toluene/Water oil-in-water concentrate emulsion absorbing Sudan IV dye from a toluene mixture in contact over the same slide (obtained by VEM technique).

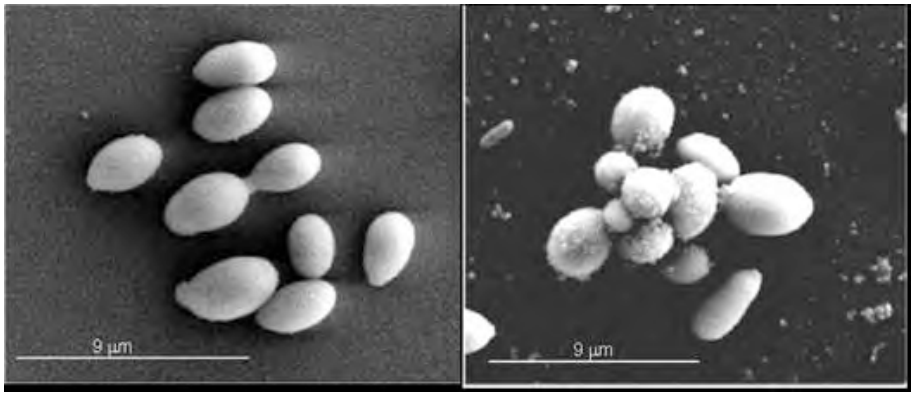

Microphotographs of *R. minuta* cells obtained by Scanning Electronic Microscopy (SEM); a) growth in YPD medium; b) in macroemulsion.

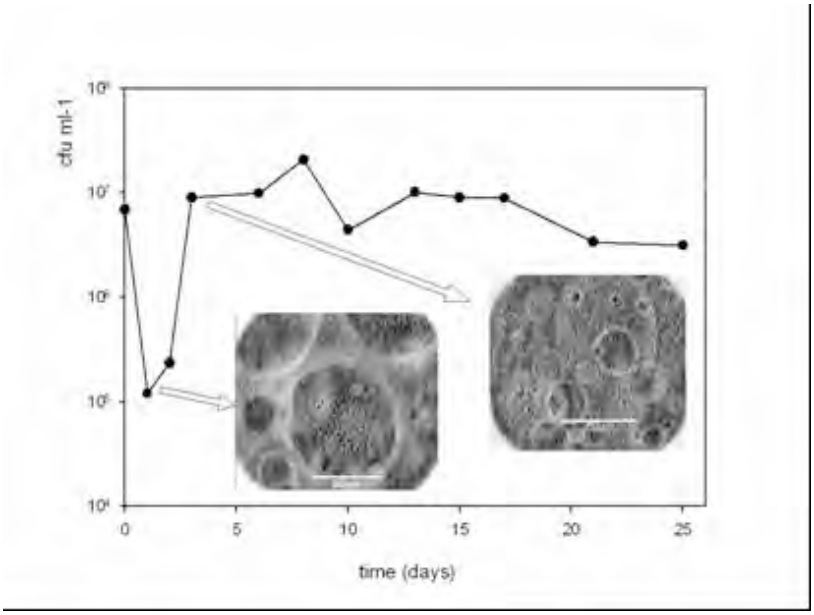

Viability of *R. minuta* in the w/o macroemulsion as a function of time. On the left microphotographs of the macroemulsion containing *R. minuta* cells after 1 day of the macroemulsion preparation are reported; on the right microphotographs of the macroemulsion after 4 days are reported.

Optical microscopy studies on particle size distribution of diameters of the dispersed phase demonstrate that the macroemulsion system is stable in terms of polidispersity. Studies on the size distribution of the macroemulsion droplet show that there are no significant effects triggered by tuning the percentage of water, the percentage of substrate, and the percentage of products.

We analyze the behavior of *Rhodotorula minuta* when hosted in the lecithin/water/isooctane macroemulsion system, with a particular interest in the "hydrolytic activity" of the yeast towards (±)-menthyl succinate ester and p-nithrophenylbutirate.

The study demonstrates that the macroemulsion system is a potentially attractive bioreactor for biotransformation reactions.

References

Cinelli G., Cuomo F., Hochkoeppler A., Ceglie A., Lopez F., *Use of Rhodotorula minuta live cells hosted in water-in-oil macroemulsion for biotrasformations reaction*, Biotechnology Progress, 2006, 22(3):689-695.

Stefan A., Palazzo G., Ceglie A., Panzavolta A. Hochkoeppler A. *Water-in-oil macroemulsions sustain long-term viability of microbial cells in organic solvent*.. Biotechnology and Bioengineering, 2003 81, 323-328.

Angelico R., Ceglie A., Hochkoeppler A., Palazzo G. and Stefan A., *Macroemulsioni acqua-in-olio a lunga stabilità, loro preparazione ed uso*. Italian Patent, 2003 n°FI2001A16.

2C – Biotechnological Processes

M. Monduzzi, A. Salis, E. Sanjust, M.C. Pinna, S. Murgia, [V. Solinas, D. Meloni, M.F. Casula, M. Pinna, (Cagliari University)], P. Adlercreutz (Lund University), E. Dumitriu (Iasi University-Bulgaria)

Aims

Enzymatic Catalysis to obtain added values products
Biocatalysis in different reaction media and solvent-free
Immobilized enzymes and their performance

Results

Three papers have been produced on the use of biocatalytic processes to obtain new products such as wax exters and sucroesters.

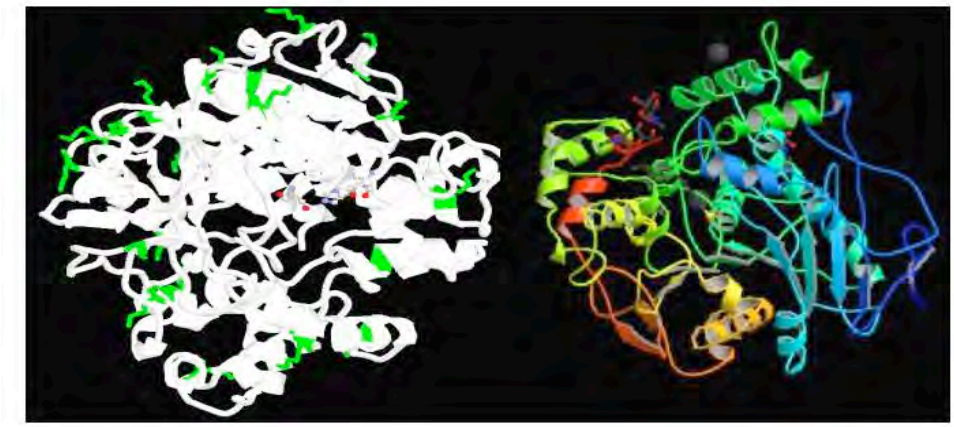

Pictures of some Lipases

Wax esters were obtained from lipase-catalysed alcoholysis of triglycerides with cetyl alcohol, using *n*-hexane as solvent. The heavy triglyceride fraction (HTF), obtained by fractionation of sheep milk fat, was used as raw material. In the natural fat mixture GCanalysis showed that palmitic, myristic, stearic and oleic acids are the most abundant fatty acids which are useful to producewax esters. Reactions were tested for different amounts of LipozymeRMIMcatalyst, and the optimum concentration of 10 mg catalyst/ml solution has been determined. The formation of the four main products, i.e. cetyl myristate, cetyl palmitate, cetyl oleate and cetyl stearate, was determined by HPLC/ELSD quantitative analysis. The optimum water activity in the reaction medium a_w = 0.35 in the case of Lipozyme RMIM, and a_w = 0.53 for Novozym 435 was found. Lipozyme RMIM (immobilised *sn*-1,3-specific lipase from *Rhizomucor miehei*) was more active than Novozym 435 (immobilised nonspecific lipase-B from *Candida antarctica*) towards wax esters production. The acyl migration of 2-monoglycerides was suggested as a crucial step

to explain the higher yields produced by the 1,3-specific lipase.

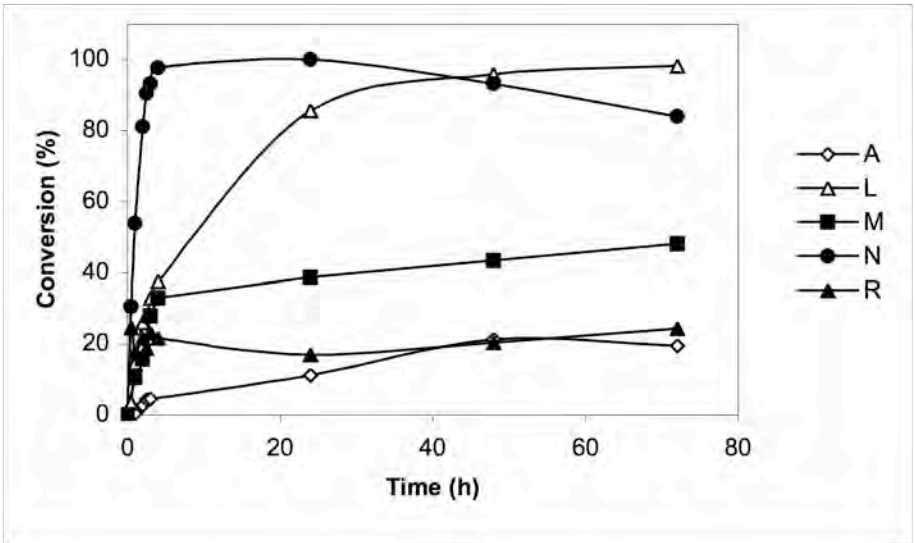

Fig. 1: Conversion of 1,2-O-isopropylidene-D-mannitol catalysed by the immobilised lipases: *Aspergillus niger* (**A**); *Rhizomucor miehei* (**L**); *Mucor javanicus* (**M**); *Candida antarctica* B (**N**), *Penicillium roqueforti* (**R**). All reactions were carried out in 2-methyl-2-butanol at 50° C.

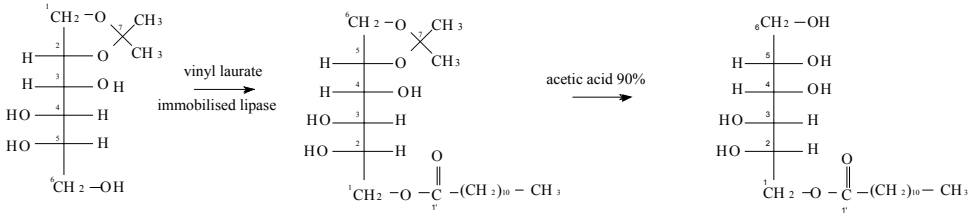

Scheme 1: Synthesis of 1-O-lauroyl-D-mannitol and C atom enumeration of reagent and products.

Two new mannitol ester based non-ionic surfactants were synthesised using immobilised lipases. The synthesis started from mannitol derivatives having two of the six hydroxyls protected by an isopropylidene group. In the acylation step five different immobilised lipases were compared, for efficiency of substrate conversion. The commercial immobilised lipase from *Candida antarctica* B (Novozym 435) gave the highest conversion in the shortest time for both substrates. Selective hydrolysis of the isopropylidene group yielded 1-O-lauroyl-D-mannitol and 1,6-di-O-lauroyl-D-mannitol. Characterisation of the products was performed by ^{13}C NMR.

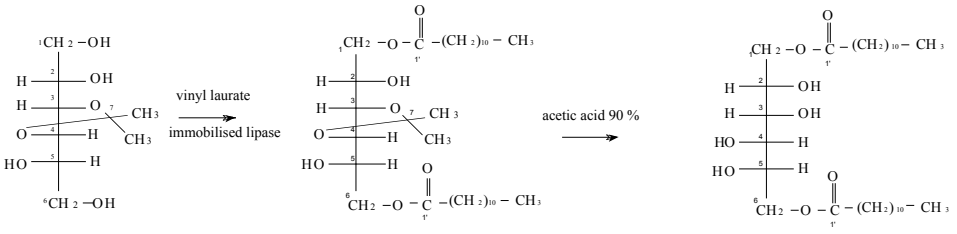

Scheme 2: Synthesis of 1,6-di-O-lauroyl-D-mannitol and C atom enumeration of reagent and products.

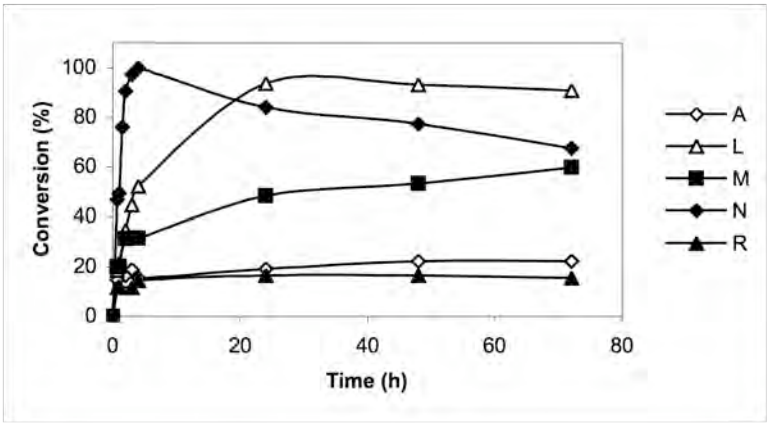

Fig. 2: Conversion of 3,4-O-isopropylidene-D-mannitol catalysed by the immobilised lipases: *Aspergillus niger* (**A**); *Rhizomucor miehei* (**L**); *Mucor javanicus* (**M**); *Candida antarctica* B (**N**), *Penicillium roqueforti* (**R**). All reactions were carried out in 2-methyl-2-butanol at 50°C.

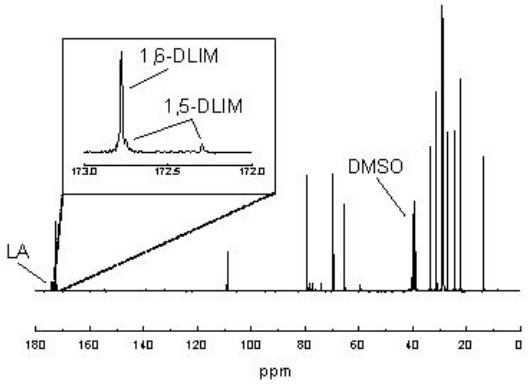

Fig. 3: ^{1}H-decoupled ^{13}C NMR spectrum of reaction products of 1,6-di-O-lauroyl-3,4-O-isopropylidene-D-mannitol (1,6-DLIM) synthesis. The signals of the isomer 1,5-di-O-lauroyl-3,4-O-isopropylidene-D-mannitol (1,5-DLIM), of the by-product lauric acid (LA), and of the solvent (DMSO) are indicated.

Table 1: ^{13}C NMR ($CDCl_3$:CD_3OD 2:1). Chemical shifts of C atoms of 1,2:4,5-di-O-isopropylidene-D-mannitol (**1**), 1-O-lauroyl-2,3:5,6-di-O-isopropylidene-D-mannitol (**2**), 1-O-lauroyl-D-mannitol (**3**), and vinyl laurate (**4**).

	d(**1**) (ppm)	d(**2**) (ppm)	d(**3**) (ppm)	d(**4**) (ppm)
C1	63.40	66.73	66.11	-
C2	70.24	69.57	69.08	-
C3	71.15	75.86	69.24	-
C4	75.20	75.41	69.27	-
C5	70.45	74.79	71.19	-
C6	66.74	63.70	63.35	-
C7,8	108.81	109.18 – 108.52	-	-
C9,10	26.02	26.13 – 26.23	-	-
C11,12	24.70	24.29 – 24.50	-	-
C1'	-	173.92	174.62	171.05
C2' (*)	-	-	-	140.69
C3' (*)	-	-	-	97.21

(*) These signals are due to the carbons of the double bond of the vinyl group in (**4**).

In the enzymatic step it has been thought that it is mainly the primary hydroxyl groups that are esterified. However, as detected from ^{13}C NMR, also other isomers were found. The formation of these isomers may be due to the non-specificity of the lipase, and to the acyl migration phenomenon.
The 1-O-lauroyl-D-mannitol, a non-ionic surfactant, was synthesised via a chemo-enzymatic pathway starting from the 1,2:4,5-di-O-isopropylidene-D-mannitol and vinyl laurate as acylation agent. The high hydrophobicity of the substrates allowed the enzymatic reaction to occur both in n-hexane and in solvent free conditions. The immobilised *Candida antarctica* lipase B was used as the catalyst of the enzymatic step. This enzyme acts differently depending on the position of the hydroxyls with respect to the isopropylidene groups. The acid selective hydrolysis of the isopropylidene groups gave the non-ionic surfactant without the presence of isomers.

Biocatalysis in different reaction media has been tested either for model reactions or to obtain added value products. *Candida antarctica* lipase B (CALB) and *Thermomyces lanuginosa* lipase (TLL) were evaluated as catalysts in different reaction media using hydrolysis of tributyrin as model reaction.
In o/w emulsions, the enzymes were used in the free form and for use in monophasic organic media, the lipases were adsorbed on porous polypropylene (Accurel EP-100). In monophasic organic media, the highest specific activity of both lipases was obtained in pure tributyrin at a water activity of >0.5 and at an enzyme loading of 10 mg/g support. With tributyrin emulsified in water, the specific activities were 2780 Amol min^{-1} mg^{-1} for TLL and 535 Amol min^{-1} mg^{-1} for CALB. Under optimal conditions in pure tributyrin, CALB expressed 49% of the activity in emulsion (264 Amol min^{-1} mg^{-1}) while TLL expressed only 9.2% (256 Amol min^{-1} mg^{-1}) of its activity in emulsion. This large decrease is probably due to the structure of TLL, which is a typical lipase with a large lid domain. Conversion between open and closed conformers of TLL involves large internal movements and catalysis probably requires more protein mobility in TLL than in CALB, which does not have a typical lid region. Furthermore, TLL lost more activity than CALB

when the water activity was reduced below 0.5, which could be due to further reduction in protein mobility.
Finally an investigation on biodiesel production using immobilized lipases has been carried out.
Oleic acid alkyl esters (biodiesel) were synthesised by biocatalysis in solvent-free conditions. Different commercial immobilised lipases, namely *Candida antarctica* B, *Rizhomucor miehei*, and *Pseudomonas cepacia*, were tested towards the reaction between triolein and butanol to produce butyl oleate. *Pseudomonas cepacia* lipase resulted to be the most active enzyme reaching 100% of conversion after 6 h. Different operative conditions such as reaction temperature, water activity, and reagent stoichiometric ratio were investigated and optimised.

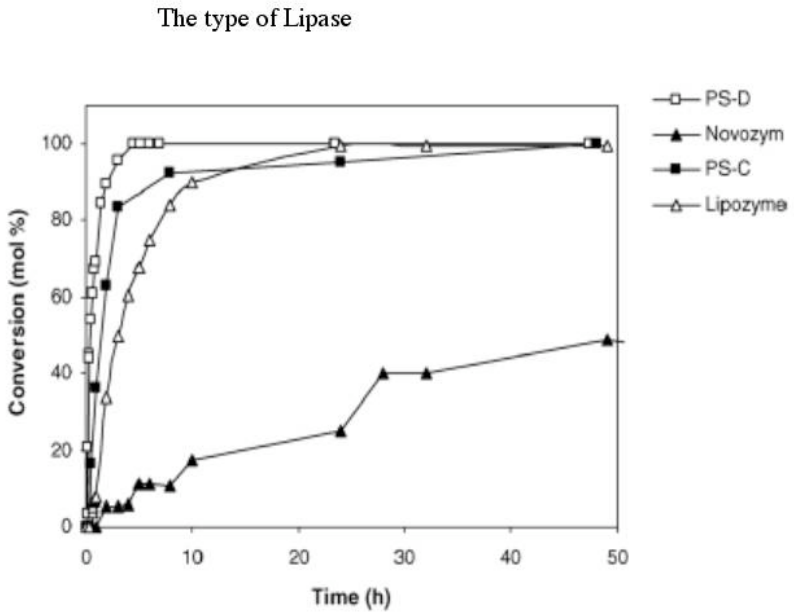

Fig. 4 – The effect of Lipase type on biodiesel production

These conditions were then used to investigate the effect of linear and branched short chain alcohols. Methanol and 2-butanol were the worst alcohols: the former, probably, due to its low miscibility with the oil and the latter because secondary alcohols usually are less reactive than primary alcohols. Conversely, linear and branched primary alcohols with short alkyl chains (C2–C4) showed high reaction rate and conversion. A mixture of linear and branched short chain alcohols that mimics the residual of ethanol distillation (fusel oil) was successfully used for oleic acid ester synthesis. These compounds are important in biodiesel mixtures since they improve low temperature properties.

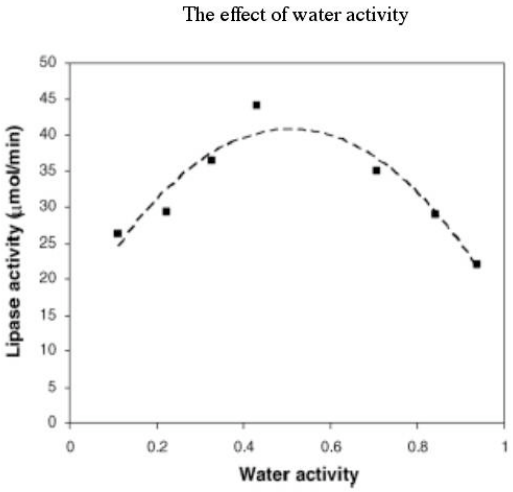

Fig. 5 – The effect of the water activity on biodiesel production

As to the immobilization process, two papers deal with Accural type supports. An innovative matrix based on nanostructured (hexagonal lattice) SiO_2 silica (SBA-15) has been tested as a suitable immobilization support for a lipase either through physical or chemical adsorption methods.
Accurel MP1004, a porous polypropylene powder, was characterised for lipase immobilisation. The particle size rangesbetween 40–80 mesh, corresponding to particle diameters of 177–420mm. The pore distribution falls between macroporous and mesoporous domains. A crude lipase preparation from *Mucor javanicus* was immobilised on Accurel MP1004 by adsorption. During the adsorption process, by measuring the variation of pore volume and of pore size distribution of mesopores as a function of enzyme loading, a significant penetration of the enzyme molecules into the pores was found to occur.
The various proteins in the crude lipase preparation are quickly adsorbed by the Accurel MP1004. However, they are progressively displaced by the lipase which shows a greater affinity for the support.

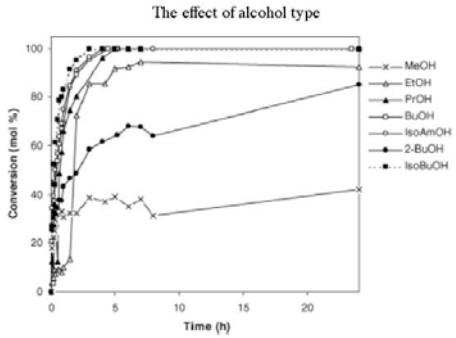

Fig. 6 – The effect of alcohol type on biodiesel production

A transesterification reaction, between glycerol tricaprylate and 1-butanol in solvent-free conditions, was catalysed by the lipase before and after the immobilisation process. The immobilisation on Accurel MP1004 improves the lipase performance both in terms of activity and of substrate conversion. Three commercial lipases (CLs), A Amano 6 (from *Aspergillus niger*), M Amano 10 (from *Mucor javanicus*), and R Amano(from *Penicillium roqueforti*) - called lipase A, M and R, respectively - were characterized in terms of carbohydrate content, protein content and enzymatic activity (p-nitrophenylacetate assay). All the CL preparations contained different proteins as observed from electrophoresis. Lipases were immobilized on Accurel MP1004 porous polypropylene by physical adsorption. The immobilization process caused a loss of enzymatic activity. The retained activity was similar for lipase M and R (about 15%). In contrast, lipase A retained only the 1.3% of the specific activity of the free lipase. The retained activity of lipases M and R seems to be due to a feature of the support, while the lower activity a of lipase A may be attributed to a strong structure distortion caused by lipase-support interaction.

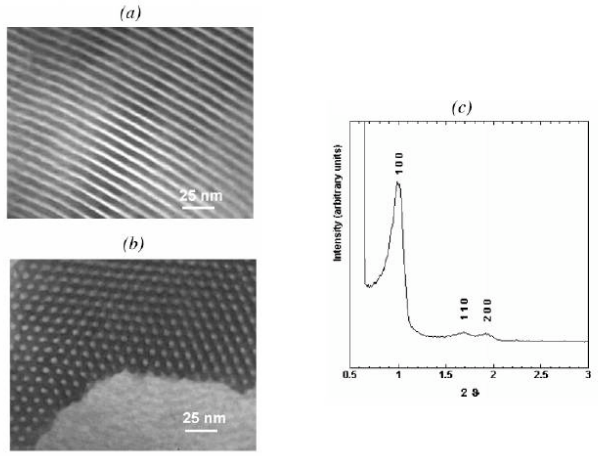

Figure 7. TEM micrographs of the SBA-15 mesoporous silica imaged in side view (a) and top view (b) and the corresponding powder X-ray diffraction pattern (c).

In another case a sample of SBA-15 mesoporous silica was synthesized and characterized by TEM, XRD, and N_2 adsorption. The sample had a high value of specific surface area (1007m^2 g^{-1}) and total pore volume (2.1 cm^3 g^{-1}). The pore diameter was 67 Å, so it was large enough to accommodate protein molecules inside the channels. Immobilization by physical adsorption of a commercial lipase preparation from *Mucor javanicus* was performed at different pH values (pH 5-8). pH6 gave the highest lipase loading and hydrolytic activity of the corresponding biocatalyst. Chemical modification of the SBA-15 via glutardialdehyde allowed also the enzyme immobilization through chemical adsorption. This preparation was active toward tributyrin hydrolysis. On the contrary, very low activity toward triolein hydrolysis was observed. The reduction of the size of the channels due the immobilization process has been suggested as a possible explanation.
Finally a review on the enzymatic catalysis in non aqueous media was performed. The most important parameters that allow to henance the activity and the stability of the enzyme are outlined.

References

Salis A., Solinas V., Monduzzi M., *Wax esters synthesis from heavy fraction of sheep milk fat and cetyl alcohol by immobilised lipases,* J. Molec. Catalysis B, 2003, 21, 167-174

Salis A., Svensson I., Solinas V., Monduzzi M., Adlercreutz P., *The atypical lipase B from candida antarctica is better adapted for organic media than the typical lipase from thermomyces lanuginosa ,* BBA - Proteins and Proteomics, 2003, 1646/1-2, 145-151

Salis A., Sanjust E., Solinas V., Monduzzi M., *Characterization of Accurel MP1004 Polypropylene powder and its use as a support for lipase immobilization,* J. Molec. Catalysis B, 2003, 24-25, 75-82

Salis A., Pinna M.C., Murgia S., Monduzzi M., Novel mannitol based non-ionic surfactants from biocatalysis, *J. Molec. Catalysis B, 2004, 27,139-146*

Pinna M.C., Salis A., Monduzzi M., *Novel mannitol based non-ionic surfactants from biocatalysis-part two- Improved sythesis*, J. Molec. Catalysis B, 2004, 27, 233-236

Salis A., Pinna M., Monduzzi M., Solinas V., *Biodiesel production in solvent free conditions by triolein and short chain alcohols through biocatalysis,* J. Biotech. 2005, 119, 291-299

Salis A., Meloni D., Ligas S., Casula M.F., Monduzzi M., Solinas V., Dumitriu E., *Physical and chemical adsorption of Mucor Javanicus Lipase on SBA-15 mesoporous silica. Synthesis, structural characterization and activity performance*. Langmuir 21, 2005, 5511-5516

Salis A., Monduzzi M., Solinas. V. *Enzymes for Biocatalysis in non aqueous media*. In Biocatalysis: Chemistry and Biology. Ed. A. Trincone. Research Signpost, Kerala. 2005, 29-53. ISBN: 81-7736-286-0

Salis A., Sanjust E., Solinas V., Monduzzi M., Commercial lipase immobilization on Accurel MP1004 porous polypropylene, Bicatalysis and Biotransf.. 2005, 23, 381-386

2C-Characterization of anti-mycobacterial pyrrole derivatives

R. Pompei

Aims

The research was aimed to the synthesis and characterization of pyrrole derivatives, obtained from the lead BM212, with a strong anti-mycobacterial activity

Results

Our work on antitubercular agents led to the identification of BM 212 as a lead compound among a series of pyrrole derivatives with good in vitro activity against mycobacteria and candidae. Further studies led us to synthesize additional pyrroles bearing the thiomorpholinomethyl moiety and different aryl substituents at N1 and C5. Some of them revealed very active, prompting us to design the new pyrrole derivatives 5-20 in the hope of increasing the activity and better understanding the influence of ortho halogens on the antimycobacterial activity. Microbiological data showed interesting in vitro activity toward Mycobacterium tuberculosis and atypical mycobacteria.

We have identified BM212 as a lead compound among a series of pyrrole derivatives with good in vitro activity against mycobacteria and candidae. First studies led us to synthesize some pyrrole compounds in which the thiomorpholine fragment was present. Some compounds revealed very active and these findings prompted us to prepare new pyrrole derivatives 2-15 in the hope of increasing the activity. The microbiological data showed interesting in vitro activity against Mycobacterium tuberculosis and atypical mycobacteria.

BACKGROUND: Over the last decade several papers have dealt with the possible interference of allergies in both the infectious disease incidence and tumour development. In the light of all these observations we analysed several tumour patients for a possible interaction between a state of allergy and tumour development and progression after primary cancer therapy. METHODS: This study included 1,055 patients with different types of solid tumours admitted consecutively between 1994 and 2002 to the Cagliari University Polyclinic. After primary surgery or medical therapy (or both), 92 allergic subjects and 182 non-allergic patients were studied over a follow-up period of 6-96 months (median 23). RESULTS: Among 1,055 tumour-bearing patients, the prevalence of allergy was found to be about 8% versus 16-37% in a population of non-tumour-bearing subjects. After primary cancer therapy, allergic patients turned out to have a 20% higher probability of being cured and about a 50% lower risk of tumour progression as compared to non-allergic ones. The observed differences were statistically significant (p=0.013). CONCLUSIONS: On the basis of our findings, we suggest that allergic subjects seem to have a better prognosis than non-allergic ones for disease outcome after cancer therapy.

References

Biava M., Porretta G.C., Deidda D., Pompei R., Tafi A., Manetti F., Antimycobacterial compounds. New pyrrole derivatives of BM212, Bioorg. Med. Chem. 2004, 12, 1453-1458

Pompei R., Lampis G., Ingianni A., Nonnis D., Ionta M.T., Massidda B., Allergy and tumour outcome after primary cancer therapy, Int. Arch. Allergy Immunol. 2004, 133, 174-178

Cottiglia F., Bonsignore L., Casu L., Deidda D., Pompei R., Casu M., Floris C., Phenolic constituents from Efhedra nebrodensis, Nat. Prod. Res. 2005, 19, 117-123

Biava M., Porretta G.C., Poce G., Deidda D., Pompei R. Tafi A., Manetti F., Antimycobacterial compounds. Optimization of the BM 212 structure, the lead compound for a new pyrrole derivative class, Bioorg. Med. Chem. 2005, 13, 1221-1230

Kondratenko R.M., Baltina L.A., Mustafina S.R., Vasil'eva E.V., Pompei R., Deidda D., Pliasunova O.A., Pokrovskii A.G., Tolstikov G.A., The synthesis and antiviral activity of glycyrrhizic acid conjugates with alpha-D-glucosamine and some glycosylamines, Bioorg. Khim (Russian) 2004, 30, 308-315

Laconi S., Molle G., Cabiddu A. Pompei R., Bioremediation of olive oil mill wastewater and production of microbial biomass. Biodegradation. 2006 Nov 14

Biava M., Porretta G.C., Poce G., Supino S., Deidda D., Pompei R. Molicotti P., Manetti F., Botta M., Antimycobacterial agents. Novel diarylpyrrole derivatives of BM212 endowed with high activity toward Mycobacterium tuberculosis and low cytotoxicity. J Med Chem. 2006 Aug 10;49(16):4946-52.

Biava M., Porretta G.C., Deidda D., Pompei R., New trends in development of antimycobacterial compounds. Infect Disord Drug Targets. 2006 Jun;6(2):159-72. Review.

Polcaro AM., Vacca A., Mascia A., Palmas S., Pompei R. and Laconi S. – Characterization of stirred tank electrochemical cell for water disinfection processes. Electrochimica Acta 2006 in press

2C – Characterization of autochtonous microflora from artisanal ewe's products

S. Cosentino, M.B. Pisano, M.E. Fadda, M. Deplano

Aims

Identification of yeasts and lactic acid bacteria throughout ripening of Fiore Sardo cheese. Phenotypic, molecular and technological characterization of the isolated strains.

Results

High counts of lactic acid bacteria and yeasts were found throughout Fiore Sardo ripening. Lactococci attained their maximum values in 48-h cheese samples, remained at a high level during the first month then decreased until disappearance, while lactobacilli reached their highest values at 1 and 3 months of ripening, then slowly decreased. Counts of enterococci increased from milk (4.4±0.59 log cfu/ml), reaching a maximum after a month (7.03±1.07 log cfu/g), then decreased to 2.05±2.21 log cfu/g at 6 months, but enterococci were still present after 9 months in two out of twelve samples (0.41±0.98 log cfu/g). Mean log yeast counts in Fiore Sardo cheese increased less than 1 unit during the first 48 h of production with respect to the initial number in the milk (from 2.64±1 to 3.06±0.9 log cfu/g, then they gradually decreased to a level of 0.65±1 log cfu/g at 9 months of ripening.

Among enterococci, Ec. faecium was the most frequently isolated species, followed by Ec. durans while Ec. faecalis was uncommon. A certain diversity in technological traits was found among enterococci isolated in our study. Proteolytic activity on casein, property considered to play an important role in cheese ripening, was detected in the majority of strains. None of the isolates could hydrolyse tributyrin, while utilization of citrate, property thought to have a positive influence on the flavour of cheese, differentiated Ec. durans isolates from others. The acidifying abilities of enterococci were generally low, and only a few strains could be considered good acid producers. As for the presence of potential pathogenic factors, only two strains of Ec. faecalis and one strain of Ec. durans were shown to produce gelatinase under the conditions of the assay. None of the strains examined in our study produced haemolysis in horse blood agar. All enterococci possessed a degree of resistance to the aminoglycosides tested, as would be predicted by their intrinsic resistance. A prevalence of multiple drug resistance was also observed. Resistance to vancomycin was not generally widespread among our strains: only one Ec. faecium and one Ec. durans strain were vancomycin resistant.

Among yeasts, the predominance of K. lactis and G. candidum in 48-h-old cheese samples suggests an important role in the first steps of ripening of Fiore Sardo for these species. Because the ability of K. lactis to ferment and assimilate lactose is considered to be one of the key properties contributing to its growth in cheeses and dairy products, this species probably participates, together with the lactic acid bacteria, to the initial acidification of the curd which takes place in the early stages of the ripening process. Similarly, G. candidum has long been the subject of biochemical and physiological studies due to its biotechnological interest. It plays an important role in competition with undesirable contaminants in the cheese, moreover, its lipases and proteases release fatty acids and peptides that contribute to the development of distinctive flavour in cheese. The overall predominance of D. hansenii in our study confirmed that this species is an important component of the microflora of Sardinian ewe's cheeses. All D. hansenii strains assimilated lactate and most (89.5%) assimilated citrate. Furthermore, a small proportion of strains showed proteolytic and lipolytic activity.

In our study, classification of the isolated strains by the use of RAPD agreed with the previous phenotypic identification. This suggests this method as an alternative to the conventional approaches to yeast identification since it is a technique that is rapid, easy to perform and rather inexpensive.

References

Fadda M.E., Mossa V., Pisano M.B., Deplano M., Cosentino S. *Occurrence and characterization of yeasts isolated from artisanal Fiore Sardo cheese*. Int. J. Food Microbiol., 2004, 95, 51-59.

Cosentino S., Pisano M.B., Corda A., Fadda M.E., Piras C. *Genotypic and technological characterization of enterococci isolated from artisanal Fiore Sardo cheese*. J. Dairy Res., 2004, 71, 444-450.

2C - Characterization of food products by ToF-SIMS and PCA

Antonio Tognazzi[a], Sandra Ristori[b], Stefania Mazzuoli[a], Silvia Focardi[a] and Claudio Rossi[a]
[a]Dipartimento di Scienze e Tecnologie Chimiche e dei Biosistemi,Università degli Studi di Siena
[b]Dipartimento di Chimica, Università degli Studi di Firenze

Aims

In recent years the analysis of agricultural products has focused on nutritional properties, which are both related to farming techniques (e.g. use of chemicals) and geographic origin. In this project we study the influence of different factors on olives and olive oil, with the aim of using extensive physico-chemical characterization to promote the final quality of this food.

Results

Extra-virgin olive oil represents one of the major high-quality agricultural product in Italy, and Tuscany ranks among the top producers. Besides the generally acknowledged good flavour and organolectic excellence of extra virgin olive oil, it has now been established that its regular use in the human diet is able to diminish the occurrence of circulatory diseases and cancer. This is mainly due to the high content of antioxidants in olives and olive oil, especially mono-unsaturated fats. However, it has been demonstrated [1] that a more subtle balance between major components and micronutrients may also play a role in determining olives and olive oil healthy properties.

Effects of chemical treatments

Chemical treatment may not only introduce traces of exogenous compounds, but it may also induce permanent alterations on plants and fruits, which compromise their overall quality. In this framework, the complexity of agricultural systems has to be taken into account during the course of investigation. In this context, fingerprint analysis is a valuable tool for complementing more conventional analytical methods.

In this study [2] we compared the chemical composition of three different groups of olives belonging to the Seggianese cultivar, that is one of the most abundant in the south of Tuscany. Samples were either taken from organic or conventional farming, and were labelled as “untreated”(UT), “treated-unwashed” (TU) and “treated-washed” (TW), according to the type of process they had undergone. Chemical treatment was carried out with an insecticide (dimethoate) and a fungicide (copper oxychloride), while washing was simply performed with cold water, according to a well established procedure. Intact olive slices and olive oil (spread as thin films on silicon wafers) were analyzed by ToF-SIMS and Principal Component Analysis (PCA) of the mass spectra was used to investigate similarities among samples. The entire ToF-SIMS spectrum is particularly suited to be used in pattern recognition and statistical analysis, since it bears high information, and it has been widely used in the characterization of complex systems.

Results showed that treated-washed olives were more similar to untreated samples. However, the washing process was not totally effective, since the treatment was able induce alterations in the olive composition (figure 1). Similar results were obtained on oils, studied with the same procedure.

Figure 2 shows the loadings for PC1(a) and PC2 (b) vs the corresponding m/z value. The loading plot indicates that lower mass peaks (i.e. m/z = 1-60) were more intense in the

treated-unwashed samples (positive loadings correspond to positive scores in Figure 1), whereas higher mass peaks were more intense in the spectra of unwashed and treated-washed samples. For the second principal component the difference between groups of samples were less clearly defined.

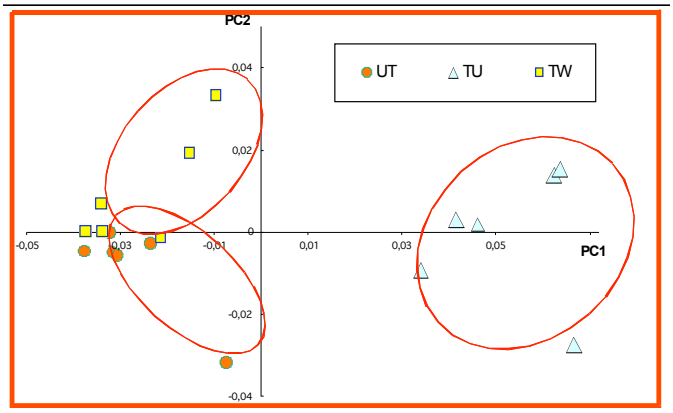

Figure 1. PC1 (90.27% of variance) and PC2 (6.16% of variance) score plot for the positive ToF-SIMS spectra of olives.

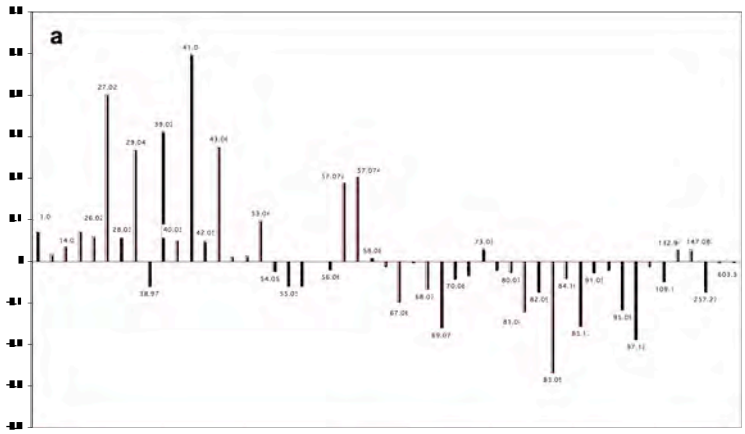

Figure 2. (a) PC1 loadings on PC1 for the score plot shown in Figure 1.

The SIMS data reported in figs 1 and 2 suggested that the chemicals used in the treatment were able to change the olive surface composition. Indeed, there were signals having higher intensity in TU than in UT or TW olive spectra, which were also found either in the dimethoate or in the copper oxychloride spectrum. For general discussion, it should be recalled that SIMS spectra of complex systems, such as the surface of intact fruits, can hardly be described by pointing out single features and a more correct description is usually obtained by statistical tools. In this respect, the results reported in figures 1 and 2 provide an overview of the analyzed samples. However, special focus has to be placed on the intermediate region of the mass spectrum, where the quasimolecular ion of dimethoate and/or copper oxychloride are expected, together with characteristic peaks of palmitic acid

(MW = 256.240), oleic acid (MW = 282.256), double chain derivatives of tripalmitin, triolein and mixed triglicerides (e.g. CH_3-CH($OCOC_{15}H_{31}$)-CH_2($OCOC_{15}H_{31}^+$), MW = 552.512; (CH_3-CH($OCOC_{15}H_{31}$)-CH_2($OCOC_{17}H_{33}^+$), MW = 578.527; CH_3-CH($OCOC_{17}H_{33}$)-CH_2($OCOC_{17}H_{33}^+$); MW = 604.543;), etc..

Fig 3 reports the positive SIMS spectra of representative olive samples and of the two chemicals used for treatment, in the 200-650 u.m.a. region.

It was observed that none of the most characteristic peaks of dimethoate and copper oxychloride had significant intensity in the spectra of treated olives and, in general, only low molecular weight species were detected. For instance, the Cu^+ peaks (at m/z ≈ 63 and m/z ≈ 65) from the fungicide and the parent ion of dimethoate ($C5H12NO3PS2^+$ at m/z ≈ 230), were not recorded in the spectra of TW or TU samples. The lack of significant amounts of the chemicals employed for the treatment was in line with data reported in the literature, since the two products used for Seggianese olives are considered among the most easily eliminable ones and, if properly administered, no trace of their presence should be retained by the edible products.

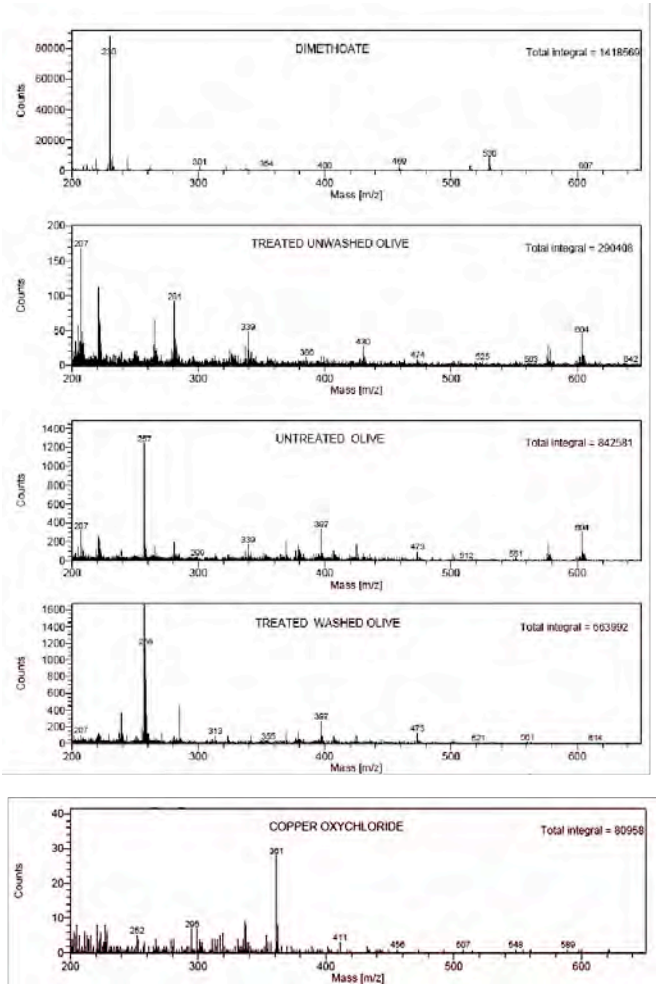

Figure 4. Intermediate (200-650 a.m.u.) region of the positive ToF-SIMS spectrum for different sample types.

Results obtained with the negative ion SIMS were in agreement with the above findings and, essentially, the same sample grouping was obtained from the principal component analysis of negative spectra. As in the case of positive ions, no peaks typical of the chemicals used in the treatment (e.g the phosphate or sulphur negative ions) showed high intensity. This implies that the difference among olive groups were due to changes induced by the chemicals (degradation of molecules present in the olives, deposition of contaminants, etc.), rather than to the presence of the chemicals themselves.
In conclusion, we observed that TU olives were appreciably different from UT and TW samples. Oils from UT and TW olives were also found to be different. Smaller differences between UT and TW specimens were detected. Distinction among sample groups was not due to the presence of the chemicals used, since most of the peaks which are specific of dimethoate and copper oxychloride SIMS spectra were not significantly more intense for TW samples. However, a general change in the ToF SIMS spectra of olives with different history was evidenced, and it was attributed to chemical modifications in the surface of treated samples.
It has been reported that pesticides, and dimethoate in particular, are able to alter the lipid biosynthesis in olives. For example, Rutter et al. showed that lipid and fatty acid patterns are affected by treatment with this pesticide, even though it rapidly disappears from the food product [3]. Our results are consistent with this finding.

Cultivar and Geographical Characterization

The quality of olives depends on many factors. Some of them are intrinsic to the fruit, such as cultivar type and geo-climatic growing conditions; other factors depends on the farming and collection modalities. All these variables are reflected on the organolectic (aroma, odour, flavour) and chemical (composition, acidity, etc.) characteristics of olives. It is therefore important to create a reliable method for the classification of olives and oils on the base of cultivar and geographic origin. For this purpose, we used ToF-SIMS and PCA and we analyzed three olive varieties (Correggiolo, Moraiolo and Leccino), obtained by organic farming. This cultivars are simultaneously grown in different geographic areas of southern Tuscany and were collected in the areas of Follonica, Murlo and Trequanda. The sample labelling is listed in Table 1.

	Leccino	**Moraiolo**	**Correggiolo**
Follonica	LF	MF	CF
Murlo	LM	MM	CM
Trequanda	LT	MT	CT

Table 1. Samples used in cultivar and geographical characterization

Preliminary results showed that a simple two dimensional analysis is not able to differentiate geographical origin and cultivar type within the same dataset. Three dimensional PCA provides a more detailed description, and in our case it was able to operate such distinction.
However, a single characteristic at a time could be appropriately handled by bi-dimensional treatment. For instance, Fig 5 shows the PC2-PC3 score plot for the three cultivars. In each graph, samples with different geographical origin were well separated.

For this analysis PC1 was not chosen, since it gave positive scores for all samples and, therefore, mainly reported on the same olive characteristics.

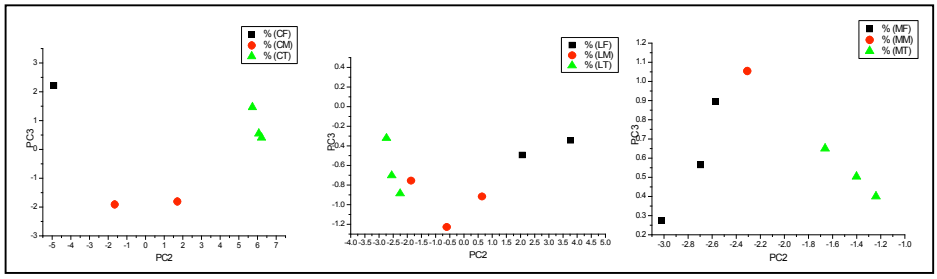

Fig. 5. PC2-PC3 score plot for the three different cultivars.

Fig. 6 shows the PC1-PC2-PC3 score plot, where samples are grouped according to both cultivar and geographical origin.

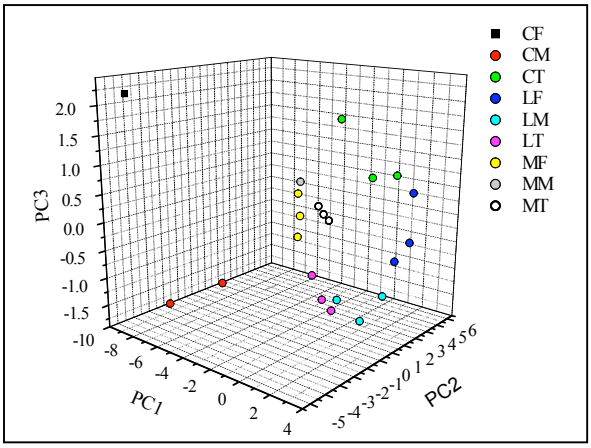

Figure 6. Three dimensional score plot for different cultivars and geographical origin.

Further studies are in progress to strengthen our method and build up a procedure for the identification of different olive types.

References

F.Visioli, C.Galli, The effects of minor constituents of olive oil on cardiovascular disease: new findings, Nutrition Review 56 (1998) 142-147.

S. Focardi, S. Ristori, S. Mazzuoli, A. Tognazzi, D. Leach-Scampavia, D. G. Castner, C. Rossi, *ToF-SIMS and PCA studies of olives and olive oil,* Colloids and Surfaces A, 2006, in the press (DOI: 10.1016/j.colsurfa.2006.01.003

A. J. Rutter, J. Sanchez, J.L. Harwood, *The effect of dimethoate on lipid biosynthesis in olive (Olea europaea) callus cultures, Phytochemistry* 47 (1998) 735-741.

2C - Enzyme activity in microemulsions

A. Ceglie, F. Lopez, L. Ambrosone, G. Palazzo, G. Colafemmina, G. Cinelli, A. Hochkoeppler

Aims

Study of the enzymatic activity of lipase at different values of W_0 and P_0 should give insight on the parameters governing the lipase activity on membrane mimetic systems.
Relationship between the enzymatic activity and the composition of the interface.

Results

The enzymatic activity of Lipase VII from *Candida rugosa* was studied in the quaternary water-in-oil microemulsion CTAB/water/pentanol/hexane. The enzyme-catalyzed hydrolysis of p-nitrophenylbutirate was found essentially independent of the water/surfactant ratio. On the other hand, the enzyme kinetics was strongly affected by the cosurfactant/surfactant ratio.
The turnover number is unaffected by the reverse micelles size and from the interfacial bromide concentration while is strongly dependent on the interfacial composition.

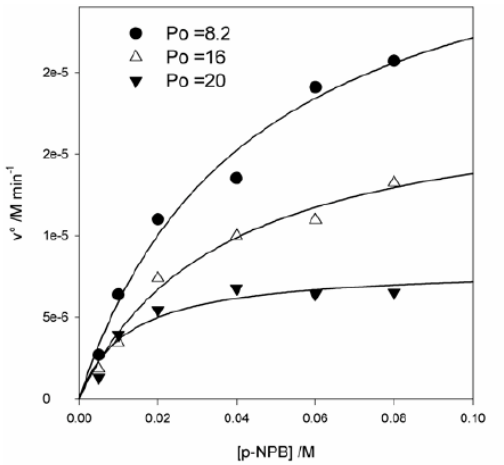

Initial rate, v_0, for the (lipase catalysed) p-NPB hydrolysis as a function of the overall p-NPB concentration in microemulsions at different P_0

References

Giuliani, S., Piana, C., Setti, L., Hochkoeppler, A., Pifferi, P.G., Williamson, G., Faulds, .B., "Synthesis of pentylferulate by a feruloyl esterase from Aspergillus niger using water-in-oil microemulsions", Biotechnology Letters, 23, 325-330, (2001)

Lopez, F., Palazzo, G., Colafemmina, G., Cinelli, G., Ambrosone, L. and Ceglie, A. "Enzymatic activity of lipase entrapped in CTAB/water/pentanol/hexane reverse micelles: a functional and microstructural inestigation", Progress Colloid & Polymer Science 123, 23-27 (2003).

2C-Enzyme and coenzyme immobilisation

E. Sanjust, A. Salis, S. Murgia, A. Rescigno, F. Sollai

Aims

Exploiting new supports and new methods for enzyme and coenzyme immobilisation.

Results

Interest towards immobilised enzymes is more and more growing as new applications in biomedicine, bioremediation, food and pharmaceutical industries are found. Supports for enzyme immobilisation should get physical and chemical stability, high affinity towards to-be-immobilised enzymes, low non-specific adsorption properties with respect to reaction products and chemicals, not involved in the enzyme-catalysed reaction. Immobilisation methods should be simple and effective. Taking into account these guidelines, some work has been made in developing preparations showing good operational stability and high retention of the original catalytic activity. Moreover, a molecularly simplified flavin has been immobilised to prepare macromolecular catalysts, capable of recycling NAD(P)+ at the expenses of molecular oxygen, with concomitant release of hydrogen peroxide. In other words, efficient b-NAD(P)H oxidase-like preparations have been obtained. Further work is in progress to study mesoporous silicas as immobilisation supports and innovative functionalised polymers to bind synthetic metalloporphins to obtain highly efficient preparations useful in a wide range of applications.

References

Amat di San Filippo, P., Rinaldi, A., Sanjust di Teulada E., *Synthetic polymeric supports for topochemical reactions, comprising also enzyme immobilization,* Materials Engineering 1989, 1, 615-620.

Amat di San Filippo, P., Fadda, M.B., Rescigno, A., Rinaldi, A., Sanjust di Teulada E., *A new synthetic polymer as a support for enzyme immobilization,* European Polymer Journal 1990, 26, 545-547.

Fadda, M. B., Rescigno, A., Rinaldi, A., Sanjust E., *Covalent coupling of Concanavalin A to commercial alumina,* Biotechnology &. Appied. Biochemistry 1992,16, 221-227.

Sanjust, E.,Curreli, N., Maullu, C., Rinaldi, A., Rescigno A., *Modified cross-linked polyvinyl alcohol as a support for protein immobilization,* Materials Engineering 1994, 5, 71-81.

Sanjust, E., Angius, C., Curreli, N., Grifi, D., Porcu, M.C., Rinaldi, A.C., Sollai, F., Rescigno, A., Rinaldi A., *New mercurated resins for covalent immobilisation*, European Polymer Journal 1997, 33, 549-551.

Sanjust, E., Curreli, N., Rescigno, A., Bannister, J.V., Cocco D., *Properties of* Thermus aquaticus •-*NADH oxidase immobilised on various supports*, Biochemistry & Molecular Biology International 1997, 41, 555-562.

Curreli, N., Oliva, S., Rescigno, A., Rinaldi, A. C., Sollai, F., Sanjust E., *Novel diazonium-functionalized support for immobilization experiments,* Journal of Applied Polymer Science 1997, 66, 1433-1438.

Sanjust, E., Cocco, D., Curreli, N., Rescigno, A., Sollai, F., Bannister J.V., *Flavin-grafted poly(vinyl alcohol): preparation and properties,* Journal of Applied Polymer Science, 2002, 85 (11), 2471-2477

2C– Enzymes and their application to waste processing and bioremediation

E. Sanjust, F. Sollai, A. Rescigno

Aims

Assessing the use of selected enzymes, also immobilised, for treatment and detoxification of solid and liquid wastes from agroindustry, dyeworks, urban wastewater plants

Results

This project has been primarily based on the enzymology of the edible fungus *Pleurotus sajor caju*. It produces upon suitable induction large amounts of the extracellular cuproenzyme laccase, able to oxidise a very wide range of phenolics and aromatic amines at the expenses of molecular oxygen. The physiological role of laccase is centred on lignin degradation, although the enzyme cannot act directly on this substrate. However the enzyme efficiently oxidised most phenolic mono- and dilignols, and is capable of involving both natural or artificial redox mediators in its action. The enzyme has been recently purified and characterised and is now under study also in the immobilised form as a tool for wastewater treatment. At least two distinct laccase forms have been singled out, arising from different culture conditions. Moreover, the fungus is capable of producing another extracellular oxidase, namely arylalcohol oxidase, a flavoenzyme releasing hydrogen peroxide as the reduction product of molecular oxygen. Arising H_2O_2 actively participates in the degradative metabolism of phenolics and aromatics.

The fungus itself has been tested as a bioremediation tool, as it actually converts a wide variety of agricultural wastes to edible biomass.

Besides *Pleurotus*, other microorganisms could be useful in waste treatment and bioremediation, so an environmental yeast, *Sporobolomyces salmonicolor*, has been isolated and tested for its ability in assimilatory removal of nitrate. The organism is now under study with concern to its main physiological and biochemical features, and preliminary work on a pilot plant has produced very promising results.

References

Sanjust, E., Pompei, R., Rescigno, A., Rinaldi, A.,Ballero, M., *Olive milling wastewater as a medium for growth of four* Pleurotus *species,* Applied Biochemistry and Biotechnology 1991, 31, 223-235.

Pompei, R., Demontis, M.G., Sanjust, E., Rinaldi, A., Ballero M., *The use of olive milling waste-water for the culture of mushrooms on perlite,* Acta Horticulturae 1994, 361, 179-185.

Sollai, F., Curreli, N., Porcu, M.C., Rescigno, A., Rinaldi, A.C., Rossino, P., Soddu , G., Sanjust E., *Effects of some substituted anthraquinones and anthrones on laccase production in* Pleurotus sajor caju, Biochemical Archives 1996,12, 7-12.

Curreli, N., Rescigno, A., Rinaldi, A., Pisu, B., Sollai, F., Sanjust E., *Degradation of juglone by* Pleurotus sajor-caju, Mycological Research, 2004, 108(8) 913-918.

Sanjust, E., Corongiu, C., Rescigno, A., Sollai, F., *Laccase induction by 4-hydroxybenzenesulfonic acid in* Pleurotus sajor-caju. The Italian Journal of Biochemistry 2004, 53, 177. Special Issue: SIB 2004, Riccione, September 28 – October 1, 2004

Sanjust, E., Rescigno, A., Sollai, F., *Laccase overproduction in* Pleurotus sajor-caju *induced by ferulic acid*, The Italian Journal of Biochemistry, 2005, 54, 103. Special Issue: SIB 2005, Riccione September 27-30, 2005.

Sollai, F., Pisu, B., Rescigno, A., Sanjust, E., Sporobolomyces salmonicolor *as a tool for nitrate removal from wastewaters*, manuscript in preparation.

2C - Formulations based on fully biocompatible surfactant systems for food, pharmaceutical and cosmetic applications

M.Monduzzi, F. Caboi, S. Mele, S. Murgia, in cooperation with P. Lazzari (Atlantis, Cagliari), T. Nylander (Lund Unversity, Sweden), H. Ljusber-Warhen (Camurus Lipid Research, Lund, Sweden), K. Larsson (Camurus Lipid Research, Lund, Sweden), N. Krog (Danisco Ingredients, Bradmont, Denmark) -

Aims

Biocompatible and stable formulations
Structural characterizations
Dynamic aspects

Results

Drug delivery systems based on liquid crystalline matrices have been developed in the recent years. The liquid crystals, generally of cubic or hexagonal space group, are formed by naturally occurring lipids such as monoglycerides or polyglycerides and phospholipids. Particularly Glycerol monooleate-based aqueous systems were considered. The aim was the preparation of high-performance biocompatible formulations which might solubilize a large variety of additives. The characterisation of the phase behavior and of the microstructural transitions occurring in multicomponent systems was performed through optical microscopy, NMR and SAXS techniques. Thermal stability of the monophasic regions and microstructural transitions vs. time were investigated, particularly when the volume fraction of the dispersed phase increases. Acyl migration and hydrolysis of the monoglyceride are the most significant phenomena, whose rate increases with increasing temperature and water content. Acyl migration in few months reaches the thermodynamic equilibrium that is G1MO:G2MO = 9:1 approximately. Hydrolysis tends to progress with storage time and often the various GMO liquid crystalline phases (lamellar and cubic) undergo a transition to a reverse hexagonal phase within 6-8 months of storage due to the formation of at least 10-12 wt% of oleic acid.

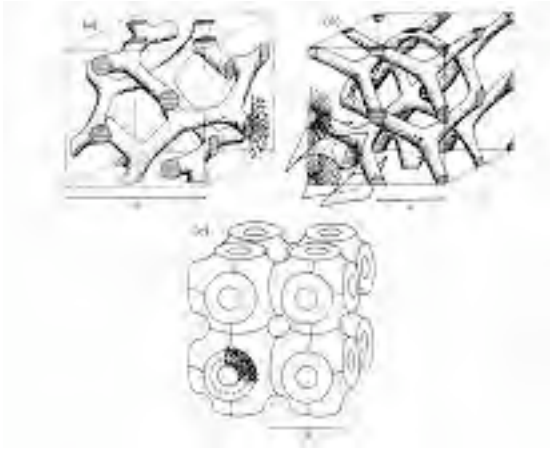

Bicontinuous cubic phases

Some additives (for instance sodium decanoate) act sinergically with oleic acid thus the reverse hexagonal phase forms within 1-2 month from preparation of the sample. Other additives such as diglycerol monooleate - a lamellar phase forming surfactant - counteract

the effect due to hydrolysis products and cubic or lamellar microstructures can be retained for years. Interestingly, GMO based systems can protect for years easily oxidazing substances such as retinol.

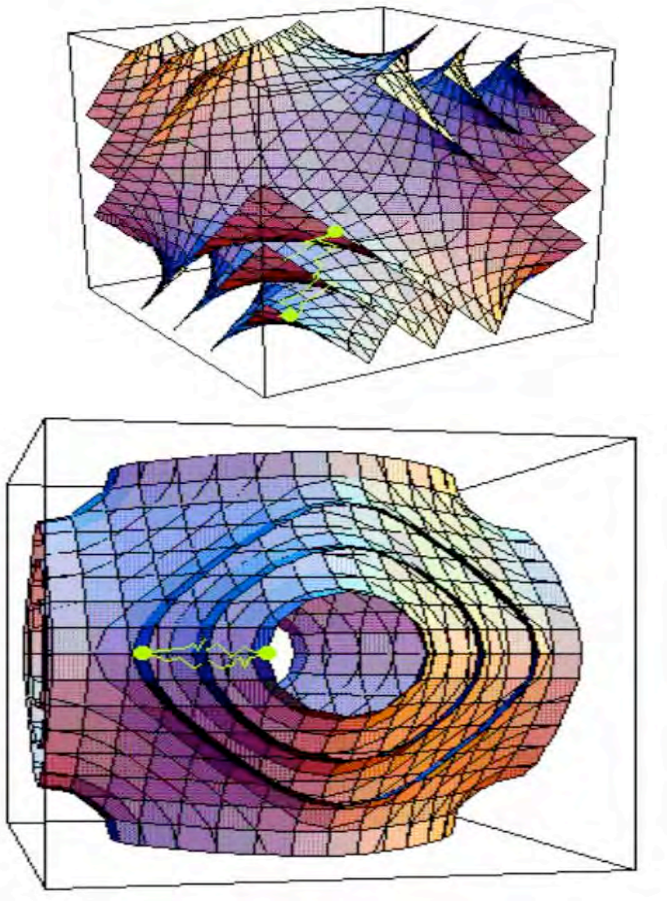

Mathematical surfaces (IPMS) of bicontinuous cubic phases

Cubic and hexagonal liquid crystalline phases of GMO can be dispersed in nanoparticles which display mostly cubic (cubosomes) and hexagonal (hexosomes) shape respectively as demonstrated by SAXS and also AFM techniques. The nanoparicles can be stabilised in aqueous solution for several months through addition of a triblock non ionic copolymer (polaxamer 407) which, besides the stabilizing action, prevents hydrolysis phenomena of the monoglycerides as shown by NMR spectra.
^{13}C NMR relaxation experiments performed on reverse micellar solutions and various liquid crystalline phases of GMO/water, GMO/water/additive and also on cubosomes and hexosomes showed that the monoolein hydrophobic skeleton is scarsely affected by the nature of the system. The local arrangement and the dynamics are retained in all systems. The significant variations of the relaxation times observed for the polar head were easily related to the interfacial curvature which is zero for lamellar and bicontinuous cubic phases and becomes negative for reverse micellar and hexagonal phases.

References

Monduzzi M., Caboi F., Nylander T., Larsson K. (1999) *Phase behavior, microstructure, and stability of three-component Systems stabilized by a fully biocompatible surfactant,* J. Surfactant & Deterg., **2**, 441

Pitzalis P., Krog N., Larsson H., Ljusberg-Wahren H., Monduzzi M., Nylander T. (2000), *Characterization of the liquid crystalline phases in the Glycerol-Monooleate/Diglycerol-Monooleate/Water System,* Langmuir, **16**, 6358-6365

Monduzzi M., Ljusberg-Wahren H., Larsson K. (2000) *A ^{13}C NMR Study of Aqueous Dispersions of Reversed Lipid Phases* Langmuir, **16**, 7355-7358

Caboi F., Amico G.S., Pitzalis P., Monduzzi M., Nylander T., Larsson K. (2001) *Addition of Hydrophilic and Lipophilic Compounds of Biological Relevance to the Monoolein/Water System. I - Phase Behavior by NMR and SAXS* Chem. Phys. Lipids, **109**, 47-62

Murgia S., Caboi F., Monduzzi M. (2001) *Addition of Hydrophilic and Lipophilic Compounds of Biological Relevance to the Monoolein/Water System. II - Dynamics by ^{13}C NMR,* Chem. Phys. Lipids, **110**, 11-17

Murgia S., Caboi F., Monduzzi M., Ljusberg-Wahren H., Nylander T. (2002) *Acyl migration and hydrolysis in monoolein based systems* Progr. Colloid Polym. Sci., **120**, 41-46

Caboi F., Murgia S., Monduzzi M., Lazzari P. (2002) *NMR investigation on Malaleuca alternifolia essential oil dispersed in the Monoolein aqueous system: phase behavior and dynamics* Langmuir, **18**,7916-7922

Mele S., Murgia S., Monduzzi M. (2003) Monoolein based liquid crystals o form long term stable emulsions Colloids & Surfaces A**, 228**, 57-63

Mele S., Murgia S., Caboi F., Monduzzi M. Biocompatible lipid formulations: Phase diagrams and microstructures from Optical Microscopy and multinuclear NMR Spectroscopy. Langmuir, submitted (2004)

2C - *In vivo* expression of antisense RNAs leads to efficient silencing in *Escherichia coli*

A. Hochkoeppler, A .Stefan

Aims

Modulation of gene expression is a useful tool to elucidate gene function and in some cases is more meaningful than complete gene inactivation. Here are analysed the effects of antisense RNAs transcribed in order to regulate the expression of specific target genes in *Escherichia coli*. The aim of this study is to understand the principles of antisense-mediated gene suppression.

Results

In prokaryotes, the silencing of specific genes by the *in vivo* expression of antisense RNAs is still a challenging phenomenon. In particular, no detailed information is available about the structural features of effective antisense molecules.

In this study the silencing of *lacZ* and *dnaQ* genes in *E. coli* has been challenged by *in vivo* expression of different antisense RNAs directed against the regulative or the coding region of the target gene. These antisense molecules were cloned into the pBAD (*ara* promoter) expression vector.

Silencing of *lacZ*

In order to determine the silencing effectiveness of these aRNAs, Western blotting analysis and β-galactosidase assays were performed. The *in vivo* stability of the antisense transcripts and the *lacZ* mRNA level were analyzed by Northern blotting. These experiments showed that the β-galactosidase activity, the protein level and the messenger concentration were significantly decreased only in bacterial populations expressing the anti-regulative antisense RNA, pBAD-areg, while bacterial cultures expressing an anti-coding antisense RNA, pBAD-acod, do not feature suppression of *lacZ* :

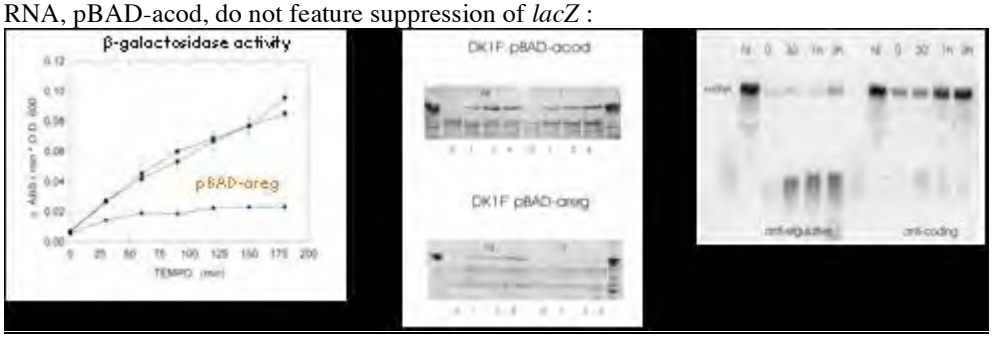

β-galactosidase activity | Western blotting | Northern blotting

Furthermore, the silencing effectiveness is correlated with a high stability *in vivo* of the antisense molecule.

Silencing of *dnaQ*

The *dnaQ* gene codes for the ε subunit of DNA polymerase III, the enzyme responsible for bacterial genome replication. This subunit primarily controls the processivity of the enzyme, independently of its proofreading function. In order to silence *dnaQ,* different aRNAs against the regulative or coding region of the gene were designed. The kinetics of binding to the target mRNA was studied *in vitro*. The same aRNAs were then expressed *in vivo* and their effect on *dnaQ* expression was evaluated (by measuring growth rate and mutation frequency).

In populations expressing the aRNA (pBAD-AR1) directed against the regulative region of the target gene the *in vivo* experiments showed a significant increase in mutation frequency correlated with a strong decrease of the growth rate in *E. coli* :

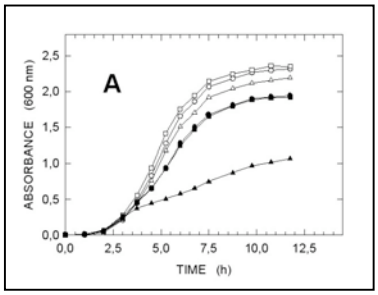

Growth rate

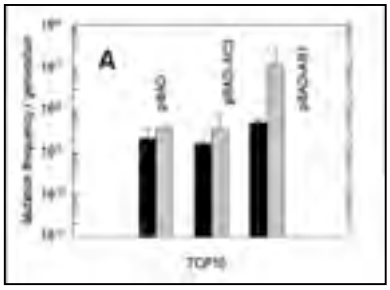

Mutation frequency

Association rate constants	
AR1:	$0{,}23\times10^{5}\ M^{-1}s^{-1}$
AC3 :	$0{,}63\times10^{5}\ M^{-1}s^{-1}$
AC4 :	$0{,}27\times10^{5}\ M^{-1}s^{-1}$

In vitro binding assays showed that the anti-coding antisense pBAD-AC3 hybridises fast the target mRNA (see table); despite this, the AC3 construct has only a moderate effect on target gene expression *in vivo:* this means that the silencing effectiveness of aRNAs cannot be predicted by *in vitro* analysis.

References

Bonoli M., Graziola M., Poggi V., Hochkoeppler A., *RNA complementary to the 5 ' UTR of mRNA triggers effective silencing in Saccharomyces cerevisiae*, Biochemical and Biophysical Research Communications, 2006, 339, 1224-1231.

Stefan A., Reggiani L., Cianchetta S., Radeghieri A., Gonzalez Vara y Rodriguez A., Hochkoeppler A., *Silencing of the gene coding for the ε subunit of DNA polymerase III slows down the growth rate of Escherichia coli populations,* FEBS Letters, 2003, 546, 295-299.

2C-Lignocellulosics: degradation and recycling

E. Sanjust, N. Curreli, A. Salis, A. Rescigno, F. Sollai

Aims

Exploring the degradation features of lignocellulosics in the view of reducing environmental impact and obtaining valuable by-products

Results

Cellulose is the most abundant biopolymer on Earth, and the same is true for lignocellulosics. Mediterranean regions produce large amounts of wheat straw, with represents an almost useless by-product. However, it contains noticeable amounts of cellulose and is rich in hemicelluloses, mainly arabinoxylans. Xylose has recently drawn much attention as the direct precursor of the non-cariogenic and non-caloric sweetener, xylitol. Therefore, some work has been devoted to optimise cellulose purification from wheat straw with concomitant xylose recovery. A mild oxidative alkaline treatment has been defined for the purpose, paralleled by a mild acidic/enzymic hydrolysis to obtain xylose syrup. Xylose recovery from a xylan-rich cereal by-product, namely wheat bran, has been developed. A novel b-glucosidase, useful for cellulose and b-glucan hydrolysis, has been purified and characterised.

References

Fadda, M. B., Curreli, N., Pompei, R., Rescigno, A.., Rinaldi, A.., Sanjust, E., *A highly active fungal ß-glucosidase. Purification and properties*, Applied Biochem. Biotechnol. 1994, 44, 263-270.

Curreli, N., Fadda, M.B., Rescigno, A., Rinaldi, A.C., Soddu, G., Sollai, F., Vaccargiu, S., Sanjust, E., Rinaldi, A., *Mild alkaline / oxidative pretreatment of wheat straw*, Process Biochemistry 1997, 32, 665-670.

Curreli, N., Agelli, M., Pisu, B., Rescigno, A., Sanjust, E., Rinaldi A.. *Complete and efficient enzymic hydrolysis of pretreated wheat straw*, Process Biochemistry 2002, 37 (9) 937-941.

Sanjust, E., Salis, A., Rescigno, A., Curreli, N., Rinaldi, A., *Note. Xylose production from durum wheat bran: enzymic versus chemical methods,* Food Science and Technology International 2004, 10, 11-14.

2C - Nanostructured Media for Bacterial Production of Fine-Chemicals

Debora Berti, Silvia Milani and Piero Baglioni (in collaboration with *F. Briganti, A. Scozzafava, Dept. of Chemistry*, University of Florence).

Aims

The purpose of the present study is the optimization of the whole-cell production of cis-dihydroxy-dihydro compounds from other less water soluble polycyclic aromatic hydrocarbons: anthracene (A in scheme 1) and phenanthrene (B in scheme 1). Such substances are converted by the naphthalene dioxygenase employed in the present study, but the biotransformation resulted in very low final yields.

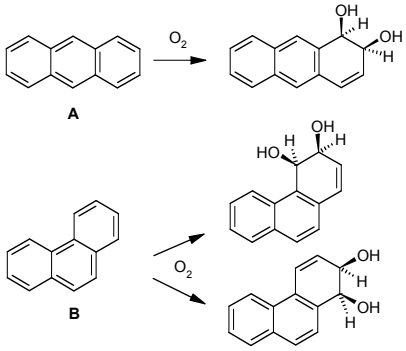

The production of large quantities of such derivatives will allow the design and synthesis of optically pure new compounds of potential industrial and pharmaceutical interest.

The particular aim of this project is the desing of a nanostructured medium where whole-cell bioconversion of polycyclic aromatic hydrocarbons for the production of fine chemicals can be performed and optimized with respect to traditional aqueous media.

Results

Industrial chemical synthesis can greatly benefit of the capabilities of enzymatic systems in terms of more gentle reaction conditions, reduced environmental pollution, and reduced costs. For oxidation reactions, the use of suitable enzymatic systems allows replacing strong oxidants with the plain oxygen molecule under mild conditions. Our interest is focused on dioxygenases which catalyze the regio- and stereo-selective dihydroxylation of a large variety of hydrocarbons, using whole cell engineered microorganisms have been developed.

Living systems accomplish high levels of selectivity and efficiency using compartmentalization. This is often realized through self assembly of amphiphatic units similar to those of synthetic surfactants which form micellar systems above the critical micellar concentration (C.M.C.). Direct micelles are able to solubilize amounts of apolar compounds in their interior. This nanophases can be seen as chemical microreactors, where hydrophobic substances stored in the apolar core can diffuse to the hydrophilic layer to take part to chemical reactions in the aqueous medium.

Kinetic bioconversion of PAH's have been performed in different o/w microemulsion media, varying surfactant type (Tween, Triton), oil nature (IPP, methyloleate, ethyloleate, glycerol trioleate) and substrate. Solubilization of PAH inside the apolar core of these nanocompartments can lead to a bulk "pseudoconcentration" three orders of magnitude higher than that in aqueous media. For a given substrate the experimental evidences that we have collected so far showed no dependence on micellar microstructure (oil content, surfactant type, etc.) whatsoever. We have interpreted this result as due to the fact that

substrate uptake by bacteria was not the rate-determining step meaning that the bioavailability of the substrate was always optimal for that bacteria number density.

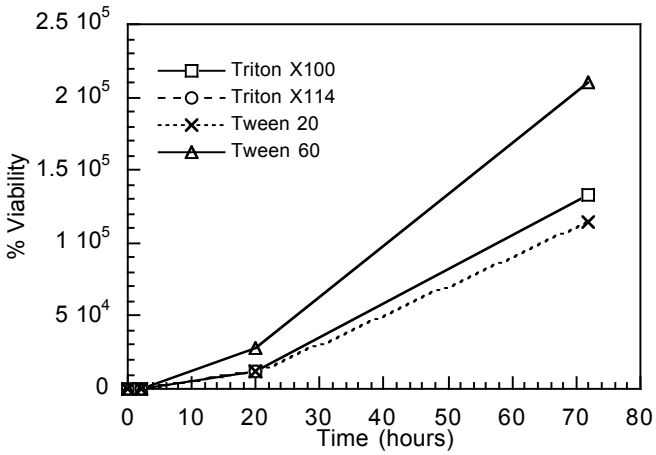

Figure1. Viability of bacterial cells suspended in some selected direct micellar solutions

Bacterial cells maintain their viability and catalytic efficiency when suspended in the different surfactant solutions employed in this study and moreover they retain viability and catalytic activity once removed from the reaction environment and resuspended again in a fresh micellar medium; this feature is rather unexpected and opens the way to scaling up procedures that take into account the reusal of cells, while in plain aqueous media cells are poisoned presumably by reaction products.

Our main achievements in this field demonstrate that the utilization of micellar phases in microbial bioconversions is milder than vigorous mixing of multiphasic media, and the effective improvement of conversion kinetics has been investigated into details for naphthalene. In such a case complete substrate conversion yielding grams of pure product per liter of culture was observed while maintaining high cell viabilities.

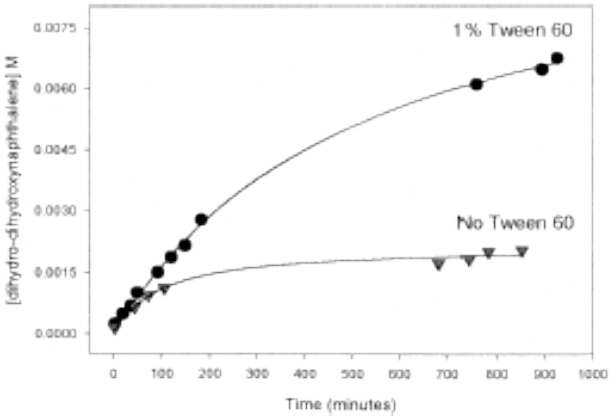

Figure2. Nanoengineered bioconversion of Naphthalene in Tween60 micellar medium compared to what obtainable in aqueous solution with excess solid substrate under vigorous stirring conditions

The latest developments of this project concern the realization and investigation of experimental conditions where some control on reaction kinetics can be exerted by proper tailoring of the micellar microstructure controlled substrate release conditions can have potential use in future application of bacterial conversion, on the other size some useful insight on the hypothesized reaction scheme can be gained.

The mechanism hypothesized consists of different steps: essentially bacteria and micelles are unperturbed by each other's presence, and their only connection is the exchange of aromatic substrate. The upload of substrate occurs from the aqueous medium and the overall conversion rates depend on the comparison of PAH's clearance operated by bacteria with respect to the supply rate to water solution operated by micellar nanocompartments.

References

Briganti, F., Randazzo, D., Scozzafava, A., Berti, D., Baglioni, P., di Gennaro, P., Galli, E., Bestetti, G. *Characterization of the Biological Conversion of Naphthalene to (+)-cis-(1R,2S)-dihydroxy-1,2-dihydronaphthalene in Direct Micellar Systems,* J. Mol. Cat. B: Enzymatic, 1999, 7, 263.

Berti, D., Randazzo, D., Briganti, F., Baglioni, P., Scozzafava, A., Di Gennaro, P., Galli, E., Bestetti, G. *Direct Micellar Systems as a Tool to Improve the Efficiency of Aromatic Substrate Conversion for Fine Chemical Production*, J. Inorg. Biochem., 2000, 79, 334-336.

D. Berti, d. Randazzo, F. Briganti, A. Scozzafava, P.di Gennaro, E. Galli, G. Bestetti, P. Baglioni, *Non-ionic Micelles promote Whole-Cell Bioconversion of Aromatic Substrates in Aqueous Environment*, Langmuir, 2002, 18 , 6015-6020.

Randazzo, D., Berti, D., Briganti, F., Baglioni, P., Scozzafava, A., Di Gennaro, P., Galli, E., Bestetti, G. *Efficient Polycyclic Aromatic Hydrocarbons Dihydroxylation in Direct Micellar Systems*, Biotechnology and Bioengineering, 74,3, 240-248 (2001).

2C – Organogel in Biotechnological processes

A. Ceglie, F. Venditti, L. Ambrosone, G. Palazzo, F. Lopez,

Aims

1) Preparation of organogel (MBGs) based on microemulsion containing a positively charged surfactant and phase diagram characterization;
2) The novel microemulsion based organogel (MBG) prepared with cationic surfactant cetyltrimethylammonium bromide (CTAB) used as support for lipase immobilization;
3) Preparation of the CTAB-silica gelatin composite obtained by hardening the organogel CTAB/water/hexane/pentanol/gelatin system with polymerization *in situ* of Tetraethoxysilane (TEOS).

Results

1) Preparation of organogel (MBGs) based on microemulsion containing a positively charged surfactant and phase diagram characterization

Reverse micelles have been used to solubilize a variety of biopolymers in apolar solvents with a low water content.In particular, the effect of gelatin solubilization on the rheological behavior of water-in-oil (w/o) microemulsions had a deep impact in several biotechnological processes. It was demonstrated that when solid gelatin is dispersed in reverse micelles at high enough water loading, a moderate warming followed by a careful decrease in temperature leads to the jellification of the whole sample, which remains fully transparent but becomes solidlike. These systems, often referred to as microemulsion-based gels or MBGs, were of outstanding importance in biotechnology because they can easily trap enzymes, retaining their catalytic activity, in organic solvents. Almost all the reported MBGs were prepared using reverse micellesmadeof bis-2-ethylhexylsodiumsuccinate (AOT), an anionic surfactant. Few exceptions are represented by microemulsions based on other anionic and nonionic surfactants. In the present contribution, we demonstrate that MBG can be made also in a w/o microemulsion stabilized by the cationic surfactant cetyltrimethylammonium bromide (CTAB).

The novel microemulsion based organogel (MBG) was prepared with cationic surfactant hexadecyltrimethylammonium bromide (CTAB). Partial phase diagram has been determined for the CTAB/water/hexane/pentanol system stabilized by gelatine. The self diffusion coefficient of water raises proportionally with W_0.

The scenario confirming the idea that also this organogel based on cationic surfactant consists of a network of rigid road of water and gelatine surrounded of surfactant and cosurfactant in equilibrium with the water droplets of the microemulsion.

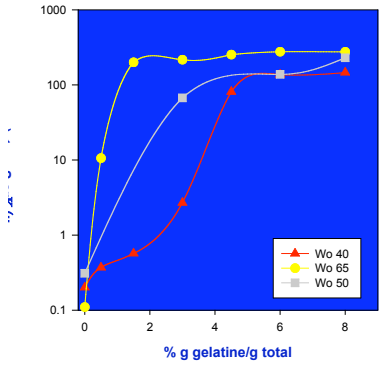

Fig.1 Conductivity of microemulsions CTAB/water/hexane/pentanol, P_0 4.8, [CTAB]=0.1M at $W_0$40, 50 and 65 as function of gelatine percentage.

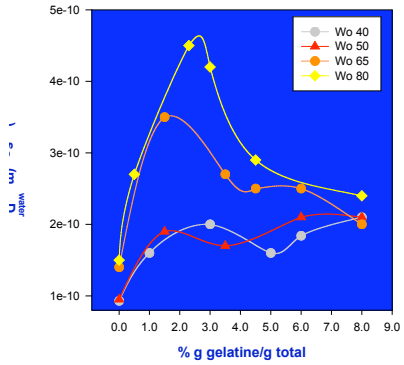

Fig.2 Self diffusion coefficient of water in CTAB/water/hexane/pentanol stabilized by gelatine as a function of gelatine percentage in systems at different W_0 measured by PFG-NMR. P_0 4.8, [CTAB]=0.1M, W_0 40,50,65,80.

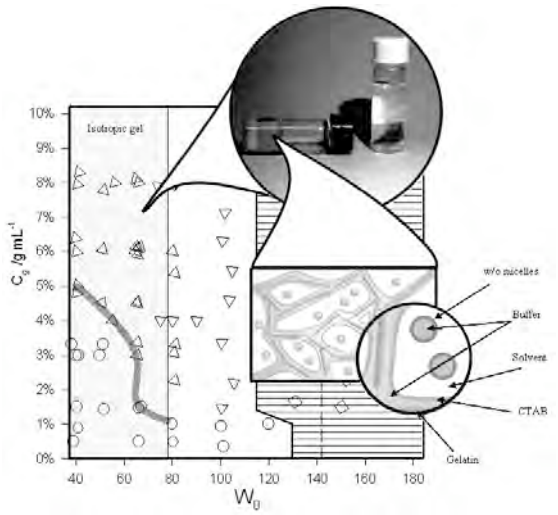

Fig.3 Schematic representation of the partial phase diagram for the CTAB MBGs. Circles, triangles and diamonds represent liquid, gel and two-phase systems, respectively. Samples at W_0 < 78 are optically isotropic (grey panel on the left). In the upper inset the optimal range of the gel and the aspect of the sample after preparation and before the solvent evaporation is reported. In the inset showed below the representation of the model proposed by Atkinson is reported.

2) The novel microemulsion based organogel (MBG) prepared with cationic surfactant cetyltrimethylammonium bromide (CTAB) used as support for lipase immobilization

Recently, immobilization of enzymes on suitable supports has represented the main goal of biotechnological applications: in particular the new technology is dealing with supports that allow high activity and high stability of products coexisting with low costs. Inside this gels, different kinds of biomolecules or dyes may be entrapped. The novel microemulsion based organogel (MBG) prepared with cationic surfactant cetyltrimethylammonium bromide (CTAB) was used as support for the immobilization of lipase from *Candida rugosa*. In this study, we found that lipase entrapped in this system is able to catalyze the esterification reaction of pentanol with caprylic acid in hexane. The maximal pentyl caprilate production of about 94% was reached in about 215 h. Recycling the immobilized enzyme was shown to be feasible, demonstrating that lipase retains its activity for several cycles. Remarkably, the enzymatic activity of lipase immobilized in the cationic MBG remained almost stable at 30 °C for at least 2 months.

Since highly reproducible results and quantitative production of pentyl caprylate was obtained at low costs, our data suggest that the novel CTAB microemulsion based gel represents a reliable tool for biotechnological applications and a commercially attractive system. The devised matrix may be generally applicable to other biologically interesting reaction systems, i.e. to bioconversion processes in organic solvents.

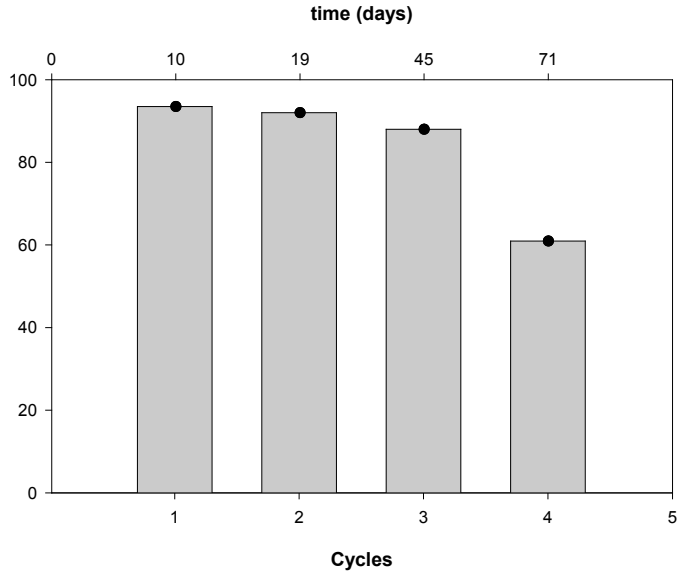

Fig.4 Yields of pentyl caprylate at 30 °C in hexane as function of run number and days passed from the sample preparation for *Candida rugosa* lipase immobilized in the CTAB microemulsion based organogel.

3) Preparation of the CTAB-silica gelatin composite obtained by hardening the organogel CTAB/water/hexane/pentanol/gelatin system with polymerization *in situ* of Tetraethoxysilane (TEOS)

A possible way to improve matrix stability, while maintaining the advantages of the microemulsion system, is the in *situ* polymerization of tetraethoxysilane that produces silica particles in CTAB microemulsion based gel. A novel composite able to remove hexavalent chromium Cr(VI) from aqueous solutions was obtained by adding the silica precursor tetraethoxysilane (TEOS) to the hexadecyltrimethylammonium bromide (CTAB) microemulsion-based gel.

The hardening process follows two essential steps after the initial collagen heat denaturation. First: the formation of aggregates via hydrophobic interactions; second: the stiffening through the inclusion of silicate inside the gelatin network. The polymerization of tetraethoxysilane (TEOS) inside the CTAB organogel leads to a formation of a material, which can be considered as a silica gelatin composite.

A current trend in the investigation over the remediation of chromium-contaminated environments calls for the development of new adsorbent materials containing positively charged surfactant, highlighting the crucial role of the surfactant. However, as the literature reads, no direct evidence of the utilization of the silica gelatin composite in general and the silica gelatin composite based on cationic surfactants for the removal process of the Cr(VI) are available. Using a new composite containing biological (gelatin) and mineral (silicate) components in the presence of a positively charged surfactant for the remediation of chromium-contaminated water could possibly be considered as a new effective method in

this matter. Furthermore, this kind of material is easy to handle and suitable to storage and manipulation processes. In the current work, we perform a physical characterization of the CTAB-silica gelatin composite obtained by hardening the organogel CTAB/water/hexane/pentanol/gelatin system and analyze the composite's behaviour in the removal process of hexavalent chromium from water at neutral pH.

References

Venditti F., Angelico R., Palazzo G., Colafemmina G., Ceglie A., Lopez F., *Hydrolysis of Tetraethoxysilane in CTAB reverse micelles: effects of the formed ethanol on the microstructure,*. Langmuir, 2006, submitted.

Venditti F., Palazzo G., Maturo L., Colafemmina G., Ceglie A., Lopez F., *Adsorption of chromate by the cationic silica-hardened organogel*, Journal of Colloid and Interface Science, 2006, submitted.

Venditti F., Lopez F., Palazzo G., Colafemmina G., Angelico R., Ambrosone L., Ceglie A., *Materiale adsorbente contenente tensioattivo cationico, sua preparazione ed uso per la rimozione di metalli da soluzioni acquose*, Italian Patent, 2006, n° IT.IP 7490.

Lopez F.,Venditti F., Cinelli G., Ceglie A., *The novel hexadecyltrimethylammonium bromide (CTAB) based organogel as reactor for ester synthesis by entrapped candida rugosa lipase*, Process Biochemistry, 2006, 41, 114-119.

Lopez F. Venditti F., Ambrosone L., Colafemmina G., Ceglie A., Palazzo P., *Gelatin Microemulsion-Based Gels with the Cationic Surfactant Cetyltrimethylammonium Bromide: A Self-Diffusion and Conductivity Study,* Langmuir, 2004, 20, 9449-9452.

Ambrosone L. and Ceglie A. *Gel stabili contenenti gelatina*, Italian Patent IT.IP 2003, n°FI2003A000237.

2C - Ovine milk: composition, dairy processing and quality controls, fractionation as a source of raw materials, no food products, and dairy wastes

M. Monduzzi, S. Cosentino, E. Sanjust, A. Rescigno, R. Pompei, S. Murgia, A. Salis, S. Mele, V. Spano, C. Pinna, in cooperation with P. Madau (Florys, Cagliari), MIUR Law 488 Projects, Ind. Lattiero Casearia F.Podda

Aims

Methodologies for analytical and nutritional certification
Methodologies for selective fractionations
Extraction of valuable by-products from dairy wastes
Selection of autochthonous lactic acid bacteria to be used as starters for ewe's cheeses

Results

A project concerning the characterisation of the ovine milk as a function of the laction stage, the influence of feeding, the dairy processing and the nature of the various wastes, is still in progress. Among the results, all the analytical procedures have been tested and new processing treatments, based on the use of CO_2 in supercritical conditions, have been employed to modify the lipid fraction of the milk.
In parallel, catalytic transesterification reactions, based on the use of immobilised lipases, to produce wax esters and biosurfactants from a milk cream fraction have been tested (see project 2C.CA1). Furthermore production of lysozyme-enriched biomass from cheese industry by-products and re-use of cheese whey to grow engineered yeasts were ascerained.
Methodologies to extract phospholipids from the cheese processing waste and an emulsifying powder from the ricotta processing waste are in progress.
In addition, methodologies to evaluate microbial activity in foods have been also investigated.

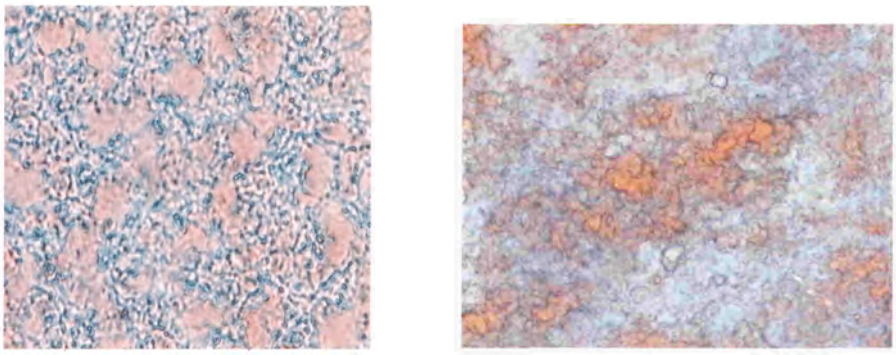

Optical microscopy of cheese samples

As a part of a project concerning the valorisation of typical Sardinian ewe's cheeses, several strains of lactic acid bacteria and yeasts have been isolated, identified and screened for their technological properties. These strains are now being tested to evaluate their potential as autochthonous starters.

References

Spano V., Madau P., Monduzzi M., Mele S., Solinas V., (2002) "*Supercritical CO_2fractionation of sheep milk fat*". Proceeding of the VIII Meeting on Supercritical Fluids "Chemical reactivity and material processing in supercritical fluids", vol. 2, 771-774

Murgia S., Mele S., Monduzzi M. (2003) Quantitat ive characterization of phospholipids in milk fat via 31P NMR using a monophasic solvent mixture. Lipids 38, 585-591

Maullu C., Lampis G., Basile T., Ingianni A., Rossolini GM and Pompei R. (1999) *Production of lysozyme-enriched biomass from cheese industry by-products*. Journal of Applied Microbiology, **86**,182-186.

Maullu C., Lampis G., Desogus A., Ingianni A., Rossolini GM and Pompei R. (1999) *High-level production of heterologous protein by engineered yeast grown in cottage cheese whey*. Applied and Environmental Microbiology, **65**, 2745-47.

Ingianni A., Pompei R. et al. (2000) *Cultural and molecular methods for the identification of Listeria monocytogenes in environmental samples and foods.,* Res. Adv. Microbiology, **1**, 61-68.

Ingianni A., Pompei R. et al. (2001) *Rapid detection of Listeria monocytogenes in foods, by a combination of PCR and DNA probe*. Molecular and Cellular Probes, **15**, 275-80.

Pompei R. et al. (1999) *Gli Streptococchi varianti nutrizionali: fisiologia e microbiologia clinica*. L'Igiene Moderna, **112**, 337-54.

Madeddu MA., Pompei R. et al. (2000) *Un terreno selettivo-differenzaile per l'isolamento degli enterococchi*. L'Igiene Moderna, **114**, 149-57.

Cosentino S., Tuberoso C.I.G., Pisano B., Satta M., Mascia V., Arzedi E., Palmas F. (1999) *In-vitro antimicrobial activity and chemical composition of sardinian Thymus essential oils*. Letters in Appl. Microbiol. , **29** (2), 130-135.

Palmas F., Cosentino S., Fadda M.E., Deplano M., Mascia V. (1999) *Microbial characteristics of Pecorino processed cheese spreads*. Lait, **79**, 607-613.

Cosentino S., Tuberoso C.I.G., Fadda M.E., Pisano B., Satta M., Mascia V., Palmas F. (1999) *Attività antimicrobica e composizione chimica di oli essenziali della Sardegna* Ig. Mod., **112**, 1411-1421.

Palmas F., Cosentino S., Fadda M.E., Deplano M., Arzedi E. (1999) *Importanza del controllo microbiologico nell'industria lattiero-casearia*. Ig. Mod., **112**, 1759-1771.

Deplano M**.,** Cosentino S., Piras C., Pisano B., Canu B., Palmas F. (2000) *Indagine sulla presenza di stipiti batterici del gen. Clostridium in campioni di Pecorino Sardo*. Atti 39° Cong. Naz. S.It.*I*., 272-274.

Cosentino S., Mascia V., Satta A., Deserra T., Palmas F. (2000) *Concentrazione di piombo in latte ovino prodotto in zone a diverso livello di inquinamento ambientale*. Atti 39° Cong. Naz. S.It.I., 352-354.

Palmas F., Cosentino S., Pisano B., Deplano M. (2000) *Acqua in uso nell'industria alimentare e qualità dei prodotti finiti*. Atti Conv. Int. Produzioni alimentari e qualità della vita**, 2**, 555-561.

Cosentino S., Fadda M.E., Deplano M., Mulargia A.F., Palmas F. (2001) *Yeasts associated with Sardinian ewe's dairy products*. Int. J. Food Microbiol. , **69**, 53-58.

Fadda M.E., Cosentino S., Deplano M., Palmas *F*. (2001) *Yeast population in Sardinian Feta cheese*. Int. J. Food Microbiol., **69**, 153-156.

Fadda M.E., Cosentino S., Pisano B., Deplano M., Palmas F. (2002) *Study of the yeasts of Fiore Sardo cheese*. Proc. Int. Conf. SFAM 2002,101-104.

Cosentino S., Pisano B., Piras C., Deplano M., Palmas F. (2002) *Characterization of lactic acid bacteria isolated from traditional Fiore Sardo cheese*. Proc. Int. Conf. SFAM 2002, ,104-107.

Cosentino S., Barra A., Pisano B., Canizza M., Pirisi F.M., Palmas F. (2003) *Composition and antimicrobial properties of sardinian Juniperus essential oils against foodborne pathogen and spoilage microorganisms*. J. Food Prot., **66**, 1288-1291,

Fadda M.E., Mossa V., Pisano M.B., Deplano M., Cosentino S. (2004) *Occurrence and characterization of yeasts isolated from artisanal Fiore Sardo cheese*. Int. J. Food Microbiol. (in press).

Cosentino S., Pisano M.B., Corda A., Fadda M.E., Piras C. (2004) *Genotypic and technological characterization of enterococci isolated from artisanal Fiore Sardo cheese*. , J. Dairy Res. in press

2C - Phase transitions and structure-properties in organic compounds

V. Massarotti, D. Capsoni, M. Bini et al.

Aims

Investigation of solid state properties of a tetrahydro hydrochloride naftalene derivative (CHF1035), a new drug for the treatment of hearth failure

Study of the racemic compound CHF1035 with binary phase diagram with one enantiomer

Characterization of polymorphism by spectral methods: Raman and ^{13}C NMR in solution and solid state

To put into evidence the different high temperature polymorphs by powder X-ray diffractometry and thermal methods

Results

The polymorphism of CHF1035 is investigated. Three different crystal forms (I, II and III) were obtained by recrystallization procedures from common organic solvents. The polymorphs have been characterized by Raman and ^{13}C NMR spectroscopy, in solution and solid state (cross polarization-MAS), powder X-ray diffractometry and thermal methods (DSC, hot stage microscopy and TGA). The diffraction patterns of Form I collected at controlled temperatures give evidence of the presence of two reversible structural rearrangements at 60<T<75°C.

The structural variations are confirmed by DSC and hot-stage spectroscopy technique. The analysis of the Raman spectra allows the identification of peculiar absorption bands for each polymorph. Form III is the stable crystal form at room temperature [21].

The polymorphism of paracetamol was investigated. Two metastable polymorphs (II and III)were obtained by appropriate thermal procedures from binary mixtures containing 10% (w/w) of hydroxypropylmethylcellulose and controlling the re-heating process it was possible to address the recrystallization into form II or III. Form III transforms either into form II or III depending on the preparatio method. The polymorphs have been characterized by micro-Fourier transform infrared spectroscopy (MFTIR) and powder X-ray diffractometry, both temperature controlled [43].

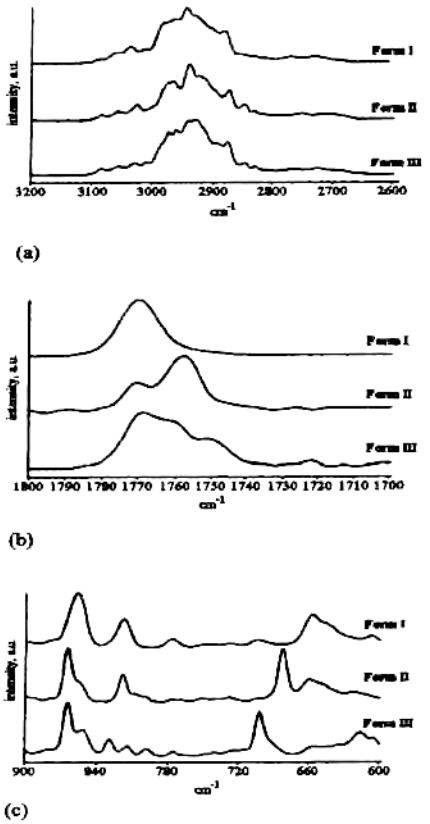

Details of Raman spectra of CHF 1035 polymorphs: (a) 3000–2600 cm^{-1} region; (b) 1800–1700 cm^{-1} region; and (c) 900–600 cm^{-1} region.

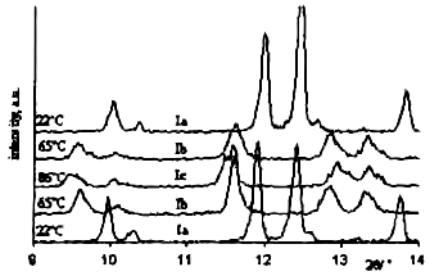

Powder X-ray diffraction patterns of CHF 1035 Form I: details of the 9–14°2θ range collected at RT, 65°C, and 86°C during the heating/cooling cycle (RT → 86°C → RT).

References

Giordano F., Rossi A., Moyano J.R., Gazzaniga A., Massarotti V., Bini M., Capsoni D., Peveri T., Redenti E., Carima L., Dagli Alberi M., Zanol M. *Polymorphism of rac –5,6-diisobutyrroyloxy –2- methylamino – 1,2,3,4 – tetrahydro-naphthalene hydrochloride (CHF1035) – I. Thermal, spectroscopic and x-ray diffraction properties*. J. Pharm. Sci. 2001, 90, 1154.

Rossi A., Savioli A., Bini M., Capsoni D., Massarotti V., Bettini R., Gazzaniga A., Sangalli M. E., Giordano F. Solid state characterization of paracetamol metastable polymorphs formed in binary mixtures with hydroxypropylmethylcellulose. Thermochimica Acta 2003, 406, 55.

2C – Physico-Chemical Properties of Pharmaceutical Systems

G. Bruni, V. Berbenni, P. Cofrancesco, C. Milanese, A. Marini

Aims

The general aim of the project is to address some of the problems relevant in the fields of preformulation and formulation of solid drugs. In particular:

- Polymorphism and polymorphic transformations;
- Thermal stability and thermal decomposition;
- Assessment of crystallinity degree and of its changes with technological operations;
- Phase diagrams characterization;
- Drug-excipient compatibility.

Results

The processes of production of drugs and dosage forms in the solid state often cause unwanted transformation of portions of the substances into amorphous state, with significant changes of properties such as stability and bio-availability. It is therefore important to quantify the relative weight of the amorphous phase, particularly when it is a small fraction (few %), either in the active ingredient or in the dosage form.

In this work we have studied the extent to which mechanical treatments cause amorphisation of perphenazine, a neuroleptic drug used in the treatment of psychosis and schizophrenia.

In particular, the amorphisation of crystalline samples has been induced by high-energy milling. The maximum level of amorphisation (~17%) is achieved with just two hours milling; longer treatments do not change the properties of the sample. The amorphous phase is kinetically stable and only half of it re-crystallizes during hours-long annealing (Fig. 1).

Furthermore, we have developed an experimental model to assess sensitivity, accuracy, and detection limit of the DSC technique in quantifying the amorphous phase. By comparing the measured and expected contents of amorphous phase in mixtures with known crystallinity degree, we show that DSC may, in principle, detect amounts of the amorphous form as low as 1% (Tab. 1).

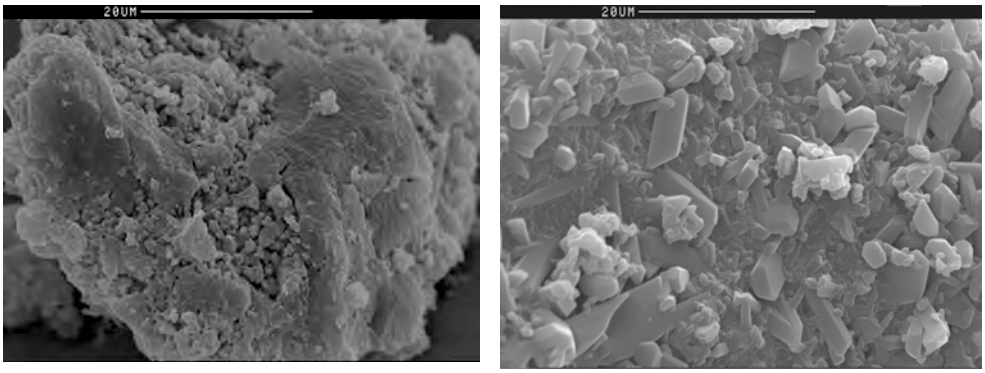

a) b)

Fig. 1 - SEM pictures of perphenazine: (a) ball milled sample; (b) ball milled sample after annealing (12 hours at 85 °C).

Mixture	Q_{exp} (% weight)	Q_{meas} (% weight)
PM_{10}	16.3	14.9
PM_{20}	14.4	13.9
PM_{50}	9.0	8.6
PM_{80}	3.7	5.4
PM_{90}	1.8	3.3
PM_{95}	0.9	1.1

Table 1. Percentage amounts of expected (Q_{exp}) and experimental (Q_{meas}) amorphous phase for mixtures.Mixtures are composed of as received and ball milled perphenazine and the subscript indicates the mass percentage fraction of the as received sample.

References

Bruni G., Milanese C., Bellazzi G., Berbenni V., Cofrancesco P., Marini A., Villa M. – Quantification of drug amorphous fraction by DSC. *J. Thermal Anal. Cal.* **2006**, under review.

Zhang G.G., Law D., Schmitt E.A., Qiu Y. – Phase transformation considerations during process development and manufacture of solid oral dosage forms. *Adv. Drug Del. Rev.* **2004**, 56, 371-390.

Willart J.F., De Gusseme A., Hemon S., Odou G., Danede F., Descamps M. – Direct crystal to glass transformation of trehalose induced by ball milling. *Solid State Comm.* **2001**, 119, 501-505.

Gupta M.K., Vanwert A., Bogner R.H. – Formation of physically stable amorphous drugs by milling with neusilin. *J. Pharm. Sci.* **2003**, 92, 536-551.

Mackin L., Sartnurak S., Thomas I., Moore S. – The impact of low levels of amorphous material (<5%) on the blending characteristics of a direct compression formulation. *Int. J. Pharm.* **2002**, 231, 213-226.

Kawakami K., Numa T., Ida Y. – Assessment of amorphous content by microcalorimetry. *J. Pharm. Sci.* **2002**, 91, 417-423.

Ahmed H., Buckton G., Rawlins D.A. – The use of isothermal microcalorimetry in the study of small degrees of amorphous content of a hydrophobic powder. *Int. J. Pharm.* **1996**, 130, 195-201.

Lefort R., De Gusseme A., Willart J.F., Danède F., Descamps M. – Solid state NMR and DSC methods for quantifying the amorphous content in solid dosage forms: an application to ball-milling of trehalose. *Int. J. Pharm.* **2004**, 280, 209-219.

2C - Polyphenol oxidases and enzymic browning

A. Rescigno, F. Sollai, E. Sanjust

Aims

Enzymatic and Nonenzymatic Food Browning and Its Prevention

Results

Enzymatic and nonenzymatyc browning reactions of amino acids and proteins with arbohydrates, oxidized lipids, and oxidized phenols cause deterioration of food during storage and processing. The loss in nutritional quality and potentially in safety is well established. Particularly, enzymatic browning is attributed to polyphenol oxidase catalyzed oxidation of polyphenols in fruits and vegetables to quinones, which, in turn, polymerize to dark melanin pigments of unknown structure, e.g. formation of brown or black spots from chlorogenic acid. Besides, reaction of polyphenol-derived quinones with free amino acids and proteins could form dark polymers. Tyrosinase and Polyphenol oxidase are copper containing enzymes , widely spread in the living world, which are the most responsible of enzymatic browning. We study catalytic and molecular properties of some vegetal enzymes as well as the role they play in some branches of food technology.

References

Olianas A., Pellegrini M., Sanjust E., Rescigno A. *Tyrosinase activity and hemocyanin in the hemolymph of the slipper lobster Scyllarides latus* J. Comparative Physiology B, 2005,175, 405-411.

Soddu G., Sanjust E., Murgia S., Rescigno A., Interference of some tryptophan metabolites in the formation of melanin *in vitro,* Pigment Cell Research , 2004, 17, 135-141.

Sanjust E., Cecchini G., Sollai F., Curreli N., and Rescigno A., *3-Hydroxykynurenine as a substrate/activator for mushroom tyrosinase*. Arch. Biochem. Biophys. 2003, 412/2, 272-278.

Rescigno, A., Sollai, F., Pisu, B., Rinaldi, A., Sanjust, E., *Tyrosinase Inhibition: General and Applied Aspects*. J. Enzym. Inhib. Medic. Chem. 2002, 17(4), 207-218.

2C - Production of Recombinant Human Monoclonal Antibodies for Diagnostic and Therapeutic Use

R. Pompei, A. Ingianni, A. Desogus, G.Lampis, S. Laconi, M.A. Madeddu (Microbiologia Cagliari); G. Rossolini (Microbiologia Siena); P. Cattani, G. Fadda (Microbiologia Roma Cattolica)

Aims

Production and testing of recombinant monoclonal antibodies against viral or microbial diseases
New antibodies for diagnostic use
New antibodies for infectious disease therapy

Results

Monoclonal antibodies have revealed a great potentiality in both diagnostic and therapeutic purposes. The conventional monoclonal antibodies are produced in murine hybridomas and thus are not always suitable for human therapeutic use. Recently a new technology for the production of human recombinant monoclonal antibodies has been realized (Williamson RA et al. 1997. Use of recombinant human antibody fragmens by Phage Display Technology. Ann. Rev. immunol. 17: 433-55). This technology allows the production of Fab antibody fragments in *E. coli* or other microorganims, with some evident advantages in terms of productivity and specificity of antibodies.
Antibodies have been already produced against Influenza A virus. They recognize a viral antigen common to most influenza viruses, probably the M matrix protein and are suitable for preparing specific diagnostic kits. Other antibodies which are in preparation are those against HHV8, a herpesvirus involved in the Kaposi's sarcoma, and against Parvovirus B19, which is responsible of some general human infectious diseases.
Other antibodies are worthy to be produced against other viral or bacterial diseases.
HHV8, the same virus mentioned above, produces a protein, named *kaposin*, which is necessary for the induction of the cell transformation. It is one of the goals of this project the production of monoclonal antibodies against this protein, with the aim of blocking the transforming activity of HHV8. Other viruses which could be candidates for the production of recombinant monoclonal antibodies are the Blue tongue virus, which infects sheeps and cows, and the African swine pest virus, which is responsible of a severe disease of pigs.

References

Biava M., Fioravanti R., Porretta GC., Sleiter GC., Deidda D., Lampis G., and Pompei R. (1999) *Synthesis and microbiological activities of pyrrole analogs of BM212, a potent antitubercular agent*. Medicinal Chem. Res., **9**, 19-34

Mai A., Sbardella G., Artico M., Massa S., Lampis G., Deidda D., and Pompei R. (1999) *N-[4-(1,1'-biphenylyl)methyl]-4-(4-thiomorpholinylmathyl)benzenamines, a new class of synthetic antituberculosis agents active against Mycobacterium avium.* , Med. Chem. Res. **9**,149-61

Biava M., Fioravanti R., Porretta GC., Sleiter GC. Deidda D., Lampis G., and Pompei R. (1999) *Antimycobacterial activity of new otho-, meta- and para-toluidine derivatives*. Il Farmaco, **54**, 721-27

Biava M., Fioravanti R., Porretta GC., Deidda D., Maullu C. and Pompei R. (1999) *New pyrrole derivatives as antimycobacterial agents analogs of BM212* Bioorg. Med. Chem. Lett., **9**, 2983-88

Costi R., Artico M., Di Santo R., Di Martino G., Massa S., Deidda D., Lampis G., Pompei R. (1999) *Pyridinylpyrrolyl analogs of isoniazid: synthesis and antimycobacterial activities* Med. Chem. Res., **9**, 408-23.

Fioravanti R., Biava M., Porretta GC., Lampis G., Maullu C. and Pompei R. (1999) *Stereospecific synthesis and antimycobacteril activity of 1-aryl-2-/1H-imidazol-1-yl)-o-(aryl)-ethanoxime ethers E' and Z oxiconazole analogs. ,* Med. Chem. Res., **9**, 249-66

Fioravanti R., Biava M., Porretta GC., Lampis G., Deidda D., Pompei R. (1999) *A new series of miconazole analogs: synthesis and in vitro antifungal and antimycobacterial activities* Med. Chem. Res, **9**, 162-75

Lampis G., Desogus A., Ingianni A., Madeddu MA., and Pompei R. (2000) *Nutritionally Variant Streptococci: Biology and Pathogenicity*. Res. Adv. In Microbiology, **1**, 1-10

Ragno R., Pompei R. et al (2000) *Antimycobacterial pyrroles; synthesis, anti-Mycobacterium tuberculosis activity and QSAR studies*. Bioorg. Med. Chem. **8**, 1423-32.

Loy G., Cottiglia F., Pompei R., Monsignore et al. (2001) *Chemical composition and cytotoxic and antimicrobial activity of Calycotome villosa (Poiret) link leaves*. Il Farmaco, **56**, 433-36,

Lampis G., Deidda D., Pinza M. and Pompei R. (2001) *Enhancement of anti-herpetic activity of glycyrrhizic acid by physiological proteins*. Antiv. Chem. Chemother. , **12**, 125-31.

Biava M., Porretta G.C., Pompei R. et al. (2003) *Importance of thiomorpholine introduction in new pyrrole derivatives as antimicrobial agents analogues of BM 212*., Bioorg. Med. Chem. **11**: 515-520

Desogus A., Pompei R. et al. (2003) *Production and characterization of a human recombinant monoclonal Fab fragment specifically directed to influenza A viruses*. Clin. Diagn. Lab. Immunol.,**10**, 680-685

Pompei R., Lampis G., Inganni A., Nonnis D., Ionta MT., Massidda B. (2004) *Allergy and tumour outcome after primary cancer therapy*. Int. Arch. Allergy Immunol., in press

2C – Selenium forms in solenium-enriched potato tubers

A. Hochkoeppler, V. Poggi

Aims

This study was aimed at identifying the main selenium forms in the selenium-enriched potatoes known by the name of "Selenella". Furthermore, the protein fraction of Selenella potatoes was investigated in order to determine the molecular mass of the main selenium-containing proteins.

Results

The knowledge of the chemical and molecular form in which nutrients occur in a food is crucial for determining its nutritional value. In fact, the form influences both the digestive and metabolic processes and it is decisive for the synthesis of biologically active compounds. The disclosure of the molecular forms of a nutrient is particularly relevant in new foods such as Selenella potatoes.

Results obtained in this research highlight the prevalence, in potato tissues, of the soluble forms of selenium: more than 50% of selenium can be extracted by a water solution even when short equilibration time intervals are applied (Table 1).

extraction time length	selenium in extract	selenium in pellet	recover y
0.5 h	59.4	25.7	85.1
1 h	54.8	15.8	70.6
1.5 h	56.8	20.1	76.9
2 h	53.7	38.6	92.3
3 h	61.5	32.9	94.4

Tab. 1 Selenium from potato (cv. Agata) tissues as partitioned in either extract or pellet upon different equilibration time intervals.

This observation is independent from the genotype: similar results were achieved considering two different potato cultivars (Agata, Primura).

Selenium determination in solutions obtained by ultrafiltration of Selenella extracts demonstrates that, independently from the genotype, about 60% of extracted selenium is included in forms with low molecular mass (Figure 1).

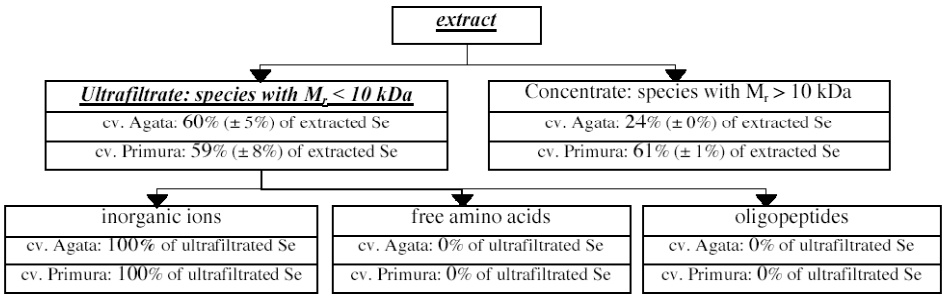

Fig. 1 Selenium forms in potatoes (cvs. Agata e Primura) extracts.

Free seleno-amino acids are not detectable: this result has been achieved using different procedures (directly, by either HPLC or LC-MS analysis, and indirectly, after determination of inorganic selenium) leading to the same conclusion (Figure 1). No selenium was found in oligopeptides precipitated by means of trichloroacetic acid. The determination of inorganic selenium in ultrafiltrates confirms these results: independently on the genotype, the 100% of the low molecular mass forms of selenium are inorganic compounds.
The amount of selenium included in species with molecular mass higher than 10 kDa (which are mainly proteins) is strongly affected by the genotype: the high molecular mass forms of selenium are about 60% of extracted selenium in tubers of potatoes cultivar Primura and about 24% of extracted selenium in tubers of potatoes cultivar Agata (Figure 1). This observation leads to the conclusion that the relevance of selenoproteins in selenium-enriched potatoes is dependent on the genotype; in other words, the observation suggests that the expression of genes encoding selenoproteins could be differently regulated in different genotypes.
The putative molecular masses of the main selenium-containing proteins were about 20 kDa or 60 kDa (Figure 2). Until now the only selenoprotein completely characterized in the plant kingdom is a 21 kDa glutathione peroxidase described in the green alga *Chlamydomonas reinhardtii*.

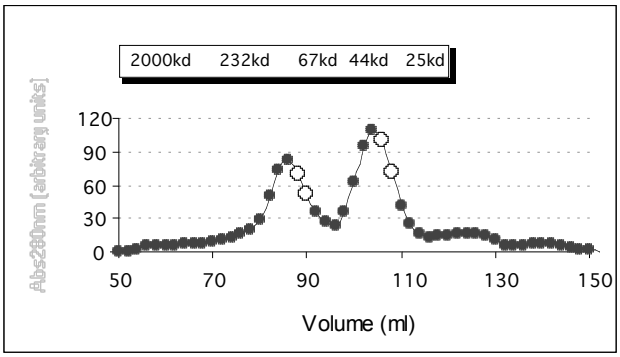

Fig. 2 Gel filtration chromatogram of potato (cv. Agata) extracts: the open circles emphasize high selenium fractions; the inset reports the elution volumes of molecular mass standard proteins.

References

Poggi V., Setti L., Bordoni A. and P. Biagi. *Vegetables as Functional Foods: Selenium-Enriched Potatoes*. In Vegetables: Growing Environment and Mineral Nutrition, Ed. R. Dris, The Haworth Press Inc., Binghamton NY. In press.

Pifferi P.G. and Poggi V., *Composition for increasing selenium and decreasing nitrate inside vegetables and use thereof*, European Patent, 2003, EP 98 103 940.

Poggi V., Arcioni A., Filippini P. and Pifferi P.G., *Foliar application of selenite and selenate to potato (Solanum tuberosum): effect of a ligand agent on selenium content of tubers*, J. Agric. Food Chem., 2000, 48, 4749-4751.

2C - Structure and oxidative stability of water-in-oil food emulsions

A. Ceglie, L. Ambrosone, M. Mosca

Aim

To study the relationships between W/O emulsion stability and the oxidative stability of the continuous oily phase.

Results

The effect of W/Olive oil emulsion structure on the susceptibility to oxidation of emulsified vegetable oils was investigated by modulating the characteristics of the water dispersed phase in different ways. First, olive oil samples were emulsified by adding a fixed water quantity in different ways in order to change the average droplet size.

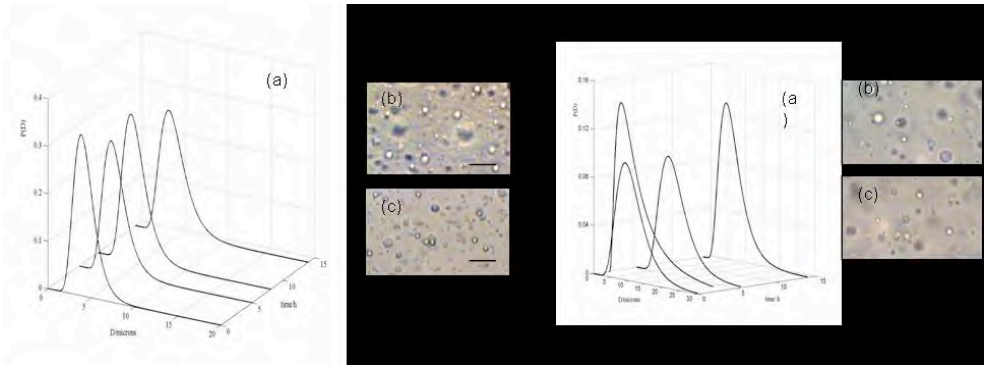

Figures 1,2 (a): (1) Droplet size distribution time evolution of filtered extra virgin olive oil emulsified with Ultraturrax for 45 min (E_{45}) and (2) for 15 min (E_{15}). (b, c): (1) Optical microscopy: representative micrographs of E_{45} emulsion at different oxidation times. Bar =20 mm (b): E_{45} just after preparation; (c): E_{45} after 14 hours of UV oxidation. (2) Optical microscopy: representative micrographs of E_{15} emulsion at different oxidation times. Bar =20 mm (b): E_{15} just after preparation; (c): E_{15} after 14 hours of UV oxidation

The results obtained from samples oxidized with UV light show that the oxidative stability of water emulsified olive oils depends on the specific surface area of the water dispersed phase. Secondly, studies on the oxidation of W/Olive oil emulsions containing different water amounts, reveal that the greater the region of emulsion stability, the longer the resistance of oil to oxidation. Moreover, it has been shown that the oxidation process affects emulsion stability to sedimentation. Finally, further evidences of the link between the oxidative stability and emulsion stability were gathered by studying lipid oxidation in W/Olive oil emulsions stabilized by edible surfactants (Spans, Sorbitan fatty acids esters). Different sorbitan fatty acid esters (Span 20, sorbitan monolaurate; Span 80, sorbitan monooleate; Span 85, sorbitan trioleate) were used to prepare water-in-olive oil emulsions which were then oxidized with UV light. The results obtained from W/O emulsions (W/Olive oil/Span) were compared to Span-olive oil and water-olive oil binary systems in order to evaluate the contribution of each component in the oxidation of emulsified olive oils.

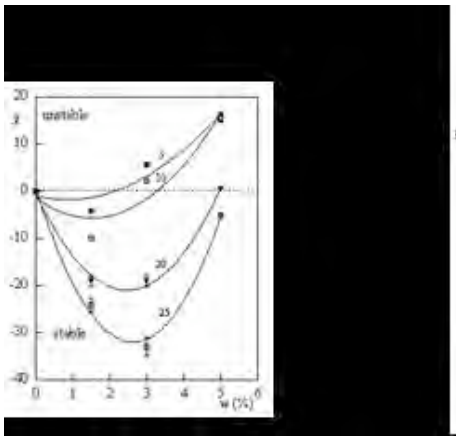

Fig.3: Peroxide value (PV) relative to a control (natural olive oil), c, of emulsified olive oils as a function of water concentration at fixed oxidation time. The numbers on the curves indicate the value in hours.

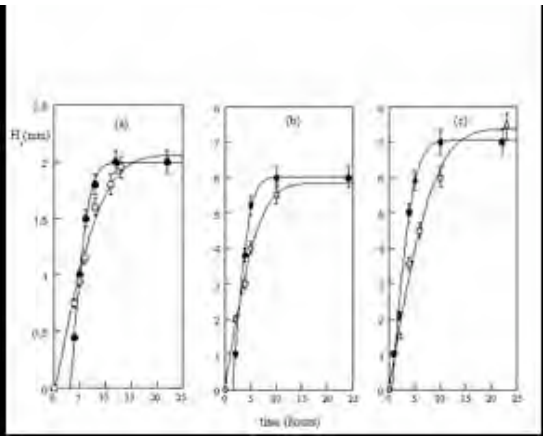

Fig.4: Height of sediment, H_s, as a function of time for water-in- olive oil emulsions with different added water. (a) H_2O = 3%(w/w); (b) H_2O = 5%(w/w);(c) H_2O = 10%(w/w); (•) oxidized sample; (o) non-oxidized sample.

The results show that the total concentration of different Span molecules as well as its distribution between the droplets and the aggregate they form in the bulk phase, have a significant impact on the oxidative behaviour of emulsified olive oils. In particular, the effectiveness of Spans in stabilizing the emulsified olive oils were related to their chemical structure and so to their ability to interact with hydroperoxides.

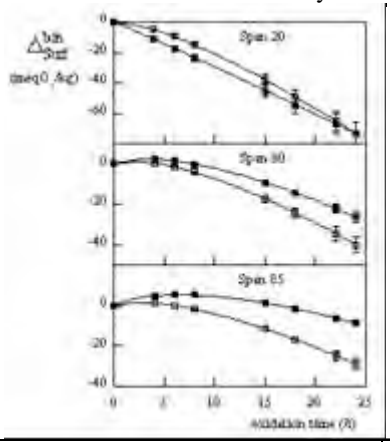

***Fig.5**: Spans Binary and Ternary relative peroxide values, Δ^{bin}_{surf} and Δ^{ter}_{surf}, as a function of the oxidation time for olive oil-Span binary systems (□) and ternary systems (□), with Span content (a) 1wt% and (b) 5wt%.*

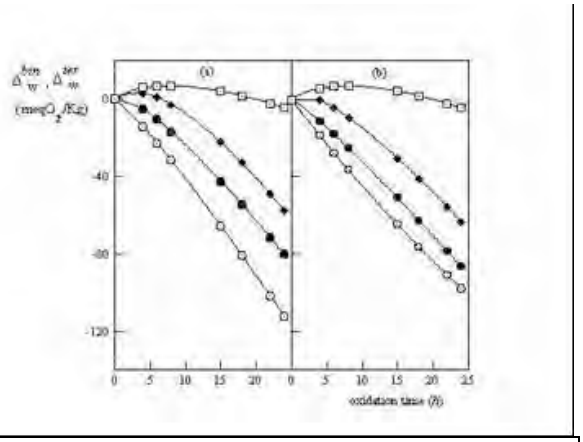

Fig.6: Water binary and ternary relative peroxide values, Δ^{bin}_{w} and Δ^{ter}_{w}, as a function of the oxidation time for olive oil-water (3wt%) binary system (□) and water-olive oil-Span ternary systems with Span content (a) 1wt% and (b) 5wt%. Span 85 (□), Span 80(□), Span 20(□).

Span 20 was more efficient in protecting the emulsified oil during the oxidation in the Span 20/olive oil binary system while Span 85 was more efficient in emulsion (ternary system). So the formation of mixed aggregate Span /hydroperoxides in the binary systems and of strong interfacial films made up of oil, Span, water can increase the oxidative stability of the emulsified oil.
Further studies are being carried out on a triolein-based model system lacking in the unsaponifiable fraction of olive oils which can greatly affect the oxidation process. The results will provide more information about the role of W/O interface in the oxidation of emulsified vegetable oils and other heterogeneous food systems.

References

Ambrosone L., Mosca M. and Ceglie A., *Impact of edile surfactants on the oxidation of olive oil in water-in-oil emulsions*, Food Hydrocolloids, 2007, in press.

Ambrosone L., Mosca M. and Ceglie A., *Oxidation of Olive oil in water-in-oil emulsions* Food Hydrocolloids, 2006, 20, 1080-1086.

Ambrosone L., Cinelli G., Mosca M. And Ceglie A., *Susceptibility of water-emulsified extra virgin olive oils to oxidation*, Journal of the American Oil Chemists' Society, 2006, 83, 165-170.

2C - Structure and stability in food emulsions

A. Ceglie, L. Ambrosone, G. Palazzo, G. Colafemmina, G. Cinelli

Aims

Structure determination in food emulsions via NMR and VEM techniques
Emulsification processes and oil an fat oxidation
Demulsification kinetics and stability of food emulsions

Results

Our approach in analysing PSGE-NMR data (see section NMR data analysis) was firstly applied to emulsion as alternative to previously proposed treatment to obtain the size distribution of water dispersed phase.
In the figure size distribution of dispersed phase of normal margarine: (a) our method to calculate size distribution by NMR data, (b) traditional method.

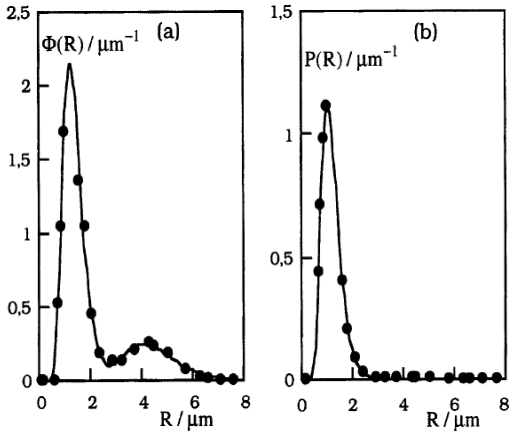

Normal margarine

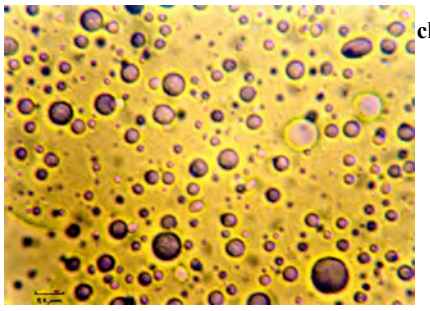

Low cholesterol

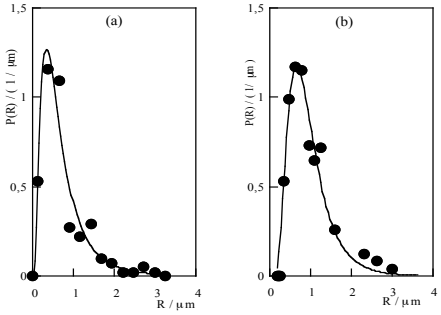

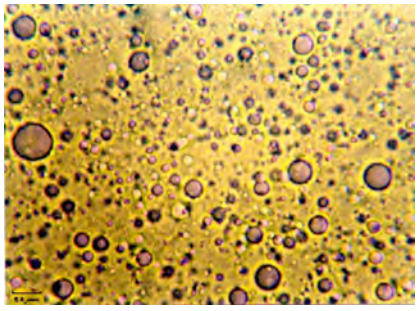

Salted butter

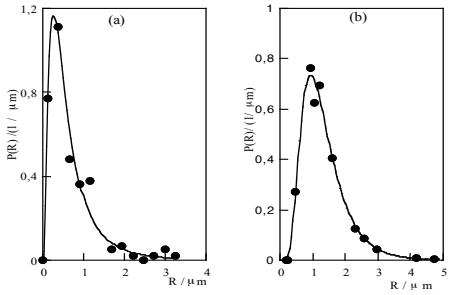

Size distribution from VEM (left) and from NMR data (right).

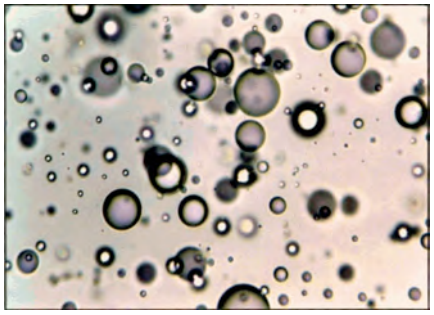

‘veiled’ extra- virgin olive oil

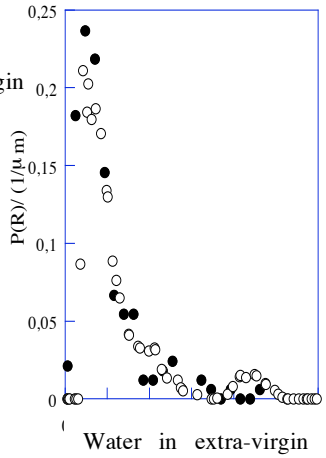

Water in extra-virgin olive oil analysed by NMR technique (empty circles) and via VEM (filled circles).

References

Ambrosone, L. and Ceglie A. Metodo ed apparato per la determinazione della polidispersità in emulsione. Italian Patent, n°FI99000044 (1999).

Colafemmina, G., Palazzo, G., Ceglie, A., Ambrosone, L., Cinelli, G. and DiLorenzo, V. “Restricted diffusion: an effective tool to investigate food emulsions”, Progress Colloid & Polymer Science 120, 23-27 (2002)

Ambrosone, L., Angelico, R., Ceglie, A., Cinelli, G. and Dilorenzo,V. “The role of water in the oxidation process of veiled extravirgin olive oils”, Journal of the American Oil Chemists’ Society 79, 577-582 (2002).

2C - Study of organic materials polymorphism

V. Massarotti, D. Capsoni, M. Bini

Aims

Study changes in crystalline structures of sodium naproxen during dehydration processes. Characterize the sodium naproxen crystal forms stable at different degree of relative humidity.

Results

The anhydrous sodium naproxen can form several hydrated phases if maintained at different relative humidities (RH). The water uptake can promote crystallographic modifications, according to the amount of water. A dihydrated form could be obtained either by crystallization in water or by exposure of the anhydrous form to a RH of 55%. The formation and characterization of a new tetrahydrated form, obtained by exposing the anhydrous sodium naproxen to RH ≥ 75% will be studied. All the hydrated compounds were characterized by the combined use of several spectroscopic (NMR), thermal (TGA and DSC) and crystallographic (room and high temperature XRPD) techniques. The thermal stability of both the dihydrated and tetrahydrated compounds was also tested.